Worldwide forest surveys reveal forty-three new species in *Phytophthora* major Clade 2 with fundamental implications for the evolution and biogeography of the genus and global plant biosecurity

T. Jung[1,2*], I. Milenković[1,3], Y. Balci[4], J. Janoušek[1], T. Kudláček[1,5], Z.Á. Nagy[1], B. Baharuddin[6], J. Bakonyi[7], K.D. Broders[8,9], S.O. Cacciola[10], T.-T. Chang[11], N.M. Chi[12], T. Corcobado[1], A. Cravador[13], B. Đorđević[1], A. Durán[14], M. Ferreira[15], C.-H. Fu[11], L. Garcia[16], A. Hieno[17], H.-H. Ho[18], C. Hong[19], M. Junaid[6], K. Kageyama[17], T. Kuswinanti[6], C. Maia[20], T. Májek[1], H. Masuya[21], G. Magnano di San Lio[22], B. Mendieta-Araica[16], N. Nasri[23], L.S.S. Oliveira[24], A. Pane[10], A. Pérez-Sierra[25], A. Rosmana[6], E. Sanfuentes von Stowasser[26], B. Scanu[27], R. Singh[15], Z. Stanivuković[28], M. Tarigan[14], P.Q. Thu[12], Z. Tomić[29], M. Tomšovský[1], S. Uematsu[30], J.F. Webber[25], H.-C. Zeng[31], F.-C. Zheng[32], C.M. Brasier[25], M. Horta Jung[1,2]

[1]*Mendel University in Brno, Faculty of Forestry and Wood Technology, Department of Forest Protection and Wildlife Management, Phytophthora Research Centre, 613 00 Brno, Czech Republic;* [2]*Phytophthora Research and Consultancy, 83131 Nussdorf, Germany;* [3]*University of Belgrade, Faculty of Forestry, 11030 Belgrade, Serbia;* [4]*USDA-APHIS Plant Protection and Quarantine, 4700 River Road, Riverdale, Maryland, 20737 USA;* [5]*University of Greifswald, Institute for Mathematics and Computer Science & Center for Functional Genomics of Microbes, 17489 Greifswald, Germany;* [6]*Departement of Plant Pest and Disease, Faculty of Agriculture, Hasanuddin University, Makassar, 90245, South Sulawesi, Indonesia;* [7]*HUN-REN Centre for Agricultural Research, Plant Protection Institute, ELKH, 1022 Budapest, Hungary;* [8]*Smithsonian Tropical Research Institute, Apartado Panamá, República de Panamá;* [9]*USDA, Agricultural Research Service, National Center for Agricultural Utilization Research, Mycotoxin Prevention and Applied Microbiology Research Unit, Peoria, IL, 61604, USA;* [10]*Department of Agriculture, Food and Environment, University of Catania, 95123 Catania, Italy;* [11]*Forest Protection Division, Taiwan Forestry Research Institute, Taipei, Taiwan;* [12]*Forest Protection Research Centre, Vietnamese Academy of Forest Sciences, 10000 Hanoi, Vietnam;* [13]*MED—Mediterranean Institute for Agriculture, Environment and Development & CHANGE—Global Change and Sustainability Institute, University of Algarve, 8005-130 Faro, Portugal;* [14]*Fiber Research and Development, Asia Pacific Resources International Limited (APRIL), 28300 Pangkalan Kerinci, Riau, Indonesia;* [15]*Plant Diagnostic Center, Department of Plant Pathology and Crop Physiology, Louisiana State University Agricultural Center, Baton Rouge, Louisiana, USA;* [16]*Universidad Nacional Agraria, Carretera Norte, Managua 11065, Nicaragua;* [17]*River Basin Research Center, Gifu University, Gifu, 501-1193, Japan;* [18]*Department of Biology, State University of New York, New Paltz, New York 12561, USA;* [19]*Hampton Roads Agricultural Research and Extension Center, Virginia Tech, Virginia Beach, VA 23455, USA;* [20]*Centre of Marine Sciences (CCMAR), University of Algarve, 8005-139 Faro, Portugal;* [21]*Forestry and Forest Products Research Institute (FFPRI), Tsukuba, Ibaraki, 305-8687, Japan;* [22]*University Mediterranea of Reggio Calabria, Department of Agriculture, 89124 Reggio Calabria, Italy;* [23]*The United Graduate School of Agricultural Science, Ehime University, Matsuyama, 790-8566, Japan;* [24]*Research and Development, Bracell, Alagoinhas, Bahia 48030-300, Brazil;* [25]*Forest Research, Alice Holt Lodge, Farnham, Surrey GU10 4LH, UK;* [26]*Laboratorio de Patología Forestal, Facultad Ciencias Forestales y Centro de Biotecnología, Universidad de Concepción, 4030000 Concepción, Chile;* [27]*Department of Agricultural Sciences, University of Sassari, Viale Italia 39A, 07100 Sassari, Italy;* [28]*University of Banja Luka, Faculty of Forestry, 78000 Banja Luka, Bosnia and Herzegovina;* [29]*Center for Plant Protection, Croatian Agency for Agriculture and Food, 10000 Zagreb, Croatia;* [30]*Laboratory of Molecular and Cellular Biology, Dept. of Bioregulation and Bio-interaction, Tokyo University of Agriculture and Technology, Fuchu, Tokyo, 183-8509, Japan;* [31]*The Institute of Bioscience and Biotechnology, Chinese Academy of Tropical Agricultural Sciences, Haikou 571101, Hainan, China;* [32]*College of Environment and Plant Protection, Hainan University, Baodoa Xincun, Danzhou City, Hainan 571737, China*

**Corresponding authors*: T. Jung, thomas.jung@mendelu.cz; dr.t.jung@gmail.com; C.M. Brasier, clive.brasier@forestresearch.gov.uk

Abstract: During 25 surveys of global *Phytophthora* diversity, conducted between 1998 and 2020, 43 new species were detected in natural ecosystems and, occasionally, in nurseries and outplantings in Europe, Southeast and East Asia and the Americas. Based on a multigene phylogeny of nine nuclear and four mitochondrial gene regions they were assigned to five of the six known subclades, 2a–c, e and f, of *Phytophthora* major Clade 2 and the new subclade 2g. The evolutionary history of the Clade appears to have involved the pre-Gondwanan divergence of three extant subclades, 2c, 2e and 2f, all having disjunct natural distributions on separate continents and comprising species with a soilborne and aquatic lifestyle and, in addition, a few partially aerial species in Clade 2c; and the post-Gondwanan evolution of subclades 2a and 2g in Southeast/East Asia and 2b in South America, respectively, from their common ancestor. Species in Clade 2g are soilborne whereas Clade 2b comprises both soil-inhabiting and aerial species. Clade 2a has evolved further towards an aerial lifestyle comprising only species which are predominantly or partially airborne. Based on high nuclear heterozygosity levels *ca*. 38 % of the taxa in Clades 2a and 2b could be some form of hybrid, and the hybridity may be favoured by an A1/A2 breeding system and an aerial life style. Circumstantial evidence suggests the now 93 described species and informally designated taxa in Clade 2 result from both allopatric non-adaptive and sympatric adaptive radiations. They represent most morphological and physiological characters, breeding systems, lifestyles and forms of host specialism found across the *Phytophthora* clades as a whole, demonstrating the strong biological cohesiveness of the genus. The finding of 43 previously unknown species from a single *Phytophthora* clade highlight a critical lack of information on the scale of the unknown pathogen threats to forests and natural ecosystems, underlining the risk of basing plant biosecurity protocols mainly on lists of named organisms. More surveys in natural ecosystems of yet unsurveyed regions in Africa, Asia, Central and South America are needed to unveil the full diversity of the clade and the factors driving diversity, speciation and adaptation in *Phytophthora*.

Key words: allopatric speciation, biodiversity, breeding systems, Gondwana, Laurasia, lifestyle, new taxa, phylogeny, sympatric species radiation.

Taxonomic novelties: New species: *Phytophthora amamensis* T. Jung, K. Kageyama, H. Masuya & S. Uematsu, *Phytophthora angustata* T. Jung, L. Garcia, B. Mendieta-Araica, & Y. Balci, *Phytophthora balkanensis* I. Milenković, Ž. Tomić, T. Jung & M. Horta Jung, *Phytophthora borneensis* T. Jung, A. Durán, M. Tarigan & M. Horta Jung, *Phytophthora calidophila* T. Jung, Y. Balci, L. Garcia & B. Mendieta-Araica, *Phytophthora catenulata* T. Jung, T.-T. Chang, N.M. Chi & M. Horta Jung, *Phytophthora celeris* T. Jung, L. Oliveira, M. Tarigan & I. Milenković, *Phytophthora curvata* T. Jung, A. Hieno, H. Masuya & M. Horta Jung, *Phytophthora distorta* T. Jung, A. Durán, E. Sanfuentes von Stowasser & M. Horta Jung, *Phytophthora excentrica* T. Jung, S. Uematsu, K. Kageyama & C.M. Brasier, *Phytophthora falcata* T. Jung, K. Kageyama, S. Uematsu & M. Horta Jung, *Phytophthora fansipanensis* T. Jung, N.M. Chi, T. Corcobado & C.M. Brasier, *Phytophthora frigidophila* T. Jung, Y. Balci, K. Broders & I. Milenković, *Phytophthora furcata* T. Jung, N.M. Chi, I. Milenković & M. Horta Jung, *Phytophthora inclinata* N.M. Chi, T. Jung, M. Horta Jung & I. Milenković, *Phytophthora indonesiensis* T. Jung, M. Tarigan, L. Oliveira & I. Milenković,

Studies in Mycology

Phytophthora japonensis T. Jung, A. Hieno, H. Masuya & J.F. Webber, *Phytophthora limosa* T. Corcobado, T. Majek, M. Ferreira & T. Jung, *Phytophthora macroglobulosa* H.-C. Zeng, H.-H. Ho, F.-C. Zheng & T. Jung, *Phytophthora montana* T. Jung, Y. Balci, K. Broders & M. Horta Jung, *Phytophthora multipapillata* T. Jung, M. Tarigan, I. Milenković & M. Horta Jung, *Phytophthora multiplex* T. Jung, Y. Balci, K. Broders & M. Horta Jung, *Phytophthora nimia* T. Jung, H. Masuya, A. Hieno & C.M. Brasier, *Phytophthora oblonga* T. Jung, S. Uematsu, K. Kageyama & C.M. Brasier, *Phytophthora obovoidea* T. Jung, Y. Balci, L. Garcia & B. Mendieta-Araica, *Phytophthora obturata* T. Jung, N.M. Chi, I. Milenković & M. Horta Jung, *Phytophthora penetrans* T. Jung, Y. Balci, K. Broders & I. Milenković, *Phytophthora platani* T. Jung, A. Pérez-Sierra, S.O. Cacciola & M. Horta Jung, *Phytophthora proliferata* T. Jung, N.M. Chi, I. Milenković & M. Horta Jung, *Phytophthora pseudocapensis* T. Jung, T.-T. Chang, I. Milenković & M. Horta Jung, *Phytophthora pseudocitrophthora* T. Jung, S.O. Cacciola, J. Bakonyi & M. Horta Jung, *Phytophthora pseudofrigida* T. Jung, A. Durán, M. Tarigan & M. Horta Jung, *Phytophthora pseudoccultans* T. Jung, T.-T. Chang, I. Milenković & M. Horta Jung, *Phytophthora pyriformis* T. Jung, Y. Balci, K.D. Boders & M. Horta Jung, *Phytophthora sumatera* T. Jung, M. Tarigan, M. Junaid & A. Durán, *Phytophthora transposita* T. Jung, K. Kageyama, C.M. Brasier & H. Masuya, *Phytophthora vacuola* T. Jung, H. Masuya, K. Kageyama & J.F. Webber, *Phytophthora valdiviana* T. Jung, E. Sanfuentes von Stowasser, A. Durán & M. Horta Jung, *Phytophthora variepedicellata* T. Jung, Y. Balci, K. Broders & I. Milenković, *Phytophthora vietnamensis* T. Jung, N.M. Chi, I. Milenković & M. Horta Jung, *Phytophthora* ×*australasiatica* T. Jung, N.M. Chi, M. Tarigan & M. Horta Jung, *Phytophthora* ×*lusitanica* T. Jung, M. Horta Jung, C. Maia & I. Milenković, *Phytophthora* ×*taiwanensis* T. Jung, T.-T. Chang, H.-S. Fu & M. Horta Jung.

Citation: Jung T, Milenković I, Balci Y, Janoušek J, Kudláček T, Nagy ZÁ, Baharuddin B, Bakonyi J, Broders KD, Cacciola SO, Chang T-T, Chi NM, Corcobado T, Cravador A, Đorđević B, Durán A, Ferreira M, Fu C-H, Garcia L, Hieno A, Ho H-H, Hong C, Junaid M, Kageyama K, Kuswinanti T, Maia C, Májek T, Masuya H, Magnano di San Lio G, Mendieta-Araica B, Nasri N, Oliveira LSS, Pane A, Pérez-Sierra A, Rosmana A, Sanfuentes von Stowasser E, Scanu B, Singh R, Stanivuković Z, Tarigan M, Thu PQ, Tomić Z, Tomšovský M, Uematsu S, Webber JF, Zeng H-C, Zheng F-C, Brasier CM, Horta Jung M (2024). Worldwide forest surveys reveal forty-three new species in *Phytophthora* major Clade 2 with fundamental implications for the evolution and biogeography of the genus and global plant biosecurity. *Studies in Mycology* **107**: 251–388. doi: 10.3114/sim.2024.107.04

Received: 20 October 2023; **Accepted:** 15 January 2024; **Effectively published online:** 27 February 2024

Corresponding editor: R.A. Samson

INTRODUCTION

The oomycete genus *Phytophthora* currently includes eight obligate biotrophic and 210 culturable necrotrophic or hemibiotrophic described species which are soil-, water- or airborne plant pathogens causing some of the most damaging diseases of horticultural and agricultural crops, forests and other natural ecosystems (Erwin & Ribeiro 1996, Yang *et al.* 2017, Jung *et al.* 2018a, 2022, Brasier *et al.* 2022, Chen *et al.* 2022, Abad *et al.* 2023a). Recently Abad *et al.* (2023a) have consolidated the formal taxonomy of the genus by designating lectotypes, epitypes or neotypes for numerous species, validating other species and providing additional taxonomic descriptions. *Phytophthora* is monophyletic and currently resolves into 15 major phylogenetic clades with numerous subclades (Yang *et al.* 2017, Brasier *et al.* 2022, Chen *et al.* 2022, Abad *et al.* 2023a). In addition, phylogenetic and phylogenomic studies demonstrated that the 20 genera of obligate biotrophic downy mildews are residing as two separate clades within the genus *Phytophthora* as a result of a paraphyletic evolutionary jump followed by rapid global radiation driven by specialization to non-woody host plants (Cooke *et al.* 2000, Thines & Choi 2016, Jung *et al.* 2017a, McCarthy & Fitzpatrick 2017, Bourret *et al.* 2018, Fletcher *et al.* 2018, 2019, Scanu *et al.* 2021, Brasier *et al.* 2022, Abad *et al.* 2023a).

At the time of the first genus-wide molecular phylogeny (Cooke *et al.* 2000) *Phytophthora* comprised around 50 known taxa, including seven species in major Clade 2: *P. botryosa*, *P. capsici*, *P. citricola*, *P. citrophthora*, *P. colocasiae*, *P. inflata* and *P. multivesiculata*. *Phytophthora inflata* was later declared a lost and invalid species (Jung & Burgess 2009). Soon, however, it was estimated that the genus might comprise as many as 600 species (Brasier 2009) and subsequent surveys in natural ecosystems, nurseries and plantations, together with a revision of the '*P. citricola* complex' using multigene phylogenetic analyses, enlarged Clade 2 to 34 described species. These reside in five evolutionary divergent subclades, Clades 2a–2e (Aragaki & Uchida 2001, Maseko *et al.* 2007, Reeser *et al.* 2007, Abad *et al.* 2008, 2011, 2023a, Hong *et al.* 2009, 2011, Jung & Burgess 2009, Scott *et al.* 2009, Bezuidenhout *et al.* 2010, Rea *et al.* 2010, Vettraino *et al.* 2011, Ginetti *et al.* 2014, Henricot *et al.* 2014, Ann *et al.* 2015, Man In't Veld *et al.* 2015, Brazee *et al.* 2017, Crous *et al.* 2017, 2020, Ruano-Rosa *et al.* 2018, Albuquerque Alves *et al.* 2019, Burgess *et al.* 2020, Bose *et al.* 2021a, Dang *et al.* 2021, Decloquement *et al.* 2021, Chen *et al.* 2022). Half of these species, including *P. acaciae*, *P. acaciivora*, *P. amaranthi*, *P. botryosa*, *P. capsici*, *P. citricola*, *P. citrophthora*, *P. colocasiae*, *P. frigida*, *P. gloveri* (previously *P. glovera*; Abad *et al.* 2011, 2023a), *P. meadii*, *P. mekongensis*, *P. mengei*, *P. multibullata*, *P. oleae*, *P. theobromicola*, *P. tropicalis* and *P.* ×*vanyenensis* cause severe root rots, bark cankers, fruit rots or leaf blights on tropical and subtropical crops, tree crops and plantation trees (Erwin & Ribeiro 1996, Aragaki & Uchida 2001, Drenth & Guest 2004, Maseko *et al.* 2007, Abad *et al.* 2011, Hong *et al.* 2009, Lamour 2013, Ann *et al.* 2015, Crous *et al.* 2017, Ruano-Rosa *et al.* 2018, Albuquerque Alves *et al.* 2019, Burgess *et al.* 2020, Dang *et al.* 2021, Decloquement *et al.* 2021, Brasier *et al.* 2022, Chen *et al.* 2022). Others, such as *P. acerina*, *P. aysenensis*, *P. elongata*, *P. multivora*, *P. pini*, *P. plurivora* and *P. siskiyouensis* are primarily pathogens of forest trees and shrubs causing root rots and bark cankers often resulting in decline and dieback (Reeser *et al.* 2007, Jung & Burgess 2009, Scott *et al.* 2009, Rea *et al.* 2010, Hong *et al.* 2011, Ginetti *et al.* 2014, Milenkovic *et al.* 2018, Jung *et al.* 2018a, Corcobado *et al.* 2020, Crous *et al.* 2020). Many of the aforementioned species plus *P. bishii* (previously *P. bisheria*; Abad *et al.* 2008, 2023a), *P. capensis*, *P. emzansi*, *P. multivesiculata*, *P. occultans*, *P. pachypleura* and *P. terminalis* also cause severe losses of a wide range of host plants in nurseries and ornamental plantings (Ilieva *et al.* 1998, Abad *et al.* 2008, Donahoo & Lamour 2008a, Moralejo *et al.* 2008, Leonberger *et al.* 2013, Pérez-Sierra & Jung 2013, Bienapfl & Balci 2014, Henricot *et al.* 2014, Prigigallo *et al.* 2015, Man In't Veld *et al.* 2015, Jung *et al.* 2016, Frankel *et al.* 2020, Mora-Sala *et al.* 2022). In contrast, *P. himalsilva*, *P. insulinativitatica* and several informally designated Clade 2 taxa have only been obtained from soil around apparently healthy vegetation in natural forests in Nepal, Christmas Island, the Cocos Islands, Taiwan and Papua New Guinea (Vettraino *et al.* 2011, Jung *et al.* 2017b, 2020, Burgess *et al.* 2021, Dang *et al.* 2021). Also, several species behaving as aggressive pathogens in invasive situations including *P. bishii*, *P. citrophthora* and *P. plurivora* in Europe and North America, *P. multivora* in Australia, Europe and

North America, and *P. elongata* in Australia have been found in 'healthy' natural ecosystems in East Asia (*P. bishii*, *P. citrophthora*, *P. elongata*, *P. plurivora*; Brasier *et al.* 2010, Bennett *et al.* 2017, Jung *et al.* 2017b, 2020) and South Africa (*P. multivora*; Oh *et al.* 2013, Tsykun *et al.* 2022).

Since 1998, we have conducted 25 *Phytophthora* surveys in natural and managed ecosystems across the Americas, Europe, Southeast and East Asia intending to better understand the diversity of the genus, its evolutionary history and the potential scale of the biosecurity threat posed to forests globally by scientifically 'unknown' tree pathogens (*cf.* Brasier 2008, Jung *et al.* 2016). Remarkably, these surveys have produced, amongst others, *ca*. 1 000 *Phytophthora* isolates preliminarily identified as belonging to 43 putative new Clade 2 taxa. Several of these have been informally taxonomically designated *e.g.* as *P. citricola* VII, *P.* taxon occultans-like, *P.* taxon ×botryosa-like and *P.* taxon ×meadii-like (Jung *et al.* 2017b), *P.* taxon botryosa-like 2, *P.* taxon meadii-like 1 and 2, *P.* taxon multivesiculata-like 1 and *P.* taxon tropicalis-like 2 (Jung *et al.* 2020), *P. valdiviana nom. prov*. (Jung *et al.* 2018b) and *P.* ×citrophthora-related1, *P.* ×citrophthora-related2 and *P.* ×citrophthora2 (Van Poucke *et al.* 2021). In this study, we used morphological and physiological criteria together with DNA sequence data from nine nuclear and four mitochondrial gene regions to characterise the 43 putative new taxa and compare them with each other and to previously known Clade 2 species. Here we describe each of them as new species and discuss the implications of our findings for the evolution and biogeography of the Clade and global biosecurity.

TERMINOLOGY

Use of the terms *Phytophthora* taxon x and *Phytophthora* sp. x

The informal term '*Phytophthora* taxon x' (*cf.* Brasier *et al.* 2003) was developed to cover situations where it was clear that a novel entity of some taxonomic level had been identified, but formal description was likely to be delayed pending further analysis to determine the level of taxonomic distinction (*e.g.* species, subspecies, variety etc; *cf.* Brasier & Rayner 1987) and because of the often considerable time required to produce the appropriate publication. This situation has arisen more frequently as more and more novel *Phytophthora* taxa are being discovered.

In this context, we do not concur with the use of the informal terminology '*Phytophthora* sp. x'. A putative new taxon is not a species (or a 'sp.') until its correct hierarchical status has been determined (as far as is reasonable), and its proposed name has been formally designated under the ICNafp (International Code of Nomenclature for algae, fungi, and plants; https://www.iapt-taxon.org) guidelines. On this basis, we consider that informal use of the term '*Phytophthora* sp. x' in the case of a putative but only partially characterised new taxon is essentially prejudicial to its eventual ranking. We have therefore confined ourselves to using the term "*Phytophthora* taxon x" throughout this manuscript.

Subclade phraseology

Naming of the subclades follows Yang *et al.* (2017), Chen *et al.* (2022) and Abad *et al.* (2023a). For brevity, throughout much of the text the main phylogenetic subclades 2a–2e of *Phytophthora* Clade 2, technically 'Clade 2 subclade a', 'Clade 2 subclade b' *etc*., are referred to as Clade 2a, Clade 2b and so on. Following Abad *et al.* (2023a), the monospecific lineage of *P. oleae* is named as subclade 2d whereas subclade 2e of Abad *et al.* (2023a) is divided into two subclades (as previously in Yang *et al.* 2017 and Chen *et al.* 2022) named here 2e and 2f. A new subclade is designated as 2g.

Definitions of 'homothallism', 'heterothallism' and sterility

Homothallism and heterothallism are somewhat archaic, quasi-morphological terms used more to describe whether gametangia are formed in single or paired *Phytophthora* cultures rather than the biological strategy this represents. We prefer a more Darwinian process-related definition that implies the organism's underlying breeding system or breeding strategy.

However, because historically these terms have been used routinely in species descriptions, we have also used them occasionally here, but with the following qualification. By *homothallic* we mean intrinsically self-fertile in a single culture and therefore often inbreeding, but this process does not preclude outbreeding in nature as a result of the fusion between antheridia and oogonia of different genotypes of the species. We will more often refer to these taxa in the text as 'self-fertile'. By *heterothallic* we mean that two mating or compatibility types (A1 and A2) are typically required to initiate gametogenesis between bisexual, largely self-incompatible individuals; but while this process promotes outcrossing, once initiated it can also lead to a significant frequency of self-fertilisation (selfing). We will refer to this breeding system in the text as A1/A2 outcrossing, or just 'A1/A2'. By *sterile* we mean an apparent lack of the intrinsic ability to form gametangia whether in a single culture or pairings with A1 or A2 isolates; but this does not exclude the possibility that an isolate or taxon may act as a 'silent' A1 or A2, inducing gametangial formation by selfing in an A2 or an A1 isolate of another species (*cf. P. gonapodyides*, Brasier *et al.* 2003).

MATERIAL AND METHODS

Phytophthora isolates

Details of all isolates used in the phylogenetic, morphological and temperature-growth studies are given in Table S1. Sampling and isolation methods from forest soil and river systems were described by Jung *et al.* (1996, 2017b, 2018b, 2020) and Pérez-Sierra *et al.* (2022). Necrotic baiting leaves or naturally fallen leaves collected from streams or the forest ground were plated onto selective PARPNH-agar (Jung *et al.* 1996, 2020). The isolates of the 43 new Clade 2 species were recovered from streams, rhizosphere soil and necrotic leaves in Valdivian rainforests in Chile; tropical or subtropical montane cloud forests in Nicaragua, Panama and Vietnam; tropical submontane to montane forests in Sumatra, Java, Sulawesi and Hainan island; tropical lowland rainforests in Nicaragua, Panama, Kalimantan, Sulawesi, Sumatra and Vietnam; subtropical monsoon forests in Japan, Taiwan and Vietnam; subtropical forests in Louisiana, USA; warm-temperate forests in Japan; cool-temperate forests in Bosnia-Herzegovina, Serbia and Japan; and Mediterranean forests in Italy and Portugal (Table S1). Isolates were also obtained from nursery plants, ornamental or horticultural plantings and amenity trees in Croatia, Germany, Hungary, the UK, Morocco and Sumatra (Table S1). In addition,

for comparative studies isolates of 11 described Clade 2 species were sourced from the culture collections of the authors (Table S1) while isolates from another seven described Clade 2 species were obtained between 2013 and 2020: *P. acaciivora* from the effluent of an *Acacia* and *Eucalyptus* nursery in Sumatra; *P. citrophthora* from rhizosphere soil and streams in temperate forests in Japan and Serbia, a subtropical monsoon forest in Taiwan and Mediterranean forests in Portugal; *P. colocasiae* from necrotic taro leaves in a tropical lowland rainforest in Sumatra; *P. pini* from rhizosphere soil and streams in temperate forests in Bosnia-Herzegovina and Serbia, subtropical forests in Louisiana, USA, and amenity plantings in Croatia, Germany and Slovakia; *P. siskiyouensis* from a bleeding bark canker of *Alnus cordata* in the UK; *P. tropicalis* from streams and naturally fallen leaves in tropical lowland and hill forests in Java, Sumatra, Nicaragua and Panama, and a subtropical monsoon forest in Taiwan; and *P.* ×*vanyenensis* from rhizosphere soil and streams in tropical lowland rainforests in Java, Sulawesi and Sumatra (Table S1). For all isolates, single hyphal tip cultures were produced under the stereomicroscope at ×20 from the margins of fresh cultures on V8-juice agar (V8A; 16 g agar, 3 g $CaCO_3$, 100 mL Campbell's V8 juice, 900 mL distilled water; Jung *et al.* 1999). Stock cultures were maintained on V8A and carrot juice agar (CA; 20 g agar, 3 g $CaCO_3$, 100 mL organic carrot juice from the company DM in Karlsruhe, Germany, 900 mL distilled water; Scanu *et al.* 2014) at 10 °C in the dark. All isolates of the 43 new *Phytophthora* spp. are preserved in the culture collection maintained at Mendel University in Brno. Ex-type cultures were deposited at the CBS culture collection (CBS) at the Westerdijk Institute, Utrecht, Netherlands (Table S1). Dried V8A cultures of the 43 ex-type isolates were deposited as holotypes in the CBS Fungarium (CBS H; also at the Westerdijk Institute).

DNA isolation, amplification and sequencing

For all *Phytophthora* isolates from Clade 2 obtained in this study or sourced from the culture collections of the authors, for the ex-epitype isolate CBS 147289 of *P. infestans* from Clade 1c and the ex-type isolate CBS 111772 of *P. pseudosyringae* from Clade 3, DNA was extracted from *ca*. 15–100 mg of mycelium scraped from 1–3-wk-old V8A cultures, placed into 2 mL homogenisation tubes (Lysis Matrix A; MP Biomedicals, Irvine, USA) and disrupted using a Precellys Evolution instrument (Bertin Technologies, Montigny-le-Bretonneux, France) until the mixture was homogenous. DNA was purified using the Monarch Genomic DNA Purification Kit (New England Biolabs, Ipswich, USA) and treated with RNase A following the manufacturer´s protocol for tissue samples. DNA was eluted with 100 µL of pre-warmed elution buffer and preserved at -80 °C for long-term storage.

Nine nuclear gene regions, *i.e*., the internal transcribed spacer region (ITS1–5.8S–ITS2) of the ribosomal RNA gene (ITS), the 5' terminal domain of the large subunit (28S-LSU) of the nuclear ribosomal RNA, heat shock protein 90 (*hsp90*), β-tubulin (*βtub*), 60S ribosomal protein L10 (*rpl10*), *TIGA* gene fusion protein (genes encoding triose-phosphate isomerase (TPI) and glyceraldehyde-3-phosphate dehydrogenase (GAPDH) fused and forming a single transcriptional unit: *tigA*), translation elongation factor 1 alpha (*tef-1α*), enolase (*enl*), *Ras*-like GTP-binding protein *YPT1* (*ras-ypt1*), and the four mitochondrial genes cytochrome-c oxidase 1 (*cox1*) and 2 (*cox2*), subunit 1 of NADH dehydrogenase (*nadh1*), and 40S ribosomal protein S10 (*rps10*) were amplified and sequenced (Table S2). The PCR amplifications were performed using a LightCycler 480 II instrument (Roche, Basel, Switzerland) or Eppendorf Mastercycler nexus GSX1 (Eppendorf, Hamburg, Germany). Table S2 provides a comprehensive overview of the PCR conditions and the primers used. All primers were synthesized by Elizabeth Pharmacon spol. s.r.o. (Brno, Czech Republic). Their annealing temperatures were estimated using a Tm calculator (http://tmcalculator.neb.com/#!/main) and adjusted empirically, according to observed PCR amplification rates.

The PCR products were visualised by gel electrophoresis (300 V; 5 min) using 2 % agarose gel stained by DNA Stain G (SERVA, Heidelberg, Germany). All amplicons were purified and sequenced in both directions by Eurofins Genomics GmbH (Cologne and Ebersberg, Germany) using the amplification primers, except for the LSU and *tigA* amplicons which required each two additional primers (Table S2). Electropherograms were quality-checked and forward and reverse reads were compiled using Geneious Prime® v. 2022.0.2 (Biomatters Ltd., Auckland, New Zealand). Pronounced double peaks were considered as heterozygous positions and labelled according to the IUPAC (International Union of Pure and Applied Chemistry; https://iupac.org) coding system. All sequences generated in this study were deposited in GenBank and accession numbers are given in Table S3.

Phylogenetic analysis

For phylogenetic analyses, the sequences obtained in this study were complemented with publicly available sequences of isolates from *Phytophthora* Clade 2 sourced from the GenBank Nucleotide Collection, many of them identified selected using the *IDphy Phytophthora* online resource (https://idtools.org/phytophthora; Abad *et al.* 2023b), and GenBank Whole-Genome Shotgun contigs (Table S3). The sequences of all loci used in the analyses were aligned using the MAFFT v. 7 (Katoh & Standley 2013) plugin within the Geneious Prime® v. 2023.3.1 software (https://www.geneious.com) by the E-INS-I strategy (ITS) or the G-INS-I strategy (all other loci). The ITS alignments in this study were manually edited and adjusted.

The phylogenetic structure of Clade 2 was studied using a 13-partition (LSU, ITS, *βtub*, *hsp90*, *tigA*, *rpl10*, *tef-1α*, *enl*, *ras-ypt1*, *cox1*, *cox2*, *nadh1*, *rps10*) dataset of 91 type and other key isolates from the 43 new and 36 previously described species and two informally designated taxa within Clade 2 with *P. infestans* from Clade 1c and *P. pseudosyringae* from Clade 3 as outgroup taxa.

The relative phylogenetic positions of the 43 new Clade 2 species within their respective subclades were studied using six separate 13-partition (LSU, ITS, *βtub*, *hsp90*, *tigA*, *rpl10*, *tef-1α*, *enl*, *ras-ypt1*, *cox1*, *cox2*, *nadh1*, *rps10*) datasets for subclades 2a (120 isolates from 6 new and 11 known species and 5 informally designated taxa); 2b (104 isolates from 9 new and 9 known species and 3 informally designated taxa); 2c (106 isolates from 15 new and 9 known species); 2e (39 isolates from 6 new and 5 known species and 1 informally designated taxon); 2f (26 isolates from 3 new and 1 known species and 1 informally designated taxon); and 2g (13 isolates from 4 new species). In all analyses, *P. infestans* from Clade 1c and *P. pseudosyringae* from Clade 3 were used as outgroup taxa.

For Maximum Likelihood (ML) analyses best-fit substitution models were selected using PartitionFinder v. 2 (Lanfear *et al.* 2016) based on the corrected Akaike Information Criterion (AICc). Each locus was considered to be a separate partition. All 84 available evolutionary models were used, including those with base frequencies estimated by maximum likelihood (the parameter models = allx;). The phylogeny was reconstructed with RAxML-NG

v. 1.1.0 (Kozlov *et al.* 2019). The MRE-based bootstopping test was applied to determine the necessary number of bootstrap replicates. The bootstopping method based on the extended majority rule (MRE) (also known as *greedy consensus*) (Pattengale *et al.* 2010) was implemented to automatically determine a sufficient number of bootstrap replicates with the cut-off value being set to 0.03 (the option --bs-cutoff 0.03). To calculate branch support values, the Transfer Bootstrap Expectation method (TBE; Lemoine *et al.* 2018) was selected. The presented ML trees represent the best-scoring trees with the TBE support values mapped onto them.

Bayesian Inference (BI) analyses were performed using BEAST v. 2 (Bouckaert *et al.* 2014). For all BI analyses Metropolis coupled MCMC (MC3) implemented in the CoupledMCMC package (Müller & Bouckaert 2020) was used with four chains – three heated and one cold. The chain length was always set to 20 M, except for the whole Clade dataset and the Clade 2a dataset where it was 40 M, and every 5 000th state was sampled. The target switch probability was set to the recommended value of 0.234 (Kone & Kofke 2005, Atchadé *et al.* 2011). Site models for individual partitions were automatically selected by model averaging implemented in the bModelTest package (Bouckaert & Drummond 2017). For all analyses, the optimised relaxed clock (Douglas *et al.* 2021), a performance-optimised version of the uncorrelated log-normal relaxed molecular clock model (Drummond *et al.* 2006), was used. The unit of branch lengths of the sampled trees was set to be substitutions per site. Parameter estimates were summarized with TreeAnnotator v. 2.6.0 (part of BEAST v. 2) and mapped onto the 50 % majority-rule consensus tree created by SumTrees v. 4.4.0 (Sukumaran & Holder 2015) from the Python library DendroPy v. 4.4.0 (Sukumaran & Holder 2010). The edge lengths of the summarizing tree were calculated as mean lengths for the corresponding edges in the input set of trees. The option 'force-rooted' was set for SumTrees telling the program to treat all the trees as rooted. The posterior estimates of the parameters were summarised with Tracer (Rambaut *et al.* 2018). The quality of the parameter estimates was assessed based on visual analysis of the trace plots and ESS values. The minimum ESS value for the parameter estimate to be considered properly sampled was 200 (standard setting). The likelihood and most of the other parameters of all the final trees were higher than 200. In all BI analyses a 25 % burn-in was used.

Phylogenetic trees were visualised in TreeGraph2 v. 2.15.0-887 beta (Stöver & Müller 2010) and/or MEGA 11 v. 11.0.11 (Tamura *et al.* 2021) and edited in figure editor programs. All datasets and trees deriving from BI and ML analyses were deposited in the Mendeley Data Repository, V1, (doi: 10.17632/8r5ww3w7mn.1).

Morphology of asexual and sexual structures

Morphological features of sporangia, oogonia, oospores, antheridia, chlamydospores, hyphal swellings and aggregations of all isolates of the 43 new species and selected isolates of related species from Clade 2 were compared with each other.

To induce the formation of sporangia, two 12–15 mm square discs were cut from the growing edge of a 3–7-d-old colony on V8A and flooded in a 90-mm-diam Petri dish with non-sterile soil extract (50 g of filtered oak forest soil in 1 000 mL of distilled water, filtered after 24 h) just above the surface of the aerial mycelium (Jung *et al.* 1996). The Petri dishes were incubated at 20 °C and natural daylight near a window and the soil extract changed after *ca*. 6 h. Shape, type of apex, caducity and special features of sporangia and the formation of hyphal swellings and aggregations were recorded after 24–48 h. For each isolate 50 sporangia were measured at ×400 using a compound microscope (Zeiss Imager.Z2), a digital camera (Zeiss Axiocam ICc3) and a biometric software (Zeiss ZEN).

The formation of chlamydospores, gametangia (oogonia and antheridia) and their characteristic features were examined on V8A (self-fertile or 'homothallic' species) or on clarified carrot agar prepared from fresh grated organic carrots (fgCA) (A1/A2 outcrossing or 'heterothallic' species; Brasier 1967) after 21–30 d growth at 20 ºC in the dark. Self-sterile isolates of *P. botryosa, P. calidophila, P. citrophthora, P. multiplex*, *P. pseudocitrophthora*, *P. pseudofrigida*, *P. obovoidea*, *P. pyriformis*, *P. tropicalis*, *P. variepedicellata*, *P. vietnamensis*, *P.* ×*australasiatica*, *P.* ×*taiwanensis* and *P.* ×*vanyenensis* were paired on V8A with A1 and A2 mating type tester strains of *P. cinnamomi* (A1: TW12; A2: MP74), *P. meadii* (A1: MYA-4042; A2: MYA-4043) and *P. acaciivora* (A1 isolate SU1735; only used for pairings with *P. pseudofrigida*) and examined after 4 wk incubation at 20 °C in the dark to determine their mating type (Jung *et al.* 2017c). Then for those species with the presence of both mating types isolates from opposite mating types were paired with each other while isolates from species with a lack of one mating type were paired with a *P. meadii* tester strain of opposite mating type using a polycarbonate membrane (Whatman Nuclepore™ Track-Etched Membranes, Sigma-Aldrich, St. Louis, MO, USA) test (Scanu *et al.* 2021). For each isolate each 50 oogonia, oospores and antheridia chosen at random were measured under a compound microscope at ×400 as described before. The oospore wall index was calculated according to Dick (1990). In addition, if present, the diameters of 50 chlamydospores per isolate were measured.

Colony morphology, growth rates and cardinal temperatures

Colony growth patterns of all 43 new Clade 2 species, one new informally designated Clade 2 taxon and 17 described Clade 2 species, *i.e.*, *P. acaciivora*, *P. acerina*, *P. botryosa*, *P. citrophthora*, *P. colocasiae*, *P. elongata*, *P. meadii*, *P. mekongensis*, *P. mengei*, *P. multivora*, *P. occultans*, *P. pachypleura*, *P. pini*, *P. plurivora*, *P. siskiyouensis*, *P. tropicalis* and *P.* ×*vanyenensis*, were described from 7-d-old cultures grown at 20 °C in the dark on V8A, CA and potato-dextrose agar (PDA; HiMedia, Mumbai, India). Colony morphologies were described according to patterns observed previously (Erwin & Ribeiro 1996, Jung & Burgess 2009, Jung *et al.* 2011, 2017c, d, 2021, 2022).

For temperature-growth relationships, representative isolates of all 43 new Clade 2 species, one new informally designated Clade 2 taxon and the 17 described Clade 2 species used for the colony morphologies (Table S1) were sub-cultured onto 90-mm-diam V8A plates and incubated for 24 h at 20 °C to stimulate onset of growth (Jung *et al.* 2002). Then three replicate plates per isolate were transferred to 10, 15, 20, 25, 27.5, 30, 32.5 and 35 °C. Radial growth was recorded after 4–14 d, before colonies reached the margin of the Petri dishes, along two lines intersecting the centre of the inoculum at right angles and the mean growth rates (mm/d) were calculated. Plates showing no growth at 25, 27.5, 30, 32.5 or 35 °C were returned to 20 °C to determine the lethal temperatures.

RESULTS

Phylogenetic results

The phylogenetic structure of Clade 2 was studied using a 13-partition (LSU, ITS, *βtub*, *hsp90*, *tigA*, *rpl10*, *tef-1α*, *enl*, *ras-ypt1*, *cox1*, *cox2*, *nadh1*, *rps10*) dataset of 91 type and other key isolates from the 43 new and 36 previously described species and three informally designated taxa within Clade 2 with *P. infestans* from Clade 1c and *P. pseudosyringae* from Clade 3 as outgroup taxa. Being largely similar, the topologies of the ML bootstrap best tree and the 50 % majority consensus rule tree derived from the BI analysis differed mainly in the relative positions of Clades 2e and 2f, and the relative positions of several taxa within Clades 2a, 2b and 2c. In contrast to the BI tree, the ML tree showed two polytomies in Clade 2c and each one polytomy in Clades 2a and 2b. Therefore, the BI tree is presented here (Fig. 1), and the ML tree is given as Fig. S1. In both analyses, the deeper phylogeny resolved six discrete clusters corresponding to known Clades 2a–2f and a new subclade designated here as Clade 2g (Fig. 1). The phylogenetic positions of most *Phytophthora* taxa were well or fully supported. In the BI analysis, the evolutionary history of the clade is characterised by the early divergence of Clade 2f followed by subsequent divergences of Clades 2e, 2d, 2c and 2b and more recently the splitting between Clades 2g and 2a (Fig. 1). The deeper phylogeny was generally well supported except for the relative position of Clade 2e which, hence, remains ambiguous (Fig. 1). The ML analysis revealed a similar evolutionary history except for Clade 2e diverging earlier than Clade 2e which was well-supported (Fig. S1).

The relative phylogenetic positions of the 43 new Clade 2 species within their respective subclades were studied using six separate 13-partition (LSU, ITS, *βtub*, *hsp90*, *tigA*, *rpl10*, *tef-1α*, *enl*, *ras-ypt1*, *cox1*, *cox2*, *nadh1*, *rps10*) datasets for subclades 2a (120 isolates from 6 new and 11 known species and 5 informally designated taxa), 2b (104 isolates from 9 new and 9 known species and 3 informally designated taxa), 2c (106 isolates from 15 new and 9 known species), 2e (39 isolates from 6 new and 5 known species and 1 informally designated taxon), 2e (26 isolates from 3 new and 1 known species and 1 informally designated taxon) and 2g (13 isolates from 4 new species). In all analyses, *P. infestans* from Clade 1c and *P. pseudosyringae* from Clade 3 were used as outgroup taxa.

Within Clade 2a both BI and ML analyses resolved 22 discrete lineages. The ML bootstrap best tree and the 50 % majority rule consensus tree derived from the BI analysis showed partly different topologies but had similar support values for most nodes. Since the ML analysis failed to resolve the deeper phylogeny and the relative positions of *P. mekongensis, P. vietnamensis* and the hybrid species *P.* ×*vanyenensis* (Fig. S2) the BI tree is presented here (Fig. 2). The BI analysis grouped the 22 taxa in two large clusters (Fig. 2). One cluster comprised a subcluster of five self-fertile (homothallic) taxa, *i.e.*, *P. himalsilva*, *P. occultans*, *P. pseudoccultans*, *P. terminalis* and *P.* taxon himalsilva-like 1, and *P.* taxon himalsilva-like 2 with unknown breeding system. *Phytophthora himalsilva* from Nepal and *P. pseudoccultans* from Taiwan proved to be closely related sister species with *P. terminalis* residing in a weakly supported, hence, ambiguous basal position to them. The separation between *P.* taxon himalsilva-like 1 and *P.* taxon himalsilva-like 2 had no support, probably because for the latter only four gene regions were available. *Phytophthora occultans* appeared in a fully supported basal position of this subcluster. The second subcluster contained the self-sterile (heterothallic) *P.* taxon awatangi and *P.* taxon germisporangia from Papua New Guinea which diverged first; the A1/A2 ('heterothallic') *P. multibullata* from Vietnam; and three sterile species, *i.e.*, the sister species *P. citrophthora* and *P.* ×*lusitanica* together with *P. pseudocitrophthora*, the latter grouping in a basal position.

In the second large cluster, the deeper phylogeny was characterised by three polytomies (trifurcations). The first one was well supported and comprised the A1/A2 hybrid species *P.* ×*taiwanensis*, a second well-supported polytomy containing the predominantly A1/A2 *P. meadii*, *P. colocasiae* and *P.* taxon meadii-like, and a third fully supported polytomy containing the A1/A2 *P. botryosa* and *P. insulinativitatica* and a cluster of four species. Within the latter, the A1/A2 *P.* ×*australasiatica* resided in a basal position to a subcluster which comprised the sterile *P. vietnamensis* and the A1/A2 *P. mekongensis* and *P.* ×*vanyenensis*. However, the nodes separating the four species were only weakly supported (BI posterior probabilities 0.77–0.78) and their relative phylogenetic positions within the subcluster remain ambiguous (Fig. 2). This was most likely caused by the high number of isolates from the hybrid species *P.* ×*australasiatica* and *P.* ×*vanyenensis* with numerous heterozygous positions in the nine nuclear gene regions, and partially by the presence of ancestors and descendants in the dataset (see below). Isolates of *P.* ×*australasiatica* showed considerable genetic variation and were grouped separately according to their origin from Japan, Panama, different regions of Vietnam and different islands of Indonesia. Isolate WPC P6310 from *T. cacao* in Indonesia, previously designated as *P.* taxon P6310 (Yang *et al.* 2017), resided within *P.* ×*australasiatica* (Fig. 2; Table S1). *Phytophthora* ×*vanyenensis* showed considerable genetic variation both within and between regions (Fig. 2; Table S1). Isolates CBS 235.30 from Sulavesi and CBS 238.28 of unknown origin, both previously designated as *P. botryosa*, resided within *P.* ×*vanyenensis*. Isolates QD30 and QD32 from *Cinnamomum cassia* plantations in the North of Vietnam, previously designated as *P.* ×*vanyenensis* (Dang *et al.* 2021), grouped with *P. mekongensis* isolates from *Citrus* plantations in the South of Vietnam (Fig. 2). The three polytomies in Clade 2a could indicate true species radiations or phylogenetic conflicts caused by reticulation events, recombination events or homoplasy (Bandelt *et al.* 1999, Posada *et al.* 2001, Cassens *et al.* 2005), or the presence of ancestors and descendents in the dataset as shown recently for the different lineages of *P. ramorum* (Jung *et al.* 2021). Across the alignments of 8 754 nuclear and 3 174 mitochondrial characters pairwise sequence differences between the Clade 2a taxa were 0.1–3.9 % and 0–6.3 %, respectively.

For Clade 2b the topologies of the 50 % majority rule consensus trees derived from the BI and ML (bootstrap best tree) analyses were mostly similar with several exceptions given below. Similar to the Clade 2a analyses, within species with highly heterozygous and diverse nuclear genes and potential interspecific hybridisation or introgression, *i.e.*, *P. multiplex*, *P. obovoidea* and *P. tropicalis*, the ML analysis had lower power of resolution than the BI analysis resulting in polytomies and a transitional placement of individual isolates (Figs 3, S3). The BI tree is presented here (Fig. 3) and the ML tree is given as supplementary material (Fig. S3). Within Clade 2b, the phylogenetic analyses revealed 21 discrete lineages (Figs 3, S3) unambiguously corresponding to the nine described species *P. amaranthi*, *P. aysenensis*, *P. capsici*, *P. gloveri*, *P. mengei*, *P. mexicana*, *P. siskiyouensis*, *P. theobromicola* and *P. tropicalis*, nine new species, *i.e.*, *P. calidophila*, *P. distorta*, *P. frigidophila*, *P. montana*, *P. multiplex*, *P. obovoidea*, *P. pyriformis*, *P. valdiviana* and

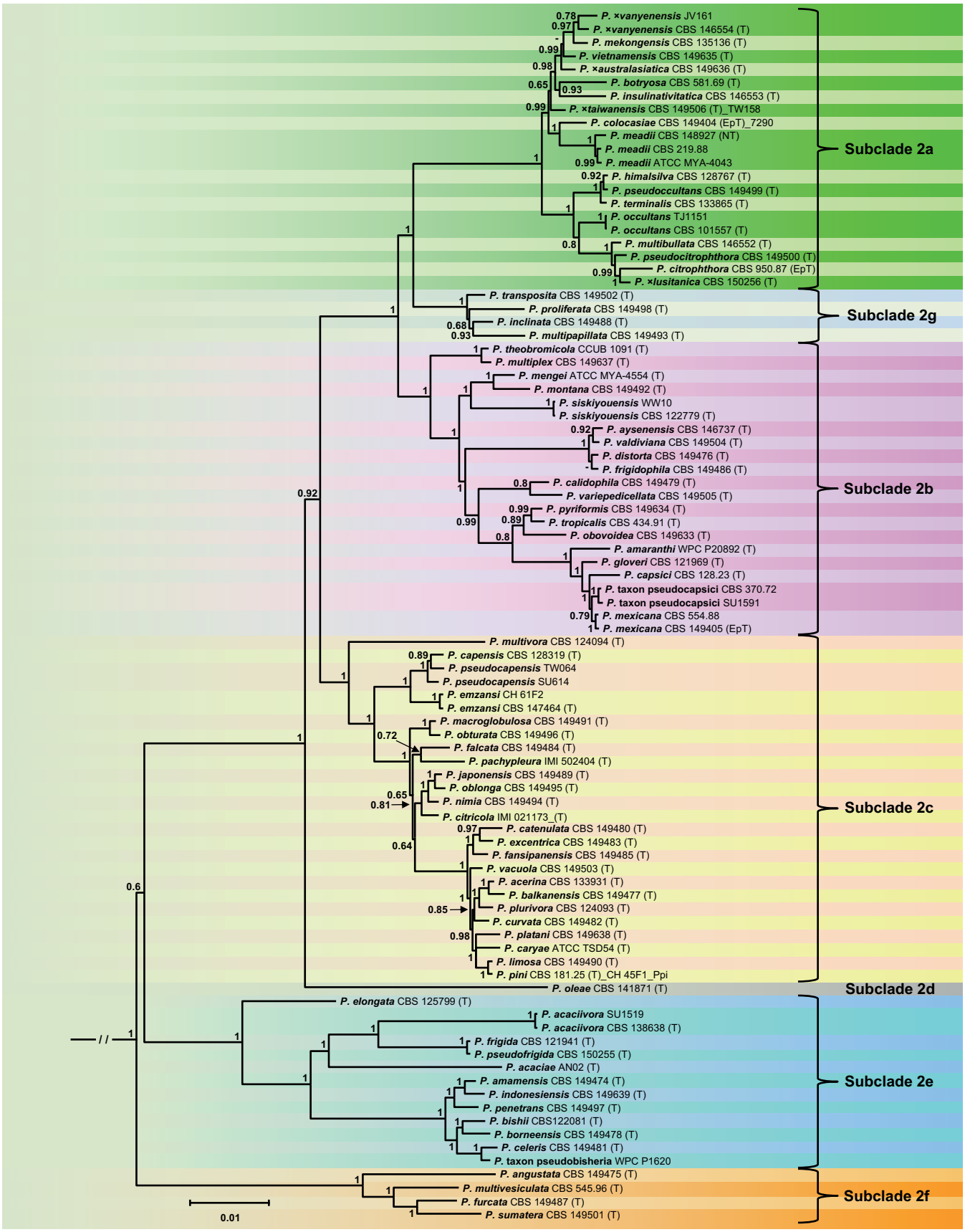

Fig. 1. Fifty percent majority rule consensus phylogram derived from Bayesian inference analysis of a concatenated thirteen-locus (LSU, ITS, *βtub*, *hsp90*, *tigA*, *rpl10*, *tef-1α*, *enl*, *ras-ypt1*, *cox1*, *cox2*, *nadh1*, *rps10*) dataset of *Phytophthora* major Clade 2. Bayesian posterior probabilities are indicated but not shown below 0.60. *Phytophthora infestans* and *P. pseudosyringae* from Clades 1c and 3, respectively, were used as outgroup taxa (not shown). (EpT), (NT) and (T) denote ex-epitype, ex-neotype and ex-type isolates. Scale bar indicates 0.01 expected changes per site per branch.

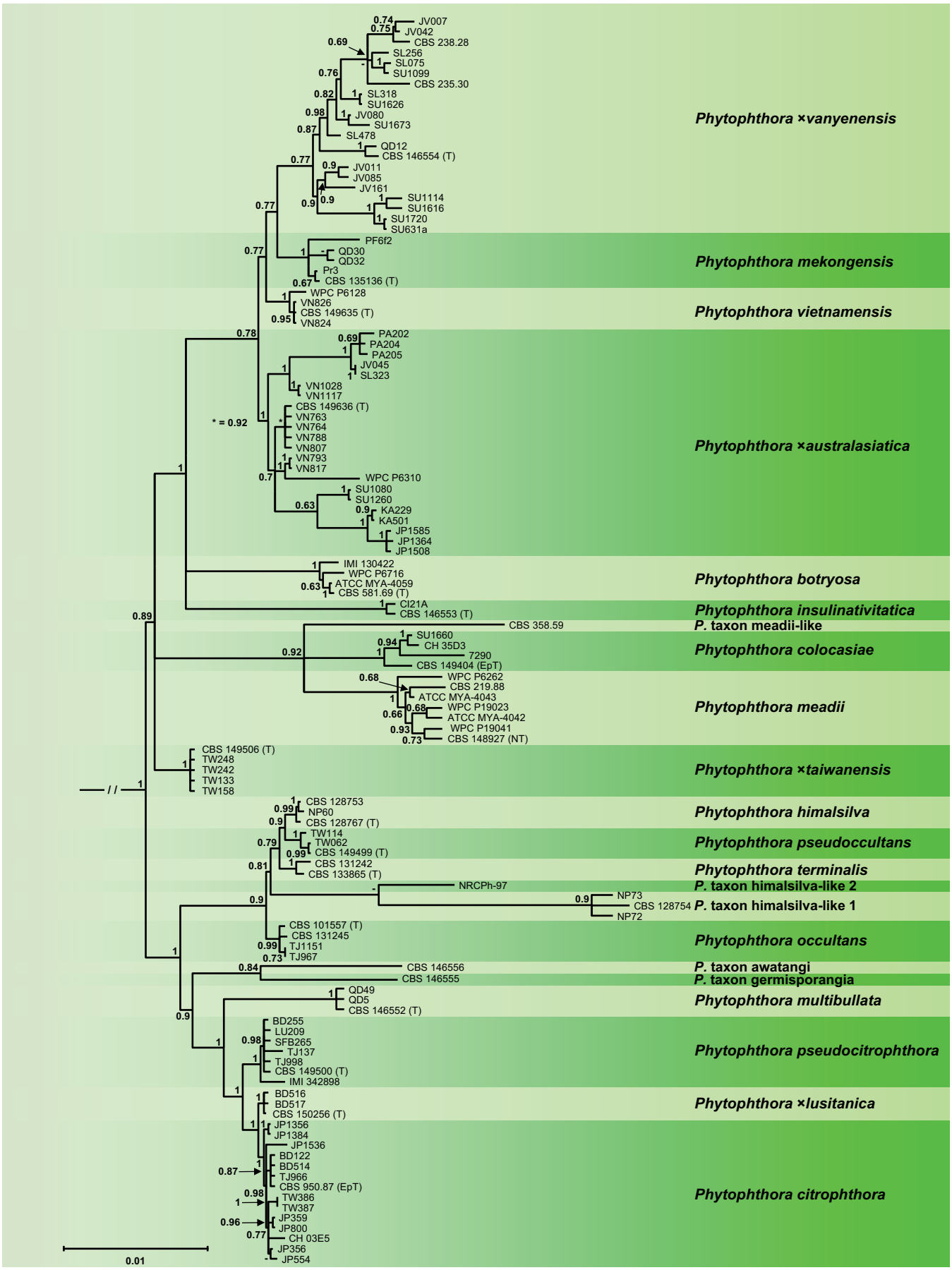

Fig. 2. Fifty percent majority rule consensus phylogram derived from Bayesian inference analysis of a concatenated thirteen-locus (LSU, ITS, *βtub*, *hsp90*, *tigA*, *rpl10*, *tef-1α*, *enl*, *ras-ypt1*, *cox1*, *cox2*, *nadh1*, *rps10*) dataset of *Phytophthora* Clade 2a. Bayesian posterior probabilities are indicated but not shown below 0.60. *Phytophthora infestans* and *P. pseudosyringae* from Clades 1c and 3, respectively, were used as outgroup taxa (not shown). (EpT), (NT) and (T) denote ex-epitype, ex-neotype and ex-type isolates. Scale bar indicates 0.01 expected changes per site per branch.

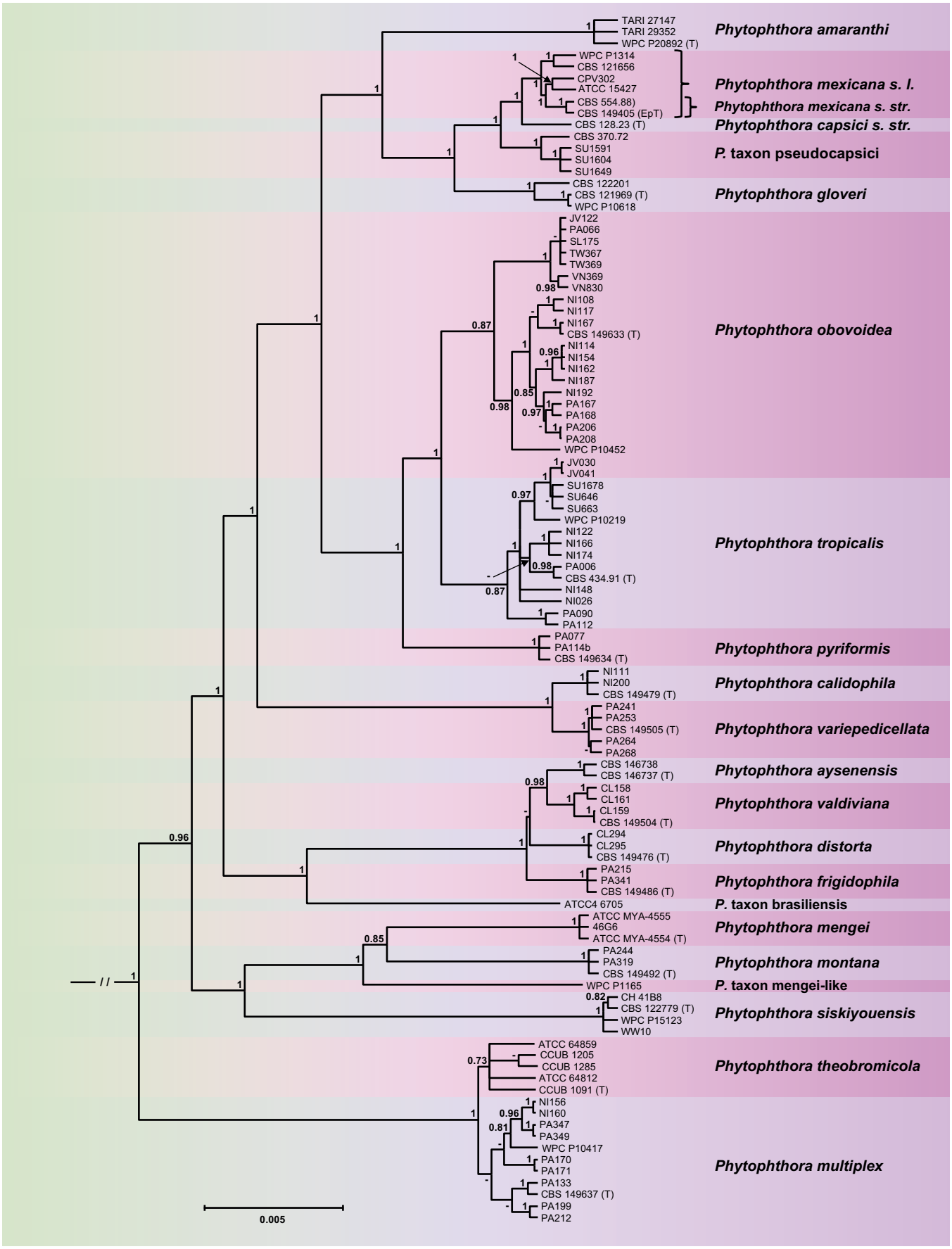

Fig. 3. Fifty percent majority rule consensus phylogram derived from Bayesian inference analysis of a concatenated thirteen -locus (LSU, ITS, *βtub*, *hsp90*, *tigA*, *rpl10*, *tef-1α*, *enl*, *ras-ypt1*, *cox1*, *cox2*, *nadh1*, *rps10*) dataset of *Phytophthora* Clade 2b. Bayesian posterior probabilities are indicated but not shown below 0.60. *Phytophthora infestans* and *P. pseudosyringae* from Clades 1c and 3, respectively, were used as outgroup taxa (not shown). (EpT) and (T) denote ex-epitype and ex-type isolates, respectively. Scale bar indicates 0.005 expected changes per site per branch.

P. variepedicellata, and three undescribed taxa, *i.e.*, the informally designated *P.* taxon brasiliensis and *P.* taxon mengei-like and *P.* taxon pseudocapsici designated here. The evolutionary history of the subclade is characterised by the fully supported early divergence of the lineage leading to the extant Central and South American sister species *P. multiplex* and *P. theobromicola* from a large cluster comprising all other known Clade 2b taxa (Figs 3, S3). Within the 'main' Clade 2b cluster, a group of self-fertile (homothallic) species from Central and North America, including the two sister species *P. mengei* and *P. montana*, *P.* taxon mengei-like and *P. siskiyouensis*, reside in a basal position. The long branch length of *P. siskiyouensis* indicates long-term isolation and evolution. All nodes were well supported (Fig. 3, S3). The next separated cluster contained three self-fertile species from Chile, *i.e.*, *P. aysenensis*, *P. distorta* and *P. valdiviana*, the self-fertile *P. frigidophila* from Panama and the distinct *P.* taxon brasiliensis in a basal position. All lineages were fully supported except *P. distorta* which was distinct but whose relative position within the cluster could not be unambiguously resolved (Figs 3, S3). An ensuing divergence of the self-sterile (heterothallic) Central American sister species *P. calidophila* and *P. variepedicellata* from a cluster including the *P. capsici* and *P. tropicalis* subclusters was also well supported (Figs 3, S3). Within the *P. capsici* subcluster the self-fertile *P. amaranthi* from Taiwan apparently diverged first followed by the splitting between the self-fertile *P. gloveri* from Brazil and a cluster of three fully supported A1/A2 lineages. One well-supported lineage comprises the ex-epitype (CBS 149405) and isolate CBS 554.88 of *P. mexicana* from Texas and Mexico, respectively, and several isolates from Mexico or the USA previously designated as *P. capsici* (CBS 121656, WPC P1314, CPV302) or *P.* aff. *capsici* (ATCC 15427; Yang *et al.* 2017), designated here as *P. mexicana sensu lato*; another with full support in the BI analysis but lower support (78.3 %) in the ML analysis the ex-type isolate of *P. capsici* (CBS 128.23) from New Mexico designated here as *P. capsici sensu stricto*; and the third *P.* taxon pseudocapsici newly designated here, fully supported and comprising three isolates obtained from Sumatra during this study. Clustering in the BI analysis with *P.* taxon pseudocapsici isolate CBS 370.72 from New Mexico previously designated as *P. capsici* grouped in the ML analysis between *P.* taxon pseudocapsici and *P. capsici s. str.* (Figs 3, S3). Within the *P. tropicalis* cluster, *P. pyriformis* from Panama resides in a well-supported basal position to the sister species *P. obovoidea* and *P. tropicalis* both of which showed considerable intraspecific variation. *Phytophthora obovoidea* contained one lineage with wide distribution in Java, Panama, Sulawesi, Taiwan and Vietnam, a more diverse group with three lineages from Nicaragua and Panama, and an isolate from southern California (WPC P10452) in a basal position (Figs 3, S3). Within *P. tropicalis*, in the BI analysis two isolates from Panama grouped in a basal position to a fully supported polytomy containing a group of isolates with Western Pacific distribution (Java, Sumatra, Tahiti), another group comprising isolates from Central America (Nicaragua, Panama) and the ex-type isolate from Hawaii, and two distinct isolates from Nicaragua (Fig. 3). In the ML analysis *P. tropicalis* is characterised by a weakly supported polytomy comprising a small cluster with the ex-type isolate and isolate PA006 from Panama; another cluster with five isolates from Nicaragua and Panama; a cluster with the Western Pacific isolates and isolate NI148 from Nicaragua in a basal position; and the distinct Nicaraguan isolate NI026 (Fig. S3). The polytomies in both analyses could result from adaptive or non-adaptive radiation or indicate phylogenetic conflicts possibly due to the presence of ancestral and descending lineages in the dataset. Within *P. obovoidea* and *P. tropicalis*, most nodes had higher support values in the BI analysis (Figs 3, S3). Across the alignments of 8 736 nuclear characters and 3 156 mitochondrial characters pairwise sequence differences between the Clade 2b taxa were 0.1–4.8 % and 0.1–4.8 %, respectively.

For the largest of the subclades, Clade 2c, both the BI and ML analyses produced trees with largely similar topology and strong support for the deeper phylogeny and most other nodes. The BI tree is presented here with both Bayesian Posterior Probability values and Maximum Likelihood bootstrap values included (Fig. 4). The phylogenetic analyses demonstrated 24 discrete lineages unambiguously corresponding to nine described species, *i.e.*, *P. acerina*, *P. capensis*, *P. caryae*, *P. citricola*, *P. emzansi*, *P. multivora*, *P. pachypleura*, *P. pini* and *P. plurivora*, and 15 new species, *i.e.*, *P. balkanensis*, *P. catenulata*, *P. curvata*, *P. excentrica*, *P. falcata*, *P. fansipanensis*, *P. japonensis*, *P. limosa*, *P. macroglobulosa*, *P. nimia*, *P. platani*, *P. oblonga*, *P. obturata*, *P. pseudocapensis* and *P. vacuola*. The overall structure of Clade 2c is characterised by the early divergence of *P. multivora* (Fig. 4), which lies in a distinct basal position, followed by the divergence of a small cluster comprising the basal *P. emzansi* and *P. capensis*, both from South Africa, and *P. pseudocapensis*, a new genetically diverse sister species of *P. capensis* that is widely distributed across Java, Sumatra, Sulawesi, Taiwan and Vietnam. Within *P. pseudocapensis* the isolates sampled from Taiwan and Vietnam grouped separately from those obtained from the different Indonesian islands, which were intermingled (Fig. 4). All lineages in this cluster received strong support values. The 'main' Clade 2c cluster comprised two separate and fully supported lineages. One lineage contained in the BI analysis two fully supported subclusters represented by eight species from East and Southeast Asia. Within one subcluster *P. macroglobulosa* from the Chinese Hainan Island and *P. obturata* from Northern Vietnam constituted closely related and fully supported sister species. *Phytophthora pachypleura* and *P. falcata* from Japan also grouped in a sister position but with lower support (0.71). Both species resided at the ends of relatively long branches indicating long-term isolation (Fig. 4). Within this subcluster the relative positions to each other of the species pairs *P. macroglobulosa*/*P. obturata* and *P. falcata/P. pachypleura* could not be resolved unambiguously as shown by low support values (Fig. 4). The ML tree differed from the BI tree in the relative position of *P. pachypleura* which formed a weakly supported polytomy with the *P. macroglobulosa* - *P. obturata* - *P. falcata* subcluster and the other subcluster. The latter comprised the ex-type and authentic type isolates of *P. citricola* from Japan and Taiwan together with a South African *P. citricola* isolate grouping in a basal position to *P. nimia* and the two sister species *P. japonensis* and *P. oblonga*, all from Japan. All nodes in this subcluster were well supported in both analyses (Fig. 4).

Within the other lineage of the 'main' Clade 2c cluster, a group of species from Southeast and East Asia apparently diverged first. These included the sister species *P. catenulata* and *P. excentrica* together with *P. fansipanensis* which resides in a basal position to them. The Taiwanese and Vietnamese populations of *P. catenulata* were closely related but grouped separately. All nodes received high support values (Fig. 4). The Japanese *P. vacuola* diverged from a cluster containing two well-supported subclusters. One subcluster comprised the sister species *P. acerina* and *P. balkanensis* with *P. plurivora* grouping basal to them and *P. curvata* from Japan basal to the whole subcluster. The three isolates of *P. acerina* from Italy were probably clonal whereas *P. balkanensis* showed some intraspecific variability: isolates from several Balkan

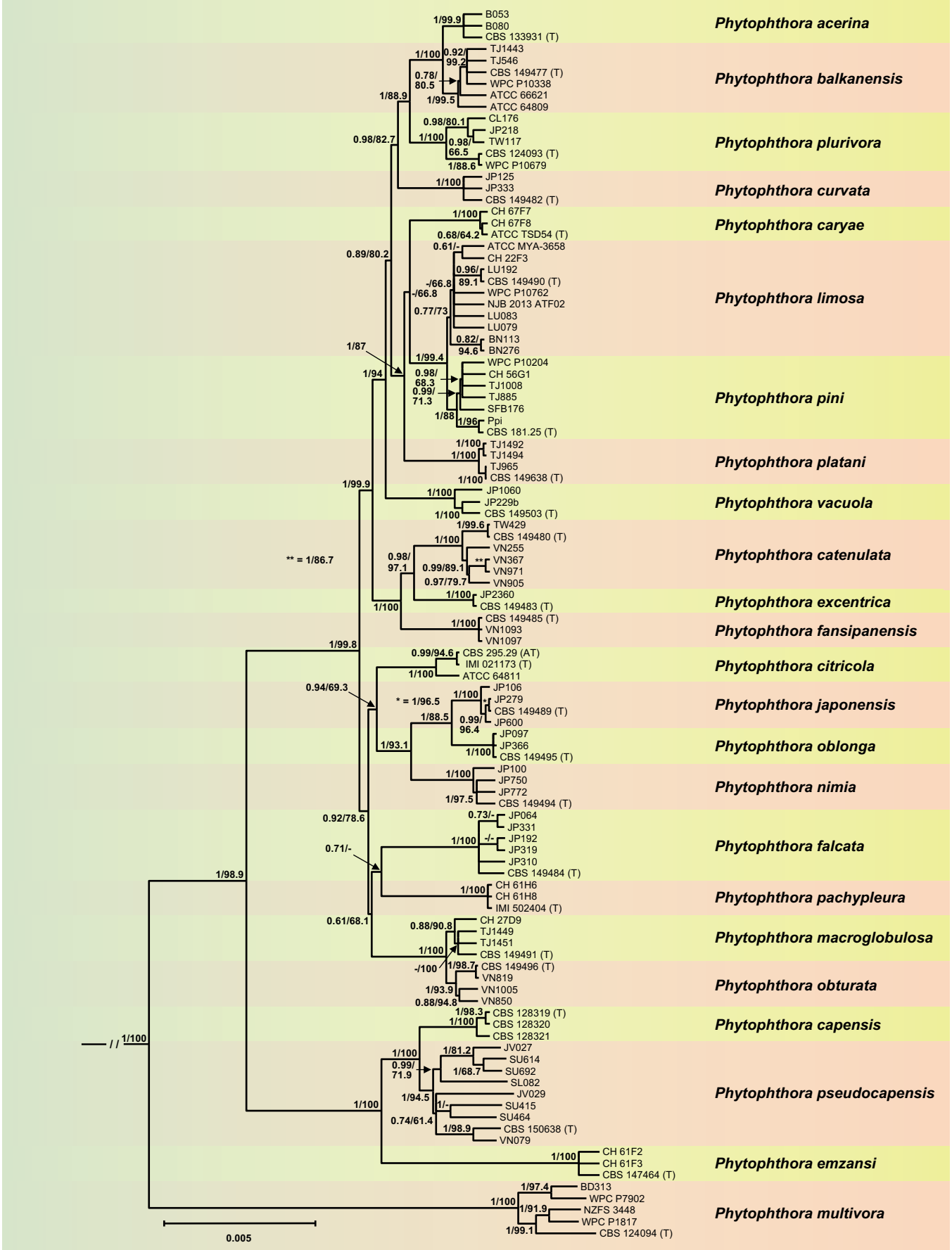

Fig. 4. Fifty percent majority rule consensus phylogram derived from Bayesian inference analysis of a concatenated thirteen-locus (LSU, ITS, *βtub*, *hsp90*, *tigA*, *rpl10*, *tef-1α*, *enl*, *ras-ypt1*, *cox1*, *cox2*, *nadh1*, *rps10*) dataset of *Phytophthora* Clade 2c. Bayesian posterior probabilities and Maximum Likelihood bootstrap values (in %) are indicated but not shown below 0.60 and 60 %, respectively. *Phytophthora infestans* and *P. pseudosyringae* from Clades 1c and 3, respectively, were used as outgroup taxa (not shown). (AT) and (T) denote ex-authentic type and ex-type isolates, respectively. Scale bar indicates 0.005 expected changes per site per branch.

countries (TJ546, TJ1443, CBS 149477) and Ireland (WPC P10338) grouping separately from those from California (ATCC 64809) and Taiwan (ATCC 66621). The *P. plurivora* isolates from Chile, Europe, Japan, Taiwan and New Zealand also showed intraspecific variability. All lineages in this subcluster were well supported (Fig. 4). In the second subcluster *P. platani* isolates from Italy and the UK resided in the BI analysis in a strongly supported basal position to three species whose isolates came either from North America or partly from Europe: the sister species *P. pini* and *P. limosa*, and *P. caryae* (Fig. 4). *Phytophthora caryae* lay in a weakly supported and hence ambiguous basal position to the latter species, probably because only 5–9 of the 13 gene regions in the individual isolates were available (Table S3). In the ML analysis, *P. caryae* and *P. platani* grouped in sister position to each other but with weak support (66.8 %). In both analyses isolates previously designated as *P.* taxon citricola III and *P.* taxon 22F3 (Yang *et al.* 2017) grouped within *P. limosa*, and isolate CH 56G1 previously designated as *P.* taxon pini-like grouped within *P. pini*. Isolates of *P. limosa* from Bosnia-Herzegovina clustered separately from US isolates but the node received only weak support. The separation between *P. limosa* and *P. pini* was, however, fully supported (Fig. 4). Across the alignments of 8 740 nuclear characters and 3 156 mitochondrial characters pairwise sequence differences between the Clade 2c taxa were 0.1–3.2 % and 0.2–4.7 %, respectively.

With Clade 2e both the BI and ML analyses produced trees with similar topology and strong support for all nodes. The BI tree is presented here with both Bayesian Posterior Probability values and Maximum Likelihood bootstrap values included (Fig. 5). Both BI and ML analyses revealed 12 discrete and fully supported lineages within Clade 2e unambiguously corresponding to the five described species *P. acaciae*, *P. acaciivora*, *P. bishii*, *P. elongata* and *P. frigida*; the six new species *P. amamensis*, *P. borneensis*, *P. celeris*, *P. indonesiensis*, *P. penetrans* and *P. pseudofrigida*; and the informally designated *P.* taxon pseudobisheria (Fig. 5). The overall structure of Clade 2e showed *P. elongata* residing in a distinct basal position to a large cluster which was characterised by the early divergence between a smaller cluster of A1/A2 species, comprising *P. acaciae* in a basal position, *P. acaciivora* and the closely related sister species *P. frigida* and *P. pseudofrigida*, and a larger cluster of self-fertile taxa with two fully supported subclusters. One subcluster comprised the sister species *P. amamensis* from the Japanese Amami Island and *P. indonesiensis* with *P. penetrans* from Panama residing in a basal position to them. The other one contained two pairs of sister taxa, *P. bishii* - *P. borneensis* and *P. celeris* - *P.* taxon pseudobisheria, respectively. It is noteworthy that within *P. indonesiensis* the populations from three different Indonesian islands formed three distinct subclusters, with the intermediate Kalimantan population grouping in a fully supported basal position to the Sumatra and Sulawesi populations (Fig. 5). Across the nuclear 8 754-character alignment and the mitochondrial 3 153-character alignment the Clade 2e taxa showed pairwise sequence differences of 0.4–6.2 % and 0.3–4.4 % (0.1 % for *P. frigida vs. P. pseudofrigida*), respectively.

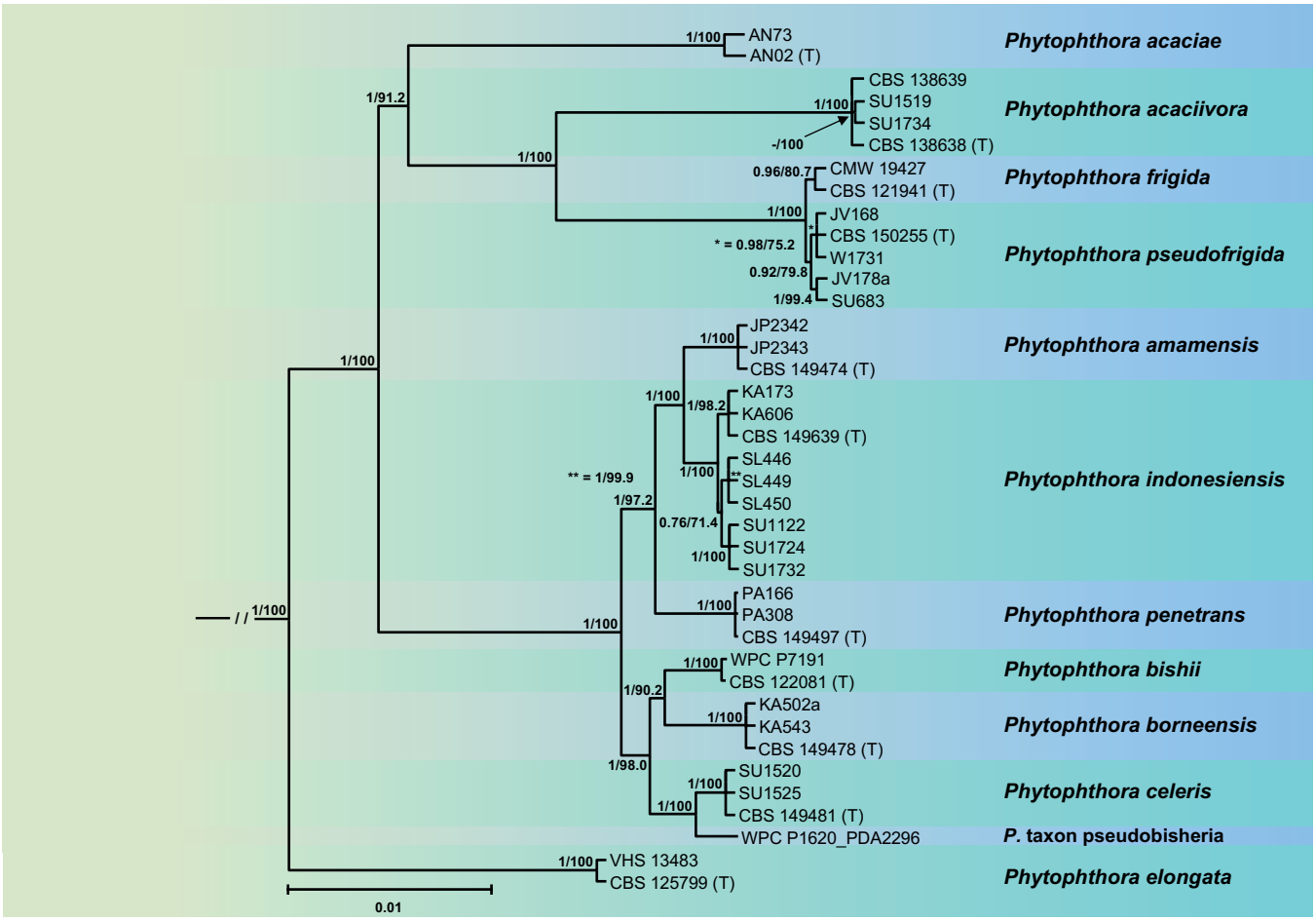

Fig. 5. Fifty percent majority rule consensus phylogram derived from Bayesian inference analysis of a concatenated thirteen-locus (LSU, ITS, *βtub*, *hsp90*, *tigA*, *rpl10*, *tef-1α*, *enl*, *ras-ypt1*, *cox1*, *cox2*, *nadh1*, *rps10*) dataset of *Phytophthora* Clade 2e. Bayesian posterior probabilities and Maximum Likelihood bootstrap values (in %) are indicated but not shown below 0.70 and 70 %, respectively. *Phytophthora infestans* and *P. pseudosyringae* from Clades 1c and 3, respectively, were used as outgroup taxa (not shown). (T) denotes ex-type isolates. Scale bar indicates 0.01 expected changes per site per branch.

For Clade 2f both the BI and ML analyses produced trees with similar topology and strong support for all nodes. The BI tree is presented here with both Bayesian Posterior Probability values and Maximum Likelihood bootstrap values included (Fig. 6). The overall structure of Clade 2f is characterised by the early divergence of *P. angustata* from Nicaragua (Fig. 6). This is followed by the separation of the North American *P.* taxon aquatilis from a cluster comprising *P. furcata* from Vietnam and *P. sumatera* in a sister position to each other, and the globally distributed *P. multivesiculata* which occurs in a fully supported basal position to the latter two species. *Phytophthora sumatera* showed high intraspecific genetic variability with isolate JV146 from Java grouping basal to three fully supported separate subclusters from Sumatra (Fig. 6). Across the nuclear 8 720-character alignment and the mitochondrial 3 153-character alignment pairwise sequence differences between the Clade 2f taxa were 0.6–2 % and 1.5–3.6 %, respectively.

Currently comprising the four new species *P. inclinata*, *P. multipapillata*, *P. proliferata* and *P. transposita*, the new Clade 2g is the smallest subclade apart from the monospecific lineage of *P. oleae* (Figs 1, 7). Both BI and ML analyses revealed two pairs of sister species, *i.e.*, *P. inclinata* from the Vietnamese Côn Lôn Island and *P. multipapillata* from Borneo; and *P. proliferata* from Cuc Phuong National Park in the North of Vietnam and *P. transposita* from the Japanese Kyushu Island. The populations of *P. multipapillata* from two different locations in East Kalimantan were grouped separately. All lineages were strongly supported. The nuclear 8 725-character alignment and the mitochondrial 3 156-character alignment of the four species showed sequence differences of 0.6–0.8 % and 1.1–1.5 %, respectively.

Nuclear gene heterozygosity. In contrast to the homozygous mitochondrial (*cox1*, *cox2*, *nadh1*, *rps10*) alignments, the nine-loci nuclear (LSU, ITS, *βtub*, *hsp90*, *tigA*, *rpl10*, *tef-1α*, *enl*, *ras-ypt1*)

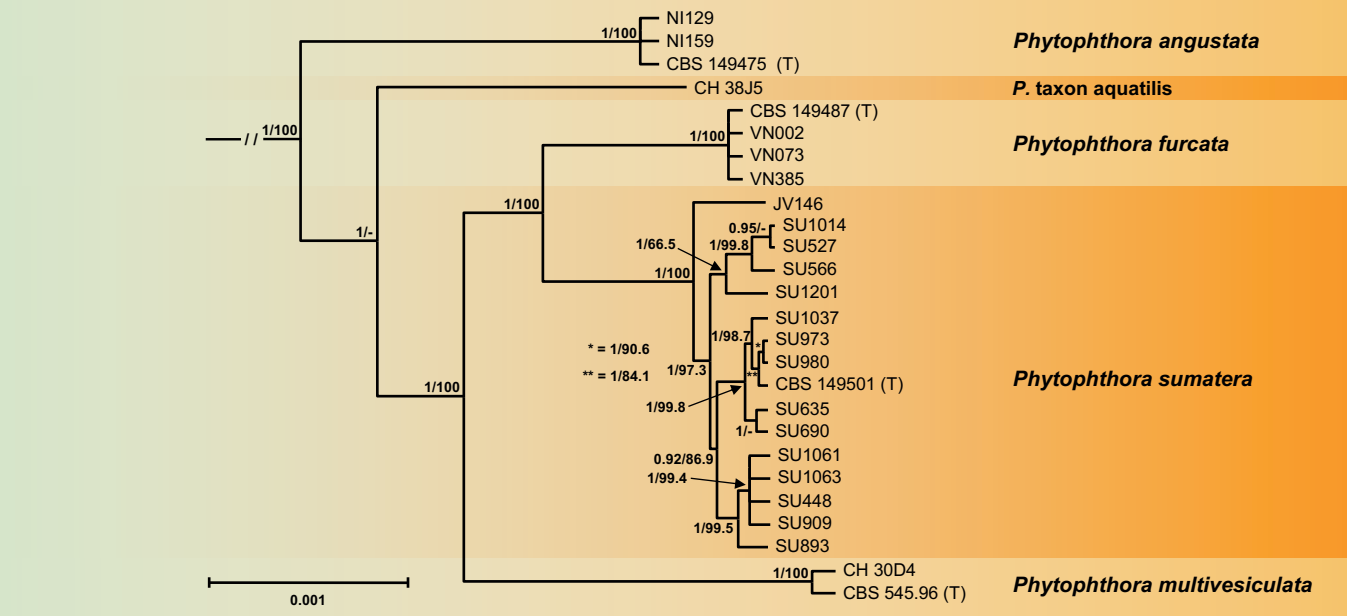

Fig. 6. Fifty percent majority rule consensus phylogram derived from Bayesian inference analysis of a concatenated thirteen-locus (LSU, ITS, *βtub*, *hsp90*, *tigA*, *rpl10*, *tef-1α*, *enl*, *ras-ypt1*, *cox1*, *cox2*, *nadh1*, *rps10*) dataset of *Phytophthora* Clade 2f. Bayesian posterior probabilities and Maximum Likelihood bootstrap values (in %) are indicated but not shown below 0.80 and 60 %, respectively. *Phytophthora infestans* and *P. pseudosyringae* from Clades 1c and 3, respectively, were used as outgroup taxa (not shown). (T) denotes ex-type isolates. Scale bar indicates 0.001 expected changes per site per branch.

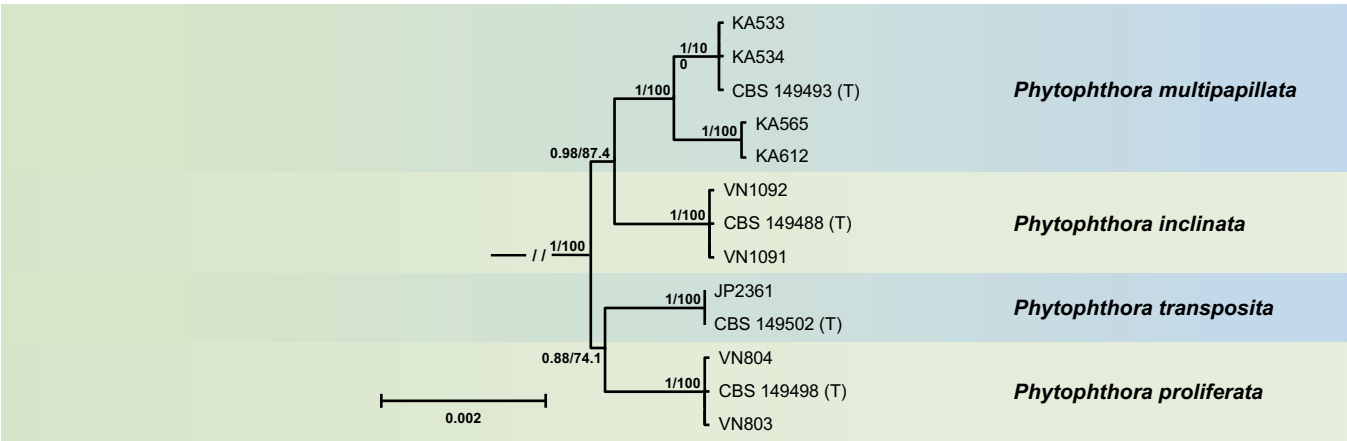

Fig. 7. Fifty percent majority rule consensus phylogram derived from Bayesian inference analysis of a concatenated thirteen-locus (LSU, ITS, *βtub*, *hsp90*, *tigA*, *rpl10*, *tef-1α*, *enl*, *ras-ypt1*, *cox1*, *cox2*, *nadh1*, *rps10*) dataset of *Phytophthora* Clade 2g. Bayesian posterior probabilities and Maximum Likelihood bootstrap values (in %) are indicated but not shown below 0.80 and 70 %, respectively. *Phytophthora infestans* and *P. pseudosyringae* from Clades 1c and 3, respectively, were used as outgroup taxa (not shown). (T) denotes ex-type isolates. Scale bar indicates 0.002 expected changes per site per branch.

alignments of all subclades contained numerous heterozygous positions. Among the 87 Clade 2 taxa with available data mean heterozygosity varied widely from close to zero to 1.27 % (Table 1). Further, within subclades 2a and 2b wide variations in heterozygosity also occurred (Table 1) according to the breeding system (Table 2) and even within some species. Relationships between these characters and interspecific hybridity were also detected. These aspects are considered in detail under the Notes on the relationship between level of heterozygosity, breeding system and interspecific hybridity below. Together with information published elsewhere (Van Poucke *et al.* 2021), they formed the basis for deciding whether a new species would be formally designated a hybrid.

Table 1. Range of mean heterozygosity across nine nuclear genes (LSU, ITS, ßtub, hsp90, tigA, rpl10, tef-1α, enl, ras-ypt1) for taxa within the Clade 2 subclades.

Subclade	No. of taxa	Heterozygosity (%)	
		Range	Mean
2a	21	0.03–1.09	0.34
2b	21	0.0–1.27	0.31
2c	24	0.03–0.18	0.09
2d	1	n/a	0
2e	11	0.02–0.06	0.12
2f	5	0.01–0.42	0.1
2g	4	0.07–0.09	0.08
All subclades	87	0.0–1.27	0.14

n/a = not applicable.

Table 2. Mean heterozygosity levels across nine nuclear genes (LSU, ITS, *ßtub*, *hsp90*, *tigA*, *rpl10*, *tef-1α*, *enl*, *ras-ypt1*) *versus* breeding systems across the subclades of *Phytophthora* Clade 2.

Subclade	Breeding system[1, 2]		
	Self-fertile	A1/A2	Sterile
2a	0.18 (5)	0.28 (12)	0.55 (4)
2b	0.10 (10)	0.54 (10)	0.09 (1)
2c	0.09 (24)	n/a	n/a
2d	0 (1)	n/a	n/a
2e	0.07 (8)	0.24 (3)	n/a
2f	0.02 (4)[3]	n/a	n/a
P. taxon aquatilis	0.42 (1)	n/a	n/a
2g	0.08 (4)	n/a	n/a
All subclades	0.09 (56)[3] 0.1 (57)	0.40 (25)	0.46 (5)

n/a = not applicable.

[1] See Terminology.

[2] No. of taxa in parentheses.

[3] Excluding *P.* taxon aquatilis.

Taxonomy

Clade 2a

For all Clade 2a species included in this study colony morphologies on CA, PDA and V8A and temperature-growth relations on V8A are presented in Figs 8–12. Morphological and physiological characters and morphometric data of the six newly described and 11 known species and five informally designated taxa in Clade 2a are given in the comprehensive Tables S4–S6. The known species *P. citrophthora* and *P. meadii* were recently validated by Abad *et al.* (2023a) and taxonomic re-descriptions given based on a newly designated epitype (*P. citrophthora*) and a newly designated neotype (*P. meadii*). However, morphometric data and growth rates from different studies often show considerable differences. To enable detailed comparisons with new species from Clade 2a, for both *P. citrophthora* and *P. meadii* isolates from different parts of the world were included in our morphological and temperature-growth studies and taxonomic descriptions without nomenclatural act are given below.

Phytophthora citrophthora (R.E. Sm. & E.H. Sm.) Leonian, Amer. J. Bot. 12 (7): 445. 1925. [MycoBank MB 251464]. Fig. 13.

Typus: **USA,** California, La Habra isolated from *Citrus* sp., collection date and collector unknown, isolated by P. Oudemans (epitype CBS 950.87 preserved in a metabolically inactive state, designated in Abad *et al.* 2023a, MBT 10008019, ex-epitype living culture CBS 950.87 = CPHST BL60 = ATCC 52231 = WPC P0479).

Morphological structures on V8A: *Sporangia* infrequently observed on solid agar and abundantly produced in non-sterile soil extract; borne predominantly terminally (95.6 %) on unbranched long or short sporangiophores or in dense or lax sympodia of 2–4 sporangia (Fig. 12O), or infrequently sessile (1.8 %; Fig. 13I) or intercalary (2.6 %); mostly ovoid, broad-ovoid or elongated-ovoid (54.7 %; Fig. 13A–E, N) or limoniform to elongated-limoniform (25.1 %; Fig. 13I, K–M, O), less frequently distorted with often two or sometimes three apices (9.3 %; Fig. 13J), obpyriform to elongated-obpyriform (6.1 %; Fig. 13F, G), ellipsoid to elongated-ellipsoid (2.5 %; Fig. 13H, O), obovoid (1 %), ampulliform (0.8 %) or pyriform (0.5 %); lateral attachment of sporangiophores (17.5 %; Fig. 13B), a conspicuous basal plug (45.2 %; Fig. 13E–H) and pedicels of variable length (av. 24.9 ± 15.9 µm; range 2.5–78.4 µm; Fig. 13B, C, K–M) commonly observed; rarely caducous (Fig. 13L, M); sporangia occasionally too big for the available cytoplasm and hence, not filled completely in the basal part, often with an additional strong plug below the cytoplasm (6.8 %; Fig. 13G); sporangial apices on solid agar exclusively papillate; in water mainly semipapillate (61.1 %; Fig. 13A, C–E, I–M, O) or less frequently papillate or semipapillate to papillate (36 %; Fig. 13B, F–H, M), occasionally nonpapillate (2.9 %); sporangial proliferation exclusively external (Fig. 13A, B, D, E, G, H, O); sporangial dimensions averaging 66.0 ± 8.3 × 36.2 ± 4.5 µm (overall range 46.5–110.2 × 23.7–48.5 µm; range of isolate means 62.5–73.9 × 30.8–39.7 µm) with a length/breadth ratio of 1.84 ± 0.31 (overall range 1.31–3.86); sporangial germination indirectly with zoospores discharged through an exit pore 3.7–9.3 µm wide (av. 5.9 ± 1.0 µm) (Fig. 13N, O). *Zoospores* limoniform to reniform whilst motile, becoming spherical (av. diam = 11.2 ± 1.3 µm) on encystment; cysts usually germinating directly forming a hypha or a microsporangium or infrequently indirectly by releasing a secondary zoospore (diplanetism). *Hyphal swellings* sometimes formed in water on sporangiophores, often close to the sporangial

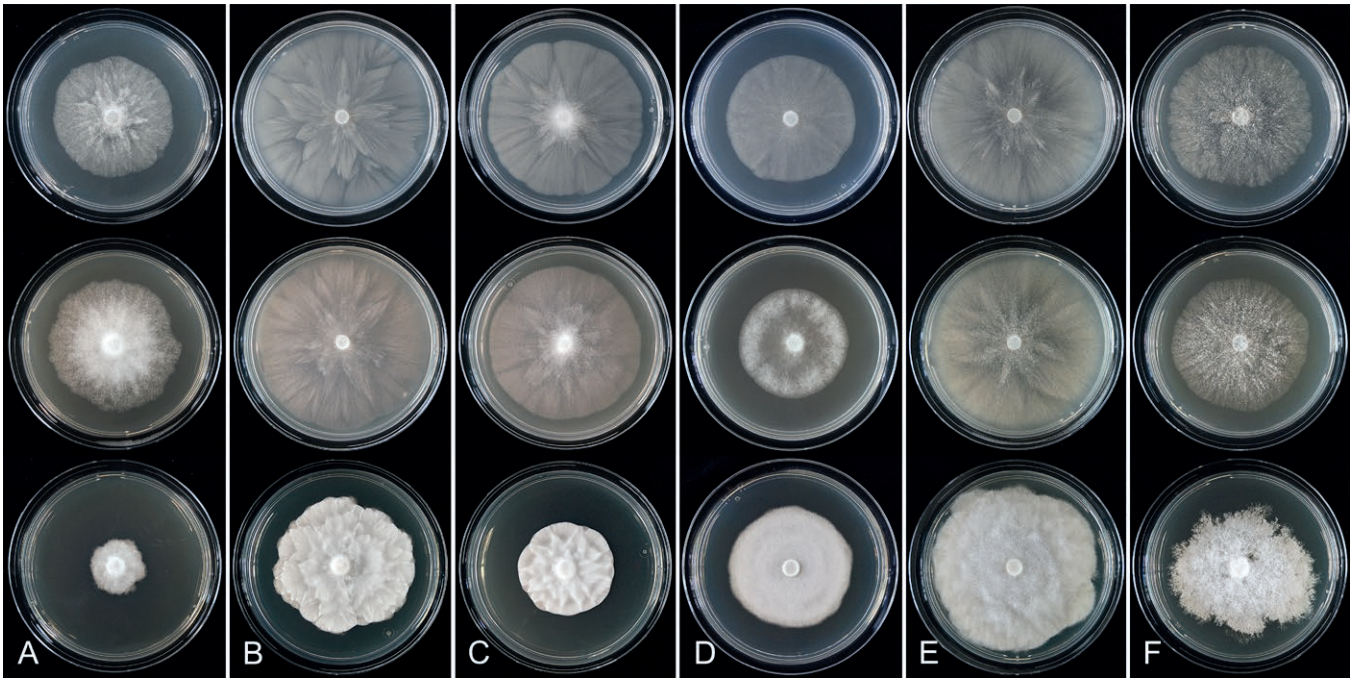

Fig. 8. Colony morphology of *Phytophthora* species from subclade 2a after 7 d growth at 20 ºC on V8-agar, carrot juice agar and potato-dextrose agar (from top to bottom). **A.** *Phytophthora botryosa* (MYA-4059). **B, C.** *Phytophthora citrophthora* (B. TW386; C. JP554). **D.** *Phytophthora colocasiae* (SU1665). **E, F.** *Phytophthora meadii* (E. MYA-4043; F. MYA-4042).

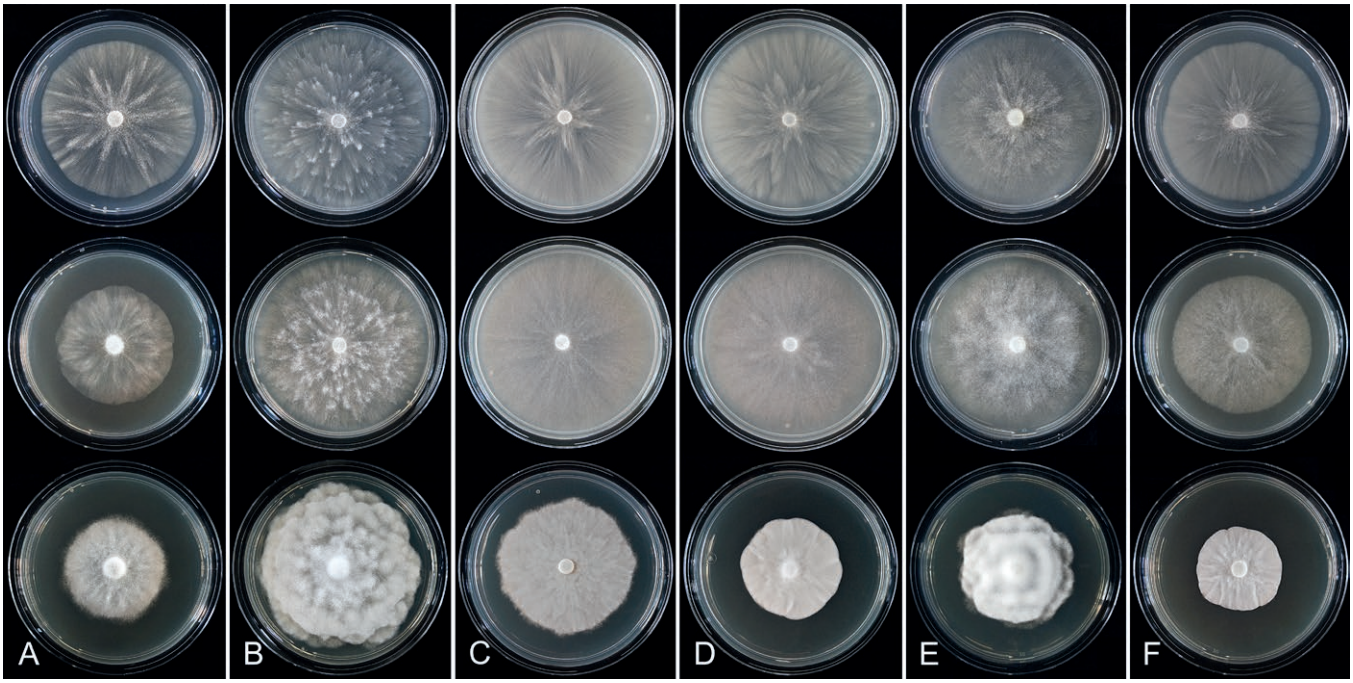

Fig. 9. Colony morphology of *Phytophthora* species from subclade 2a after 7 d growth at 20 ºC on V8-agar, carrot juice agar and potato-dextrose agar (from top to bottom). **A.** *Phytophthora mekongensis* (ex-type CBS 135136). **B.** *Phytophthora occultans* (TJ967). **C, D.** *Phytophthora pseudocitrophthora* (C. TJ133; D. ex-type CBS 149500). **E.** *Phytophthora pseudoccultans* (ex-type CBS 149499). **F.** *Phytophthora vietnamensis* (ex-type CBS 149635).

base, subglobose to globose, limoniform or irregular (Fig. 13D); diam 14.8 ± 4.1 µm (range 7.0–20.3 µm). *Chlamydospores* not observed. *Hyphal aggregations* commonly formed. *Oogonia* not observed in single culture; in mating tests with A1 and A2 mating type isolates of *P. meadii* two of the nine tested isolates (TW386 and TW387) stimulated the production of oogonia in the A2 isolate MYA-4043 of *P. meadii* and, hence, were of silent A2 mating type. The other seven isolates were sterile.

Culture characteristics: Colonies on V8A and CA mostly submerged with scanty aerial mycelium, stellate or faintly stellate; on PDA dense felty-cottony, with rosaceous or stellate patterns (Fig. 8).

Cardinal temperatures and growth rates: On V8A optimum 27.5 °C with 6.8 ± 0.58 mm/d radial growth, maximum 30–<32.5 °C, minimum <10 °C (Fig. 12), lethal temperature 35 °C. At 20 °C on V8A, CA and PDA 5.6 ± 0.53 mm/d, 4.7 ± 0.49 mm/d and 2.6 ± 0.48 mm/d, respectively.

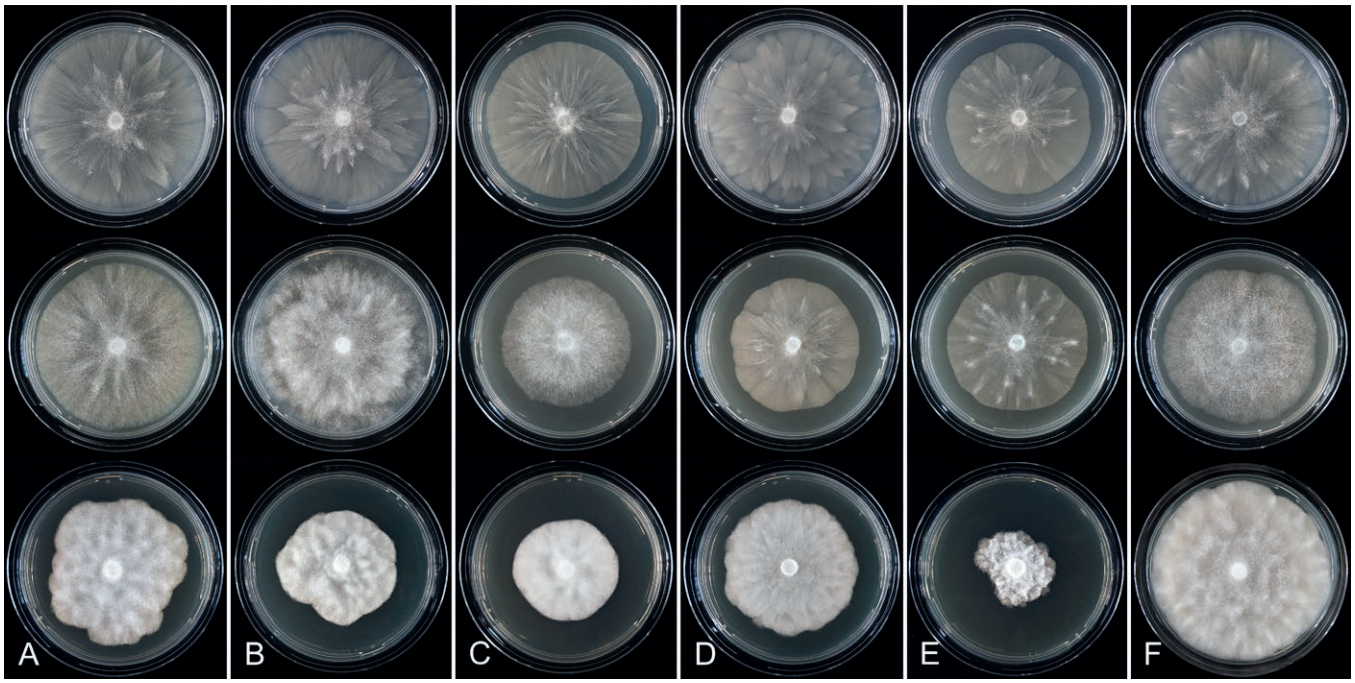

Fig. 10. Colony morphology of *Phytophthora* species from subclade 2a after 7 d growth at 20 ºC on V8-agar, carrot juice agar and potato-dextrose agar (from top to bottom). **A–D.** *Phytophthora* ×*australasiatica* (A. ex-type CBS 149636; B. JP1364; C. PA205; D. SU1084). **E.** *Phytophthora* ×*lusitanica* (ex-type CBS 150256). **F.** *Phytophthora* ×*taiwanensis* (ex-type CBS 149506).

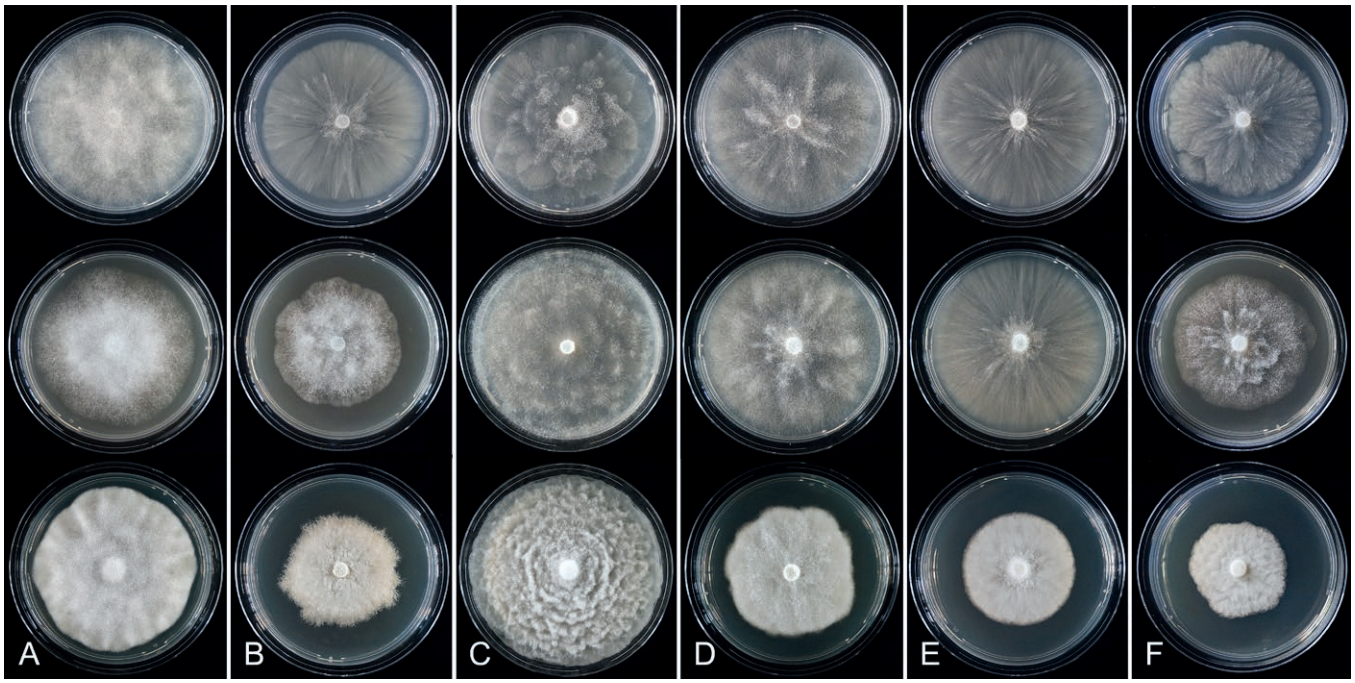

Fig. 11. Colony morphology of *Phytophthora* species from subclade 2a after 7 d growth at 20 ºC on V8-agar, carrot juice agar and potato-dextrose agar (from top to bottom). **A, B.** *Phytophthora* ×*taiwanensis* (A. TW168; B. TW248). **C–F.** *Phytophthora* ×*vanyenensis* (C. JV014; D. JV009; E. SL318; F. SU631a).

Materials examined: **Japan**, Kyushu, isolated from necrotic baiting leaves floating in forest streams; May 2017, *T. Jung, A. Hieno & K. Kageyama* (JP359, JP554); isolated from a naturally fallen necrotic leaf of *Neolitsea sericea* collected from the forest ground, Feb. 2017, *H. Masuya* (JP976); Amami-Ōshima, isolated from a naturally fallen tree leaf floating in a stream running through a subtropical lowland forest, Nov. 2018, *T. Jung & M. Horta Jung* (JP1356); Okinawa, isolated from a naturally fallen tree leaf floating in a stream running through a subtropical lowland forest, Nov. 2018, *T. Jung & S. Uematsu* (JP1536). **Portugal**, Tavira, isolated from necrotic baiting leaves floating in the Rio Séqua, Sep. 2012, *T. Jung & M. Horta Jung* (BD513, BD514); isolated from naturally fallen fruits of *Citrus sinensis* floating in the Rio Séqua running through *Citrus* orchards, Sep. 2011, *T. Jung & M. Horta Jung* (BD786, BD787, BD788). **Spain**, Galicia, isolated from rhizosphere soil of planted *Citrus sinensis*, before 2013, O. Aguin (TJ966 = EFA-16). **Taiwan**, Fushan, isolated from rhizosphere soil of *Quercus tarokoensis*, 2013, T. Jung, T.-T. Chang & M. Horta Jung (TW386, TW387).

Phytophthora meadii McRae, J. Bombay Nat. Hist. Soc. 25: 760. 1918. [MycoBank MB 120866]. Fig. 14.

Neotypus: **India**, Kerala State, Palapilly Region isolated from *Hevea brasiliensis*, 2001, unknown collector (**neotype** CBS H-25073 designated in Abad *et al.* 2023a, MBT 10008019, dried culture on V8A; ex-neotype living culture CBS 148927 = NRRL 64146 = WPC P19007).

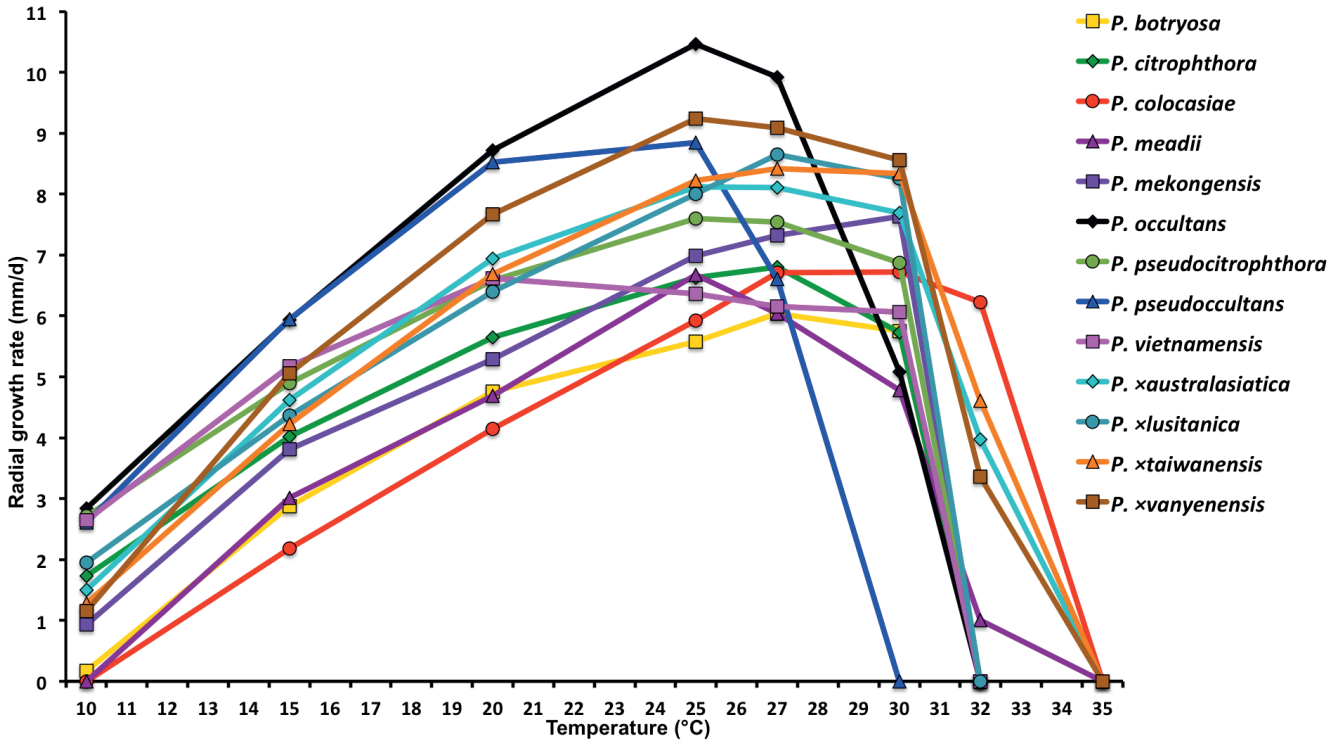

Fig. 12. Mean radial growth rates of seven known and five new *Phytophthora* species from subclade 2a on V8-agar at different temperatures: *P. botryosa* (2 isolates); *P. citrophthora* (13 isolates); *P. colocasiae* (3 isolates); *P. meadii* (2 isolates); *P. mekongensis* (2 isolates); *P. occultans* (2 isolates); *P. pseudocitrophthora* (9 isolates); *P. pseudoccultans* (3 isolates); *P. vietnamensis* (5 isolates); *P. ×australasiatica* (28 isolates); *P. ×lusitanica* (4 isolates); *P. ×taiwanensis* (14 isolates); *P. ×vanyenensis* (33 isolates).

Morphological structures on V8A: *Sporangia* infrequently observed on solid agar and abundantly produced in non-sterile soil extract; borne almost exclusively terminally (99.2 %) on unbranched long or short sporangiophores or in dense or lax sympodia of 2–6 sporangia, or rarely intercalary (0.8 %; Fig. 14H); mostly ovoid to elongated ovoid (47.7 %; Fig. 14A–C, I, J) or obpyriform to elongated-obpyriform (28 %; Fig. 14E–H, L), less frequently distorted with often two or sometimes three apices (14.6 %; Fig. 14K), limoniform to elongated-limoniform (4.5 %), ellipsoid (2.5 %; Fig. 14D), pyriform (1.5 %) or subglobose; lateral attachment of sporangiophores (11.4 %; Fig. 14E, H), a widening of the sporangiophore towards the sporangial base (14.4 %; Fig. 14E, G) and vacuoles (7.3 %; Fig. 14H) commonly observed; sporangia frequently too big for the available cytoplasm and hence, not filled completely in the basal part, often with a strong plug below the cytoplasm (17.7 %; Fig. 14D, F, G); mostly (65.8 %) with pedicels of variable length (av. 22.7 ± 9.2 µm; range 7.3–46.4 µm; Fig. 14A–D, F, I, J) and caducous (Fig. 14I, J), but 34.2 % of sporangia without pedicel and persistent (Fig. 14K); sporangial apices on solid agar exclusively papillate, but in water mainly semipapillate to shallow papillate (77.2 %; Fig. 14A–D, G–K) with a smooth transition between both forms or less frequently nonpapillate and mostly pointed (22.8 %; Fig. 14E, F); sporangial proliferation exclusively external (Fig. 14A–C, F, K); sporangial dimensions averaging 44.5 ± 5.6 × 30.3 ± 4.9 µm (overall range 29.4–59.7 × 17.5–43.5 µm; range of isolate means 43.5–45.5 × 27.1–33.5 µm) with a length/breadth ratio of 1.5 ± 0.28 (overall range 1.13–2.45); sporangial germination indirectly with zoospores discharged through an exit pore 4.0–10.5 µm wide (av. 6.4 ± 1.2 µm) (Fig. 14L). *Zoospores* limoniform to reniform whilst motile, becoming spherical (av. diam = 10.4 ± 0.7 µm) on encystment; cysts germinating directly forming a hypha or a microsporangium. *Hyphal swellings* are sometimes formed in water on sporangiophores, usually close to the sporangial base, subglobose to globose or limoniform. *Chlamydospores* infrequently formed in solid agar in single cultures, but abundantly produced in mating tests; globose to subglobose, borne intercalary or sessile (Fig. 14M–Q), sometimes catenulate (Fig. 14M) or with radiating hyphae (Fig. 14P); dimensions 28.0 ± 3.3 µm (overall range 23.1–34.3 µm); with relatively thin (Fig. 14M–O) or thick wall (Fig. 14P, Q) averaging 1.11 ± 1.0 µm (range 0.35–3.5 µm); often golden-brown (Fig. 14M–P). *Hyphae* in solid agar often coralloid and swollen (Fig. 14R). *Hyphal aggregations* are commonly formed (Fig. 14S). *Oogonia* not observed in single cultures, but commonly produced in mating tests between A1 and A2 mating type isolates ('heterothallic' breeding system); mostly sessile with short thin stalks and rounded base, globose to slightly subglobose (Fig. 14T–Y), often slightly excentric (30 %; Fig. 14V–X); wall predominantly smooth (87.5 %; Fig. 14T–V, Y) or occasionally slightly wavy (12.5 %; Fig. 14W, X); oogonial diam 31.7 ± 4.2 µm (overall range 21.5–40.5 µm); slightly aplerotic to aplerotic (Fig. 14T–Y). *Oospores* globose, usually with one large lipid globule (Fig. 14U–Y) or infrequently with multiple smaller globules (6 %; Fig. 14T); diam 27.1 ± 3.6 µm (overall range 18.3–34.0 µm) wall thickness 1.46 ± 0.24 µm (overall range 1.13–2.07 µm), oospore wall index 0.29 ± 0.03; high abortion rate of 66 % after 4 wk (Fig. 14Z). *Antheridia* exclusively amphigynous and cylindrical or subglobose, sometimes curved, and unicellular (Fig. 14T–Z); dimensions 15.2 ± 2.3 × 13.4 ± 1.3 µm.

Culture characteristics: Colonies on V8A and CA submerged to appressed with scanty aerial mycelium, radiate to stellate or faintly radiate on V8A, and stellate or radiate on CA; on PDA dense felty-cottony and petaloid or dense felty with a stoloniferous pattern (Fig. 8).

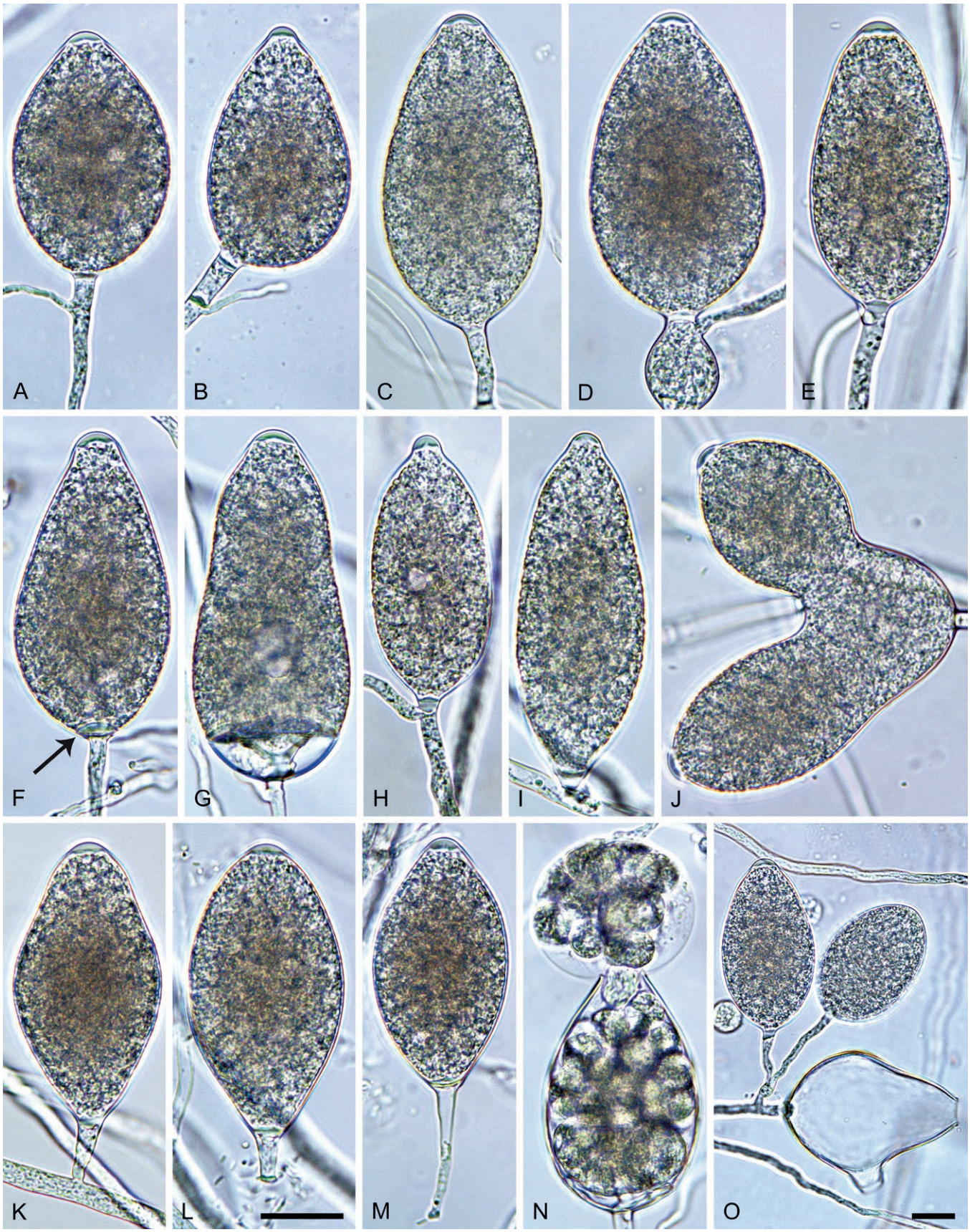

Fig. 13. *Phytophthora citrophthora*. **A–M.** Semipapillate and papillate sporangia formed on V8-agar in soil extract. **A–I, K.** Ovoid, limoniform, obpyriform or ellipsoid persistent sporangia. **A, B, D, E, G, H.** External proliferation. **F.** Conspicuous basal plug (arrow). **G.** Cytoplasm not filling the sporangium. **J.** Bilobed persistent sporangium. **L, M.** Caducous limoniform sporangia with varying pedicel length. **N.** Ovoid sporangium releasing zoospores. **O.** Dense sporangial sympodium. Images: A, N. BD122; B. JP1356; C–G, J, L, M, O. BD786; H, I. JP554; K. TW386. Scale bars = 20 µm; L applies to A–N.

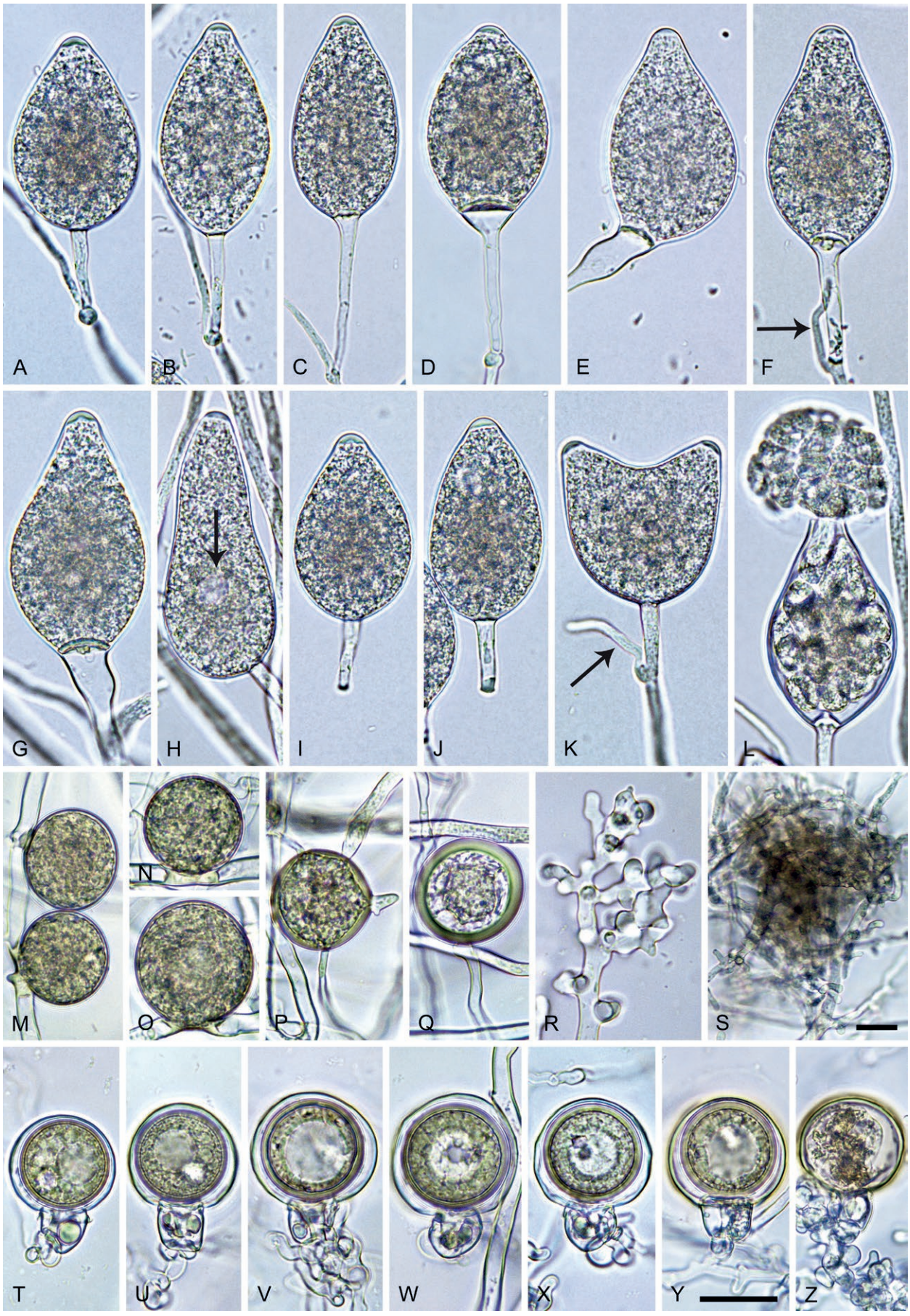

Fig. 14. *Phytophthora meadii*. **A–L.** Sporangia formed on V8-agar (V8A) in soil extract. **A–D, F–J.** Ovoid, obpyriform and ellipsoid sporangia with semipapillate or papillate apices. **A–D, F, G, I, J.** Medium-length to long pedicels. **E.** Nonpapillate obpyriform sporangium. **A–C, F, K.** External proliferation (arrows). **H.** Vacuole (arrow). **I, J.** Caducous sporangia. **K.** Bilobed semipapillate sporangium. **L.** Zoospore releases. **M–Q.** Chlamydospores formed in solid carrot agar (fgCA). **R.** Coralloid hypae in solid V8A. **S.** Hyphal aggregation in solid V8A. **T–Y.** Oogonia with slightly aplerotic to aplerotic oospores and amphigynous unicellular antheridia, formed in mating test in solid fgCA. **Z.** Aborted oogonium. Images: A–C, E–R. MYA-4043; D, S. MYA-4042; T–Z. MYA-4042 × MYA-4043. Scale bars = 20 µm; Y applies to A–R, T–Z.

Cardinal temperatures and growth rates: On V8A optimum 25 °C with 6.67 ± 2.85 mm/d radial growth, maximum 32.5 °C, minimum >10–<15 °C (Fig. 12), lethal temperature 35 °C. At 20 °C on V8A, CA and PDA 4.68 ± 1.0 mm/d, 5.18 ± 0.7 mm/d and 4.78 ± 0.97 mm/d, respectively.

Materials examined: **India**, Karnataka, Beligundi, isolated from a leaf of Coorg orange (*Citrus reticulata*), 1992, *S.D. Sawant* (MYA-4043 = NRRL 64250 = IMI 403509 = WPC P10191 = CH 22G5 = MEGp75 = TJ1112); Nittur village isolated from a leaf of Coorg orange, 1992, *S.D. Sawant* (MYA-4042 = WPC P10190 = CH 22G4 = MEGp74 = TJ1149*)*.

Phytophthora pseudocitrophthora T. Jung, S.O. Cacciola, J. Bakonyi & M. Horta Jung, ***sp. nov.*** MycoBank MB 847265. Fig. 15.

Etymology: The name refers to the morphological similarity and phylogenetic relatedness to *P. citrophthora*.

Typus: **Italy,** Sicily, Pantalica Nature Reserve, isolated from rhizosphere soil of *Platanus orientalis* in a riparian forest, May 2013, *T. Jung & S.O. Cacciola* (**holotype** CBS H-25124, dried culture on V8A, ex-holotype living culture CBS 149500 = TJ798).

Morphological structures on V8A: *Sporangia* infrequently observed on solid agar and abundantly produced in non-sterile soil extract; borne predominantly terminally (99.1 %) on unbranched long or short sporangiophores or in dense or lax sympodia of 2–8 sporangia (Fig. 15O), or rarely intercalary (0.8 %; Fig. 15J); mostly ovoid, broad-ovoid or elongated-ovoid (63.7 %; Fig. 15A–E, H, M, O) or limoniform to elongated-limoniform (20 %; Fig. 15F, G, N, O), less frequently distorted with often two or sometimes three apices (7.4 %; Fig. 15K), obpyriform to elongated-obpyriform (6.2 %; Fig. 15I, L), ellipsoid to elongated-ellipsoid (1.2 %; Fig. 15J), subglobose, pyriform, obturbinate, obovoid or ampulliform (each 0.3 %); lateral attachment of sporangiophores (23.1 %; Fig. 15B, D, L) and a conspicuous basal plug (42.9 %; Fig. 15E–I, M, N) commonly observed; sporangiophores sometimes widening towards the sporangial base (6.9 %; Fig. 15E); sporangia occasionally too big for the available cytoplasm and hence, not filled completely in the basal part, often with an additional strong plug below the cytoplasm (4.9 %; Fig. 15F, G); predominantly (86.3 %) with pedicels of variable length (av. 24.8 ± 13.6 µm; range 4.4–90.1 µm; Fig. 15A–M, O); infrequently caducous (Fig. 15L, M); sporangial apices on solid agar exclusively papillate; in water mainly papillate (75.9 %; Fig. 15A–I, L, O) or less frequently semipapillate (14.6 %; Fig. 15K) or nonpapillate and mostly pointed (9.5 %; Fig. 15J); sporangial proliferation exclusively external (Fig. 15A–E, K, O); sporangial dimensions averaging 61.6 ± 7.6 × 36.0 ± 4.0 µm (overall range 39.3–89.4 × 20.5–45.5 µm; range of isolate means 54.4–71.5 × 32.8–39.8 µm) with a length/breadth ratio of 1.73 ± 0.26 (overall range 1.12–2.68); sporangial germination indirectly with zoospores discharged through an exit pore 3.7–7.3 µm wide (av. 5.3 ± 0.7 µm) (Fig. 15M, N). *Zoospores* limoniform to reniform whilst motile, becoming spherical (av. diam = 10.7 ± 0.9 µm) on encystment; cysts usually germinating directly forming a hypha or a microsporangium or infrequently indirectly by releasing a secondary zoospore (diplanetism). *Hyphal swellings* sometimes formed in water on sporangiophores, often close to the sporangial base, subglobose to globose, limoniform or irregular (Fig. 15A); diam 13.0 ± 6.1 µm (range 5.6–21.7 µm). *Chlamydospores* not observed. *Hyphal aggregations* commonly formed (Fig. 15P). *Oogonia* not observed in single culture; in mating tests with A1 and A2 mating type isolates of *P. meadii* one of the 10 tested isolates (TJ133) stimulated the production of a few oogonia in the A1 isolate MYA-4042 of *P. meadii* and, hence, was a silent A2 mating type, whereas the other nine isolates were sterile.

Culture characteristics: Colonies on V8A mostly submerged with scanty aerial mycelium, stellate to radiate; on CA submerged to appressed with limited aerial mycelium and faint radiate pattern; on PDA dense felty-cottony and mostly appressed, with a radiate pattern (Fig. 9).

Cardinal temperatures and growth rates: On V8A optimum 25 °C with 7.59 ± 1.15 mm/d radial growth, maximum 30–<32.5 °C, minimum <10 °C (Fig. 12), lethal temperature 35 °C. At 20 °C on V8A, CA and PDA 6.59 ± 0.59 mm/d, 5.62 ± 0.17 mm/d and 3.45 ± 0.45 mm/d, respectively.

Additional materials examined: **Hungary**, Répceszemere, isolated from *Syringa vulgaris*, Sep. 2008, *J. Bakonyi* (TJ133 = JA149); Gencsapáti, isolated from *Abies procera*, Aug. 2009, *J. Bakonyi* (TJ137 = JA333). **Morocco**, Marrakech, isolated from rhizosphere soil of planted *Citrus limon* in a garden, Jan. 2012, *T. Jung* (TJ995); isolated from rhizosphere soil of planted *Myrthus communis* in a garden, Jan. 2012, *T. Jung* (TJ998). **Portugal**, Parque Natural Sintra-Cascais, isolated from a baiting leaf of *Quercus suber* floating in a stream running through planted forests, Mar. 2015, *T. Jung & C. Maia* (BD255); Tavira, isolated from a naturally fallen fruit of *Citrus sinensis* floating in the Rio Séqua river running through *Citrus* orchards, Sep. 2011, *T. Jung & M. Horta Jung* (BD505). **Serbia**, Fruska Gora National Park, isolated from rhizosphere soil of *Quercus petraea* in a planted forest, Apr. 2012, *I. Milenković* (SFB265). **Spain**, Mallorca, unknown, 2010, *E.M. Moralejo* (TJ065 = P300 = P4142); Valencia, isolated from rhizosphere soil of planted *Pistacia lentiscus*, 2010, *A. Pérez-Sierra* (TJ480 = 917b). **USA**, Louisiana, Little Bayou Sara, isolated from a naturally fallen necrotic leaf floating in a forest stream, Mar. 2020, *T. Corcobado & T. Majek* (LU209).

Phytophthora pseudoccultans T. Jung, T.-T. Chang, I. Milenković & M. Horta Jung, ***sp. nov.*** MycoBank MB 847272. Fig. 16.

Etymology: The name refers to the morphological similarity to *P. occultans*.

Typus: **Taiwan**, Fushan, isolated from a baiting leaf floating in a tributary of Ha-pen River running through subtropical *Castanopsis-Machilus* forest, Mar. 2013, *T. Jung & T.-T. Chang* (**holotype** CBS H-25123, dried culture on V8A, ex-holotype living culture CBS 149499 = TW044).

Morphological structures on V8A: Sporangia rarely observed on solid agar but produced abundantly in non-sterile soil extract; typically borne terminally (94 %) in dense or lax sympodia of 2–4 sporangia (Fig. 16L) or on unbranched long or short lateral sporangiophores, or intercalary (6 %; Fig. 16E); apices papillate (Fig. 16A–J, L); mostly ovoid, broad-ovoid or elongated ovoid (62.1 %; Fig. 16A–C, I, L), less frequently distorted and often bi- or tripapillate (18.4 %; Fig. 16G, H), limoniform to elongated-limoniform (10.2 %; Fig. 16F, J), obpyriform to broad-obpyriform (4.5 %; Fig. 16D), ellipsoid to elongated-ellipsoid (2 %; Fig. 16E), obovoid (2 %) or pyriform (0.8 %); lateral attachment of the sporangiophore (35 %; Fig. 16B, C, G–I) common; mostly with pedicels (69.9 %; Fig. 16A, B, D, F, I, J) averaging 17.3 ± 8.1 µm in length (range 4.3–38.1 µm) and caducous (Fig. 16I, J); infrequently with a vacuole (Fig. 16L); sporangial proliferation exclusively external (Fig. 16A, F, L); sporangial dimensions averaging 57.9 ± 6.3 ´ 36.0 ± 3.6 µm (overall range 42.6–77.9 ´ 28.2–45.1 µm; range of isolate means 56.9–58.9 ´ 35.3–36.6 µm) with a length/breadth ratio of 1.62 ± 0.23

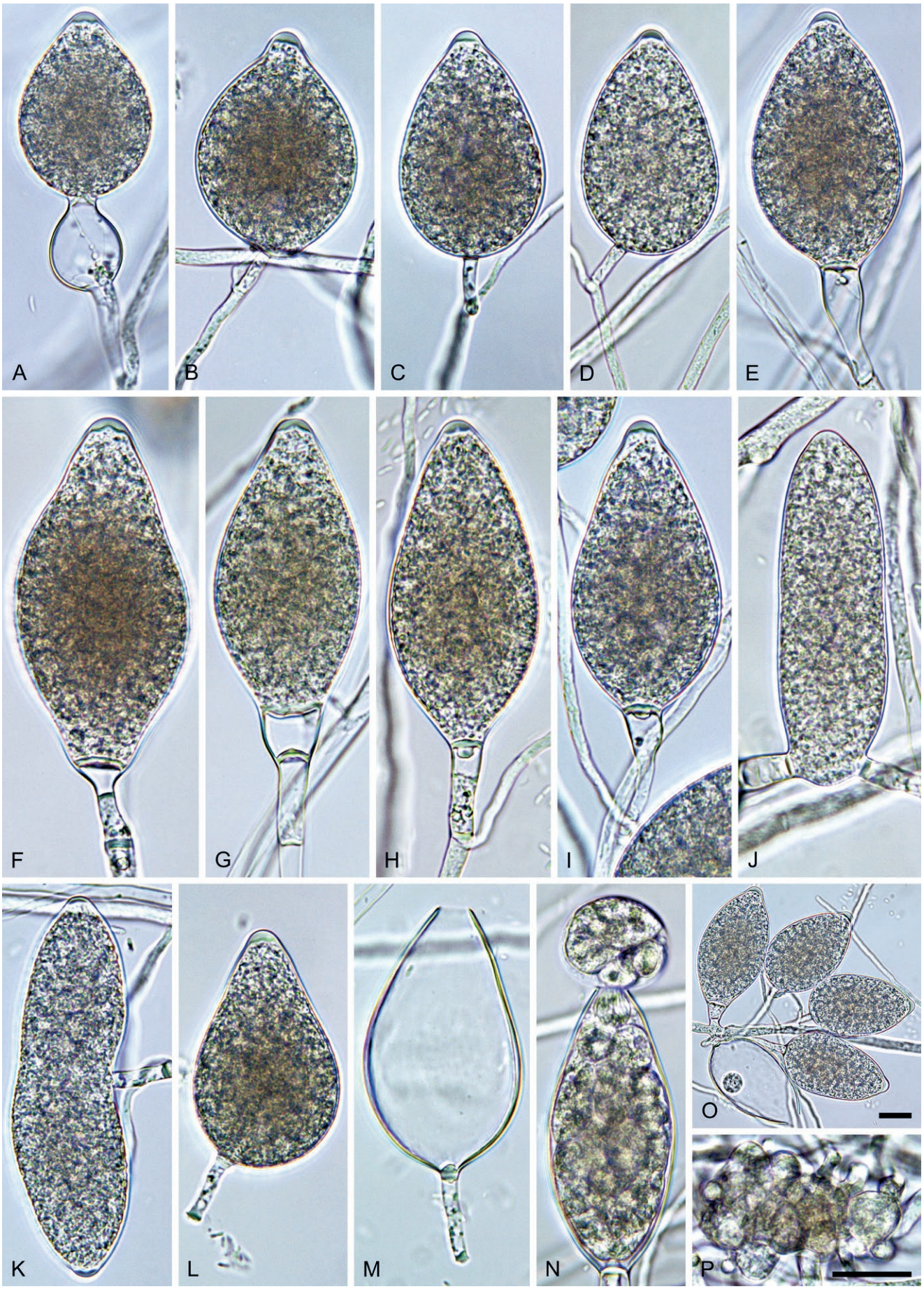

Fig. 15. *Phytophthora pseudocitrophthora*. **A–O.** Sporangia formed on V8-agar (V8A) in soil extract. **A–I.** Ovoid, limoniform or obpyriform sporangia with papillate apices and medium-length to long pedicels. **A–C, E, H.** External proliferation. **F, G.** Cytoplasm not completely filling the sporangia. **J.** Ellipsoid, intercalary nonpapillate sporangium. **K.** Distorted sporangium with two semipapillate apices. **L, M.** Caducous sporangia. **N.** Zoospore release. **O.** Dense sporangial sympodium. **P.** Hyphal aggregation formed in solid V8A. Images: A, G–J, M, N, P. Ex-type CBS 149500; B–D. BD505; E. TJ998; F. TJ133; K. TJ995; L. TJ065; O. TJ480. Scale bars = 20 µm; P applies to A–N, P.

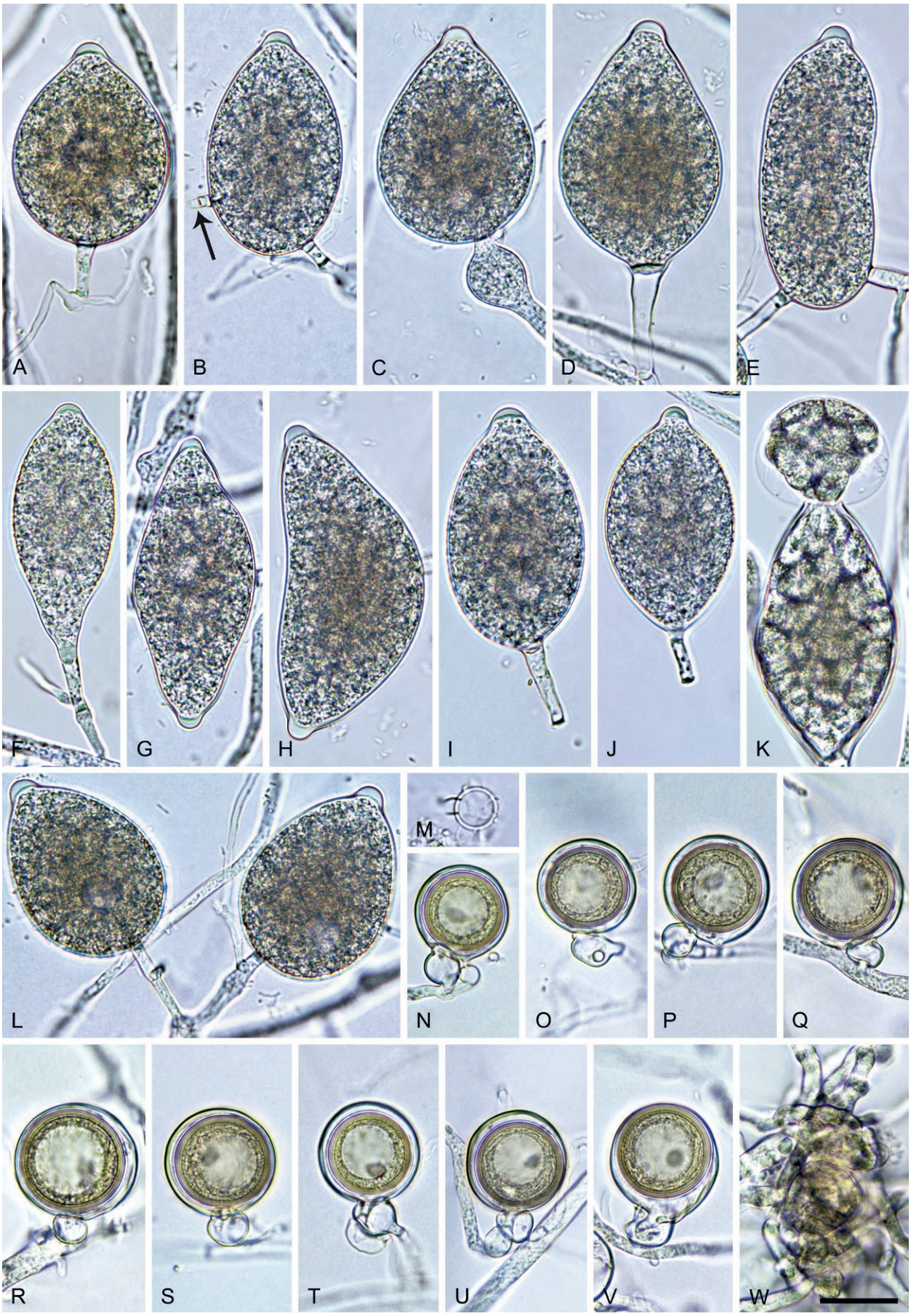

Fig. 16. *Phytophthora pseudoccultans*. **A–L.** Sporangia formed on V8-agar (V8A) in soil extract. **A–J, L.** Papillate sporangia. **A–F, I–L.** Ovoid, obpyriform, ellipsoid and limoniform sporangia. **A, B, D-F, I, J, L.** Pedicels. **B.** Hyphal extension (arrow). **E.** Intercalary sporangium. **G, H.** Distorted, bipapillate sporangia. **I, J.** Caducous sporangia. **K.** Zoospore release. **L.** Beginning sporangial sympodium. **M.** Empty zoospore cyst after releasing a secondary zoospore (diplanetism). **N–V.** Oogonia with near-plerotic to slightly aplerotic oospores produced in solid V8A. **N–S.** Paragynous antheridia. **T–V.** Amphigynous antheridia. **W.** Hyphal aggregation formed in solid V8A. Images: A–E, G–I, L, M, O–T, W. Ex-type CBS 149499; F, J, K, N, U, V. TW062. Scale bar = 20 µm; W applies to A–W.

(overall range 1.24–2.47); sporangial germination usually indirectly with zoospores discharged through an exit pore 4.8–7.8 µm wide (av. 6.6 ± 0.8 µm) (Fig. 16K). *Zoospores* limoniform to reniform whilst motile, becoming spherical (av. diam = 10.4 ± 0.7 µm) on encystment; cysts mostly germinating directly or by releasing a secondary zoospore (= diplanetism; Fig. 16M). *Hyphal swellings* infrequently produced in water on sporangiophores and hyphae; globose to subglobose or limoniform, often close to the sporangial base (Fig. 16C); dimensions 10.8 ± 2.3 µm. *Chlamydospores* not observed. *Oogonia* abundantly produced in single culture ('homothallic' breeding system), mostly sessile without stalk or on short thin stalks, with rounded base, smooth-walled, globose to slightly subglobose (93 %; Fig. 16N–U) or sometimes slightly elongated (7 %; Fig. 16V); oogonial diam 28.8 ± 2.6 µm (overall range 22.4–35.3 µm; range of isolate means 27.8–29.7 µm); nearly plerotic to slightly aplerotic (Fig. 16N–V). *Oospores* globose with a large lipid globule (Fig. 16N–V); diam 24.3 ± 2.4 µm (overall range 18.8–33.3 µm; range of isolate means 23.5–25.2 µm) wall thickness 1.37 ± 0.22 µm (overall range 1.02–2.48 µm), oospore wall index 0.3 ± 0.04; abortion rate 9–21 % (av. 15 %) after 4 wk. *Antheridia* predominantly paragynous and club-shaped, ovoid or subglobose (77 %; Fig. 16N–S) or less frequently amphigynous, unicellular and club-shaped to cylindrical (23 %; Fig. 16T–V); sometimes two antheridia attached to one oogonium (4 %); dimensions 11.4 ± 2.3 × 8.7 ± 1.6 µm.

Culture characteristics: Colonies on V8A mostly submerged to appressed with limited aerial mycelium and a radiate pattern; on CA shallow cottony with submerged margin and a faint radiate pattern; on PDA cottony and petaloid (Fig. 9).

Cardinal temperatures and growth rates: On V8A optimum 25 °C with 8.85 ± 0.71 mm/d radial growth, maximum 27.5–<30 °C, minimum <10 °C (Fig. 12), lethal temperature 30–32.5 °C. At 20 °C on V8A, CA and PDA 8.53 ± 2.04 mm/d, 6.05 ± 0.43 mm/d and 4.09 ± 0.28 mm/d, respectively.

Additional materials examined: **Taiwan**, Fushan, isolated from a baiting leaf floating in Cu-keng River, Mar. 2013, *T. Jung, M. Horta Jung & T.-T. Chang* (TW062); Tunyuan, isolated from rhizosphere soil of *Quercus variabilis* in montane, temperate, seasonally dry *Quercus–Pinus* forest, Mar. 2013, *T. Jung, M. Horta Jung & T.-T. Chang* (TW114).

Phytophthora vietnamensis T. Jung, N.M. Chi, I. Milenković & M. Horta Jung, ***sp. nov.*** MycoBank MB 847280. Fig. 17.

Etymology: The name refers to the origin of all known isolates in Vietnam.

Typus: **Vietnam**, Sapa, Xin Chài Mountain, isolated from rhizosphere soil of *Alnus nepalensis* in montane, temperate *Alnus* forest, Mar. 2016, *T. Jung & N.M. Chi* (**holotype** CBS H-25190, dried culture on V8A, ex-holotype living culture CBS 149635 = VN368).

Morphological structures on V8A: *Sporangia* infrequently observed on solid agar but abundantly produced in non-sterile soil extract; borne mostly terminally (91.6 %) on unbranched long or short sporangiophores (Fig. 17B, I) or in dense or lax sympodia of 2–5 sporangia, or less frequently intercalary (8.4 %; Fig. 17C, H, O); mostly ovoid to broad-ovoid (52.2 %; Fig. 17A–E, K) or obpyriform, broad-obpyriform or elongated-obpyriform (28.4 %; Fig. 17F–H, L), less frequently distorted with often two or sometimes three apices (9.6 %; Fig. 17M), limoniform to elongated-limoniform (5.6 %; Fig. 17J), ampulliform (3.6 %; Fig. 17I, O) or obovoid (0.6 %); sporangial apices predominantly papillate (92.6 %; Fig. 16B, D–I, L, M), sometimes semipapillate (4.8 %; Fig. 17A, C, J) or nonpapillate and pointed (2.6 %; Fig. 17K); frequently curved (20.8 %; Fig. 17G–I); lateral attachment of sporangiophores (54.4 %; Fig. 17E–G, K, L), small vacuoles (32.9 %; Fig. 17F–I) and a conspicuous basal plug (22.8 %; Fig. 17A, F, J, O) commonly observed; predominantly (72.8 %) with short- to medium-length pedicels (9.7 ± 4.3 µm; range 2.1–34.2 µm; Fig. 17A–C, J–L); often caducous (Fig. 17K–M); sporangial proliferation exclusively external (Fig. 17A, B, D, F, O); sporangial dimensions averaging 63.3 ± 7.2 × 42.4 ± 4.5 µm (overall range 42.3–100.1 × 29.3–54.1 µm; range of isolate means 61.8–67.2 × 40.8–44.5 µm) with a length/breadth ratio of 1.51 ± 0.28 (overall range 1.13–2.83); sporangial germination indirectly with zoospores discharged through an exit pore 4.0–9.2 µm wide (av. 6.1 ± 0.7 µm) (Fig. 17N, O). *Zoospores* limoniform to reniform whilst motile, becoming spherical (av. diam = 10.2 ± 1.1 µm) on encystment; cysts germinating directly forming a hypha or a microsporangium. *Hyphal swellings* sometimes formed in water on sporangiophores, often close to the sporangial base, subglobose to globose, limoniform or irregular (Fig. 17E); diam 13.6 ± 4.7 µm (range 5.8–23.7 µm). *Chlamydospores* not observed. *Oogonia* not observed in single cultures or in mating tests with A1 and A2 mating type isolates of *P. meadii* (sterile breeding system).

Culture characteristics: Colonies on V8A mostly submerged with scanty aerial mycelium and a radiate pattern; on CA submerged to appressed with limited aerial mycelium and faint radiate pattern; on PDA dense-felty and appressed with limited aerial mycelium and a radiate pattern (Fig. 9).

Cardinal temperatures and growth rates: On V8A optimum 20 °C with 6.62 ± 0.8 mm/d radial growth but growing only slightly slower at 25, 27.5 and 30 °C, maximum 30–<32.5 °C, minimum <10 °C (Fig. 12), lethal temperature 32.5–<35 °C. On CA and PDA at 20 °C 4.48 ± 0.12 mm/d and 2.72 ± 0.08 mm/d, respectively.

Additional materials examined: **Vietnam**, Sapa, Xin Chài Mountain, isolated from rhizosphere soil of *Alnus nepalensis* in montane, temperate *Alnus* forest, Mar. 2016, *T. Jung, M. Horta Jung & N.M. Chi* (VN824, VN825, VN826, VN827).

Phytophthora ×australasiatica T. Jung, N.M. Chi, M. Tarigan & M. Horta Jung, ***sp. nov.*** MycoBank MB 847287. Fig. 18.

Etymology: The name refers to the hybrid status and the origin of most known isolates in the south of Asia (*australis* Latin = southern).

Typus: **Vietnam**, Cuc Phuong National Park, isolated from mixed rhizosphere soil of *Allophylus cobbe, Ficus* sp. and *Homalium* sp. in tropical lowland rainforest, Mar. 2016, *T. Jung, & N.M. Chi* (**holotype** CBS H-25191, dried culture on V8A, ex-holotype living culture CBS 149636 = VN812).

Morphological structures on V8A: *Sporangia* infrequently observed on solid agar and abundantly produced in non-sterile soil extract; borne mostly terminally (96.7 %) in dense or lax sympodia of 2–6 sporangia (Fig. 18L, M) or rarely on unbranched long or short sporangiophores, less frequently intercalary or sessile (3.3 %; Fig. 18F, G); mostly ovoid, broad-ovoid or elongated ovoid (61.8 %; Fig. 18A, B, I, K, L), less frequently distorted with often two or sometimes three apices or bilobed (16.2 %; Fig. 18G, H), limoniform to elongated limoniform (9 %; Fig. 18C, M), obpyriform

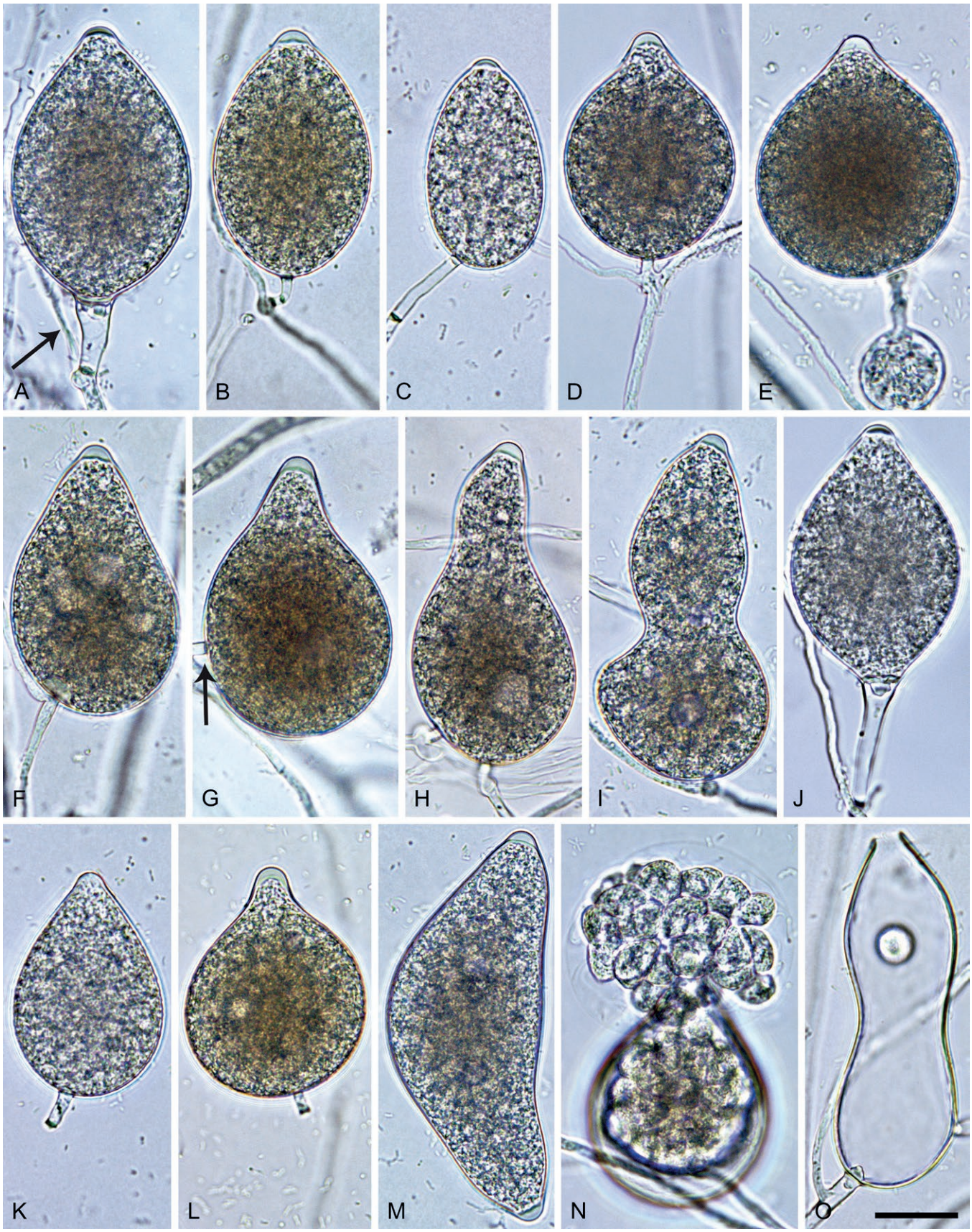

Fig. 17. *Phytophthora vietnamensis*. **A–O.** Sporangia formed on V8-agar (V8A) in soil extract. **A–J, L.** Ovoid, obpyriform, ampulliform or limoniform sporangia with papillate or semipapillate apices. **A–C, J–L.** Short to long pedicels. **A, B, D, F, O.** External proliferation (arrow in A). **C, H, O.** Intercalary sporangia. **G.** Lateral attachment (arrow). **K–M.** Caducous sporangia. **K.** Nonpapillate apex. **M.** Bipapillate sporangium. **N.** Zoospore release. **O.** Ampulliform sporangium after zoospore release. Images: A, C–E, I–K, M, O. Ex-type CBS 149635; B, F–H, L, N. CBS 149635. Scale bar = 20 µm; O applies to A–O.

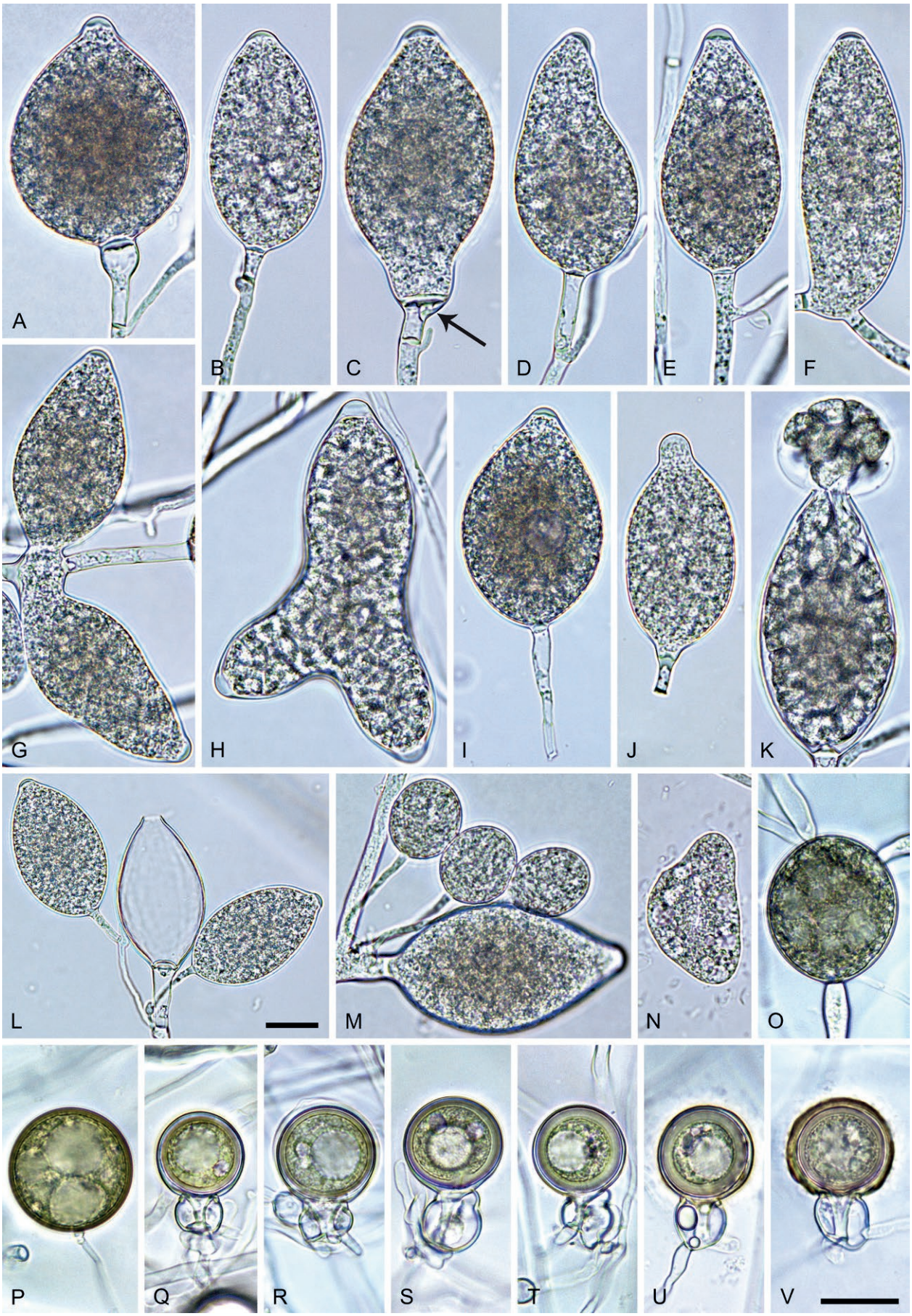

Fig. 18. *Phytophthora* ×*australasiatica*. **A–M.** Sporangia formed on V8-agar (V8A) in soil extract. **A–I.** Papillate or semipapillate sporangial apices. **A–F, I–M.** Ovoid, obpyriform, ellipsoid or limoniform sporangia. **A–C, I, J, L.** Medium-length to long pedicels. **F, G.** Intercalary insertion. **G.** Bilobed sporangium. **H.** Trilobed sporangium before zoospore release. **A, C–E, K–M.** External proliferation. **I, J.** Caducous sporangia. **J.** Nonpapillate apex. **K.** Zoospore release. **L.** Sporangial sympodium. **N.** Large multinucleate zoospore. **O, P.** Chlamydospores formed in carrot agar (fgCA). **Q–V.** Oogonia with plerotic oospores and amphigynous unicellular antheridia, formed in fgCA in mating tests. Images: A, C, G, J, M, N, P. Ex-type CBS 149636; B. SU658; D, E. JP1585; F. KA501; H. PA205; K, O. PA201; I, L. SU1087; Q, R. JP1538 × JP1364; S, T, V. CBS 149636 × VN1028; U. SL323 × VN1028. Scale bars = 20 µm; V applies to A–K, M–V.

to elongated-obpyriform (7.1 %; Fig. 18D, E, J), ellipsoid to elongated ellipsoid (2.6 %; Fig. 18F), obovoid (2.3 %), ampulliform (0.5 %), pyriform (0.3 %), mouse-shaped (0.1 %) or sickle-shaped (0.1 %); lateral attachment of sporangiophores (25.6 %; Fig. 18A, B, D, I, J) and a conspicuous basal plug (48.8 %; Fig. 18A, C, G, J–L) commonly observed; sometimes with a vacuole (Fig. 18I) or with sporangiophores widening towards the sporangial base (0.5 %; Fig. 18A); predominantly (74.8 %) with pedicels of variable length (av. 16.4 ± 9.4 µm; range 2.0–70.4 µm; Fig. 18A–D, I, J, L) and often caducous (Fig. 18I, J), but 25.2 % of sporangia without pedicel and persistent (Fig. 18E, F, M); sporangial apices on solid agar mostly papillate, but in water variable ranging from papillate (30.1 %; Fig. 18A, E) and semipapillate (68.7 %; Fig. 18B–D, F, G, I, L) to nonpapillate (1.2 %; Fig. 18J); sporangial proliferation exclusively external (Fig. 18A, C–E, K–M), sometimes with 2 or 3 sporangiophores arising from the same point close to a sporangial base (Fig. 18M); sporangial dimensions averaging 62.4 ± 8.6 × 36.9 ± 5.0 µm (overall range 31.0–100.8 × 20.2–69.0 µm; range of isolate means 49.1–75.0 × 29.1–41.2 µm) with a length/breadth ratio of 1.7 ± 0.23 (overall range 0.67–3.7); sporangial germination indirectly with zoospores discharged through an exit pore 3.4–10.4 µm wide (av. 6.0 ± 0.9 µm) (Fig. 18K). *Zoospores* limoniform to reniform whilst motile (Fig. 18N), becoming spherical (av. diam = 10.3 ± 0.9 µm) on encystment; sometimes unusually large and multinucleate (Fig. 18N); cysts germinating directly by forming a hypha or a microsporangium or infrequently indirectly by releasing a secondary zoospore (diplanetism). *Hyphal swellings* rarely formed in water on sporangiophores, subglobose to globose, limoniform or irregular; diam 13.7 ± 4.6 µm. *Chlamydospores* rarely produced in single culture but commonly produced in mating tests between A1 and A2 mating type isolates; globose (85 %) or subglobose (15 %), borne intercalary, sessile or terminal, with one or multiple lipid globules (Fig. 18O, P), sometimes with radiating hyphae (15 %; Fig. 18O); diam 36.9 ± 4.7 µm (range 28.0–47.6 µm); walls often turning golden-brown during maturation (Fig. 18P); wall diam 1.1 ± 0.5 µm (range 0.4–2.1 µm). *Oogonia* not observed in single culture, but commonly produced in mating tests between A1 and A2 mating type isolates ('heterothallic' breeding system; 35 tested isolates from Japan, Java, Kalimantan, Panama, Sulawesi, Sumatra and Vietnam belonging to the A1 mating type and 6 isolates from Japan and Vietnam to the A2 mating type); globose to slightly subglobose, smooth-walled (Fig. 18Q–U) or rarely with a thicker, slightly wavy wall (Fig. 18V), mostly sessile with short to medium-sized, often thin stalks and rounded base (76.9 %; Fig. 18S–V), less frequently with short tapering base (23.1 %; Fig. 18Q, R); sometimes oogonial wall turning golden-brown during maturation (Fig. 18V); oogonial diam 27.1 ± 2.9 µm (overall range 16.1–38.4 µm; range of means in different mating combinations 25.0–31.2 µm); nearly plerotic to plerotic (Fig. 18Q–V). *Oospores* globose with one large lipid globule (Fig. 18Q–V); diam 24.5 ± 2.7 µm (overall range 14.8–34.6 µm; range of means in different mating combinations 22.2–28.4 µm); wall thickness 1.22 ± 0.28 µm (overall range 0.6–2.59 µm), oospore wall index 0.27 ± 0.05; high abortion rate of 76.6 % (48–66 %) after 4 wk. *Antheridia* exclusively amphigynous, cylindrical, subglobose or irregular, and unicellular (Fig. 18Q–V); dimensions 15.2 ± 2.5 × 14.1 ± 1.7 µm.

Culture characteristics: Colonies variable between isolates; on V8A submerged to appressed with limited aerial mycelium and radiate or stellate patterns; on CA either submerged to appressed with limited aerial mycelium and radiate to striate pattern, or appressed with limited woolly mycelium and faint radiate pattern or uniform; on PDA either appressed, dense felty and uniform with stoloniferous margin or woolly-cottony and petaloid (Fig. 10).

Cardinal temperatures and growth rates: On V8A optimum at 25 °C (9 tested isolates) or 27.5 °C (21 isolates) with 8.12 ± 1.32 and 8.11 ± 1.44 mm/d radial growth, respectively; maximum 30–<32.5 °C (10 isolates) or 32.5–<35 °C (18 isolates); minimum <10 °C (Fig. 12), lethal temperature 35 °C. At 20 °C on V8A, CA and PDA 6.64 ± 0.89 mm/d, 4.98 ± 0.53 mm/d and 3.84 ± 0.58 mm/d, respectively.

Additional materials examined: **Indonesia**, Java, Bandung area, isolated from a naturally fallen, necrotic leaf of an unidentified tree species collected from the ground in a tropical rainforest, Feb. 2019, *T. Jung & M. Junaid* (JV045); Kalimantan, Balikpapan area, isolated from a naturally fallen, necrotic leaf of an unidentified tree species floating in a stream running through a lowland rainforest, Feb. 2019, *T. Jung & M. Tarigan* (KA229); isolated from rhizosphere soil of *Gmelina* sp. in a lowland rainforest, Feb. 2019, *T. Jung & M. Tarigan* (KA501); Sulawesi, Palanro, isolated from rhizosphere soil of *Mangifera indica* and *Szygium* sp. in a tropical lowland rainforest, May 2019, *T. Jung & M. Junaid* (SL323); Sumatra, Padang area, isolated from naturally fallen, necrotic leaves of unidentified tree species floating in a stream running through a tropical rainforest, Sep. 2018, *T. Jung, M. Tarigan & T. Corcobado* (SU637, SU658); isolated from rhizosphere soil of unidentified tree species in a tropical rainforest, Sep. 2018, *T. Jung, M. Tarigan & T. Corcobado* (SU1080, SU1084, SU1087, SU1093, SU1260). **Japan**, Amami-Ōshima, Sumiyou, isolated from a naturally fallen, necrotic leaf of an unidentified tree species floating in a stream running through a subtropical monsoon forest, Nov. 2018, *T. Jung, K. Kageyama & M. Horta Jung* (JP1364); Okinawa, isolated from naturally fallen, necrotic leaves of unidentified tree species floating in streams running through subtropical monsoon forests, Nov. 2018, *T. Jung, A. Hieno, H. Masuya & S. Uematsu* (JP1508, JP1538, JP1585). **Panama**, Herrera, El Montoso Reserva Forestal, isolated from naturally fallen, necrotic leaves of unidentified tree species collected from the ground in a tropical lowland rainforest, Nov. 2019, *K. Broders & Y. Balci* (PA201, PA202, PA203, PA205, PA330, PA332, PA334). **Vietnam**, Cuc Phuong National Park, isolated from mixed rhizosphere soil of *Allophylus cobbe, Ficus* sp. and *Homalium* sp. in a tropical lowland rainforest, Mar. 2016, *T. Jung, N.M. Chi & M. Horta Jung* (VN763, VN764, VN788, VN793, VN807, VN808, VN809, VN810, VN811, VN813, VN814, VN815, VN816, VN817, VN1086, VN1087, VN1088); Côn Đảo National Park, Côn Lôn Island, isolated from rhizosphere soil of *Canarium album, Hopea* sp. and *Leucaena leucocephala* in a tropical lowland rainforest, April 2017, *N.M. Chi* (VN1028, VN1116, VN1117, VN1118, VN1119).

Phytophthora ×lusitanica T. Jung, M. Horta Jung, C. Maia & I. Milenković, ***sp. nov.*** MycoBank MB 849628. Fig. 19.

Etymology: The name refers to the hybrid status and the origin of all known isolates from Portugal (*lusitanica* Latin = from Lusitania which is the old Roman name for Portugal).

Typus: **Portugal,** Algarve, Tavira, isolated from a baiting leaf floating in Rio Séqua, Jul. 2011, *T. Jung & M. Horta Jung* (**holotype** CBS H-25293, dried culture on V8A, ex-holotype living culture CBS 150256 = BD518).

Morphological structures on V8A: *Sporangia* infrequently observed on solid agar and abundantly produced in non-sterile soil extract; borne predominantly terminally (99 %) on unbranched long or short sporangiophores (Fig. 19F, H) or in dense or lax sympodia of 2–5 sporangia (Fig. 19O), or rarely intercalary (1 %; Fig. 19K); mostly ovoid, broad-ovoid or elongated-ovoid (40.9 %; Fig. 19A, B, L, N, O), distorted with often two or three or rarely four apices (22.6 %; Fig. 19G–J) or obpyriform to elongated-obpyriform (18.5 %; Fig. 19E, F, M), less frequently limoniform to elongated-limoniform (9 %; Fig. 19C, O), obovoid (5 %; Fig. 19D) or ampulliform (1 %); lateral attachment

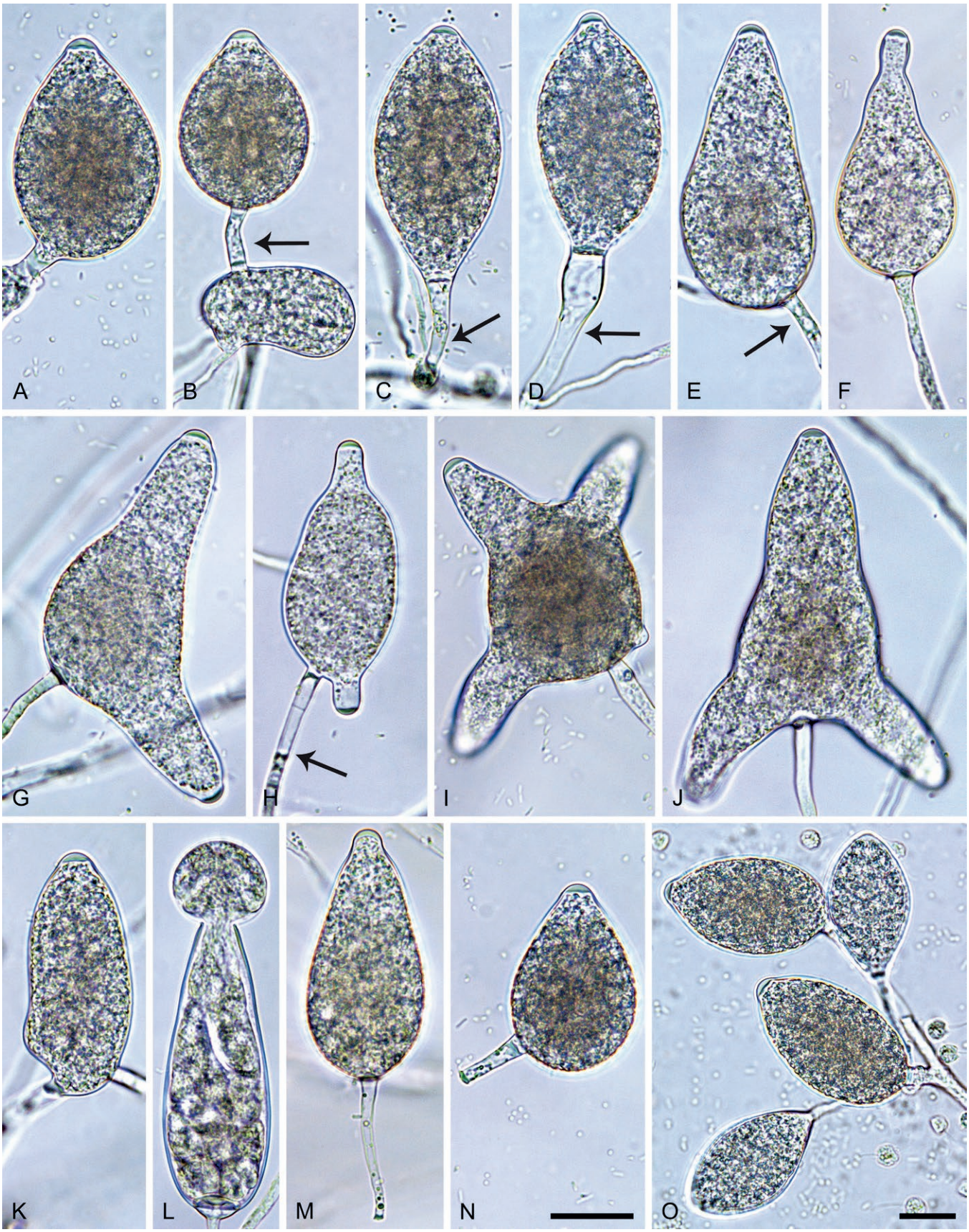

Fig. 19. *Phytophthora* ×*lusitanica*. **A–O.** Semipapillate to papillate sporangia formed on V8-agar flooded in extract. **A–F, K–O.** Ovoid, obovoid, limoniform or obpyriform sporangia. **B–E, H, M, N.** Medium-length to long pedicels (arrows). **B.** Hyphal swelling. **C, D.** External proliferation. **G–J.** Distorted sporangia with 2–4 apices. **K.** Intercalary sporangium. **L.** Zoospore release. **M, N.** Caducous sporangia. **O.** Dense sporangial sympodium. Images: A–C, G, I, K, N, O. Ex-type CBS 150256; D. BD517; E, F, H, J, L, M. BD516. Scale bars = 20 µm; N applies to A–N.

of sporangiophores (38 %; Fig. 19A, E, G, H, N) and pedicels (51.3 %) of variable length (av. 18.8 ± 10.7 µm; range 3.2–50.6 µm; Fig. 19B–E, H, M, N) common; infrequently caducous (1.9 %; Fig. 19M, N); seldom with a conspicuous basal plug (1 %; Fig. 19L); sporangiophores sometimes widening towards the sporangial base (1.9 %; Fig. 19D); in water semipapillate to papillate (Fig. 19A–K, M–O); sporangial proliferation exclusively external (Fig. 19C, D, O); sporangial dimensions averaging 53.9 ± 8.6 × 32.5 ± 4.7 µm (overall range 34.1–79.8 × 22.5–48.3 µm; range of isolate means 48.1–61.5 × 29.9–37.5 µm) with a length/breadth ratio of 1.67 ± 0.27 (overall range 1.15–2.43); sporangial germination indirectly with zoospores discharged through an exit pore 4.5–7.5 µm wide (av. 5.9 ± 0.6 µm) (Fig. 19L). *Zoospores* limoniform to reniform whilst motile, becoming spherical (av. diam = 10.6 ± 0.9 µm) on encystment. *Hyphal swellings* occasionally formed in water on sporangiophores, often close to the sporangial base, subglobose to globose, limoniform, ovoid or irregular (Fig. 19B); diam 11.6 ± 3.2 µm (range 5.3–18.3 µm). *Chlamydospores* or *hyphal aggregations* not observed. *Oogonia* not observed in single culture; in mating tests with A1 and A2 mating type isolates of *P. meadii* all four tested isolates stimulated abundant production of oogonia in the A1 isolate MYA-4042 of *P. meadii* and, hence, were a silent A2 mating type.

Culture characteristics: Colonies on V8A and CA mostly submerged with scanty aerial mycelium and radiate pattern; on PDA dense felty with limited aerial mycelium, irregular margins and a faint petaloid pattern (Fig. 10).

Cardinal temperatures and growth rates: On V8A optimum 27.5 °C with 8.65 ± 1.17 mm/d radial growth, maximum 30–<32.5 °C, minimum <10 °C (Fig. 12), lethal temperature 35 °C. At 20 °C on V8A, CA and PDA 6.4 ± 1.04 mm/d, 4.55 ± 0.57 mm/d and 2.55 ± 0.47 mm/d, respectively.

Additional materials examined: **Portugal,** Algarve, Tavira, isolated from a baiting leaf floating in Rio Séqua, Jul. 2011, *T. Jung & M. Horta Jung* (BD515, BD516, BD517).

Phytophthora ×taiwanensis T. Jung, T.-T. Chang, H.-S. Fu & M. Horta Jung, ***sp. nov.*** MycoBank MB 847288. Fig. 20.

Etymology: The name refers to the hybrid status and the origin of all known isolates in Taiwan.

Typus: **Taiwan**, Hualien County, isolated from rhizosphere soil of *Styrax suberifolia* in a subtropical, evergreen lowland monsoon forest, Aug. 2013, *T. Jung & T.-T. Chang* (**holotype** CBS H-25130, dried culture on V8A, ex-holotype living culture CBS 149506 = TW161).

Morphological structures on V8A: *Sporangia* infrequently observed on solid agar and abundantly produced in non-sterile soil extract; borne almost exclusively terminally (99.4 %) in dense or lax sympodia of 2–6 sporangia (Fig. 20K) or less frequently on unbranched long or short sporangiophores, or rarely intercalary or sessile (0.6 %); ovoid to elongated-ovoid (31.7 %; Fig. 20A, K), obpyriform to elongated-obpyriform (19.3 %; Fig. 20B, C), limoniform to elongated-limoniform (18.2 %; Fig. 20I, K), distorted with often two or sometimes three or four apices (16.5 %; Fig. 20E–G), ellipsoid to elongated ellipsoid (8.4 %; Fig. 20D, J), less frequently mouse-shaped (3.1 %) or pyriform (2.8 %; Fig. 20H); lateral attachment of sporangiophores (16.6 %; Fig. 20B, C, E), vacuoles (14.4 %; Fig. 20B, C, K) and a curved apex (11.9 %; Fig. 20D) commonly observed; sometimes sporangiophores widening towards the sporangial base (1.2 %); predominantly (80.4 %) with pedicels of variable length (av. 15.4 ± 5.9 µm; range 4.8–58.0 µm; Fig. 20A, C, D, G–I) and often caducous (Fig. 20G–I), but 19.6 % of sporangia without pedicel and persistent (Fig. 20B, E); sporangial apices on solid agar exclusively papillate, but in water variable ranging from papillate (40.7 %; Fig. 20A, E, F) and semipapillate (50.1 %; Fig. 20B, C, G–I, K) to nonpapillate (10.2 %; Fig. 20D); sporangial proliferation exclusively external (Fig. 20B, E, F, K); sporangial dimensions averaging 61.9 ± 11.0 × 31.9 ± 5.0 µm (overall range 23.7–123.1 × 17.3–52.1 µm; range of isolate means 45.1–79.5 × 26.5–42.3 µm) with a length/breadth ratio of 1.95 ± 0.32 (overall range 1.21–3.38); sporangial germination indirectly with zoospores discharged through an exit pore 3.4–9.9 µm wide (av. 6.3 ± 1.2 µm) (Fig. 20J). *Zoospores* limoniform to reniform whilst motile (Fig. 20L), becoming spherical (av. diam = 11.7 ± 1.2 µm) on encystment; sometimes with multiple nuclei (Fig. 20L); cysts germinating directly by forming a hypha or a microsporangium. *Hyphal swellings* rarely formed in water on sporangiophores, subglobose to globose, limoniform or irregular; diam 12.6 ± 2.0 µm. *Chlamydospores* rarely produced in single culture but infrequently produced in mating tests with tester strains of *P. meadii*; globose to subglobose, borne intercalary, sessile or terminal, with one or multiple lipid globules (Fig. 20M, N); diam 30.8 ± 3.5 µm (range 27.3–34.3 µm). *Oogonia* not observed in single culture, but commonly produced in mating tests with the A2 mating type isolate MYA-4043 of *P. meadii* ('heterothallic' breeding system; all 18 tested isolates belonging to the A1 mating type); globose to slightly subglobose, smooth-walled, mostly sessile with short to medium-sized, often thin stalks and rounded base (87.4 %; Fig. 20O–S, U, V), less frequently with short tapering base (12.6 %; Fig. 20T); sometimes appearing comma-shaped due to an angle between the oogonial stalk and the bearing hypha (Fig. 20V); oogonial diam 25.6 ± 2.1 µm (overall range 20.0–30.9 µm; range of means in different mating combinations 23.2–26.3 µm); nearly plerotic to plerotic (Fig. 20O–V). *Oospores* globose, usually with one large lipid globule (Fig. 20O–R, T–V) or infrequently with multiple smaller globules (4.4 %; Fig. 20S); diam 22.9 ± 1.9 µm (overall range 18.1–29.1 µm; range of means in different mating combinations 20.6–23.8 µm); wall thickness 1.19 ± 0.21 µm (overall range 0.72–2.13 µm), oospore wall index 0.28 ± 0.04; high abortion rate of 67 % (42–96 %) after 4 wk. *Antheridia* exclusively amphigynous, cylindrical or subglobose, predominantly unicellular (95.5; Fig. 20P–T), rarely bicellular and slightly curved (4.5 %; Fig. 20O, U, V); dimensions 13.3 ± 2.0 × 12.5 ± 1.5 µm.

Culture characteristics: Colonies variable between isolates; on V8A submerged to appressed with limited aerial mycelium and radiate or stellate patterns; on CA either submerged to appressed with limited aerial mycelium and radiate to striate pattern, or appressed with limited woolly mycelium and faint radiate pattern or uniform; on PDA either appressed, dense felty and uniform with stoloniferous margin or woolly-cottony and petaloid (Figs 10, 11).

Cardinal temperatures and growth rates: On V8A optimum at 25 °C (4 isolates), 27.5 °C (4 isolates) or 30 °C (6 isolates) with 8.23 ± 0.95, 8.42 ± 1.17 and 8.33 ± 1.17 mm/d radial growth, respectively; maximum 30–<32.5 °C (2 isolates) or 32.5–<35 °C (12 isolates); minimum <10 °C (Fig. 12), lethal temperature 32.5 °C (1 isolate), 35 °C (10 isolates) or >35 °C (3 isolates). At 20 °C on V8A, CA and PDA 6.68 ± 0.85 mm/d, 4.98 ± 0.62 mm/d and 4.68 ± 0.78 mm/d, respectively.

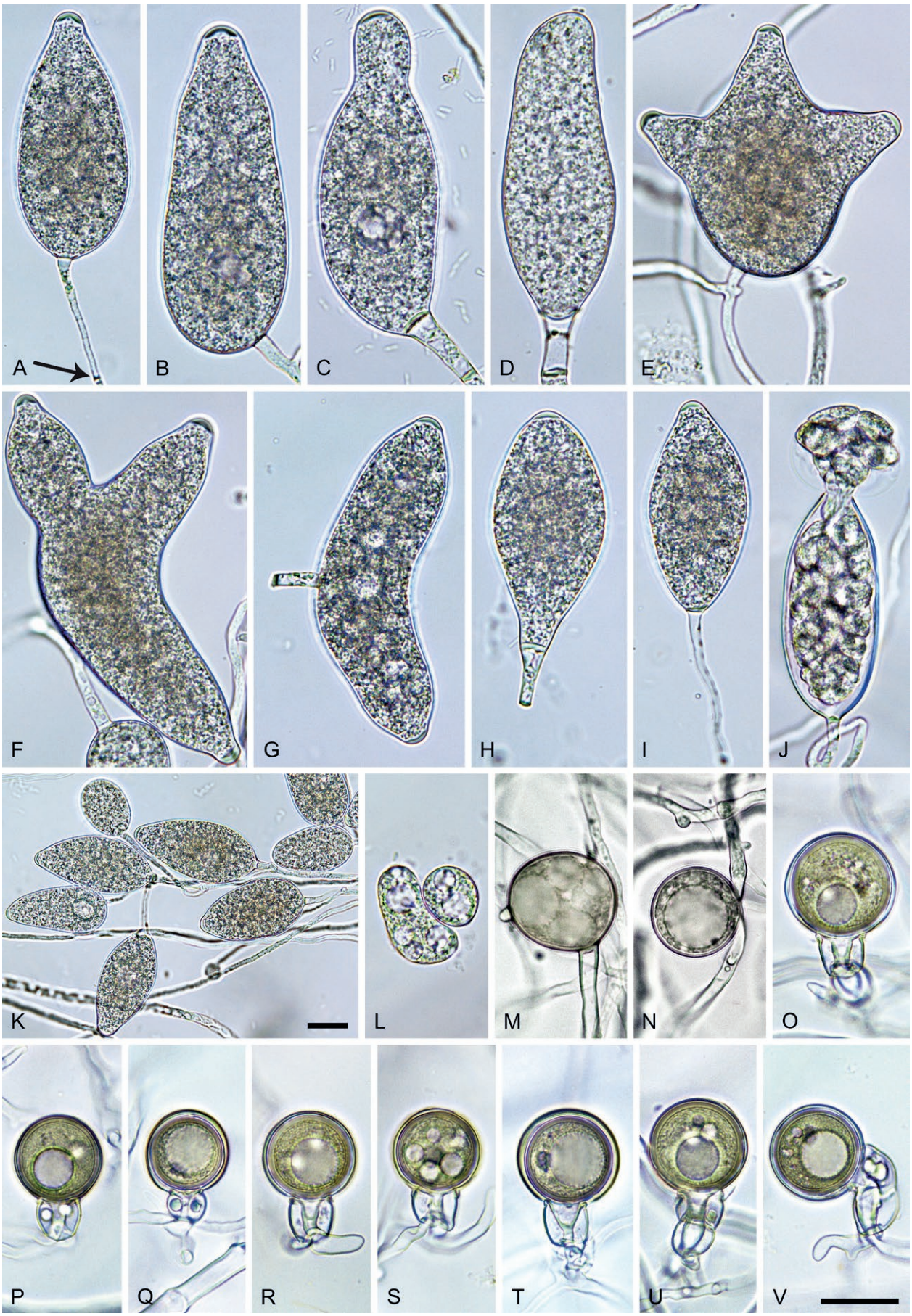

Fig. 20. *Phytophthora* ×*taiwanensis*. **A–K.** Sporangia formed on V8-agar in soil extract. **A–D, H–K.** Elongated ovoid, obpyriform, pyriform, limoniform or ellipsoid sporangia. **E–G.** Distorted bi- or trilobed sporangia. **A–C, E–I, L.** Semipapillate to papillate apices. **D.** Nonpapillate apex. **A, C, D, G–J.** Medium-length to long pedicels (arrow in A). **B, E, F.** External proliferation. G, H. Caducous sporangia. **J.** Zoospore release. **K.** Dense sporangial sympodium. **L.** Multinucleate zoospores. **M, N.** Chlamydospores formed in carrot agar (fgCA). **O–V.** Oogonia with near-plerotic to plerotic oospores and amphigynous antheridia, formed in fgCA in polycarbonate membrane mating tests. **O, U, V.** Bicellular antheridia. **P–R.** Unicellular antheridia. Images: A, B, E–G, I–K, G, M–O, Q, T–V. Ex-type CBS 149506; C, D. TW158; H, P, R, S. TW133; L. TW172. Scale bars = 20 µm; V applies to A–J, L–V.

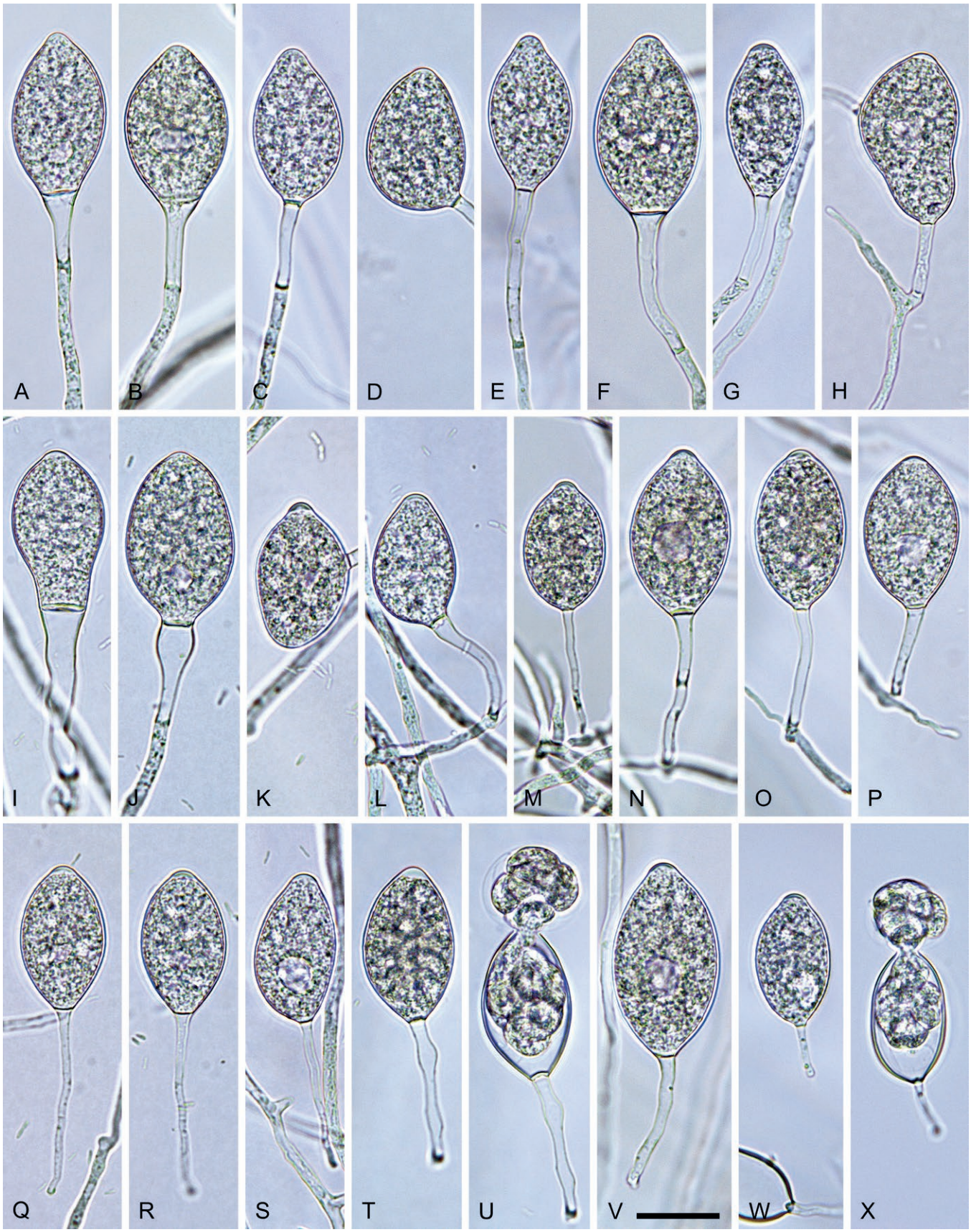

Fig. 21. *Phytophthora botryosa*. **A–F.** Ovoid, limoniform, pyriform and ellipsoid sporangia with medium-length to long pedicels formed on V8-agar in soil extract. **A–F, I, J, N, P, S, V.** Nonpapillate sporangia. **G, H, L, M, O, Q, R, W.** Semipapillate sporangia. **K, T.** Papillate sporangia. **H.** Intercalary sporangium with external proliferation. **P–X.** Caducous sporangia. **U.** Zoospore release. Images: A, D, H–L, P–U. Ex-type CBS 581.69; B, C, E–G, M–O, V–X. MYA-4059. Scale bar = 20 µm; V applies to A–X.

Additional materials examined: **Taiwan**, Hualien County, isolated from rhizosphere soil of *S. suberifolia* in a subtropical, evergreen lowland monsoon forest, Aug. 2013, *T. Jung, T.-T. Chang & M. Horta Jung* (TW158, TW162, TW163); isolated from rhizosphere soil of *Cinnamomum camphora* in a subtropical, evergreen lowland monsoon forest, Aug. 2013, *T. Jung, T.-T. Chang & M. Horta Jung* (TW165, TW167, TW168, TW172, TW173, TW379); isolated from mixed rhizosphere soil of a subtropical, evergreen lowland monsoon forest, Aug. 2013, *T. Jung, M. Horta Jung & T.-T. Chang* (TW248, TW249); isolated from a baiting leaf floating in Xiao-Qingshui Creek running through a subtropical, evergreen lowland monsoon forest, Aug. 2013, *T. Jung, M. Horta Jung & T.-T. Chang* (TW133, TW135); Taitung County, isolated from rhizosphere soil of *Trema orientalis* in a subtropical, evergreen lowland monsoon forest, Aug. 2013, *T. Jung, M. Horta Jung & T.-T. Chang* (TW242, TW243, TW244).

Notes on Clade 2a taxa: Across the nuclear (LSU, ITS, *βtub*, *hsp90*, *tigA*, *rpl10*, *tef-1α*, *enl*, *ras-ypt1*) 8 754-character alignment and the mitochondrial (*cox1*, *cox2*, *nadh1* and *rps10*) 3 174-character alignment pairwise sequence differences between the 11 known and six newly described *Phytophthora* species and five informally designated taxa in Clade 2a were 0.1–3.9 % and 0–6.3 %, respectively. In addition, the six new and the seven known Clade 2a species examined (*P. botryosa*, *P. citrophthora*, *P. colocasiae*, *P. meadii*, *P. mekongensis*, *P. occultans* and *P.* ×*vanyenensis*) developed distinctive colony morphologies on V8A, CA and PDA at 20 °C (Figs 8–11). In addition, the five new species can be separated from each other and from other Clade 2a species by a combination of morphological (Figs 13–22) and physiological characters (Fig. 12) of which the most discriminating are highlighted in bold in Tables S4–S6.

The ex-type isolate CBS 581.69 and key isolate MYA-4059 of *P. botryosa* produced larger sporangia than originally reported by Chee (1969) (39.1 × 22.6 *vs.* 28 × 15 µm). Furthermore, they were only partly caducous and had variable apices (12 % papillate, 42 % semipapillate, 36 % nonpapillate) while those in the original description were fully caducous and exclusively papillate (Table S4; Fig. 21). These discrepancies most likely reflect differences between sporangia formed in water (this study) and sporangia produced on solid agar (Chee 1969).

Phytophthora meadii key isolates MYA-4043 and MYA-4042 used in the present study originate from India like the isolates McRae (1918) based the original description on and like the ex-neotype isolate CBS 148127 designated by Abad *et al.* (2023a). The sporangia formed by isolates MYA-4043 and MYA-4042 (44.5 × 30.3 µm; Table S5) were on average slightly larger than those reported by Oudemans & Coffey (1991) (38.5 × 24.7 µm; Table S4) for seven isolates and considerably larger than in the original description by McRae (1918) (20–44 × 16–29 µm) and those reported by Abad *et al.* (2023a) (17–44 × 15–29 µm) for the ex-neotype isolate CBS 148927. However, sporangial l/b ratios and pedicel lengths were comparable between this study and Oudemans & Coffey (1991). The breeding system of *P. meadii* is still a conundrum. While McRae (1918) described *P. meadii* as 'homothallic' later studies found evidence of heterothallism (Peries & Dantanarayana 1965; Rajalakshmy *et al.* 1985, Sansome *et al.* 1990, Abad *et al.* 2023a). In a mating study, 45 of 50 Indian rubber isolates were described as 'heterothallic' (A1/A2) with 31 and 14 belonging to the A1 and A2 mating type, respectively; two isolates were described as 'homothallic' (possibly weakly self-fertile A2s as described in Sansome *et al.* 1990), and three isolates were sterile (Rajalakshmy *et al.* 1985). Sizes and morphological features of oogonia produced in a mating test between isolates A1 and A2 isolates MYA-4042 and MYA-4043 were comparable to those reported by Rajalakshmy *et al.* (1985) and Erwin & Ribeiro (1996), and their optimum and maximum temperatures for growth were in accordance with Erwin & Ribeiro (1996) (Tables S4, S5). Sansome *et al.* (1990) described both diploidy and polyploidy in A1 and A2 isolates of *P. meadii* from Sri Lanka, the former associated with meiotic instability, sterility and smaller oogonia.

Despite being one of the oldest known and most widespread *Phytophthora* species *P. citrophthora* is still poorly characterised, probably reflecting the erroneous inclusion of other species with diverging characters during the pre-molecular era. Using isozyme patterns Mchau & Coffey (1994) provided a redescription of the species based on a worldwide collection of 77 isolates. However, their isozyme analysis demonstrated that Indonesian and Brazilian isolates from cocoa (*Theobroma cacao*) trees constituted distinct electrophoretic subgroups CTR2 and CTR3 which were phylogenetically separate from the largest electrophoretic subgroup CTR1 from diverse hosts and geographical locations. Recently, the Brazilian cocoa isolates have been described as *P. theobromicola* residing within Clade 2b (Decloquement *et al.* 2021). As the morphometric and physiological data provided by Mchau & Coffey (1994) were not assigned to their subgroups they cannot be used for species comparisons. The morphological characters, the morphometric data and the cardinal temperatures for growth of the 13 *P. citrophthora* isolates in this study were largely in agreement with the data given by Abad *et al.* (2023a) for the ex-epitype isolate CBS 950.87 except for the production of chlamydospores by the ex-epitype. In the present study "*P. citrophthora*-like" isolates from a wide range of hosts, ecosystems and locations formed three separate phylogenetic groups. The group containing the ex-epitype isolate of *P. citrophthora* from *Citrus* in California, *Citrus* isolates from Portugal and Spain and a range of isolates from natural ecosystems in warm-temperate and subtropical regions of Japan and Taiwan is considered to be the original *P. citrophthora*. Another group, comprising isolates from diverse hosts in nurseries and gardens in Europe and Morocco and streams in Portugal, Serbia and Louisiana, USA, is described here as *P. pseudocitrophthora*. The third group, a hybrid between *P. citrophthora* as the maternal parent and another Clade 2a species as the paternal parent, was only obtained from the Rio Séqua in the South of Portugal and is described here as *P.* ×*lusitanica*. The sporangia of the three species are similar, with a low degree of caducity in most isolates (Tables S4–S6; Figs 13, 15, 19). However, the proportions of papillate, semipapillate and nonpapillate sporangia differ considerably between *P. citrophthora* (36 %, 61.1 % and 2.9 %, respectively) and *P. pseudocitrophthora* (75.9 %, 14.6 % and 9.5 %, respectively) while the sporangia of *P.* ×*lusitanica* are mostly a transition between semipapillate and papillate (Figs 12, 14, 18). Furthermore, in *P. citrophthora* sporangia are on average slightly longer (66.0 µm) than in *P. pseudocitrophthora* (61.6 µm) and much longer than in *P.* ×*lusitanica* (53.9 µm) with a higher l/b ratio (1.84 *vs.* 1.73 *vs.* 1.67), form frequently larger sympodia (2–8 *vs.* 2–4 *vs.* 2–4 sporangia) and have a higher frequency of pedicels (86 % *vs.* 37 % *vs.* 51.3 %). In addition, *P.* ×*lusitanica* has higher proportions of sporangia with two, three or four apices (22.6 %) than *P citrophthora* (9 %) and *P. pseudocitrophthora* (7.4 %). *Phytophthora citrophthora*, *P. pseudocitrophthora* and *P.* ×*lusitanica* are self-sterile, failing to produce oogonia in mating tests with A1 and A2 tester strains of *P. cinnamomi* and *P. meadii*. However, two of the 13 tested isolates of *P. citrophthora* and all four tested isolates of *P.* ×*lusitanica* are silent A1s and one of the nine tested isolates of *P. pseudocitrophthora* is a silent A2 mating type. The large subgroup CTR1 in Mchau & Coffey (1994) was also self-sterile, with 15 of

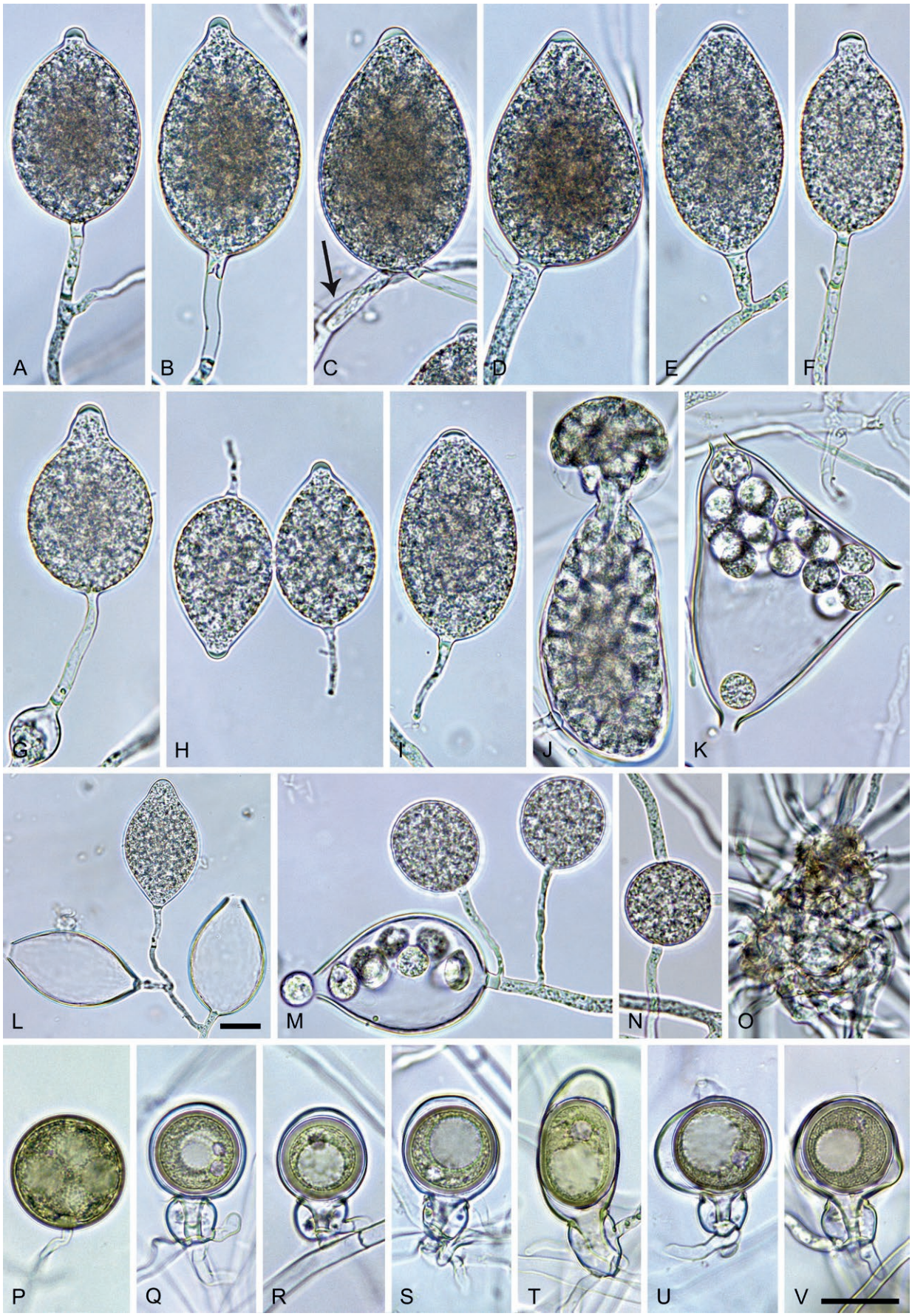

Fig. 22. *Phytophthora ×vanyenensis*. **A–M.** Sporangia formed on V8-agar (V8A) in soil extract. **A–I.** Ovoid, ellipsoid or obpyriform sporangia with papillate or semipapillate apices. **A–C, F–I.** Medium length to long pedicels. **A, C, D, F.** External proliferation (arrow in C). **C.** Intercalary sporangium. **H, I.** Caducous sporangia. **J, M.** Zoospore release. **K.** Distorted sporangium with three apices and zoospore cysts. **L.** Sympodium with a nonpapillate sporangium. **M.** Beginning sporangial sympodium. **N.** Hyphal swelling in water. **O.** Hyphal aggregation in V8A. **P.** Chlamydospore in carrot agar (fgCA). **Q–V.** Oogonia with oospores and amphigynous unicellular antheridia formed in fgCA in mating tests. **T–V.** Elongated or excentric oogonia. Images: A, B, K. SU1615; C, O. SU631a; D, E, I, L, M. SL318; F, G. JV102; H, P. JV042; J. SU1055; N. SU1099; Q–S, U. SL075 × SL478; T. JV004 × CBS 235.30; V. SL075 × SL327. Scale bars = 20 µm; V applies A–K, M–V.

56 isolates being silent A2s. *Phytophthora peudocitrophthora* has a slightly lower optimum temperature of growth than *P. citrophthora* and *P.* ×*lusitanica* (25 *vs.* 27.5 *vs.*27.5 °C) and shows on average slightly faster growth between 10 and 30 °C than *P. citrophthora* whereas *P.* ×*lusitanica* grows faster than the other two species between 25 and 30 °C (Tables S4–S6; Fig. 12). Like subgroup CTR1 of Mchau & Coffey (1994), none of the 28 isolates of *P. citrophthora*, *P. pseudocitrophthora* and *P.* ×*lusitanica* examined in this study produced chlamydospores.

Crous *et al.* (2017) reported that no gametangia were produced in mating tests between *P. mekongensis* and A1 and A2 tester strains of *P. nicotianae* and *P. citrophthora* and concluded that *P. mekongensis* has a sterile breeding system. However, in this study, the ex-type isolate CBS 135136 and isolate PF6f2 of *P. mekongensis* both produced abundant oogonia when mated with A1 isolate MYA-4042 of *P. meadii* demonstrating it has an A1/A2 breeding system and that they are all of A2 mating type. Since the abortion rate of these selfed oogonia was 100 % and no A1 isolates of *P. mekongensis* are currently known it remains unclear whether the A1/A2 system is fully functional.

Phytophthora pseudoccultans can be discriminated from *P. occultans* by having on average considerably larger sporangia (57.9 × 36.0 *vs.* 47 × 30 µm) which are exclusively papillate, the production of hyphal swellings, a lower maximum temperature for growth (27.5–<30 *vs.* 30–<32.5 °C) and by showing slower growth between 20 and 27.5 °C (Man In't Veld *et al.* 2015; Table S5; Fig. 12). *Phytophthora terminalis* differs from *P. pseudoccultans* by its considerably smaller sporangia (41.7 × 30.4 µm) and sporangial l/b ratio (1.37 *vs.* 1.62) (Man In't Veld *et al.* 2015; Table S5).

Phytophthora vietnamensis can be distinguished from all other self-sterile species in Clade 2a by having a fully sterile breeding system and a low optimum temperature for growth of 20 °C (Tables S4–S6, Fig. 12). *Phytophthora* ×*australasiatica* can be easily discriminated from other self-sterile species in Clade 2a by having considerably larger sporangia than *P. botryosa*, *P. insulinativitatica*, *P. meadii*, *P. mekongensis* and *P. multibullata* and larger oogonia than *P. multibullata* (Crous *et al.* 2017, Dang *et al.* 2021; Tables S4–S6). Both *P.* ×*australasiatica* and *P.* ×*taiwanensis* differ from *P. citrophthora*, *P. pseudocitrophthora*, *P. vietnamensis* and *P.* ×*lusitanica* by having functional A1/A2 breeding systems (Tables S4–S6; Figs 13, 15, 17–20); from the exclusively semipapillate and host specific *P. colocasiae* by producing on average 30 % and 41 % papillate sporangia, respectively, and by their different and wider host ranges (Erwin & Ribeiro 1996; Tables S4, S6); from *P.* ×*vanyenensis* by having on average higher sporangial l/b ratios and larger chlamydospores, and the high proportion of excentric and elongated oogonia in *P.* ×*vanyenensis* (Table S6; Figs 18, 20, 22); and from *P. multibullata* by their considerably larger sporangia and faster growth (Dang *et al.* 2021; Tables S5, S6). *Phytophthora* ×*australasiatica* can be distinguished from *P.* ×*taiwanensis* by its higher proportion of ovoid sporangia (62 *vs.* 32 %), its lower sporangial l/b ratio (1.7 *vs.* 1.95) and by not producing bicellular antheridia (Table S6; Figs 18, 20). The morphological data and cardinal temperatures of the 35 isolates of *P.* ×*vanyenensis* in this study largely concurred with the original description (Dang *et al.* 2021). However, in the present study, *P.* ×*vanyenensis* produced chlamydospores (which were particularly abundant in mating tests) and exhibited a considerably faster growth rate (Table S6).

Several new Clade 2a species described here were previously known under informal names, *i.e.*, *P. pseudoccultans* as *P.* taxon occultans-like (Jung *et al.* 2017b), *P. vietnamensis* as *P.* taxon meadii-like 1 (Jung *et al.* 2020), *P.* ×*australasiatica* as *P.* taxon botryosa-like 2 and *P.* taxon meadii-like 2 (Jung *et al.* 2020) and *P.* ×citrophthora-related2 (Van Poucke *et al.* 2021), *P.* ×*lusitanica* as *P.* ×citrophthora2 (Van Poucke *et al.* 2021), and *P.* ×*taiwanensis* as *P.* taxon ×botryosa-like and *P.* taxon ×meadii-like (Jung *et al.* 2017b) and *P.* ×citrophthora-related1 (Van Poucke *et al.* 2021).

Clade 2b

For all Clade 2b species included in this study colony morphologies on CA, PDA and V8A and temperature-growth relations on V8A are presented in Figs 23–26. Morphological and physiological characters and morphometric data of the nine known and nine newly described species and three informally designated taxa in Clade 2b are given in the comprehensive Tables S7–S9. The known species *P. tropicalis* was included in the morphological and temperature-growth studies and a taxonomic description is given below to enable detailed comparisons with new closely related species from Clade 2b.

Phytophthora calidophila T. Jung, Y. Balci, L. Garcia & B. Mendieta-Araica, ***sp. nov.*** MycoBank MB 847289. Fig. 27.

Etymology: The name refers to the high maximum temperature for growth and the fast growth at 30 °C (*calidus* Latin = warm, hot; *philos* Greek = friend, loving).

Typus: **Nicaragua**, Matagalpa, Selva Negra, isolated from a necrotic lesion on a naturally fallen leaf of a non-identified tree species collected from the ground in a lower montane tropical forest, Nov. 2017, *Y. Balci, L. Garcia & B. Mendieta-Araica* (**holotype** CBS H-25101, dried culture on V8A, ex-holotype living culture CBS 149479 = NI112).

Morphological structures on V8A: *Sporangia* abundantly produced in non-sterile soil extract; borne terminally in lax sympodia of 2–4 sporangia or on unbranched sporangiophores (99.2 %; Fig. 27A–I) or rarely intercalary (0.8 %; Fig. 27K); ovoid, broad-ovoid or elongated-ovoid (38.0 %; Fig. 27A, B, H), ellipsoid to elongated-ellipsoid (16.6 %; Fig. 27C–E, K, L), pyriform or elongated-pyriform (15.4 %; Fig. 27M), limoniform to elongated-limoniform (14.2 %; Fig. 27F, N), obovoid (10.8 %; Fig. 27G) or less frequently obpyriform to elongated-obpyriform (2.6 %; Fig. 27I) or distorted, often with two apices (2.4 %; Fig. 27J); apices papillate (37 %; Fig. 27H, J, N), semipapillate (38 %; Fig. 27A, F, I, L, M) or nonpapillate and often pointed (25 %; Fig. 27B–E, G, K); lateral attachment of sporangiophores (5.6 %; Fig. 27D) or a swelling on the sporangiophore close to the sporangial base (2.4 %; Fig. 27B) infrequently observed; predominantly caducous (82 %; Fig. 27L–N) with pedicel length ranging from 8.0 to 52.4 µm (av. 24.3 ± 11.6 µm) (Fig. 27A, C–I, L–N); sporangial proliferation exclusively external (Fig. 27A, F, H); sporangial dimensions averaging 49.2 ± 5.6 × 27.5 ± 2.8 µm (overall range 32.0–66.9 × 20.7–33.8 µm; range of isolate means 47.5–51.0 × 26.3–28.5 µm) with a length/breadth ratio of 1.79 ± 0.18 (overall range 1.31–2.55; sporangial germination indirectly with zoospores discharged through an exit pore 2.4–6.3 µm wide (av. 4.2 ± 0.9 µm). *Zoospores* limoniform to reniform whilst motile becoming spherical (av. diam = 9.3 ± 1.3 µm) on encystment. *Hyphal swellings* subglobose, limoniform or irregular, infrequently formed in water on sporangiophores (Fig. 27B) or in solid agar on hyphae (Fig. 27Z), 11.6 ± 2.8 µm. *Chlamydospores* not observed. *Oogonia* not observed in single cultures, but abundantly produced by all eight tested isolates in polycarbonate mating tests with the A2 mating type isolate PA172 of *P. multiplex* (A1/A2 or 'heterothallic' breeding system; all tested isolates mating type A1); mostly sessile or terminal on short to medium-length, sometimes curved lateral

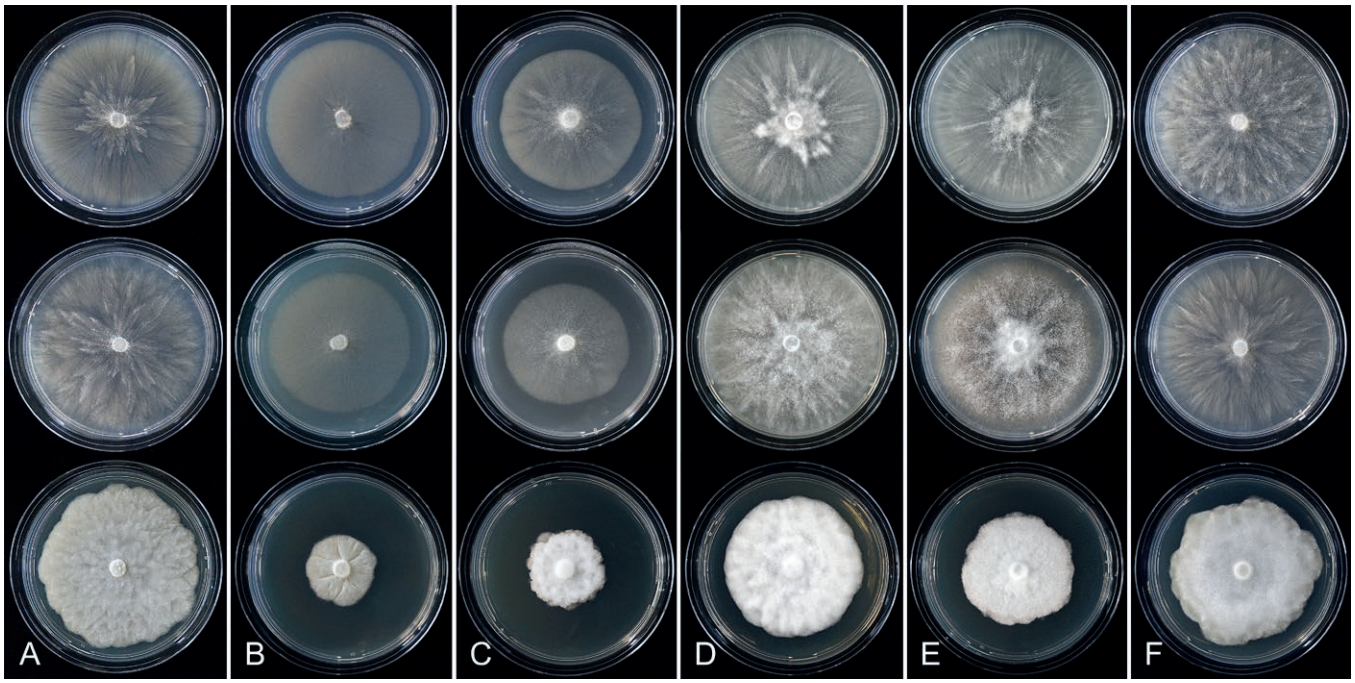

Fig. 23. Colony morphology of *Phytophthora* species from subclade 2b after 7 d growth at 20 ºC on V8-agar, carrot juice agar and potato-dextrose agar (from top to bottom). **A.** *Phytophthora calidophila* (ex-type CBS 149479). **B.** *Phytophthora distorta* (ex-type CBS 149476). **C.** *Phytophthora frigidophila* (ex-type CBS 149486). **D.** *Phytophthora mengei* (TJ1109). **E.** *Phytophthora montana* (ex-type CBS 149492). **F.** *Phytophthora pyriformis* (PA214).

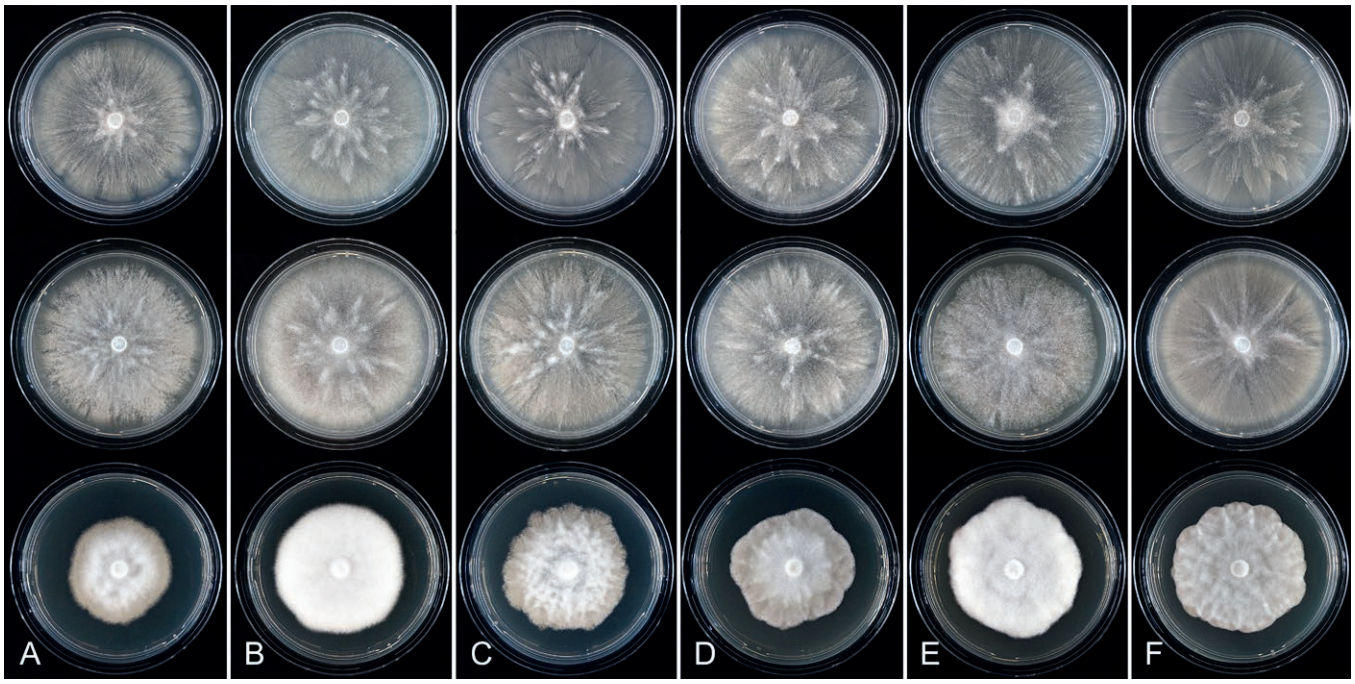

Fig. 24. Colony morphology of *Phytophthora* species from subclade 2b after 7 d growth at 20 ºC on V8-agar, carrot juice agar and potato-dextrose agar (from top to bottom). **A–C.** *Phytophthora obovoidea* (A. ex-type CBS 149633; B. PA208; C. VN830). **D–F.** *Phytophthora tropicalis* (D. PA112; E. SU663a; F. TW343).

hyphae, smooth-walled, globose to slightly subglobose (Fig. 27O–Y), sometimes slightly excentric (4 %; Fig. 27Y), with a short or medium-length tapering (57.4 %; Fig. 27O, R–T, W–Y) or non-tapering stalk (42.6 %; Fig. 27P, Q, U, V) which is sometimes inclined (Fig. 27U, V); oogonial diam 25.2 ± 2.8 µm (overall range 18.6–33.2 µm; range of isolate means 23.6–27.6 µm); nearly plerotic to plerotic (Fig. 27O–Y). *Oospores* globose with one or, less frequently, several medium-large lipid globules (Fig. 27O–Y); mean diam 22.6 ± 2.8 µm (overall range 10.5–30.9 µm; range of isolate means 21.1–24.8 µm); wall thickness 1.28 ± 0.16 µm (overall range 0.87–1.91 µm), oospore wall index 0.3 ± 0.04; abortion 32–56 % (av. 41 %) after 4 wk. *Antheridia* exclusively amphigynous and cylindrical or subglobose, sometimes asymmetric, unicellular (Fig. 27O–Y); dimensions 15.3 ± 2.8 × 13.9 ± 1.5 µm. *Hyphal aggregations* observed in all isolates (Fig. 27A, B).

Culture characteristics: Colonies on V8A and CA submerged to appressed with limited aerial mycelium and radiate patterns; dense-felty and shallow cottony on PDA with a rosaceous pattern (Fig. 23).

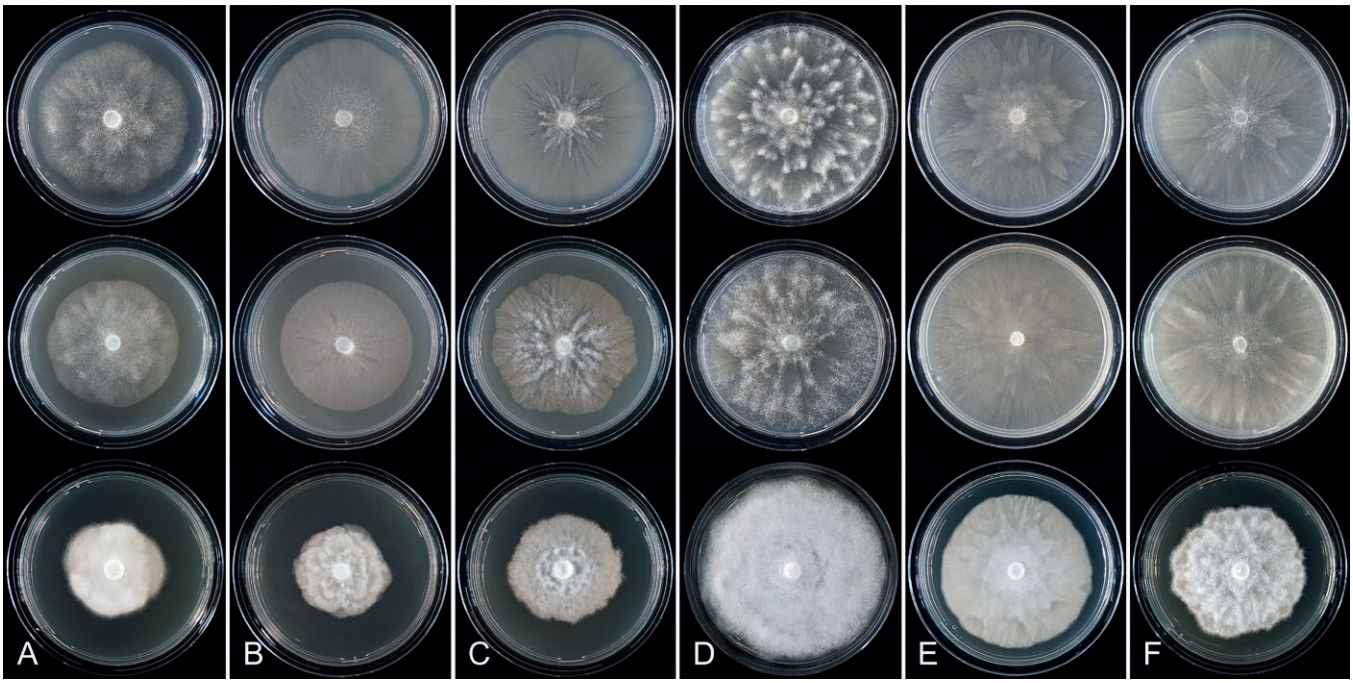

Fig. 25. Colony morphology of *Phytophthora* species from subclade 2b after 7 d growth at 20 ºC on V8-agar, carrot juice agar and potato-dextrose agar (from top to bottom). **A.** *Phytophthora siskiyouensis* (WW10). **B.** *Phytophthora valdiviana* (ex-type CBS 149504). **C.** *Phytophthora variepedicellata* (ex-type CBS 149505). **D.** *Phytophthora multiplex* (isolate PA171). **E, F.** *Phytophthora* taxon pseudocapsici (E. CH 26G2; F. SU1649).

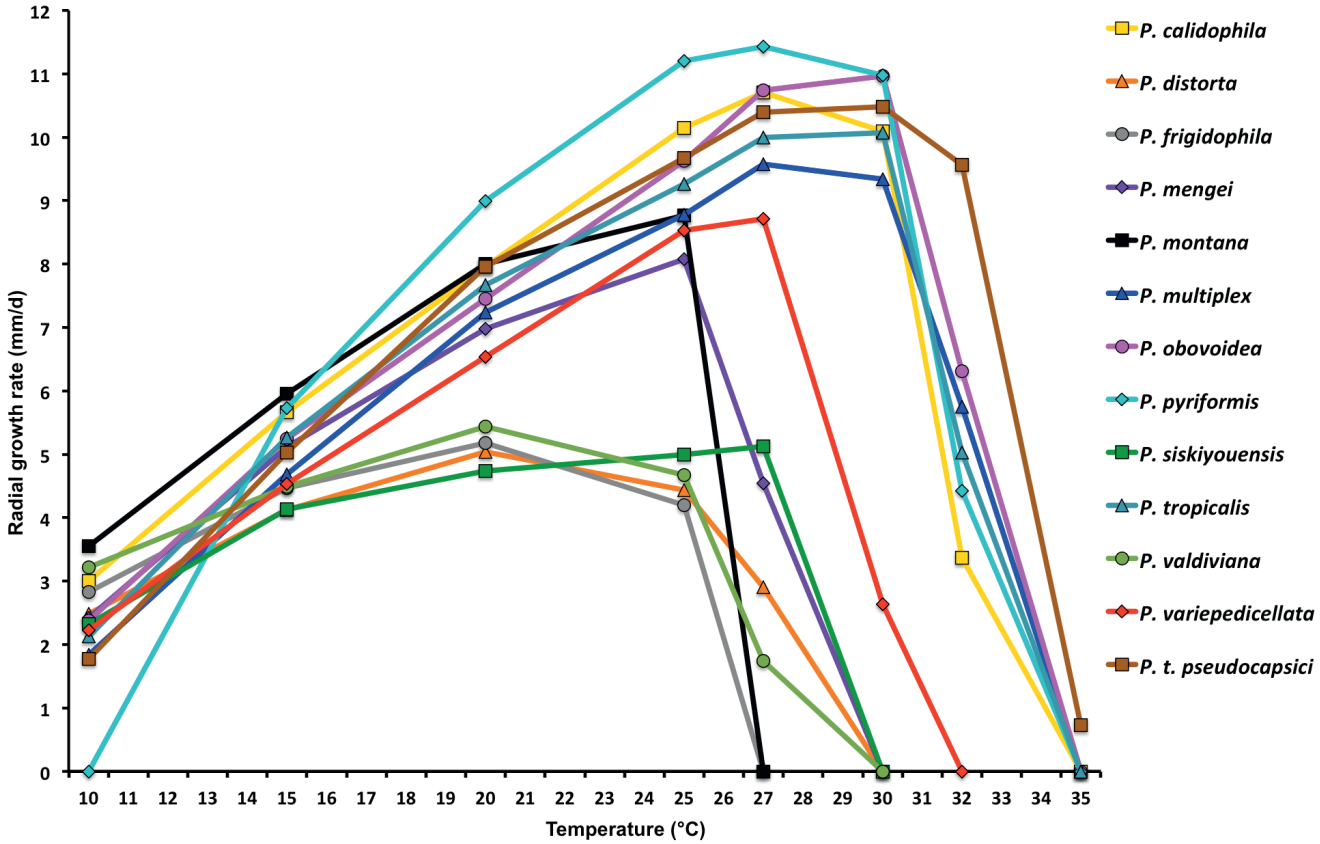

Fig. 26. Mean radial growth rates of five known and nine new *Phytophthora* species from subclade 2b on V8-agar at different temperatures: *P. calidophila* (8 isolates); *P. distorta* (4 isolates); *P. frigidophila* (4 isolates); *P. mengei* (3 isolates); *P. montana* (5 isolates); *P. multiplex* (11 isolates); *P. obovoidea* (22 isolates); *P. pyriformis* (6 isolates); *P. siskiyouensis* (1 isolate); *P. tropicalis* (12 isolates); *P. valdiviana* (5 isolates); *P. variepedicellata* (5 isolates); *P.* taxon pseudocapsici (6 isolates).

Cardinal temperatures and growth rates: On V8A optimum 27.5 °C with 10.7 ± 0.3 mm/d radial growth, maximum 32.5–<35 °C, minimum <10 °C (Fig. 26), lethal temperature 35 °C. At 20 °C on V8A, CA and PDA 7.96 ± 0.47 mm/d, 5.73 ± 0.14 mm/d and 5.33 ± 0.15 mm/d, respectively.

Additional materials examined: **Nicaragua**, Matagalpa, Selva Negra, isolated from necrotic lesions on naturally fallen leaves of a non-identified tree species collected from the ground in a lower montane tropical forest, Nov. 2017, *Y. Balci, L. Garcia & B. Mendieta-Araica* (NI11, NI198, *NI199, NI200, NI201, NI202, NI203).*

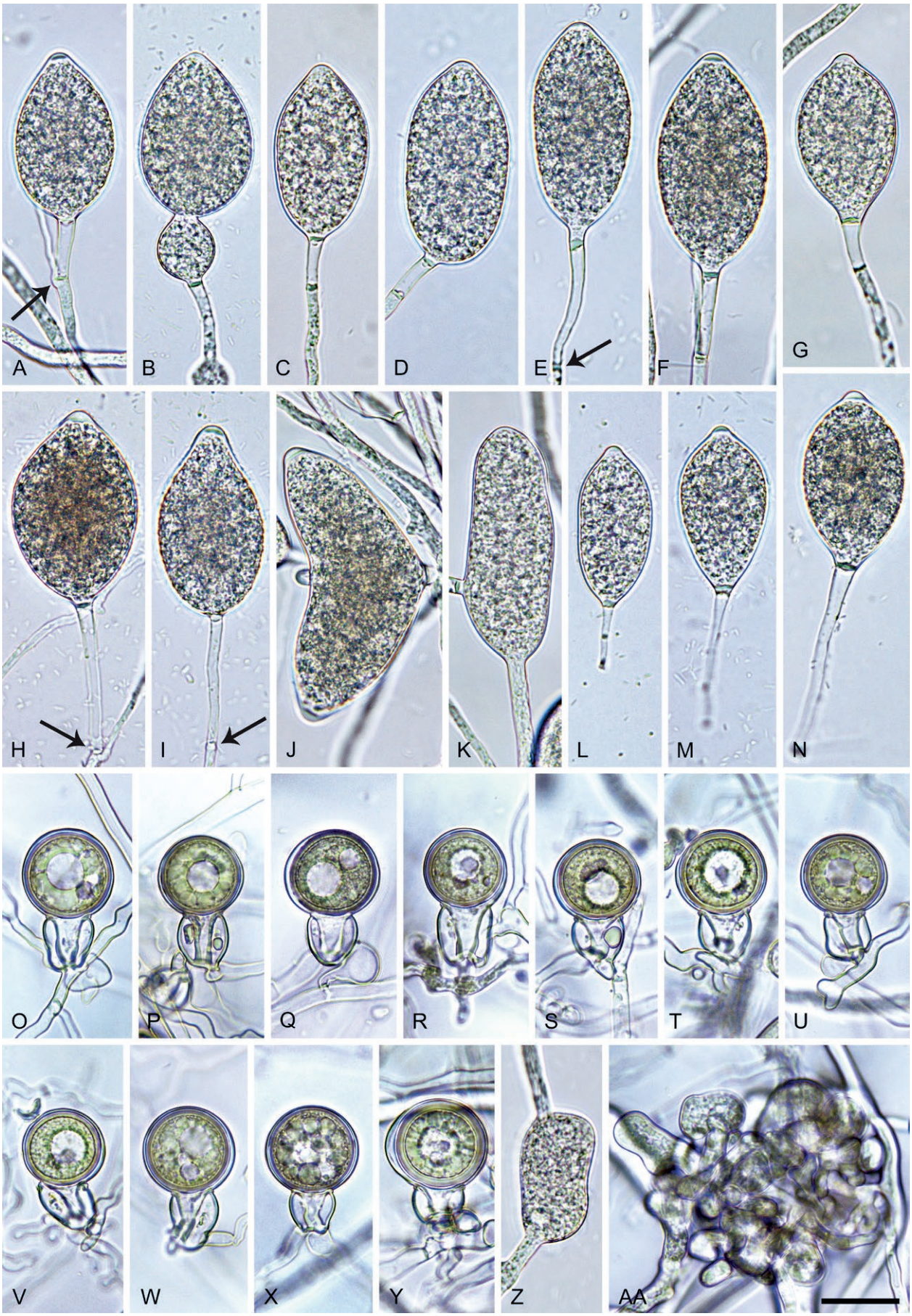

Fig. 27. *Phytophthora calidophila*. **A–N.** Sporangia formed on V8-agar (V8A) in soil extract. **A–I, K–N.** Ovoid, ellipsoid, obovoid, obpyriform, pyriform and limoniform sporangia. **A–I, L–N.** Medium-length to long pedicels (arrows in E, H, I pointing at basal pedicel septum). **A–G, I–M.** Nonpapillate to semipapillate apices. **H, M.** Papillate apices. **A, F, H.** External proliferation (arrow in A). **J.** Bipapillate sporangium. **K.** Intercalary sporangium. **L–N**. Caducous sporangia. **O–Y.** Oogonia with near-plerotic to plerotic oospores and amphigynous unicellular antheridia, formed in carrot agar in polycarbonate membrane mating tests. **Z.** Hyphal swelling in water. **AA.** Hyphal aggregation in V8A. Images: A–G, I, K, M, O, R–T, X, Y, AA. Ex-type CBS 149479; H, J, L, N, P, Q, U–W, Z. NI111. Scale bar = 20 µm; AA applies to A–AA.

Phytophthora distorta T. Jung, A. Durán, E. Sanfuentes von Stowasser & M. Horta Jung, ***sp. nov.*** MycoBank MB 847290. Fig. 28.

Etymology: The name refers to the distorted asymmetric shapes of many sporangia.

Typus: **Chile**, Valdivian region, isolated from a baiting leaf floating in the Valdivia River, Nov. 2014, *T. Jung, A. Durán & E. Sanfuentes von Stowasser* (**holotype** CBS H-25098, dried culture on V8A, ex-holotype living culture CBS 149476 = CL181).

Morphological structures on V8A: *Sporangia* occasionally formed in solid agar but abundantly produced in non-sterile soil extract; borne terminally (61.9 %) in dense or lax sympodia of 2–5 sporangia or on long or short unbranched sporangiophores, or intercalary (38.1 %; Fig. 28A, F, H); shapes distorted-asymmetric often with two or three apices (43.9 %; Fig. 28B, C, F–H), ovoid, broad ovoid or elongated ovoid (38.6 %; Fig. 28A, D, I, J), less frequently obpyriform to elongated obpyriform (7.5 %; Fig. 28E), limoniform (4.0 %), ellipsoid (1.5 %), obovoid (1.5 %), pyriform (1 %), turbinate (1 %) or ampulliform (1 %); lateral attachment of the sporangiophore (47 %; Fig. 28B, C, G, I, J) and pedicels (34 %; Fig. 28C, F, J) common; sporangia sometimes too big for the available cytoplasm and hence, not filled completely in the basal part, with a strong plug below the cytoplasm (15.2 %; Fig. 28D, G, H); apices papillate (33.7 %; Fig. 28E, H, J) or more frequently semipapillate (66.3 %; Fig. 28A–D, F, G) with a smooth transition between both forms; sporangial dimensions averaging 57.0 ± 8.0 × 40.1 ± 4.8 µm (overall range 41.1–97.0 × 26.2–51.7 µm; range of isolate means 53.4–61.1 × 37.8–41.2 µm) with a length/breadth ratio of 1.43 ± 0.2 (overall range 1.04–2.39); pedicel length 17.1 ± 15.3 µm (range 1.8–80.1 µm); sporangia formed on solid agar occasionally caducous; in water caducity not observed; sporangial proliferation exclusively external (Fig. 28A–C, F–H); sporangial germination indirectly with zoospores discharged through an exit pore of 4.0–8.9 µm (av. 6.4 ± 1.0 µm) (Fig. 28I). *Zoospores* limoniform to reniform whilst motile, becoming spherical (av. diam = 10.6 ± 1.1 µm) on encystment; cysts germinating mostly directly by producing hyphae or indirectly by releasing a secondary zoospore (diplanetism). *Hyphal swellings* commonly produced on sporangiophores and hyphae, globose to subglobose, pyriform, limoniform or irregular, often catenulate (Fig. 28T). *Chlamydospores* not observed. *Oogonia* abundantly produced in single culture ('homothallic' breeding system), on short, thin and mostly non-tapering stalks (Fig. 28K–S); smooth-walled, globose to subglobose with round base (Fig. 28K–S), sometimes slightly bend to comma-shaped (2 %; Fig. 28Q); av. oogonial diam 29.0 ± 2.5 µm with an overall range of 21.6–34.4 µm and a range of isolate means of 27.4–30.6 µm; predominantly slightly aplerotic to aplerotic (92 %; Fig. 28K–O, R) or infrequently nearly plerotic (8 %; Fig. 28P, Q). *Oospores* globose to subglobose with a large lipid globule, often turning golden-brown during maturation (Fig. 28K–R); av. diam 24.8 ± 1.8 µm with an overall range of 19.1–29.6 µm and a range of isolate means of 23.2–26.1 µm; wall diam 1.89 ± 0.22 µm (overall range 1.49–2.46 µm) and oospore wall index 0.39 ± 0.03; abortion 28–54 % (av. 41.8 %; Fig. 28R, S) after 4 wk. *Antheridia* amphigynous, cylindrical or subglobose, unicellular (Fig. 28K–S), sometimes with finger-like projections (Fig. 28M); occasionally with an additional paragynous antheridium (Fig. 28R); dimensions 16.8 ± 2.2 × 14.0 ± 1.5 µm.

Culture characteristics: Colonies on V8A and CA submerged and faintly striate; on PDA dense-felty with radiating raised lobes separated by trenches (Fig. 23).

Cardinal temperatures and growth rates: On V8A optimum 20.0 °C with 5.04 ± 0.54 mm/d radial growth, maximum 27.5–<30 °C, minimum <10 °C (Fig. 26), lethal temperature 30 °C. On CA and PDA at 20 °C 4.55 ± 0.11 mm/d and 2.48 ± 0.33 mm/d, respectively.

Additional materials examined: **Chile**, Valdivian region, isolated from a baiting leaf floating in the Valdivia River, Nov. 2014, *T. Jung, A. Durán & E. Sanfuentes von Stowasser* (CL294, CL295, CL296).

Phytophthora frigidophila T. Jung, Y. Balci, K. Broders & I. Milenković, ***sp. nov.*** MycoBank MB 847291. Fig. 29.

Etymology: The name refers to the low cardinal temperatures for growth (*frigidus* Latin = cold, cool; *philos* Greek = friend, loving).

Typus: **Panama**, Volcano Baru, isolated from necrotic lesion on a naturally fallen leaf of a non-identified tree species collected from the ground in a tropical cloud forest, Nov. 2019, *K.D. Broders & Y. Balci* (**holotype** CBS H-25108, dried culture on V8A, ex-holotype living culture CBS 149486 = PA213A).

Morphological structures on V8A: *Sporangia* not observed in solid agar but abundantly produced in non-sterile soil extract; borne mostly terminally (95.4 %;) in dense or lax sympodia of 2–4 sporangia (Fig. 29M) or on unbranched sporangiophores or less frequently intercalary (3.2 %; Fig. 29E) or sessile (1.4 %; Fig. 29M); sporangia predominantly papillate (85.8 %; Fig. 29A, B, E, H–M), infrequently semipapillate (10.2 %; Fig. 29C, F, G) or nonpapillate (4 %; Fig. 29D, M), often with a pointed apex; mostly with pedicels (65.2 %; Fig. 29A–D, F–L) averaging 18.3 ± 13.7 µm in length (range 2.5–62.0 µm) and caducous (Fig. 29J–L); predominantly ovoid, broad ovoid or elongated ovoid (61.6 %; Fig. 29A, B, E, G, J–M), less frequently limoniform to elongated-limoniform (14.4 %; Fig. 29D, H, M), obpyriform to elongated-obpyriform (11.6 %; Fig. 29I), pyriform (3.6 %; Fig. 29C), ampulliform (2.8 %), ellipsoid (1.6 %), mouse-shaped (2 %; Fig. 29F), obovoid (1.2 %) or subglobose (1.2 %); bi- or tripapillate sporangia not observed; sporangia sometimes too big for the available cytoplasm and, hence, not filled completely in the basal part, with or without a strong plug below the cytoplasm (11.9 %; Fig. 29G–I); lateral attachment of the sporangiophore (17.6 %; Fig. 29F, G) and a reinforcement of the sporangial base by a laminar basal plug (16.4 %; Fig. 29F) common; sporangial dimensions averaging 55.9 ± 7.8 × 33.5 ± 3.0 µm (overall range 36.6–83.0 × 24.5–42.2 µm; range of isolate means 52.2–58.6 × 32.5–34.3 µm) with a length/breadth ratio of 1.68 ± 0.25 (overall range 1.24–3.07); sporangial proliferation exclusively external (Fig. 29A–D, M); sporangial germination indirectly with zoospores discharged through an exit pore of 4.3–9.4 µm (av. 5.5 ± 0.9 µm). *Zoospores* limoniform to reniform whilst motile, becoming spherical (av. diam = 10.7 ± 0.9 µm) on encystment; cysts germinating mostly directly by producing hyphae or indirectly by releasing a secondary zoospore (diplanetism). *Hyphal swellings* frequently formed on sporangiophores, usually close to the sporangial base, ovoid, subglobose or limoniform (Fig. 29A, M), dimensions 14.3 ± 4.5 µm (range 8.0–23.3 µm). *Chlamydospores* not observed. *Oogonia* produced in single culture ('homothallic' breeding system), predominantly close to the edge of the Petri dish; mostly sessile or terminal on short to medium-length, sometimes curved lateral hyphae, smooth-walled, globose to subglobose (85.5 %; Fig. 29N–

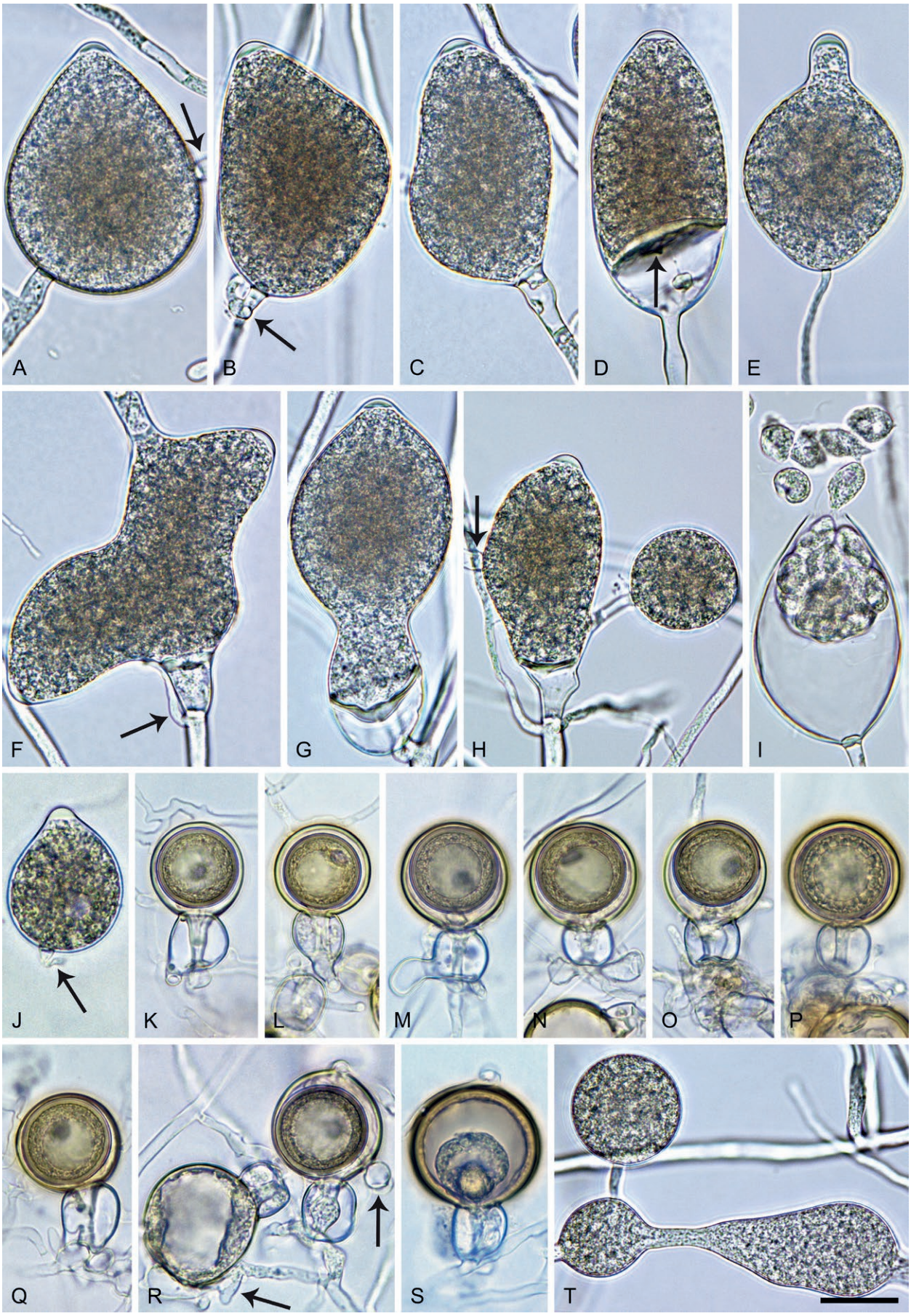

Fig. 28. *Phytophthora distorta*. **A–J.** Sporangia formed on V8-agar (V8A) in soil extract. **A–I, J.** Semipapillate to papillate sporangia. **A, D, E, G, I, J.** Ovoid, obpyriform and ampulliform sporangia. **B, C, F, H.** Distorted sporangia. **A–C, F, H.** External proliferation (arrows in B, F). **A, F, H.** Intercalary (arrows in A, H). **C, F, J.** Medium-length pedicels (arrow in J). **D, G.** Cytoplasm partially filling the sporangia. **I.** Zoospore release. **J.** Caducous sporangium. **K–S.** Oogonia with near-plerotic or aplerotic oospores and amphigynous antheridia, formed in solid V8A. **R.** Additional paragynous antheridia (arrows); left oogonium aborted. **S.** Aborted oogonium. **T.** Catenulate hyphal swellings in water. Images: A, C–F, H, J–T. Ex-type CBS 149476; B, G. CL296; I. CL295. Scale bar = 20 µm; T applies to A–T.

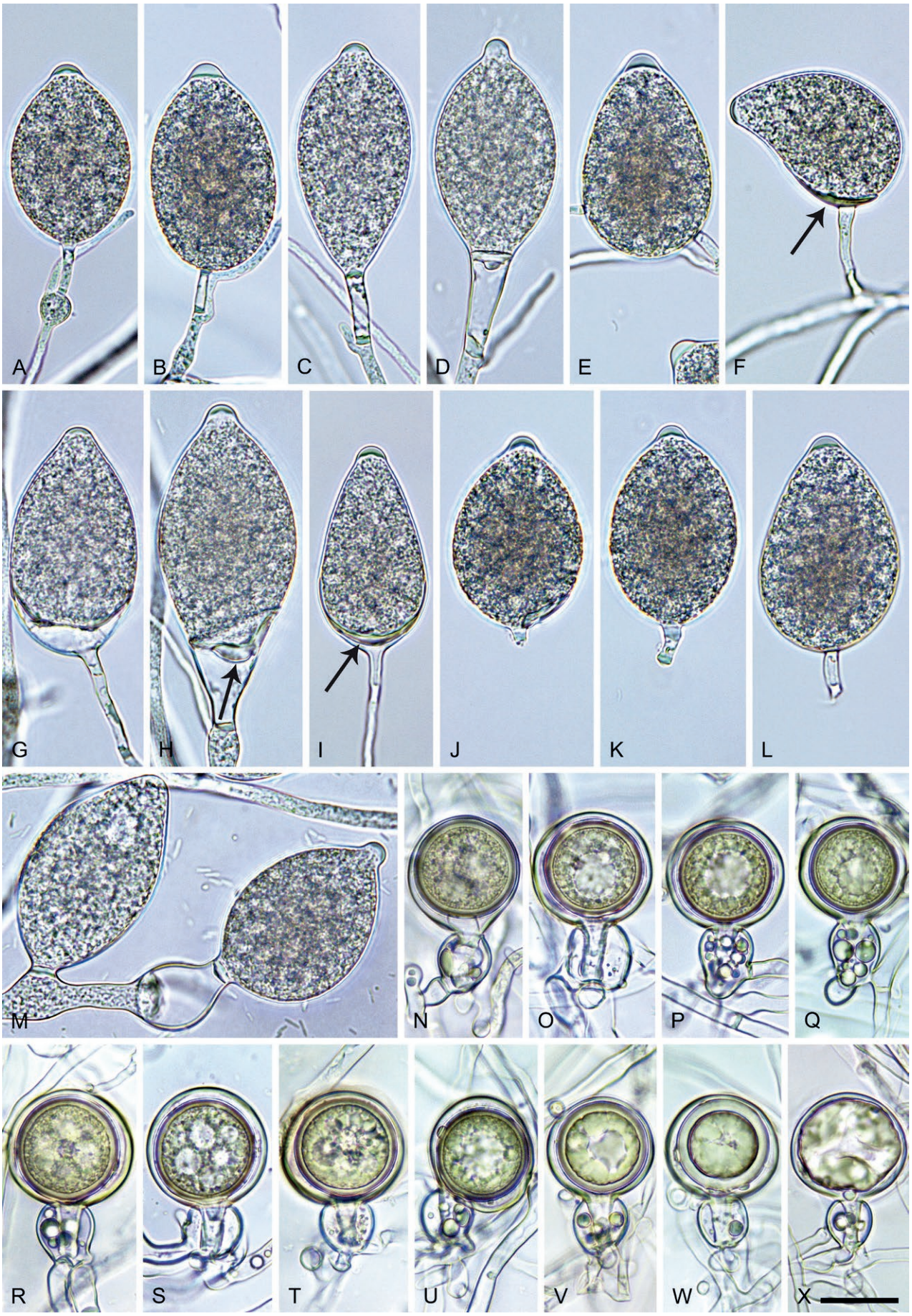

Fig. 29. *Phytophthora frigidophila*. **A–M.** Ovoid, pyriform, limoniform, obpyriform and mouse-shaped sporangia formed on V8-agar in soil extract. **A–C, E–L.** Papillate or semipapillate apices. **A–L.** Pedicels with variable length. **A–D.** External proliferation. **F, H, I.** Thick plugs below cytoplasm (arrows). **G–I.** Sporangia partially filled with cytoplasm. **J–L.** Caducous sporangia. **M.** Sympodium with nonpapillate (left) and papillate sporangium and hyphal swelling. **N–W.** Oogonia with aplerotic oospores and amphigynous unicellular antheridia, formed in solid carrot agar. **V, W.** Aborted oospores. **X.** Oogonium aborted before oospore formation. Images: A, E–G, I–W. Ex-type CBS 149486; B–D, H, X; PA215A. Scale bar = 20 µm; X applies to A–X.

T, V–X), excentric and/or comma-shaped (14.5 %; Fig. 29U), with a short or medium-length, mostly non-tapering stalk (Fig. 29N–X); av. oogonial diam 30.7 ± 4.1 µm with an overall range of 20.0–40.9 µm and a range of isolate means of 31.2–34.9 µm; predominantly slightly aplerotic to aplerotic (88.5 %; Fig. 29O–W) or infrequently nearly plerotic (11.5 %; Fig. 29N). *Oospores* globose to subglobose with one medium-large or several small lipid globules (Fig. 29N–U); av. diam 25.5 ± 3.4 µm with an overall range of 20.5–35.1 µm and a range of isolate means of 23.7–27.6 µm; wall diam 1.57 ± 0.2 µm (overall range 1.13–2.06 µm) and oospore wall index 0.33 ± 0.04; abortion rate after 4 wk very high, av. 94 % (range 85–99 %) with oogonia aborting after (Fig. 29V, W) or before oospore formation (Fig. 29X). *Antheridia* amphigynous, cylindrical, limoniform, subglobose or irregular, unicellular (Fig. 29N–X); 16.8 ± 2.5 × 15.2 ± 2.5 µm.

Culture characteristics: Colonies on V8A and CA submerged to appressed with scanty aerial mycelium, radiate on V8A and faintly radiate on CA; on PDA dense felty-cottony with a petaloid pattern (Fig. 23).

Cardinal temperatures and growth rates: On V8A optimum 20 °C with 5.18 ± 0.02 mm/d radial growth, maximum 25–<27.5 °C, minimum <10 °C (Fig. 26), lethal temperature 32.5–<35 °C. On CA and PDA at 20 °C 4.05 ± 0.14 mm/d and 2.51 ± 0.21 mm/d, respectively.

Additional materials examined: **Panama**, Volcano Baru, isolated from necrotic lesions on naturally fallen leaves of a non-identified tree species collected from the ground in a tropical cloud forest, Nov. 2019, *K.D. Broders & Y. Balci* (PA338, PA339, PA340); isolated from necrotic lesions on naturally fallen leaves of a non-identified tree species floating in a stream running through a tropical cloud forest, Nov. 2019, *K.D. Broders & Y. Balci* (PA215, PA341, PA342, PA343).

Phytophthora montana T. Jung, Y. Balci, K. Broders & M. Horta Jung, ***sp. nov.*** MycoBank MB 847292. Fig. 30.

Etymology: The name refers to the mountainous habitat of the known isolates (*montana* Latin = mountainous).

Typus: **Panama**, Volcano Baru, isolated from a necrotic lesion on a naturally fallen leaf of a non-identified tree species collected from the ground in a tropical cloud forest, Nov. 2019, *K.D. Broders & Y. Balci* (**holotype** CBS H-25115, dried culture on V8A, ex-holotype living culture CBS 149492 = PA243).

Morphological structures on V8A: *Sporangia* occasionally observed in solid agar but abundantly produced in non-sterile soil extract; borne mostly terminally (86.2 %) in dense or lax sympodia of 2–9 sporangia (Fig. 30K) or on unbranched sporangiophores, or less frequently intercalary (13.8 %; Fig. 30C, D, G); non-caducous with semipapillate apices (Fig. 30A–I); predominantly ovoid, broad ovoid or elongated-ovoid (66.8 %; Fig. 30A–C, J), less frequently limoniform to elongated-limoniform (9.3 %; Fig. 30F), distorted and often with two apices (7.7 %; Fig. 30H, I), obturbinate (6.6 %; Fig. 30E), obpyriform to elongated-obpyriform (3.2 %; Fig. 30D), ellipsoid to elongated-ellipsoid (2.8 %), obovoid (1.6 %), ampulliform (0.8 %; Fig. 30G), subglobose (0.8 %) or mouse-shaped (0.4 %); lateral attachment of the sporangiophore (38.8 %; Fig. 30E, H), a conspicuous basal plug (65.6 %; Fig. 30B, C, F–H) and pedicels (19.1 %; Fig. 30A, C) common; pedicel length variable, averaging 25.3 ± 18.1 µm (range 4.8–87.9 µm); sporangial dimensions averaging 54.1 ± 6.1 × 37.0 ± 3.5 µm (overall range 37.2–78.8 × 25.1–44.2 µm; range of isolate means 51.2–57.7 × 35.4–38.0 µm) with a length/breadth ratio of 1.47 ± 0.19 (overall range 1.12–2.56); sporangial proliferation exclusively external (Fig. 30C, E, K); sporangial germination indirectly with zoospores discharged through an exit pore of 3.7–8.7 µm (av. 5.8 ± 0.8 µm; Fig. 30J). *Zoospores* limoniform to reniform whilst motile, becoming spherical (av. diam = 10.8 ± 0.7 µm) on encystment; cysts germinating directly. *Hyphal swellings* infrequently formed on sporangiophores, ovoid, subglobose or limoniform, dimensions 17.7 ± 5.6 µm (range 11.6–29.1 µm). *Chlamydospores* not observed. *Oogonia* produced in single culture ('homothallic' breeding system); mostly sessile or terminal on short to medium-length, sometimes curved lateral hyphae, smooth-walled (98 %; Fig. 30L–P, R–V) or rarely with a nipple-like wart at the apex (Fig. 30Q), globose to subglobose (88 %; Fig. 30L–N, R–V) or slightly elongated (12 %; Fig. 30O–Q), sometimes slightly bend (19.5 %; Fig. 30M, T), with a rounded (75.5 %; Fig. 30L, R–U) or short tapering base (24.5 %; Fig. 30M–Q, V); av. oogonial diam 28.0 ± 3.0 µm with an overall range of 17.8–36.6 µm and a range of isolate means of 27.2–28.5 µm; nearly plerotic to plerotic (66.5 %; Fig. 30M–R, U, V) or slightly aplerotic to aplerotic (33.5 %; Fig. 30L, S, T). *Oospores* globose to subglobose with one or sometimes two medium-large or large lipid globules (Fig. 30L–V), turning golden-brown during maturation (Fig. 30U, V; av. diam 24.9 ± 2.6 µm with an overall range of 15.7–31.3 µm and a range of isolate means of 24.4–25.3 µm; wall diam 1.34 ± 0.2 µm (overall range 0.72–1.94 µm) and oospore wall index 0.29 ± 0.03; abortion rate after 4 wk 56 % (range 28–76 %). *Antheridia* paragynous, club-shaped, ovoid or subglobose (82 %; Fig. 30L–Q, U, V) or less frequently amphigynous, cylindrical and unicellular (18 %; Fig. 30R–T); sometimes a second paragynous antheridium attached to the oogonial wall (Fig. 30O); dimensions 12.2 ± 2.1 × 9.0 ± 1.3 µm.

Culture characteristics: Colonies on V8A and CA submerged to appressed with limited aerial mycelium, striate to radiate on V8A and radiate on CA; on PDA appressed, dense felty-cottony and uniform to faintly radiate (Fig. 23).

Cardinal temperatures and growth rates: On V8A optimum 25.0 °C with 8.77 ± 0.46 mm/d radial growth, maximum 25–<27.5 °C, minimum <10 °C (Fig. 26), lethal temperature 30 °C. At 20 °C on V8A, CA and PDA 8.01 ± 0.17 mm/d, 5.93 ± 0.07 mm/d and 3.61 ± 0.09 mm/d, respectively.

Additional materials examined: **Panama**, Volcano Baru, isolated from necrotic lesions on naturally fallen leaves of a non-identified tree species collected from the ground in a tropical cloud forest, Nov. 2019, *K.D. Broders & Y. Balci* (PA244, PA318, PA319, PA320).

Phytophthora multiplex T. Jung, Y. Balci, K. Broders & M. Horta Jung, ***sp. nov.*** MycoBank MB 847300. Figs 31, 32.

Etymology: The name refers to the diverse set of morphological structures (*multiplex* Latin = diverse).

Typus: **Panama**, Parque National Sobernia, isolated from a necrotic lesion on a naturally fallen leaf of a non-identified tree species in a tropical lowland rainforest, Nov. 2019, *K.D. Broders & Y. Balci* (**holotype** CBS H-25192, dried culture on V8A, ex-holotype living culture CBS 149637 = PA061).

Morphological structures on V8A: *Sporangia* common abundantly produced in non-sterile soil extract; borne terminally (97.2 %) on

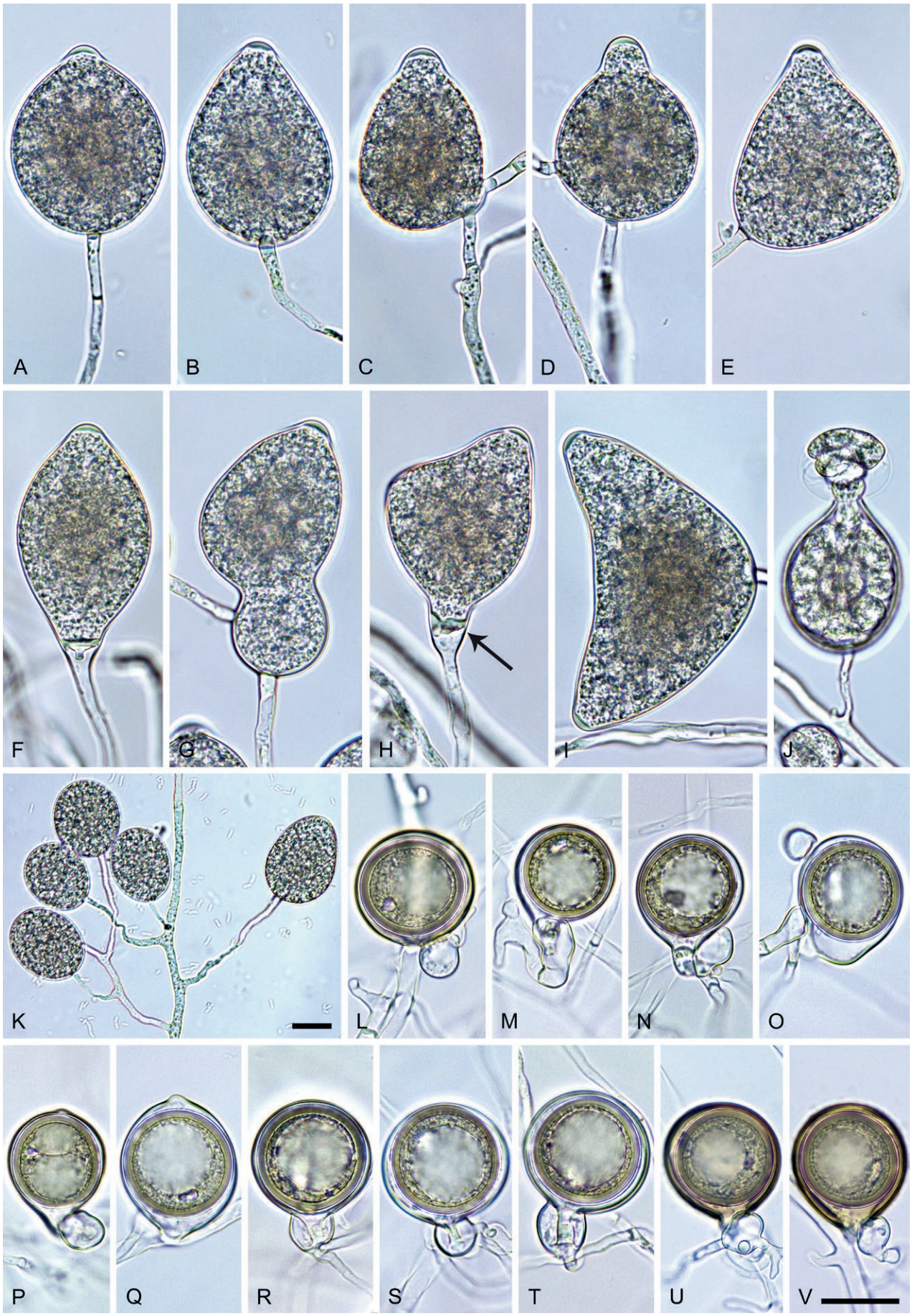

Fig. 30. *Phytophthora montana*. **A–K.** Sporangia formed on V8-agar in soil extract. **A–I.** Semipapillate apices. **A–G, J.** Ovoid, Obpyriform, obturbinate, limoniform and ampulliform sporangia. **H.** Distorted sporangium. **I.** Bilobed sporangium. **A, C.** With pedicels. **C, D, G.** Intercalary sporangia. **C, E.** External proliferation. **J.** Zoospore release. **K.** Dense sympodium with immature sporangia. **L–V.** Oogonia with near-plerotic to plerotic oospores, formed in carrot agar. **L–Q, U, V.** Paragynous antheridia. **O.** Two antheridia. **O–Q.** Slightly elongated oogonia. **R–T.** Amphigynous antheridia. **S, T.** Slightly bend to comma-shaped oogonia. Images: A–C, E, G–I, K–N, P, T–V. Ex-type CBS 149492; D, F, J, O, Q–S; PA319. Scale bars = 20 µm; V applies to A–J, L–V.

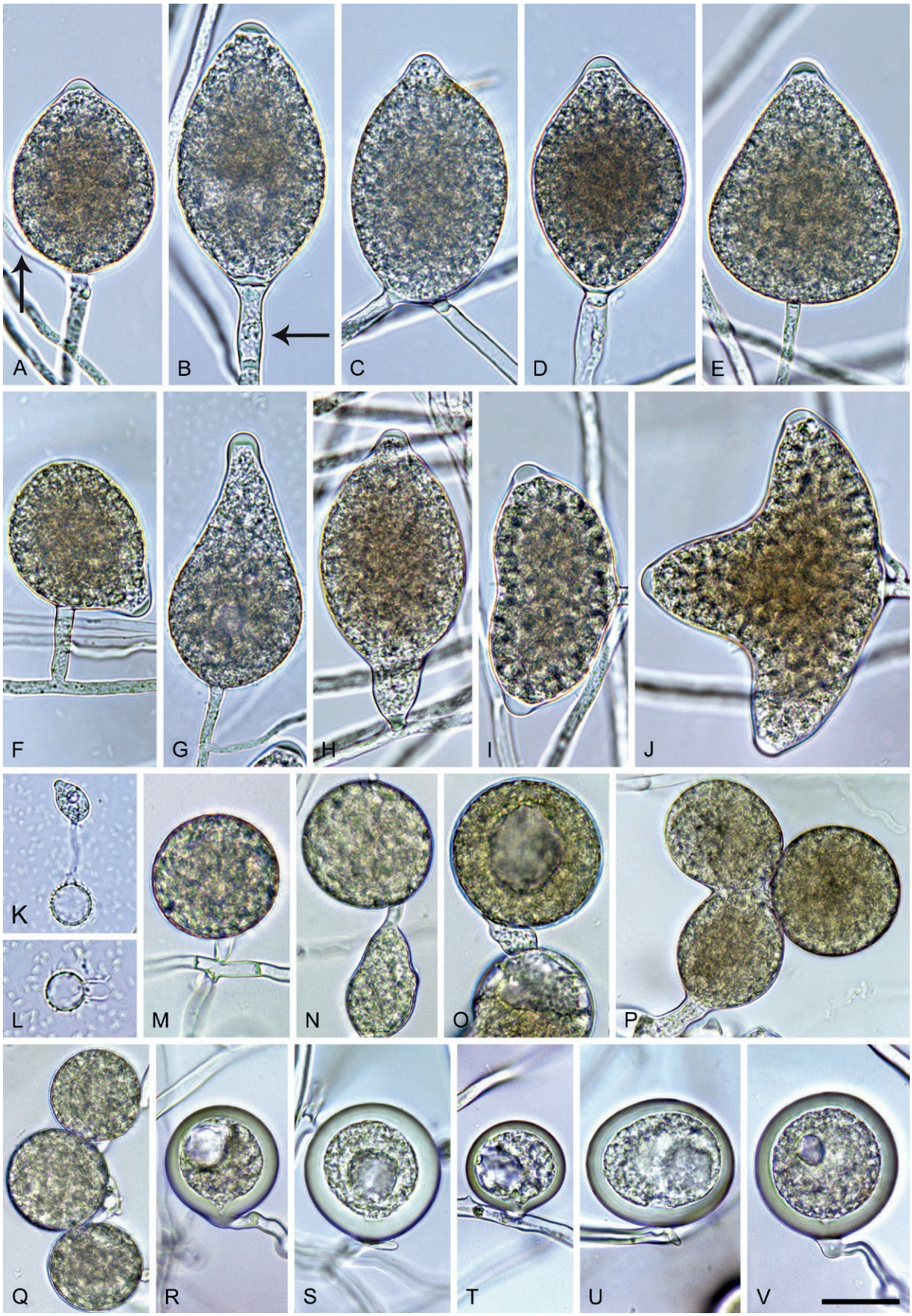

Fig. 31. *Phytophthora multiplex*. **A–J.** Sporangia formed on V8-agar (V8A) in soil extract. **A, B, D–J.** Papillate or semipapillate sporangia. **A–H.** Ovoid, limoniform, obturbinate and obpyriform sporangia. **A, B, G, J.** External proliferation (arrow in A). **B.** Medium-length pedicel (arrow). **C.** Nonpapillate intercalary sporangium. **I, J.** Distorted, bi- and tripapillate sporangia before zoospore release. **K.** Zoospore cyst germinating by forming a microsporangium. **L.** Empty cyst after release of secondary zoospore (diplanetism). **M–Q.** Thin-walled globose chlamydospores and swellings formed in V8A. **R–V.** Extremely thick-walled globose to subglobose chlamydospores formed in carrot agar in mating tests. Images: A, C, D, F, J, M, N, P, Q. Ex-type CBS 149637; B. PA038; E, H. NI160; G, I, K, L. PA212; O. PA133; R–V. Ex-type CBS 149637 × PA172. Scale bar = 20 µm; V applies to A–V.

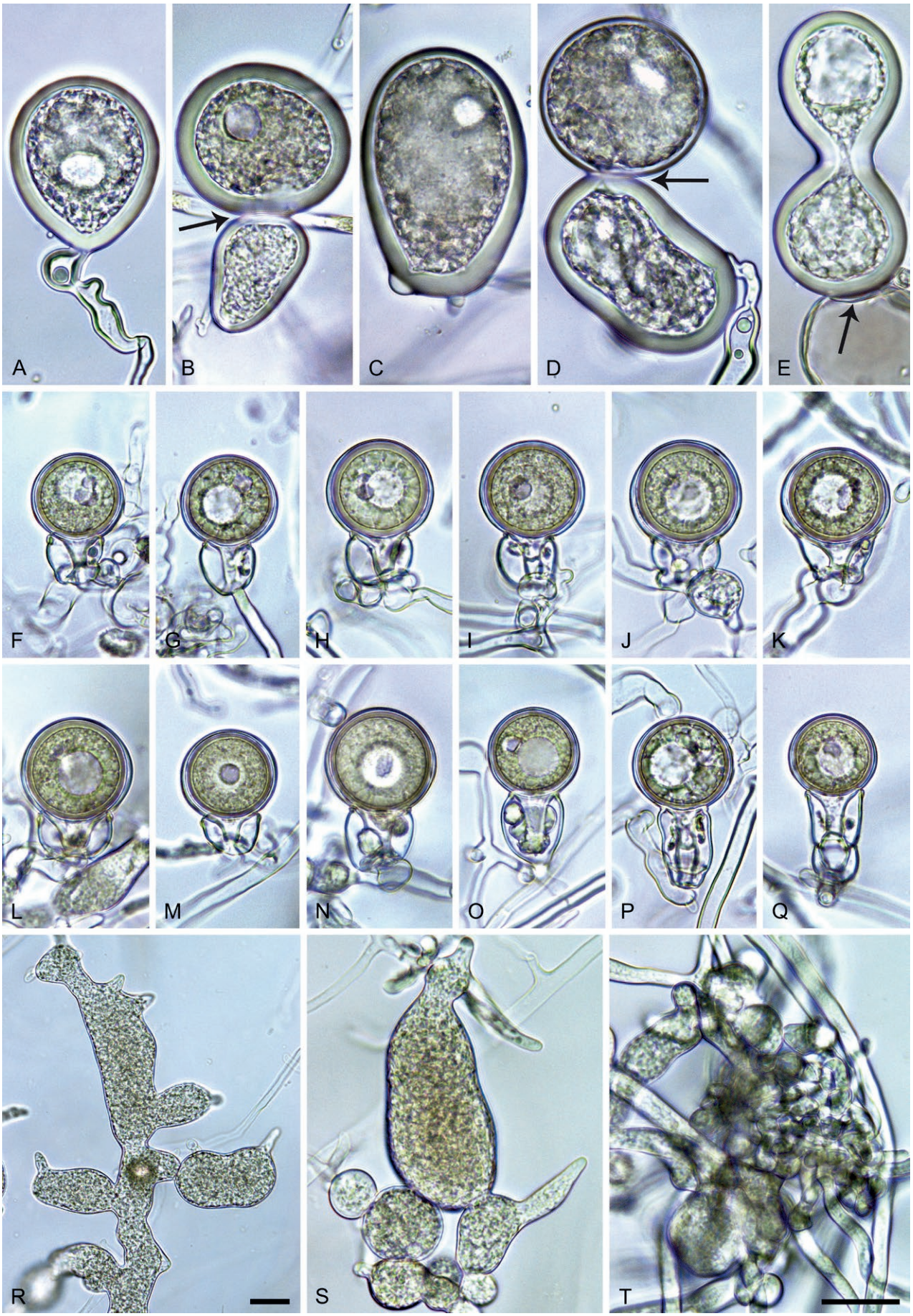

Fig. 32. *Phytophthora multiplex*. **A–E.** Extremely thick-walled chlamydospores with variable shapes formed in solid carrot agar (fgCA) in mating tests. **D, E.** New chlamydospore arising (arrow) from other chlamydospores. **F–Q.** Globose to subglobose, smooth-walled oogonia with near-plerotic to plerotic oospores, formed in fgCA in mating tests. **F–O.** Unicellular amphigynous antheridia. **P, Q.** Bicellular amphigynous antheridia. **R, S.** Catenulate irregular hyphal swellings formed in V8A. **T.** Dense hyphal aggregation in V8A. Images: A–D, F–O. Ex-type CBS 149637 × PA172; E, P, Q. PA133 × PA172; R. Ex-type CBS 149637; S, T. PA133. Scale bars = 20 µm; T applies A–Q, S, T.

unbranched long or short sporangiophores (Fig. 31F) or in dense or lax sympodia of 2–4 sporangia, or infrequently intercalary (1.6 %; Fig. 31C) or sessile (1.2 %; Fig. 31H); apices mostly papillate (89.9 %; Fig. 31A, D, E, G, I, J) or infrequently semipapillate (8.3 %; Fig. 31B, F, H) or nonpapillate and pointed (1.8 %; Fig. 31C); non-caducous, mostly ovoid, broad-ovoid or elongated ovoid (54.4 %; Fig. 31A–C, F), distorted and often bi- or tripapillate (18 %; Fig. 31I, J), limoniform to elongated-limoniform (16.7 %; Fig. 31D, H) or less frequently obpyriform to elongated obpyriform (5.6 %; Fig. 31G), pyriform (3.2 %), obturbinate (1.3 %; Fig. 31E), ellipsoid (0.6 %) or subglobose (0.2 %); lateral attachment of sporangiophores (13.2 %; Fig. 31F), pedicels (26.9 %; Fig. 31B) and vacuoles (11.8 %; Fig. 31G) commonly observed; pedicel length ranging from 3.1 to 82.6 µm (av. 20.7 ± 12.9 µm); sporangial proliferation exclusively external (Fig. 31A, B, G, J); sporangial dimensions averaging 60.0 ± 8.8 × 37.0 ± 5.1 µm (overall range 20.8–81.9 × 21.2–52.9 µm; range of isolate means 42.6–68.3 × 29.8–41.0 µm) with a length/breadth ratio of 1.63 ± 0.2 (overall range 0.71–2.45; sporangial germination indirectly with zoospores discharged through an exit pore 2.3–9.8 µm wide (av. 5.3 ± 1.0 µm). *Zoospores* limoniform to reniform whilst motile, becoming spherical (av. diam = 10.0 ± 1.0 µm) on encystment; cysts germinating directly forming a hypha or a microsporangium or indirectly by releasing a secondary zoospore (diplanetism) (Fig. 31K, L). *Hyphal swellings* infrequently formed in water on sporangiophores, subglobose to globose or limoniform, 5.3 ± 1.0 µm; frequently formed on solid agar, globose to subglobose, limoniform, irregular or coralloid (Fig. 31N, Fig. 32R, S). *Chlamydospores* formed in solid agar infrequently in single culture and abundantly in mating tests between A1 and A2 mating type isolates; borne terminally, intercalary or sessile (Fig. 31M–O, Q–V, Fig. 32A, C), sometimes catenulate (Fig. 31Q), or by emergence from another chlamydospore (Fig. 31P, Fig. 32B, D, E); globose to subglobose (68.4 %; Fig. 31M–V, Fig. 32B, D), pyriform (10 %), ellipsoid (8.3 %; Fig. 32C, D), irregular (8.3 %; Fig. 32B), ampulliform (3.3 %; Fig. 32E) or obovoid (1.7 %; Fig. 32A); often containing lipid globules (51.6 %; Fig. 31O, R–U, Fig. 32E); dimensions 47.9 ± 17.1 × 42.6 ± 8.9 µm (overall range 25.2–128.9 × 23.1–65.8 µm); with thin (Fig. 31M–Q) or thick wall (Fig. 31R–V, Fig. 32A–E), on average 4.0 ± 1.7 µm thick (range 0.7–8.4 µm). *Oogonia* not observed in single culture, but abundantly produced in mating tests between the two A2 mating type isolates PA172A and PA161 and the 10 A1 isolates ('heterothallic' breeding system); with short stalks, terminal on short to medium-length, sometimes curved lateral hyphae or sessile, smooth-walled, globose to slightly subglobose with a rounded or short-tapering base (Fig. 32F–Q); oogonial diam 26.6 ± 2.7 µm (overall range 18.6–35.5 µm; range of means in different mating combinations 25.5–28.7 µm); plerotic or nearly plerotic (Fig. 32F–Q). *Oospores* globose with a medium-sized lipid globule (Fig. 32F–Q); mean diam 23.8 ± 2.5 µm (overall range 17.8–33.0 µm; range of means in different mating combinations 22.9–26.0 µm); wall thickness 1.34 ± 0.21 µm (overall range 0.86–2.17 µm), oospore wall index 0.3 ± 0.04; abortion 24–52 % (av. 40.3 %) after 4 wk. *Antheridia* exclusively amphigynous and cylindrical or subglobose, unicellular (96.7 %: Fig. 32F–O) or infrequently bicellular with the basal cell being smaller than the upper cell (3.3 %; Fig. 32P, Q); dimensions 17.3 ± 2.9 × 15.3 ± 1.6 µm. *Hyphal aggregations* observed in all isolates (Fig. 32T).

Culture characteristics: Colonies on V8A and CA appressed with limited aerial mycelium, chrysanthemum-like on V8A, and radiate on CA; dense felty-cottony on PDA with a faint petaloid pattern (Fig. 25).

Cardinal temperatures and growth rates: On V8A optimum 27.5 °C with 9.58 ± 1.04 mm/d radial growth, maximum 32.5–<35 °C (10 isolates) or 30–32.5 °C (1 isolate), minimum <10 °C (Fig. 26), lethal temperature 35 °C. At 20 °C on V8A, CA and PDA 7.24 ± 0.72 mm/d, 5.17 ± 0.4 mm/d and 5.12 ± 0.51 mm/d, respectively.

Additional materials examined: **Nicaragua**, Diriomo, Mombacho volcano, isolated from naturally fallen necrotic leaves of unidentified rainforest trees collected from the ground in a tropical cloud forest, Nov. 2017, *Y. Balci, L. Garcia & B. Mendieta-Araica* (NI156, NI160). **Panama**, Parque National Sobernia, isolated from necrotic lesions on naturally fallen leaves of non-identified tree species in a tropical lowland rainforest, Nov. 2019, *K.D. Broders & Y. Balci* (PA038, PA065, PA133); Parque National de Campana, isolated from necrotic lesions on naturally fallen leaves of non-identified tree species in a tropical lowland rainforest, Nov. 2019, *K.D. Broders & Y. Balci* (PA170, PA171, PA172); El Montoso, Reserva Forestal, isolated from necrotic lesions on naturally fallen leaves of non-identified tree species in a tropical lowland rainforest, Nov. 2019, *K.D. Broders & Y. Balci* (PA199, PA212).

Phytophthora obovoidea T. Jung, Y. Balci, L. Garcia & B. Mendieta-Araica, ***sp. nov.*** MycoBank MB 847293. Fig. 33.

Etymology: The name refers to the obovoid shape of many sporangia.

Typus: **Nicaragua**, Diriomo, Mombacho volcano, isolated from a naturally fallen necrotic leaf of an unidentified rainforest tree collected from the ground in a tropical cloud forest, Nov. 2017, *Y. Balci, L. Garcia & B. Mendieta-Araica* (**holotype** CBS H-25188, dried culture on V8A, ex-holotype living culture CBS 149633 = NI168).

Morphological structures on V8A: *Sporangia* common on solid agar and abundantly produced in non-sterile soil extract; borne predominantly terminally (97.6 %) in dense or lax sympodia of 2–10 sporangia (Fig. 33N) or sometimes on unbranched long or short sporangiophores (Fig. 33D), less frequently intercalary (1.2 %) or sessile (1.2 %; Fig. 33A); ovoid, broad-ovoid or elongated ovoid (38.7 %; Fig. 33A, J, L–N), obovoid (25.1 %; Fig. 33B, C, H, I), limoniform to elongated-limoniform (22.8 %; Fig. 33E, F, N), or less frequently ellipsoid (5.2 %; Fig. 33D), distorted, often with two apices (3.6 %; Fig. 33K), pyriform (3.2 %; Fig. 33G), obpyriform to elongated obpyriform (1 %) or ampulliform (0.4 %); usually with pedicels of variable length ranging from 3.2 to 142.1 µm (av. 30.2 ± 17.9 µm) (83.6 %; Fig. 33B–M) and caducous (Fig. 33I–M); lateral attachment of sporangiophores rare (0.2 %; Fig. 33H); apices papillate (77.4 %; Fig. 33A, B, D, G, I, J), less frequently semipapillate (16.5 %; Fig. 33C, F, H) or nonpapillate (6.1 %; Fig. 33E, K); sporangial proliferation exclusively external (Fig. 33F, G, N); sporangial dimensions averaging 51.5 ± 7.0 × 30.2 ± 3.4 µm (overall range 24.3–89.2 × 19.7–44.9 µm; range of isolate means 46.8–59.8 × 27.2–35.4 µm) with a length/breadth ratio of 1.71 ± 0.2 (overall range 0.81–3.19; sporangial germination indirectly with zoospores discharged through an exit pore 1.9–9.8 µm wide (av. 4.8 ± 1.1 µm) (Fig. 33M). *Zoospores* limoniform to reniform whilst motile, becoming spherical (av. diam = 10.2 ± 0.8 µm) on encystment; cysts germinating directly forming a hypha or a microsporangium or indirectly by releasing a secondary zoospore (diplanetism). *Hyphal swellings* infrequently formed in water on sporangiophores, subglobose to globose or limoniform, 12.1 ± 3.3 µm. *Chlamydospores* commonly formed in solid agar; borne terminally, intercalary or sessile (Fig. 33O–R), sometimes catenulate (Fig. 33R); globose to subglobose (95.2 %; Fig. 33O–R), ovoid (3.2 %) or ellipsoid (1.6 %), usually containing one or

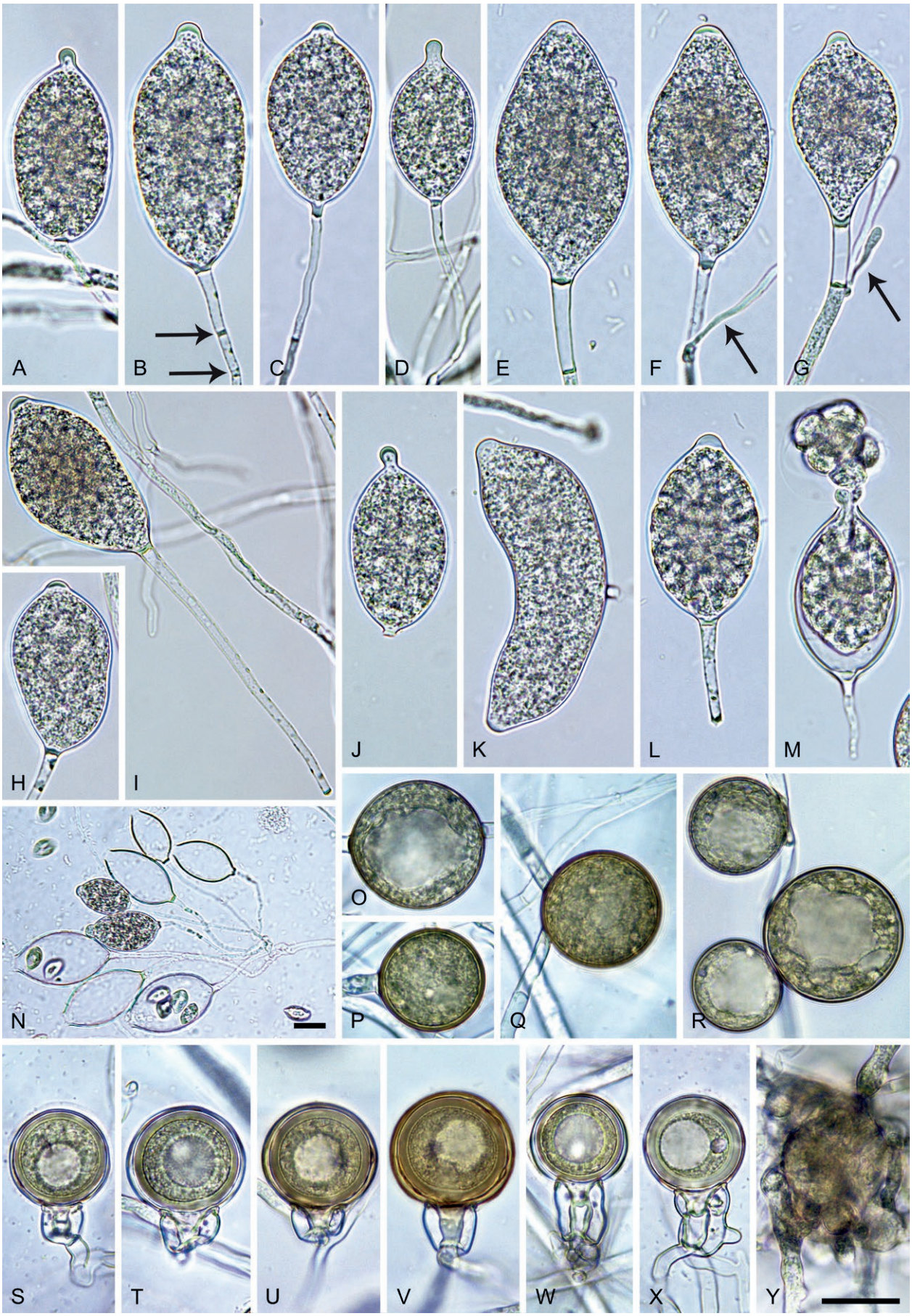

Fig. 33. *Phytophthora obovoidea*. **A–N.** Sporangia formed on V8-agar in soil extract. **A–J, L–N.** Obovoid, ovoid, limoniform and pyriform sporangia. **A–D, F–J, L.** Papillate or semipapillate apices. **E, K.** Nonpapillate apices. **B–M.** Short to very long pedicels. **B.** Double pedicel (arrows). **F, G.** External proliferation (arrows). **I–M.** Caducous sporangia. **K.** Bilobed sporangium. **N.** Dense sporangial sympodium. **O–R.** Globose thick-walled chlamydospores in carrot agar (fgCA). **O, Q.** Intercalary. **P.** Terminal. **R.** Catenulate. **S–X.** Globose oogonia with plerotic or near-plerotic oospores and amphigynous antheridia, formed in fgCA in mating tests. **X.** Bicellular antheridium. **Y.** Dense hyphal aggregation in V8A. Images: A–D, J, K, M, P–R. Ex-type CBS 149633; E, F, H, I. NI187; G. VN828; L, O, Y. PA212; N. VN369; S–X. TW367 × ex-type CBS 149633. Scale bars = 20 µm; Y applies to A–M, O–Y.

more vacuoles and turning golden-brown during maturation (Fig. 33O–R); diam 29.8 ± 4.2 µm (overall range 20.3–39.8 µm); wall 1.35 ± 0.34 µm thick (range 0.84–2.8 µm). *Oogonia* not observed in single cultures, but abundantly produced in mating tests between A1 and A2 mating type isolates ('heterothallic' breeding system); globose to slightly subglobose with a rounded base and a short, sometimes slightly tapering stalk, sessile or terminal on short to medium-length, sometimes curved lateral hyphae, smooth-walled (Fig. 33S–X); oogonial diam 27.6 ± 3.2 µm (overall range 20.0–40.6 µm; range of means in different mating combinations 24.9–29.6 µm); plerotic or nearly plerotic (Fig. 33S–X). *Oospores* globose with a medium-sized or large lipid globule (Fig. 33S–X); mean diam 23.9 ± 2.7 µm (overall range 17.5–36.5 µm; range of means in different mating combinations 21.9–25.4 µm); wall thickness 1.48 ± 0.17 µm (overall range 1.17–2.3 µm), oospore wall index 0.33 ± 0.04; abortion 32–56 % (av. 41.3 %) after 4 wk. *Antheridia* exclusively amphigynous and cylindrical or subglobose, unicellular (95.3 %; Fig. 33S–W) or infrequently bicellular (3.3 %; Fig. 33X); basal septum of the oogonial stalks mostly inside the antheridium (Fig. 33S, T, V–X); dimensions 14.4 ± 2.7 × 14.5 ± 1.6 µm. *Hyphal aggregations* observed in all isolates (Fig. 33Y).

Culture characteristics: Colonies on V8A submerged to appressed with limited aerial mycelium and radiate to stellate patterns; on CA appressed with limited or woolly aerial mycelium and a radiate pattern; on PDA dense felty-cottony or woolly with a faint petaloid pattern or uniform (Fig. 24).

Cardinal temperatures and growth rates: On V8A optimum 30 °C with 10.98 ± 0.99 mm/d radial growth but growing only slightly slower at 27.5 °C (10.74 ± 0.91 mm/d), maximum 32.5–<35 °C, minimum <10 °C (Fig. 26), lethal temperature 35 °C (13 isolates) or >35 °C (9 isolates). At 20 °C on V8A, CA and PDA 7.45 ± 0.95 mm/d, 5.29 ± 0.46 mm/d and 3.77 ± 0.56 mm/d, respectively.

Additional materials examined: **Indonesia**, Java, Bandung area, isolated from a naturally fallen necrotic leaf of an unidentified rainforest tree floating in a stream below waterfall Tilu Leuwi Opat, Feb. 2019, *T. Jung, M. Tarigan & L. Oliveira* (JV122); Sulawesi, Gowa district, isolated from a naturally fallen necrotic leaf of an unidentified tree floating in a stream running through a submontane rainforest, Jun. 2019, *T. Jung, M. Junaid & M. Horta Jung* (SL175). **Nicaragua**, Diriomo, Mombacho volcano, isolated from naturally fallen necrotic leaves of unidentified rainforest trees collected from the ground in a tropical cloud forest, Nov. 2017, *Y. Balci, L. Garcia & B. Mendieta-Araica* (NI154, NI162, NI167); Rivas, Maderas Volcano, isolated from a naturally fallen necrotic leaf of an unidentified rainforest tree collected from the ground in a tropical cloud forest, Nov. 2017, *Y. Balci, L. Garcia & B. Mendieta-Araica* (NI187); Matagalpa, Selva Negra, isolated from naturally fallen necrotic leaves of unidentified rainforest trees collected from the ground in a tropical cloud forest, Nov. 2017, *Y. Balci, L. Garcia & B. Mendieta-Araica* (NI108, NI114, NI117). **Panama**, Parque National Sobernia, isolated from a naturally fallen necrotic leaf of an unidentified tree collected from the ground in a tropical lowland rainforest, Nov. 2019, *K.D. Broders & Y. Balci* (PA066); Parque National de Campana, isolated from naturally fallen necrotic leaves of unidentified trees collected from the ground in a tropical lowland rainforest, Nov. 2019, *K.D. Broders & Y. Balci* (PA167, PA168); El Montoso Reserva Forestal, isolated from naturally fallen necrotic leaves of unidentified trees in a tropical lowland rainforest, Nov. 2019, *K.D. Broders & Y. Balci* (PA206, PA208, PA211). **Taiwan**, Taichung County, isolated from baiting leaves floating in tributaries of Da-jia River, Sep. 2013, *T. Jung, M. Horta Jung & T.-T. Chang* (TW343, TW367, TW369). **Vietnam**, Sapa, Xin Chài Mountain, isolated from rhizosphere soil of *Alnus nepalensis* in a montane, temperate *Alnus* forest, Mar. 2016, *T. Jung, M. Horta Jung & N.M. Chi* (VN369, VN802, VN828, VN829, VN830).

Phytophthora pyriformis T. Jung, Y. Balci, K.D. Boders & M. Horta Jung, ***sp. nov.*** MycoBank MB 847297. Fig. 34.

Etymology: The name refers to the pyriform shape of many sporangia.

Typus: **Panama**, Parque National Sobernia, isolated from a naturally fallen necrotic leaf of an unidentified tree collected from the ground in a tropical lowland rainforest, Nov. 2019, *K.D. Broders & Y. Balci* (**holotype** CBS H-25189, dried culture on V8A, ex-holotype living culture CBS 149634 = PA106).

Morphological structures on V8A: *Sporangia* common on solid agar and abundantly produced in non-sterile soil extract; borne predominantly terminally (99.4 %) in dense or lax sympodia of 2–6 sporangia (Fig. 34M) or on unbranched long or short sporangiophores, less frequently intercalary (0.6 %; Fig. 34A); mostly pyriform to elongated-pyriform (33.5 %; Fig. 34A, D, E, H), limoniform to elongated-limoniform (27.1 %; Fig. 34F, G, I, J, M) or obovoid to elongated-obovoid (16.5 %; Fig. 34C), less frequently ovoid, broad-ovoid or elongated ovoid (14.8 %; Fig. 34B, M), ellipsoid (4 %; Fig. 34K), distorted, usually with two or sometimes three apices (2.3 %; Fig. 32L), subglobose (1.2 %) or obpyriform to elongated-obpyriform (0.6 %); almost exclusively with pedicels of variable length ranging from 6.5 to 156.7 µm (av. 62.5 ± 27.3 µm) (99.1 %; Fig. 34A–K, M) and caducous (Fig. 34G, I–K); most sporangia with a conspicuous basal plug, often protruding into the sporangiophore (93.5 %; Fig. 34A, C–J, M); lateral attachment of sporangiophores rare (2 %); apices mostly papillate (90.8 %; Fig. 34B–H, J, K) or infrequently semipapillate (6.2 %; Fig. 34I) or nonpapillate (3 %; Fig. 34A), often pointed; sporangial proliferation exclusively external (Fig. 34B–G, M); sporangial dimensions averaging 54.2 ± 7.3 × 30.2 ± 3.1 µm (overall range 31.1–77.0 × 20.6–39.3 µm; range of isolate means 48.3–57.6 × 27.3–32.2 µm) with a length/breadth ratio of 1.8 ± 0.19 (overall range 0.97–2.89); sporangial germination indirectly with zoospores discharged through an exit pore 2.8–9.1 µm wide (av. 4.0 ± 0.7 µm) (Fig. 34L). *Zoospores* limoniform to reniform whilst motile, becoming spherical (av. diam = 10.6 ± 0.7 µm) on encystment; cysts germinating directly forming a hypha. *Hyphal swellings* rarely formed in water on sporangiophores, subglobose to globose, limoniform or ellipsoid. *Chlamydospores* commonly formed in solid agar; borne terminally on long or short lateral hyphae or sessile (Fig. 34N–Q), less frequently intercalary; globose to subglobose (95.2 %; Fig. 34N–Q), ellipsoid (4.7 %) or ovoid (3.3 %), usually containing one or more vacuoles and turning golden- to dark-brown during maturation (Fig. 34N–Q); diam 29.7 ± 3.7 µm (overall range 21.2–39.4 µm); wall 1.31 ± 0.24 µm thick (range 0.84–2.0 µm). *Oogonia* not observed in single culture, but abundantly produced in mating tests with A2 mating type isolates NI168, PA047 and PA168 of *P. obovoidea* ('heterothallic' breeding system; all tested isolates belonging to the A1 mating type); globose to slightly subglobose with a rounded base and a short, sometimes slightly tapering stalk, sessile or terminal on short to medium-length, sometimes curved lateral hyphae, smooth-walled (Fig. 34R–X); oogonial diam 25.5 ± 2.6 µm (overall range 19.4–32.3 µm; range of means in different mating combinations 22.4–27.9 µm); plerotic or nearly plerotic (Fig. 34R–X). *Oospores* globose with a medium-sized or large lipid globule (Fig. 34R–X); mean diam 22.7 ± 2.5 µm (overall range 16.7–32.2 µm; range of means in different mating combinations 19.8–25.2 µm); wall thickness 1.37 ± 0.16 µm (overall range 0.92–1.86 µm), oospore wall index 0.32 ± 0.04; abortion 16–44 % (av. 23.7 %) after 4 wk. *Antheridia* exclusively amphigynous, cylindrical

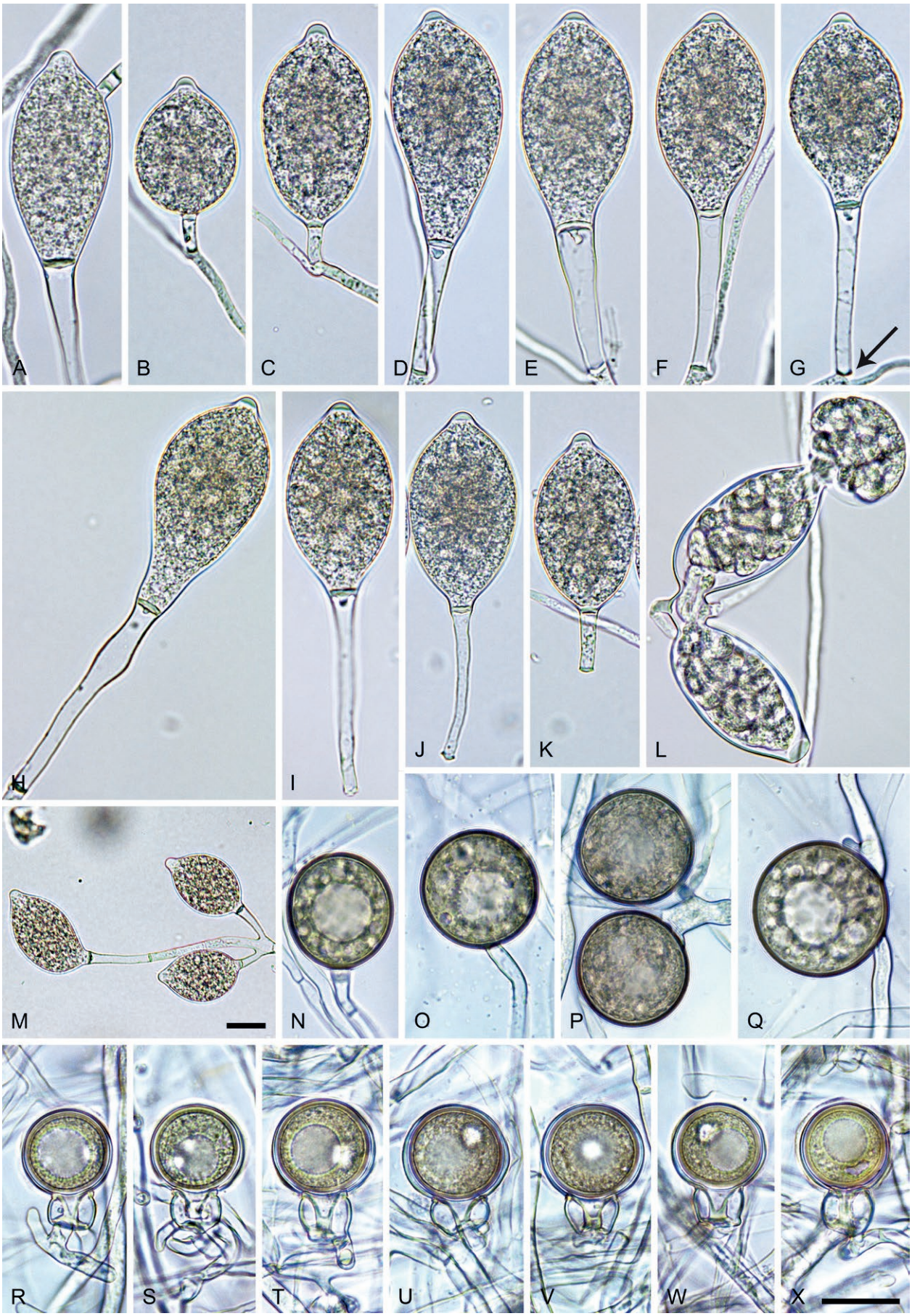

Fig. 34. *Phytophthora pyriformis*. **A–M.** Sporangia formed on V8-agar in soil extract. **A–K, M.** Pyriform, ovoid, obovoid, limoniform and ellipsoid sporangia with medium-length to long pedicels. **A.** Nonpapillate, intercalary sporangium. **B–H, J, K.** Papillate apices. **B–G.** External proliferation. **J.** Semipapillate apex. **I–K.** Caducous sporangia. **L.** Bilobed intercalary sporangium releasing zoospores. **M.** Lax sporangial sympodium. **N–Q.** Globose to subglobose, thick-walled chlamydospores in carrot agar (fgCA). **N–P.** Terminal. **Q.** Sessile. **R–X.** Globose oogonia with near-plerotic to plerotic oospores and unicellular amphigynous antheridia, formed in fgCA in polycarbonate membrane mating tests. Images: A, C–F, H, J, K, N–X. Ex-type CBS 149634; B, G, M. PA114; I. PA077; L. PA066. Scale bars = 20 µm; X applies to A–L, N–X.

or subglobose and unicellular (Fig. 34R–X); dimensions 14.2 ± 2.1 × 14.6 ± 1.5 µm. *Hyphal aggregations* not observed.

Culture characteristics: Colonies on V8A and CA submerged to appressed with limited aerial mycelium and radiate to stellate patterns; on PDA dense felty-cottony with a petaloid pattern (Fig. 23).

Cardinal temperatures and growth rates: On V8A optimum 27.5 °C with 11.43 ± 0.53 mm/d radial growth but growing only slightly slower at 25 and 30 °C with 11.21 ± 0.34 and 10.98 ± 0.78 mm/d, maximum 32.5–<35 °C, minimum >10–15 °C (Fig. 26), lethal temperature 35 °C (2 isolates) or >35 °C (4 isolates). At 20 °C on V8A, CA and PDA 9.0 ± 0.65 mm/d, 5.76 ± 0.04 mm/d and 4.85 ± 0.23 mm/d, respectively.

Additional materials examined: **Panama**, Parque National Sobernia, isolated from naturally fallen necrotic leaves of an unidentified tree species collected from the ground in a tropical lowland rainforest, Nov. 2019, *K.D. Broders & Y. Balci* (PA076, PA077, PA079, PA104, PA113, PA114).

Phytophthora tropicalis Aragaki & J.Y. Uchida, Mycologia 93: 139. 2001. [MycoBank MB 467732]. Fig. 35.

Typus: **USA**, Hawaii, Keaau, isolated from an inflorescence of *Macadamia integrifolia*, Jan. 1975, *M. Aragaki* (**holotype** CBS 434.91 preserved in a metabolically inactive state, ex-holotype living culture CBS 434.91 = ATCC 76651 = MYA-4218 = NRRL 64471 = WPC P10329).

Morphological structures on V8A: *Sporangia* common on solid agar and abundantly produced in non-sterile soil extract; borne predominantly terminally (99.6 %) in dense or lax sympodia of 2–9 sporangia (Fig. 35A, L) or sometimes on unbranched long or short sporangiophores (Fig. 35G), rarely intercalary (0.4 %); limoniform to elongated-limoniform (50.4 %; Fig. 35A, C, E, I, K, L), ovoid, broad-ovoid or elongated ovoid (21.7 %; Fig. 35A, F, J), less frequently pyriform (7.1 %; Fig. 35B, H), obovoid (6.9 %), distorted, often with two apices (5 %; Fig. 35D), obpyriform to elongated obpyriform (4.4 %; Fig. 35G) or ellipsoid (4.3 %); predominantly (98.6 %) with pedicels of variable length ranging from 2.9 to 100.1 µm (av. 33.9 ± 18.8 µm) (Fig. 35A–L) and caducous (Fig. 35G–J); lateral attachment of sporangiophores rare (0.1 %); apices fluent transition from semipapillate to papillate (95.1 %; Fig. 35A–J, L), infrequently nonpapillate and often pointed (4.9 %; Fig. 35B); sporangial proliferation exclusively external (Fig. 35A–D, K, L); sporangial dimensions averaging 55.8 ± 6.9 × 31.1 ± 3.8 µm (overall range 26.3–87.7 × 21.0–39.6 µm; range of isolate means 52.6–59.2 × 26.0–33.9 µm) with a length/breadth ratio of 1.81 ± 0.24 (overall range 0.89–2.67); sporangial germination indirectly with zoospores discharged through an exit pore 2.6–8.0 µm wide (av. 4.8 ± 1.0 µm) (Fig. 35K). *Zoospores* limoniform to reniform whilst motile, becoming spherical (av. diam = 10.6 ± 0.9 µm) on encystment; cysts germinating directly forming a hypha or a microsporangium or indirectly by releasing a secondary zoospore (diplanetism). *Hyphal swellings* infrequently formed in water on sporangiophores, subglobose to globose, limoniform or irregular, 12.1 ± 3.1 µm. *Chlamydospores* commonly formed in solid agar; borne terminally, intercalary or sessile (Fig. 35M–P), sometimes catenulate (Fig. 35N); globose to subglobose (85 %; Fig. 35M, N, P), ovoid (3 %) or ellipsoid- to pyriform-elongated (12 %; Fig. 35O), usually containing one or more lipid globules and turning golden-brown during maturation (Fig. 35M, N); diam 29.8 ± 4.2 µm (overall range 20.3–39.8 µm); wall 1.48 ± 0.5 µm thick (range 0.84–4.8 µm). *Oogonia* not observed in single culture, but abundantly produced in mating tests between A1 and A2 mating type isolates ('heterothallic' breeding system); globose to slightly subglobose (97 %) or rarely slightly excentric (3 %) with a rounded base and a short, sometimes slightly tapering stalk, sessile or terminal on short to medium-length, sometimes curved lateral hyphae, smooth-walled (Fig. 35Q–U); oogonial diam 27.3 ± 3.2 µm (overall range 20.6–35.6 µm; range of means in different mating combinations 24.8–30.2 µm); plerotic or nearly plerotic (Fig. 35Q–T). *Oospores* globose with a medium-sized or less frequently a large lipid globule (Fig. 35Q–T); mean diam 23.6 ± 2.2 µm (overall range 18.1–31.6 µm; range of means in different mating combinations 22.4–25.2 µm); wall thickness 1.35 ± 0.15 µm (overall range 0.91–1.75 µm), oospore wall index 0.31 ± 0.03; abortion 30–40 % (av. 35 %; Fig. 35U) after 4 wk. *Antheridia* exclusively amphigynous and cylindrical or subglobose, unicellular (Fig. 35Q–U); basal septum of the oogonial stalks often inside the antheridium (Fig. 35S–U); dimensions 13.0 ± 2.8 × 12.8 ± 2.2 µm. *Hyphal aggregations* observed in all isolates (Fig. 35V).

Culture characteristics: Colonies on V8A and CA submerged to appressed with limited aerial mycelium and stellate to radiate patterns; on PDA dense felty-cottony or woolly with a faint petaloid pattern or uniform (Fig. 24).

Cardinal temperatures and growth rates: On V8A optimum 30 °C with 10.08 ± 1.27 mm/d radial growth but growing only slightly slower at 27.5 °C (10.0 ± 0.82 mm/d), maximum 32.5–<35 °C, minimum <10 °C (Fig. 26), lethal temperature 35 °C (3 isolates) or >35 °C (9 isolates). At 20 °C on V8A, CA and PDA 7.7 ± 0.9 mm/d, 5.56 ± 0.42 mm/d and 4.51 ± 0.41 mm/d, respectively.

Materials examined: **Indonesia**, Java, Bandung area, isolated from naturally fallen necrotic leaves of unidentified trees floating in streams running through montane rainforests, Feb. 2019, *T. Jung & M. Tarigan* (JV030, JV041); Sumatra, Western Sumatra, isolated from naturally fallen necrotic leaves of unidentified trees floating in streams running through lowland and montane rainforests, Sep. 2018 and Feb. 2019, *T. Jung, M. Tarigan & L. Oliveira* (SU646, SU663, SU1678). **Nicaragua**, Driamba, isolated from a naturally fallen necrotic leaf of an unidentified tree floating in a stream running through a lowland rainforest, Nov. 2017, *Y. Balci, L. Garcia & B. Mendieta-Araica* (NI026); Diriomo, Mombacho Volcano, isolated from naturally fallen necrotic leaves of unidentified rainforest trees floating in a stream running through a tropical cloud forest, Nov. 2017, *Y. Balci, L. Garcia & B. Mendieta-Araica* (NI148, NI166, NI174). **Panama**, Parque National Sobernia, isolated from naturally fallen necrotic leaves of unidentified trees collected from the ground in a tropical lowland rainforest, Nov. 2019, *K.D. Broders & Y. Balci* (PA006, PA090, PA112).

Phytophthora valdiviana T. Jung, E. Sanfuentes von Stowasser, A. Durán & M. Horta Jung, ***sp. nov.*** MycoBank MB 847298. Fig. 36.

Etymology: The name refers to the origin of all known isolates in the Valdivian region of Chile.

Typus: **Chile**, Valdivian region, Parque Oncol, isolated from a baiting leaf floating in a stream running through a Valdivian rainforest, Nov. 2014, *T. Jung, E. Sanfuentes von Stowasser & A. Durán* (**holotype** CBS H-25128, dried culture on V8A, ex-holotype living culture CBS 149504 = CL157).

Morphological structures on V8A: *Sporangia* not observed in solid agar but abundantly produced in non-sterile soil extract, mostly inside the colonies rather than at the growing margins; borne terminally on mostly long or short unbranched sporangiophores or less frequently in

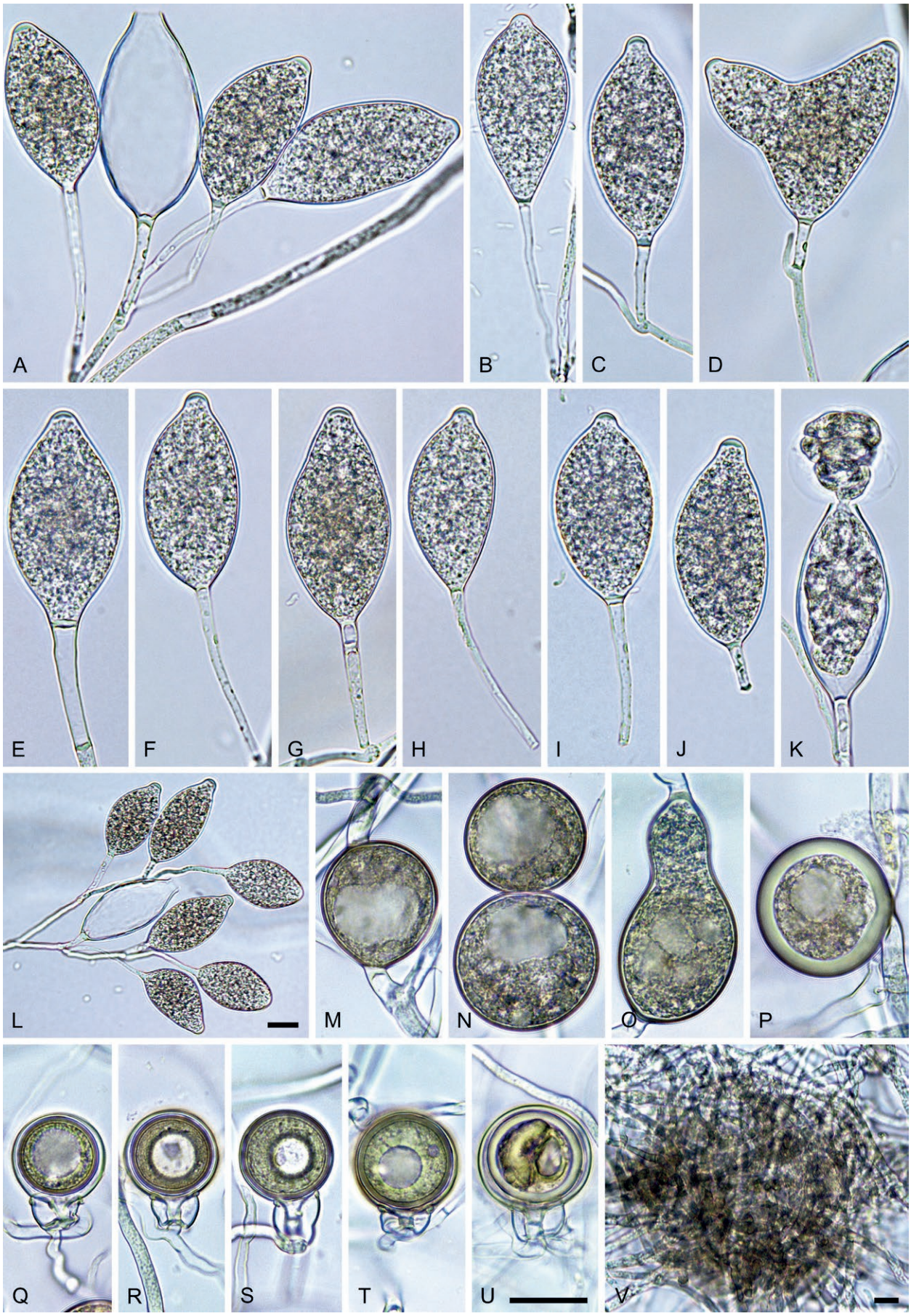

Fig. 35. *Phytophthora tropicalis*. **A–L.** Sporangia with medium-length to long pedicels, formed on V8-agar (V8A) in soil extract. **A–C, E–L.** Limoniform, pyriform, ovoid and obpyriform sporangia. **D.** Bilobed sporangium. **A–D, K, L.** External proliferation. **A, L.** Dense sporangial sympodia. **A, C–J.** Semipapillate and papillate apices. **B.** Nonpapillate apex. **H–J.** Caducous sporangia. **K.** Zoospore release. **M–O.** Thick-walled chlamydospores in V8A. **M, O.** Intercalary. **N.** Catenulate. **P.** Exteremely thick-walled sessile chlamydospore formed in carrot agar (fgCA) in mating test. **Q–U.** Globose oogonia with near-plerotic to plerotic oospores and amphigynous antheridia, formed in fgCA in mating tests. **U.** Aborted oospore. **V.** Hyphal aggregation in V8A. Images: A–C, F, H, J, L, M. NI122; D, G, K, V. NI174; E. NI148; I. NI166; N–P. SU663 × NI174; Q, U. PA112 × NI122; R–T. SU663 × NI174. Scale bars = 20 µm; U applies to A–K, M–U.

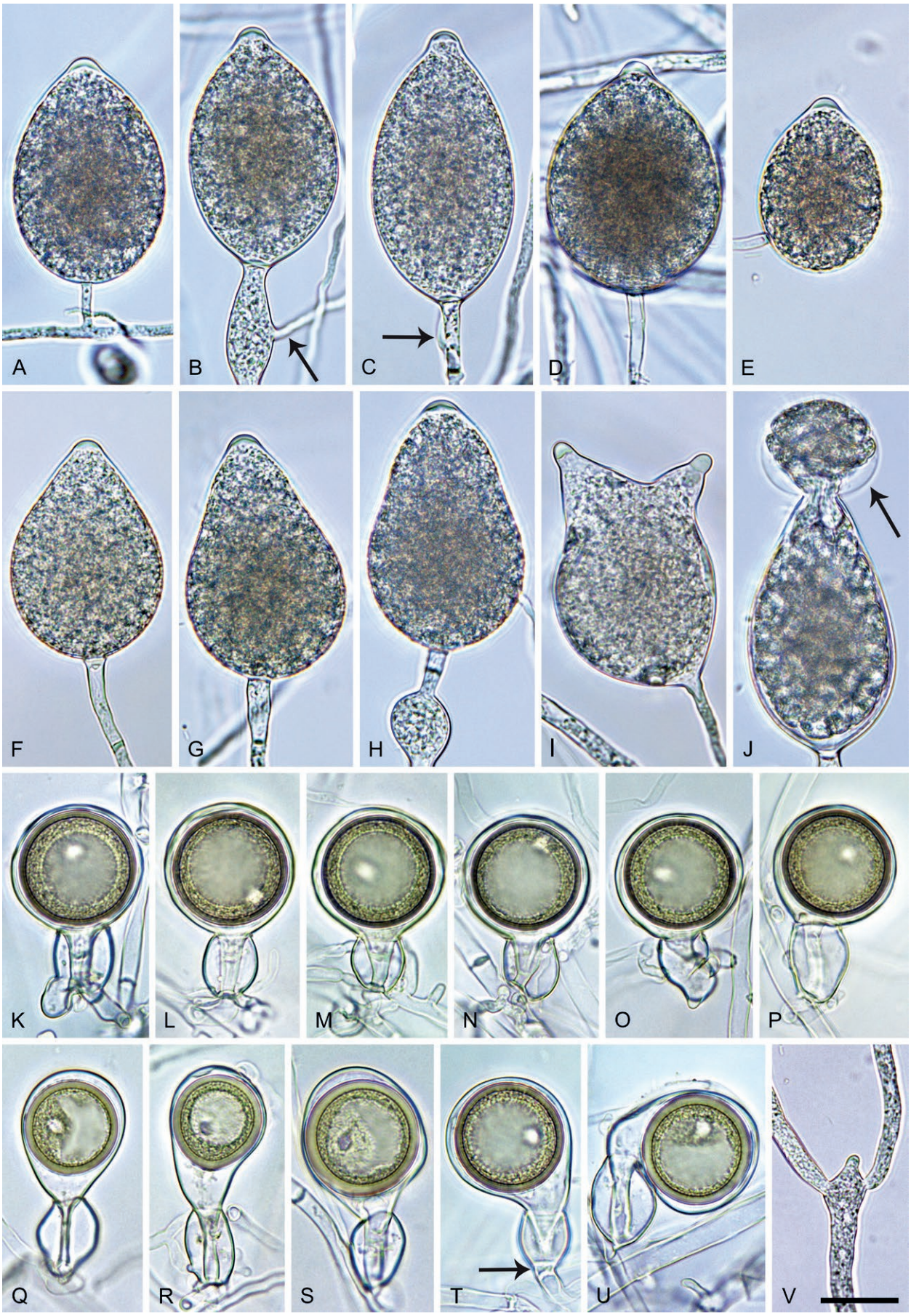

Fig. 36. *Phytophthora valdiviana*. **A–J.** Semipapillate and papillate sporangia formed on V8-agar (V8A) in soil extract. **A–H, J.** Ovoid, obpyriform and limoniform sporangia. **I.** Bipapillate sporangium. **C, D, F–H.** Short to medium-length pedicels. **B, C.** External proliferation (arrows). **H.** With hyphal swelling. **J.** Zoospore release into short-lived vesicle (arrow). **K–U.** Oogonia with slightly aplerotic to near-plerotic oospores and amphigynous antheridia, formed in V8A. **K–P.** Globose to subglobose oogonia. **Q–S.** Elongated oogonia with tapering funnel-like bases. **T, U.** Elongated comma-shaped oogonia. **T.** Bicellular antheridium with small basal cell (arrow). **V.** Sympodial hyphal branching. Images: A, D–G, J, K–P, T; Ex-type CBS 149504; B, C, I, R, S. CL158; H, V. CL159; Q, U. CL161. Scale bar = 20 µm; V applies to A–V.

dense or lax sympodia of 2–4 sporangia; papillate (51.5 %; Fig. 36A, D, E, I) or semipapillate (48.5 %; Fig. 36B, C, F–H), often with a pointed apex non-caducous, predominantly ovoid, broad ovoid or elongated ovoid (70 %; Fig. 36A–F, J), less frequently obpyriform to elongated obpyriform (15.2 %; Fig. 36G, H), distorted and often with two or three apices (6.8 %; Fig. 36I), ellipsoid (3.2 %), limoniform (2.8 %), subglobose (1.2 %) or ampulliform (0.8 %); lateral attachment of the sporangiophore (25.2 %; Fig. 36E, G–I) and pedicels (55.4 %; Fig. 36C, D, F–H) common; sporangial dimensions averaging 61.4 ± 10.4 × 38.4 ± 6.4 µm (overall range 31.0–101.0 × 17.8–54.2 µm; range of isolate means 58.0–65.3 × 35.3–43.4 µm) with a length/breadth ratio of 1.62 ± 0.28 (overall range 0.92–3.15); pedicel length 14.1 ± 6.1 µm (range 2.5–33.2 µm); sporangial proliferation exclusively external (Fig. 36B, C); sporangial germination indirectly with zoospores discharged through an exit pore of 3.8–9.4 µm (av. 6.9 ± 1.1 µm) into a short-lived vesicle (Fig. 36J). *Zoospores* limoniform to reniform whilst motile, becoming spherical (av. diam = 11.8 ± 2.4 µm) on encystment; cysts germinate mostly directly by producing hyphae or indirectly by releasing a secondary zoospore (diplanetism). *Hyphal swellings* infrequently produced on sporangiophores, usually close to the sporangial base, ovoid, subglobose or limoniform (Fig. 36B, H). *Chlamydospores* not observed. *Oogonia* abundantly produced in single culture ('homothallic' breeding system), (Fig. 36K–U); smooth-walled, globose to subglobose (68 %; Fig. 36K–P) or elongated (32 %; Fig. 36Q–U), often slightly bend to comma-shaped (29.6 %; Fig. 36P, T, U), with round (62.4 %; Fig. 36K–P) or long tapering, often funnel-like bases (37.6 %; Fig. 36Q–U) which sometimes become very thin (Fig. 36Q); av. oogonial diam 33.2 ± 3.5 µm with an overall range of 20.0–40.9 µm and a range of isolate means of 31.2–34.9 µm; slightly aplerotic to plerotic (Fig. 36K–P, R–U) or infrequently aplerotic (Fig. 36Q). *Oospores* globose to subglobose with a large lipid globule (Fig. 36K–U); av. diam 30.3 ± 2.9 µm with an overall range of 19.2–37.1 µm and a range of isolate means of 28.6–32.0 µm; wall diam 2.42 ± 0.3 µm (overall range 1.72–3.26 µm) and oospore wall index 0.41 ± 0.05; abortion 2–12 % (av. 6.2 %) after 4 wk. *Antheridia* amphigynous, cylindrical, limoniform, subglobose or irregular, predominantly unicellular (Fig. 36K–S, U) or rarely bicellular with the basal cell being very small (Fig. 33T), 19.0 ± 2.7 × 15.2 ± 1.5 µm. *Hyphae* often branch sympodially in a monochasium or dichasium with the bearing hypha ending with a short tip (Fig. 36V).

Culture characteristics: Colonies on V8A and CA submerged to appressed, faintly striate to radiate on V8A and faintly radiate on CA; on PDA dense felty-cottony with a petaloid pattern (Fig. 25).

Cardinal temperatures and growth rates: On V8A optimum 20.0 °C with 5.43 ± 0.38 mm/d radial growth, maximum 27.5–<30 °C, minimum <10 °C (Fig. 26), lethal temperature 30–32.5 °C. On CA and PDA at 20 °C 3.84 ± 0.35 mm/d and 2.86 ± 0.15 mm/d, respectively.

Additional materials examined: **Chile**, Valdivian region, Parque Oncol, isolated from a baiting leaf floating in a stream running through a Valdivian rainforest, Nov. 2014, *T. Jung, E. Sanfuentes von Stowasser & A. Durán* (CL158, CL159, CL160, CL161).

Phytophthora variepedicellata T. Jung, Y. Balci, K. Broders & I. Milenković, ***sp. nov.*** MycoBank MB 847299. Fig. 37.

Etymology: The name refers to the variable length of the sporangial pedicels.

Typus: **Panama**, Volcano Baru, isolated from a necrotic lesion on a naturally fallen leaf of a non-identified tree species collected from the ground in a tropical cloud forest, Nov. 2019, *K.D. Broders & Y. Balci* (**holotype** CBS H-25129, dried culture on V8A, ex-holotype living culture CBS 149505 = PA254).

Morphological structures on V8A: *Sporangia* common on solid agar and abundantly produced in non-sterile soil extract; borne terminally in dense or lax sympodia of 2–8 sporangia (98.4 %; Fig. 37K, M) or rarely intercalary (1.6 %; Fig. 37C, M); apices semipapillate (59.5 %; Fig. 37A, C–I, K) or papillate (40.5 %; Fig. 37B, J), sometimes slightly asymmetric or curved (9.2 %; Fig. 37K); mostly ovoid or elongated ovoid (59.6 %; Fig. 37B, C, M), limoniform to elongated-limoniform (19.4 %; Fig. 37D, E, J, M) or less frequently distorted usually with two apices (6.5 %; Fig. 37F, G); obpyriform to elongated obpyriform (5.3 %; Fig. 37A), pyriform or elongated-pyriform (3.9 %), ellipsoid (2.3 %; Fig. 37H), obovoid (1.3 %; Fig. 37I), ampulliform (1.2 %; Fig. 37M) or mouse-shaped (0.5 %; Fig. 37K); lateral attachment of sporangiophores (26.3 %; Fig. 37K, M), small vacuoles (43.7 %; Fig. 37D, F–H, J) and a conspicuous basal plug (95.9 %; Fig. 37B, D, E, G, I, J, L) common; mostly caducous with variable pedicel length ranging from 4.0 to 75.0 µm (96.7 %; av. 19.2 ± 10.0 µm) (Fig. 37H–L), sometimes two sporangia are shed together (Fig. 37K); sporangial proliferation exclusively external (Fig. 37A, D–G, K, M); sporangial dimensions averaging 42.4 ± 8.5 × 24.7 ± 3.2 µm (overall range 20.2–88.7 × 18.6–43.3 µm; range of isolate means 36.3–56.9 × 22.9–27.0 µm) with a length/breadth ratio of 1.72 ± 0.27 (overall range 0.63–2.64; sporangial germination indirectly with zoospores discharged through an exit pore 3.3–7.2 µm wide (av. 4.9 ± 0.8 µm) (Fig. 37L). *Zoospores* limoniform to reniform whilst motile, sometimes with ring-like flagella ends, becoming spherical (av. diam = 9.5 ± 1.2 µm) on encystment. *Hyphal swellings* rarely formed on sporangiophores, subglobose, limoniform or deltoid (Fig. 37M), 13.3 ± 1.9 µm. *Chlamydospores* not observed. *Oogonia* not observed in single cultures, but abundantly produced by all seven tested isolates in polycarbonate membrane mating tests with the A1 mating type isolate PA133 of *P. multiplex* ('heterothallic' breeding system; all tested isolates mating type A2); with short stalks, terminal on short to medium-length, sometimes curved lateral hyphae or sessile, smooth-walled, globose to slightly subglobose with a rounded base (Fig. 37N–V); oogonial diam 25.8 ± 2.8 µm (overall range 21.0–37.3 µm; range of isolate means 25.0–27.1 µm); nearly plerotic to plerotic (Fig. 37N–V). *Oospores* globose with a large lipid globule (Fig. 37N–V); mean diam 22.6 ± 2.3 µm (overall range 17.0–30.0 µm; range of isolate means 21.9–23.9 µm); wall thickness 1.32 ± 0.24 µm (overall range 0.78–2.15 µm), oospore wall index 0.31 ± 0.05; abortion 40–80 % (av. 56 %) after 4 wk. *Antheridia* almost exclusively amphigynous and cylindrical or subglobose, unicellular (Fig. 37N–U), but a few paragynous club-shaped antheridia were rarely observed (Fig. 37V); dimensions of amphigynous antheridia 17.6 ± 3.8 × 15.5 ± 1.9 µm. *Hyphal aggregations* observed in all isolates (Fig. 37W).

Culture characteristics: Colonies on V8A and CA submerged to appressed, radiate with a stellate centre and scanty aerial mycelium on V8A, and radiate with limited aerial mycelium on CA; dense-felty on PDA with a petaloid centre and a uniform margin (Fig. 25).

Cardinal temperatures and growth rates: On V8A optimum 27.5 °C with 8.72 ± 0.55 mm/d radial growth, maximum 27.5–30 °C (2 isolates) or 30–<32.5 °C (3 isolates), minimum <10 °C (Fig. 26),

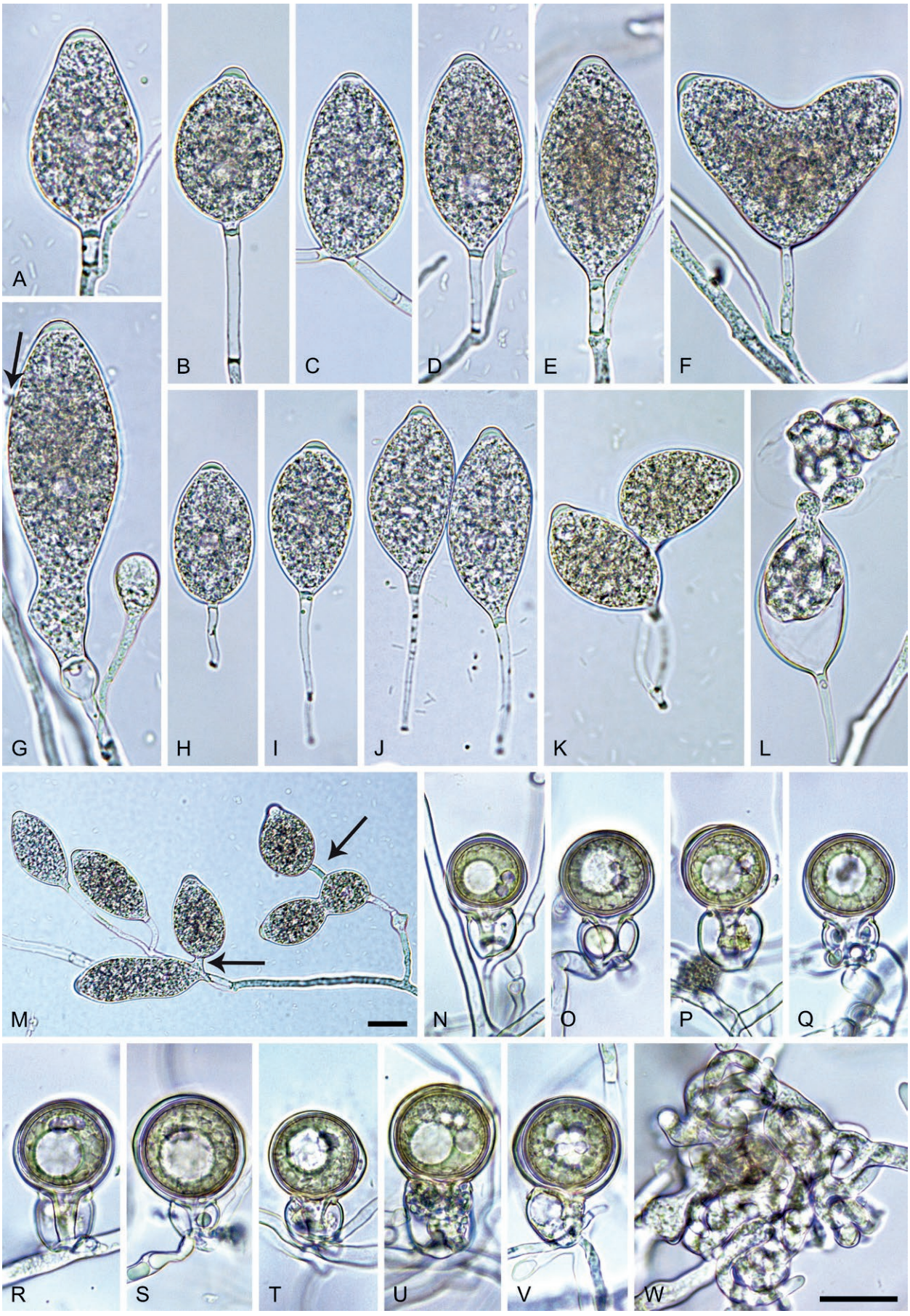

Fig. 37. *Phytophthora variepedicellata*. **A–M.** Sporangia with variable pedicel lengths, formed on V8-agar (V8A) in soil extract. **A–E, H–M.** Obpyriform, ovoid, limoniform, ellipsoid and mouse-shaped sporangia. **C.** Intercalary sporangium. **F.** Bilobed sporangium. **G.** Intercalary (arrow) distorted sporangium. **A, D–G.** External proliferation. **H–L.** Caducous sporangia. **L.** Zoospore release. **M.** Dense sporangial sympodium. **N–V.** Globose to subglobose oogonia with near-plerotic to plerotic oospores, formed in carrot agar in polycarbonate membrane mating tests. **N–U.** Unicellular amphigynous antheridia. **V.** Paragynous antheridium. **W.** Hyphal aggregation in V8A. Images: A, D, E, G, J, M, N, Q–S, V, W. Ex-type CBS 149505; B, C, H, I. PA241; F, K. PA268; L, O, P, T, U. PA264; Scale bars = 20 µm; W applies to A–L, N–W.

lethal temperature 32.5 °C. At 20 °C on V8A, CA and PDA 6.54 ± 0.68 mm/d, 4.7 ± 0.28 mm/d and 4.2 ± 0.63 mm/d, respectively.

Additional materials examined: **Panama**, Volcano Baru, isolated from necrotic lesions on naturally fallen leaves of a non-identified tree species collected from the ground in a tropical cloud forest, Nov. 2019, *K.D. Broders & Y. Balci* (PA241, PA242, PA253, PA264, PA267, PA268).

Notes on Clade 2b taxa: Across the nuclear (LSU, ITS, *βtub*, *hsp90*, *tigA*, *rpl10*, *tef-1α*, *enl*, *ras-ypt1*) 8 736-character alignment and the mitochondrial (*cox1*, *cox2*, *nadh1* and *rps10*) 3 156-character alignment pairwise sequence differences between the nine known and nine newly described species and three informally designated taxa in Clade 2b were 0.1–4.8 % and 0.1–4.8 %, respectively. In addition, the 13 Clade 2b taxa examined developed distinctive colony morphologies on V8A, CA and PDA at 20 °C (Figs 23–25). In addition, the nine new species are separated from each other and the other Clade 2b species by a combination of morphological (Figs 27–37) and physiological (Fig. 26) characters of which the most discriminating are highlighted in bold in Tables S7–S9.

Full sexual sterility clearly separates *P. theobromicola* from all other Clade 2b species (Tables S7–S9). Nine of the 18 Clade 2b species are self-fertile ('homothallic') and can be discriminated by a combination of morphological and physiological characters.

Phytophthora distorta can be distinguished from *P. amaranthi* by having a much lower degree of caducity (*ca.* 1.0 *vs.* 20–30 %), much thinner oospore walls (1.89 *vs.* 3.6 µm) and lower optimum and maximum temperatures for growth (20 and 27.5–30 °C *vs.* 24 and 32 °C) (Ann *et al.* 2016; Table S7); from *P. aysenensis* by producing both papillate and semipapillate sporangia which are on average considerably larger and sometimes caducous, the presence of hyphal swellings and by having predominantly aplerotic oospores with considerably thinner walls (1.89 *vs.* 3.2 µm) (Crous *et al.* 2020; Table S7; Fig. 28); from *P. gloveri* by the production of papillate sporangia, occasional caducity, on average smaller oogonia with almost exclusively amphigynous antheridia, the occurrence of hyphal swellings and a lower optimum temperature for growth (20 *vs.* 25 °C) (Abad *et al.* 2011; Table S7); from *P. mengei*, which has exclusively semipapillate persistent sporangia, by producing a considerable proportion of papillate sporangia, by occasional sporangial caducity, larger oogonia with almost exclusively aplerotic oospores, different antheridial insertion (amphigynous *vs.* paragynous) and slower growth between 15 and 27.5 °C (Hong *et al.* 2009; Tables S7, S8; Fig. 26); from *P. montana* by the production of papillate sporangia, occasional sporangial caducity, the absence of tapering oogonial bases, the much lower frequency of excentric, elongated or comma-shaped oogonia (2 *vs.* 19.5 %), mostly aplerotic oospores, lower optimum (20 *vs.* 25 °C) and slightly higher maximum temperature (27.5–30 *vs.* 25–27.5 °C) for growth and slower growth between 10 and 25 °C (Tables S7, S8; Figs 26, 28, 30); from *P. siskiyouensis* by the production of papillate sporangia, often in sympodia, the absence of paragynous antheridia, and having considerably lower optimum temperature for growth (20 *vs.* 27.5 °C) (Reeser *et al.* 2007; Tables S7, S8; Fig. 26); and from the co-occurring *P. valdiviana* by occasional sporangial caducity and by having a much higher proportion of distorted sporangia with often two apices (44 *vs.* 7 %), exclusively rounded non-tapering oogonial bases, much lower frequency of excentric, elongated or comma-shaped oogonia (2 *vs.* 32 %) and almost exclusively aplerotic oospores; (Tables S7, S9; Figs 28, 36). *Phytophthora frigidophila* differs from *P. distorta* by the absence of distorted sporangia with two apices, its much lower proportion of semipapillate sporangia (10.2 *vs.* 66.3 %), much higher oospore abortion rate (94 *vs.* 46 %) and slightly lower maximum temperature for growth (25–27.5 *vs.* 27.5–30 °C) (Table S7; Figs 26, 28, 29). Its low optimum temperature for growth of 20 °C separates *P. frigidophila* from *P. amaranthi*, *P. gloveri*, *P. mengei*, *P. montana* and *P. siskiyouensis* (Abad *et al.* 2011, Ann *et al.* 2016; Tables S7, S9; Fig. 26). In addition, *P. frigidophila* can be easily distinguished from all other seven self-fertile Clade 2b species by its predominant sporangial caducity (Reeser *et al.* 2007, Hong *et al.* 2009, Abad *et al.* 2011, Ann *et al.* 2016, Crous *et al.* 2020; Tables S7–S9; Figs 28–30, 36).

The production of dense sympodia with up to nine sporangia discriminates *P. montana* from *P. distorta*, *P. frigidophila*, *P. mengei*, *P. siskiyouensis* and *P. valdiviana*. In addition, *P. montana* has a lower proportion of pedicellate sporangia (19 %) than *P. distorta* (34 %), *P. frigidophila* (65 %) and *P. valdiviana* (55 %), and its lack of sporangial caducity distinguish it from *P. amaranthi*, *P. distorta*, *P. frigidophila* and *P. siskiyouensis* (Reeser *et al.* 2007, Hong *et al.* 2009, Ann *et al.* 2016; Tables S7–S9). *Phytophthora valdiviana* differs from all other self-fertile Clade 2b species except *P. montana* by its high proportion of oogonia with tapering bases (37.6 %) and elongated or comma-like shapes (32 %) (Reeser *et al.* 2007, Hong *et al.* 2009, Abad *et al.* 2011, Ann *et al.* 2016, Crous *et al.* 2020; Tables S7–S9; Figs 28–30, 36). Furthermore, it can easily be distinguished from *P. amaranthi*, *P. gloveri*, *P. mengei*, *P. montana* and *P. siskiyouensis* by its lower optimum temperature for growth of 20 °C (Abad *et al.* 2011, Ann *et al.* 2016; Tables S7–S9; Fig. 26).

Eight species and *P.* taxon pseudocapsici from Clade 2b share an A1/A2 ('heterothallic') breeding system and can be discriminated by a combination of morphological and physiological characters. The morphometric data, morphological characters and cardinal temperatures of the 12 isolates of *P. tropicalis* examined in this study were largely congruent with the original description by Aragaki & Uchida (2001) except for the sporangial apices which were a blurred transition between semipapillate and papillate (95.1 %) or nonpapillate (4.9 %) rather than exclusively papillate, and having on average considerably shorter sporangial pedicels (34 *vs.* 87 µm) in this study (Table S9; Fig. 35). It is noteworthy, that all 12 isolates examined in this study had a functional A1/A2 breeding system (six isolates A1, six isolates A2) in contrast to the 53 isolates examined in the study of Aragaki & Uchida (2001) of which eight were found to be A1, one A2 and 44 isolates were fully sterile. For comparisons with the five newly described A1/A2 Clade 2b species, the *P. tropicalis* data from the present study will be used.

The *P. capsici* - *P. mexicana* species complex remains unresolved and further multigene phylogenetic and phenotypic studies of a high number of isolates, representing a wide range of host plants, geographical locations and all electrophoretic types of the isozyme study of Mchau & Coffey (1995), will be needed to define and characterise the species in the complex. In the isozyme population study of Mchau & Coffey (1995), the ex-type isolate of *P. capsici* and ex-epitype isolate WPC P646 of *P. mexicana* and a high number of isolates designated as *P. capsici* grouped as electrophoretic types ET4 and ET15, respectively, within the diverse isozyme group CapA comprising 18 different electrophoretic types. In our multigene phylogenetic analysis, the *P. capsici* ex-type resided separately from a group including *P. mexicana* and several isolates designated as *P. capsici* or *P.* aff. *capsici* and another distinct group designated here as *P.* taxon pseudocapsici which included isolates from Sumatra and one old isolate from Mexico (CBS 370.72 = WPC P6190), previously designated as *P.*

capsici in Mchau & Coffey (1995), where it belonged to ET4 like the *P. capsici* ex-type, and in the multigene phylogeny of Yang *et al.* (2017). Either the whole complex has to be considered as one genetically and phenotypically highly variable species which would then be named *P. capsici*, which due to its earlier description in 1922 would have priority over *P. mexicana* (described in 1923); or many isolates currently designated as *P. capsici* would have to be re-designated as *P. mexicana* or described as one or two separate species more closely related to *P. mexicana* than *P. capsici*, and *P.* taxon pseudocapsici be erected to species status. For the phenotypic comparisons of the new A1/A2 Clade 2b species with known species, the data of CapA from Mchau & Coffey (1995) but without isolates WPC P646 and WPC P6190 will be used for *P. capsici*.

Phytophthora calidophila can be discriminated from *P. multiplex*, *P. obovoidea*, *P. pyriformis* and *P. tropicalis* by producing a comparatively high proportion of sporangia with semipapillate (38 %) or nonpapillate (25 %) apices (Tables S7–S9; Figs 27, 31, 33–35). In addition, *P. calidophila* differs from *P. capsici* in having considerably shorter pedicels (on average 24.3 *vs.* 78.4 µm), smaller oogonia and an inability to grow at 35 °C (Mchau & Coffey 1995; Table S7; Fig. 24); from *P. mexicana s. str.*, *P. multiplex* and *P. theobromicola* by producing caducous sporangia (Erwin & Ribeiro 1996; Decloquement *et al.* 2021; Tables S7–S9); from *P. multiplex*, *P. pyriformis* and *P. tropicalis* by having a much higher proportion of oogonia with tapering bases (Tables S7–S9; Figs 27, 32, 34, 35); and from *P. variepedicellata* by its high proportion of oogonia with tapering bases (57.4 *vs.* 0 %) and its higher maximum temperature (32.5–<35 *vs.* 27.5–32.5 ° C) (Tables S7, S9; Figs 26, 27, 37). *Phytophthora obovoidea*, previously informally designated as *P.* taxon tropicalis-like 2 (Jung *et al.* 2020), can be distinguished from *P. calidophila* by producing chlamydospores and dense sympodia with up to 10 sporangia and by almost exclusively having rounded oogonial bases (Tables S7, S8; Figs 27, 33); from *P. pyriformis* by having a lower proportion of papillate (77 *vs.* 91 %), pyriform (3 *vs.* 34 %) and pedicellate sporangia (84 *vs.* >99 %), on average shorter pedicel length (30.2 *vs.* 62.5 µm), often higher numbers of sporangia per sympodium (max. 10 *vs.* max. 6) and higher optimum temperature for growth (30 *vs.* 27.5 °C); from *P. tropicalis* by producing mostly papillate sporangia (77.4 %) with a higher proportion of obovoid shapes (25 *vs.* 7 %) and a lower frequency of pedicels (84 *vs*. 99 %), and slightly higher optimum temperature for growth (30 *vs*. 27.5–30 °C); and from *P. variepedicellata* by having larger sporangia (52 *vs*. 42 µm) which are more often papillate (77 *vs*. 41 %), the production of chlamydospores and higher optimum and maximum temperatures for growth (Tables S7–S9; Figs 26, 33–35, 37). *Phytophthora* taxon pseudocapsici has considerably longer sporangia than both *P. capsici* and *P. mexicana* (58 *vs.* 46 and 45 µm) and differs from *P. mexicana* by having caducous sporangia (Tables S7–S9; Mchau & Coffey 1995, Erwin & Ribeiro 1996). *Phytophthora pyriformis* is differentiated from all other Clade 2b species by its inability to grow at 10 °C (Fig. 26), and from all other A1/A2 Clade 2b species by having the highest proportion of pyriform sporangia (33 %) and the fastest growth at 25 °C (Tables S7–S9; Figs 26, 27, 31, 33–35, 37); and from all other A1/A2 Clade 2b species except *P. capsici* by having on average the longest sporangial pedicels (Tables S7–S9; Figs 27, 31, 33–35, 37). *Phytophthora variepedicellata* has on average the smallest sporangia of all A1/A2 Clade 2b species. In addition, its high proportion (59.5 %) of semipapillate sporangia separates *P. variepedicellata* from *P. obovoidea*, *P. pyriformis*, *P. tropicalis* and *P. multiplex* (Tables S7–S9; Figs 31, 33–35, 37).

A lack of sporangial caducity discriminates *P. mexicana*, *P. multiplex* and *P. theobromicola* from the caducous airborne *P. calidophila*, *P. capsici*, *P. obovoidea*, *P. pyriformis*, *P. tropicalis*, *P. variepedicellata* and *P.* taxon pseudocapsici (Erwin & Ribeiro 1996, Decloquement *et al.* 2021; Tables S7–S9; Figs 27, 31, 33–35, 37). In addition, *P. multiplex* differs from its closest relative, the sterile *P. theobromicola*, by its functional A1/A2 breeding system with both A1 and A2 isolates; in producing on average larger chlamydospores (48 *vs*. 30 µm) and larger sporangia (60 × 37 *vs*. 52 × 35.5 µm) with a slightly higher l/b ratio (1.63 *vs.* 1.5), mostly in dense sympodia with up to 14 sporangia instead of simple sporangiophores as in *P. theobromicola*, and by having a higher optimum temperature for growth (27.5 *vs.* 20–25 °C) (Decloquement *et al.* 2021; Tables S8, S9; Figs 31, 32).

Clade 2c

For all Clade 2c species included in this study colony morphologies on CA, PDA and V8A and temperature-growth relations on V8A are presented in Figs 38–43. Morphological and physiological characters and morphometric data of the nine known and 15 newly described species in Clade 2c are given in the comprehensive Tables S10–S13.

Phytophthora balkanensis I. Milenković, Ž. Tomić, T. Jung & M. Horta Jung, ***sp. nov.*** MycoBank MB 847307. Fig. 44.

Etymology: The name refers to the occurrence in natural forests in the Balkans.

Typus: **Bosnia and Herzegovina**, Teslić municipality, isolated from rhizosphere soil of *Alnus glutinosa* in a riparian forest, May 2019, *I. Milenković* (**holotype** CBS H-25099, dried culture on V8A, ex-holotype living culture CBS 149477 = BN286).

Morphological structures on V8A: Sporangia rarely observed on solid agar but produced abundantly in non-sterile soil extract; typically borne terminally in dense or lax sympodia of 2–8 sporangia (Fig. 44N) or on unbranched sporangiophores (Fig. 44E); non-caducous, predominantly ovoid, broad-ovoid or elongated ovoid (60.7 %; Fig. 44A–D, K, L, N), less frequently ellipsoid to elongated-ellipsoid (17.1 %; Fig. 44F, G, J), limoniform to elongated limoniform (9.7 %; Fig. 44H), distorted and often with two or three apices (9 %; Fig. 44I, M, N), obpyriform to elongated-obpyriform (2.1 %; Fig. 44E), obovoid (1 %) or pyriform (0.4 %); apices predominantly semipapillate (98 %; Fig. 44A–I) or rarely nonpapillate (2 %; Fig. 44M); lateral attachment of the sporangiophore (6.8 %; Fig. 44B) and pedicels (28 %; Fig. 44A–C, F–H, J) commonly observed; sporangial proliferation exclusively external (Fig. 44A, C, D, H, N); sporangial dimensions averaging 55.5 ± 7.4 × 34.7 ± 4.7 µm (overall range 37.2–79.5 × 23.0–53.2 µm; range of isolate means 50.7–59.7 × 33.2–37.8 µm) with a length/breadth ratio of 1.61 ± 0.18 (overall range 1.2–2.16); pedicel length 21.2 ± 11.9 µm (range 2.2–53.6 µm); sporangial germination usually indirectly with zoospores discharged through an exit pore 4.9–11.4 µm wide (av. 7.9 ± 1.2 µm) (Fig. 44K, L). *Zoospores* limoniform to reniform whilst motile, sometimes with ring-like flagella ends (Fig. 44L), becoming spherical (av. diam = 10.7 ± 0.8 µm) on encystment; cysts germinating directly. *Hyphal swellings* rarely produced in water on sporangiophores and hyphae; globose to subglobose or limoniform. *Chlamydospores* not observed. *Oogonia* abundantly produced in single culture ('homothallic' breeding system), terminal on short to medium-length, often curved lateral hyphae or sessile,

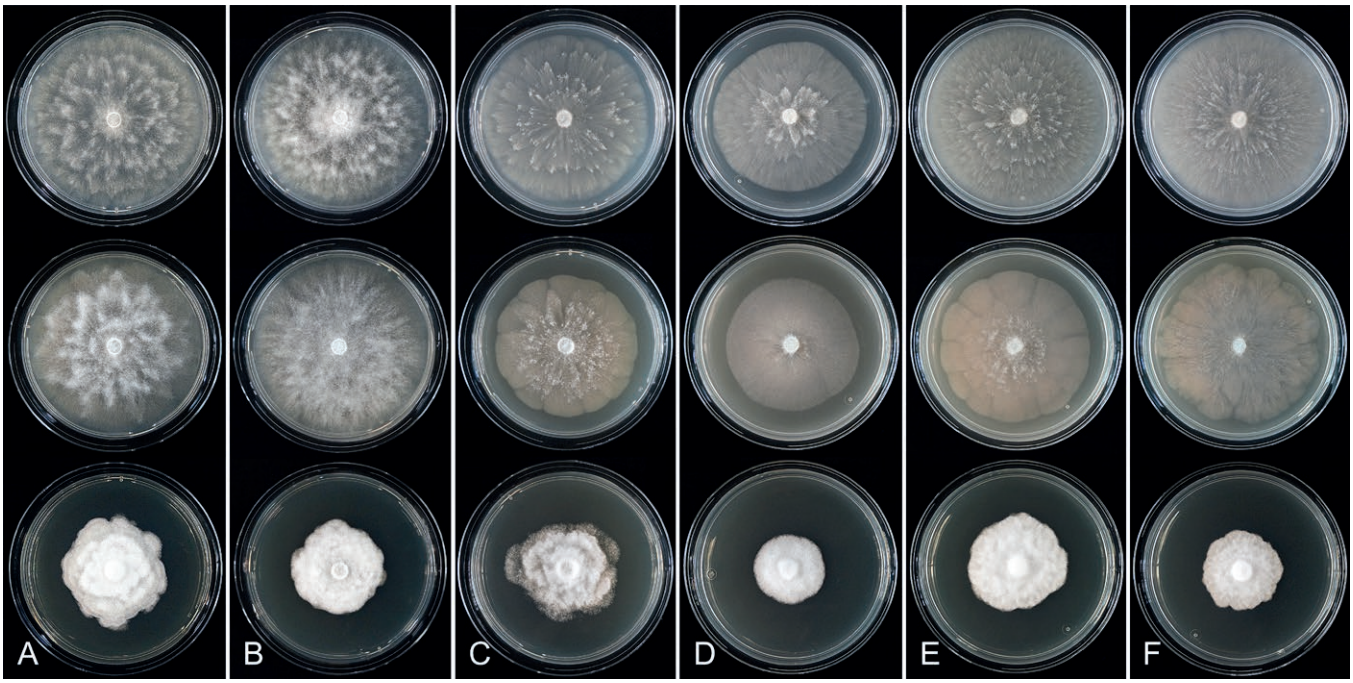

Fig. 38. Colony morphology of *Phytophthora* species from subclade 2c after 7 d growth at 20 ºC on V8-agar, carrot juice agar and potato-dextrose agar (from top to bottom). **A.** *Phytophthora acerina* (ex-type CBS 133931). **B.** *Phytophthora balkanensis* (ex-type CBS 149477). **C.** *Phytophthora catenulata* (ex-type CBS 149480). **D.** *Phytophthora curvata* (ex-type CBS 149482). **E.** *Phytophthora excentrica* (ex-type CBS 149483). **F.** *Phytophthora falcata* (ex-type CBS 149484).

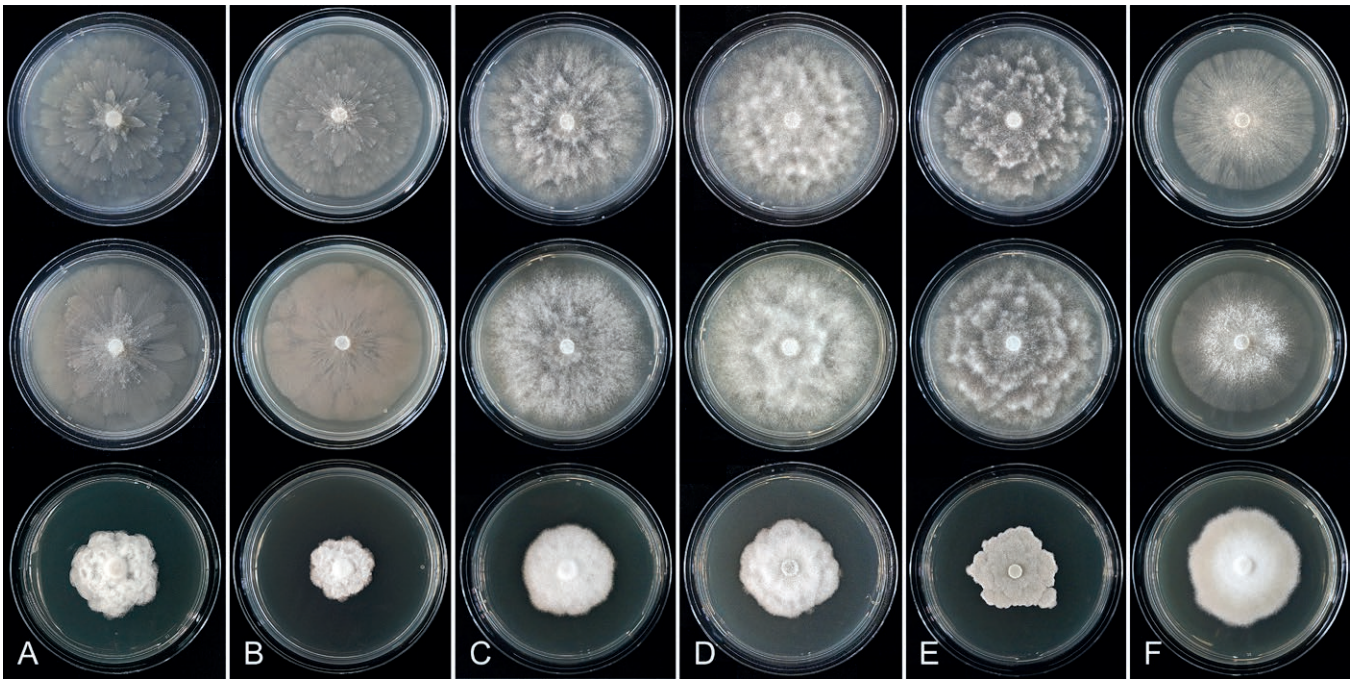

Fig. 39. Colony morphology of *Phytophthora* species from subclade 2c after 7 d growth at 20 ºC on V8-agar, carrot juice agar and potato-dextrose agar (from top to bottom). **A.** *Phytophthora fansipanensis* (ex-type CBS 149485). **B.** *Phytophthora japonensis* (ex-type CBS 149489). **C, D.** *Phytophthora limosa* (C. ex-type CBS 149490; D. LU083). **E.** *Phytophthora macroglobulosa* (ex-type CBS 149491). **F.** *Phytophthora multivora* (ex-type CBS 124094).

smooth-walled, globose to slightly subglobose (87 %; Fig. 44O–R, U), sometimes slightly excentric (Fig. 44P, U), or slightly elongated (13 %; Fig. 44S, T), with a rounded (89.5 %; Fig. 44O–Q, S–U) or a short tapering base (10.5 %; Fig. 44R); oogonial diam 30.1 ± 3.0 µm (overall range 17.3–35.9 µm; range of isolate means 28.9–31.0 µm); slightly aplerotic to aplerotic (64 %; Fig. 44P, R–U) or nearly plerotic (36 %; Fig. 44O, Q). *Oospores* globose with a large lipid globule (Fig. 44O–U); diam 26.5 ± 2.5 µm (overall range 14.4–31.6 µm; range of isolate means 25.6–27.2 µm) wall thickness 1.55 ± 0.27 µm (overall range 0.69–2.39 µm), oospore wall index 0.31 ± 0.04; abortion rate 2–18 % (av. 8 %) after 4 wk. *Antheridia* predominantly paragynous and club-shaped, ovoid or subglobose (99.5 %; Fig. 44O–T) or rarely amphigynous and cylindrical (0.5 %; Fig. 44U); infrequently two antheridia attached to one oogonium (6.4 %; Fig. 44O, S); dimensions 12.3 ± 2.7 × 8.2 ± 1.4 µm.

Culture characteristics: Colonies on V8A and CA appressed with limited aerial mycelium, chrysanthemum-like on V8A and faintly radiate on CA; on PDA dense-felty to felty-cottony with a faint petaloid pattern (Fig. 38).

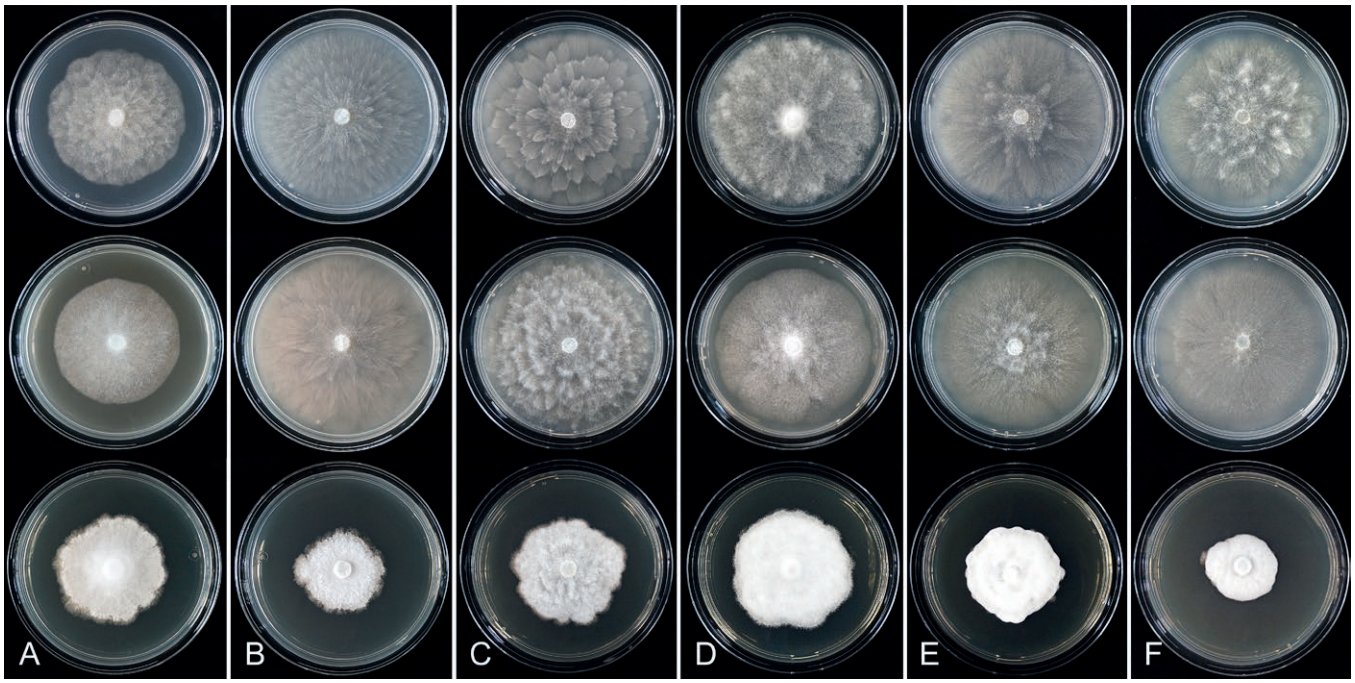

Fig. 40. Colony morphology of *Phytophthora* species from subclade 2c after 7 d growth at 20 °C on V8-agar, carrot juice agar and potato-dextrose agar (from top to bottom). **A.** *Phytophthora nimia* (ex-type CBS 149494). **B.** *Phytophthora oblonga* (ex-type CBS 149495). **C.** *Phytophthora obturata* (ex-type CBS 149496). **D.** *Phytophthora pachypleura* (ex-type IMI 502404). **E, F.** *Phytophthora platani* (E. ex-type CBS 149638; F. TJ1492).

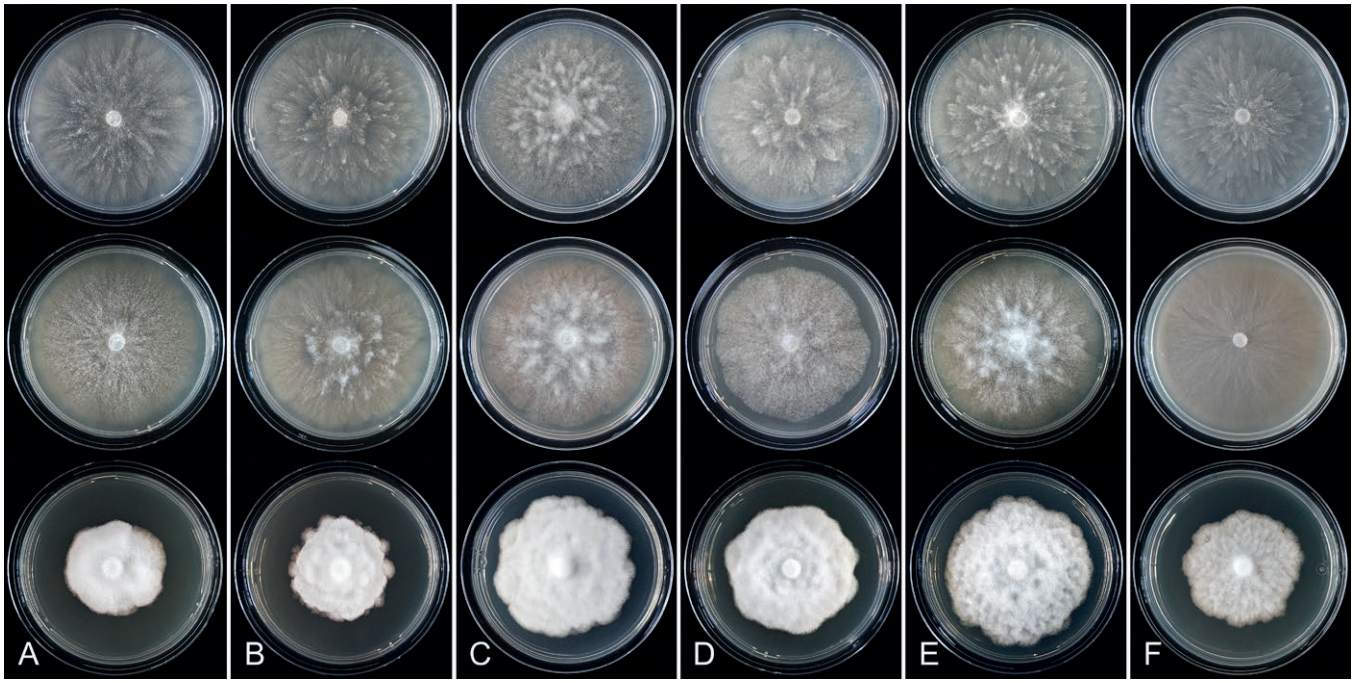

Fig. 41. Colony morphology of *Phytophthora* species from subclade 2c after 7 d growth at 20 °C on V8-agar, carrot juice agar and potato-dextrose agar (from top to bottom). **A.** *Phytophthora pini* (isolate SFB183). **B.** *Phytophthora plurivora* (ex-type CBS 124093). **C–E**. *Phytophthora pseudocapensis* (C. ex-type CBS 150638; D. JV027; E. VN079). **F.** *Phytophthora vacuola* (ex-type CBS 149503).

Cardinal temperatures and growth rates: On V8A optimum 25 °C with 8.65 ± 0.17 mm/d radial growth, maximum 30–<32.5 °C, minimum <10 °C (Fig. 42), lethal temperature 32.5–35 °C. At 20 °C on V8A, CA and PDA 7.71 ± 0.2 mm/d, 5.96 ± 0.13 mm/d and 2.89 ± 0.23 mm/d, respectively.

Additional materials examined: **Bosnia and Herzegovina**, Teslić municipality, isolated from rhizosphere soil of *Alnus glutinosa* in a riparian forest, May 2019, *I. Milenković* (BN289); Ozren Mountain, isolated from a small stream running through a mixed oak forest, May 2019, *I. Milenković* (BN117). **Serbia**, Željin Mountain, isolated from a small stream running through a natural *Fagus sylvatica* forest, May 2017, *I. Milenković* (SFB880). **Croatia**, Zagreb, isolated from nursery-grown *Rubus fruticosus* seedling, Mar. 2017, *Ž. Tomić* (TJ546).

Phytophthora catenulata T. Jung, T.-T. Chang, N.M. Chi & M. Horta Jung, ***sp. nov.*** MycoBank MB 847308. Fig. 45.

Etymology: The name refers to the catenulate swellings formed in water on sporangiophores and hyphae.

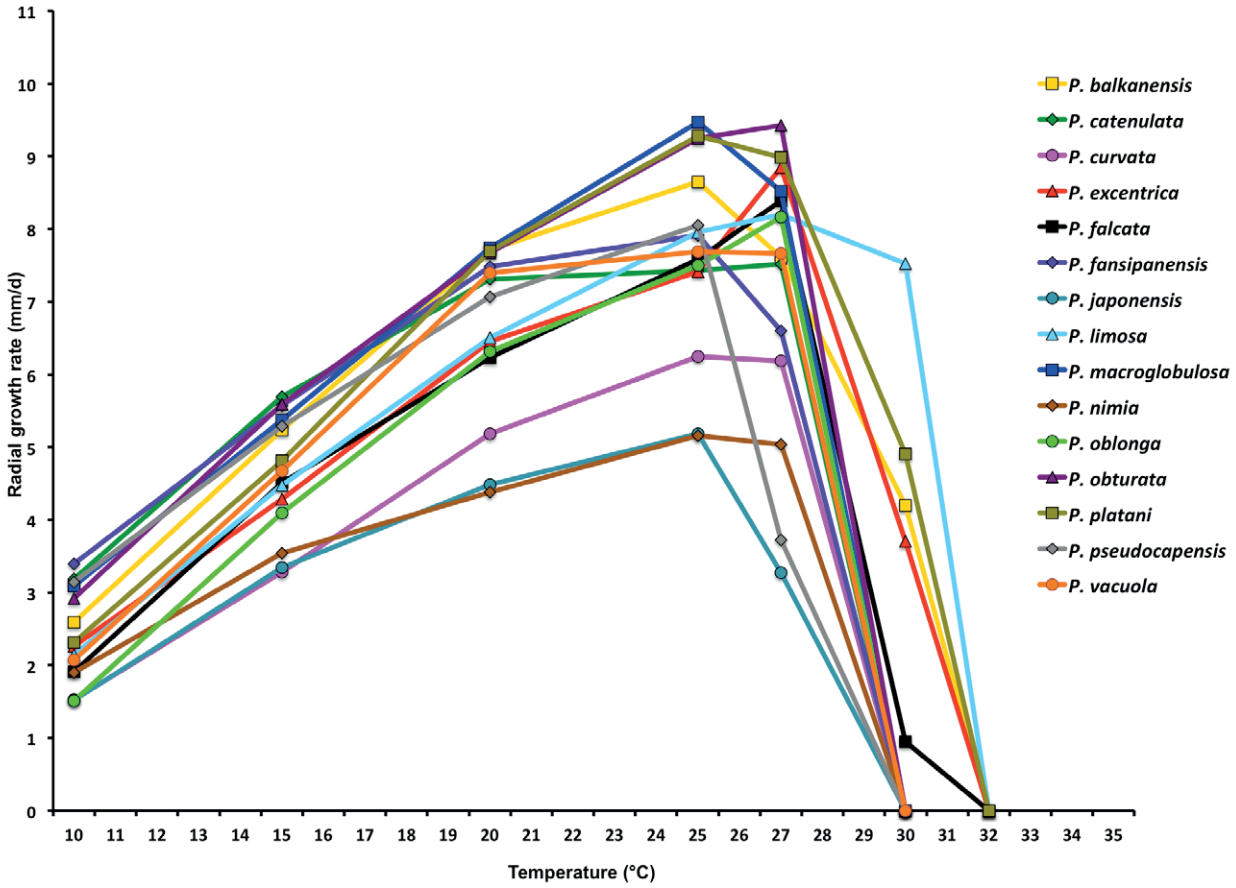

Fig. 42. Mean radial growth rates of 15 new *Phytophthora* species from subclade 2c on V8-agar at different temperatures: *P. balkanensis* (8 isolates); *P. catenulata* (10 isolates); *P. curvata* (3 isolates); *P. excentrica* (2 isolates); *P. falcata* (7 isolates); *P. fansipanensis* (5 isolates); *P. japonica* (4 isolates); *P. limosa* (5 isolates); *P. macroglobulosa* (4 isolates); *P. nimia* (4 isolates); *P. oblonga* (4 isolates); *P. obturata* (8 isolates); *P. platani* (11 isolates); *P. pseudocapensis* (11 isolates); *P. vacuola* (2 isolates).

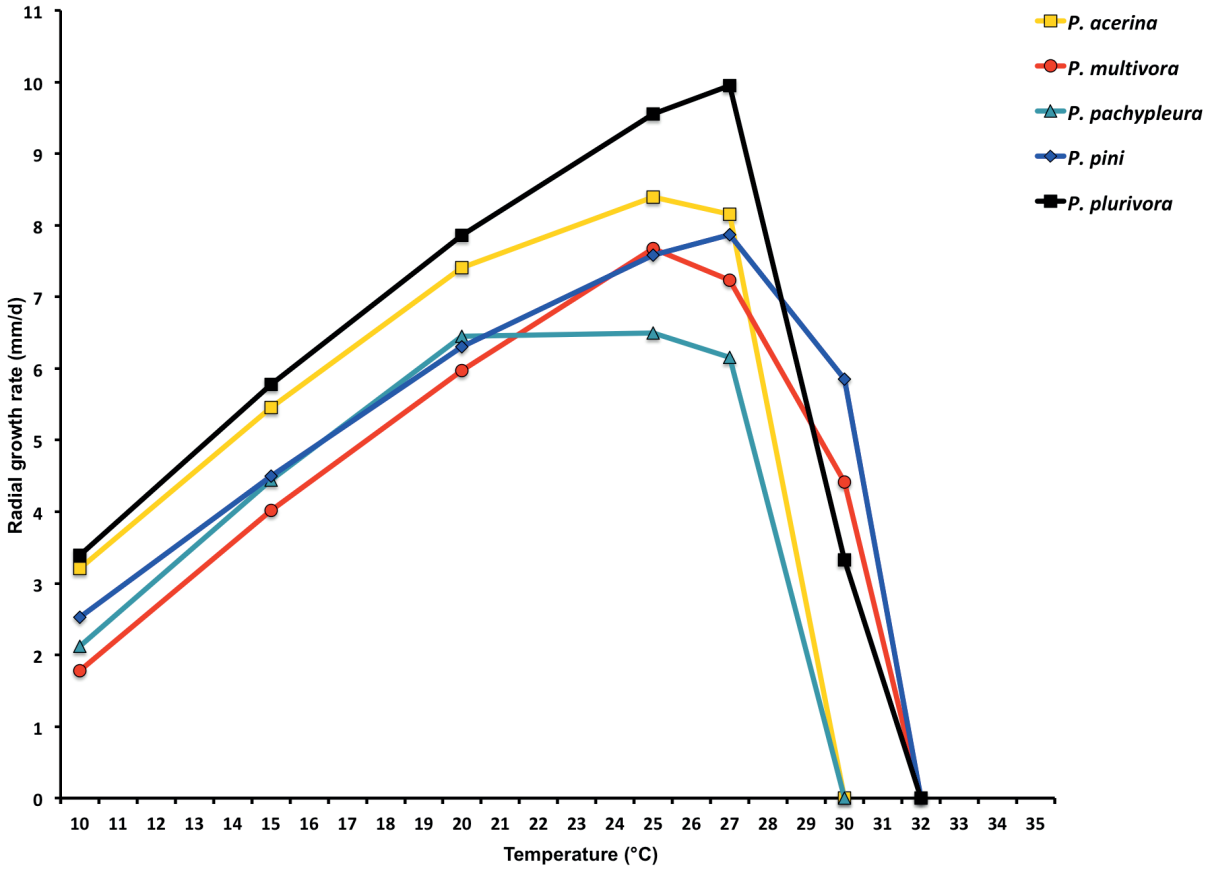

Fig. 43. Mean radial growth rates of five known *Phytophthora* species from subclade 2c on V8-agar at different temperatures: *P. acerina* (1 isolate); *P. multivora* (1 isolate); *P. pachypleura* (1 isolate); *P. pini* (7 isolates); *P. plurivora* (2 isolates).

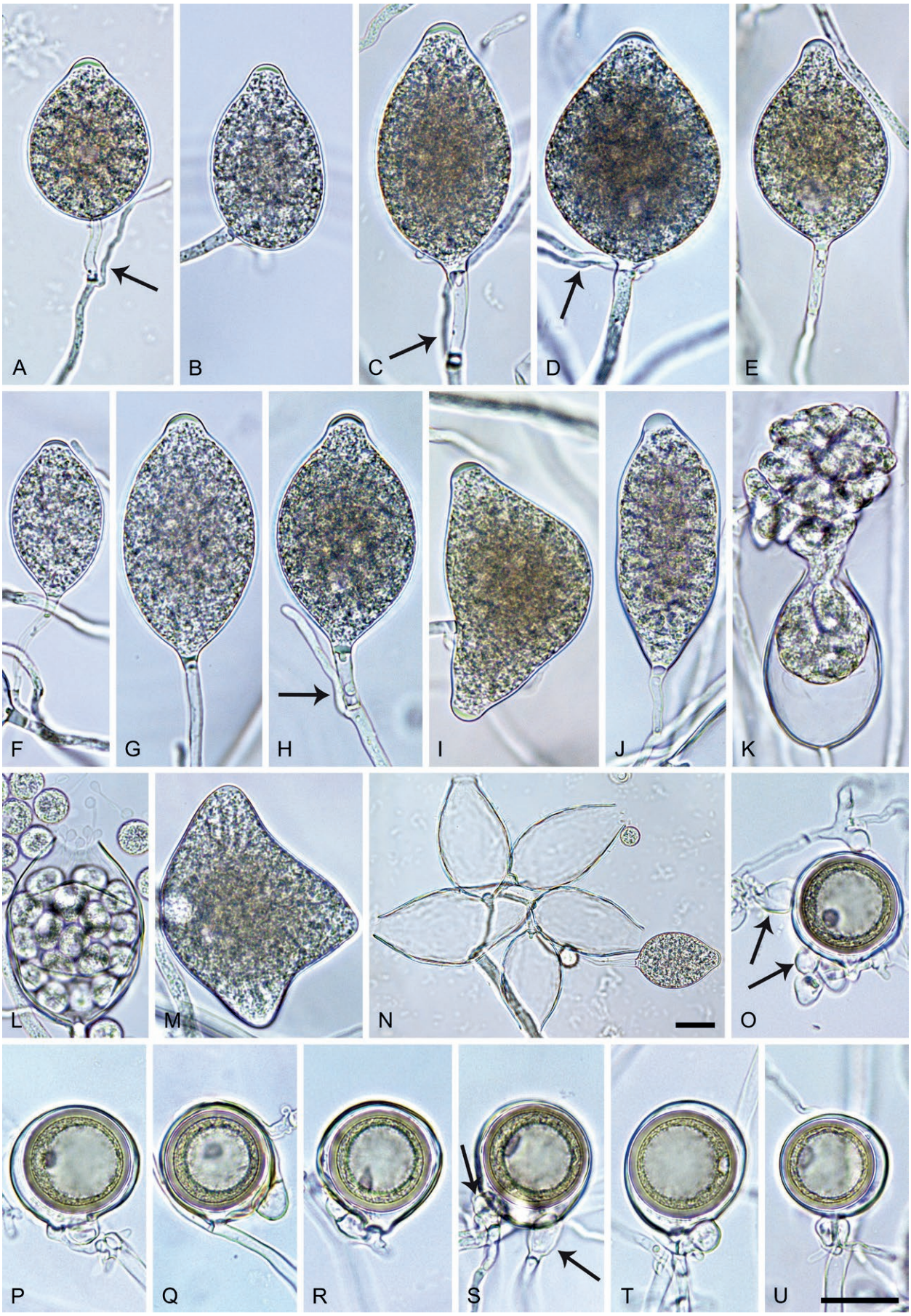

Fig. 44. *Phytophthora balkanensis*. **A–N.** Persistent sporangia formed on V8-agar (V8A) in soil extract. **A–H, J–L, N.** Ovoid, obpyriform, limoniform and ellipsoid sporangia. **A–I.** Sporangia with flat semipapillate apices. A, C, D, H. External proliferation (arrows). A, C, E**–H.** Medium-length to long pedicels. I. Bilobed sporangium. J. Swollen apex before zoospore release. K, L. Zoospore release. L. Ring-like zoospore flagella ends. M. Trilobed nonpapillate sporangium. **N.** Dense sporangial sympodium. **O–U.** Subglobose, slightly elongated or slightly excentric oogonia with near-plerotic to slightly aplerotic oospores, formed in V8A. **O–T.** Paragynous antheridia. **O, S.** Two antheridia (arrows). **U.** Amphigynous antheridium. Images: A, D, L, R, T, U. TJ546; B, E–K, N, O–Q, S. Ex-type CBS 149477; C, M. BN117. Scale bars = 20 µm; U applies to A–M, O–U.

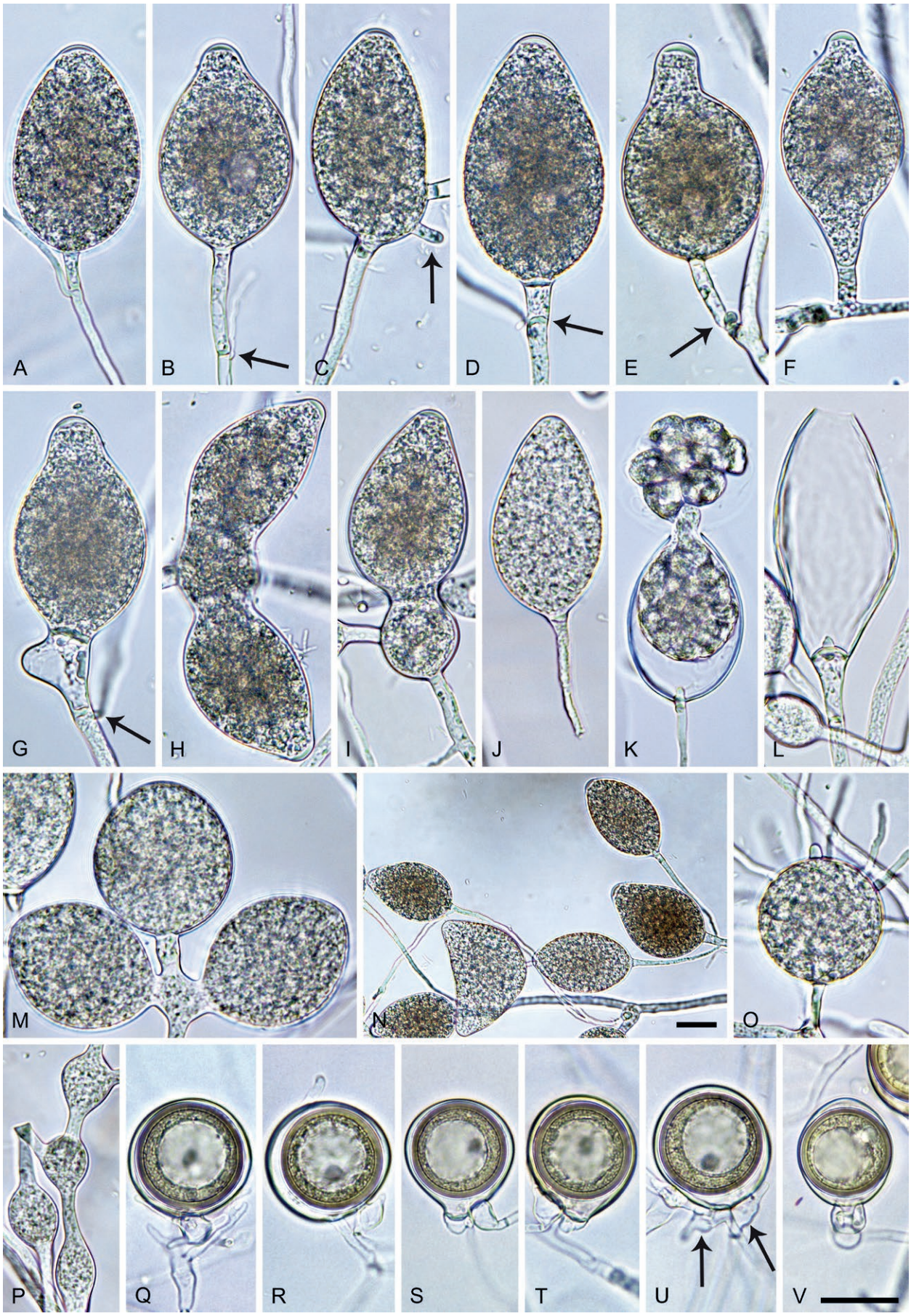

Fig. 45. *Phytophthora catenulata*. **A–N.** Sporangia formed on V8-agar (V8A) in soil extract. **A–G, I–L, N.** Ovoid, obpyriform, limoniform, ampulliform and ellipsoid sporangia. **A–I.** Flat semipapillate apices. **A, B, D, E, G, J.** Pedicels (arrows in D, E). **A, B, D, E, G, I.** External proliferation (arrows in B, G). **C.** Intercalary sporangium with hyphal appendix (arrow). **H.** Bilobed intercalary sporangium. **J.** Caducous sporangium. **K.** Zoospore release. **M.** Developing sporangial sympodium. **N.** Sporangial sympodium. **O, P.** Hyphal swellings in water. **O.** Radiating hyphae. **P.** Catenulate. **Q–V.** Oogonia with near-plerotic to aplerotic oospores, formed in V8A. **Q–U.** Paragynous antheridia. **V.** Amphigynous antheridium. Images: A, C, E, H, K, N–P, Q, R, V. Ex-type CBS 149480; B, D, F, G, J, L, M, S–U. VN367; I. VN1011. Scale bars = 20 µm; V applies to A–M, O–V.

Typus: **Taiwan**, Tunyuan, isolated from rhizosphere soil of *Quercus variabilis* in a montane, temperate, seasonally dry *Quercus–Pinus* forest, Mar. 2013, *T. Jung, T.-T. Chang & M. Horta Jung* (**holotype** CBS H-25102, dried culture on V8A, ex-holotype living culture CBS 149480 = TW115).

Morphological structures on V8A: Sporangia rarely observed on solid agar but produced abundantly in non-sterile soil extract; typically borne terminally (96.4 %) in dense or lax sympodia of 2–8 sporangia (Fig. 45M, N) or rarely on unbranched sporangiophores, or intercalary (3.6 %; Fig. 45C, H, I); predominantly ovoid, broad-ovoid or elongated ovoid (75.4 %; Fig. 45A–D, J, K, N), less frequently limoniform to elongated limoniform (10.9 %; Fig. 45F, L), ellipsoid to elongated-ellipsoid (5.5 %; Fig. 45N), obpyriform to elongated-obpyriform (4.3 %; Fig. 45E, G), obovoid (2 %), subglobose (0.5 %), ampulliform (0.4 %; Fig. 45I), sickle-shaped (0.4 %), distorted and usually with two apices (0.4 %; Fig. 45H) or pyriform (0.2 %) ; apices predominantly semipapillate (97 %; Fig. 45A–I) or rarely nonpapillate (3 %; Fig. 45J); lateral attachment of the sporangiophore (15.3 %), pedicels (34 %; Fig. 45A, B, D, E, G, J, L), an asymmetric apex (13.6 %; Fig. 45E) and a conspicuous basal plug protruding into the empty sporangium (28.5 %; Fig. 45K, L) commonly observed; sporangial caducity rare (<1 %; Fig. 45J); sporangial proliferation almost exclusively external (Fig. 45A, B, D, E, G, I, N) or infrequently by a sporangiophore emerging laterally from a sporangium (Fig. 45I); sporangial dimensions averaging 57.4 ± 6.8 × 35.7 ± 4.3 µm (overall range 34.0–85.5 × 18.7–47.3 µm; range of isolate means 53.6–64.4 × 32.5–39.4 µm) with a length/breadth ratio of 1.62 ± 0.19 (overall range 1.14–2.54); pedicel length 15.3 ± 8.7 µm; sporangial germination usually indirectly with zoospores discharged through an exit pore 4.5–15.6 µm wide (av. 8.4 ± 1.2 µm) (Fig. 45K, L). *Zoospores* limoniform to reniform whilst motile, becoming spherical (av. Diam = 10.3 ± 1.3 µm) on encystment; mostly germinating directly although diplanetism occurred in all isolates. *Hyphal swellings* abundantly produced in water on sporangiophores and hyphae; globose to subglobose, often with radiating hyphae (Fig. 45O), or limoniform to deltoid and often catenulate (Fig. 45P); dimensions 13.9 ± 4.5 µm (range 6.1–29.7 µm). *Chlamydospores* not observed. *Oogonia* abundantly produced in single culture ('homothallic' breeding system), terminal on short to medium-length, often curved lateral hyphae, smooth-walled, globose to slightly subglobose (86.7 %; Fig. 45Q–U), sometimes slightly excentric (Fig. 45R, U), or slightly elongated (13.3 %; Fig. 45V), with a rounded (93.7 %; Fig. 45Q, R, U, V) or a short tapering base (6.3 %; Fig. 45S, T); oogonial diam 28.2 ± 2.4 µm (overall range 20.9–36.9 µm; range of isolate means 27.2–29.9 µm); nearly plerotic to plerotic (60.5 %; Fig. 45Q, S, T, V) or slightly aplerotic to aplerotic (39.5 %; Fig. 45R, U). *Oospores* globose with a large lipid globule (Fig. 45Q–V); diam 25.1 ± 1.9 µm (overall range 19.3–33.3 µm; range of isolate means 24.0–26.5 µm) wall thickness 1.63 ± 0.31 µm (overall range 0.9–2.5 µm), oospore wall index 0.34 ± 0.06; abortion rate 2–6 % (av. 4 %) after 4 wk. *Antheridia* predominantly paragynous and club-shaped, ovoid or subglobose (95.8 %; Fig. 45Q–U) or rarely amphigynous and cylindrical (4.2 %; Fig. 45V); sometimes two antheridia attached to one oogonium (Fig. 45U); dimensions 12.4 ± 2.5 × 7.3 ± 1.3 µm.

Culture characteristics: Colonies on V8A and CA mostly submerged to appressed, chrysanthemum-like to radiate on V8A and faintly petaloid on CA; on PDA dense-felty with irregular submerged margins and a petaloid pattern (Fig. 38).

Cardinal temperatures and growth rates: Optimum 27.5 °C with 7.52 ± 0.9 mm/d radial growth on V8A, maximum 27.5–<30 °C, minimum <10 °C (Fig. 42), lethal temperature 30–32.5 °C. At 20 °C on V8A, CA and PDA 7.31 ± 0.7 mm/d, 4.33 ± 0.3 mm/d and 3.14 ± 0.38 mm/d, respectively.

Additional materials examined: **Taiwan**, Tunyuan, isolated from rhizosphere soil of *Q. variabilis* in a montane, temperate, seasonally dry *Quercus–Pinus* forest, Mar. 2013, *T. Jung, M. Horta Jung & T.-T. Chang* (TW429, TW430). **Vietnam**, Sapa, Xin Chài Mountain, isolated from rhizosphere soil of *Alnus nepalensis* in a montane, temperate *Alnus* forest, Mar. 2016, *T. Jung, M. Horta Jung & N.M. Chi* (VN367, VN1103, VN1104, VN1105); Fansipan Mountain, isolated from naturally fallen leaves floating in streams running through a montane evergreen cloud forest, Mar. 2017, *T. Jung, B. Scanu & N.M. Chi* (VN905, VN971, VN1011); Sau Chua Mountain, isolated from a naturally fallen leaf floating in a stream running through a montane *Chamaecyparis* forest, Mar. 2017, *T. Jung, C.M. Brasier & N.M. Chi* (VN966).

Phytophthora curvata T. Jung, A. Hieno, H. Masuya & M. Horta Jung, ***sp. nov.*** MycoBank MB 847309. Fig. 46.

Etymology: The name refers to the high proportion of curved sporangial shapes.

Typus: **Japan**, Shikoku Island, Ichinomata, isolated from rhizosphere soil of a mature *Abies firma* tree in a warm-temperate submontane mixed forest, May 2017, *T. Jung & A. Hieno* (**holotype** CBS H-25104, dried culture on V8A, ex-holotype living culture CBS 149482 = JP126).

Morphological structures on V8A: Sporangia rarely observed on solid agar but produced abundantly in non-sterile soil extract; typically borne terminally in dense or lax sympodia of 2-4 sporangia (Fig. 46L) or less frequently on unbranched short or long sporangiophores; non-caducous, ovoid, broad-ovoid or elongated ovoid (41 %; Fig. 46A–C, L), mouse-shaped (24 %; Fig. 46E–H), distorted and often with two apices (23 %; Fig. 46I–L) or less frequently obpyriform to elongated-obpyriform (6 %), ellipsoid (4 %; Fig. 46D) and subglobose (2 %); apices papillate (48 %; Fig. 46B, E, G, J) or semipapillate (52 %; Fig. 46A, C, D, H, I, K, L); curved apices (37.4 %; Fig. 46C–I) and lateral attachment of the sporangiophore (16 %; Fig. 46G, I, L) commonly observed; sporangial proliferation exclusively external (Fig. 46A–C, E, F, H, L); sporangial dimensions averaging 54.5 ± 5.7 × 33.6 ± 4.0 µm (overall range 42.2–64.4 × 24.5–41.7 µm; range of isolate means 52.6–56.1 × 32.6–35.2 µm) with a length/breadth ratio of 1.63 ± 0.15 (overall range 1.24–2.04); sporangial germination usually indirectly with zoospores discharged through an exit pore 4.8–7.6 µm wide (av. 6.2 ± 0.8 µm). *Zoospores* limoniform to reniform whilst motile, becoming spherical (av. Diam = 10.4 ± 1.9 µm) on encystment. *Hyphal swellings* infrequently produced in water on sporangiophores; limoniform or subglobose, usually close to the sporangial base (Fig. 46B, I); dimensions 9.4–30.6 µm). *Chlamydospores* not observed. *Oogonia* abundantly produced in single culture ('homothallic' breeding system), terminal on short to medium-length, often curved lateral hyphae, smooth-walled, globose to slightly subglobose (62 %; Fig. 46M–R), or comma-shaped (38 %; Fig. 46S–U), with a round (54 %; Fig. 46M, P–R) or a short tapering, often curved base (46 %; Fig. 46N, O, S–U); oogonial diam 27.3 ± 4.5 µm (overall range 18.3–33.1 µm; range of isolate means 25.5–28.6 µm); nearly plerotic to plerotic (54.4 %; Fig. 46N, P, Q, S, U) or slightly aplerotic to aplerotic (45.6 %; Fig. 46M, O, R, T). *Oospores* globose with a large lipid globule (Fig. 46M, O, Q, R, T); diam 22.3 ± 4.0 µm (overall range 15.7–28.5

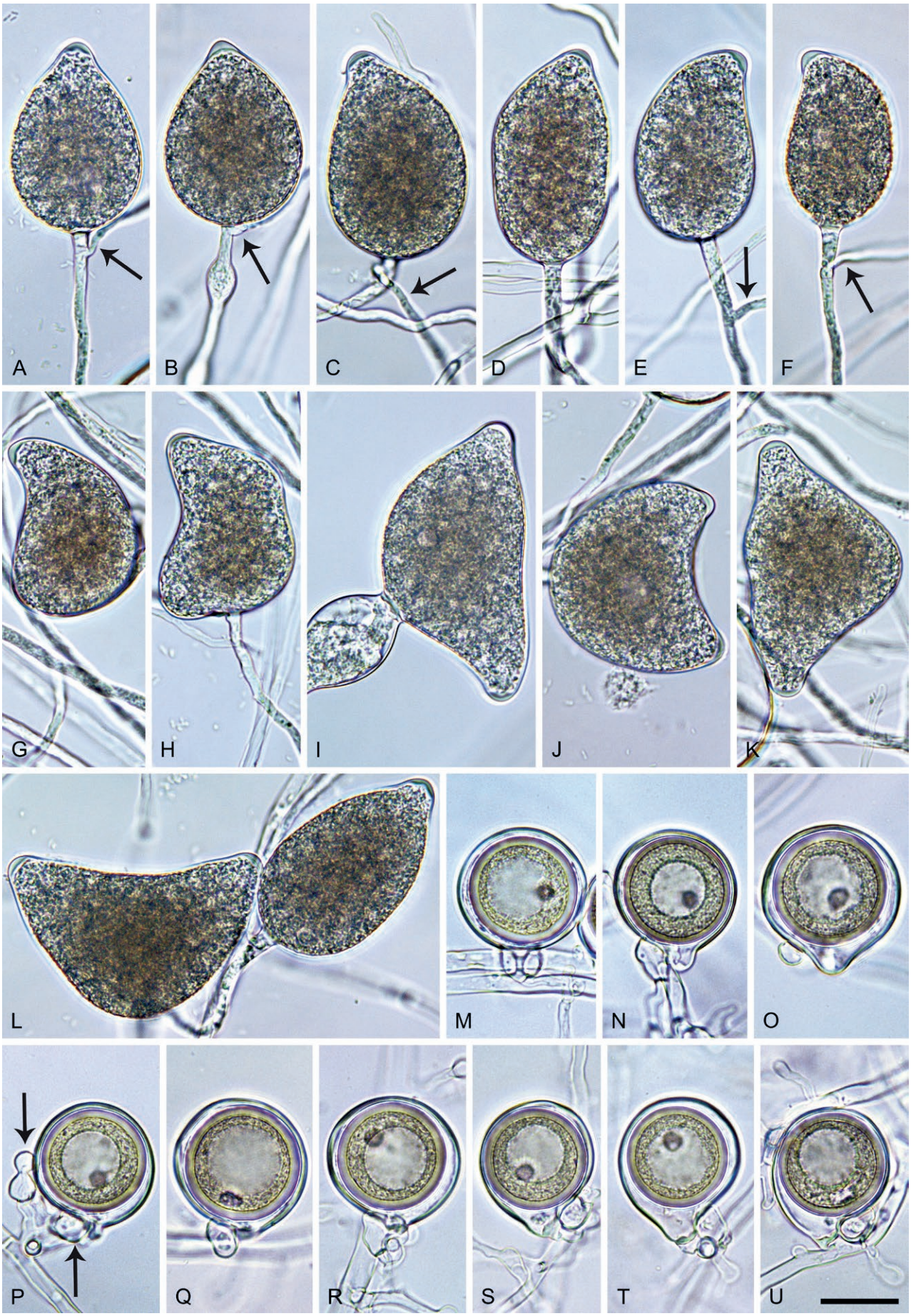

Fig. 46. *Phytophthora curvata*. **A–L.** Semipapillate to papillate sporangia without pedicels, formed on V8-agar (V8A) in soil extract. **A–H, J, L.** Ovoid, ellipsoid, mouse- and sickle-shaped sporangia. **C–J.** Curved apices. **A–F.** External proliferation (arrows). **I–L.** Bilobed sporangia. **I.** Hyphal swelling close to sporangium base. **L.** Beginning sporangial sympodium. **M–U.** Oogonia with aplerotic to near-plerotic oospores, formed in V8A. **M–R.** Globose to subglobose oogonia. **S–U.** Comma-shaped oogonia. **M.** Amphigynous antheridium. **N–U.** Paragynous antheridia. Images: A–U. Ex-type CBS 149482. Scale bar = 20 µm; U applies to A–U.

µm; range of isolate means 21.5–23.6 µm); wall thickness 1.69 ± 0.32 µm (overall range 0.96–2.46 µm), oospore wall index 0.38 ± 0.04; abortion rate 2–7 % (av. 3.7 %) after 4 wk. *Antheridia* almost exclusively paragynous and club-shaped, ovoid, globose to subglobose or irregular (99.3 %; Fig. 46N–U), or rarely amphigynous, unicellular and cylindrical (Fig. 46M); sometimes two antheridia attached to the same oogonium (Fig. 46P); dimensions 12.3 ± 1.9 ´ 9.0 ± 1.6 µm.

Culture characteristics: Colonies on V8A appressed with limited aerial mycelium, chrysanthemum-like to radiate; on CA submerged and uniform to faintly radiate; on PDA woolly and uniform (Fig. 38).

Cardinal temperatures and growth rates: On V8A optimum 25 °C with 6.25 ± 0.22 mm/d radial growth, maximum 27.5–<30 °C, minimum <10 °C (Fig. 42), lethal temperature 32.5 °C. At 20 °C on V8A, CA and PDA 5.18 ± 0.17 mm/d, 4.48 ± 0.25 mm/d and 2.29 ± 0.06 mm/d, respectively.

Additional materials examined: **Japan**, Shikoku Island, Ichinomata, isolated from rhizosphere soil of a mature *A. firma* tree in a warm-temperate submontane mixed forest, May 2017, *T. Jung, A. Hieno & H. Masuya* (JP125, JP333).

Phytophthora excentrica T. Jung, S. Uematsu, K. Kageyama & C.M. Brasier, ***sp. nov.*** MycoBank MB 847310. Fig. 47.

Etymology: The name refers to the common production of excentric and asymmetric oogonia and sporangia.

Typus: **Japan**, Shikoku Island, Ichinomata, isolated from rhizosphere soil of *Torreya nucifera* in a warm-temperate submontane forest, May 2017, *T. Jung & S. Uematsu* (**holotype** CBS H-25105, dried culture on V8A, ex-holotype living culture CBS 149483 = JP461).

Morphological structures on V8A: Sporangia produced abundantly in non-sterile soil extract; typically borne terminally (93.8 %) in dense or lax sympodia of 2–8 sporangia (Fig. 47N) or on unbranched short (Fig. 47G) or long sporangiophores, less frequently intercalary (6.2 %); non-caducous, predominantly ovoid, broad-ovoid or elongated ovoid (76 %; Fig. 47A–C, E, G, M, N), less frequently distorted and often with two apices (8 %; Fig. 47J, K), obpyriform to elongated-obpyriform (4 %; Fig. 47L), limoniform to elongated limoniform (4 %; Fig. 47H, N), subglobose (3 %; Fig. 47D), ellipsoid (2 %; Fig. 47F), mouse-shaped (2 %; Fig. 47I) or obovoid (1 %); apices semipapillate (81.2 %; Fig. 47A–G, I, K) or papillate (13.1 %; Fig. 47J) with a smooth transition between both forms, or infrequently nonpapillate (5.7 %; Fig. 47H); lateral attachment of the sporangiophore (46 %; Fig. 47D–F, I–M), asymmetric shapes of the apex or the whole sporangium (25 %; Fig. 47I–L), pedicels (34 %; Fig. 47A–C, H), and conspicuous basal plugs, sometimes protruding backwards into the sporangiophore (24 %; Fig. 47C) common; sporangial proliferation exclusively external (Fig. 47A–C, M, N); sporangial dimensions averaging 56.9 ± 4.9 × 38.0 ± 3.4 µm (overall range 46.7–72.5 × 31.2–45.1 µm; range of isolate means 55.7–58.1 × 37.4–38.6 µm) with a length/breadth ratio of 1.5 ± 0.18 (overall range 1.2–2.22); pedicel length 16.7 ± 16.9 µm (range 5.7–62.5 µm); sporangial germination indirectly with zoospores discharged through an exit pore 5.3–9.0 µm wide (av. 7.3 ± 0.8 µm). *Zoospores* limoniform to reniform whilst motile, becoming spherical (av. Diam = 11.0 ± 1.4 µm) on encystment; cysts usually germinate directly. *Hyphal swellings* commonly produced in water on sporangiophores and hyphae; globose to subglobose, ellipsoid or limoniform, sometimes with radiating hyphae (Fig. 47O, P); dimensions 24.3 ± 9.4 µm. *Chlamydospores* not observed. *Oogonia* abundantly produced in single culture ('homothallic' breeding system), terminal on short to medium-length, often curved lateral hyphae or sessile (Fig. 47Q–W), smooth-walled, globose to subglobose (47 %; Fig. 47Q, R), slightly to markedly excentric (44 %; Fig. 47S–V) or less frequently elongated (9 %; Fig. 47W), mostly with a round (82 %; Fig. 47R–U, W) or a short-tapering base (18 %; Fig. 47Q, V); oogonial diam 30.6 ± 3.5 µm (overall range 17.5–37.9 µm; range of isolate means 29.9–31.3 µm); nearly plerotic to plerotic (96 %; Fig. 47Q–W) or rarely aplerotic (4 %). *Oospores* globose with a large lipid globule (Fig. 47Q–W); diam 26.6 ± 3.1 µm (overall range 15.2–32.4 µm; range of isolate means 26.2–27.0 µm); wall thickness 1.64 ± 0.27 µm (overall range 0.87–2.22 µm), oospore wall index 0.33 ± 0.03; abortion rate 5 % after 4 wk. *Antheridia* almost exclusively paragynous and club-shaped, ovoid, globose to subglobose or irregular (Fig. 47Q–W); dimensions 11.8 ± 2.9 × 8.1 ± 1.8 µm. *Hyphal aggregations* commonly produced (Fig. 47X).

Culture characteristics: Colonies on V8A and CA mostly submerged with scanty aerial mycelium, chrysanthemum-like on V8A and petaloid with large petals on CA; on PDA dense felty-cottony with a faint petaloid pattern (Fig. 38).

Cardinal temperatures and growth rates: On V8A optimum 27.5 °C with 8.85 ± 0.14 mm/d radial growth, maximum 30 °C, minimum <10 °C (Fig. 42), lethal temperature 30–<32.5 °C. At 20 °C on V8A, CA and PDA 6.46 ± 0.15 mm/d, 4.98 ± 0.04 mm/d and 3.32 ± 0.09 mm/d, respectively.

Additional materials examined: **Japan**, Shikoku Island, Ichinomata, isolated from rhizosphere soil of *T. nucifera* in a warm-temperate submontane forest, May 2017, *T. Jung & S. Uematsu* (JP2360).

Phytophthora falcata T. Jung, K. Kageyama, S. Uematsu & M. Horta Jung, ***sp. nov.*** MycoBank MB 847311. Fig. 48.

Etymology: The name refers to the common production of curved and often sickle-shaped sporangia in all known isolates (*falcata* Latin = sickle-shaped).

Typus: **Japan**, Shikoku Island, Ichinomata, isolated from a baiting leaf floating in a stream running through a diverse warm-temperate forest, May 2017, *T. Jung & K. Kageyama* (**holotype** CBS H-25106, dried culture on V8A, ex-holotype living culture CBS 149484 = JP065).

Morphological structures on V8A: Sporangia rarely observed on solid agar but produced abundantly in non-sterile soil extract; typically borne terminally (99.2 %) in dense or lax sympodia of 2–5 sporangia (Fig. 48L) or less frequently on unbranched short or long sporangiophores, or rarely intercalary (0.8 %); mostly ovoid, broad-ovoid or elongated ovoid (44.8 %; Fig. 48A–C, J, L) or curved, sickle-shaped or mouse-shaped (34.2 %; Fig. 48D–G, K), less frequently obpyriform to elongated-obpyriform (10.6 %; Fig. 48H), distorted and often with two or three apices (4.2 %; Fig. 48I, L), limoniform to elongated limoniform (2.4 %), ampulliform (2 %) or ellipsoid to elongated-ellipsoid (1.8 %); apices mostly semipapillate (87.2 %; Fig. 48B, C, E, F, H–J) or less frequently papillate (12.8 %; Fig. 48A, D, G) with a smooth transition between both forms; lateral attachment of the sporangiophore (18 %; Fig. 48E, G–I, K), pedicels (51.6 %; Fig. 48A–C, G, J), and conspicuous basal plugs, often protruding backwards into the sporangiophore (44.8 %; Fig. 48B, C) common;

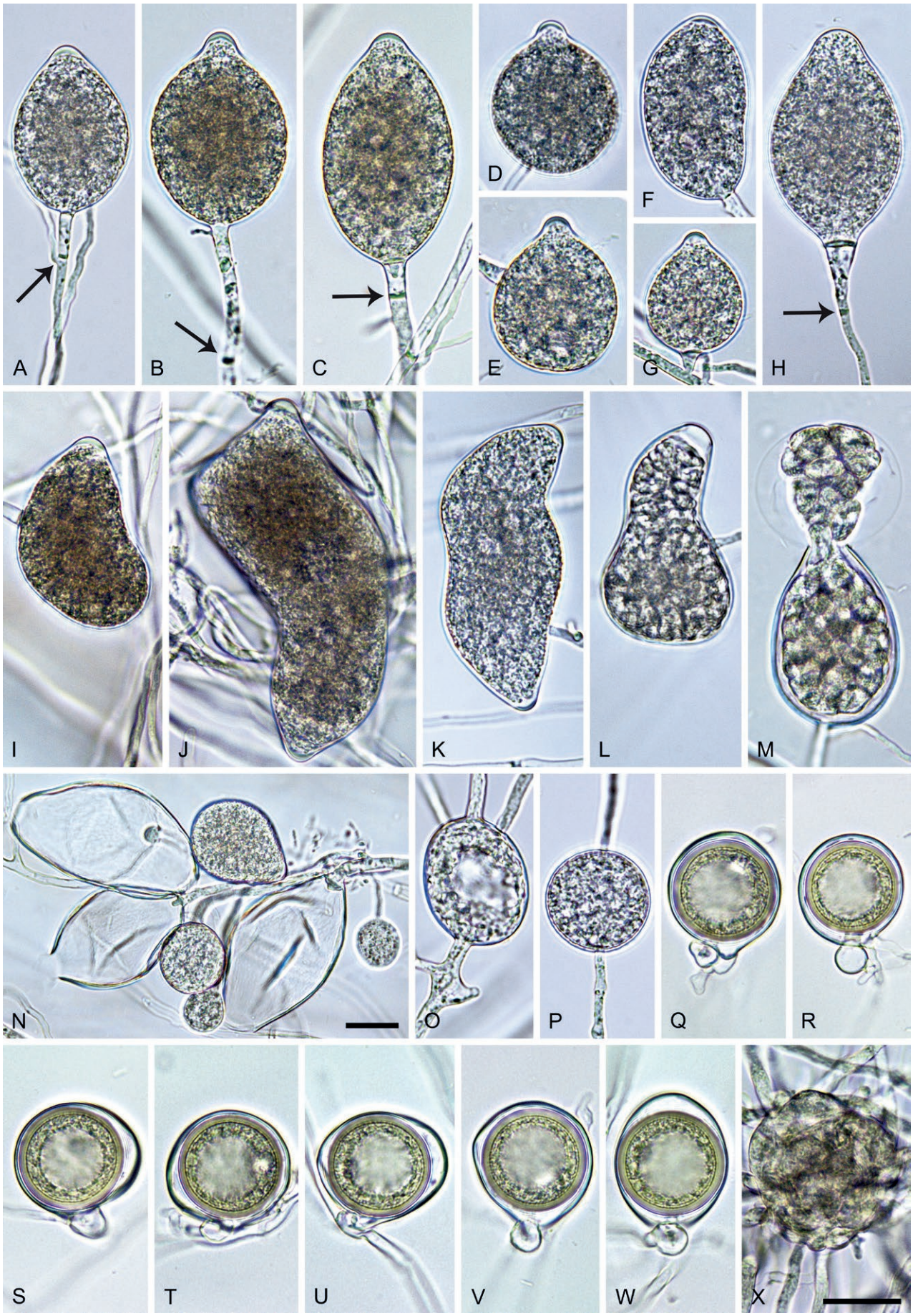

Fig. 47. *Phytophthora excentrica*. **A–N.** Sporangia formed on V8-agar (V8A) in soil extract. **A–I, L–N.** Ovoid, subglobose, ellipsoid, limoniform, mouse-shaped and obpyriform sporangia. **A–G, I, K.** Semipapillate apices. **H.** Nonpapillate apex. **J.** Papillate apex. **A–C, H.** Medium-length to long pedicels (arrows in B, C, H). **A, M, N.** External proliferation (arrow in A). **J, K.** Distorted with two apices. **M.** Zoospore release. **N.** Dense sporangial sympodium. **O, P.** Intercalary hyphal swellings in water. **Q–W.** Oogonia with near-plerotic to plerotic oospores and paragynous antheridia, formed in V8A. **Q, R.** Subglobose oogonia. **S–V.** Excentric oogonia. **W.** Elongated oogonium. **X.** Hyphal aggregation in V8A. Images: A–X. Ex-type CBS 149483. Scale bars = 20 µm; X applies to A–M, O–X.

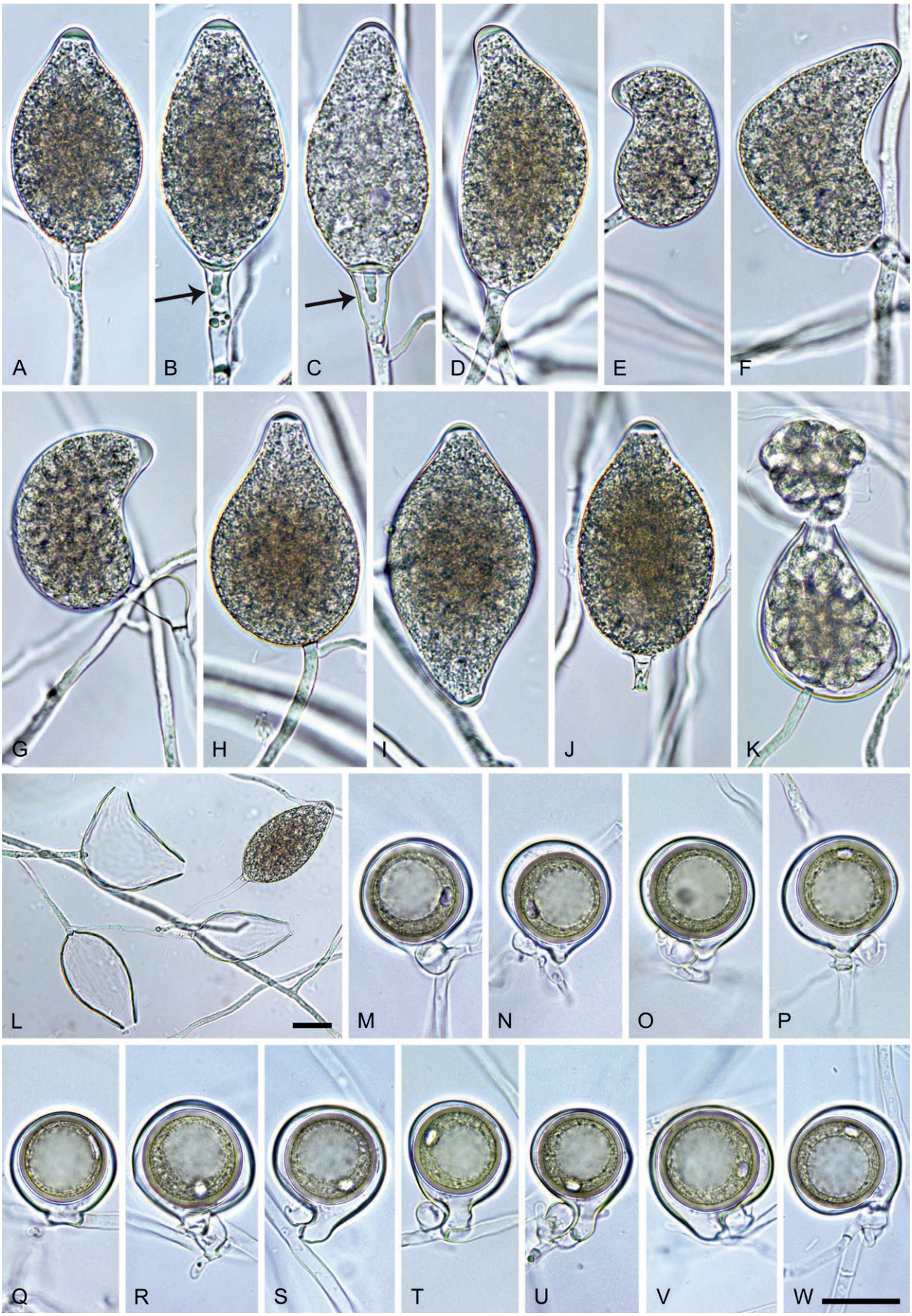

Fig. 48. *Phytophthora falcata*. **A–L.** Sporangia formed on V8-agar (V8A) in soil extract. **A–J.** Semipapillate and papillate apices. **A–H, J–L.** Ovoid, obpyriform, mouse- and sickle-shaped sporangia. **A–C, J.** Pedicels with variable lengths. **B, C.** conspicuous basal plug protruding into the pedicel (arrows). **A–C, H.** External proliferation. **I.** Distorted sporangium with two apices. **J.** Caducous sporangium. **K.** Zoospore release. **L.** Sporangial sympodium. **M–W.** Globose, subglobose and excentric oogonia with near-plerotic to aplerotic oospores and paragynous antheridia, formed in V8A. **Q.** Intercalary oogonium. **S–U.** Tapering oogonia bases. **W.** Comma-shaped oogonium. Images: A–D, F, J, L–Q, T, U. Ex-type CBS 149484; E, JP310; G–I, K. JP719; R. JP253. S, V, W. JP807. Scale bars = 20 µm; W applies to A–K, M–W.

sporangiophores sometimes widening towards the sporangial base (2 %; Fig. 48C); predominantly non-caducous, but caducity occasionally (<1 %) observed in all isolates (Fig. 48J); sporangial proliferation exclusively external (Fig. 48A–C, H, L); sporangial dimensions averaging 58.8 ± 7.1 × 31.6 ± 4.6 µm (overall range 40.0–79.5 × 17.7–45.3 µm; range of isolate means 54.9–64.9 × 29.6–34.9 µm) with a length/breadth ratio of 1.88 ± 0.25 (overall range 1.33–2.8); pedicel length 23.1 ± 12.2 µm (range 1.7–66.9 µm); sporangial germination usually indirectly with zoospores discharged through an exit pore 4.1–8.7 µm wide (av. 6.1 ± 0.9 µm). *Zoospores* limoniform to reniform whilst motile, becoming spherical (av. Diam = 10.4 ± 1.4 µm) on encystment; cysts usually germinate directly. *Hyphal swellings* infrequently produced in water on sporangiophores and hyphae; globose to subglobose or limoniform (Fig. 48G); dimensions 13.5 ± 0.8 µm. *Chlamydospores* not observed. *Oogonia* abundantly produced in single culture ('homothallic' breeding system), terminal on short to medium-length, often curved lateral hyphae or sessile (Fig. 48M–P, R–W), or occasionally intercalary (Fig. 48Q), smooth-walled, globose to slightly subglobose (87 %; Fig. 48M–V), or comma-shaped (13 %; Fig. 48W), often excentric (23.5 %; Fig. 48N, P, R, V, W) with a round (54 %; Fig. 48M–R, W) or a tapering, often curved base (46 %; Fig. 48S–V); oogonial diam 28.3 ± 2.8 µm (overall range 18.8–35.4 µm; range of isolate means 27.4–29.6 µm); slightly aplerotic to aplerotic (68.5 %; Fig. 48N, P–S, W) or nearly plerotic (31.5 %; Fig. 48M, O, T, U). *Oospores* globose with a large lipid globule (Fig. 48M–W); diam 23.8 ± 2.5 µm (overall range 16.1–30.0 µm; range of isolate means 23.0–25.0 µm); wall thickness 1.47 ± 0.2 µm (overall range 0.87–2.07 µm), oospore wall index 0.33 ± 0.03; abortion rate 0–1 % (av. 0.5 %) after 4 wk. *Antheridia* almost exclusively paragynous and club-shaped, ovoid, globose to subglobose or irregular (Fig. 48M–P, R–W), sometimes with finger-like projections (Fig. 48R, U); dimensions 10.8 ± 2.0 × 8.1 ± 1.4 µm.

Culture characteristics: Colonies on V8A and CA mostly submerged to appressed with scanty aerial mycelium, radiate on V8A and petaloid on CA; on PDA dense-felty with a faint petaloid pattern (Fig. 38).

Cardinal temperatures and growth rates: On V8A optimum 27.5 °C with 8.39 ± 0.49 mm/d radial growth, maximum 27.5–<30 °C (5 isolates) or 30 °C (2 isolates), minimum <10 °C (Fig. 42), lethal temperature 30–<32.5 °C. At 20 °C on V8A, CA and PDA 6.23 ± 0.36 mm/d, 5.29 ± 0.1 mm/d and 2.47 ± 0.21 mm/d, respectively.

Additional materials examined: **Japan**, Honshu Island, Takayama, isolated from a baiting leaf floating in a stream running through a montane riparian *Alnus irsute* forest, May 2017, *T. Jung & A. Hieno* (JP253); isolated from rhizosphere soil of *A. irsute* in two montane riparian forests, May 2017, *T. Jung, C.M. Brasier & J.F. Webber* (JP319, JP807); Kyushu Island, Takakuma, isolated from a naturally fallen leaf floating in a stream running through a warm-temperate *Castanopsis* forest, May 2017, *T. Jung & S. Uematsu* (JP310): Shikoku Island, Ichinomata, isolated from rhizosphere soil of a mature *Abies firma* tree in a warm-temperate submontane mixed forest, May 2017, *T. Jung & H. Masuya* (JP331); isolated from a naturally fallen leaf floating in a stream running through a submontane *Quercus*-Abies-Tsuga forest, May 2017, *T. Jung & M. Horta Jung* (JP719).

Phytophthora fansipanensis T. Jung, N.M. Chi, T. Corcobado & C.M. Brasier, ***sp. nov.*** MycoBank MB 847312. Fig. 49.

Etymology: The name refers to the origin of the first isolates from a forest stream at the Fansipan Mountain in Vietnam.

Typus: **Vietnam**, Sapa, Fansipan Mountain, isolated from a baiting leaf floating in a stream running through a montane evergreen cloud forest, Mar. 2017, *T. Jung & N.M. Chi* (**holotype** CBS H-25107, dried culture on V8A, ex-holotype living culture CBS 149485 = VN970).

Morphological structures on V8A: *Sporangia* not observed in solid agar but abundantly produced in non-sterile soil extract; borne terminally in lax or dense sympodia of 2–5 sporangia (Fig. 49K) or less frequently on unbranched sporangiophores (Fig. 49D, H) or rarely intercalary (1.5 %; Fig. 49F, I); sporangia semipapillate (Fig. 49A–G, I, K) non-caducous, predominantly ovoid, broad ovoid or elongated ovoid (80.4 %; Fig. 49A–E, H, J, K), less frequently limoniform (8.6 %; Fig. 49G), obpyriform to elongated obpyriform (5.6 %; Fig. 49F), distorted and often with two or three apices (2.4 %; Fig. 49I, K), ellipsoid (1.5 %), obovoid (0.5 %), sickle-shaped (0.5 %) or ampulliform (0.5 %); special features like lateral attachment of the sporangiophore (24.2 %; Fig. 49E, K) and pedicels (34.8 %; Fig. 49B, D, G, I), vacuoles (Fig. 49D–F) and swellings close to the sporangial base (Fig. 49H, K) common; small hyphal appendices (Fig. 49E) occasionally observed; sporangial dimensions averaging 53.3 ± 5.0 × 34.5 ± 3.5 µm (overall range 40.3–65.0 × 26.8–42.9 µm; range of isolate means 52.6–54.9 × 34.1–34.8 µm) with a length/breadth ratio of 1.55 ± 0.15 (overall range 1.27–2.18); pedicel length 13.1 ± 6.3 µm (range 3.5–37.8); sporangial proliferation exclusively external (Fig. 49A–C, E, G, K); sporangial germination indirectly with zoospores discharged through an exit pore of 5.4–10.4 µm (av. 7.2 ± 0.8 µm; Fig. 47J). *Zoospores* limoniform to reniform whilst motile (Fig. 49J), becoming spherical (av. Diam = 10.2 ± 1.1 µm) on encystment; cysts germinating directly by producing hyphae. *Hyphal swellings* on sporangiophores common, liminiform, ovoid or subglobose (Fig. 49H, K), 14.9 ± 5.2 µm (7.9–27.9 µm). *Chlamydospores* not observed. *Oogonia* abundantly produced in single culture ('homothallic' breeding system), on short, often curved stalks (74 %; Fig. 49L, M, Q–U) or sessile (26 %; Fig. 49N–P); smooth-walled, globose to subglobose (80 %; Fig. 49L–Q) or slightly elongated (20 %; Fig. 49R–U), with a round (72.7 %; Fig. 49L–P, S, U) or tapering base (27.3 %; Fig. 49Q, R, T); av. Diam 28.0 ± 2.2 µm with an overall range of 21.3–32.4 µm and a range of isolate means of 27.3–28.4 µm; slightly aplerotic to aplerotic (84 %; Fig. 49N–Q, S–U) or nearly plerotic to plerotic (16.0 %; Fig. 49L, M, R). *Oospores* globose with a large lipid globule (Fig. 49L–U), turning golden-brown during maturation (Fig. 49N–U); av. Diam 23.3 ± 1.4 µm with an overall range of 18.8–27.9 µm and a range of isolate means of 23.3–23.5 µm; wall diam 1.64 ± 0.19 µm (overall range 1.2–2.27 µm) and oospore wall index 0.37 ± 0.03; abortion rate after 4 wk very low (1–2 %; av. 1.3 %). *Antheridia* 1-celled, mostly paragynous and club-shaped, ovoid or subglobose (96 %; Fig. 49L–T) or infrequently amphigynous and cylindrical (4 %; Fig. 49U); 11.5 ± 2.3 × 7.4 ± 1.1 µm.

Culture characteristics: Colonies on V8A and CA appressed to submerged with a chrysanthemum-like pattern on V8A and a chrysanthemum-like to stellate pattern on CA; and petaloid and felty-cottony on PDA (Fig. 39).

Cardinal temperatures and growth rates: Optimum 25.0 °C with 7.92 ± 0.28 mm/d radial growth on V8A, maximum 27.5–<30 °C, minimum <10 °C (Fig. 42), lethal temperature 32.5–35 °C. At 20 °C on V8A, CA and PDA 7.49 ± 0.14 mm/d, 5.93 ± 0.15 mm/d and 3.0 ± 0.12 mm/d, respectively.

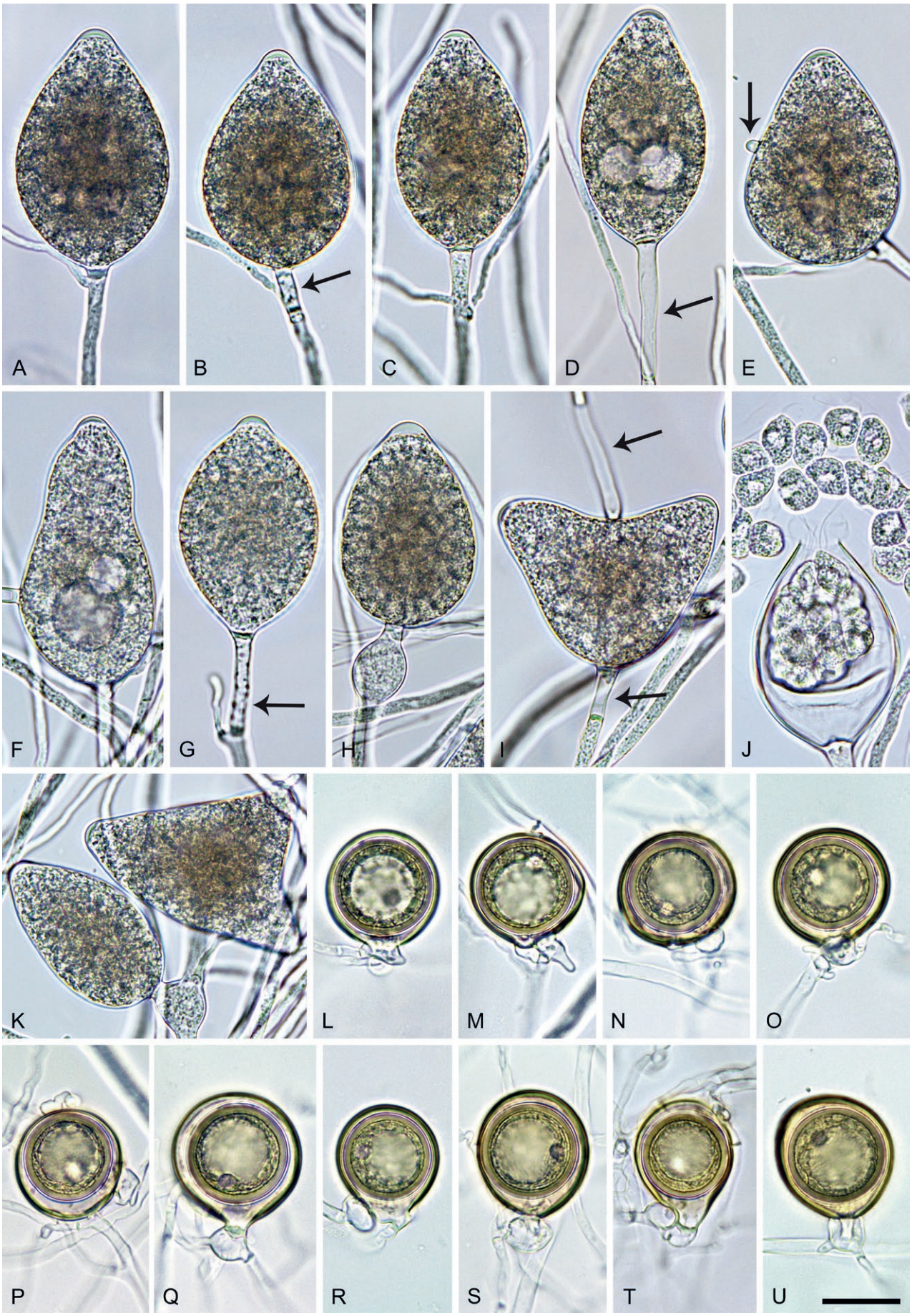

Fig. 49. *Phytophthora fansipanensis*. **A–K.** Sporangia formed on V8-agar (V8A) in soil extract. **A–I, J, K.** Ovoid, obpyriform and limoniform sporangia. **A–G, I, K.** Semipapillate apices. **A–C, E, G.** External proliferation. **B, D, F, I.** Medium-length to long pedicels (arrows). **H.** Swollen apex before zoospore release and hyphal swelling. **I.** Bilobed intercalary sporangium. **J.** Zoospore release. **K.** Sympodium with ovoid and trilobed sporangia and hyphal swelling. **L–U.** Oogonia with near-plerotic to aplerotic oospores, formed in V8A. **L–T.** Paragynous antheridia. **L–Q.** Globose to subglobose oogonia. **R–U.** Slightly elongated oogonia. **U.** Amphigynous antheridium. Images: A–C, G, J–P, U. Ex-type CBS 149485; D, F, I. VN1095; E, H, Q–T. VN1097. Scale bar = 20 µm; U applies to A–U.

Additional materials examined: **Vietnam**, Sapa, Fansipan Mountain, isolated from baiting leaves floating in a stream running through a montane evergreen cloud forest, Mar. 2017, *T. Jung, N.M. Chi & T. Corcobado* (VN1093, VN1095, VN1097, VN1099).

Phytophthora japonensis T. Jung, A. Hieno, H. Masuya & J.F. Webber, ***sp. nov.*** MycoBank MB 847314. Fig. 50.

Etymology: Name refers to the distribution in several Japanese islands.

Typus: **Japan**, Kyushu Island, Aya, isolated from a baiting leaf floating in a stream running through a warm-temperate mixed forest, May 2017, *T. Jung & A. Hieno* (**holotype** CBS H-25112, dried culture on V8A, ex-holotype living culture CBS 149489 = JP467).

Morphological structures on V8A: Sporangia produced abundantly in non-sterile soil extract; typically borne terminally (98 %) in dense or lax sympodia of 2–8 sporangia (Fig. 50I, K, L) or less frequently on unbranched long or short sporangiophores (Fig. 50E), or rarely intercalary (2 %); predominantly ovoid, broad-ovoid or elongated ovoid (70.6 %; Fig. 50A–E, G, I) or distorted and often with two apices (24.1 %; Fig. 50H–L), infrequently ellipsoid or elongated-ellipsoid (2.7 %; Fig. 50F, L),), obpyriform (1.4 %), limoniform (0.8 %) or obovoid (0.4 %); apices semipapillate, sometimes curved or laterally displaced (17 %; Fig. 50H, I, L); non-caducous; a conspicuous basal plug (15.6 %; Fig. 50K, L), pedicels (11.3 %; Fig. 50B) and small swellings close to the sporangial base (2 %; Fig. 50F) infrequently observed; sporangial proliferation exclusively external (Fig. 50A–C, G–L); sporangial dimensions averaging 55.0 ± 5.8 × 36.8 ± 3.8 µm (overall range 39.1–69.3 × 27.0–47.1 µm; range of isolate means 51.8–56.8 × 36.0–37.5 µm) with a length/breadth ratio of 1.5 ± 0.13 (overall range 1.24–1.89); pedicel length 11.3 ± 6.2 µm (range 5.2–22.0 µm); sporangial germination indirectly with zoospores discharged through an exit pore 4.5–9.9 µm wide (av. 6.9 ± 1.0 µm) (Fig. 50K, L). *Zoospores* limoniform to reniform whilst motile, becoming spherical (av. Diam = 10.4 ± 1.0 µm) on encystment; cysts germinating directly. *Hyphal swellings* rarely produced in water on sporangiophores, globose to subglobose, ovoid or limoniform (Fig. 50F). *Chlamydospores* not observed. *Oogonia* abundantly produced in single culture ('homothallic' breeding system), terminal on short, sometimes curved lateral hyphae or sessile, smooth-walled, globose to slightly subglobose (Fig. 50M–U), sometimes slightly excentric (16.7 %; Fig. 50Q, R, U), usually with a rounded (86 %; Fig. 50M–S, U) or infrequently a short tapering base (14 %; Fig. 50T); oogonial diam 28.9 ± 2.6 µm (overall range 17.3–33.6 µm; range of isolate means 28.4–29.3 µm); nearly plerotic to plerotic (Fig. 50M–U). *Oospores* with a large lipid globule, globose (Fig. 50M–T) or rarely subglobose (Fig. 50U); diam 25.2 ± 2.4 µm (overall range 15.5–29.8 µm; range of isolate means 24.8–25.6 µm) wall thickness 1.56 ± 0.23 µm (overall range 1.06–2.24 µm), oospore wall index 0.33 ± 0.04; abortion rate 1–2 % (av. 1.3 %) after 4 wk. *Antheridia* exclusively paragynous and club-shaped, ovoid or subglobose (Fig. 50M–U); dimensions 11.1 ± 2.0 × 8.0 ± 1.5 µm.

Culture characteristics: Colonies on V8A appressed with scanty aerial mycelium and a chrysanthemum-like pattern; on CA submerged to appressed with a faint petaloid pattern; on PDA dense-felty with irregular margins and a faint petaloid pattern (Fig. 39).

Cardinal temperatures and growth rates: On V8A optimum at 25 °C with 5.18 ± 0.09 mm/d radial growth, maximum 27.5–<30 °C, minimum <10 °C (Fig. 42), lethal temperature 30–32.5 °C. At 20 °C on V8A, CA and PDA 4.48 ± 0.02 mm/d, 4.07 ± 1.67 mm/d and 1.92 ± 0.28 mm/d, respectively.

Additional materials examined: **Japan**, Kyushu Island, Aya, isolated from rhizosphere soil of *Machilus thunbergii* and *Castanopsis cuspidata* in a warm-temperate *Fagaceae-Lauraceae* forest, May 2017, *T. Jung & A. Hieno* (JP542, JP744); Kyushu Island, Takakuma, isolated from rhizosphere soil of *Lithocarpus edulis* in a warm-temperate *Fagaceae-Lauraceae* forest on volcanic soil, May 2017, *T. Jung & J.F. Webber* (JP279); isolated from a baiting leaf floating in a stream running through a warm-temperate *Fagaceae-Lauraceae* forest on volcanic soil, May 2017, *T. Jung & M. Horta Jung* (JP541); Shikoku Island, Satayama, isolated from a baiting leaf floating in a stream running through a warm-temperate *Fagaceae-Lauraceae* forest, May 2017, *T. Jung & H. Masuya* (JP600); Shikoku Island, Ichinomata, isolated from a baiting leaf floating in a stream running through a mixed *Quercus*-Torreya-Tsuga forest, May 2017, *T. Jung & H. Masuya* (JP106, JP107).

Phytophthora limosa T. Corcobado, T. Majek, M. Ferreira & T. Jung, ***sp. nov.*** MycoBank MB 847315. Fig. 51.

Etymology: The name refers to the occurrence in muddy soils (*limosa* Latin = muddy).

Typus: **USA**, Louisiana, Clark Creek, isolated from riverbank soil in a mixed subtropical forest, March 2020, *T. Corcobado & T. Majek* (**holotype** CBS H-25113, dried culture on V8A, ex-holotype living culture CBS 149490 = LU185).

Morphological structures on V8A: Sporangia rarely observed on solid agar but produced abundantly in non-sterile soil extract; borne terminally in dense or lax sympodia of 2–4 sporangia (Fig. 51M); non-caducous, ovoid, broad-ovoid or elongated ovoid (55.4 %; Fig. 51A, B, K–M), mouse- or sickle-shaped (15.5 %; Fig. 51C), distorted with often two apices (9.6 %; Fig. 51H, J), limoniform to elongated limoniform (8.2 %; Fig. 51D, G, I), obpyriform to elongated-obpyriform (7.2 %; Fig. 51E, F), ellipsoid to elongated-ellipsoid (3.8 %), pyriform (0.2 %) or obovoid (0.1 %); apices predominantly semipapillate (81.1 %; Fig. 51A–F, J, L, M), less frequently papillate (16.2 %; Fig. 51H, I) or rarely nonpapillate (2.7 %; Fig. 51G), frequently curved or laterally displaced (18.6 %; Fig. 51B, C, H, I); lateral attachment of the sporangiophore (10 %; Fig. 51L) and pedicels (35.6 %; Fig. 51A, C, F, H) commonly observed; sporangial proliferation exclusively external (Fig. 51A, B, D, E, H, L, M) with sometimes two new sporangiophores arising from the same node (Fig. 51L); sporangial dimensions averaging 52.7 ± 7.0 × 31.9 ± 3.1 µm (overall range 37.3–72.2 × 21.9–39.8 µm; range of isolate means 49.2–56.6 × 31.2–32.4 µm) with a length/breadth ratio of 1.66 ± 0.19 (overall range 1.25–2.6); pedicel length 23.9 ± 12.3 µm (range 8.1–57.9 µm); sporangial germination usually indirectly with zoospores discharged through an exit pore 4.9–11.2 µm wide (av. 6.9 ± 1.4 µm) (Fig. 51K). *Zoospores* limoniform to reniform whilst motile, becoming spherical (av. diam = 11.4 ± 1.9 µm) on encystment; cysts germinating directly. *Hyphal swellings* infrequently produced in water on sporangiophores; limoniform or ellipsoid, 14.1 ± 5.2 µm. *Chlamydospores* not observed. *Oogonia* abundantly produced in single culture ('homothallic' breeding system), terminal on short to medium-length, often curved lateral hyphae or sessile, smooth-walled, globose to slightly subglobose (64 %; Fig. 51N, O, Q, S, T), excentric (21 %; Fig. 51R, U), or elongated (15 %; Fig. 51P, V), with a rounded (84 %; Fig. 51N–R, U) or a short tapering base (16 %; Fig. 51S, T); oogonial diam 30.5 ± 3.3 µm (overall range 18.8–39.7 µm; range of isolate means

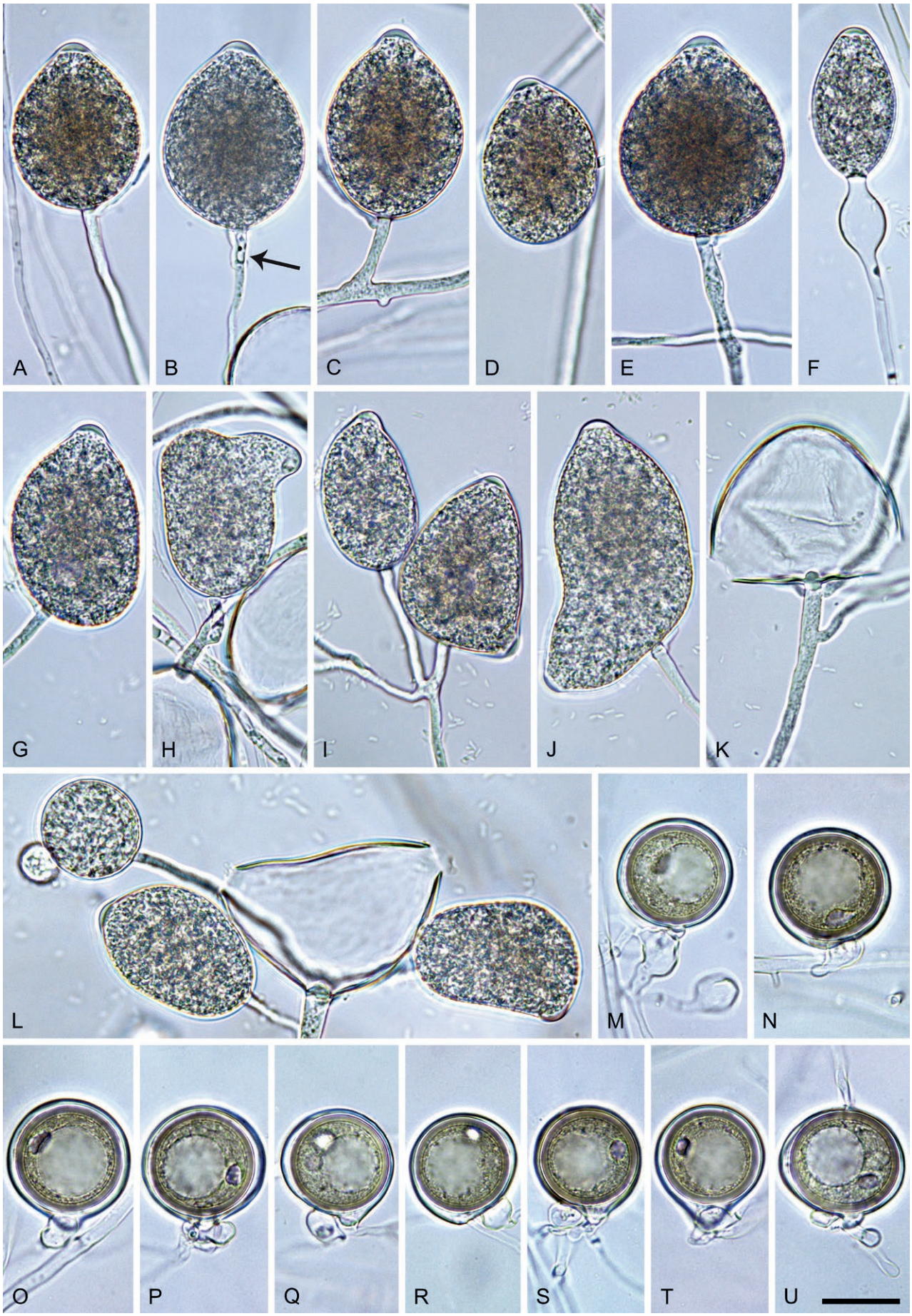

Fig. 50. *Phytophthora japonensis*. **A–L.** Sporangia formed on V8-agar (V8A) in soil extract. **A–J, L.** Semipapillate apices. **A–C, G–L.** External proliferation. **A–G, I, L.** Ovoid and ellipsoid sporangia. **B.** Medium-length pedicel. **F.** Long pedicel and hyphal swelling. **H.** Distorted sporangium with laterally displaced apex. **I–L.** Distorted sporangia with two apices. **I, L.** Dense sporangial sympodia. **M–U.** Globose to subglobose oogonia with near-plerotic to plerotic oospores and paragynous antheridia formed in solid V8A. **Q, R, U.** Slightly excentric oogonia. Images: A–C, H, K, L, N, O, R–U. Ex-type CBS 149489; D, G, I, J, P. JP542; E, F, M, Q. JP279. Scale bar = 20 µm; U applies to A–U.

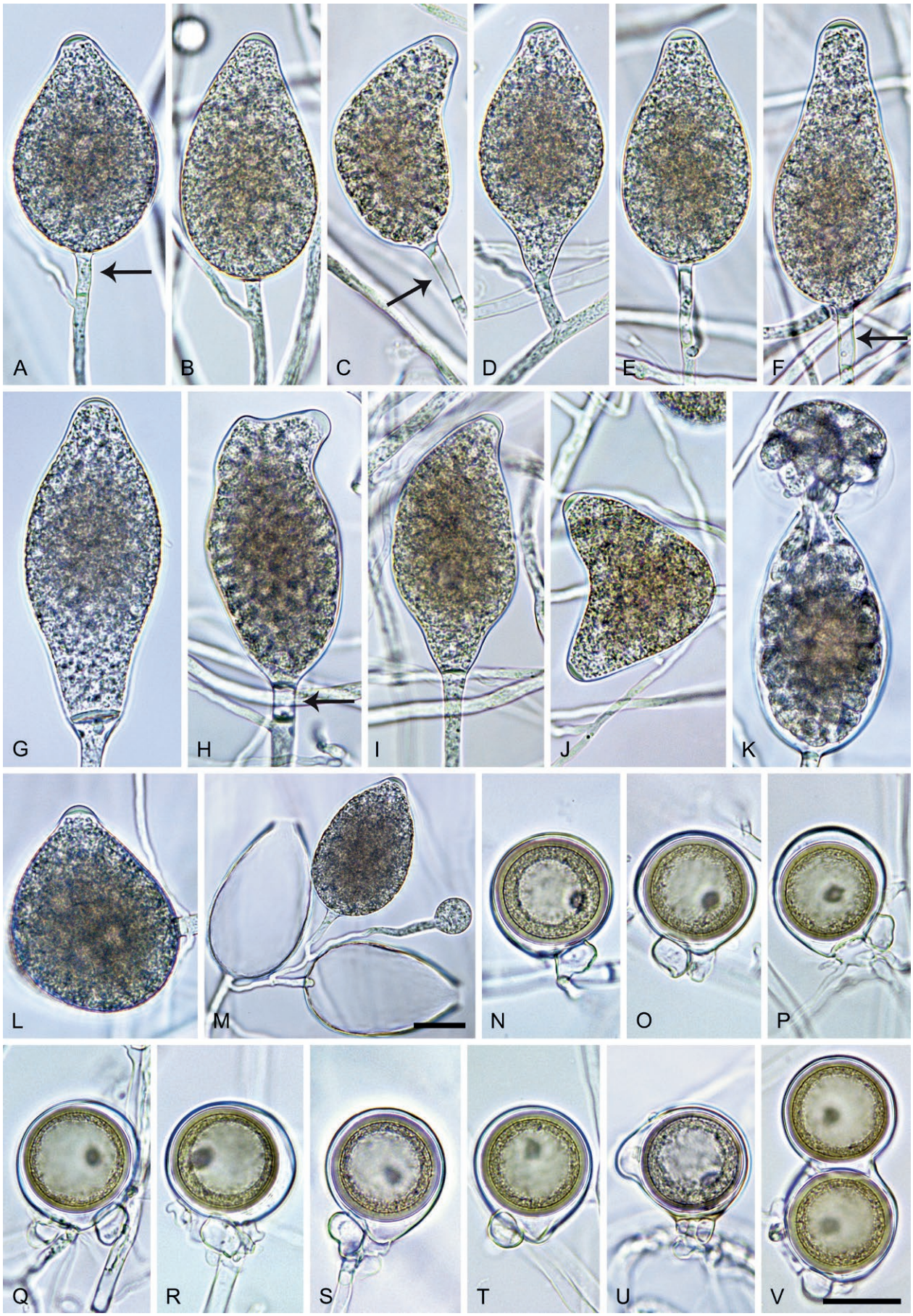

Fig. 51. *Phytophthora limosa*. **A–M.** Sporangia formed on V8-agar (V8A) in soil extract. **A–G, I, J–M.** Ovoid, limoniform, obpyriform and mouse-shaped sporangia. **A, B, D–G, J, L, M.** Semipapillate apices. **A, C, E, F, H.** Medium-length pedicels (arrows). **A, B, D, E, H, L.** External proliferation. **B.** Swollen apex before zoospore release. **H, I.** Papillate apices. **H.** Distorted sporangium with displaced apex. **J.** Bilobed sporangium. K. Zoospore release. M. Dense sympodium. **N–V.** Subglobose to globose, excentric or elongated oogonia with plerotic to aplerotic oospores, formed in V8A. **N–T, U.** Paragynous antheridia. **U.** Amphigynous antheridium. **V.** Elongated oogonium with two oospores. Images: A–C, E, F, I, J, L, N, P, Q, S–V. Ex-type CBS 149490; D, G, H, LU079; K, M. BN113; O, R. LU083. Scale bars = 20 µm; V applies to A–L, N–V.

29.5–31.2 µm); nearly plerotic to plerotic (75.7 %; Fig. 51N, O, S–V) or slightly aplerotic to aplerotic (24.3 %; Fig. 51P–R); in rare cases two oospores inside of one oogonium (Fig. 51V). *Oospores* globose with a large lipid globule (Fig. 51N–V); diam 27.2 ± 3.1 µm (overall range 16.3–36.5 µm; range of isolate means 26.1–28.1 µm) wall thickness 1.52 ± 0.27 µm (overall range 0.72–2.31 µm), oospore wall index 0.3 ± 0.04; abortion rate 0–17 % (av. 7.3 %) after 4 wk. *Antheridia* almost exclusively paragynous and club-shaped, ovoid or subglobose (99.5 %; Fig. 51N–T, V) or rarely amphigynous and cylindrical (0.5 %; Fig. 51U); rarely two antheridia attached to one oogonium (Fig. 51Q); dimensions 12.4 ± 2.2 × 9.3 ± 1.6 µm.

Culture characteristics: Colonies on V8A and CA appressed with limited aerial mycelium, chrysanthemum-like on V8A and faintly radiate on CA; on PDA dense-felty and uniform (Fig. 39).

Cardinal temperatures and growth rates: On V8A optimum 27.5 °C with 8.2 ± 0.83 mm/d radial growth, maximum 30–<32.5 °C, minimum <10 °C (Fig. 42), lethal temperature 32.5–35 °C. At 20 °C on V8A, CA and PDA 6.51 ± 0.45 mm/d, 5.93 ± 0.12 mm/d and 3.04 ± 0.17 mm/d, respectively.

Additional materials examined: **USA**, Louisiana, Clark Creek, isolated from riparian soil of a streambank in a mixed subtropical forest, March 2020, *T. Corcobado & T. Majek* (LU192); Louisiana, JC "Sonny" Gilbert, isolated from naturally fallen *Magnolia* leaves floating in a stream running through a mixed subtropical forest, March 2020, *T. Corcobado & T. Majek* (LU079, LU083). **Bosnia-Herzegovina**, Ozren Mountain, isolated from a necrotic leaf floating in a forest stream, Apr. 2019, *I. Milenković* (BN113); Teslić, isolated from rhizosphere soil of a riparian *Alnus glutinosa* tree, May 2019, I. *Milenković* (BN276, BN277).

Phytophthora macroglobulosa H.-C. Zeng, H.-H. Ho, F.-C. Zheng & T. Jung, ***sp. nov.*** MycoBank MB 847316. Fig. 52.

Etymology: The name refers to the large size of the lipid globule in most oospores.

Typus: **China**, Hainan Island, Wuzhi Mountain, isolated from soil in a tropical montane forest, 1999, *H.-C. Zeng, H.-H. Ho & F.-C. Zheng* (**holotype** CBS H-25114, dried culture on V8A, ex-holotype living culture CBS 149491 = TJ917 = FFM 2 2-2).

Morphological structures on V8A: *Sporangia* not observed in solid agar but abundantly produced in non-sterile soil extract; borne terminally on unbranched sporangiophores (Fig. 52A, E) or in dense or lax sympodia of 2–4 sporangia (Fig. 52L); non-caducous, predominantly ovoid, broad ovoid or elongated ovoid (77.2 %; Fig. 52A–D, L), less frequently ellipsoid to elongated-ellipsoid (9.4 %; Fig. 52E, F), obpyriform to elongated obpyriform, sometimes asymmetric (6.4 %; Fig. 52G, H), distorted with usually two or three apices (3 %; Fig. 52J), mouse-shaped (3 %; Fig. 52I, K), limoniform (0.6 %) or obovoid (0.4 %); apices semipapillate (Fig. 52A–J); vacuoles (18.2 %; Fig. 52F–H) common and pedicels (6.5 %) infrequently observed; sporangial dimensions averaging 61.2 ± 6.5 × 39.1 ± 3.9 µm (overall range 42.6–79.3 × 28.5–47.6 µm; range of isolate means 59.4–64.5 × 38.4–39.4) with a length/breadth ratio of 1.58 ± 0.19 (overall range 1.25–2.29); pedicel length 22.5 ± 14.9 µm (range 4.2–49.0 µm); sporangial proliferation exclusively external (Fig. 52B, D, F, L); sporangial germination indirectly with zoospores discharged through an exit pore of 6.6–10.8 µm (av. 8.5 ± 0.9 µm) (Fig. 52K). *Zoospores* limoniform to reniform whilst motile, becoming spherical, ovoid or sometimes irregular on encystment; cysts with an av. diam of 11.0 ± 1.8 µm, germinating mostly directly by producing hyphae or sometimes indirectly by releasing a secondary zoospore (diplanetism). *Hyphal swellings* on sporangiophores are rare, ovoid, limoniform or subglobose. *Hyphal aggregations* are infrequently produced. *Chlamydospores* not observed. *Oogonia* abundantly produced in single culture ('homothallic' breeding system), on short, often curved stalks (82 %) or sessile (18 %); globose to subglobose with round bases (94 %; Fig. 52M–T, V) or short tapering bases (6 %; Fig. 52U) and smooth or slightly wavy walls; av. diam 31.5 ± 2.8 µm with an overall range of 21.9–38.7 µm (range of isolate means 31.1–32.1 µm); slightly aplerotic to aplerotic (59 %; Fig. 52M–O, Q–T) or nearly plerotic (41 %; Fig. 52P, U, V). *Oospores* globose with a large lipid globule, often almost entirely filling the oospore (Fig. 52O, R, T–V); av. diam 26.9 ± 2.4 µm with an overall range of 18.5–32.3 µm (range of isolate means 26.5–27.3 µm); wall diam 1.58 ± 0.21 µm (overall range 1.13–2.22 µm) and oospore wall index 0.31 ± 0.03; abortion 22 % (6–34 %) after 4 wk. *Antheridia* almost exclusively paragynous (99.3 %), 1-celled and club-shaped, ovoid, limoniform or subglobose (Fig. 52M–U) or rarely amphigynous (Fig. 52V); 11.9 ± 2.3 × 7.7 ± 1.4 µm.

Culture characteristics: Colonies appressed with limited aerial mycelium and petaloid pattern on V8A and CA; appressed and dense-felty with a petaloid pattern on PDA (Fig. 39).

Cardinal temperatures and growth rates: On V8A optimum 25 °C with 9.47 ± 0.16 mm/d radial growth, maximum 27.5–<30 °C, minimum <10 °C (Fig. 42), lethal temperature 32.5–<35 °C. At 20 °C on V8A, CA and PDA 7.74 ± 0.04 mm/d, 5.93 ± 0.2 mm/d and 2.66 ± 0.24 mm/d, respectively.

Additional materials examined: **China**, Hainan Island, Wuzhi Mountain, isolated from soil in a tropical montane forest, 1999, *H.-C. Zeng, H.-H. Ho & F.-C. Zheng* (TJ1449, TJ1451).

Phytophthora nimia T. Jung, H. Masuya, A. Hieno & C.M. Brasier, ***sp. nov.*** MycoBank MB 847318. Fig. 53.

Etymology: The name refers to the infrequent occurrence of sporangia which are too big for the available cytoplasm and reduce the effective volume by the production of big plugs inside the sporangia (*nimia* Latin = too big).

Typus: **Japan**, Kyushu Island, Takakuma, isolated from rhizosphere soil of *Castanopsis sieboldii* in a warm-temperate *Fagaceae-Lauraceae* forest on volcanic soil, May 2017, *T. Jung & H. Masuya* (**holotype** CBS H-25117, dried culture on V8A, ex-holotype living culture CBS 149494 = JP490).

Morphological structures on V8A: Sporangia produced abundantly in non-sterile soil extract; typically borne terminally in dense or lax sympodia of 2–8 sporangia (97.7 %; Fig. 53B, M), or less frequently intercalary (1.8 %; Fig. 53C, H) or sessile (0.5 %; Fig. 53F); predominantly ovoid, broad-ovoid or elongated ovoid (75.1 %; Fig. 53A, B, J, K, M), less frequently ellipsoid to elongated-ellipsoid (8.5 %; Fig. 53C, G, L), obpyriform to elongated obpyriform (7 %; Fig. 53D), limoniform or elongated limoniform (6 %; Fig. 53B), pyriform to elongated pyriform (2.5 %; Fig. 53E, F) or distorted often with two apices (0.9 %; Fig. 53H, I); apices semipapillate (Fig. 53A–I, K, M); predominantly persistent but a few caducous sporangia (<1 %; Fig. 53B, K) were present in most isolates; infrequently sporangia too big for the available cytoplasm resulting in the production of big conspicuous plugs inside the sporangia to reduce the effective sporangial volume (3.7 %; Fig. 53B, F, H);

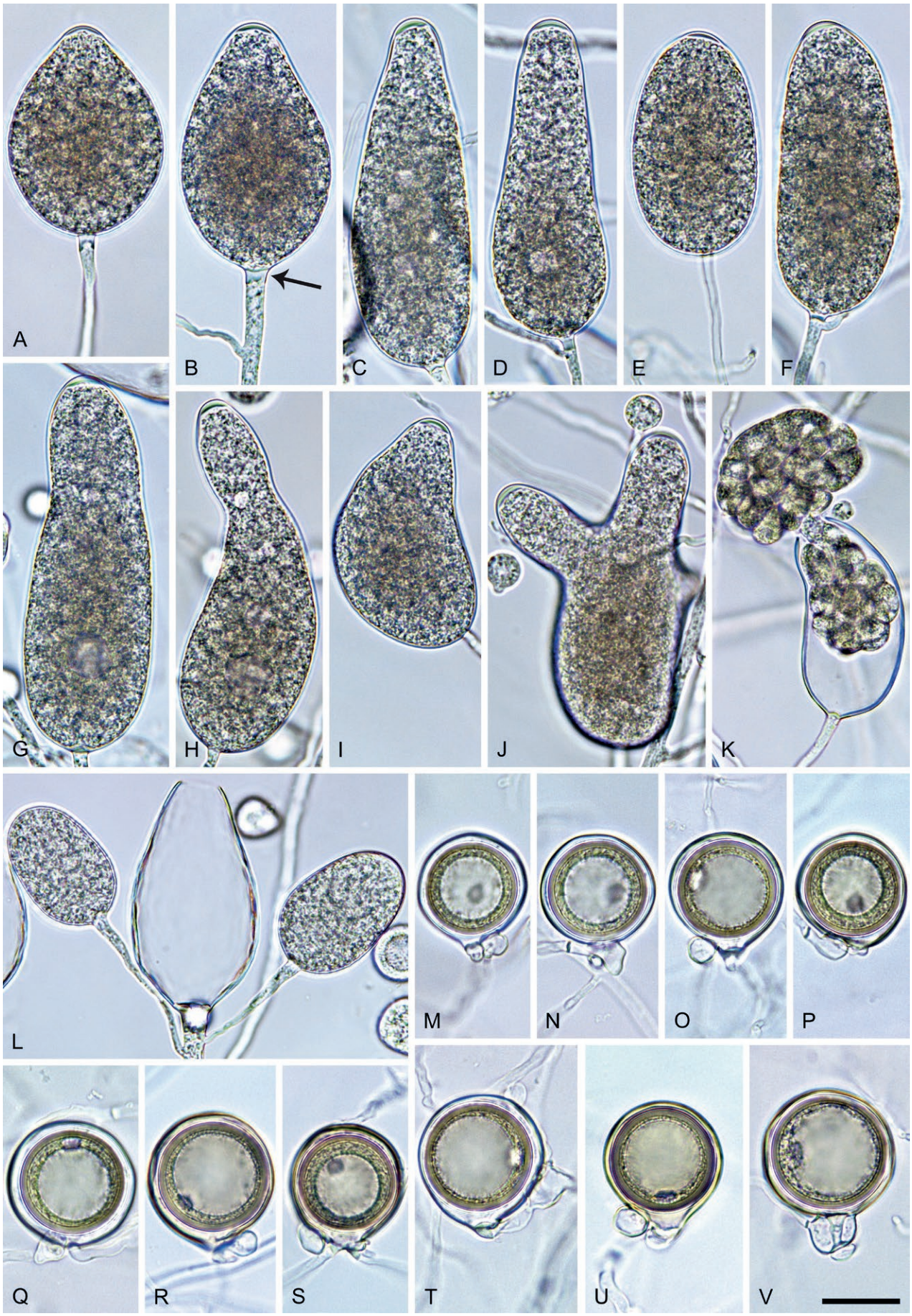

Fig. 52. *Phytophthora macroglobulosa*. **A–L.** Sporangia formed on V8-agar (V8A) in soil extract. **A–J.** Semipapillate apices. **A–I, K, L.** Ovoid, ellipsoid, obpyriform and mouseshaped, often elongated sporangia. **B, D, F, L.** External proliferation. **B.** Thick basal plug (arrow). **F–H.** Sporangia with vacuoles. **J.** Distorted multilobed sporangium. **K.** Zoospore release. **L.** Dense sympodium. **M–V.** Globose to subglobose oogonia with slightly aplerotic to near-plerotic oospores, formed in solid V8A. **M–U.** Oogonia with smooth walls and paragynous antheridia. **V.** Oogonium with slightly wavy wall and amphigynous antheridium. Images: A, M, N, P, Q. TJ1449. B–L, O, R–V Ex-type CBS 149491; Scale bar = 20 µm; V applies to A–V.

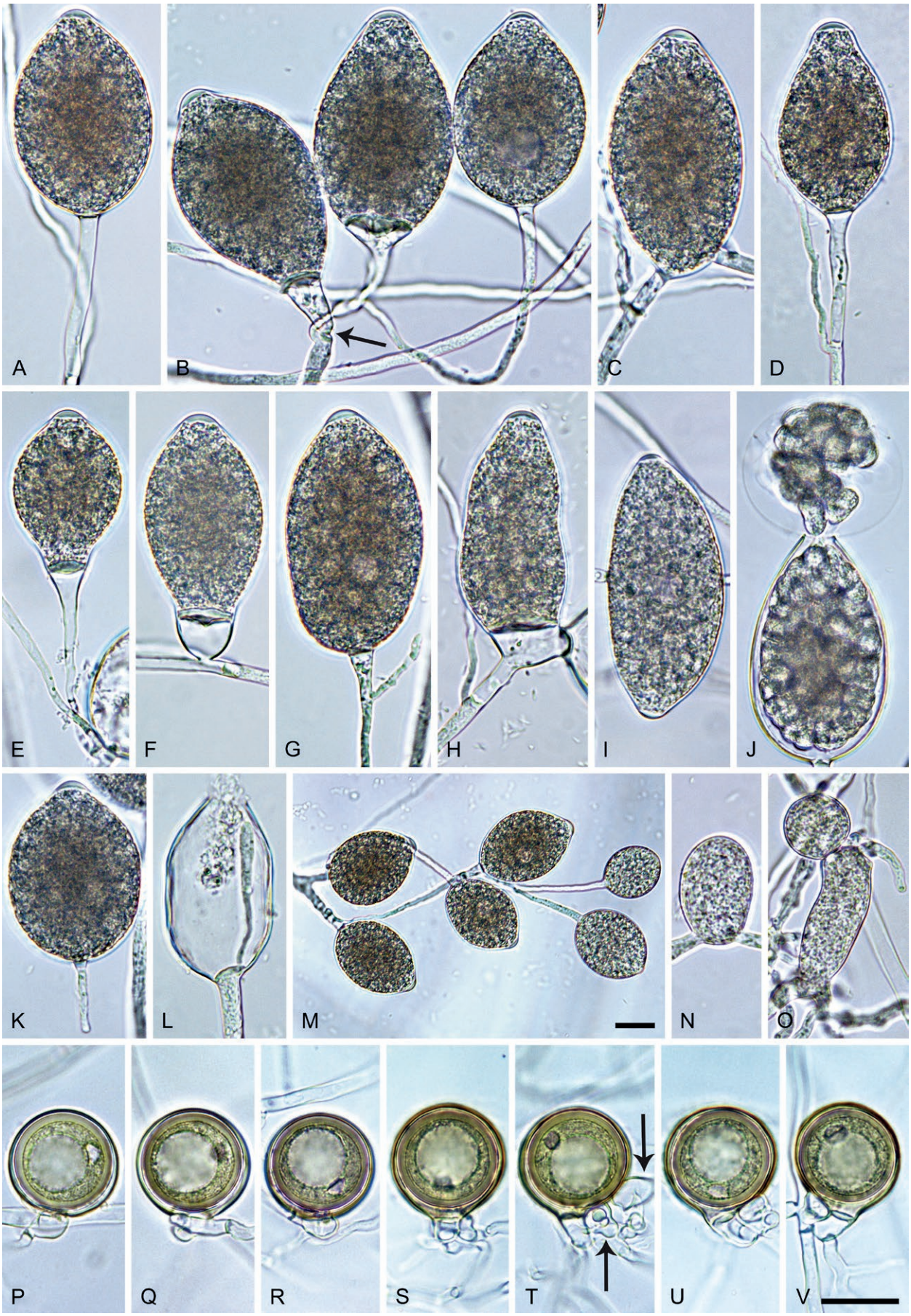

Fig. 53. *Phytophthora nimia*. **A–M.** Sporangia formed on V8-agar (V8A) in soil extract. **A–I, K.** Semipapillate apices. **A–G, J–M.** Ovoid, ellipsoid, obpyriform and pyriform sporangia. **A–E, G, H, M.** External proliferation. **A–E, G.** Medium-length to long pedicels. **B.** Dense sympodium; one sporangium shedding from sporangiophore (arrow). **C–I.** Intercalary sporangia. **F, H.** Thick plugs below cytoplasm. **H, I.** Distorted sporangia. **I.** Two apices. **J.** Zoospore release. **K.** Caducous sporangium. **L.** Internal extended proliferation. **M.** Dense sympodium. **N, O.** Hyphal swellings on V8A in soil extract. **P–V.** Globose to subglobose oogonia with near-plerotic to plerotic oospores and paragynous antheridia, formed in V8A. **T.** Oogonium with two antheridia. Images: A, B, G, H, K, L, O, Q, T–V. Ex-type CBS 149494; C, M, N. JP772; D–F, R, S. JP750; I, J, P. JP100. Scale bars = 20 µm; V applies to A–L, N–V.

lateral attachment of the sporangiophore (6 %;) pedicels (49 %; Fig. 53A–E, K) and a widening of the sporangiophore towards the sporangium (4.5 %; Fig. 53B, E) commonly observed; sporangial proliferation almost exclusively external (Fig. 53A–E, G, H, M), internal extended proliferation rarely occurring in several isolates (Fig. 53L); sporangial dimensions averaging 54.2 ± 6.7 × 35.0 ± 5.0 µm (overall range 30.0–72.6 × 22.4–62.3 µm; range of isolate means 52.2–56.8 × 33.9–36.1 µm) with a length/breadth ratio of 1.56 ± 0.2 (overall range 0.68–2.53); pedicel length 21.7 ± 15.9 µm (range 3.8–91.1 µm); sporangial germination indirectly with zoospores discharged through an exit pore 4.4–9.4 µm wide (av. 6.8 ± 0.8 µm) (Fig. 53J, L). *Zoospores* limoniform to reniform whilst motile, becoming spherical (av. diam = 11.2 ± 1.5 µm) on encystment; cysts usually germinate directly but diplanetism occurs in all isolates. *Hyphal swellings* infrequently produced in water on sporangiophores and hyphae; globose to subglobose, ovoid, ellipsoid or allantoid (Fig. 53N, O). *Chlamydospores* not observed. *Oogonia* abundantly produced in single culture ('homothallic' breeding system), terminal on short to medium-length, sometimes curved lateral hyphae or sessile, smooth-walled, globose to slightly subglobose (Fig. 53P–V), predominantly with a rounded (90.7 %; Fig. 53P–U) or a very short tapering base (9.3 %; Fig. 53V); oogonial diam 27.5 ± 2.6 µm (overall range 19.3–34.8 µm; range of isolate means 26.4–28.2 µm); nearly plerotic to plerotic (Fig. 53P–V). *Oospores* globose with a large lipid globule (Fig. 53P–V); diam 23.9 ± 2.3 µm (overall range 16.8–30.8 µm; range of isolate means 23.4–24.5 µm) wall thickness 1.62 ± 0.21 µm (overall range 1.08–2.17 µm), oospore wall index 0.35 ± 0.03; abortion rate 1–6 % (av. 3 %) after 4 wk. *Antheridia* exclusively paragynous and club-shaped, ellipsoid or subglobose (Fig. 53P–V); sometimes two antheridia attached to one oogonium (0.7 %; Fig. 53T); dimensions 11.5 ± 2.1 × 8.0 ± 1.6 µm.

Culture characteristics: Colonies on V8A rosaceous with limited aerial mycelium; on CA uniform and appressed with scanty aerial mycelium; on PDA uniform with irregular submerged margins, dense-felty appressed with limited aerial mycelium in the centre (Fig. 40).

Cardinal temperatures and growth rates: On V8A optimum at 25 °C with relatively slow radial growth of 5.15 ± 0.08 mm/d, maximum 27.5–<30 °C, minimum <10 °C (Fig. 42), lethal temperature 30–32.5 °C. At 20 °C on V8A, CA and PDA 4.38 ± 0.26 mm/d, 4.27 ± 0.18 mm/d and 3.58 ± 0.1 mm/d, respectively.

Additional materials examined: **Japan**, Kyushu Island, Takakuma, isolated from rhizosphere soil of *C. sieboldii* in a warm-temperate *Fagaceae-Lauraceae* forest on volcanic soil, May 2017, *T. Jung & H. Masuya* (JP750, JP772); Shikoku Island, Satayama, isolated from the rhizosphere of a mature *M. thunbergii* tree in a warm-temperate *Fagaceae-Lauraceae* forest, May 2017, *T. Jung & A. Hieno* (JP100).

Phytophthora oblonga T. Jung, S. Uematsu, K. Kageyama & C.M. Brasier, ***sp. nov.*** MycoBank MB 847306. Fig. 54.

Etymology: The name refers to the production of elongated oogonia and oospores (*oblonga* Latin = elongated).

Typus: **Japan**, Shikoku Island, Satayama, isolated from the rhizosphere of a mature *Machilus thunbergii* tree in a warm-temperate *Fagaceae-Lauraceae* forest, May 2017, *T. Jung & S. Uematsu* (**holotype** CBS H-25118, dried culture on V8A, ex-holotype living culture CBS 149495 = JP367).

Morphological structures on V8A: Sporangia produced infrequently on solid agar and abundantly in non-sterile soil extract; typically borne terminally (99.3 %) in dense or lax sympodia of 2–8 sporangia (Fig. 54K) or rarely intercalary (0.7 %); predominantly ovoid, broad-ovoid or elongated ovoid (80.3 %; Fig. 54A, B, G, J–M), less frequently obpyriform or elongated obpyriform (10 %; Fig. 54C–E), distorted and mostly with two apices (3.8 %; Fig. 54H, I), limoniform or elongated limoniform (1.8 %), mouse-shaped (1.7 %; Fig. 54F), ellipsoid or elongated-ellipsoid (1.4 %) or obovoid (1 %); apices usually semipapillate (92 %; Fig. 54A–F, I, L) or infrequently nonpapillate (8 %; Fig. 54G, H), sometimes curved or asymmetric (19.3 %; Fig. 54B, C, F–H); sporangia formed in water predominantly (>99 %) persistent but sporangia formed on solid agar almost exclusively caducous (>99 %; Fig. 54L, M); lateral attachment of the sporangiophore (12.3 %; Fig. 54C, E, F, L, M), pedicels (13.3 %; Fig. 54D, I, L, M), vacuoles (24.4 %; Fig. 54B, D–F, H) and a conspicuous basal plug (33.3 %; Fig. 54I) commonly observed; sporangial proliferation mostly external (Fig. 54A, B, D, G, H, K) or infrequently internal in an extended way (Fig. 54G); sporangial dimensions averaging 56.1 ± 6.6 × 37.2 ± 4.7 µm (overall range 38.4–72.1 × 23.8–48.6 µm; range of isolate means 53.1–58.9 × 34.8–39.8 µm) with a length/breadth ratio of 1.52 ± 0.15 (overall range 1.2–2.02); pedicel length 15.1 ± 7.1 µm (range 7.3–32.9 µm); sporangial germination indirectly with zoospores discharged through an exit pore 5.6–11.6 µm wide (av. 8.3 ± 1.1 µm) (Fig. 54G, J, K, M). *Zoospores* limoniform to reniform whilst motile, becoming spherical (av. diam = 11.6 ± 1.4 µm) on encystment; cysts germinating directly. *Hyphal swellings* rarely produced in water on sporangiophores and hyphae; globose to subglobose or limoniform (Fig. 54N). *Chlamydospores* not observed. *Oogonia* abundantly produced in single culture ('homothallic' breeding system), terminal on short to medium-length, sometimes curved lateral hyphae or sessile, smooth-walled, globose to subglobose (48.1 %) with a rounded (85.2 %; Fig. 54O–Q) or a very short tapering base (14.8 %; Fig. 54R), or slightly elongated to tube-like or ampulliform elongated, usually with a tapering base (51.9 %; Fig. 54S–W); often comma-shaped (26 %; Fig. 54S, T, V, W); oogonial diam 26.6 ± 3.3 µm (overall range 15.0–38.9 µm; range of isolate means 24.9–28.6 µm); oogonial length ranging from 18.7 to 77.6 µm; nearly plerotic to plerotic (Fig. 54O–W). *Oospores* globose to subglobose with 1 large lipid globule (Fig. 54O–R) or slightly elongated to tube-like or ampulliform elongated with 1 or 2 large lipid globules (Fig. 54S–W); diam 23.6 ± 2.6 µm (overall range 12.3–30.5 µm; range of isolate means 23.0–24.8 µm), wall thickness 1.47 ± 0.2 µm (overall range 0.82–2.36 µm), oospore wall index 0.33 ± 0.03; abortion rate 1–8 % (av. 4.4 %) after 4 wk. *Antheridia* almost exclusively paragynous and club-shaped, ellipsoid or subglobose (99.5 %; Fig. 54O–W) or rarely amphigynous and cylindrical (0.5 %); sometimes two antheridia attached to one oogonium (0.4 %); dimensions 11.5 ± 2.1 × 7.6 ± 1.5 µm.

Culture characteristics: Colonies on V8A and CA submerged to suppressed with scanty aerial mycelium; on V8A chrysanthemum-like to radiate and on CA stellate; on PDA uniform with irregular submerged margins, dense-felty appressed (Fig. 40).

Cardinal temperatures and growth rates: On V8A optimum at 27.5 °C with 8.17 ± 0.11 mm/d radial growth, maximum 27.5–<30 °C, minimum <10 °C (Fig. 42), lethal temperature 30–32.5 °C. At 20 °C on V8A, CA and PDA 6.32 ± 0.17 mm/d, 5.71 ± 0.03 mm/d and 2.83 ± 0.11 mm/d, respectively.

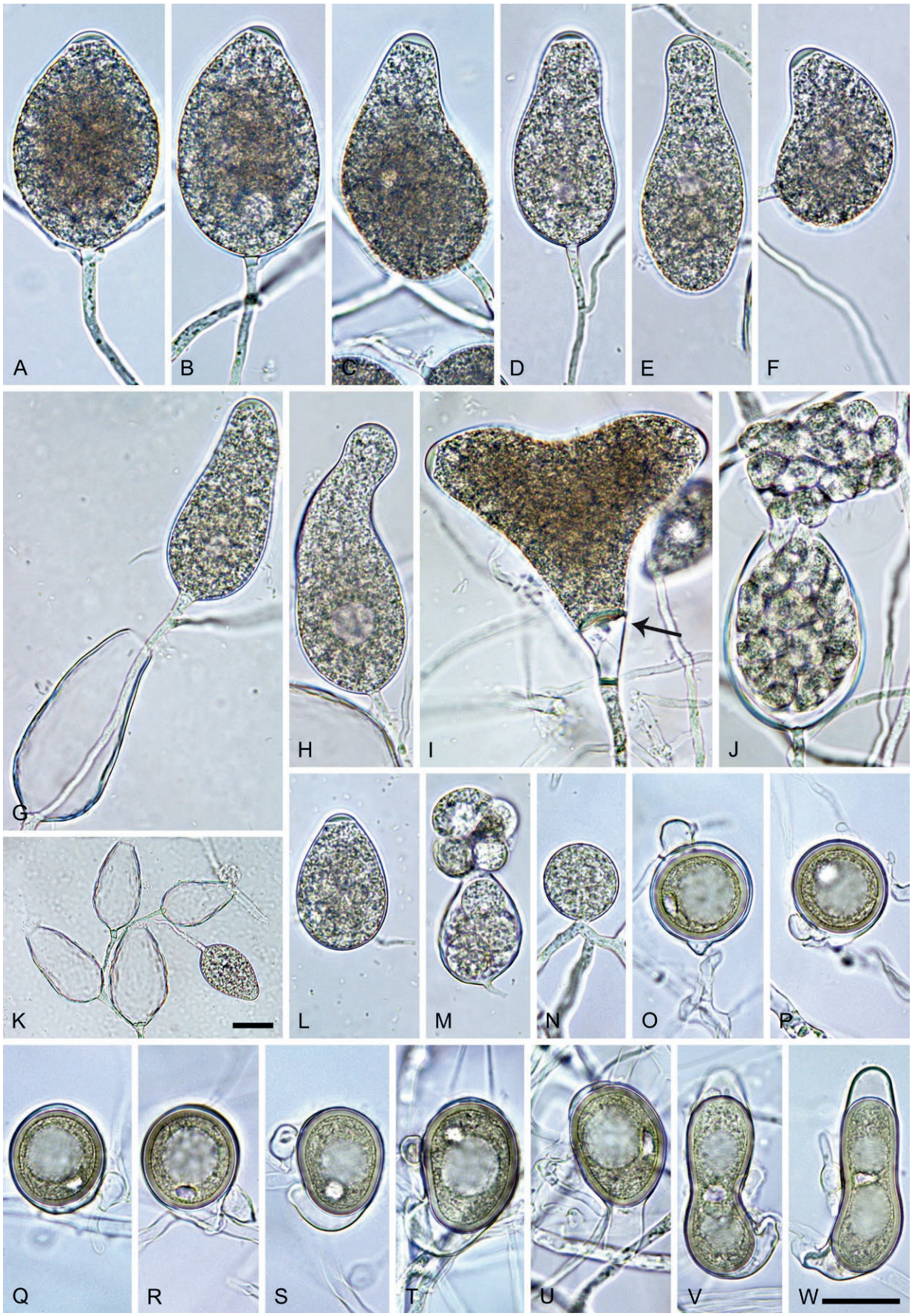

Fig. 54. *Phytophthora oblonga*. **A–K.** Sporangia formed on V8-agar (V8A) in soil extract. **A–F, I.** Semipapillate, often curved apices. **G, H.** Nonpapillate apices, **A–G, J, K.** Ovoid, obpyriform and mouse-shaped sporangia. **A, B, D, H, K.** External proliferation. **D, I.** Medium-length pedicels. **D–F, H.** Sporangia with vacuoles. **G.** Internal extended proliferation. **H.** Distorted sporangium with curved nonpapillate apex. **I.** Bilobed sporangium with thick basal plug (arrow) below the cytoplasm. **J.** Zoospore release. **K.** Dense sympodium. **L, M.** Ovoid, caducous sporangia with pedicels, formed on solid V8A. **M.** Zoospore release. **N.** Hyphal swelling on V8A in soil extract. **O–W.** Oogonia with near-plerotic to plerotic oospores and paragynous antheridia, formed in V8A. **O–R.** Globose to subglobose oogonia. **S–W.** Elongated oogonia. Images: A, D, E, G, H, K, M, O, P, S, V. Ex-type CBS 149495; B, C, I, L, W. JP366; F, J, N, Q, R, T, U. JP097. Scale bars = 20 µm; W applies to A–J, L–W.

Additional materials examined: **Japan**, Shikoku Island, Satayama, isolated from the rhizosphere of a mature *M. thunbergii* tree in a warm-temperate *Fagaceae-Lauraceae* forest, May 2017, *T. Jung & S. Uematsu* (JP366); isolated from the rhizosphere of a mature *C. sieboldii* tree in a warm-temperate *Fagaceae-Lauraceae* forest, May 2017, *T. Jung & K. Kageyama* (JP097).

Phytophthora obturata T. Jung, N.M. Chi, I. Milenković & M. Horta Jung, ***sp. nov.*** MycoBank MB 847301. Fig. 55.

Etymology: The name refers to the conspicuous basal plug which is formed in many sporangia and often protrudes backwards into the sporangiophore (*obturata* Latin = plugged).

Typus: **Vietnam**, Ba Vì National Park, isolated from rhizosphere soil of *Meliosma arnottiana* in a subtropical humid evergreen forest, Mar. 2016, *T. Jung & N.M. Chi* (**holotype** CBS H-25119, dried culture on V8A, ex-holotype living culture CBS 149496 = VN528).

Morphological structures on V8A: Sporangia produced abundantly in non-sterile soil extract; typically borne terminally in dense or lax sympodia of 2–9 sporangia (Fig. 55M) or less frequently on unbranched long or short sporangiophores (Fig. 55A, H), or intercalary (2.5 %); predominantly ovoid, broad-ovoid or elongated ovoid (64.1 %; Fig. 55A–D, G, K, M, N), less frequently ellipsoid or elongated-ellipsoid (14.5 %; Fig. 55E), limoniform or elongated limoniform (11.5 %; Fig. 55F, L), distorted and usually with two apices (4.2 %; Fig. 55J), obpyriform (3 %; Fig. 55H), ampulliform (1.5 %), obovoid (1 %) or pyriform to elongated pyriform (0.2 %; Fig. 55I); apices semipapillate (Fig. 55A–J, M, N); usually persistent but a few caducous sporangia (0.2 %; Fig. 55N) and sporangia with a constriction of the sporangiophore enabling caducity (3.7 %; Fig. 55L) were present in all isolates; a conspicuous basal plug often protruding backward into the sporangiophore (55.7 %; Fig. 55C, F, I, L), lateral attachment of the sporangiophore (9.8 %; Fig. 55G, H), pedicels (49.6 %; Fig. 55A, B, E, F, H, I, K, L, N), slightly asymmetric shapes (11.6 %; Fig. 55G–I), a widening of the sporangiophore towards the sporangial base (1.2 %; Fig. 55C) and small sporangiophore swellings close to the sporangial base (0.7 %; Fig. 55D) commonly observed; sporangial proliferation exclusively external (Fig. 55F, M); sporangial dimensions averaging 53.9 ± 6.5 × 34.0 ± 4.3 µm (overall range 34.0–84.1 × 20.4–57.5 µm; range of isolate means 49.4–57.0 × 30.4–37.6 µm) with a length/breadth ratio of 1.6 ± 0.2 (overall range 0.97–2.48); pedicel length 15.6 ± 9.4 µm (range 1.5–62.5 µm); sporangial germination usually indirectly with zoospores discharged through an exit pore 3.7–10.3 µm wide (av. 7.5 ± 1.0 µm) (Fig. 55K, L). *Zoospores* limoniform to reniform whilst motile, often with flagella ends forming a ring (Fig. 55O); becoming spherical (av. diam = 11.0 ± 1.6 µm) on encystment; cysts mostly germinating directly although diplanetism occurred in all isolates. *Hyphal swellings* produced in water on sporangiophores and hyphae; globose to subglobose, ovoid, limoniform, deltoid or irregular (Fig. 55D, H, M, P), sometimes catenulate (Fig. 55P); dimensions 13.8 ± 4.7 µm (range 6.4–37.9 µm). *Chlamydospores* not observed. *Oogonia* abundantly produced in single culture ('homothallic' breeding system), terminal on short to medium-length, sometimes curved lateral hyphae or sessile, smooth-walled, globose to slightly subglobose (82.3 %; Fig. 55Q–W) or slightly elongated (17.7 %; Fig. 55X, Y), usually with a rounded (84.6 %; Fig. 55Q, S, U–X) or a short tapering base (15.4 %; Fig. 55R, T, Y); oogonial diam 26.0 ± 2.9 µm (overall range 17.4–35.1 µm; range of isolate means 22.7–27.1 µm); nearly plerotic to plerotic (96.4 %; Fig. 55Q–W) or slightly aplerotic (3.6 %; Fig. 55X, Y). *Oospores* globose with a large lipid globule (Fig. 55Q–Y); diam 23.7 ± 2.5 µm (overall range 15.6–32.2 µm; range of isolate means 21.0–24.8 µm) wall thickness 1.81 ± 0.24 µm (overall range 1.1–2.48 µm), oospore wall index 0.39 ± 0.04; abortion rate 1–6 % (av. 2.3 %) after 4 wk. *Antheridia* exclusively paragynous and club-shaped, ovoid or subglobose (Fig. 55Q–Y); sometimes two antheridia attached to one oogonium (Fig. 55W); dimensions 12.1 ± 2.4 × 6.9 ± 1.0 µm.

Culture characteristics: Colonies on V8A submerged to appressed with a chrysanthemum-like pattern; on CA appressed with scanty aerial mycelium and a chrysanthemum-like pattern; on PDA dense-felty with irregular margins and a faint petaloid pattern (Fig. 40).

Cardinal temperatures and growth rates: On V8A optimum at 25 °C (2 isolates) or 27.5 °C (6 isolates) with 9.43 ± 0.59 mm/d radial growth at 27.5 °C, maximum 27.5–<30 °C, minimum <10 °C (Fig. 42), lethal temperature 32.5–35 °C. At 20 °C on V8A, CA and PDA 7.67 ± 0.34 mm/d, 5.69 ± 0.11 mm/d and 3.6 ± 0.14 mm/d, respectively.

Additional materials examined: **Vietnam**, Ba Vì National Park, isolated from rhizosphere soil of *M. arnottiana* in a subtropical humid evergreen forest, Mar. 2016, *T. Jung, M. Horta Jung & N.M. Chi* (VN819, VN820, VN821, VN822, VN823); Sapa, Sau Chua Mountain, isolated from naturally fallen leaves floating in a stream running through a montane *Chamaecyparis* forest, Mar. 2017, *T. Jung, B. Scanu & N.M. Chi* (VN850, VN1005, VN1013).

Phytophthora platani T. Jung, A. Pérez-Sierra, S.O. Cacciola & M. Horta Jung, ***sp. nov.*** MycoBank MB 847302. Fig. 56.

Etymology: The name refers to the isolation of all known isolates from necrotic tissue and rhizosphere soil of *Platanus* trees.

Typus: **Italy**, Sicily, Pantalica Nature Reserve, isolated from the rhizosphere of *Platanus orientalis* in a riparian forest, May 2013, *T. Jung & S.O. Cacciola* (**holotype** CBS H-25121, dried culture on V8A, ex-holotype living culture CBS 149638 = TJ812).

Morphological structures on V8A: *Sporangia* not observed in solid agar but abundantly produced in non-sterile soil extract; borne terminally in lax or dense sympodia of 2–15 sporangia (Fig. 56M) or less frequently on unbranched sporangiophores or intercalary (2.9 %; Fig. 56E); sporangia almost exclusively semipapillate (99 %; Fig. 56A–G, M) or rarely papillate (1 %; Fig. 56H), mostly ovoid, broad ovoid or elongated ovoid (54.3 %; Fig. 56A–C, G), less frequently limoniform to elongated-limoniform (18.9 %; Fig. 56I, L), obpyriform to elongated obpyriform (6.5 %; Fig. 56F), pyriform (4.3 %; Fig. 56D), distorted and often with two or three apices (8.4 %; Fig. 56G, H, K), ellipsoid (3.8 %; Fig. 56J), obovoid (3.2 %) or ampulliform (0.6 %; Fig. 56E); special features like lateral attachment of the sporangiophore (22.3 %; Fig. 56A, B, F, G), pedicels (41.1 %; Fig. 56A–D) and an often conspicuous basal plug (82.9 %; Fig. 56C, D, I, K, L) common; swellings close to the sporangial base (0.9 %; Fig. 56B) infrequently observed; almost exclusively non-caducous but a few caducous sporangia breaking-off at a constriction of the sporangiophore (0.9 %; Fig. 56C) were present in all isolates; proliferation external (Fig. 56E, M) and less frequently internal in a nested and extended way (Fig. 56J–M), or rarely by emergence from the wall of a mature sporangium (Fig. 56G); sporangial dimensions averaging 53.6 ± 8.1 × 34.0 ± 4.6 µm (overall range 29.3–91.6 × 21.1–56.3 µm; range of isolate

Fig. 55. *Phytophthora obturata*. **A–N.** Sporangia formed on V8-agar (V8A) in soil extract. **A–J, N.** Semipapillate apices. **A–I, K–N.** Ovoid, ellipsoid, limoniform and obpyriform sporangia. **A, B, E, F, H, I, K, L, N.** Short to medium-length pedicels (arrows). **C, E, I, K.** Thick plugs below cytoplasm. **D.** Hyphal swelling. **F, M.** External proliferation. **J.** Distorted sporangium with two apices and hyphal extension. **K.** Zoospore release. **L.** After zoospore release, with constriction of pedicel (arrow). **M.** Dense sympodium. **N.** Caducous sporangium. **O.** Zoospores with ring-like flagella ends (arrows). **P.** Catenulate hyphal swellings on V8A in soil extract. **Q–Y.** Globose, subglobose or elongated oogonia with plerotic to slightly aplerotic oospores and paragynous antheridia formed in V8A. **W.** Two antheridia (arrows). Images: A, B, E, H, J, M, N–S, X, Y. Ex-type CBS 149496; C, D, F, G, K, T–W. VN850; I, L. VN1005. Scale bars = 20 µm; Y applies to A–L, N–Y.

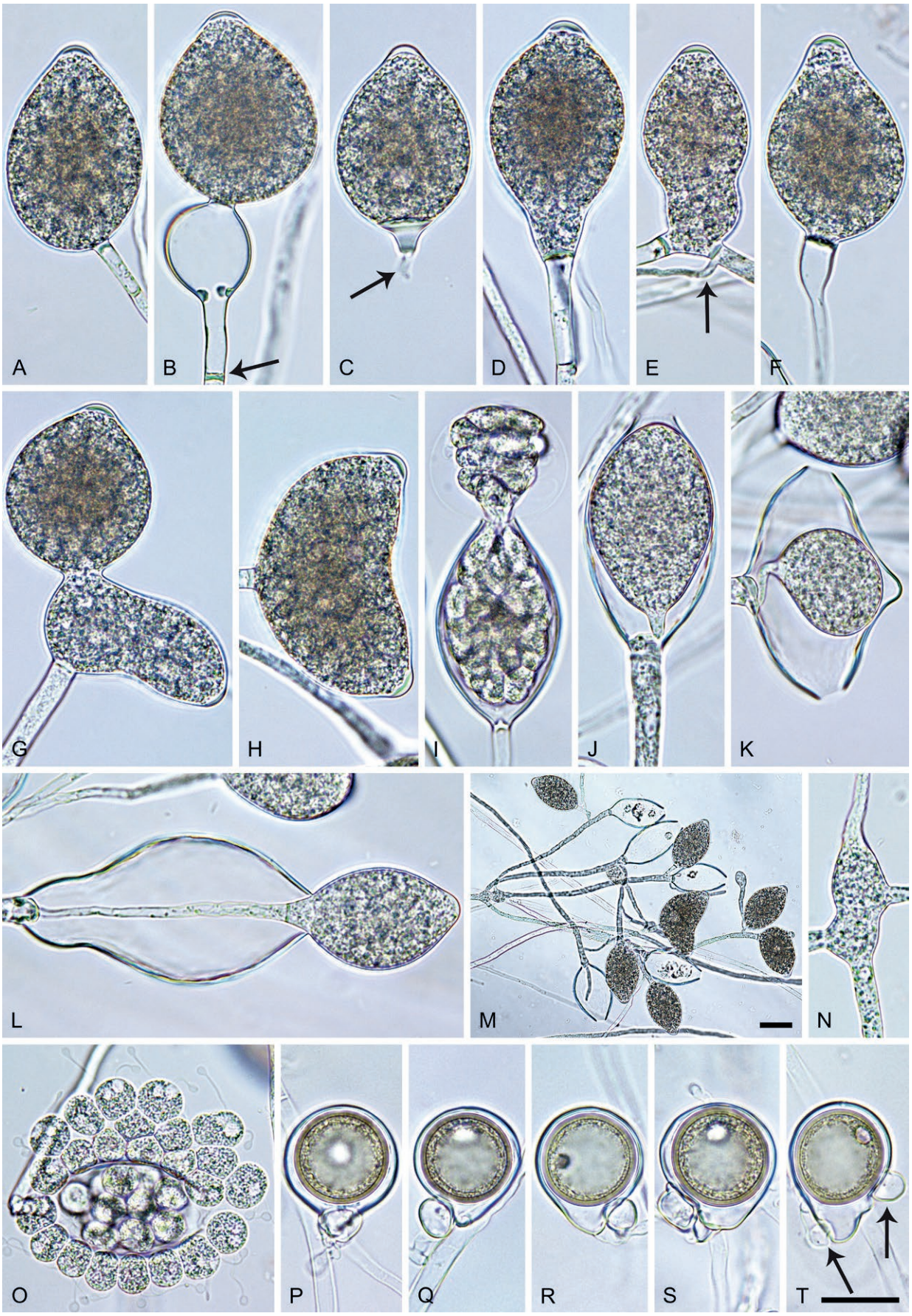

Fig. 56. *Phytophthora platani*. **A–M.** Sporangia formed on V8-agar (V8A) in soil extract. **A–F, I, J, L, M.** Ovoid, pyriform, ampulliform, obpyriform and limoniform sporangia. **A–G.** Semipapillate apices. **A–D.** Short to long pedicels (arrows in B, C). **B.** Pedicel swelling. **C.** Caducous sporangium. **E.** Intercalary sporangium with external proliferation (arrow). **G.** Ovoid sporangium arising from distorted sporangium. **H.** Bipapillate sporangium. **I.** Zoospore release. **J, K.** Internal nested proliferation. **L.** Internal extended proliferation. **M.** Dense compound sympodium. **N.** Hyphal swelling on V8A in soil extract. **O.** Zoospores with ring-like flagella ends. **P–T.** Subglobose to elongated oogonia with near-plerotic to slightly aplerotic oospores and paragynous antheridia formed in V8A. **T.** Two antheridia (arrows). Images: A, E, Q. APS_272a; B, D, F, G, J, M–O, R, T. Ex-type CBS 149638; C, H, I, K, L, P, S. VN965. Scale bars = 20 µm; T applies to A–L, N–T.

means 48.7–63.8 × 30.1–37.6 µm) with a length/breadth ratio of 1.59 ± 0.22 (overall range 1.15–2.57); pedicel length 20.8 ± 11.3 µm (range 1.4–62.6 µm); sporangial germination indirectly with zoospores discharged through an exit pore of 4.0–10.4 µm (av. 6.7 ± 1.1 µm; Fig. 56I–L). *Zoospores* limoniform, subglobose or reniform whilst motile, often with ring-like flagella ends (Fig. 56O), becoming spherical (av. diam = 10.5 ± 1.0 µm) on encystment; cysts predominantly germinating directly by producing hyphae or less frequently by releasing a secondary zoospore (diplanetism). *Hyphal swellings* commonly produced in water, close to the sporangial base or at sporangiophore nodes; limoniform, subglobose, deltoid or irregular (Fig. 56M, N), 15.2 ± 2.9 µm (range 11.0–22.4 µm). *Chlamydospores* not observed. *Oogonia* abundantly produced in single culture ('homothallic' breeding system), on short, often curved stalks (87.6 %; Fig. 56R–T) or sessile (12.4 %; Fig. 56P, Q); smooth-walled, globose to subglobose with a short tapering base (80.4 %; Fig. 56P–R) or slightly elongated (19.6 %; Fig. 56S, T), sometimes slightly excentric (13.6 %; Fig. 56S); av. diam 30.5 ± 2.6 µm with an overall range of 16.2–39.7 µm and a range of isolate means of 29.2–31.1 µm; slightly aplerotic to aplerotic (61.2 %; Fig. 56P, Q, S) or nearly plerotic to plerotic (38.8 %; Fig. 56R, T). *Oospores* globose or subglobose with a large lipid globule (Fig. 56P–T); av. diam 26.3 ± 2.3 µm with an overall range of 14.5–34.5 µm and a range of isolate means of 25.2–27.3 µm; wall diam 1.4 ± 0.22 µm (overall range 0.69–3.53 µm) and oospore wall index 0.29 ± 0.04; abortion rate after 4 wk 1–13 % (av. 5 %). *Antheridia* 1-celled, almost exclusively paragynous and club-shaped, ovoid or subglobose (99.8 %; Fig. 56P–T) or rarely amphigynous and cylindrical (0.2 %); sometimes two antheridia attached to one oogonium (Fig. 56T); 12.3 ± 2.4 × 9.1 ± 1.8 µm.

Culture characteristics: Colonies on V8A and CA appressed to submerged with scanty aerial mycelium and a stellate pattern on V8A and a faint radiate pattern on CA; dense felty-cottony with a faint petaloid on PDA (Fig. 40).

Cardinal temperatures and growth rates: On V8A optimum 25.0 °C with 9.28 ± 0.37 mm/d radial growth, maximum 30–<32.5 °C, minimum <10 °C (Fig. 42), lethal temperature 32.5–35 °C. At 20 °C on V8A, CA and PDA 7.73 ± 0.36 mm/d, 5.82 ± 0.28 mm/d and 2.38 ± 0.17 mm/d, respectively.

Additional materials examined: **Italy**, Sicily, Pantalica Nature Reserve, isolated from the rhizosphere of *P. orientalis* in a riparian forest, May 2013, *T. Jung & S.O. Cacciola* (TJ1446, TJ1447, TJ1448); Sicily, Irminio Nature Reserve, isolated from the rhizosphere of *P. orientalis* in a riparian forest, May 2013, *T. Jung & S.O. Cacciola* (TJ965, TJ1349, TJ1350, TJ1351, TJ1352). **UK**, London, isolated from rhizosphere soil, a necrotic root and a bark canker on a branch of a roadside *Platanus* × *acerifolia* tree, Mar. 2020, *A. Pérez-Sierra* (TJ1492 = APS_272a, TJ1493 = APS_272b, TJ1494 = APS_272c).

Phytophthora pseudocapensis T. Jung, T.-T. Chang, N.M. Chi & M. Horta Jung, ***sp. nov.*** MycoBank MB 850536. Fig. 57.

Etymology: The name refers to the morphological similarity and phylogenetic relatedness to *P. capensis*.

Typus: **Taiwan**, Fushan, isolated from a baiting leaf floating in a tributary of Ha-pen River running through a subtropical *Castanopsis-Machilus* forest, Mar. 2013, *T. Jung & T.-T. Chang* (**holotype** CBS H-25296, dried culture on V8A, ex-holotype living culture CBS 150638 = TW045).

Morphological structures on V8A: Sporangia produced infrequently on solid agar and abundantly in non-sterile soil extract; typically borne terminally (96 %) in dense or lax sympodia of 2–6 sporangia (Fig. 57M) or rarely on unbranched sporangiophores, or intercalary (4 %; Fig. 57D); non-caducous, predominantly ovoid, broad-ovoid or elongated ovoid (68.2 %; Fig. 57A–C, K, M, N), less frequently obpyriform to elongated-obpyriform (18.6 %; Fig. 57E–H), limoniform to elongated limoniform (5.1 %; Fig. 57D), distorted and usually with two apices (2.5 %; Fig. 57J), subglobose (2.5 %; Fig. 57I), ellipsoid to elongated-ellipsoid (1.8 %), mouse-shaped (0.5 %; Fig. 57H), sickle-shaped (0.4 %) or pyriform (0.4 %); apices papillate (47.8 %; Fig. 57B, C, E, G, I), semipapillate (46.3 %; Fig. 57A, D, H, J, M) or infrequently nonpapillate (5.9 %; Fig. 57F); lateral attachment of the sporangiophore (26.8 %; Fig. 57E, G, H) and pedicels (46.3 %; Fig. 57B, C, F, G, N) common; a conspicuous basal plug (5.2 %; Fig. 57D) infrequently observed; sporangial proliferation exclusively external (Fig. 57B, D, E, G, K, M); sporangial dimensions averaging 55.9 ± 7.9 × 37.4 ± 4.5 µm (overall range 36.3–93.2 × 23.9–50.3 µm; range of isolate means 46.1–63.5 × 34.0–42.1 µm) with a length/breadth ratio of 1.5 ± 0.21 (overall range 1.09–2.51); pedicel length 33.0 ± 7.7 µm (5.3–86.8 µm); sporangial germination usually indirectly with zoospores discharged through an exit pore 4.2–8.2 µm wide (av. 6.0 ± 0.7 µm) (Fig. 57K). *Zoospores* limoniform to reniform whilst motile, becoming spherical (av. diam = 10.2 ± 10.8 µm) on encystment. *Hyphal swellings* infrequently produced in water on sporangiophores; subglobose to limoniform, sometimes catenulate (Fig. 57L, M); dimensions 13.6 ± 2.0 µm (range 11.9–16.8 µm). *Chlamydospores* not observed. *Oogonia* abundantly produced in single culture ('homothallic' breeding system), terminal on short to medium-length lateral hyphae, smooth-walled, globose to slightly subglobose (60 %; Fig. 57O–R, T, X), slightly excentric to excentric (28.6 %; Fig. 57S, U, V), or slightly elongated (11.4 %; Fig. 57W), with a rounded (77.8 %; Fig. 57P–R, U–X) or a short tapering base (22.2 %; Fig. 57O, S, T); oogonial diam 26.3 ± 2.6 µm (overall range 19.3–35.7 µm; range of isolate means 24.1–29.6 µm); nearly plerotic to plerotic (62.5 %; Fig. 57O, P, T, X) or slightly aplerotic to aplerotic (37.5 %; Fig. 57Q–S, U–W). *Oospores* globose with a large lipid globule (Fig. 57O–X); diam 22.5 ± 2.2 µm (overall range 16.8–29.6 µm; range of isolate means 20.7–25.2 µm) wall thickness 1.13 ± 0.22 µm (overall range 0.7–1.8 µm), oospore wall index 0.27 ± 0.05; abortion rate 10–35 % (av. 19.2 %) after 4 wk. *Antheridia* predominantly paragynous and club-shaped, ovoid or subglobose (86.6 %; Fig. 57O–V) or less frequently amphigynous and cylindrical (13.4 %; Fig. 57W, X); dimensions 13.0 ± 2.8 × 9.0 ± 1.7 µm. *Hyphal aggregations* observed in all isolates (Fig. 57Y).

Culture characteristics: Colonies on V8A and CA appressed with limited aerial mycelium, radiate to stellate on V8A and radiate on CA; on PDA dense-felty with a petaloid pattern (Fig. 41).

Cardinal temperatures and growth rates: Optimum 25 °C with 8.1 ± 0.44 mm/d radial growth on V8A, maximum 27.5–<30 °C, minimum <10 °C (Fig. 42), lethal temperature 30–32.5 °C. At 20 °C on V8A, CA and PDA 7.1 ± 0.51 mm/d, 5.38 ± 0.31 mm/d and 4.84 ± 0.31 mm/d, respectively.

Additional materials examined: **Taiwan**, Fushan, isolated from a baiting leaf floating in Cu-keng River, Mar. 2013, *T. Jung, M. Horta Jung & T.-T. Chang* (TW064). **Indonesia**, Java, Bandung, isolated from naturally fallen necrotic leaves of unidentified tree species floating in streams running through tropical montane rainforests, Feb. 2019, *T. Jung, M. Tarigan & M. Junaid* (JV027, JV029); Sulawesi, Pali, isolated from a naturally fallen

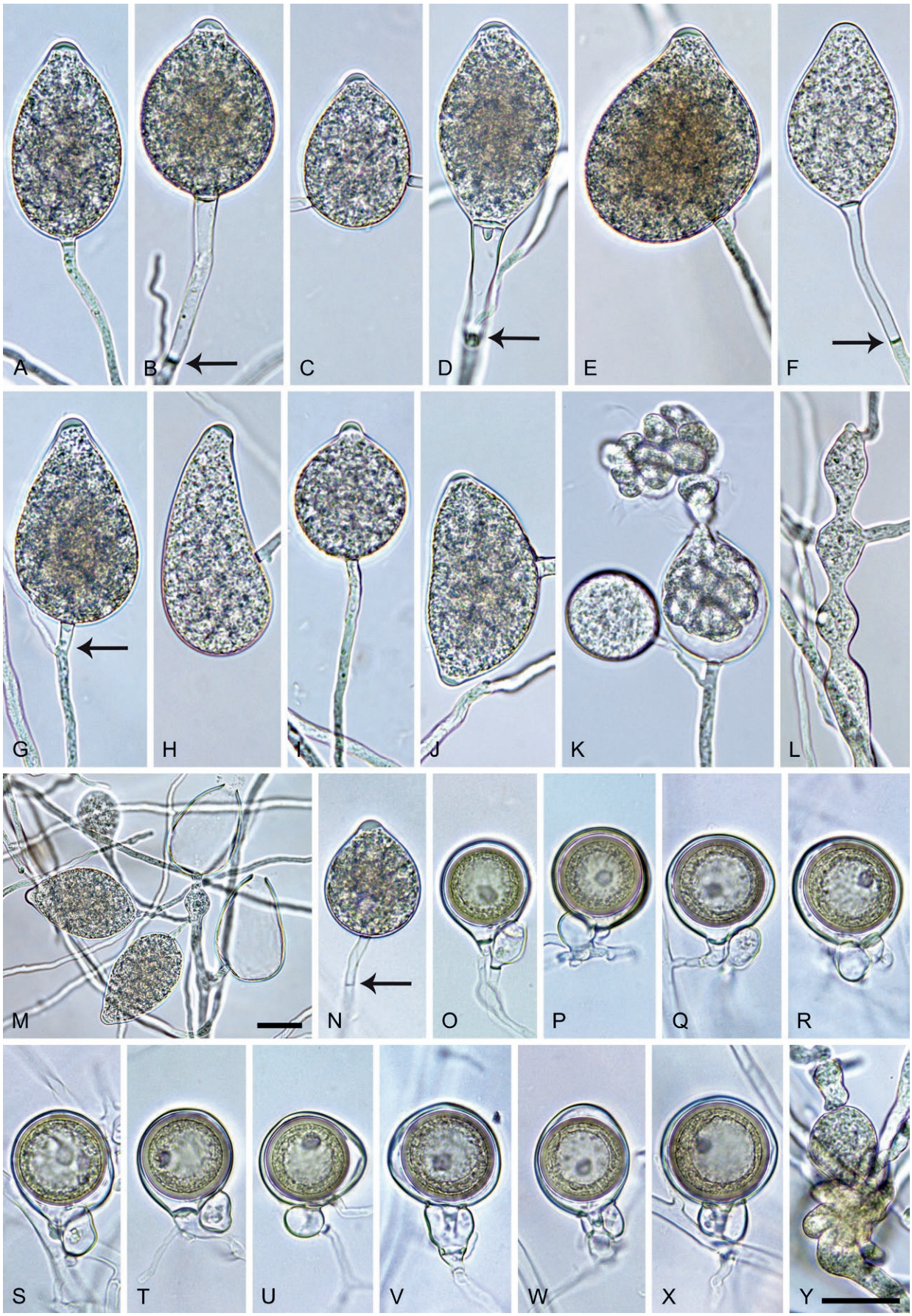

Fig. 57. *Phytophthora pseudocapensis*. **A–N.** Structures formed on V8-agar (V8A) in soil extract. **A–K, M.** Sporangia. **A–I, K, M.** Ovoid, limoniform, obpyriform, mouse-shaped and subglobose sporangia. **A, D, H, J.** Semipapillate apices. **B, C, E, G, I.** Papillate apices. **B, D, F, G.** Short to long pedicels (arrows). **B, D, E, G, K, M.** External proliferation. **C.** Intercalary sporangium. **F.** Nonpapillate apex. **J.** Two apices. **K.** Zoospore release. **L.** Catenulate hyphal swellings. **M.** Dense sympodium. **N.** Ovoid papillate sporangium with medium-length pedicel (arrow) formed on solid V8A. **O–X.** Globose, subglobose, slightly excentric or elongated oogonia with near-plerotic to slightly aplerotic oospores, formed in V8A. **O–V.** Paragynous antheridia. W, X. Amphigynous antheridia. **Y.** Hyphal aggregation in V8A. Images: A, B, D, F, H, L, O, P, T, U, X. Ex-type CBS 150638; C, G, P, S. SU415; E, M. JV027; J, K, Q, R, V, W. TW064; I, N. VN079; X. JV029. Scale bars = 20 µm; Y applies to A–L, N–Y.

necrotic leaf of an unidentified tree species floating in a stream running through a tropical montane rainforest, May 2019, *T. Jung, M. Junaid & M. Horta Jung* (SL082); Sumatra, Lake Toba, isolated from naturally fallen necrotic leaves of unidentified tree species floating in streams running through tropical montane rainforests, Aug. 2018, *T. Jung, M. Tarigan & I. Milenković* (SU415, SU464, SU614); Sumatra, Padang, isolated from a naturally fallen necrotic leaf of an unidentified tree species floating in a stream running through a tropical hill rainforest, Sep. 2018, *T. Jung, M. Tarigan & T. Corcobado* (SU692). **Vietnam**, Sapa, Fansipan Mountain, isolated from a baiting leaf floating in a stream running through a montane evergreen cloud forest, Mar. 2016, *T. Jung, N.M. Chi & M. Horta Jung* (VN079); isolated from a baiting leaf floating in a stream running through a montane evergreen cloud forest, Mar. 2016, *T. Jung, N.M. Chi & C.M. Brasier* (VN974).

Phytophthora vacuola T. Jung, H. Masuya, K. Kageyama & J.F. Webber, ***sp. nov.*** MycoBank MB 847305. Fig. 58.

Etymology: The name refers to the common production of sporangia with vacuoles.

Typus: **Japan**, Honshu Island, Takayama, isolated from a baiting leaf floating in a stream running through a montane riparian *Quercus crispula* forest, May 2017, *T. Jung & K. Kageyama* (**holotype** CBS H-25127, dried culture on V8A, ex-holotype living culture CBS 149503 = JP229).

Morphological structures on V8A: Sporangia produced abundantly in non-sterile soil extract; typically borne terminally (99 %) on unbranched long or short sporangiophores or in dense or lax sympodia of 2–4 sporangia (Fig. 58M) or rarely intercalary (1 %); mostly ovoid, broad-ovoid or elongated ovoid (58 %; Fig. 58A–C, M) or less frequently mouse-shaped (13.5 %; Fig. 58D, E, J, L), obpyriform to elongated-obpyriform (11.5 %; Fig. 58G, H), ellipsoid or elongated-ellipsoid (7.5 %; Fig. 58F), limoniform or elongated limoniform (5.5 %; Fig. 58I), ampulliform (2.5 %; Fig. 58K) or distorted (1.5 %); sporangia with more than one apex not observed; apices often curved or laterally displaced (36.8 %; Fig. 58D–F, I–L), predominantly papillate (77.3 %; Fig. 58B, E–H, J, K, M) or less frequently semipapillate (22.7 %; Fig. 58A, C, D, I) with a smooth transition between both forms; non-caducous; vacuoles (30.4 %; Fig. 58A, C, E, G, H, J, K), lateral attachment of the sporangiophore (24 %; Fig. 58B, D, J, L) commonly observed; infrequently with pedicels (6 %; Fig. 58C, M) of 21.4 ± 7.5 µm (range 16.0–26.7 µm) length; sporangial proliferation exclusively external (Fig. 58A, F, G, M); sporangial dimensions averaging 55.5 ± 6.7 × 35.9 ± 3.6 µm (overall range 38.9–90.9 × 24.3–43.2 µm; range of isolate means 54.9–56.1 × 34.8–37.1 µm) with a length/breadth ratio of 1.55 ± 0.21 (overall range 1.27–2.42); sporangial germination indirectly with zoospores discharged through an exit pore 5.0–8.4 µm wide (av. 6.8 ± 0.9 µm) (Fig. 58L). *Zoospores* limoniform to reniform whilst motile, becoming spherical (av. diam = 10.7 ± 1.1 µm) on encystment; cysts germinating directly. *Hyphal swellings* produced infrequently in water on sporangiophores and hyphae; globose to subglobose, ovoid or limoniform (Fig. 57A). *Chlamydospores* not observed. *Oogonia* abundantly produced in single culture ('homothallic' breeding system), terminal on short to medium-length, sometimes curved lateral hyphae or sessile, with smooth (Fig. 58N, O, Q, S–X) or slightly wavy wall (Fig. 58P, R); globose to slightly subglobose (58 %; Fig. 58N–S), elongated (22 %; Fig. 58V–X) or comma-shaped (20 %; Fig. 58T, U), often slightly excentric (29 %; Fig. 58R–T); with a rounded (88 %; Fig. 58N–Q, S, W, X) or less frequently a short tapering base (12 %; Fig. 58R, T–V); oogonial diam 27.9 ± 2.9 µm (overall range 21.4–36.1 µm; range of isolate means 26.6–29.2 µm); nearly plerotic to plerotic (53 %; Fig. 58N–Q, V–X) or slightly aplerotic (47 %; Fig. 58R–X). *Oospores* globose with a large lipid globule (Fig. 58N–X); diam 23.9 ± 2.3 µm (overall range 18.2–30.4 µm; range of isolate means 22.9–25.0 µm) wall thickness 1.73 ± 0.28 µm (overall range 1.23–2.48 µm), oospore wall index 0.37 ± 0.04; abortion rate 8–12 % (av. 10 %) after 4 wk. *Antheridia* predominantly paragynous and club-shaped, ellipsoid or subglobose (98 %; Fig. 58O–X), occasionally amphigynous and cylindrical (2 %; Fig. 58N); dimensions 12.0 ± 2.2 × 8.7 ± 1.5 µm.

Culture characteristics: Colonies on V8A and CA appressed to submerged with scanty aerial mycelium, radiate to stellate on V8A and faintly radiate on CA; on PDA felty-cottony with a faint stellate pattern (Fig. 41).

Cardinal temperatures and growth rates: On V8A optimum at 25 °C with 7.69 ± 1.44 mm/d radial growth, maximum 27.5–<30 °C, minimum <10 °C (Fig. 42), lethal temperature 30–32.5 °C. At 20 °C on V8A, CA and PDA 7.39 ± 0.96 mm/d, 4.93 ± 0.06 mm/d and 2.99 ± 0.88 mm/d, respectively.

Additional materials examined: **Japan**, Honshu Island, Takayama, isolated from a baiting leaf floating in a stream running through a montane *Q. crispula* forest, May 2017, *T. Jung & K. Kageyama* (JP229b); Honshu Island, Appi, isolated from the rhizosphere of an *Alnus hirsuta* tree in a riparian forest, Jun. 2017, *T. Jung & H. Masuya* (JP1060).

Notes on Clade 2c taxa: Across the nuclear (LSU, ITS, *βtub*, *hsp90*, *tigA*, *rpl10*, *tef-1α*, *enl*, *ras-ypt1*) 8 740-character alignment and the mitochondrial (*cox1*, *cox2*, *nadh1* and *rps10*) 3 156-character alignment pairwise sequence differences between the nine known and 15 newly described *Phytophthora* species in Clade 2c were 0.1–3.2 % and 0.2–4.7 %, respectively. The 15 new and the five known Clade 2c species examined (*viz. P. acerina*, *P. multivora*, *P. pachypleura*, *P. pini* and *P. plurivora*) developed distinctive colony morphologies on V8A, CA and PDA at 20 °C (Figs 38–41). In addition, the 15 new species are separated from each other and other Clade 2c species by a combination of morphological (Figs 44–58) and physiological (Figs 42, 43) characters of which the most discriminating are highlighted in bold in Tables S10–S13.

The seven isolates of *P. pini* examined in this study showed several morphological and morphometric differences to the re-description of this species by Hong *et al.* (2011), most notably larger sporangia (55.6 × 35.4 *vs.* 47.4 × 31.5 µm), the occurrence of papillate (5.7 %) and nonpapillate (1.7 %) sporangia and aplerotic oospores (38 %), lower maximum (30–<32.5 *vs.* 35 °C) and slightly higher optimum temperature (27.5 *vs.* 25 °C) for growth (Table S13). For the following phenotypic comparisons within Clade 2c species, the *P. pini* data from this study will be used.

The sporangia of the majority of species in Clade 2c have exclusively semipapillate apices, *i.e.*, *P. acerina*, *P. capensis*, *P. caryae*, *P. citricola*, *P. fansipanensis*, *P. japonensis*, *P. macroglobulosa*, *P. multivora*, *P. nimia*, *P. obturata*, *P. pachypleura* and *P. plurivora*, or predominantly semipapillate apices, *i.e.*, *P. balkanensis*, *P. catenulata*, *P. emzansi*, *P. excentrica*, *P. falcata, P. limosa*, *P. oblonga*, *P. pini* and *P. platani* (Jung & Burgess 2009, Scott *et al.* 2009, Ginetti *et al.* 2014, Henricot *et al.* 2014, Brazee *et al.* 2017; Tables S10–S13; Figs 44, 45, 47–56). However, several species are clearly distinguished by producing, in addition to semipapillate sporangia, a significant proportion of either papillate sporangia, *i.e.*, *P. curvata* (48 %), *P. excentrica* (13 %), *P. falcata* (13 %), *P. limosa* (16.2 %) and *P. vacuola* (77.3 %), or nonpapillate sporangia, *i.e.*, *P. emzansi* (10 %), *P. excentrica* (6 %) and *P. oblonga* (8 %). *Phytophthora pseudocapensis* is characterised by

Fig. 58. *Phytophthora vacuola*. **A–M.** Ovoid, ellipsoid, obpyriform, limoniform and mouse-shaped, mostly elongated sporangia formed on V8-agar (V8A) in soil extract. **A, C, D, I.** Semipapillate apices. **B, E–H, J, K, M.** Papillate apices. **D–F, I–L.** Curved apices. **A.** Hyphal swelling. **A, C, E, G, H, J, K.** Sporangia with vacuoles. **A, F, G, M.** External proliferation. **C.** Short pedicel (arrow). **L.** Zoospore release. **M.** Sympodium and medium-length pedicel (arrow). **N–X.** Oogonia with smooth or wavey walls and plerotic to slightly aplerotic oospores, formed in V8A. **N.** Amphigynous antheridium. **O–X.** Paragynous antheridia. **N–Q.** Subglobose to globose oogonia. **R–X.** Excentric, comma-shaped or elongated oogonia. Images: A–K, M, P–U, X. Ex-type CBS 149503; L, O. JP229b; N, V, W, JP1060. Scale bar = 20 µm; X applies to A–X.

having high proportions of both papillate (47.8 %) and semipapillate (46.3 %) sporangia and, in addition, also produces nonpapillate sporangia (5.9 %). In contrast, sporangial apices are exclusively papillate in *P. capensis* and predominantly papillate in *P. vacuola* (77.3 %) (Bezuidenhout *et al.* 2010, Bose *et al.* 2021a; Tables S10–S13; Figs 46–48, 51, 54, 57, 58).

High sporangial l/b ratios separate *P. citricola* (1.73 ± 0.28), *P. emzansi* (1.8–1.9), *P. falcata* (1.88 ± 0.25), *P. limosa* (1.76 ± 0.19), *P. multivora* (1.7 ± 0.22) and *P. pachypleura* (1.82 ± 0.05) from the majority of Clade 2c species which tend, on average, to form more squat sporangia (Tables S10–S13). In water the sporangia of most Clade 2c species, except *P. curvata*, are partially pedicellate with the proportion of pedicels ranging widely from only 6–16.5 % in *P. japonensis*, *P. macroglobulosa*, *P. oblonga* and *P. vacuola* to 42.7–51.6 % in *P. falcata*, *P. nimia*, *P. obturata*, *P. pini*, *P. platani* and *P. pseudocapensis* (Tables S10–S13; Figs 44–58). In contrast to the majority of Clade 2c species with exclusively persistent sporangia, *P. catenulata*, *P. falcata*, *P. nimia*, *P. oblonga*, *P. obturata* and *P. platani* show a low level of caducity (<1 %) in water (Tables S10–S13; Figs 45, 48, 53–56). It is noteworthy that *P. oblonga* commonly forms sporangia on solid agar which are predominantly caducous (Fig. 54).

Apart from *P. capensis* (Bezuidenhout *et al.* 2010), all species from Clade 2c show external sporangial proliferation and form sympodia. *Phytophthora acerina*, *P. emzansi*, *P. macroglobulosa* and *P. pachypleura* can be discriminated by forming only simple lax sympodia whereas the other Clade 2c species form both lax and dense, sometimes compound sympodia (Bezuidenhout *et al.* 2010, Ginetti *et al.* 2014, Henricot *et al.* 2014; Tables S10–S13; Figs 44–58). In several species, including *P. balkanensis*, *P. catenulata*, *P. excentrica*, *P. japonensis*, *P. nimia*, *P. oblonga* and *P. obturata*, the sympodia can contain up to 8 or 9 sporangia. In *P. platani* sympodia with up to 15 sporangia have been observed (Fig. 56). Internal sporangial proliferation occurs only in three Clade 2c species, clearly discriminating them from all other 2c species. *Phytophthora nimia* and *P. oblonga* show only occasional internal extended proliferation (Figs 53, 54) whereas in *P. platani* both extended and nested internal proliferation are relatively frequent (Fig. 56).

Moreover, the occurrence of some sporangial and hyphal features or their comparatively high proportions discriminate several Clade 2c species from other 2c species, *e.g.* the common occurrence of catenulate hyphal swellings in *P. catenulata*; high proportions of curved, mouse- or sickle-shaped sporangia in *P. curvata* (24 %), *P. falcata* (34.2 %) and *P. limosa* (15.5 %), distorted sporangia with often two or three apices in *P. curvata* (23 %) and *P. japonensis* (24.1 %) (Tables S10–S12), or ellipsoid sporangia in *P. pachypleura* (27 %; Henricot *et al.* 2014); the high frequency of curved or asymmetric sporangial apices in *P. curvata* (34.7 %), and *P. vacuola* (38.6 %) (Figs 46, 58); in *P. obturata* the high proportion (55.7 %) of sporangia with a conspicuous basal plug, often protruding backwards into the sporangiophore (Fig. 55); and the high proportion (30.4 %) of sporangia containing vacuoles in *P. vacuola* (Fig. 58).

All known and new species in Clade 2c are intrinsically self-fertile. Comparatively high proportions of oogonia with tapering instead of rounded bases distinguish *P. caryae* (53 %), *P. curvata* (46 %), *P. falcata* (46 %), *P. oblonga* (59 %) and *P. platani* (80.4 %) from other Clade 2c species (Brazee *et al.* 2017; Tables S10–S13; Figs 44–58). Likewise, a high proportion of excentric, elongated or comma-shaped oogonia discriminate *P. curvata* (38 %), *P. excentrica* (53 %), *P. falcata* (36.5 %), *P. limosa* (36 %), *P. oblonga* (51.9 %), *P. platani* (33.2 %) and *P. vacuola* (42 %) from other Clade 2c species (Tables S10–S13; Figs 44–58). *Phytophthora oblonga* differs from all other species by having particularly elongated oogonia (up to 77.6 µm; Fig. 54). The oospore wall index, *i.e.*, the proportion of the oospore volume occupied by the oospore wall, is particularly high in *P. pachypleura* (0.71; Henricot *et al.* 2014), *P. capensis* (0.56; Bezuidenhout *et al.* 2010) and *P. multivora* (0.52; Scott *et al.* 2009), and moderately high in *P. obturata* (0.39), *P. curvata* (0.38), *P. acerina* (Ginetti *et al.* 2014), *P. fansipanensis* and *P. vacuola* (all 0.37) (Tables S10–S13). Relatively high abortion rates are typical for *P. acerina* (38.5 %; Ginetti *et al.* 2014), *P. caryae* (46 %; Brazee *et al.* 2017), *P. emzansi* (42–46 %; Bezuidenhout *et al.* 2010) and *P. macroglobulosa* (22 %). The latter species is also characterised by having particularly large lipid globules, sometimes filling the oospore almost entirely (Fig. 52). *Phytophthora emzansi* is the only species in Clade 2c with exclusively amphigynous antheridia (Bezuidenhout *et al.* 2010) while the antheridia in all other Clade 2c species are predominantly paragynous and only infrequently amphigynous, *i.e.*, *P. pseudocapensis* (13.4 %), *P. catenulata* (4.2 %) and *P. fansipanensis* (4 %); predominantly paragynous and rarely (<1 %) amphigynous, *i.e.*, *P. balkanensis*, *P. citricola* (Jung & Burgess 2009), *P. curvata*, *P. excentrica*, *P. falcata*, *P. limosa*, *P. multivora* (Scott *et al.* 2009), *P. oblonga*, *P. pini*, *P. platani* and *P. plurivora* (Jung & Burgess 2009); or exclusively paragynous (all other Clade 2c species) (Tables S10–S13).

Except for *P. emzansi* which grows optimally at 20 °C, all species from Clade 2c have an optimum temperature for growth of 25 or 27.5 °C (Jung & Burgess 2009, Bezuidenhout *et al.* 2010, Brazee *et al.* 2017, Bose *et al.* 2021a; Tables S10–S13; Figs 42, 43). *Phytophthora limosa* from subtropical forests in Louisiana, USA and *P. transposita* from a warm-temperate forest in Kyushu, Japan show fast growth at 30 °C, discriminating them from *P. balkanensis*, *P. excentrica*, *P. falcata*, *P. multivora*, *P. pini*, *P. platani* and *P. plurivora* with moderate to slow growth at 30 °C and all other Clade 2c species which have maximum temperatures below 30 °C (Tables S10–S13; Figs 42, 43).

Several new Clade 2c species described here were previously known under informal names, *i.e.*, *P. balkanensis* as *P. citricola* E (Jung & Burgess 2009); *P. catenulata* as *P. citricola* VII (Jung *et al.* 2017b, 2020); *P. fansipanensis* as *P. citricola* VIII and *P. obturata* as *P. citricola* IX (Jung *et al.* 2020); *P. macroglobulosa* as *P.* sp. citricola-like VIII and *P. limosa* as *P.* sp. 22F3 (Yang *et al.* 2017). Isolates of *P. pseudocapensis* were previously designated as *P. capensis* (Jung *et al.* 2017b, 2020).

Clade 2e

For all Clade 2e species included in this study, colony morphologies on CA, PDA and V8A and temperature-growth relations on V8A are presented in Figs 59–62. Morphological and physiological characters and morphometric data of the five known and six newly described species and one informally designated taxon in Clade 2e are given in the comprehensive Tables S14 and S15.

Phytophthora amamensis T. Jung, K. Kageyama, H. Masuya & S. Uematsu, ***sp. nov.*** MycoBank MB 847319. Fig. 63.

Etymology: The name refers to the origin of the first isolates on the Japanese island of Amami-Ōshima.

Typus: **Japan**, Amami-Ōshima, Kasari, isolated from a naturally fallen tree leaf floating in a stream running through a subtropical lowland forest, Nov. 2018, *T. Jung & K. Kageyama* (**holotype** CBS H-25096, dried culture on V8A, ex-holotype living culture CBS 149474 = JP1340).

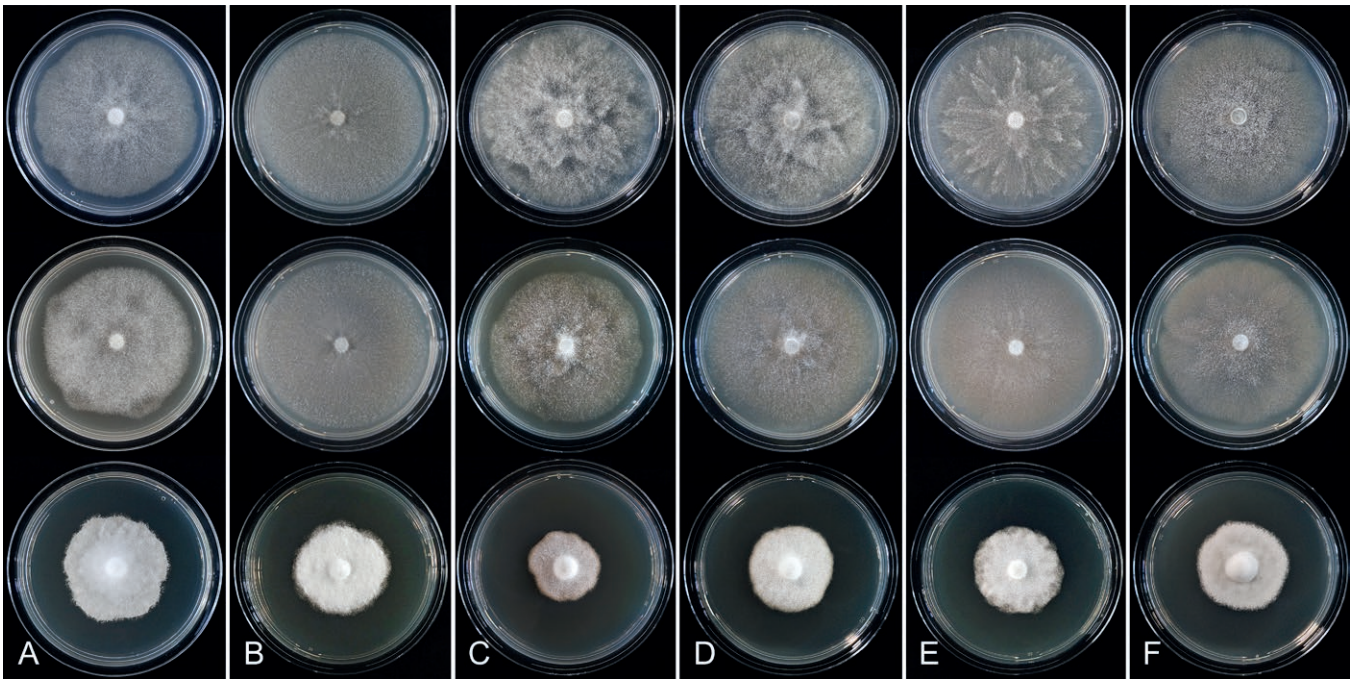

Fig. 59. Colony morphology of *Phytophthora* species from subclade 2e after 7 d growth at 20 ºC on V8-agar, carrot juice agar and potato-dextrose agar (from top to bottom). **A.** *Phytophthora acaciivora* (isolate SU1734). **B.** *Phytophthora amamensis* (ex-type CBS 149474). **C, D.** *Phytophthora borneensis* (C. ex-type CBS 149478; D. KA595). **E.** *Phytophthora celeris* (SU1509). **F.** *Phytophthora elongata* (ex-type CBS 125799).

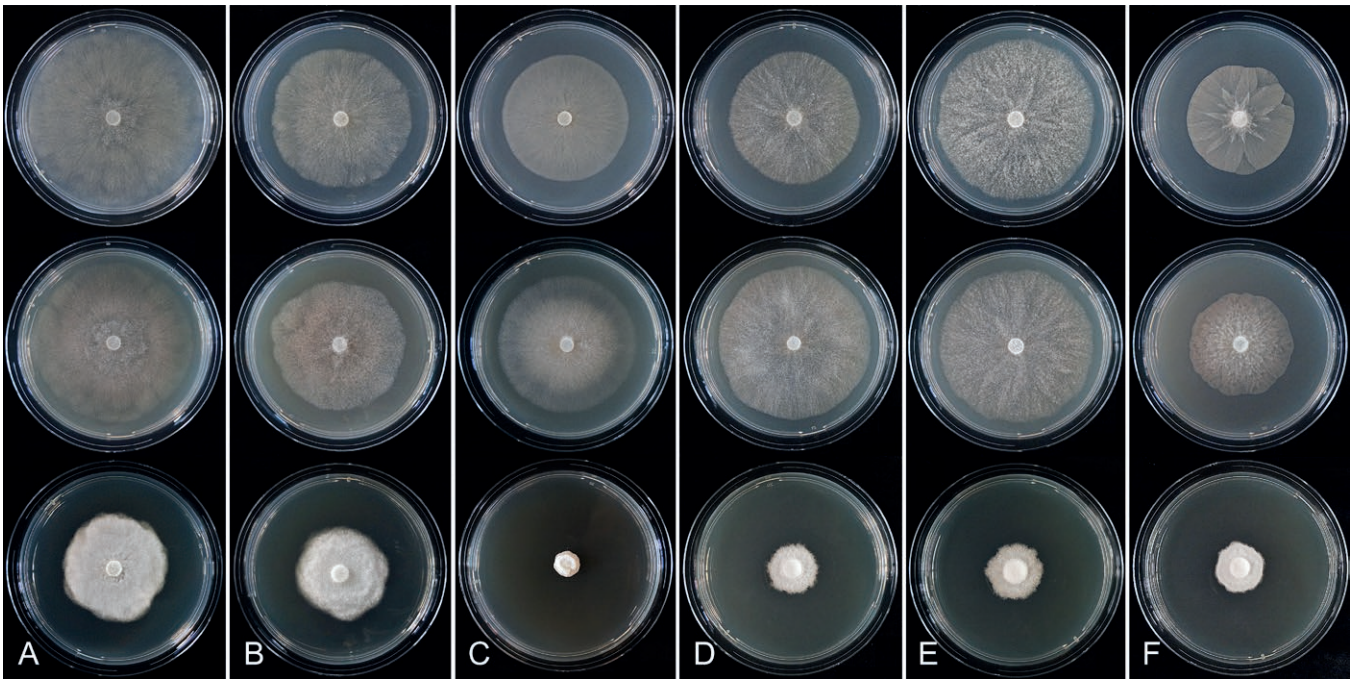

Fig. 60. Colony morphology of *Phytophthora* species from subclade 2e after 7 d growth at 20 ºC on V8-agar, carrot juice agar and potato-dextrose agar (from top to bottom). **A–C.** *Phytophthora indonesiensis* (A. ex-type CBS 149639; B. SL446; C. SU1131). **D–F.** *Phytophthora pseudofrigida* (D. ex-type CBS 150255; E. JV168; F. JV165).

Morphological structures on V8A: *Sporangia* not observed in solid agar but abundantly produced in non-sterile soil extract; borne terminally, on unbranched sporangiophores or in lax sympodia of 2–3 sporangia (Fig. 63E), or infrequently on short lateral hyphae (Fig. 63A); non-caducous, predominantly ovoid to elongated ovoid (56.5 %; Fig. 63A, B, E, J) or obpyriform to elongated-obpyriform (39 %; Fig. 63C–F, L), ampulliform (2.5 %; Fig. 63G, H), elongated-ellipsoid (1.5 %; Fig. 63I) or limoniform (0.5 %); a curved, laterally displaced apex (12 %; Fig. 63I) or a pedicel (10 %; Fig. 63F, L) sometimes, and a conspicuous basal plug (47 %; Fig. 63F, L) commonly observed; apices predominantly shallow semipapillate (89.6 %; Fig. 63B–E, G–I), less frequently papillate (5.4 %; Fig. 63A) or nonpapillate (5 %; Fig. 63F) with a smooth transition between all types; sporangial proliferation exclusively external (Fig. 63B–H, J–L); sporangial dimensions averaging 56.5 ± 7.5 × 30.6 ± 3.6 µm (overall range 39.5–75.5 × 22.6–42.0 µm; range of isolate means 53.0–59.1 × 29.2–31.9 µm) with a length/breadth ratio of 1.85 ± 0.18 (overall range 1.41–2.82); pedicel length varying from 4.3 to 89.4 µm (av. 29.0 ± 21.0 µm); sporangial germination usually indirectly with zoospores discharged through an exit pore 4.5–7.8

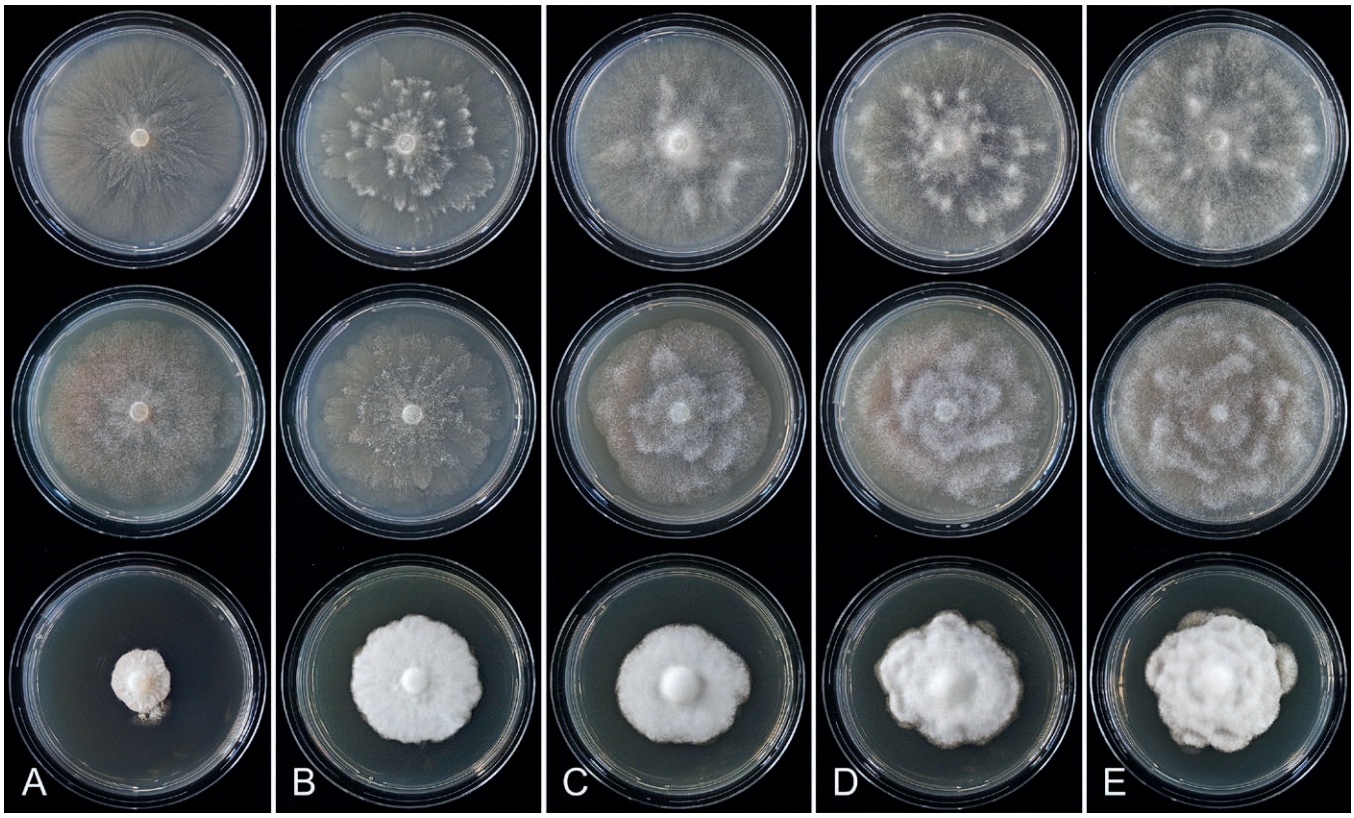

Fig. 61. Colony morphology of *Phytophthora* species after 7 d growth at 20 °C on V8-agar, carrot juice agar and potato-dextrose agar (from top to bottom). **A.** *Phytophthora penetrans* (ex-type CBS 149497) from subclade 2e. **B–E.** From subclade 2f. **B.** *Phytophthora angustata* (ex-type CBS 149475). **C.** *Phytophthora furcata* (ex-type isolate CBS 149487). **D, E.** *Phytophthora sumatera* (D. ex-type CBS 149501; E. JV146).

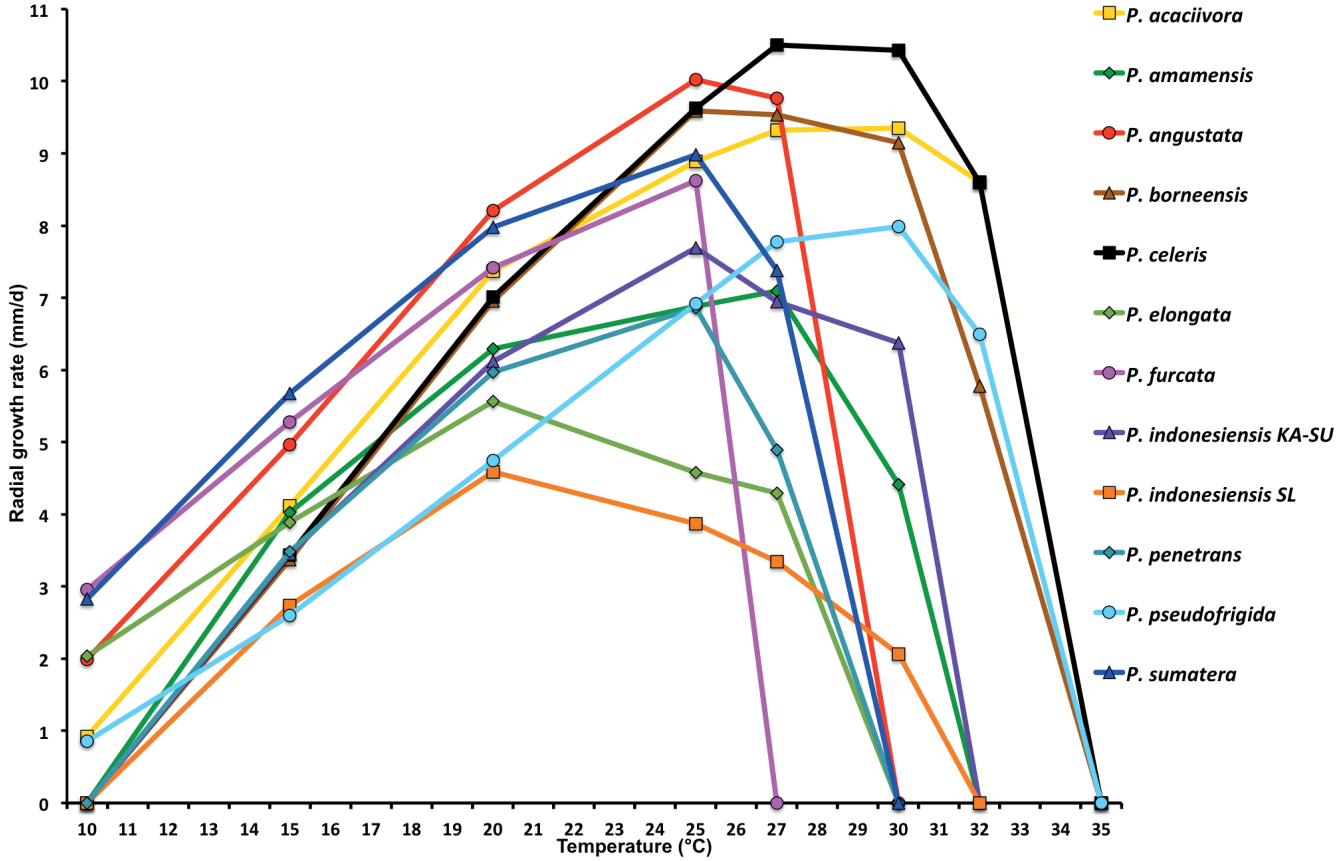

Fig. 62. Mean radial growth rates of three known and eight new *Phytophthora* species on V8-agar at different temperatures: From subclade 2e *P. acaciivora* (4 isolates); *P. amamensis* (4 isolates); *P. borneensis* (7 isolates); *P. celeris* (6 isolates); *P. elongata* (5 isolates); *P. frigida* (5 isolates); *P. indonesiensis* (9 isolates from Kalimantan and Sumatra; 3 isolates from Sulawesi); *P. penetrans* (5 isolates). From subclade 2f, *P. angustata* (6 isolates); *P. furcata* (6 isolates); *P. sumatera* (9 isolates).

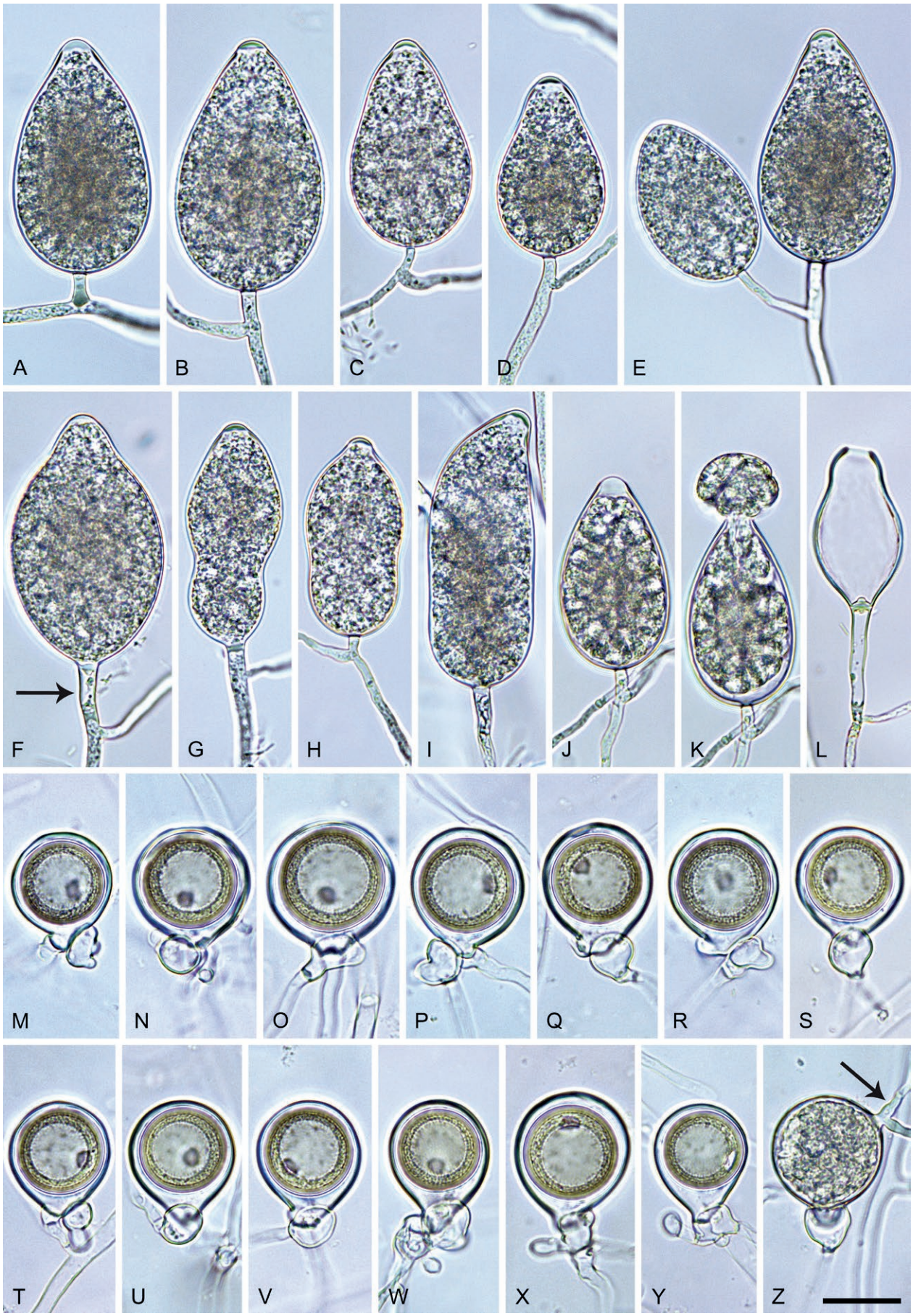

Fig. 63. *Phytophthora amamensis*. **A–L.** Ovoid, obpyriform, ampulliform and ellipsoid sporangia formed on V8-agar (V8A) in soil extract. **A–M. A.** Papillate apex. **B–E, G–I. S**semipapillate apices. **B–H, J–L.** External proliferation. **F.** Nonpapillate sporangium with medium-length pedicel (arrow). **I.** Curved apex. **J.** Swollen apex before zoospore release. **K.** Zoospore release. **L.** After zoospore release, with conspicuous basal plug and long pedicel. **M–Y.** Subglobose oogonia with slightly aplerotic to aplerotic oospores and paragynous antheridia formed in V8A. **Z.** Oogonium with paragynous antheridium and oospore germinating (arrow). Images: A, B, D, E, G, L, M–P, S, V, X, Z. Ex-type CBS 149474; C, H, Q, R, W. JP2342; F, I–K. T, U, Y. JP2341. Scale bar = 20 µm; Z applies to A–Z.

µm wide (av. 6.0 ± 0.7 µm) (Fig. 63K, L). *Zoospores* limoniform to reniform whilst motile, becoming spherical (av. diam = 10.2 ± 0.8 µm) on encystment. *Hyphal swellings* and *chlamydospores* not observed. *Oogonia* abundantly produced in single culture ('homothallic' breeding system), sessile or terminal on short to medium-length, often curved lateral hyphae, smooth-walled, globose to subglobose (64 %; Fig. 63M–P, R–T, Z) or elongated (36 %; Fig. 63Q, U–Y), with a nearly round base (26 %; Fig. 63M–O, Z) or a tapering base (74 %; Fig. 63P–Y); oogonial diam 26.4 ± 2.3 µm (overall range 17.5–31.6 µm; range of isolate means 25.5–27.2 µm); slightly aplerotic to aplerotic (Fig. 63M–Y). *Oospores* globose with a large lipid globule (Fig. 63M–Y); diam 22.5 ± 1.9 µm (overall range 16.4–27.8 µm; range of isolate means 22.1–23.1 µm) wall thickness 1.49 ± 0.21 µm (overall range 0.54–2.2 µm), oospore wall index 0.35 ± 0.03; abortion 8–35 % (av. 21 %) after 4 wk; after 2 mo at 20 °C many oospores germinating with 1 or 2 hyphae (Fig. 63Z). *Antheridia* exclusively paragynous and club-shaped, ovoid, subglobose or irregular (Fig. 62M–Z); 13.4 ± 2.2 × 10.5 ± 1.9 µm.

Culture characteristics: Colonies on V8A and CA mostly submerged to appressed and faintly radiate to striate; on PDA dense-felty, uniform with irregular submerged margins (Fig. 59).

Cardinal temperatures and growth rates: Optimum 27.5 °C with 7.1 ± 0.07 mm/d radial growth on V8A, maximum 30–<32.5 °C, minimum >10–15 °C (Fig. 62), lethal temperature 32.5–35 °C. At 20 °C on V8A, CA and PDA 6.29 ± 0.09 mm/d, 5.28 ± 0.13 mm/d and 3.24 ± 0.07 mm/d, respectively.

Additional materials examined: **Japan**, Amami-Ōshima, Kasari, isolated from naturally fallen tree leaves floating in a stream running through a subtropical lowland forest, Nov. 2018, *T. Jung & K. Kageyama* (JP2341, JP2342, JP2343).

Phytophthora borneensis T. Jung, A. Durán, M. Tarigan & M. Horta Jung, ***sp. nov.*** MycoBank MB 847320. Fig. 64.

Etymology: The name refers to the origin of the first isolates in Borneo.

Typus: **Indonesia**, Kalimantan, Balikpapan, isolated from rhizosphere soil of *Horsfieldia grandis* in a tropical lowland rainforest, Feb. 2019, *T. Jung & M. Tarigan* (**holotype** CBS H-25100, dried culture on V8A, ex-holotype living culture CBS 149478 = KA527).

Morphological structures on V8A: *Sporangia* not observed in solid agar but abundantly produced in non-sterile soil extract; borne terminally, on unbranched sporangiophores or in dense or lax sympodia of 2–4 sporangia (Fig. 64F, G); non-caducous, mostly ovoid, broad-ovoid or elongated ovoid (57.5 %; Fig. 64A, B, F–I) or obpyriform (33.5 %; Fig. 64C), less frequently ellipsoid (4.5 %), obovoid (2 %), limoniform (1.5 %; Fig. 64D) or distorted, usually with two apices (1 %; Fig. 64E); sporangiophores sometimes slightly laterally attached to the sporangia (18.5 %; Fig. 64A, H); conspicuous basal plugs, often covering the sporangial base and protruding into the sporangium, (62.5 %; Fig. 64D, F–I) common; pedicels infrequently (12.3 %) observed; sporangial apices semipapillate (57 %; Fig. 64A, E, F) or nonpapillate (43 %; Fig. 64B–D) and sometimes pointed (Fig. 64D); sporangial proliferation mostly external (Fig. 64A, F–H) or sometimes internal in an extended way (Fig. 64I); sporangial dimensions averaging 60.9 ± 11.4 × 38.4 ± 5.5 µm (overall range 33.9–83.4 × 24.4–53.5 µm; range of isolate means 54.9–70.6 × 35.6–41.5 µm) with a length/breadth ratio of 1.58 ± 0.17 (overall range 1.15–2.22); pedicel length 16.2 ± 5.6 µm (range 8.2–29.7 µm); sporangial germination usually indirectly with zoospores discharged through an exit pore 3.5–11.6 µm wide (av. 7.1 ± 1.3 µm) (Fig. 64F–I). *Zoospores* limoniform to reniform whilst motile, becoming spherical (av. diam = 10.9 ± 1.1 µm) on encystment. *Hyphal swellings* and *chlamydospores* not observed. *Oogonia* abundantly produced in single culture ('homothallic' breeding system), terminal on short to medium-length, thin, sometimes (22 %) curved lateral hyphae, smooth-walled, globose to slightly subglobose (Fig. 64J–V), mostly with a rounded (81 %; Fig. 64J–R) or sometimes with a tapering base (19 %; Fig. 64S–V); oogonial wall predominantly smooth (Fig. 64J–L, N–P, S–V) or less frequently slightly wavy (Fig. 64M, Q, R); oogonial diam 26.2 ± 2.8 µm (overall range 17.8–36.3 µm; range of isolate means 24.2–28.7 µm); slightly aplerotic to aplerotic (63 %; Fig. 64J–R) or nearly plerotic (37 %; Fig. 64S–V). *Oospores* globose with a large lipid globule (Fig. 64J–V); mean diam 22.3 ± 2.3 µm (overall range 12.9–27.8 µm; range of isolate means 20.7–24.2 µm); wall thickness 1.62 ± 0.25 µm (overall range 0.87–2.06 µm), oospore wall index 0.35 ± 0.03; abortion 23–50 % (av. 41 %) after 4 wk. *Antheridia* exclusively paragynous and club-shaped, ovoid, or subglobose (Fig. 64J–V); 10.5 ± 2.1 × 7.8 ± 1.1 µm.

Culture characteristics: Colonies stellate to petaloid and appressed with limited aerial mycelium on V8A; faintly radiate to uniform and mostly submerged on CA; and uniform and felty-cottony on PDA (Fig. 59).

Cardinal temperatures and growth rates: Optimum 25–27.5 °C with 9.6 ± 0.13 and 9.5 ± 0.42 mm/d radial growth on V8A at 25 and 27.5 °C, respectively, maximum 32.5–<35 °C, minimum >10–15 °C (Fig. 62), lethal temperature 35 °C. At 20 °C on V8A, CA and PDA 6.96 ± 0.22 mm/d, 5.4 ± 0.19 mm/d and 3.02 ± 1.08 mm/d, respectively.

Additional materials examined: **Indonesia**, Kalimantan, Balikpapan, isolated from rhizosphere soil of *H. grandis* in a tropical lowland rainforest, Feb. 2019, *T. Jung, M. Tarigan & M. Junaid* (KA528, KA529, KA530, KA531); isolated from rhizosphere soil of *Gmelina uniflora* in a tropical lowland rainforest, Feb. 2019, *T. Jung & M. Tarigan* (KA502a); isolated from rhizosphere soil of *Macaranga* sp. in a tropical lowland rainforest, Feb. 2019, *T. Jung & M. Tarigan* (KA543, KA595a).

Phytophthora celeris T. Jung, L. Oliveira, M. Tarigan & I. Milenković, ***sp. nov.*** MycoBank MB 847321. Fig. 65.

Etymology: The name refers to the fast growth in culture (*celeris* Latin = fast).

Typus: **Indonesia**, Sumatra, Kerinci, isolated from a nursery effluent, Nov. 2018, *T. Jung & M. Tarigan* (**holotype** CBS H-25103, dried culture on V8A, ex-holotype living culture CBS 149481 = SU1500).

Morphological structures on V8A: *Sporangia* not observed in solid agar but abundantly produced in non-sterile soil extract; borne terminally on mostly long unbranched sporangiophores or less frequently in lax sympodia of 2–4 sporangia (Fig. 65C); sporangia shallow semipapillate (77 %; Fig. 65A–G, J), less frequently nonpapillate (19 %; Fig. 65H, I) or rarely papillate (4 %; Fig. 65G), non-caducous, predominantly ovoid, broad ovoid or elongated ovoid (75.6 %; Fig. 65A–C, G, I, K), less frequently obpyriform to elongated obpyriform (10.4 %; Fig. 65E, J), limoniform (7.6 %; Fig. 65D), ampulliform (3.8 %; Fig. 65F–H), ellipsoid (1.8 %) or obovoid

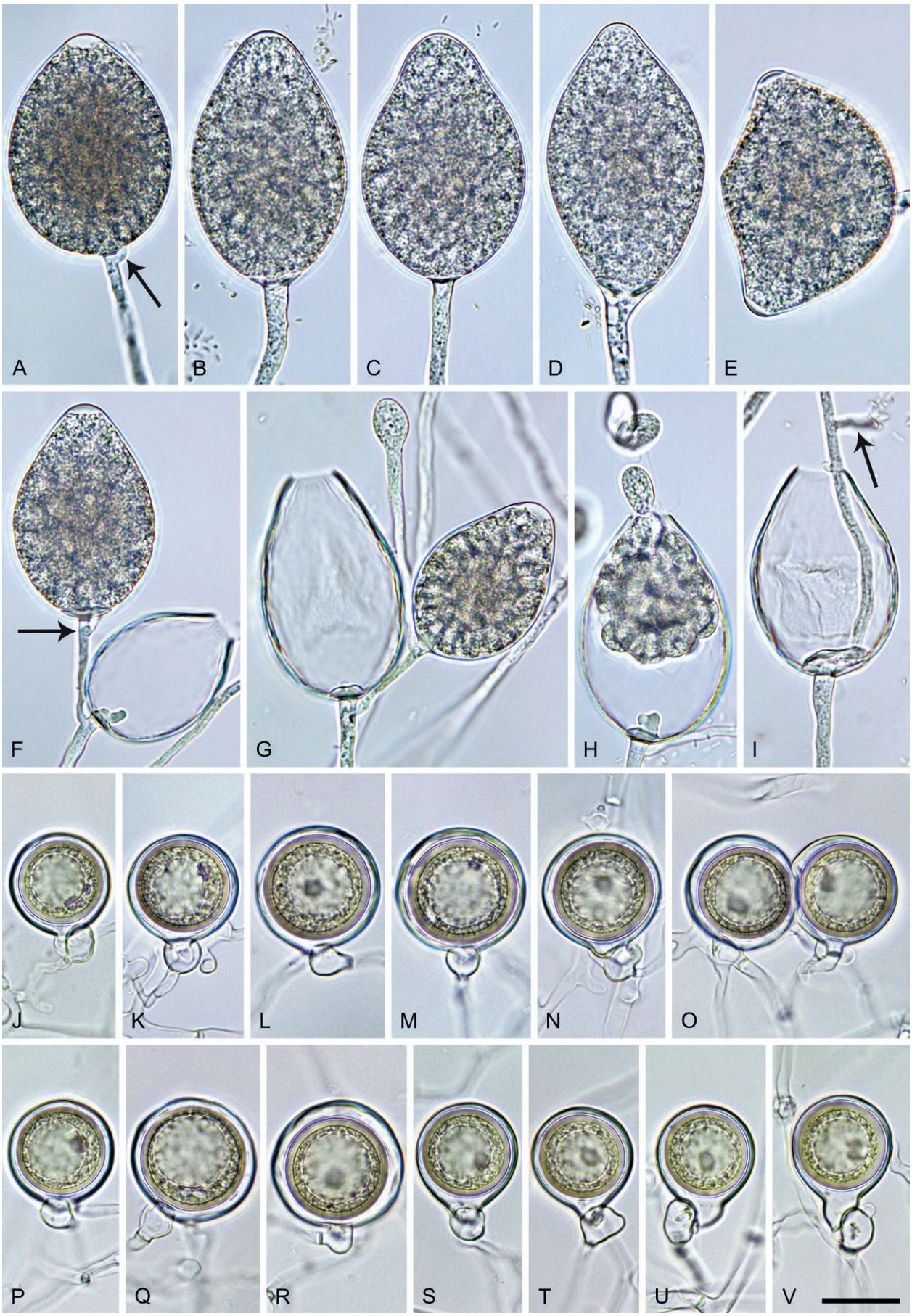

Fig. 64. *Phytophthora borneensis*. **A–I.** Sporangia formed on V8-agar (V8A) in soil extract. **A–D, F–I.** Ovoid and obpyriform sporangia. **A, F–H.** External proliferation (arrows in A, F). **A.** Swollen apex before zoospore release. **B–D.** Nonpapillate apices. **E, F.** Semipapillate apices. **E.** Distorted sporangium with two apices. **F, G.** Sympodia. **F–I.** Conspicuous basal plugs. **H.** Zoospore release. **I.** Internal extended proliferation with new sporangiophore branching outside the sporangium (arrow). **J–V.** Globose to subglobose oogonia with near-plerotic to aplerotic oospores and paragynous antheridia, formed in V8A. **J–R.** With round bases. **S–V.** With tapering bases. Images: A, E, J, P, Q, S–U. KA595a; B–D, G–I, K–O, R, V. Ex-type CBS 149478; F. KA532. Scale bar = 20 µm; V applies to A–V.

Fig. 65. *Phytophthora celeris*. **A–K.** Ovoid, limoniform, obpyriform and ampulliform sporangia formed on V8-agar (V8A) in soil extract. **A–G, J.** Semipapillate apices. **C, D, G.** External proliferation (arrows in D, G). **C.** Sympodium; mature sporangium with short pedicel. **E.** Long pedicel. **G.** Ovoid sporangium with papillate apex and hyphal extension. **H, I.** Nonpapillate sporangia. **I, J.** Sporangiophores with swellings. **K.** Zoospore release. **L.** Zoospore cyst germinating by forming a microsporangium. **M.** Two-mo-old oogonium with oospore germinating by forming two sporangia (arrows). **N–V.** Globose to subglobose oogonia with smooth or wavey walls, slightly aplerotic to aplerotic oospores and paragynous antheridia, formed in V8A. **W.** Hyphal aggregation formed in V8A. Images: A, E–G, I, J, L–S, W. Ex-type CBS 149481; B. SU1505; C, D, K, SU1535; H, SU1525; T–V. SU1511. Scale bar = 20 µm; W applies to A–W.

(0.8 %); lateral attachment of the sporangiophore (28 %; Fig. 65B, F, G) and pedicels (35.6 %; Fig. 65C, E) common; sporangial dimensions averaging 42.6 ± 12.6 × 27.1 ± 5.4 µm (overall range 13.7–112.0 × 9.4–40.0 µm; range of isolate means 34.1–55.4 × 24.2–29.1 µm) with a length/breadth ratio of 1.58 ± 0.37 (overall range 1.13–3.11); pedicel length 41.1 ± 20.0 µm (range 7.3–96.4 µm); sporangial proliferation exclusively external (Fig. 65C, D, G); sporangial germination indirectly with zoospores discharged through an exit pore of 3.6–10.1 µm (av. 6.8 ± 1.2 µm) into a short-lived vesicle (Fig. 65K). *Zoospores* limoniform to reniform whilst motile (Fig. 65K), becoming spherical (av. diam = 11.0 ± 1.8 µm) on encystment; cysts germinating directly by producing hyphae or microsporangia (Fig. 65L) or indirectly by releasing a secondary zoospore (diplanetism). *Hyphal swellings* on sporangiophores common, ovoid or subglobose (Fig. 65I, J). *Chlamydospores* not observed. *Oogonia* abundantly produced in single culture ('homothallic' breeding system), on short, thin and often curved stalks (Fig. 65M–V); globose to subglobose with round non-tapering bases (Fig. 65N–V) and smooth (Fig. 65M–Q) or slightly wavy walls (Fig. 65R–V); av. diam 29.3 ± 2.2 µm with an overall range of 23.0–36.2 µm and a range of isolate means of 28.7–31.1 µm; slightly aplerotic (Fig. 65N–Q, T) to aplerotic (Fig. 65R, S, U, V). *Oospores* globose with a large lipid globule (Fig. 65N–V); in 2-mo-old cultures many oospores germinate by producing 1 or 2 sporangia (Fig. 65M); av. diam 24.1 ± 2.1 µm with an overall range of 17.2–33.6 µm and a range of isolate means of 22.3–25.7 µm; wall diam 1.46 ± 0.15 µm (overall range 1.22–1.84 µm) and oospore wall index 0.32 ± 0.03; abortion 12–40 % (av. 28 %) after 4 wk. *Antheridia* paragynous, 1-celled, and club-shaped, ovoid or subglobose (Fig. 65M–V); 12.2 ± 2.2 × 9.3 ± 1.4 µm. *Hyphal aggregations* common in all isolates (Fig. 65W).

Culture characteristics: Colonies are stellate and appressed with limited aerial mycelium on V8A; faintly striate to radiate and mostly submerged on CA; and faintly petaloid and felty-cottony on PDA (Fig. 59).

Cardinal temperatures and growth rates: On V8A optimum 27.5–30 °C with 10.5 ± 0.3 mm/d and 10.43 ± 0.63 mm/d radial growth, respectively, maximum 32.5–<35 °C, minimum >10–15 °C (Fig. 62), lethal temperature 35 °C. At 20 °C on V8A, CA and PDA 7.01 ± 0.22 mm/d, 5.35 ± 0.57 mm/d and 2.68 ± 0.12 mm/d, respectively.

Additional materials examined: **Indonesia**, Sumatra, Kerinci, isolated from a nursery effluent, Nov. 2018, *T. Jung, M. Tarigan, L. Oliveira & I. Milenković* (SU1505, SU1511, SU1520, SU1525, SU1535).

Phytophthora indonesiensis T. Jung, M. Tarigan, L. Oliveira & I. Milenković, ***sp. nov.*** MycoBank MB 847323. Fig. 66.

Etymology: The name refers to the distribution of this species across the Indonesian archipelago.

Typus: **Indonesia**, North Kalimantan, Malinau, isolated from a naturally fallen tree leaf floating in a tributary of Sesayap River in a tropical lowland rainforest, Feb. 2019, *T. Jung & M. Tarigan* (**holotype** CBS H-25111, dried culture on V8A, ex-holotype living culture CBS 149639 = KA174).

Morphological structures on V8A: *Sporangia* not observed in solid agar but abundantly produced in non-sterile soil extract; borne mostly terminally on unbranched sporangiophores or in dense or lax sympodia of 2–6 sporangia (Fig. 66K), or sometimes intercalary (Fig. 66F); sporangia semipapillate (88.2 %; Fig. 66A, C–G, K), often with a pointed apex (Fig. 66D, G), or less frequently papillate (11.8 %; Fig. 66B); usually non-caducous but a few caducous sporangia occur in all isolates (Fig. 66G); predominantly ovoid, broad ovoid or elongated ovoid (76.7 %; Fig. 66A, B, H, K), less frequently obpyriform, broad-obpyriform or elongated obpyriform (14 %; Fig. 66F, G), limoniform (3.5 %; Fig. 66C, I), obovoid (2.8 %; Fig. 66D), subglobose (2.2 %), ellipsoid (0.4 %; Fig. 66E), ampulliform (0.2 %) or distorted with two apices (0.2 %; Fig. 65J); slightly asymmetric shapes (26.7 %; Fig. 66B, E, I), a conspicuous protruding basal plug (25.1 %; Fig. 66I), lateral attachment of the sporangiophore (33.6 %; Fig. 66B, J) and medium-length pedicels (32.7 %; Fig. 66A, B, E–G) common; sporangial dimensions averaging 60.8 ± 8.6 × 42.5 ± 5.4 µm (overall range 36.8–85.6 × 26.6–83.5 µm; range of isolate means 52.0–68.0 × 37.2–46.7 µm) with a length/breadth ratio of 1.44 ± 0.19 (overall range 0.62–2.3); pedicel length 22.2 ± 13.9 µm (range 3.4–77.8 µm); sporangial proliferation exclusively external (Fig. 66C, H, K); sporangial germination indirectly with zoospores discharged through an exit pore of 4.8–9.9 µm (av. 7.4 ± 0.9 µm) into a short-lived vesicle (Fig. 66H). *Zoospores* limoniform to reniform whilst motile, becoming spherical (av. diam = 11.0 ± 1.8 µm; Fig. 66I) on encystment; cysts germinating directly by producing hyphae (Fig. 66I). *Hyphal swellings* on sporangiophores ovoid or subglobose (Fig. 66K, L), 14.7 ± 0.6 µm. *Chlamydospores* not observed. *Oogonia* abundantly produced in single culture ('homothallic' breeding system); sessile or on short, often curved stalks (Fig. 66M–S); globose to subglobose (66 %; Fig. 66P–S) or elongated (34 %; Fig. 66M–O), with short or long tapering, sometimes funnel-shaped or curved bases (46 %; Fig. 66M–Q) or round non-tapering bases (54 %; Fig. 66R, S), and smooth (Fig. 66M–Q, S) or, less frequently, slightly wavy walls (Fig. 66R); av. diam 26.7 ± 3.8 µm with an overall range of 15.0–43.4 µm and a range of isolate means of 23.8–29.7 µm; plerotic or near-plerotic (82 %; Fig. 66M–Q, S) or less frequently aplerotic (18 %; Fig. 66R). *Oospores* globose with a large lipid globule (Fig. 66M–R) or rarely with multiple smaller lipid globules (Fig. 66S); av. diam 23.5 ± 3.2 µm with an overall range of 13.0–35.9 µm and a range of isolate means of 21.3–26.0 µm; wall diam 1.72 ± 0.35 µm (overall range 0.96–2.7 µm) and oospore wall index 0.38 ± 0.05; abortion rate 3–9 % (av. 7 %) after 4 wk. *Antheridia* paragynous, 1-celled, and club-shaped, ovoid, subglobose or irregular (Fig. 66M–S); 11.5 ± 6.0 × 8.1 ± 1.4 µm. *Hyphal aggregations* common in all isolates (Fig. 66T).

Culture characteristics: Colony morphologies varying between isolates from different islands; isolates from Kalimantan and Sumatra faintly radiate and largely submerged to appressed on V8A and CA, and faintly petaloid and dense-felty appressed on PDA; isolates from Sulawesi faintly striate to uniform and submerged on V8A and CA, and uniform, dense-felty with very slow growth on PDA (Fig. 60).

Cardinal temperatures and growth rates: On V8A isolates from Kalimantan and Sumatra optimum at 25.0 °C with 7.7 ± 0.8 mm/d radial growth, maximum 30.0–<32.5 °C, minimum >10–15 °C (Fig. 62), lethal temperature 35 °C; at 20 °C on V8A, CA and PDA 6.12 ± 0.14 mm/d, 4.6 ± 0.33 mm/d and 3.85 ± 0.59 mm/d, respectively. Isolates from Sulawesi optimum at 20 °C with radial growth of 4.6 ± 0.17 mm/d on V8A, 4.52 ± 0.1 mm/d on CA and 0.82 ± 0.02 mm/d on PDA; maximum 30.0–<32.5 °C, minimum >10–15 °C (Fig. 62), lethal temperature 35 °C.

Additional materials examined: **Indonesia**, North Kalimantan, Malinau, isolated from naturally fallen leaves floating in a tributary of Sesayap River in a tropical lowland rainforest, Feb. 2019, *T. Jung, M. Tarigan & M. Junaid*

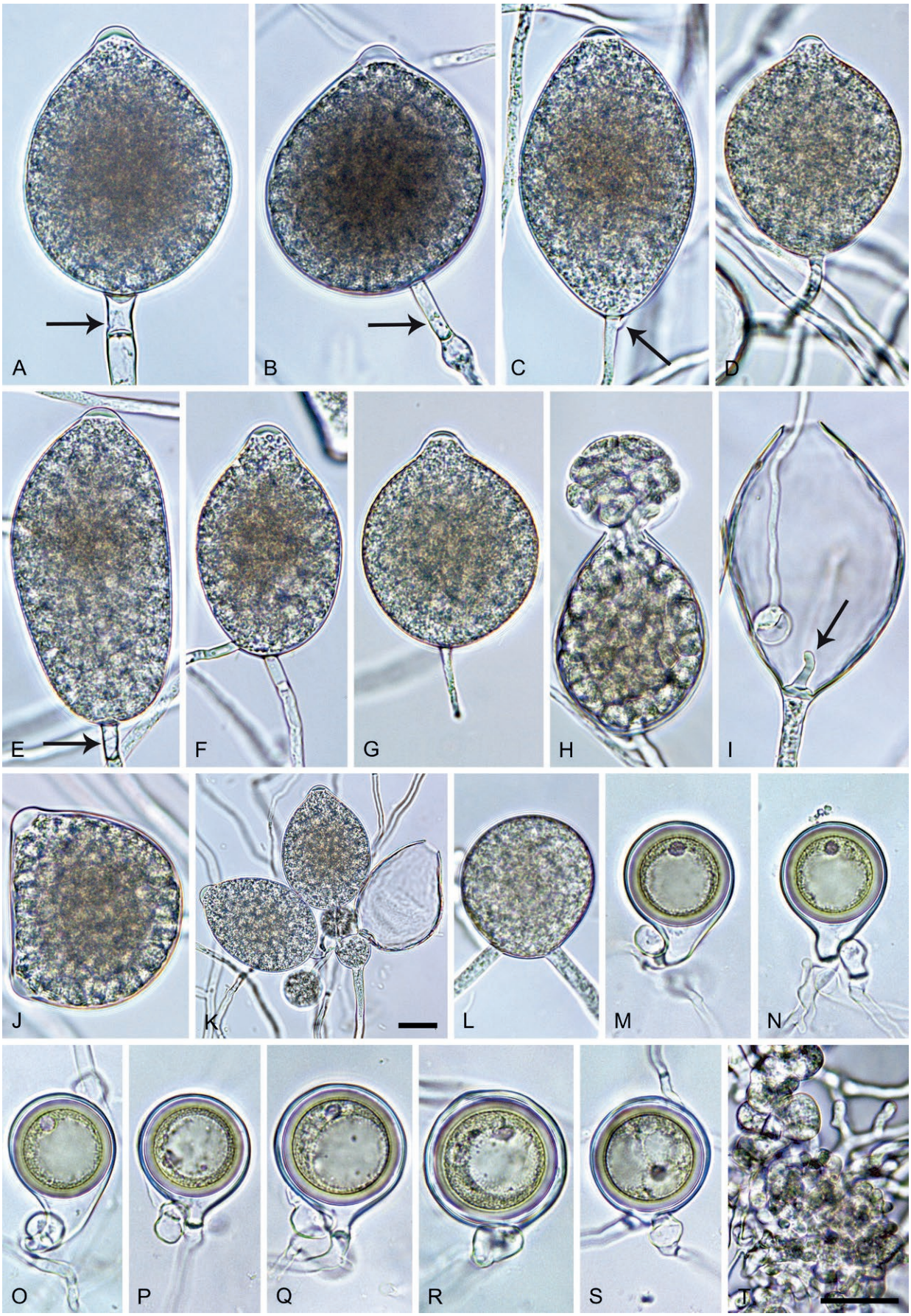

Fig. 66. *Phytophthora indonesiensis*. **A–K.** Sporangia formed on V8-agar (V8A) in soil extract. **A–I, K.** Ovoid, limoniform, obovoid, ellipsoid and obpyriform sporangia. **A, C–G.** Semipapillate apices. **B.** Papillate apex. **A, B, E, F.** Medium-length pedicels (arrows in A, B, E). C, H, K. External proliferation (arrow in C). F. Intercalary sporangium. G. Caducous sporangium. H. Zoospore release. **I.** After zoospore release, with conspicuous protruding basal plug (arrow) and germinating zoospore cyst. **J.** Distorted sporangium with two apices. **K.** Dense sporangial sympodium and globose hyphal swelling. **L.** Intercalary hyphal swelling on V8A in soil extract. **M–S.** Oogonia with plerotic to aplerotic oospores, tapering or round bases and paragynous antheridia, formed in V8A. **T.** Hyphal aggregation formed in V8A. Images: A, B, I, P–R, T. SL449; C, J. SL446; D–H, K, L–O, S. Ex-type CBS 149639; Scale bars = 20 µm; T applies to A–J, L–T.

(KA173, KA606); West Sumatra, Padang, isolated from rhizosphere soil of an unidentified tree in a tropical hill rainforest, Sep. 2018, *T. Jung, L. Oliveira & I. Milenković* (SU1122, SU1131, SU1724, SU1726, SU1728, SU1732); South Sulawesi, Lembang, isolated from rhizosphere soil of *Cinnamomum iners* in a tropical mountain rainforest, May 2019, *T. Jung & M. Junaid* (SL446, SL449, SL450).

Phytophthora penetrans T. Jung, Y. Balci, K. Broders & I. Milenković, ***sp. nov.*** MycoBank MB 847324. Fig. 67.

Etymology: The name refers to the occasional penetration of the sporangial wall by sporangiophores in internally proliferating sporangia.

Typus: **Panama**, Parque Nacional de Campana, isolated from necrotic lesion on a naturally fallen leaf of a non-identified tree species in a tropical lowland rainforest, Nov. 2019, *K.D. Broders & Y. Balci* (**holotype** CBS H-25120, dried culture on V8A, ex-holotype living culture CBS 149497 = PA165).

Morphological structures on V8A: *Sporangia* not observed in solid agar but abundantly produced in non-sterile soil extract; borne terminally, usually in dense or lax sympodia of 2–6 sporangia (Fig. 67J); non-caducous, predominantly ovoid, broad-ovoid or elongated ovoid (70.5 %; Fig. 67A, B, F–J), less frequently obpyriform (22.2 %; Fig. 67C), limoniform (3.3 %; Fig. 67E, J), ellipsoid (3 %; Fig. 67F) or obovoid (1 %; Fig. 67D); lateral attachment of the sporangiophore (16.5 %; Fig. 67B), medium-length pedicels (32.8 %; Fig. 67A, E, G, H) and a conspicuous thick basal plug (84.5 %; Fig. 67A, C, E, G–I), frequently protruding with one or two long tips into the sporangium (Fig. 67H), commonly observed; apices semipapillate (Fig. 67A–E, J); sporangial proliferation mostly external (Fig. 67D–F, J) or infrequently internal in an extended way with 1–2 sporangiophores arising from beside the sporangial basal plug and often penetrating the lateral wall of the empty sporangium (Fig. 67H, I); sporangial dimensions averaging 56.7 ± 9.8 × 36.8 ± 4.3 µm (overall range 37.4–94.2 × 26.9–50.1 µm; range of isolate means 50.0–69.2 × 34.2–41.3 µm) with a length/breadth ratio of 1.53 ± 0.15 (overall range 1.22–2.28); pedicel length 21.9 ± 15.8 µm (range 3.0–89.0 µm); sporangial germination usually indirectly with zoospores discharged through an exit pore 5.3–10.8 µm wide (av. 7.7 ± 1.0 µm) (Fig. 67F–I). *Zoospores* limoniform to reniform whilst motile, becoming spherical (av. diam = 10.4 ± 1.0 µm) on encystment. *Hyphal swellings* on sporangiophores subglobose, limoniform or irregular, 17.4 ± 5.5 µm. *Chlamydospores* not observed. *Oogonia* abundantly produced in single culture ('homothallic' breeding system), terminal on short to medium-length, often curved lateral hyphae, smooth-walled, globose to slightly subglobose (94.8 %; Fig. 67K–S), sometimes slightly excentric (Fig. 67K, O), or elongated (5.2 %; Fig. 67K), often with a short or long tapering base (77 %; Fig. 67L–N, P–T); oogonial diam 29.3 ± 3.0 µm (overall range 18.1–38.5 µm; range of isolate means 27.5–31.8 µm); slightly aplerotic to aplerotic (68 %; Fig. 67K–P) or nearly plerotic (32 %; Fig. 67Q–T). *Oospores* globose with a large lipid globule (Fig. 67K–T); diam 25.4 ± 2.6 µm (overall range 15.7–32.8 µm; range of isolate means 24.0–27.7 µm) wall thickness 2.0 ± 0.3 µm (overall range 1.3–3.1 µm), oospore wall index 0.41 ± 0.04; abortion rate 2–46 % (av. 20 %) after 4 wk. *Antheridia* exclusively paragynous and club-shaped, ovoid or subglobose (Fig. 67K–T); sometimes two antheridia attached to one oogonium (Fig. 67M); 11.5 ± 2.1 × 7.8 ± 1.3 µm.

Culture characteristics: Colonies on V8A and CA mostly submerged to appressed, stellate on V8A and faintly radiate on CA; on PDA dense-felty, radiate, often with irregular sectors growing from the margin with submerged margins (Fig. 61).

Cardinal temperatures and growth rates: On V8A optimum 25 °C with 6.86 ± 0.28 mm/d radial growth, maximum 27.5–<30 °C, minimum >10–15 °C (Fig. 62), lethal temperature 30–32.5 °C. At 20 °C on V8A, CA and PDA 5.97 ± 0.15 mm/d, 5.14 ± 0.13 mm/d and 1.76 ± 0.09 mm/d, respectively.

Additional materials examined: **Panama**, Parque Nacional de Campana, isolated from necrotic lesions on naturally fallen leaves of unidentified tree species in tropical lowland forests, Nov. 2019, *K.D. Broders & Y. Balci* (PA166, PA304, PA306, PA308, PA309, PA311, PA313).

Phytophthora pseudofrigida T. Jung, A. Durán, M. Tarigan & M. Horta Jung, ***sp. nov.*** MycoBank MB 849627. Fig. 68.

Etymology: The name refers to the phylogenetic relatedness and morphological similarities to *P. frigida*.

Typus: **Indonesia**, Sumatra, Lake Toba, isolated from a naturally fallen necrotic leaf of an unidentified tree species floating in a stream running through a tropical montane rainforest, Aug. 2018, *T. Jung & M. Tarigan* (**holotype** CBS H-25294, dried culture on V8A, ex-holotype living culture CBS 150255 = SU588).

Morphological structures on V8A: *Sporangia* infrequently observed in solid agar and abundantly produced in non-sterile soil extract; borne predominantly terminally (87 %) on long or short sporangiophores (Fig. 68A, D–G, J), mostly unbranched or infrequently in lax sympodia of 2–3 sporangia, or intercalary (13.3 %; Fig. 68B, C); sporangia exclusively papillate (Fig. 68A–J), non-caducous, predominantly ovoid, broad ovoid or elongated ovoid (74.7 %; Fig. 68A–G), less frequently obpyriform to elongated obpyriform (19.1 %; Fig. 68H–J), subglobose (2.6 %), limoniform (2.4 %), or mouse-shaped (1.2 %); lateral attachment of the sporangiophore frequent (55.4 %; Fig. 68B, D, F, H, I), pedicels (12 %; Fig. 68G) or a constriction of the sporangiophore (4.8 %; Fig. 68E, G) infrequent; sporangial dimensions averaging 60.3 ± 7.2 × 39.9 ± 4.7 µm (overall range 28.7–74.2 × 23.8–49.0 µm; range of isolate means 58.6–61.3 × 38.3–41.3 µm) with a length/breadth ratio of 1.52 ± 0.16 (overall range 1.19–2.07); pedicel length 20.9 ± 14.8 µm (range 4.0–50.0 µm); sporangial proliferation exclusively external (Fig. 68A, B, D); sporangial germination indirectly with zoospores discharged through an exit pore of 5.3–9.6 µm (av. 7.1 ± 1.3 µm) into a short-lived vesicle. *Zoospores* limoniform to reniform whilst motile, becoming spherical (av. diam = 10.6 ± 0.9 µm) on encystment. *Hyphal swellings* not observed. *Chlamydospores* globose to subglobose, 31.5–43.6 µm (av. diam 37.6 ± 6.0 µm), with golden-brown thick walls (wall diam 2.3 ± 0.8 µm) (Fig. 68S, T). *Oogonia* not observed in single cultures, but abundantly produced by all five tested isolates in polycarbonate membrane mating tests with the A2 mating type isolate SU1735 of *P. acaciivora* (A1/A2 or 'heterothallic' breeding system; all tested isolates mating type A1); predominantly globose to subglobose (86 %; Fig. 68K–P, R) or infrequently elongated (14 %; Fig. 68Q), with smooth walls and almost exclusively (99 %) tapering bases (Fig. 68K–V); av. diam 25.1 ± 2.9 µm with an overall range of 19.2–31.6 µm and a range of isolate means of 24.9–25.3 µm; predominantly plerotic (76 %; Fig. 68M–R) or less frequently aplerotic (Fig. 68K, L). *Oospores* globose (Fig. 68K–P, R) or rarely elongated (Fig. 68Q) with a large lipid globule; av. diam 21.6 ± 2.2 µm with an overall range of 16.8–26.6 µm and a range of isolate means of 21.1–22.4 µm; wall diam

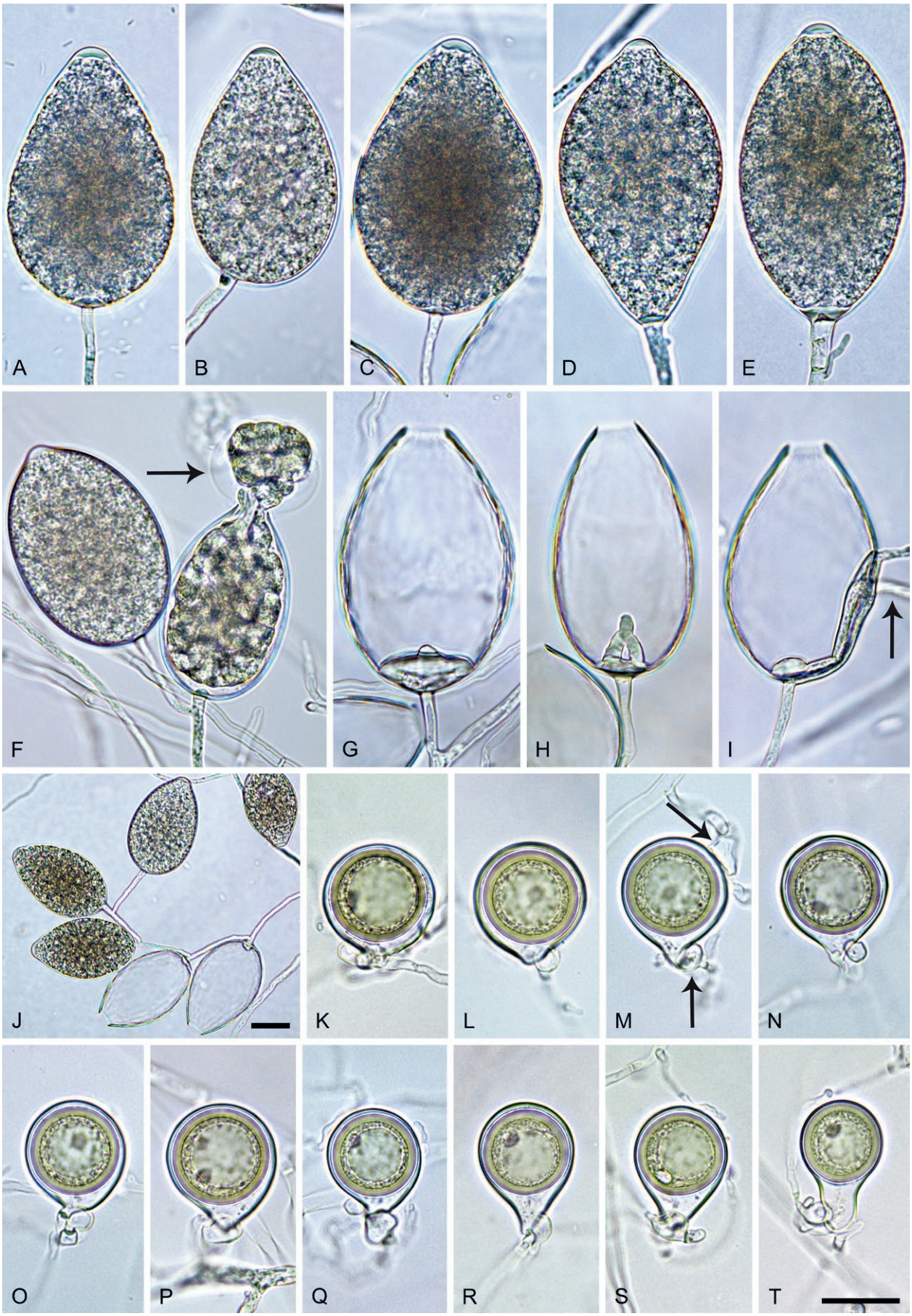

Fig. 67. *Phytophthora penetrans*. **A–J.** Ovoid, obpyriform, pyriform and limoniform sporangia formed on V8-agar (V8A) in soil extract. **A–E, J.** Semipapillate apices. **A, E, G, H.** Medium-length pedicels. **D–F, J.** External proliferation. **F.** Sympodium with immature sporangium and sporangium releasing zoospores into short-lived vesicle (arrow). **G–I.** After zoospore release, with large basal plugs. **H.** Basal plug with two protruding tips. **I.** Internal extended proferation with new sporangiophores penetrating the sporangial wall (arrow). **J.** Dense sympodium. **K–T.** Smooth-walled oogonia with mostly tapering bases, near-plerotic to plerotic oospores and paragynous antheridia formed in V8A. M. Two antheridia (arrows). Images: A–C, E, G, I, K, R–T. Ex-type CBS 149497; D, F, J, P, Q. PA166; H, L–O, PA309. Scale bars = 20 µm; T applies to A–I, K–T.

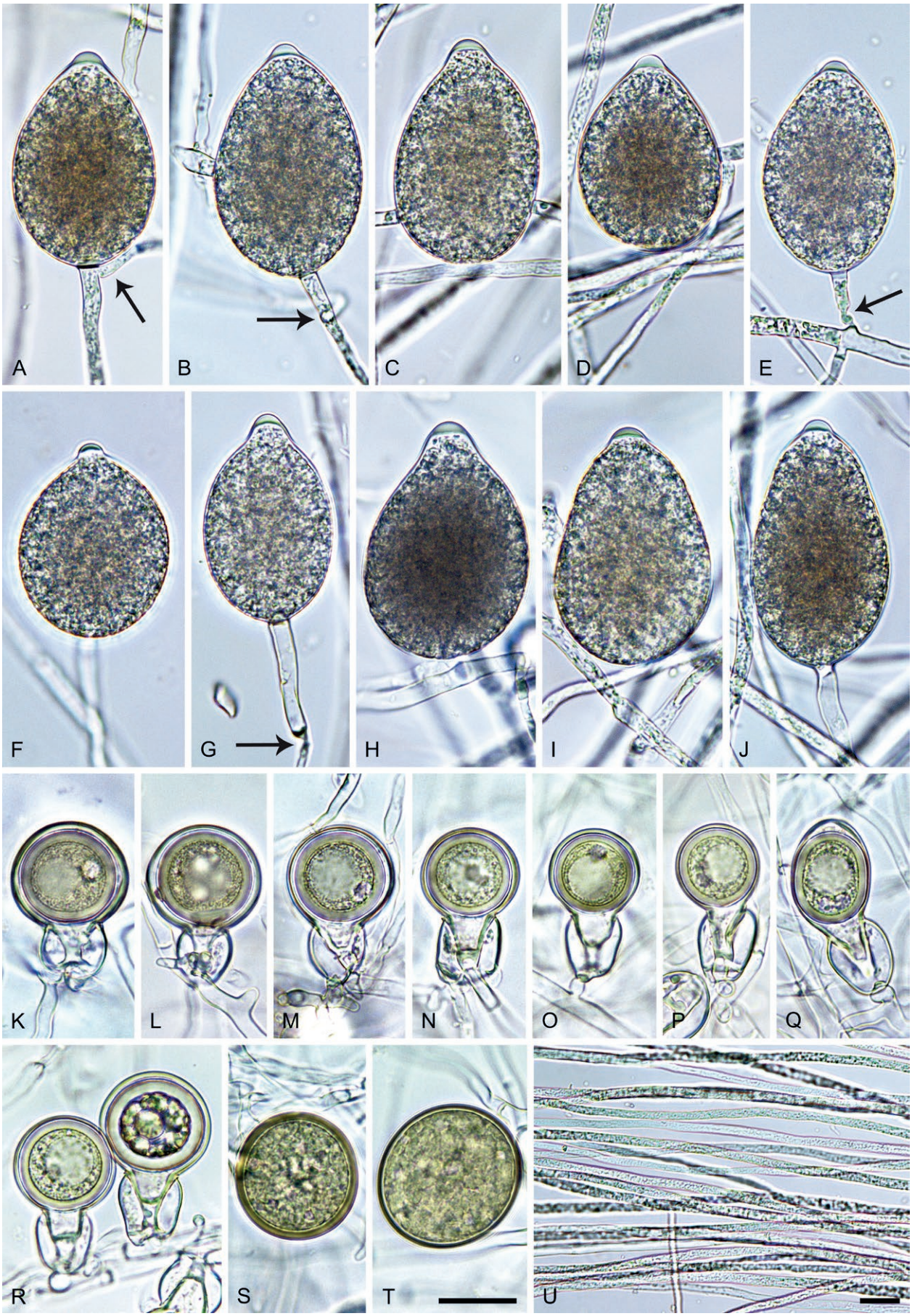

Fig. 68. *Phytophthora pseudofrigida*. **A–L.** Papillate sporangia formed on V8-agar (V8A) in soil extract. **A–F.** Ovoid sporangia. **G–J.** Obpyriform sporangia. **A, B.** External proliferation (arrows). **B, C.** Intercalary sporangia. **D, F, H, I.** Laterally attached sporangiophores. **E, G.** Sporangiophore constrictions (arrows). **G.** Long pedicel. **K–T.** Structures formed in carrot agar in polycarbonate membrane mating tests. **K–R.** Oogonia with tapering bases, near-plerotic to plerotic oospores and amphigynous antheridia. **P.** Bicellular antheridium. **Q.** Elongated oogonium and oospore. **R.** Oogonium on the right with aborted oospore. **S, T.** Thick-walled chlamydospores. **U.** Unbranched hyphae in V8A. Images: A, B, D–F, I, J, K–M, O, Q, S–U. Ex-type CBS 150255; C, G, H, N, JV168; P, R. SU1280. Scale bars = 20 µm; T applies to A–T.

1.61 ± 0.31 µm (overall range 0.84–2.29 µm) and oospore wall index 0.38 ± 0.05; abortion 68–83 % (av. 76 %; Fig. 68R) after 4 wk. *Antheridia* amphigynous, 1-celled (Fig. 68L, M, O, Q, R) or 2-celled with the basal cell being significantly smaller (Fig. 68K, N, P), and cylindrical to subcylindrical (Fig. 68K–R); 18.0 ± 2.2 × 15.5 ± 1.6 µm. *Hyphae* often with long unbranched sections (Fig. 68U).

Culture characteristics: Colonies are submerged to appressed with very limited aerial mycelium on V8A and CA, striate or stellate on V8A and faintly striate or chrysanthemum-like on CA; and uniform, appressed and felty-cottony on PDA (Fig. 60).

Cardinal temperatures and growth rates: On V8A optimum 30 °C with 8.0 ± 0.76 mm/d radial growth but with almost similar growth of 7.9 ± 0.61 mm/d at 27.5 °C, maximum 32.5–<35 °C, minimum <10 °C (Fig. 62), lethal temperature 35 °C. At 20 °C on V8A, CA and PDA 4.74 ± 0.77 mm/d, 4.07 ± 0.63 mm/d and 1.44 ± 0.07 mm/d, respectively.

Additional materials examined: **Indonesia**, Java, Bandung area, isolated from a naturally fallen necrotic leaf of an unidentified tree species floating in a stream running through a tropical montane *Pinus merkusii* forest, Mar. 2019, *T. Jung, M. Tarigan & L. Oliveira* (JV168); Java, Papandayan Mountain, isolated from a naturally fallen necrotic leaf of an unidentified tree species floating in a stream running through a tropical montane forest, Mar. 2019, *T. Jung, M. Tarigan & L. Oliveira* (JV178a); Sumatra, Padang, isolated from naturally fallen necrotic leaves floating in a forest stream in a tropical hill rainforest, Sep. 2018*, T. Jung, M. Tarigan, T. Corcobado & I. Milenković* (SU683, SU1280).

Notes on Clade 2e taxa: Across the nuclear (LSU, ITS, *βtub*, *hsp90*, *tigA*, *rpl10*, *tef-1α*, *enl*, *ras*-ypt1) 8 754-character alignment and the mitochondrial (*cox1*, *cox2*, *nadh1* and *rps10*) 3 153-character alignment the five known and six newly described *Phytophthora* species from Clade 2e showed pairwise sequence differences of 0.4–6.2 % and 0.1–4.4 %, respectively. The six new and the two known Clade 2e species examined (*viz*. *P. acaciivora* and *P. elongata*) developed distinctive colony morphologies on V8A, CA and PDA at 20 °C (Figs 59–61). It should be noted that colony morphologies of both *P. pseudofrigida* and *P. indonesiensis* are highly variable (Fig. 60). In addition, the six new species can be discriminated from each other and other Clade 2e species by a combination of morphological (Figs 63–68) and physiological characters (Fig. 62) of which the most discriminating are highlighted in bold in Tables S14 and S15.

The four Indonesian isolates of *P. acaciivora* examined in this study differed from the original description of this species which was based on three Vietnamese isolates by having higher optimum (27.5–30 *vs*. 25 °C) and lower maximum (32.5–35 *vs*. >37.5 °C) temperatures for growth (Burgess *et al*. 2020; Table S14; Fig. 62).

The five isolates of *P. pseudofrigida* from Java and Sumatra examined in this study showed considerable morphological and morphometric differences from its sister species *P. frigida* (Maseko *et al.* 2007), most notably much larger sporangia (60.3 × 39.9 *vs*. 33 × 27 µm), larger chlamydospores (37.6 *vs*. 25 µm), smaller oogonia (25 *vs*. 33 µm), lack of sporangial caducity and a higher optimum temperature for growth (30 *vs*. 25 °C) (Table S14; Figs 62, 68). *Phytophthora acaciae*, *P. acaciivora*, *P. frigida* and *P. pseudofrigida* are distinguished from the other Clade 2e species by their exclusively papillate sporangia (Maseko *et al.* 2007, Albuquerque Alves *et al.* 2019, Burgess *et al.* 2020; Tables S14, S15; Fig. 68). In contrast, the sporangia of *P. bishii*, *P. elongata*, *P. penetrans* and *P.* taxon AUS 2E (previously *P.* taxon elongata-like) are exclusively semipapillate (Abad *et al.* 2008, Rea *et al.* 2010; Tables S14, S15; Fig. 67). Three new Clade 2e species produce predominantly semipapillate sporangia and varying proportions of papillate (*P. amamensis* 5.4 %; *P. celeris* 4 %, *P. indonesiensis* 11.8 %) or nonpapillate sporangia (*P. amamensis* 5 %, *P. celeris* 19 %) (Tables S14, S15; Figs 63, 65, 66). *Phytophthora borneensis* can be discriminated from all other Clade 2e species by producing semipapillate (57 %) and nonpapillate (43 %) sporangia in almost similar proportions (Tables S14, S15; Fig. 64). *Phytophthora celeris* differs from *P. acaciae*, *P. acaciivora* and the other five new Clade 2e species by having considerably smaller sporangia (on average 42.6 *vs*. 51–60.3 µm). In addition, with 41.1 ± 20.0 µm the pedicels of *P. celeris* are on average considerably longer than in all other Clade 2e species (av. 11.3–29.0 µm) (Tables S14, S15). *Phytophthora amamensis* and *P. acaciivora* have mostly slender sporangia with high sporangial l/b ratios (1.85 and 1.73, respectively) separating them from all other species with more squat sporangia (Tables S14, S15). Two new species from Indonesia, *P. borneensis* and *P. indonesiensis*, are discriminated from the other four new species by the occasional production of sporangia with two apices (Figs 63–68). *Phytophthora borneensis*, *P. indonesiensis* and *P. penetrans* share the production of large conspicuous basal plugs which often protrude into the sporangium, but the frequency differs between these three species ranging from 25.1 % in *P. indonesiensis* to 62.5 % in *P. borneensis* and 84.5 % in *P. penetrans*. The latter species also differs from the other two species by frequently forming two long tips protruding from the basal plug into the sporangium. The occurrence of internal extended proliferation differentiates *P. borneensis* and *P. penetrans* from all other species in Clade 2e which exclusively show external sporangial proliferation (Maseko *et al.* 2007, Abad *et al.* 2008, Albuquerque Alves *et al.* 2019, Burgess *et al.* 2020; Tables S14, S15; Figs 63–68). *Phytophthora penetrans* differs from *P. borneensis* and all currently known *Phytophthora* species by producing internally proliferating sporangiophores which occasionally penetrate the lateral wall of the empty sporangium (Fig. 67). The frequent formation of dense hyphal aggregations distinguishes *P. celeris* and *P. indonesiensis* from the other Clade 2e species (Maseko *et al.* 2007, Abad *et al.* 2008, Albuquerque Alves *et al.* 2019, Burgess *et al.* 2020; Tables S14, S15; Figs 63–68).

The A1/A2 breeding systems of *P. acaciae*, *P. acaciivora*, *P. frigida* and *P. pseudofrigida* readily discriminate them from all other species in Clade 2e which are intrinsically self-fertile (Maseko *et al.* 2007, Albuquerque Alves *et al.* 2019, Burgess *et al.* 2020; Tables S14, S15). *Phytophthora bishii* differs from the other self-fertile species by producing on average larger oogonia (Abad *et al.* 2008) whereas *P. elongata* can easily be identified because of its long oogonial stalks (Rea *et al.* 2010; Tables S14, S15). High proportions of oogonia with tapering bases distinguish *P. amamensis* (74 %) and *P. penetrans* (77 %) from *P. borneensis* (19 %), *P. celeris* (0 %) and *P. indonesiensis* (46 %) (Tables S14, S15; Figs 63–67). Comparatively high frequencies of slightly elongated oogonia also differentiate *P. amamensis* (36.0 %) and *P. indonesiensis* (34 %) from *P. penetrans* (5.2 %), *P. borneensis* and *P. celeris* (both 0 %) (Tables S14, S15; Figs 63–67). In *P. indonesiensis* most oospores (82 %) are near-plerotic to plerotic whereas in the other four new self-fertile Clade 2e species most oospores are slightly aplerotic or aplerotic (Tables S14, S15; Figs 63–67).

At 35 °C *P. acaciae* has the highest maximum temperature for growth followed by *P. acaciivora*, *P. borneensis*, *P. celeris* and *P. pseudofrigida* (all 32.5–<35 °C). At 20 °C *P. elongata* and montane isolates of *P. indonesiensis* have the lowest optimum temperatures

within Clade 2e, followed by *P. acaciae* (24 °C), *P. frigida*, *P. penetrans*, lowland isolates of *P. indonesiensis* and *P.* taxon AUS 2E (all 25 °C), *P. bishii* (26 °C), *P. borneensis* (25–27.5 °C), *P. amamensis* (27.5 °C), *P. acaciivora* and *P. celeris* (27.5–30 °C) and *P. pseudofrigida* (30 °C) (Maseko *et al.* 2007, Abad *et al.* 2008, Rea *et al.* 2010, Albuquerque Alves *et al.* 2019, Burgess *et al.* 2020; Tables S14, S15; Fig. 62).

Clade 2f

For all Clade 2f species included in this study colony morphologies on CA, PDA and V8A and temperature-growth relations on V8A are presented in Figs 61 and 62, respectively. Morphological and physiological characters and morphometric data of one known and the three newly described species and one informally designated taxon in Clade 2f are given in the comprehensive Table S16.

Phytophthora angustata T. Jung, L. Garcia, B. Mendieta-Araica & Y. Balci, ***sp. nov.*** MycoBank MB 847326. Fig. 69.

Etymology: The name refers to the tapering oogonial bases (*angustata* Latin = tapering).

Typus: **Nicaragua**, Diriomo, Mombacho Volcano, isolated from a naturally fallen necrotic leaf of an unidentified rainforest tree collected from the ground in a tropical cloud forest, Nov. 2017, *Y. Balci, L. Garcia & B. Mendieta-Araica* (**holotype** CBS H-25097, dried culture on V8A, ex-holotype living culture CBS 149475 = NI121).

Morphological structures on V8A: *Sporangia* not observed on solid agar but abundantly produced in non-sterile soil extract; borne terminally in dense or lax sympodia of 2–4 sporangia (Fig. 69G) or on unbranched long or short sporangiophores (Fig. 69A, B); non-caducous, mostly ovoid or elongated ovoid (83.7 %; Fig. 69A, B, F–H, I, K), less frequently limoniform or elongated-limoniform (7.4 %; Fig. 69C), obpyriform to elongated-obpyriform (3.9 %), ampulliform (2.3 %; Fig. 69D, H), ellipsoid to elongated ellipsoid (1.4 %) or club-shaped (1.3 %; Fig. 69E); lateral attachment of the sporangiophore (18.7 %; Fig. 69B, E) and a conspicuous basal plug (34.7 %; Fig. 69E–G, K) common; apices nonpapillate (Fig. 69A–E, H); sporangial proliferation external (Fig. 69G) and more frequently internal in a nested way (Fig. 69G–I), sometimes with the new sporangium partly protruding out of the old sporangium (Fig. 69H), or in an extended way (Fig. 69J, K), sometimes with multiple sporangiophores inside the empty proliferating sporangium (Fig. 69K); sporangial dimensions averaging 65.9 ± 6.6 ´ 35.6 ± 2.5 µm (overall range 50.7–98.0 × 27.3–41.8 µm; range of isolate means 61.9–69.4 × 33.9–36.7 µm) with a length/breadth ratio of 1.85 ± 0.16 (overall range 1.53–2.83); sporangial germination indirectly with zoospores discharged through an exit pore 7.6–14.8 µm wide (av. 10.6 ± 1.6 µm) (Fig. 69F, G, I–K). *Zoospores* limoniform to reniform whilst motile, sometimes with ring-like flagella ends, becoming spherical (av. diam = 10.7 ± 0.6 µm) on encystment; cysts germinating directly or less frequently indirectly by releasing a secondary zoospore (diplanetism). *Hyphal swellings* infrequently formed in water, globose to subglobose, limoniform or irregular, sometimes catenulate (Fig. 69L), av. diam 12.5 ± 0.3 µm. *Chlamydospores* not observed. *Oogonia* abundantly produced in single culture ('homothallic' breeding system), terminal on short or medium-length, often curved lateral hyphae; predominantly globose to subglobose (65.9 %; Fig. 69M–S), elongated (27.3 %; Fig. 69T–W) or comma-shaped (6.8 %; Fig. 69X), with short (34 %; Fig. 69M–S) or long tapering, often (38 %) funnel-like bases (66 %; Fig. 69T–W); smooth-walled (Fig. 69M–X); oogonial diam 31.1 ± 2.3 µm (overall range 25.5–38.2 µm; range of isolate means 29.6–32.7 µm); nearly plerotic to plerotic (Fig. 69M–X). *Oospores* globose with a large lipid globule (Fig. 69M–X); diam 29.3 ± 2.2 µm (overall range 23.9–35.3 µm; range of isolate means 27.8–30.8 µm) wall thickness 2.05 ± 0.28 µm (overall range 1.29–3.0 µm), oospore wall index 0.36 ± 0.04; abortion rate 3–17 % (av. 8.7 %) after 4 wk. *Antheridia* almost exclusively (>99 %) paragynous, club-shaped, subglobose, limoniform or irregular (Fig. 69M–X); dimensions 12.8 ± 1.9 × 8.7 ± 1.2 µm.

Culture characteristics: Colonies on V8A and CA submerged to appressed with scanty aerial mycelium, chrysanthemum-like to stellate on V8A and petaloid to stellate on CA; on PDA dense-cottony with a faint radiate pattern (Fig. 61).

Cardinal temperatures and growth rates: On V8A optimum 25 °C with 10.02 ± 0.23 mm/d radial growth, maximum 27.5–<30 °C, minimum <10 °C (Fig. 62), lethal temperature 32.5 °C. At 20 °C on V8A, CA and PDA 8.21 ± 0.48 mm/d, 5.36 ± 0.06 mm/d and 3.65 ± 0.27 mm/d, respectively.

Additional materials examined: **Nicaragua**, Diriomo, Mombacho Volcano, isolated from naturally fallen necrotic leaves of unidentified rainforest trees collected from the ground in a tropical cloud forest, Nov. 2017, *Y. Balci, L. Garcia & B. Mendieta-Araica* (NI124, NI129, NI157, NI159, NI165).

Phytophthora furcata T. Jung, N.M. Chi, I. Milenković & M. Horta Jung, ***sp. nov.*** MycoBank MB 847327. Fig. 70.

Etymology: The name refers to the frequent furcation of sporangiophores inside proliferating empty sporangia (*furcata* Latin = furcated).

Typus: **Vietnam**, Sapa, Fansipan Mountain, isolated from rhizosphere soil of *Meliosma henryi* and *Neolitsea merilliana* in a montane evergreen cloud forest, Mar. 2016, *T. Jung, N.M. Chi & M. Horta Jung* (**holotype** CBS H-25109, dried culture on V8A, ex-holotype living culture CBS 149487 = VN035).

Morphological structures on V8A: *Sporangia* infrequently observed on solid agar but abundantly produced in non-sterile soil extract; borne terminally in dense or lax sympodia of 2–5 sporangia (Fig. 70J) or on unbranched long or short sporangiophores; non-caducous, mostly ovoid or elongated ovoid (70.7 %; Fig. 70A–D, G, J), less frequently limoniform or elongated-limoniform (14.3 %; Fig. 70F), obpyriform to elongated-obpyriform (10.7 %; Fig. 70E), ellipsoid to elongated ellipsoid (2.7 %) or mouse-shaped (1.6 %); lateral attachment of the sporangiophore (6.7 %; Fig. 70H) and a conspicuous basal plug (10 %; Fig. 70F) occasionally observed; apices almost exclusively nonpapillate (99.7 %; Fig. 70A–D, F, J) or rarely shallow semipapillate (0.3 %), sometimes curved (9.7 %; Fig. 70I); sporangial proliferation both external (Fig. 70A, D, E, J) and internal in a nested (Fig. 70I) or extended way (Fig. 70G, H), often with the sporangiophore furcating inside the empty proliferating sporangium (Fig. 70H); sporangial dimensions averaging 56.4 ± 8.6 × 32.8 ± 3.4 µm (overall range 27.4–99.2 × 17.1–41.6 µm; range of isolate means 49.8–61.3 × 29.8–35.0 µm) with a length/breadth ratio of 1.72 ± 0.22 (overall range 1.32–2.63); sporangial germination indirectly with zoospores discharged through an exit pore 6.5–16.0 µm wide (av. 11.6 ± 1.8 µm) (Fig. 70G–J). *Zoospores* limoniform to reniform whilst motile, becoming spherical (av. diam = 10.4 ± 0.8 µm) on encystment. *Hyphal swellings* abundantly

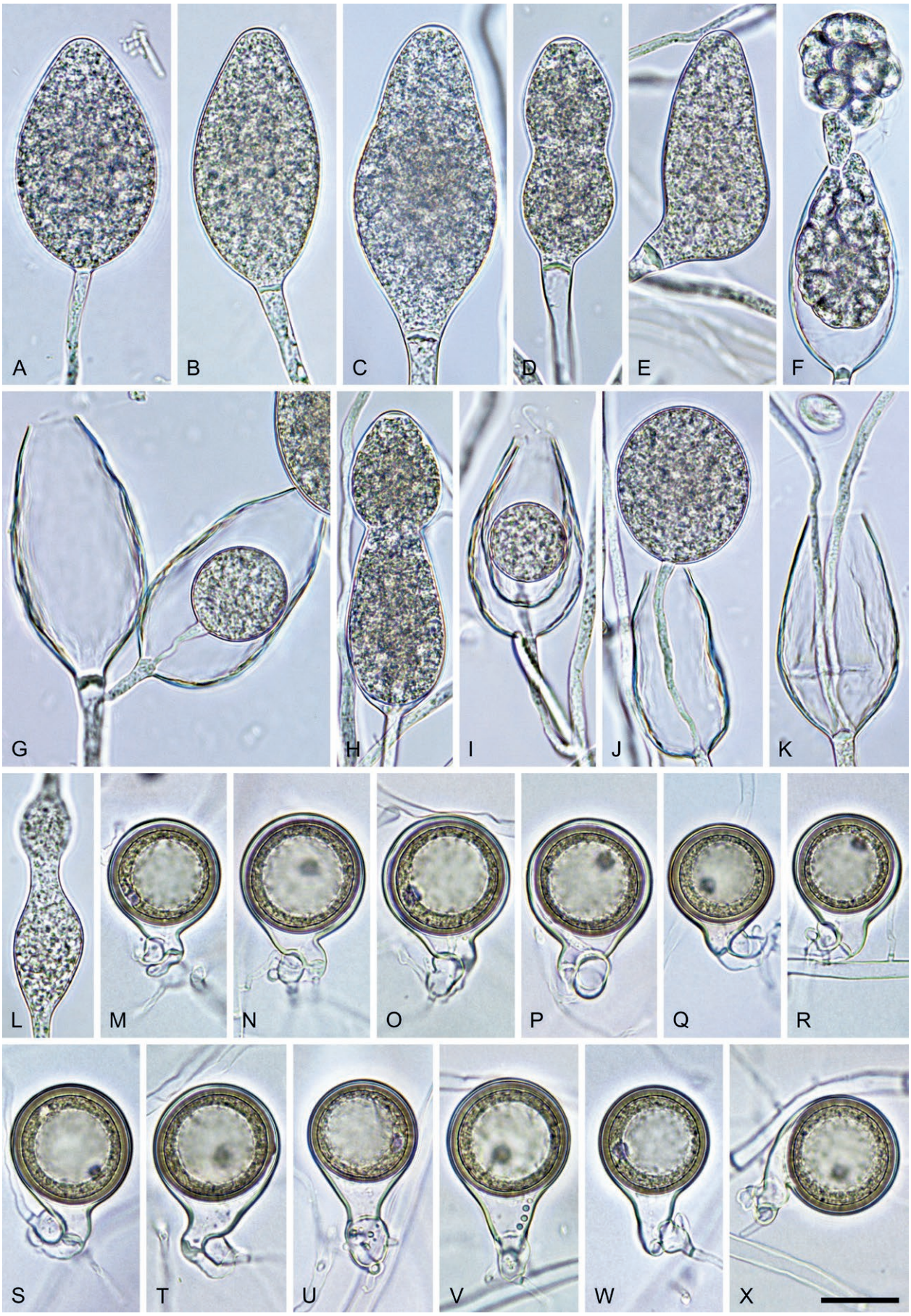

Fig. 69. *Phytophthora angustata*. **A–K.** Ovoid, limoniform, ampulliform and club-shaped sporangia formed on V8-agar (V8A) in soil extract. **A–E.** Nonpapillate sporangia. **E–G.** Conspicuous basal plugs. **F.** Zoospore release. **G.** External and internal nested proliferation. **H.** Internal nested proliferation with new ampulliform sporangium protruding out of the old sporangium. **I.** Internal nested proliferation. **J.** Internal extended proliferation. **K.** Internal extended proliferation with two new sporangiophores. **L.** Catenulate hyphal swellings on V8A in soil extract. **M–X.** Smooth-walled oogonia with tapering bases, near-plerotic to plerotic oospores and paragynous antheridia formed in V8A. **X.** Comma-shaped oogonium. Images: A, D, E, G, I, J, L, M–R, T. Ex-type CBS 149475; B, NI159; C, F. NI164; H, K. NI124; S, W, X. NI165; U, V. NI129. Scale bar = 20 µm; X applies to A–X.

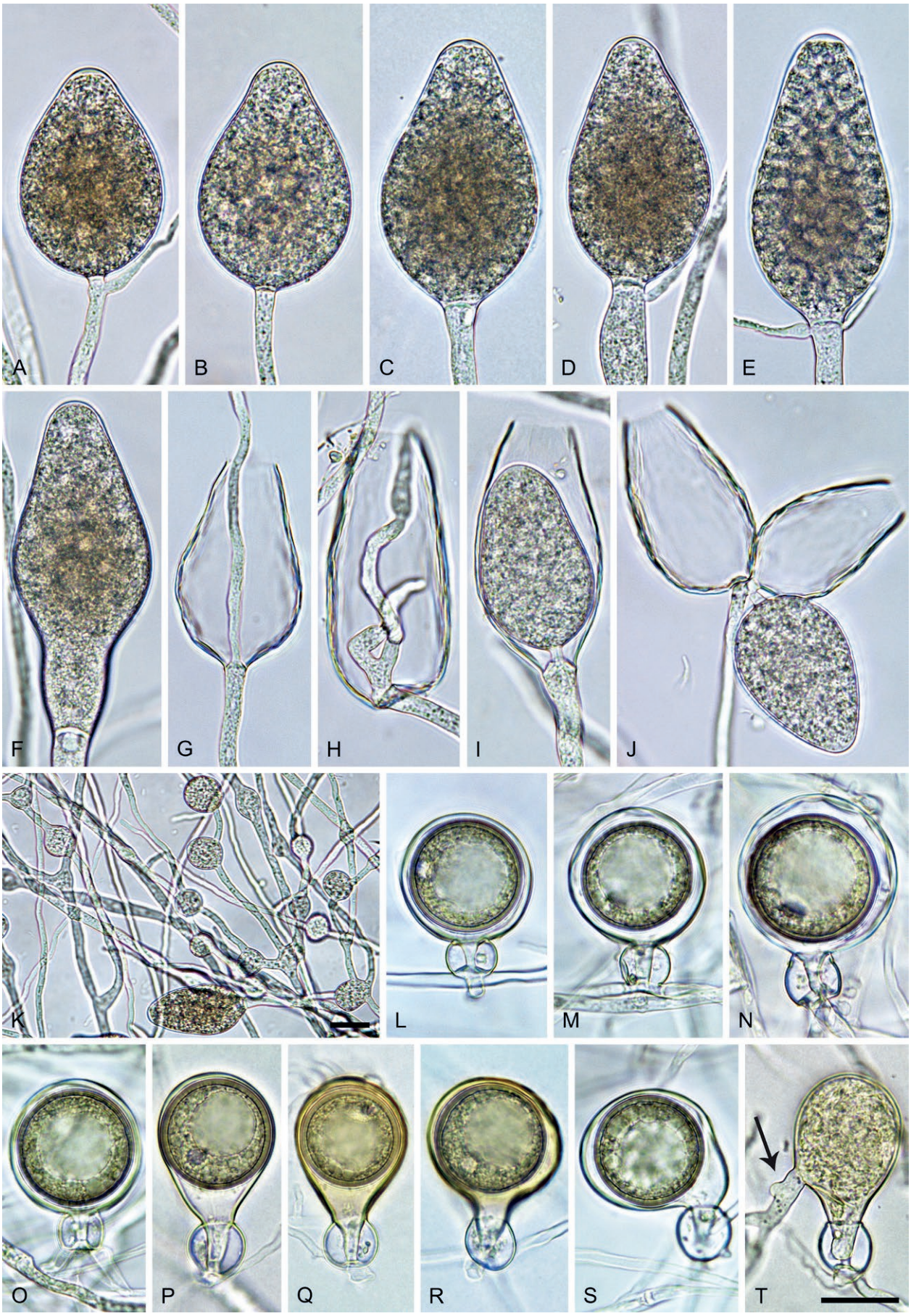

Fig. 70. *Phytophthora furcata*. **A–K.** Structures formed on V8-agar (V8A) in soil extract. **A–J.** Ovoid, obpyriform and limoniform sporangia. **A–D, F.** Nonpapillate sporangia. **A, D, E.** External proliferation. **D.** Widening sporangiophore. **E.** Swollen apex before zoospore release. **G, H.** Internal extended proliferation. **H.** Sporangiophore furcating inside empty sporangium. I. Internal nested proliferation. **J.** Dense sympodium. **K.** Catenulate hyphal swellings and sporangium. **L–S.** Oogonia with aplerotic to near plerotic oospores and amphigynous antheridia, formed in V8A. **L–O.** Globose to subglobose oogonia with round bases. **M, N.** Wavy oogonial walls. **P–S.** Elongated, excentric or comma-shaped oogonia with tapering bases. **T.** Oogonium with germinating oospore. Images: A, G, L, Q. VN002; B, D, F, I–K, M–P, S, T. Ex-type CBS 149487; C, VN073; E, H, R. VN384. Scale bars = 20 µm; T applies to A–J, L–T.

formed in water, globose to subglobose, limoniform or irregular, usually catenulate (Fig. 70K), av. diam 13.6 ± 5.3 µm (range 6.5–58.1 µm). *Chlamydospores* not observed. *Oogonia* abundantly produced in single culture ('homothallic' breeding system), sessile, predominantly globose to subglobose (59.7 %; Fig. 70L–O), elongated (15.7 %; Fig. 70P, Q), slightly excentric (19.3 %; Fig. 70R, S) or comma-shaped (5.3 %; Fig. 70S), with a rounded base and short thin stalk (34 %; Fig. 70L–O) or with a long tapering, frequently (24 %) funnel-like base (66 %; Fig. 70P–T); oogonial wall smooth (Fig. 70L, O–T) or slightly wavy (Fig. 70M, N); oogonial diam 31.4 ± 3.1 µm (overall range 19.8–40.4 µm; range of isolate means 29.6–33.0 µm); slightly aplerotic to aplerotic (50.7 %; Fig. 70M, N, R, S) or nearly plerotic to plerotic (49.3 %; Fig. 70L, O–Q). *Oospores* globose with a large lipid globule (Fig. 70L–S); diam 28.5 ± 2.6 µm (overall range 16.1–36.1 µm; range of isolate means 27.3–29.8 µm) wall thickness 1.94 ± 0.28 µm (overall range 0.91–2.79 µm), oospore wall index 0.36 ± 0.04; abortion rate 16–37 % (av. 25.2 %) after 4 wk; after 2 mo at 20 °C most oospores germinating (Fig. 70T). *Antheridia* exclusively amphigynous and unicellular, subglobose to cylindrical (Fig. 70L–T); dimensions 15.0 ± 1.8 × 13.3 ± 1.4 µm.

Culture characteristics: Colonies on V8A and CA appressed with limited aerial mycelium, stellate on V8A and petaloid on CA; on PDA uniform, dense-cottony and dome-shaped (Fig. 61).

Cardinal temperatures and growth rates: On V8A optimum 25 °C with 8.62 ± 0.41 mm/d radial growth, maximum 25–<27.5 °C, minimum <10 °C (Fig. 62), lethal temperature 27.5 °C. At 20 °C on V8A, CA and PDA 7.42 ± 0.18 mm/d, 4.91 ± 0.18 mm/d and 3.48 ± 0.25 mm/d, respectively.

Additional materials examined: **Vietnam**, Sapa, Fansipan Mountain, isolated from rhizosphere soil of *M. henryi* and *N. merilliana* in a montane evergreen cloud forest, Mar. 2016, *T. Jung, N.M. Chi & M. Horta Jung* (VN002, VN036, VN384, VN385); isolated from a baiting leaf floating in a stream running through a montane evergreen cloud forest, Mar. 2016, *T. Jung, N.M. Chi & M. Horta Jung* (VN073).

Phytophthora sumatera T. Jung, M. Tarigan, I. Milenković & A. Durán, ***sp. nov.*** MycoBank MB 847328. Fig. 71.

Etymology: The name refers to the origin of all known isolates in Sumatra (Sumatera is the Indonesian name for Sumatra).

Typus: **Indonesia**, Sumatra, Lake Toba, isolated from a naturally fallen necrotic leaf of an unidentified tree species floating in a stream running through a tropical montane rainforest, Aug. 2018, *T. Jung, M. Tarigan & I. Milenković* (**holotype** CBS H-25125, dried culture on V8A, ex-holotype living culture CBS 149501 = SU521).

Morphological structures on V8A: *Sporangia* abundantly produced in non-sterile soil extract; borne terminally on unbranched long or short sporangiophores (Fig. 71A, C, D, G) or in dense sympodia of 2–4 sporangia (Fig. 71E, J–L); non-caducous, predominantly ovoid or elongated ovoid (80.7 %; Fig. 71A–C, F, I–L), less frequently obpyriform to elongated-obpyriform (17.4 %; Fig. 71D, E, G), ellipsoid or elongated ellipsoid (1.3 %), limoniform or elongated-limoniform (0.3 %) or ampulliform (0.3 %); lateral attachment of the sporangiophore (11.7 %; Fig. 71B) and a conspicuous, mostly non-protruding basal plug (24.7 %; Fig. 71E, G, J–L) commonly observed; apices exclusively nonpapillate (Fig. 71A, B, D, E, K, L), appearing semipapillate immediately before zoospore release (Fig. 71C, G); sporangial proliferation both external (Fig. 71E, F, H, J–L) and internal in a nested (Fig. 71G, H) or extended way (Fig. 71I); sporangial dimensions averaging 48.5 ± 8.6 × 32.2 ± 4.1 µm (overall range 34.5–77.5 × 22.3–48.7 µm; range of isolate means 42.1–60.3 × 29.2–35.8 µm) with a length/breadth ratio of 1.51 ± 0.16 (overall range 1.2–2.23); sporangial germination indirectly with zoospores discharged through an exit pore 5.5–13.2 µm wide (av. 8.5 ± 1.2 µm) (Fig. 71F–L). *Zoospores* limoniform to reniform whilst motile, sometimes with ring-like flagella-ends (Fig. 71M), becoming spherical (av. diam = 10.7 ± 0.9 µm) on encystment; Cysts germinating directly or by releasing a secondary zoospore (diplanetism). *Hyphal swellings* frequently formed in water, globose to subglobose, limoniform, ovoid or irregular, often catenulate (Fig. 71N), av. diam 15.4 ± 3.6 µm (range 7.0–27.0 µm). *Chlamydospores* not observed. *Oogonia* abundantly produced in single culture ('homothallic' breeding system), sessile or on short to medium-length lateral hyphae; globose to subglobose (56.5 %; Fig. 71O, R, W), comma-shaped (33.5 %; Fig. 71S–U) or excentric and/or elongated (10 %; Fig. 71V) with a short tapering or more frequently a long tapering, sometimes (18 %) funnel-like base (Fig. 71O–W); oogonial wall smooth (Fig. 71O, P, R–V) or slightly wavy (Fig. 71Q, W); oogonial diam 32.1 ± 3.9 µm (overall range 23.3–41.6 µm; range of isolate means 30.2–34.2 µm); slightly aplerotic to aplerotic (56.5 %; Fig. 71S–W) or nearly plerotic to plerotic (43.5 %; Fig. 71O–R). *Oospores* globose with a large lipid globule (Fig. 71O–W); diam 27.7 ± 3.4 µm (overall range 19.4–38.7 µm; range of isolate means 25.9–28.8 µm) wall thickness 1.36 ± 0.2 µm (overall range 0.78–2.02 µm), oospore wall index 0.27 ± 0.04; abortion rate 6–21 % (av. 15.8 %) after 4 wk; sometimes turning golden-brown to dark-brown during maturation (Fig. 71W). *Antheridia* exclusively amphigynous and unicellular, subglobose to cylindrical (Fig. 71O–W), sometimes intercalary (Fig. 71R); dimensions 13.8 ± 1.8 × 12.2 ± 1.2 µm.

Culture characteristics: Colonies on V8A and CA appressed with limited aerial mycelium, radiate on V8A and petaloid on CA; on PDA felty-cottony and dome-shaped with petaloid pattern and submerged margin (Fig. 61).

Cardinal temperatures and growth rates: On V8A optimum 25 °C with 8.98 ± 0.44 mm/d radial growth, maximum 27.5–<30 °C, minimum <10 °C (Fig. 62), lethal temperature 32.5 °C. At 20 °C on V8A, CA and PDA 7.98 ± 0.36 mm/d, 5.72 ± 0.09 mm/d and 3.57 ± 0.44 mm/d, respectively.

Additional materials examined: **Indonesia**, Java, Bandung area, isolated from a naturally fallen necrotic leaf of an unidentified tree species floating in a stream running through a tropical montane *Pinus merkusii* forest, Mar. 2019, *T. Jung, M. Tarigan & L. Oliveira* (JV146); Sumatra, Lake Toba, isolated from a naturally fallen necrotic leaf of an unidentified tree species floating in a stream running through a tropical montane rainforest, Aug. 2018, *T. Jung, M. Tarigan & I. Milenković* (SU566); isolated from rhizosphere soil of an unidentified tree species in a tropical montane rainforest, Aug. 2018, *T. Jung, M. Tarigan & I. Milenković* (SU909, SU973, SU1037); isolated from rhizosphere soil of a declining *Eucalyptus* sp. in a montane forest plantation, Aug. 2018, *T. Jung, M. Tarigan & I. Milenković* (SU1061); Sumatra, Padang, isolated from a naturally fallen necrotic leaf of an unidentified tree species floating in a stream running through a tropical lowland rainforest, Sep. 2018, *T. Jung, M. Tarigan & L. Oliveira* (SU635); Sumatra, Gulung Talang, isolated from a naturally fallen necrotic leaf of an unidentified tree species floating in a stream running through a tropical submontane rainforest, Sep. 2018, *T. Jung, M. Tarigan & L. Oliveira* (SU690).

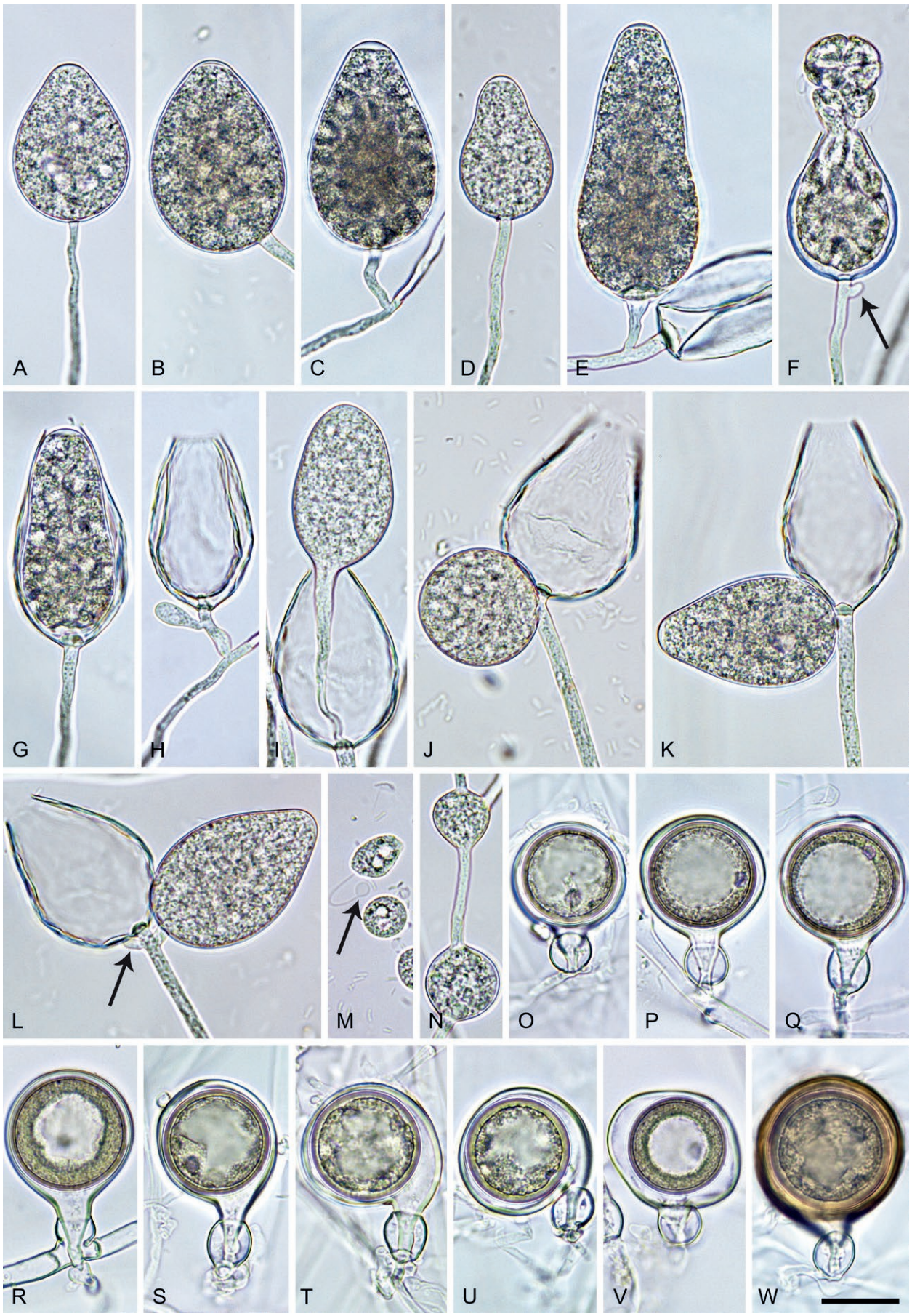

Fig. 71. *Phytophthora sumatera*. **A–N.** Structures formed on V8-agar (V8A) in soil extract. **A–L.** Ovoid and obpyriform sporangia. **A, B, D, E, K, L.** Nonpapillate apices. **C, G.** Swollen apices before zoospore release. **C, E, F, H, J–L.** External proliferation (arrows in F, L). **F.** Zoospore release. **G, H.** Internal nested proliferation. **I.** Internal extended proliferation. **J, K.** Dense sympodia with sessile sporangia. **M.** Zoospores with ring-like flagella ends (arrow). **N.** Catenulate hyphal swellings. **O–W.** Oogonia with near-plerotic to aplerotic oospores, tapering bases and amphigynous antheridia formed in V8A. **O–R, W.** Subglobose to globose oogonia. **S–U.** Comma-shaped oogonia. **V.** Excentric oogonium. Images: A, D, F, G, I, L, N, P, R, U, W. Ex-type CBS 149501; B, J, SU1061; C, E, H, K, O, S, T, JV146; M, Q. SU973; V. SU1037. Scale bar = 20 µm; W applies to A–W.

Notes on Clade 2f taxa: Across the nuclear (LSU, ITS, *βtub*, *hsp90*, *tigA*, *rpl10*, *tef-1α*, *enl*, *ras*-ypt1) 8 720-character alignment and the mitochondrial (*cox1*, *cox2*, *nadh1* and *rps10*) 3 153-character alignment pairwise sequence differences between *P. multivesiculata*, the informally designated *Phytophthora* taxon aquatilis and the three new *Phytophthora* species from Clade 2f taxa were 0.6–2 % and 1.5–3.6 %, respectively. *Phytophthora angustata*, *P. furcata*, previously informally designated as *P.* taxon multivesiculata-like 1 (Jung *et al.* 2020), and *P. sumatera* developed distinctive colony morphologies on V8A, CA and PDA at 20 °C (Fig. 61). In addition, they are distinguished from each other and other Clade 2f species by a combination of morphological (Figs 69–71) and physiological characters (Fig. 62) of which the most discriminating are highlighted in bold in Table S16.

The sporangia of the three new Clade 2f species are exclusively (*P. angustata*, *P. sumatera*) or almost exclusively (*P. furcata*) nonpapillate whereas those of *P. multivesiculata* are both nonpapillate and semipapillate (Ilieva *et al.* 1998; Figs 69–71). *Phytophthora* taxon aquatilis exclusively forms semipapillate sporangia (Hong *et al.* 2012). Their larger average sporangial dimensions discriminate *P. angustata* (65.9 × 35.6 µm) and *P. furcata* (56.4 × 32.8 µm) from *P. multivesiculata* (45 × 33 µm), *P. sumatera* (48.5 × 32.2 µm) and *P.* taxon aquatilis (45.9 × 29.7 µm). Furthermore, the sporangia of *P. angustata* and *P. furcata* have higher l/b ratios (1.85 and 1.72, respectively) than those of *P. multivesiculata* (1.43), *P. sumatera* (1.51) and *P.* taxon aquatilis (1.6). According to Hong *et al.* (2012) the latter taxon differs from all other Clade 2f species by the caducity of its sporangia, although sporangia reported as being caducous in fig. 7 of Hong *et al.* (2012) do not show caducity, and the absence of internal sporangial proliferation. In contrast, *P. angustata*, *P. furcata*, *P. multivesiculata* and *P. sumatera* exclusively produce persistent sporangia with internal nested and extended proliferation (Ilieva *et al.* 1998; Table S16; Figs 69–71).

All five taxa in Clade 2f are intrinsically self-fertile. *Phytophthora multivesiculata* and *P.* taxon aquatilis produce on average much larger oogonia (41 and 38.2 µm) than the three new Clade 2f species (31.1–32.1 µm). The three new species are also distinguished from *P.* taxon aquatilis by having a comparatively high frequency of elongated, excentric or comma-shaped oogonia (34–44 %) and exclusively (*P. angustata*, *P. sumatera*) or predominantly (*P. furcata*) tapering oogonial bases (Ilieva *et al.* 1998; Hong *et al.* 2012; Table S16). In *P. angustata* and *P.* taxon aquatilis oospores are almost exclusively plerotic (Hong *et al.* 2012; Fig. 69) whereas *P. furcata* and *P. sumatera* produce both plerotic and aplerotic oospores in almost equal proportions (Table S16; Figs 70, 71). In *P. multivesiculata* oospores are mostly aplerotic (Ilieva *et al.* 1998). After 4 wk at 20 °C the oospore abortion rate is higher in *P. furcata* (25.2 %) than in *P. angustata* (8.7 %) and *P. sumatera* (15.8 %). The almost exclusively paragynous attachment of their antheridia discriminate *P. angustata* and *P.* taxon aquatilis from *P. furcata* and *P. sumatera* which have exclusively amphigynous antheridia, and *P. multivesiculata* with 95 % amphigynous and 5 % paragynous antheridia. *Phytophthora multivesiculata* and the three new Clade 2f species share the abundant production of catenulate hyphal swellings in water whereas *P.* taxon aquatilis does not form hyphal swellings (Ilieva *et al.* 1998, Hong *et al.* 2012; Table S16; Figs 69–71).

With 25 °C *P. angustata*, *P. furcata* and *P. sumatera* have a higher optimum temperature for growth than *P. multivesiculata* and *P.* taxon aquatilis (both 20 °C). In contrast, the maximum temperature for growth is higher in *P. multivesiculata* (30 °C) and *P.* taxon aquatilis 30–<35 °C) than in *P. angustata*, *P. sumatera* (both 27.5–<30 °C) and *P. furcata* (25–<27.5 °C) (Hong *et al.* 2012; Table S16; Fig. 62). *Phytophthora multivesiculata* shows the slowest growth of all Clade 2f species (Hong *et al.* 2012; Table S16).

Clade 2g

For all known Clade 2g species, colony morphologies on CA, PDA and V8A and temperature-growth relations on V8A are presented in Figs 72 and 73, respectively. Morphological and physiological characters and morphometric data of the four newly described species in Clade 2g are given in the comprehensive Table S17.

Phytophthora inclinata N.M. Chi, T. Jung, M. Horta Jung & I. Milenković, ***sp. nov.*** MycoBank MB 847313. Fig. 74.

Etymology: The name refers to the occurrence of sporangial apices with inclined papillae.

Typus: **Vietnam**, Côn Đảo National Park, Côn Lôn Island, isolated from rhizosphere soil of *Ailanthus triphysa* and *Chukrasia tabularis* in a tropical lowland rainforest, Apr. 2017, *N.M. Chi* (**holotype** CBS H-25110, dried culture on V8A, ex-holotype living culture CBS 149488 = VN1023).

Morphological structures on V8A: Sporangia rarely observed on solid agar but produced abundantly in non-sterile soil extract; typically borne terminally (94.5 %) on unbranched short or long sporangiophores (Fig. 74D, E) or in dense or lax sympodia of 2–4 sporangia (Fig. 74B, K), or less frequently intercalary (4.5 %; Fig. 74G, H) or sessile (1 %); predominantly ovoid, broad-ovoid or elongated ovoid (77.5 %; Fig. 74A–E, J, K), less frequently obpyriform to elongated-obpyriform (7.6 %; Fig. 74G), subglobose (5.5 %; Fig. 74F), limoniform to elongated limoniform (4.5 %), distorted and often with two apices (3.5 %; Fig. 74I), ellipsoid (0.5 %), obovoid (0.5 %) or ampulliform (0.4 %; Fig. 74H); apices semipapillate (51.5 %; Fig. 74A–C, H, I) or papillate (48.5 %; Fig. 74D–G, K); lateral attachment of the sporangiophore (39 %; Fig. 74A, C, F), pedicels (21 %; Fig. 74A, E, I), an asymmetric apex, often with inclined papilla or semipapilla (27 %; Fig. 74B, K) and short hyphal appendices (Fig. 74F) commonly observed; usually non-caducous, but a few sporangia with constrictions of the sporangiophore (Fig. 74E), potentially enabling caducity, present in all isolates; sporangial proliferation exclusively external (Fig. 74B, K); sporangial dimensions averaging 51.8 ± 6.6 × 36.1 ± 5.0 µm (overall range 34.2–84.6 × 24.7–57.6 µm; range of isolate means 44.6–57.8 × 33.0–38.7 µm) with a length/breadth ratio of 1.45 ± 0.21 (overall range 1.06–2.37); pedicel length 18.7 ± 13.2 µm (range 2.9–78.0 µm); sporangial germination usually indirectly with zoospores discharged through an exit pore 4.9–8.8 µm wide (av. 6.6 ± 0.7 µm). *Zoospores* limoniform to reniform whilst motile, becoming spherical (av. diam = 10.0 ± 0.9 µm) on encystment; cysts mostly germinating directly although diplanetism was infrequently observed in all isolates. *Hyphal swellings* abundantly produced in water on sporangiophores and hyphae; globose to subglobose, limoniform, deltoid or irregular and often catenulate (Fig. 74L); dimensions 13.7 ± 3.1 µm (range 7.9–22.7 µm). *Chlamydospores* not observed. *Oogonia* abundantly produced in single culture ('homothallic' breeding system), terminal on short to medium-length, often curved lateral hyphae, smooth-walled, globose to slightly subglobose (94.5 %; Fig. 74M–V), or slightly elongated (5.5 %; Fig. 74W), with a round (64.5 %; Fig. 74M–O, Q, R, V, W) or a short tapering, often curved base (35.5 %; Fig. 74P, S–U); sometimes comma-shaped (9.9 %; Fig. 74V, W); oogonial

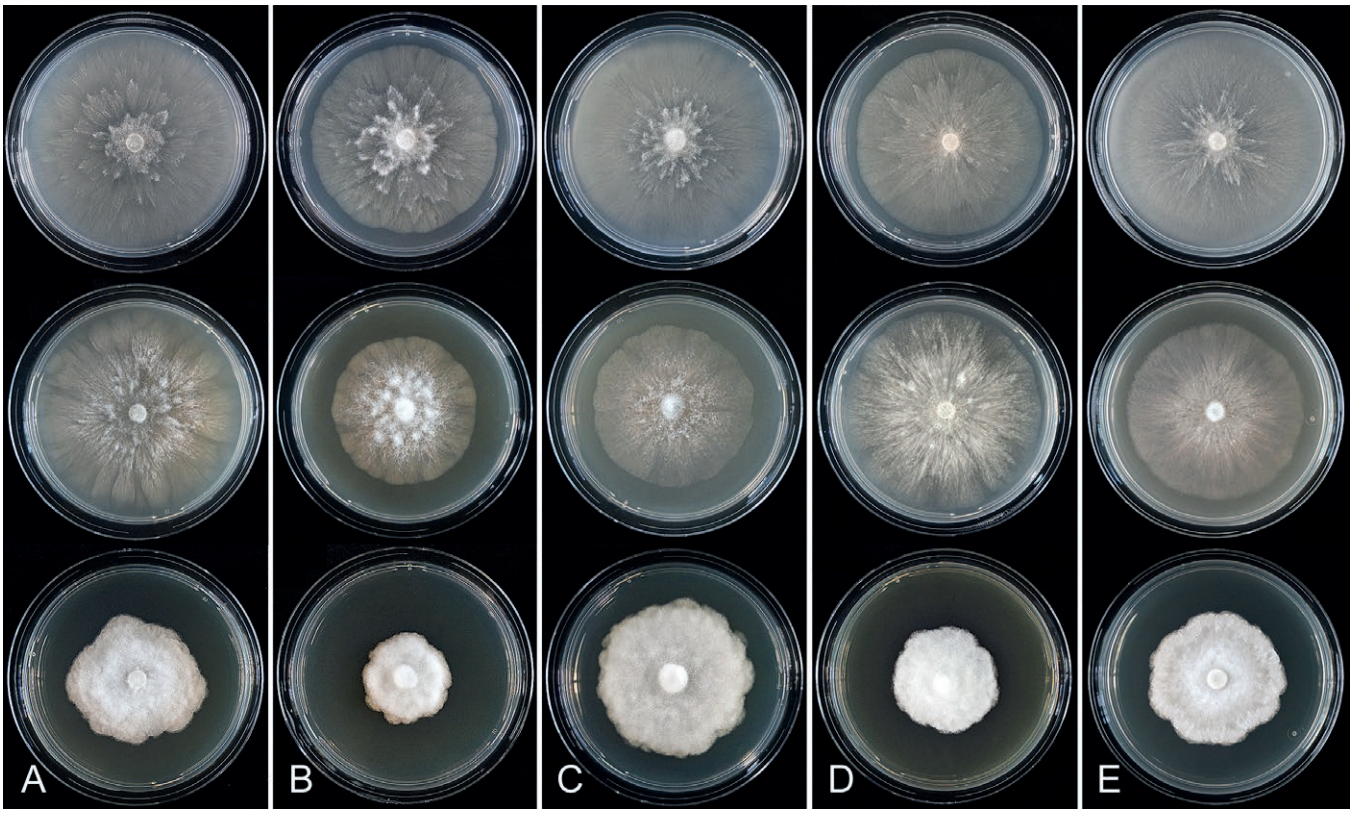

Fig. 72. Colony morphology of *Phytophthora* species from subclade 2g after 7 d growth at 20 ºC on V8-agar, carrot juice agar and potato-dextrose agar (from top to bottom). **A.** *Phytophthora inclinata* (ex-type CBS 149488). **B, C.** *Phytophthora multipapillata* (B. ex-type CBS 149493; C. KA565). **D.** *Phytophthora proliferata* (ex-type CBS 149498). **E.** *Phytophthora transposita* (ex-type CBS 149502).

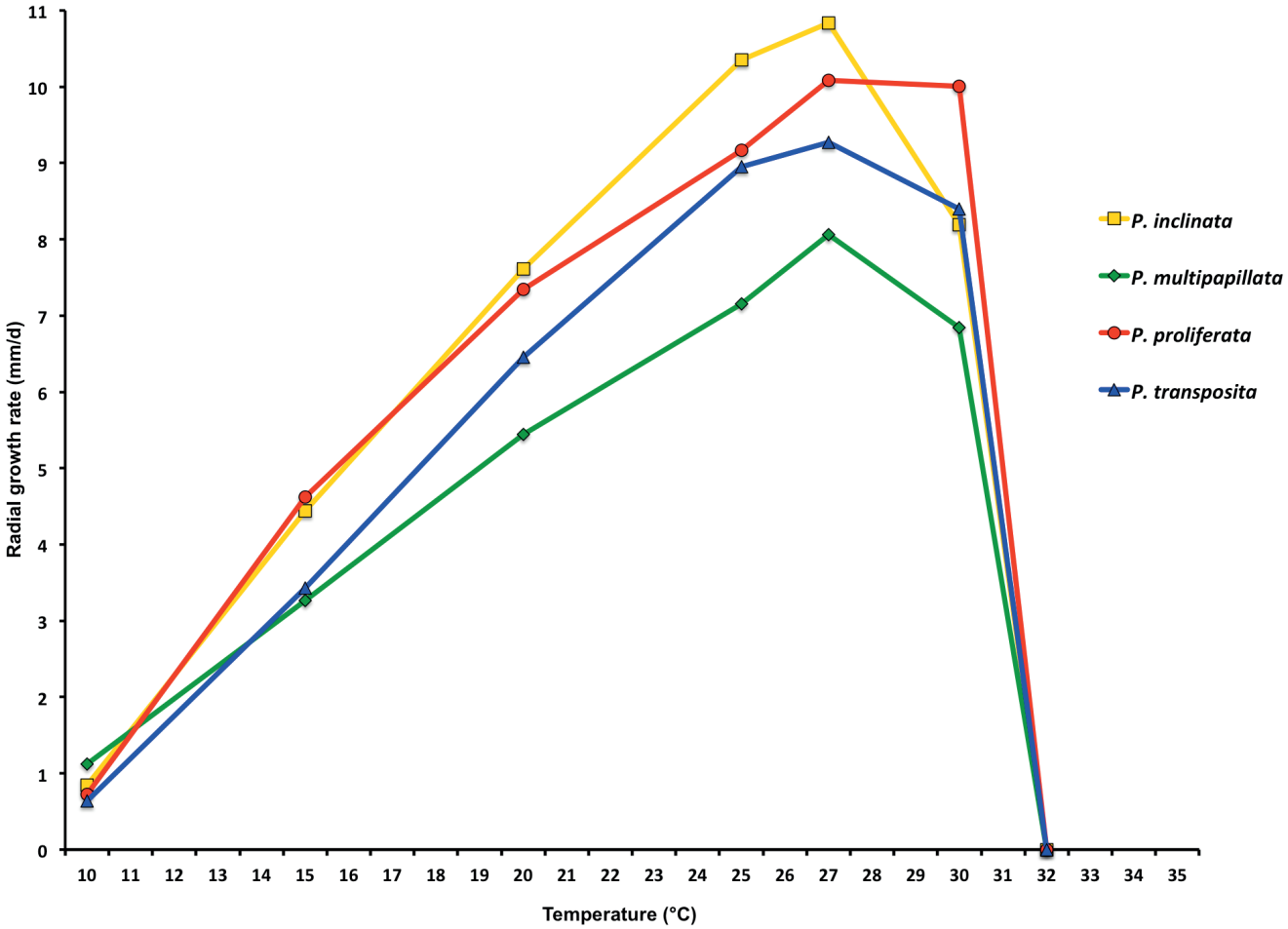

Fig. 73. Mean radial growth rates of four new *Phytophthora* species from subclade 2g on V8-agar at different temperatures: *P. inclinata* (5 isolates); *P. multipapillata* (7 isolates); *P. proliferata* (4 isolates); *P. transposita* (2 isolates).

Fig. 74. *Phytophthora inclinata*. **A–L.** Structures formed on V8-agar (V8A) in soil extract. **A–K.** Sporangia. **A–H, J, K.** Ovoid, obpyriform and ampulliform sporangia. **A–C, H, I.** Semipapillate apices. **A, I.** Pedicels (arrows). **B, K.** Inclined apices and external proliferation. **D–G, K.** Papillate apices. **E.** Constricted sporangiophore. **F.** Hyphal extension (arrow). **G, H.** Intercalary sporangia. **J.** Zoospore release. **L.** Catenulate hyphal swellings. **M–W.** Oogonia with near-plerotic to slightly aplerotic oospores and paragynous antheridia formed in V8A. **M–V.** Subglobose to globose oogonia. **S–V.** Tapering curved bases. **W.** Comma-shaped oogonium. Images: A, D, E–G, K–O, Q, S–U, W. Ex-type CBS 149488; B, C, I, J, P, R. VN1092; H, V. VN1091. Scale bar = 20 µm; W applies to A–W.

diam 25.4 ± 1.9 µm (overall range 14.6–29.8 µm; range of isolate means 24.7–25.7 µm); nearly plerotic to plerotic (81 %; Fig. 74M–U) or slightly aplerotic (19 %; Fig. 74V, W). *Oospores* globose with a large lipid globule (Fig. 74M–W); diam 22.5 ± 1.8 µm (overall range 12.3–26.6 µm; range of isolate means 22.3–22.8 µm); wall thickness 1.38 ± 0.22 µm (overall range 0.76–2.09 µm), oospore wall index 0.32 ± 0.05; abortion rate 0–3 % (av. 1.3 %) after 4 wk. *Antheridia* exclusively paragynous and club-shaped, ovoid, globose to subglobose or irregular (Fig. 74M–W), sometimes with finger-like projections (Fig. 74O, P); dimensions 11.4 ± 1.8 × 8.6 ± 1.4 µm.

Culture characteristics: Colonies on V8A and CA mostly submerged to appressed with scanty aerial mycelium, chrysanthemum-like to stellate on V8A and radiate on CA; on PDA dense-felty with irregular margins and a faint petaloid pattern (Fig. 72).

Cardinal temperatures and growth rates: Optimum 27.5 °C with 10.83 ± 0.15 mm/d radial growth on V8A, maximum 30–<32.5 °C, minimum slightly below 10 °C (Fig. 73), lethal temperature 32.5–35 °C. At 20 °C on V8A, CA and PDA 7.61 ± 0.14 mm/d, 5.38 ± 0.31 mm/d and 3.43 ± 0.06 mm/d, respectively.

Additional materials examined: **Vietnam**, Côn Đảo National Park, Côn Lôn Island, isolated from rhizosphere soil of *A. triphysa* and *C. tabularis* in a tropical lowland rainforest, April 2017, *N.M. Chi* (VN1089, VN1090, VN1091, VN1092).

Phytophthora multipapillata T. Jung, M. Tarigan, I. Milenković & M. Horta Jung, ***sp. nov.*** MycoBank MB 847317. Fig. 75.

Etymology: The name refers to the frequent production of bi- or tripapillate sporangia (*multi* Latin = many).

Typus: **Indonesia**, Kalimantan, Balikpapan, isolated from rhizosphere soil of *Paraserianthes falcataria* in a tropical lowland rainforest, Feb. 2019, *T. Jung & M. Tarigan* (**holotype** CBS H-25116, dried culture on V8A, ex-holotype living culture CBS 149493 = KA532).

Morphological structures on V8A: Sporangia produced abundantly in non-sterile soil extract; typically borne terminally (88.5 %) on unbranched long or short sporangiophores (Fig. 75A, B) or in dense or lax sympodia of 2–5 sporangia (Fig. 75L), or intercalary (2.5 %) or sessile (6.5 %; Fig. 75F); mostly ovoid, broad-ovoid or elongated ovoid (58.7 %; Fig. 75A, B, G, K, L), distorted with two or three apices (22.3 %; Fig. 75I, J, L) or less frequently obpyriform to elongated-obpyriform (5.5 %; Fig. 75C, D, F), mouse-shaped (5 %; Fig. 75H), obovoid or elongated obovoid (4 %; Fig. 75E), ellipsoid or elongated-ellipsoid (2.5 %), limoniform or elongated limoniform (2 %); apices often asymmetric or curved (24.5 %; Fig. 75B, C, F, I, L), semipapillate and often pointed (84.5 %; Fig. 75A–D, G, I, J, L), less frequently papillate (14.5 %; Fig. 75E, H) or nonpapillate (1 %; Fig. 75F); usually persistent but a few caducous sporangia (<1 %; Fig. 75H) were present in all isolates; lateral attachment of the sporangiophore (27 %; Fig. 75D, E, G, H) and pedicels (46 %; Fig. 75A, B, D, H) commonly observed; sporangial proliferation exclusively external (Fig. 75H, L); sporangial dimensions averaging 60.4 ± 6.2 × 33.9 ± 4.0 µm (overall range 42.5–75.0 × 22.6–43.1 µm; range of isolate means 57.3–62.6 × 33.2–35.4 µm) with a length/breadth ratio of 1.8 ± 0.2 (overall range 1.22–2.6); pedicel length 30.2 ± 12.9 µm (range 6.3–55.6 µm); sporangial germination indirectly with zoospores discharged through an exit pore 4.6–8.1 µm wide (av. 6.3 ± 0.8 µm) (Fig. 75K). *Zoospores* limoniform to reniform whilst motile, becoming spherical (av. diam = 10.5 ± 0.8 µm) on encystment; cysts germinating directly. *Hyphal swellings* produced in water on sporangiophores and hyphae; globose to subglobose, ovoid, limoniform or deltoid (Fig. 75C, M). *Chlamydospores* not observed. *Oogonia* abundantly produced in single culture ('homothallic' breeding system), terminal on short to medium-length, sometimes curved lateral hyphae or sessile, smooth-walled, globose to slightly subglobose (79.6 %; Fig. 75N–S), slightly elongated (2.4 %; Fig. 75T) or comma-shaped (18 %; Fig. 75U, V), usually with a rounded (90.4 %; Fig. 75N–S) or a short tapering base (9.6 %; Fig. 75T–V); oogonial diam 27.2 ± 1.4 µm (overall range 22.9–31.2 µm; range of isolate means 26.8–27.7 µm); slightly aplerotic (53.6 %; Fig. 75N–Q) or nearly plerotic to plerotic (46.4 %; Fig. 75R–V). *Oospores* globose with a large lipid globule (Fig. 75N–V); diam 24.0 ± 1.2 µm (overall range 20.3–29.6 µm; range of isolate means 23.8–24.4 µm) wall thickness 1.18 ± 0.17 µm (overall range 0.69–1,7 µm), oospore wall index 0.27 ± 0.03; abortion rate 1–14 % (av. 6.4 %) after 4 wk. *Antheridia* exclusively paragynous and club-shaped, ellipsoid or subglobose (Fig. 75N–V), occasionally with finger-like projections (12.8 %; Fig. 75P); sometimes two antheridia attached to one oogonium; dimensions 13.5 ± 3.0 × 8.3 ± 1.2 µm.

Culture characteristics: Colonies on V8A and CA appressed with limited aerial mycelium, chrysanthemum-like to stellate on V8A and faintly radiate on CA; on PDA felty-cottony with a faint petaloid pattern (Fig. 72).

Cardinal temperatures and growth rates: On V8A optimum at 27.5 °C with 8.06 ± 0.43 mm/d radial growth, maximum 30–<32.5 °C, minimum <10 °C (Fig. 73), lethal temperature 32.5–35 °C. At 20 °C on V8A, CA and PDA 5.44 ± 0.26 mm/d, 4.66 ± 0.27 mm/d and 3.43 ± 0.81 mm/d, respectively.

Additional materials examined: **Indonesia**, Kalimantan, Balikpapan, isolated from rhizosphere soil of *P. falcataria* in a tropical lowland rainforest, Feb. 2019, *T. Jung & M. Tarigan* (KA533, KA534); isolated from rhizosphere soil of *Diospyros pilosanthera* in a tropical lowland rainforest, Feb. 2019, *T. Jung, M. Tarigan & M. Junaid* (KA565, KA612, KA613, KA614).

Phytophthora proliferata T. Jung, N.M. Chi, I. Milenković & M. Horta Jung, ***sp. nov.*** MycoBank MB 847303. Fig. 76.

Etymology: The name refers to the regular external and internal nested and extended proliferation of sporangia.

Typus: **Vietnam**, Cuc Phuong National Park, isolated from rhizosphere soil of *Anogeissus acuminata* and *Taxotrophis macrophylla* in a tropical lowland rainforest, Mar. 2016, *T. Jung, & N.M. Chi* (**holotype** CBS H-25122, dried culture on V8A, ex-holotype living culture CBS 149498 = VN686).

Morphological structures on V8A: *Sporangia* not observed in solid agar but abundantly produced in non-sterile soil extract; borne terminally, in dense or lax sympodia of 2–5 sporangia (Fig. 76L) or on short lateral hyphae (Fig. 76B, F, J), or less frequently intercalary (2 %; Fig. 76D) or sessile (0.5 %; Fig. 76C); non-caducous, predominantly ovoid, broad-ovoid or elongated ovoid (69 %; Fig. 76A–E, I–L), less frequently limoniform or elongated-limoniform (11.5 %; Fig. 76G), ellipsoid (10.5 %; Fig. 76L), subglobose (3 %), distorted and often with two or three apices (2 %; Fig. 76H, M), obovoid (1.5 %), obpyriform (1.5 %; Fig. 76F), pyriform (0.5 %) or ampulliform (0.5 %); lateral attachment of the sporangiophore common (31.5 %; Fig. 76B, E); pedicels infrequent (4 %), 15.1 ±

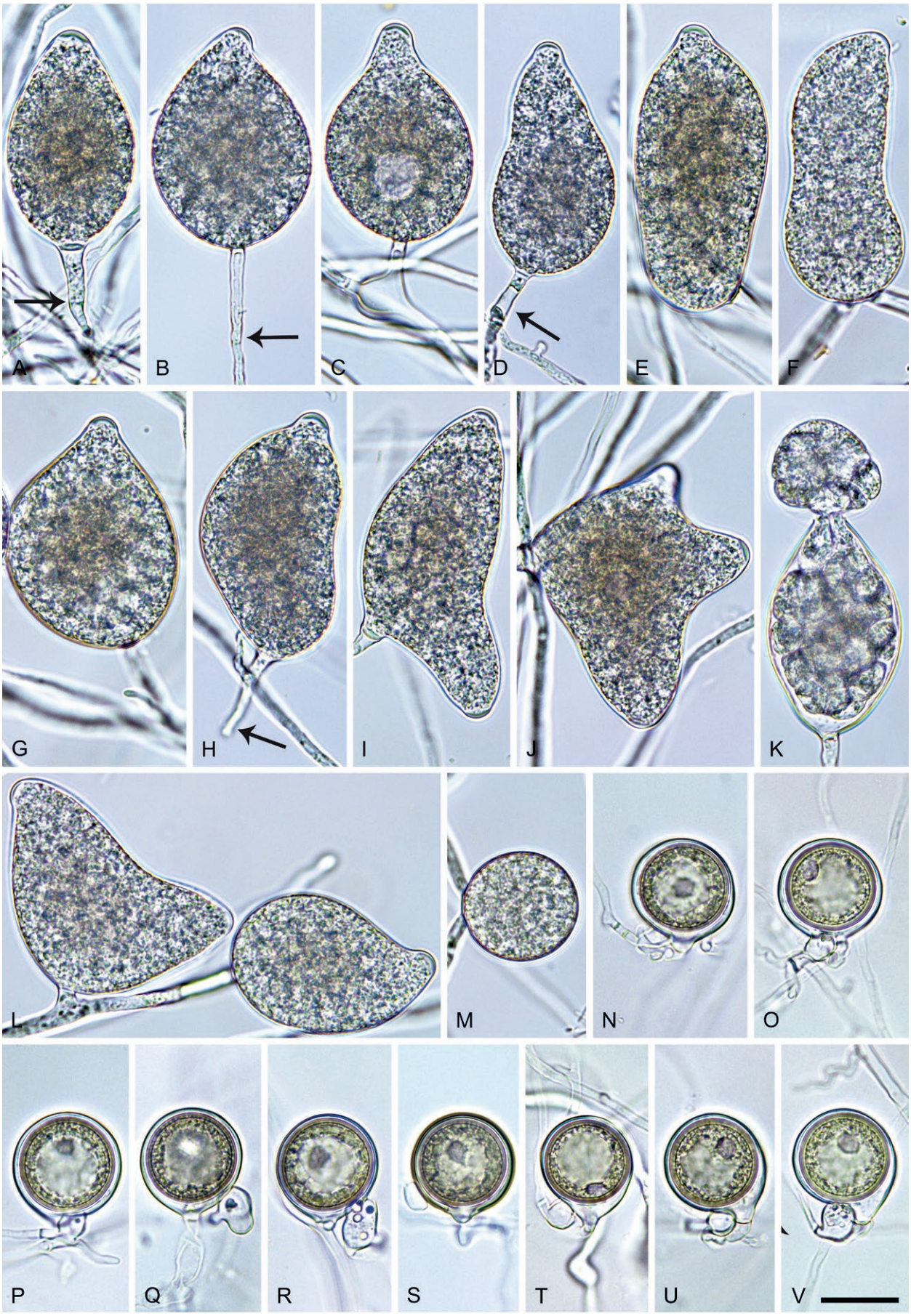

Fig. 75. *Phytophthora multipapillata*. **A–L.** Sporangia formed on V8-agar (V8A) in soil extract. **A–H, L.** Ovoid, obpyriform, obovoid and mouse-shaped sporangia. **A–D, F, G, I, J, L.** Semipapillate apices. E, H. Papillate apices. A, B, D, H. Medium-length pedicels (arrows). **H, I.** External proliferation. F. Intercalary sporangium. H. Caducous sporangium. I, J, L. Sporangia with multiple apices. K. Zoospore release. **L.** Sympodium. **M.** Intercalary hyphal swelling on V8A in soil extract. **N–V.** Oogonia with slightly aplerotic to plerotic oospores and paragynous antheridia formed in V8A. **N–S.** Globose to subglobose oogonia. **T.** Slightly elongated oogonium. **U, V.** Comma-shaped oogonia with tapering bases. Images: A, C, E–H, M, N, P–S, V. Ex-type CBS 149493; B, D, I, K, L, O, T, U. KA565; J. KA534; Scale bar = 20 µm; V applies to A–V.

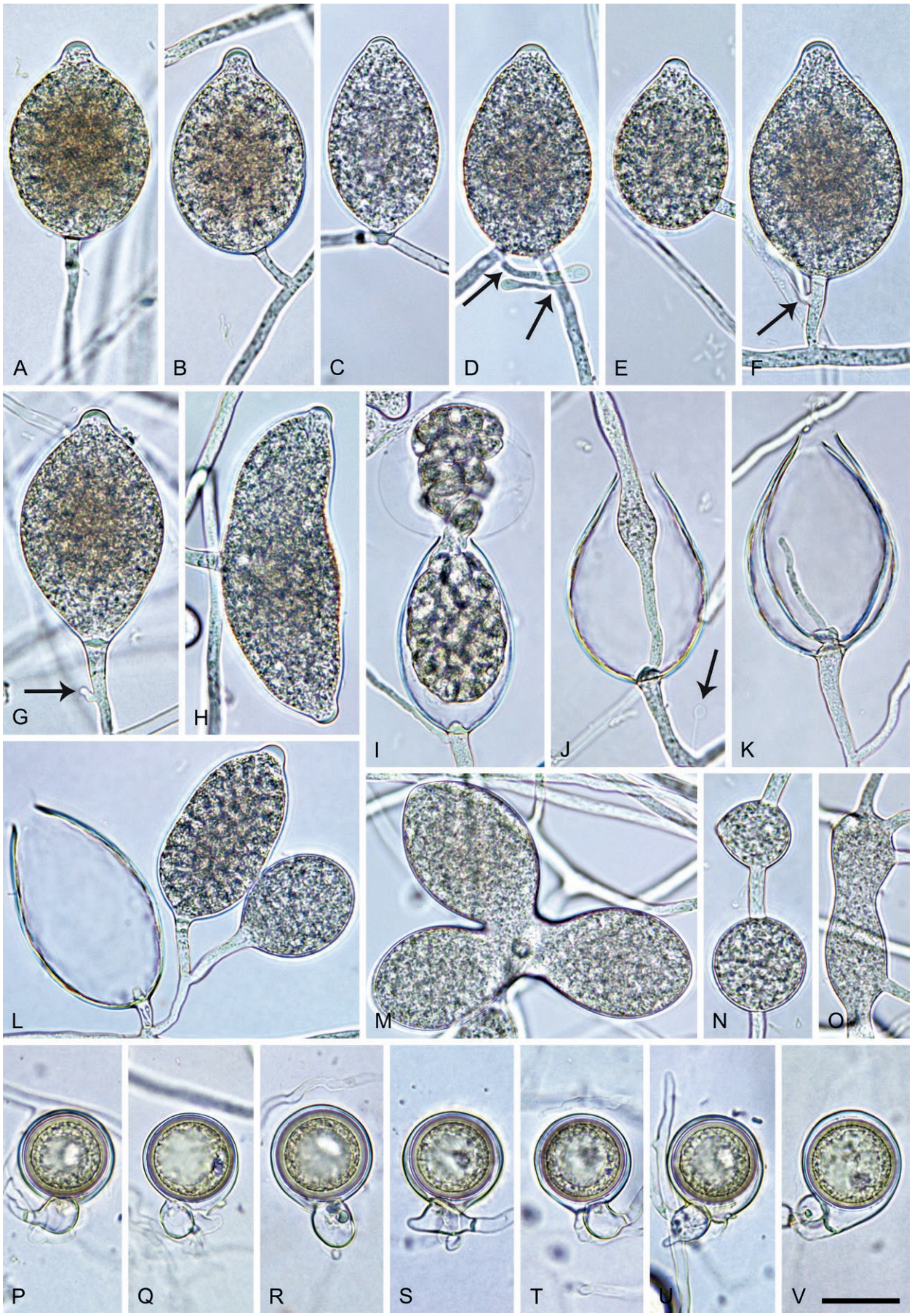

Fig. 76. *Phytophthora proliferata*. **A–M.** Sporangia formed on V8-agar (V8A) in soil extract. **A–G, I–L.** Ovoid, obpyriform and limoniform sporangia. **A, B, G, L.** Papillate apices. **C–F, H.** Semipapillate apices. **A, D, F, G, K, L.** External proliferation (arrows in D, F, G). **C.** Sessile sporangium. **D.** Intercalary sporangium. **H.** Bilobed sporangium. **I.** Zoospore release. **J.** Internal extended proliferation and zoospore flagella with ring-like end (arrow). **K.** Internal nested and extended proliferation. **L.** Dense sympodium. M. Immature trilobed sporangium. **N, O.** Hyphal swellings on V8A in soil extract. **N.** Catenulate. **P–V.** Oogonia with slightly aplerotic to plerotic oospores and paragynous antheridia formed in V8A. **P–T.** Globose to subglobose oogonia. **U, V.** Slightly elongated oogonia. Images: A, G, O, VN804; B, C–E, H, I, J, K, L, M, R–V. Ex-type CBS 149498; F, N, P, Q. VN803. Scale bar = 20 µm; V applies to A–V.

7.5 µm (range 3.6–50.5 µm); apices papillate (44 %; Fig. 76A, B, G, L) or semipapillate (56 %; Fig. 76C–F, H); sporangial proliferation external (Fig. 76D, F, G, I, K, L) or less frequently internal in an extended (Fig. 76J, K) or nested way (Fig. 76K); sporangial dimensions averaging 49.1 ± 6.8 × 31.3 ± 4.2 µm (overall range 29.6–67.5 × 20.3–42.2 µm; range of isolate means 46.4–52.3 × 28.3–34.9 µm) with a length/breadth ratio of 1.58 ± 0.19 (overall range 1.17–2.26); sporangial germination indirectly with zoospores discharged through an exit pore 4.6–8.9 µm wide (av. 6.6 ± 0.9 µm) (Fig. 76I–L). *Zoospores* limoniform to reniform whilst motile, sometimes with ring-like flagella ends (Fig. 76J), becoming spherical (av. diam = 10.8 ± 1.3 µm) on encystment. *Hyphal swellings* infrequently formed in water, globose to subglobose, limoniform or irregular, sometimes catenulate (Fig. 76N, O), av. diam 10.1 ± 2.8 µm. *Chlamydospores* not observed. *Oogonia* abundantly produced in single culture ('homothallic' breeding system), terminal on short to medium-length, often curved lateral hyphae, smooth-walled, globose to slightly subglobose (88 %; Fig. 76P–T) or slightly elongated (12 %; Fig. 76U, V), usually with a round (72.5 %; Fig. 76P–U) or less frequently with a tapering base (27.5 %; Fig. 76V); oogonial diam 26.5 ± 2.0 µm (overall range 15.1–31.0 µm; range of isolate means 26.2–27.1 µm); nearly plerotic to plerotic (97 %; Fig. 76P–U), rarely slightly aplerotic (3 %; Fig. 76V). *Oospores* globose with a large lipid globule (Fig. 76P–V); diam 23.7 ± 1.8 µm (overall range 13.0–28.1 µm; range of isolate means 22.9–24.2 µm) wall thickness 1.61 ± 0.25 µm (overall range 0.92–2.25 µm), oospore wall index 0.35 ± 0.04; abortion rate 2–19 % (av. 10.5 %) after 4 wk. *Antheridia* exclusively paragynous and club-shaped, ovoid or globose to subglobose (Fig. 76P–V); 13.5 ± 2.3 × 9.3 ± 1.2 µm.

Culture characteristics: Colonies on V8A and CA mostly submerged to appressed, stellate on V8A and radiate on CA; on PDA felty-cottony with a faint petaloid pattern (Fig. 72).

Cardinal temperatures and growth rates: On V8A optimum 27.5 °C with 10.1 ± 0.17 mm/d radial growth, maximum 30–<32.5 °C, minimum slightly below 10 °C (Fig. 73), lethal temperature 32.5–35 °C. At 20 °C on V8A, CA and PDA 7.34 ± 0.13 mm/d, 5.47 ± 0.2 mm/d and 3.06 ± 0.14 mm/d, respectively.

Additional materials examined: **Vietnam**, Cuc Phuong National Park, isolated from rhizosphere soil of *A. acuminata* and *T. macrophylla* in a tropical lowland rainforest, Mar. 2016, *T. Jung, M. Horta Jung & N.M. Chi* (VN803, VN804, VN805, VN806).

Phytophthora transposita T. Jung, K. Kageyama, C.M. Brasier & H. Masuya, ***sp. nov.*** MycoBank MB 847304. Fig. 77.

Etymology: The name refers to the high proportion of sporangia with laterally displaced sporangiophore attachment and laterally displaced or curved apices (*transposita* Latin = displaced).

Typus: **Japan**, Kyushu Island, Aya, isolated from rhizosphere soil of *Zanthoxylum ailanthoides* in a warm-temperate mixed forest, May 2017, *T. Jung & K. Kageyama* (**holotype** CBS H-25126, dried culture on V8A, ex-holotype living culture CBS 149502 = JP583).

Morphological structures on V8A: Sporangia produced abundantly in non-sterile soil extract; typically borne terminally (98 %) in dense or lax sympodia of 2–5 sporangia (Fig. 77M) or less frequently on unbranched long or short sporangiophores (Fig. 77F), or intercalary (2 %); non-caducous, predominantly ovoid, broad-ovoid or elongated ovoid (64 %; Fig. 77A–E, J, M), less frequently obpyriform or elongated-obpyriform (11 %; Fig. 77H), distorted and often with two apices (7.6 %; Fig. 77K, L), limoniform or elongated limoniform (6 %; Fig. 77G), mouse-shaped (5 %; Fig. 77I, M), obovoid (4 %; Fig. 77F) or ampulliform (2.4 %); apices semipapillate (50 %; Fig. 77A–D, G–I, M), papillate (32.6 %; Fig. 77E, F, K) or nonpapillate (17.4 %; Fig. 77J, M), often curved or laterally displaced (28.3 %; Fig. 77B–D, I–K, M); lateral attachment of the sporangiophore (49.1 %; Fig. 77A–D, I, M) and vacuoles (21.7 %; Fig. 77D, I, K) commonly observed; empty sporangia often with a conspicuous protruding basal plug (40 %; Fig. 77L); rarely (4 %) with short pedicels < 10 µm (Fig. 77M); sporangial proliferation exclusively external (Fig. 77E, J–M); sporangial dimensions averaging 61.0 ± 8.5 × 31.5 ± 3.1 µm (overall range 48.1–79.8 × 25.5–37.9 µm; range of isolate means 60.4–61.6 × 30.7–32.3 µm) with a length/breadth ratio of 1.96 ± 0.32 (overall range 1.4–2.74); sporangial germination usually indirectly with zoospores discharged through an exit pore 4.6–6.7 µm wide (av. 5.6 ± 0.6 µm) (Fig. 77L). *Zoospores* limoniform to reniform whilst motile, becoming spherical (av. diam = 11.0 ± 1.0 µm) on encystment. *Hyphal swellings* rarely produced in water on sporangiophores; globose to subglobose, ovoid, limoniform or irregular (Fig. 77M); dimensions 10.9–23.6 µm. *Chlamydospores* not observed. *Oogonia* abundantly produced in single culture ('homothallic' breeding system), terminal on short to medium-length, sometimes curved lateral hyphae or sessile, smooth-walled, globose to slightly subglobose (72 %; Fig. 77N–R) or slightly comma-shaped (28 %; Fig. 77S–V), with a rounded (54 %; Fig. 77N–R) or a tapering base (46 %; Fig. 77S–V); oogonial diam 24.8 ± 1.3 µm (overall range 22.1–27.3 µm; range of isolate means 24.2–25.4 µm); nearly plerotic to plerotic (98 %; Fig. 77N–V) or slightly aplerotic (2 %). *Oospores* globose with a large lipid globule (Fig. 77N–V); diam 21.1 ± 1.1 µm (overall range 18.4–22.7 µm; range of isolate means 20.8–21.4 µm), wall thickness 1.52 ± 0.19 µm (overall range 1.07–2.02 µm), oospore wall index 0.37 ± 0.03; abortion rate 7 % after 4 wk; after 2 mo at 20 °C many oospores germinating by producing one or multiple sporangia (Fig. 77W). *Antheridia* exclusively paragynous and club-shaped, ovoid or subglobose (Fig. 77N–V), sometimes with finger-like projections (Fig. 77R, V); dimensions 12.6 ± 2.5 × 7.9 ± 1.3 µm.

Culture characteristics: Colonies on V8A submerged to appressed with limited aerial mycelium and a radiate pattern; on CA submerged to appressed with scanty aerial mycelium and a striate pattern; on PDA appressed, felty-woolly in the centre and dense-felty at the irregular margins, without pattern (Fig. 72).

Cardinal temperatures and growth rates: On V8A optimum at 27.5 °C with 9.28 ± 0.18 mm/d radial growth, maximum 30–<32.5 °C, minimum <10 °C (Fig. 73), lethal temperature 32.5–35 °C. At 20 °C on V8A, CA and PDA 6.46 ± 0.17 mm/d, 4.82 ± 0.07 mm/d and 3.77 ± 0.07 mm/d, respectively.

Additional materials examined: **Japan**, Kyushu Island, Aya, isolated from rhizosphere soil of *Z. ailanthoides* in a warm-temperate mixed forest, May 2017, *T. Jung & K. Kageyama* (JP2361).

Notes on Clade 2g taxa: Across the nuclear (LSU, ITS, *βtub*, *hsp90*, *tigA*, *rpl10*, *tef-1α*, *enl*, *ras*-ypt1) 8 725-character alignment and the mitochondrial (*cox1*, *cox2*, *nadh1* and *rps10*) 3 156-character alignment the four new species from Clade 2g showed sequence differences of 0.6–0.8 % and 1.1–1.5 %, respectively. The four new Clade 2g species developed distinctive colony morphologies on V8A, CA and PDA at 20 °C (Fig. 72). In addition, they are

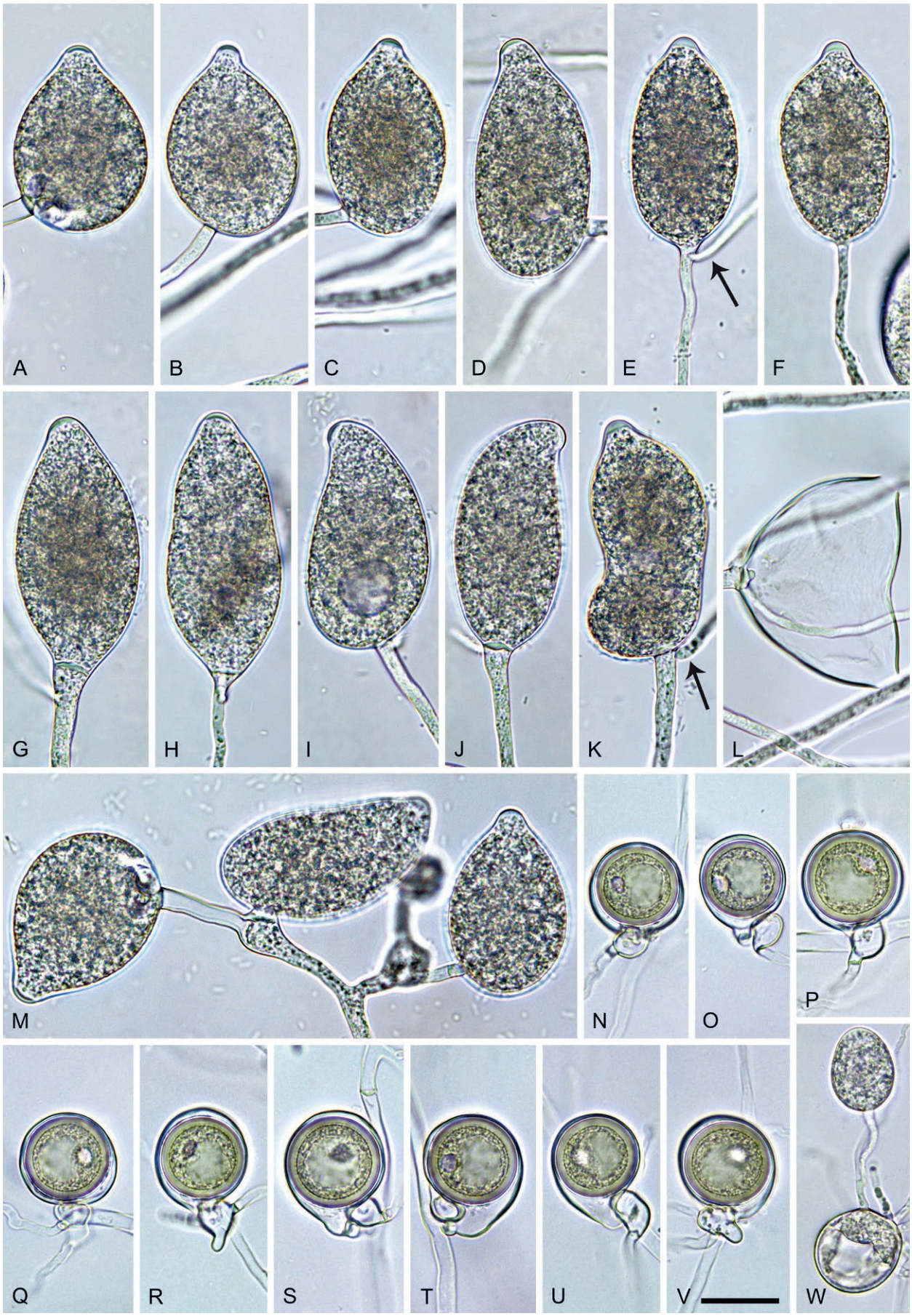

Fig. 77. *Phytophthora transposita*. **A–M.** Sporangia formed on V8-agar (V8A) in soil extract. **A–J, M.** Ovoid, obovoid, limoniform, obpyriform and mouse-shaped sporangia. **A–D, G–J, M.** Semipapillate apices. **E, F, K.** Papillate apices. **D, I, J.** Curved, laterally displaced apices. **A–D, I, M.** Laterally attached sporangiophores. **E, G, I–M.** External proliferation (arrows in E, K). **K.** Distorted sporangium. **L.** Sporangium with two apices, after zoospore release. **M.** Dense sympodium with semipapillate and nonpapillate sporangia and hyphal swellings. **N–V.** Oogonia with near-plerotic to plerotic oospores and paragynous antheridia formed in V8A. **N–R.** Subglobose to globose oogonia. **S–V.** Comma-shaped oogonia with tapering bases. **W.** Oospore germinating by producing a sporangium. Images: A–C, E, H, J–O, Q, R, U–W. CBS 149502; D, F, G, I, P, S, T. JP2361. Scale bar = 20 µm; V applies to A–W.

separated from each other by a combination of morphological (Figs 74–77) and physiological (Fig. 73) characters of which the most discriminating are highlighted in bold in Table S17.

Three of the four species in Clade 2g, *i.e.*, *P. inclinata*, *P. proliferata* and *P. transposita*, share having high proportions of both semipapillate (50–56 %) and papillate (33–48.5 %) sporangia while in *P. multipapillata* sporangia are predominantly semipapillate (84.5 %) and less frequently papillate (14.5 %) or nonpapillate (1 %) (Table S17; Figs 74–77). *Phytophthora transposita* differs from the other three Clade 2g species by having a comparatively high proportion of nonpapillate sporangia (17 %).

High sporangial l/b ratios separate *P. multipapillata* (1.8 ± 0.2) and *P. transposita* (1.96 ± 0.32) from *P. inclinata* (1.45 ± 0.21) and *P. proliferata* (1.58 ± 0.19) (Table S17). Furthermore, in *P. multipapillata* 46 % of sporangia are pedicellate and occasionally show caducity (<1 %) whereas in the other three species sporangia are exclusively persistent with much lower proportions of pedicels (4–21 %) (Table S17; Figs 74–77). In addition, *P. multipapillata* has higher proportions of sporangia with more than one apex than the other Clade 2g species (22 % *vs*. 2–8 %) (Table S17). *Phytophthora proliferata* differs from the other three species by having internal nested and extended sporangial proliferation (Table S17; Figs 74–77).

All four species in Clade 2g are intrinsically self-fertile with exclusively paragynous antheridia and low oospore abortion rates. *Phytophthora multipapillata* differs from the other three species by having a considerably smaller proportion of oogonia with tapering bases (9.6 *vs*. 27.5–46 %) and a lower oospore wall index (0.27 *vs*. 0.32–0.37) (Table S17; Figs 74–77).

The four Clade 2g species have identical optimum (27.7 °C) and maximum temperatures (<32.5 °C) for growth but their growth rates differ with *P. multipapillata* being the slowest species between 20 and 30 °C and *P. inclinata* and *P. proliferata* showing the fastest growth at 27.5 and 30 °C, respectively (Fig. 73).

Several new Clade 2g species described here were previously known under informal names, *i.e.*, *P. inclinata* as *P. citricola* XI and *P. proliferata* as *P. citricola* X (Jung *et al.* 2020).

Notes on geographical distribution and host and habitat associations of Clade 2 taxa

Apart from *P. celeris*, which was detected together with *P. acaciivora* in effluents from an *Acacia* and eucalypt nursery in Sumatra, and several isolates of *P. pseudocitrophthora* from nursery plants in Hungary and Spain all the newly described Clade 2 species were isolated either (i) from forest streams (*P. amamensis*, *P. balkanensis*, *P. catenulata*, *P. distorta*, *P. falcata*, *P. fansipanensis*, *P. frigidophila*, *P. furcata*, *P. indonesiensis*, *P. japonensis*, *P. limosa*, *P. obovoidea*, *P. obturata*, *P. pseudocapensis*, *P. pseudocitrophthora*, *P. pseudofrigida*, *P. pseudoccultans*, *P. sumatera*, *P. vacuola*, *P. valdiviana*, *P.* ×*australasiatica*, *P.* ×*lusitanica*, *P.* ×*taiwanensis*); (ii) from rhizosphere soil of forest trees (*P. balkanensis*, *P. borneensis*, *P. catenulata*, *P. curvata*, *P. excentrica*, *P. falcata*, *P. furcata*, *P. inclinata*, *P. indonesiensis*, *P. japonensis*, *P. limosa*, *P. macroglobulosa*, *P. multipapillata*, *P. nimia*, *P. oblonga*, *P. obovoidea*, *P. obturata*, *P. platani*, *P. proliferata*, *P. pseudocitrophthora*, *P. pseudoccultans*, *P. sumatera*, *P. transposita*, *P. vacuola*, *P. vietnamensis*, *P.* ×*australasiatica*, *P.* ×*taiwanensis*); or (iii) from naturally fallen leaves under the forest canopy (*P. angustata*, *P. calidophila*, *P. frigidophila*, *P. montana*, *P. multiplex*, *P. obovoidea*, *P. penetrans*, *P. pyriformis*, *P. variepedicellata*, *P.* ×*australasiatica*). On a purely visual basis, no above-soil stem or foliar symptoms were observed in associated vegetation. It should be noted that, besides being found in the rhizosphere of healthy *Platanus orientalis* trees in two riparian forests in Sicily, *P. platani* has also been isolated from aerial bark cankers and necrotic roots of a declining planted mature *Platanus* × *acerifolia* tree in London, UK.

Clade 2a taxa

Clade 2a now comprises 22 taxa, *i.e.*, 11 known and six newly described species and five informally designated taxa, with the majority distributed along a belt stretching from South Asia via Southeast Asia to the subtropical islands of the Japanese archipelago (Figs 78, 79).

Both mating types of *P. meadii* are widespread across the southern part of the Indian subcontinent and Sri Lanka where it has been recognized as the main cause of bark cankers, pod rot and abnormal leaf fall of introduced rubber (*Hevea brasiliensis*) trees and also damages other crops, including areca nut (*Areca catechu*), *Citrus* and vanilla (Peries & Dantanarayana 1965, Peries & Fernando 1966, Rajalakshmy *et al.* 1985, Erwin & Ribeiro 1996, Bai & Thomas 2000, Drenth & Guest 2004, Krishnan *et al.* 2019, Patil *et al.* 2022). Records of *P. meadii* from elsewhere (*cf*. Erwin & Ribeiro 1996, Drenth & Guest 2004) lack molecular verification and, hence, could be of other morphologically similar species (*e.g*. *P. insulinativitatica*, *P. mekongensis*, *P. multibullata*, *P. vietnamensis*, *P.* ×*australasiatica*, *P.* ×*taiwanensis* and *P.* ×*vanyenensis*).

Phytophthora colocasiae may be host-specific, causing the economically important taro (*Colocasia esculenta*) leaf blight. It is distributed from India throughout Southeast Asia and Papua New Guinea to Japan and Hawaii. Exclusive findings of A1 mating type isolates in India (Nath *et al.* 2013) and, in an early study, Hawaii (Ko 1979), and of A2 isolates in Taiwan, Vietnam, Papua New Guinea and several Pacific islands (Tyson & Fullerton 2007, Lin & Ko 2008, Shresta *et al.* 2014) and, in a recent study, also Hawaii (Ann *et al.* 1986) suggest that *P. colocasiae* is introduced in these regions, probably on plant material and adhering soil (Zentmyer 1988). Recently, Feng *et al.* (2022) reported self-sterile A1 or A2 mating type isolates and self-fertile A2 and A1A2 isolates from Japan but in a highly unbalanced ratio of 3:63:32:2. In contrast, Zhang *et al.* (1994) found a more balanced A1: A2: A0 (A0 = sterile) ratio of 49:36:15 in 280 *P. colocasiae* isolates sampled across Hainan Island, South China, and suggested Hainan and adjacent regions in Southeast Asia to be within the centre of origin of the species. This is supported by the isolation of *P. colocasiae* from leaf spots on wild taro plants growing in riparian lowland rainforest in Sumatra in the present study.

Phytophthora taxon meadii-like (isolate CBS 358.59, erroneously designated in the CBS collection as *P. palmivora*, in the WPC collection as *P. meadii* and at GenBank (accession no. MH760162 as *P. colocasiae*) was only isolated from *H. brasiliensis* in Sri Lanka.

Phytophthora botryosa, only known from and possibly native to Malaysia, Thailand and Vietnam where both mating types co-occur, poses a serious threat to the introduced *H. brasiliensis*, currently the only known host (Chee 1969, Erwin & Ribeiro 1996, Drenth & Guest 2004, Krishnan *et al.* 2019).

Phytophthora vietnamensis (previously *P.* taxon meadii-like 1) occurs in a montane *Alnus nepalensis* forest in the North of Vietnam, close to the border with China (Jung *et al.* 2020 and this study) and in a *Elettaria cardamomum* plantation in India (isolate WPC P6128 designated as *P. meadii* in Blair *et al.* 2008; see Fig. 2).

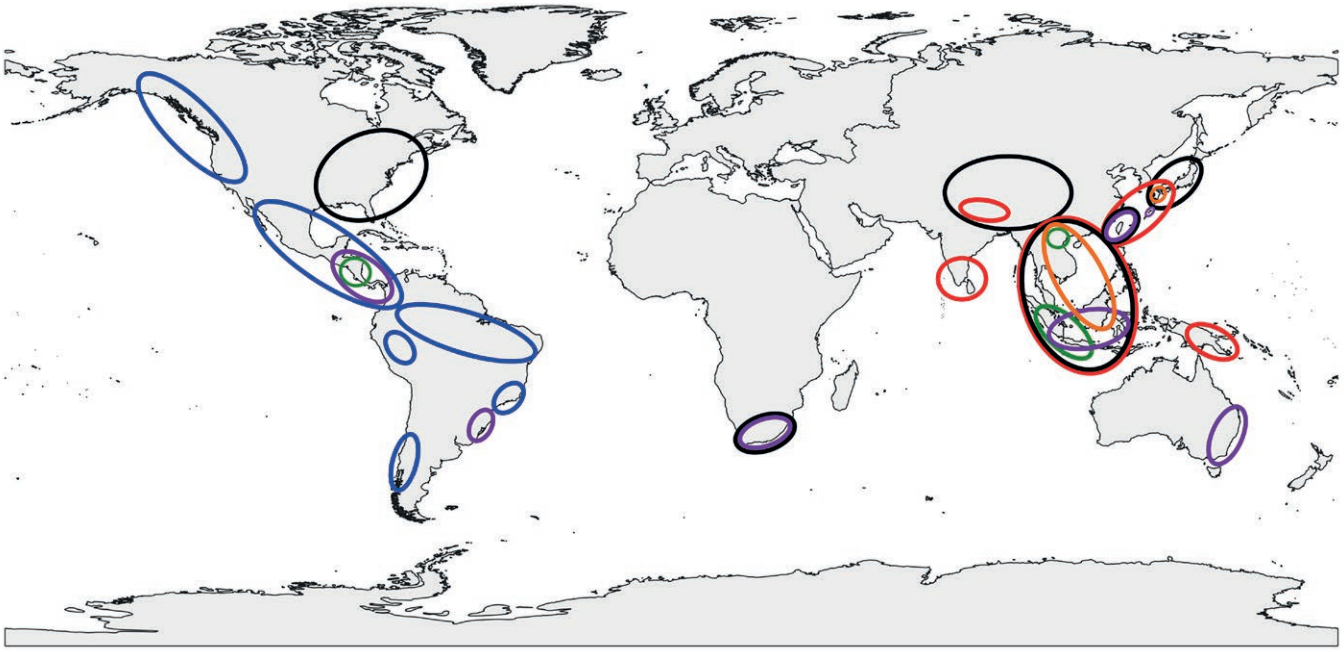

Fig. 78. Natural global biogeography of *Phytophthora* Clade 2. Colours indicate the subclades: Clade 2a = red; Clade 2b = blue; Clade 2c = black; Clade 2e = purple; Clade 2f = green; Clade 2g = orange.

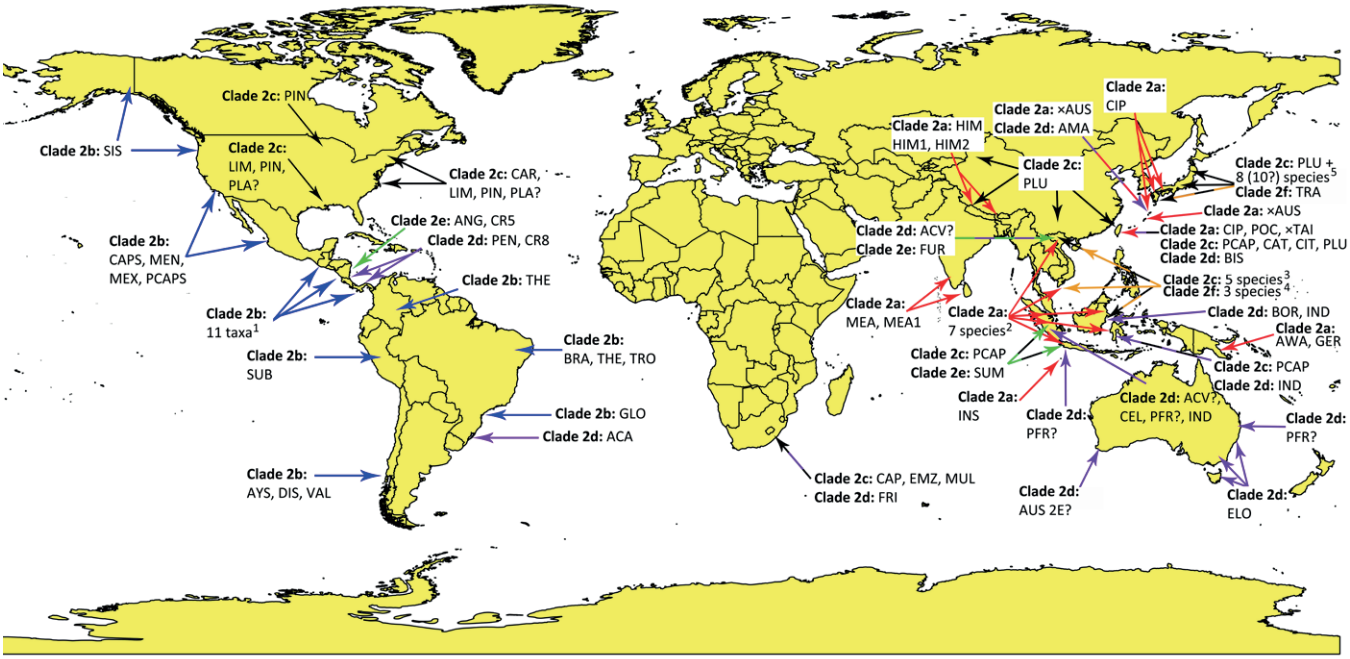

Fig. 79. Natural global biogeography of *Phytophthora* Clade 2. Colours of arrows indicate the subclades: Clade 2a = red; Clade 2b = blue; Clade 2c = black; Clade 2e = purple; Clade 2f = green; Clade 2g = orange. Species codes: ACA = *P. acaciae*; ACV = *P. acaciivora*; AMA = *P. amamensis*; ANG = *P. angustata*; AUS2E = *P.* taxon AUS 2E; AYS = *P. aysenensis*; BAL = *P. balkanensis*; BIS = *P. bishii*; BOR = *P. borneensis*; BRA = *P.* taxon brasiliensis; CAP = *P. capensis*; CAPS = *P. capsici*; CAR = *P. caryae*; CAT = *P. catenulata*; CEL = *P. celeris*; CIP = *P. citrophthora*; CIT = *P. citricola*; CR5 = *P.* taxon Costa Rica 5; CR8 = *P.* taxon Costa Rica 8; DIS = *P. distorta*; ELO = *P. elongata*; EMZ = *P. emzansi*; FRI = *P. frigida*; FUR = *P. furcata*; GLO = *P. gloveri*; HIM = *P. himalsilva*; HIM1 = *P.* taxon himalsilva-like 1; HIM2 = *P.* taxon himalsilva-like 2; IND = *P. indonesiensis*; INS = *P. insulinativitatica*; LIM = *P. limosa*; MEA = *P. meadii*; MEA1 = *P.* taxon meadii-like; MEN = *P. mengei*; MEX = *P. mexicana*; MUL = *P. multivora*; PCAP = *P. pseudocapensis*; PCAPS = *P.* taxon pseudocapsici; PEN = *P. penetrans*; PFR = *P. pseudofrigida*; PIN = *P. pini*; PLA = *P. platani*; PLU = *P. plurivora*; POC = *P. pseudoccultans*; SIS = *P. siskiyouensis*; SUB = *P.* taxon subnubulis; SUM = *P. sumatera*; THE = *P. theobromicola*; TRA = *P. transposita*; TRO = *P. tropicalis*; VAL = *P. valdiviana*; ×AUS = *P.* ×*australasiatica*; ×TAI = *P.* ×*taiwanensis*. Diversity hotspots: 1 = *P. calidophila*, *P. capsici*, *P. frigidophila*, *P. mengei*, *P. montana*, *P. multiplex*, *P. obovoidea*, *P. pyriformis*, *P. tropicalis*, *P. variepedicellata*, *P.* taxon mengei-like. 2 = *P. botryosa*, *P. colocasiae*, *P. mekongensis*, *P. multibullata*, *P. vietnamensis*, *P.* ×*australasiatica*, *P.* ×*vanyenensis*. 3 = *P. catenulata*, *P. fansipanensis*, *P. macroglobulosa*, *P. obturata*, *P. pseudocapensis*. 4 = *P. inclinata*, *P. multipapillata*, *P. proliferata*. 5 = *P. citricola*, *P. curvata*, *P. excentrica*, *P. falcata*, *P. japonensis*, *P. nimia*, *P. oblonga*, *P. vacuola* and most likely *P. acerina*, *P. balkanensis* and *P. pachypleura*.

Phytophthora mekongensis and *P. multibullata* are currently only known from plantations of *Citrus grandis* (*P. mekongensis*) and the introduced *Cinnamomum cassia* (both species) in Vietnam (Crous *et al.* 2017, Puglisi *et al.* 2017, Dang *et al.* 2021, this study), and it seems likely that they are native to the natural forests surrounding the affected plantations. For *P. multibullata* this is supported by the co-occurrence of both mating types in the affected plantations (Dang *et al.* 2021).

Phytophthora ×*vanyenensis*, which was first described from Vietnamese *C. cassia* plantations (Dang *et al.* 2021), and *P.* ×*australasiatica* overlap widely, being found so far from northern Vietnam to Java, Sumatra and Sulawesi. Both species co-occur at several sites in Indonesia. Their functional A1/A2 breeding systems, with both mating types present at several sites, suggest they are native to the region. In addition, *P.* ×*australasiatica* was found in native forests on Kalimantan, on the subtropical Amami and Okinawa islands in the Ryukyu Islands chain between Taiwan and southwest Japan, and in a tropical lowland rainforest in Panama. Since no other Clade 2a species has been found in our surveys in Panama and Nicaragua or - apart from the globally distributed *P. citrophthora* - elsewhere in Central or South America, *P.* ×*australasiatica* has probably been introduced from Asia to Panama.

Phytophthora insulinativitatica was described from a tropical rainforest on Christmas Island *ca*. 350 km south of Java and Sumatra (Dang *et al.* 2021), where the occurrence of both mating types (and its unique phylogenetic position within Clade 2a; Fig. 2) indicates it might be indigenous to this remote outpost. One isolate of *P. insulinativitatica* was recently obtained from a tiny coral island belonging to the remote Cocos Islands atoll in the Indian Ocean (Burgess *et al.* 2021), *ca*. 1 000 km west of Christmas Island and southwest of Java and Sumatra.

Phytophthora citrophthora was commonly isolated from numerous streams in native healthy forests on the subtropical Japanese islands of Kyushu, Amami and Okinawa and in Taiwan. Its centre of origin lays therefore most probably within the subtropical regions of East Asia. In contrast, in Europe, North and South America, South Africa and India *P. citrophthora* is considered an introduced invasive pathogen causing severe diseases of *Citrus* spp. and a wide range of other host plants in horticultural and ornamental nurseries and plantings (Rojic & Cancino 1975, MacDonald *et al.* 1994, Mchau & Coffey 1994, Erwin & Ribeiro 1996, Ferguson & Jeffers 1999, Themann *et al.* 2002, Schwingle *et al.* 2007, Alvarez *et al.* 2008, Donahoo & Lamour 2008a, Savita & Nagpal 2012, Moralejo *et al.* 2009, Pane *et al.* 2009, Salamone *et al.* 2011, Leonberger *et al.* 2013, Bienapfl & Balci 2014, Meitz-Hopkins *et al.* 2014, Parke *et al.* 2014, Prigigallo *et al.* 2015, Jung *et al.* 2016, Burgess *et al.* 2021, Mora-Sala *et al.* 2022). However, many previous records of *P. citrophthora* may be of the morphologically similar and closely related *P. pseudocitrophthora*.

Phytophthora pseudocitrophthora was discovered in this study on *Citrus limon* and a range of other host plants in nurseries and plantings in Europe and Morocco. It was isolated previously from a citrus tree in California (isolate WPC P10142, designated as *P. citrophthora*). It was also found in forest streams in Portugal, Louisiana and Connecticut (isolate NJB2013-HR-27; Brazee *et al.* 2016), USA, and in the rhizosphere of riparian *Platanus orientalis* in Sicily, possibly a result of ornamental and forest outplanting in the catchment areas. *Phytophthora pseudocitrophthora* was also isolated from soil in a remote, montane broadleaved forest in Nepal (isolate PCRh7-1; Vettraino *et al.* 2011), from *Prunus persica* in China (isolate WPC P3243) and from *Malus pumila* in South Korea (isolate CBS 111339) (see Table S1). It seems likely to be native to East Asia.

The only known isolates of *P.* ×*lusitanica* are from the Rio Séqua in the South of Portugal where its relatives *P. citrophthora* and *P. pseudocitrophthora* were also recovered. Since it is a hybrid with *P. citrophthora* as its maternal parent *P.* ×*lusitanica* was most likely introduced from East Asia.

Phytophthora himalsilva and *P.* taxon himalsilva-like 1 (previously *P. himalsilva* in Vettraino *et al.* 2011, and *P.* aff. himalsilva in Yang *et al.* 2017) are plausibly endemic to a remote area of western Nepal, occurring naturally in the rhizosphere of several tree species in healthy, mixed sub-tropical forests (Vettraino *et al.* 2011).

Phytophthora taxon himalsilva-like 2 (isolate NRCPh-97, designated as *P. citrophthora* in Das *et al.* 2016), a sister taxon of *P.* taxon himalsilva-like 1, was only recorded from a citrus nursery in East Sikkim, India close to Nepal.

Phytophthora pseudoccultans and *P.* ×*taiwanensis* are only known from rhizosphere soil and streams in healthy subtropical forests of Taiwan where they are most likely endemic.

Phytophthora occultans and *P. terminalis* are exclusively known as invasive pathogens in horticultural and ornamental nurseries and plantings in Europe and, in case of *P. occultans*, also in the USA (Reeser *et al.* 2012, Nechwatal *et al.* 2014, Man In't Veld *et al.* 2015, this study). Since their closest relatives *P. himalsilva*, *P. pseudoccultans*, *P.* taxon himalsilva-like 1 and *P.* taxon himalsilva-like 2 are native to South and Southeast Asia, it seems likely that *P. occultans* and *P. terminalis* also originate from these regions.

Phytophthora taxon awatangi and *P.* taxon germisporangia are only known from disturbed rainforests in Papua New Guinea (Dang *et al.* 2021).

Clade 2b taxa

Clade 2b now comprises 22 taxa, *i.e.*, nine known and nine new species and the undescribed *P.* taxon brasiliensis, *P.* taxon mengei-like, *P.* taxon pseudocapsici and *P.* taxon subnubulis, of which 21 taxa (95.5 %) are distributed in the Americas from Alaska to the Valdivian region in Chile.

Phytophthora siskiyouensis has the most northerly known distribution of all Clade 2 taxa and occurs commonly in forest streams in Alaska and Oregon occasionally causing bark cankers in *Alnus rubra* and *Notholithocarpus densiflorus* and shoot blight of *Umbellularia californica* (Reeser *et al.* 2007, 2011, Sims *et al.* 2015a, b). It is also associated with bark cankers and mortality of introduced European *Alnus glutinosa* trees in Victoria, Australia (Smith *et al.* 2006, Burgess *et al.* 2021) and planted riparian *Alnus incana* trees in the UK (Pérez-Sierra *et al.* 2015), in both cases certainly introduced.

Phytophthora mengei is distributed from California to Guatemala causing root rot and bark cankers on cultivated avocado (*Persea americana*) with high disease incidences since the early 20th Century (Hong *et al.* 2009, Bezuidenhout *et al.* 2010). It has only once been recorded from another continent and another host species, *i.e.*, from *Vigna unguiculata* in Queensland, Australia (ITS GenBank accession no. GU258661.1; erroneously submitted as *P. siskiyouensis*; Burgess *et al.* 2021). It is therefore most probably endemic to Central America, perhaps as a relatively benign pathogen on coevolved wild avocados and other neotropical *Persea* species. This is supported by the probably endemic co-occurrence of its closest relative, *P. montana*, and two other new Clade 2b species, *P. frigidophila* and *P. variepedicellata*, in a remote natural cloud forest near the peak of the Barú Volcano in Panama.

All three species were exclusively found in naturally fallen tree leaves of this cloud forest together with the recently described aerial oomycete *Synchrospora medusiformis* (Jung *et al.* 2023) and a yet undescribed aerial *Phytophthora* species from Clade 8 (Y. Balci, K. Broders & T. Jung unpublished results) which is related to the undescribed *Phytophthora madida nom. prov*. recently found in Chile (Jung *et al.* 2018b).

Phytophthora taxon mengei-like, which grouped in the multigene phylogeny in a basal position to the sister species *P. mengei* and *P. montana*, is another avocado pathogen only known from Guatemala (isolate WPC P1165; Bezuidenhout *et al.* 2010) where it is most likely endemic.

Phytophthora calidophila was obtained only from a montane rainforest in Nicaragua where it co-occurred with *P. obovoidea*. The latter species is widespread in both montane and lowland rainforests across Nicaragua and Panama and was also found scattered in Java, Sulawesi, Taiwan and Vietnam. The co-occurrence of both mating types in the same stands and high genetic variability indicates that Nicaragua and Panama may lie within the origin of *P. obovoidea*, whereas all isolates from Southeast Asia were clonal (Fig. 3) and exclusively A1s.

Phytophthora tropicalis, the sister species of *P. obovoidea*, is a globally distributed, often damaging pathogen with a wide host range including many tropical crops and ornamentals (Aragaki & Uchida 2001, Gerlach & Schubert 2001, Drenth & Guest 2004, Cerqueira *et al.* 2006, Leahy 2006, Pane *et al.* 2009, Uchida & Kadooka 2013, Jung *et al.* 2016, Luongo *et al.* 2016, Chávez-Ramírez *et al.* 2021). Under its previous designation as *P. capsici* electrophoretic type CAP2, *P. tropicalis* was shown to cause pod rot of cocoa in the Americas, whereas in tropical regions of Africa and Asia the disease is mainly caused by *P. megakarya*, *P. palmivora* and occasionally other *Phytophthora* species (Brasier and Griffith 1979, Mchau & Coffey 1995, Aragaki & Uchida 2001, McMahon & Purwantara 2004; Chávez-Ramírez *et al.* 2021). In the present surveys, both mating types of *P. tropicalis* were common in tropical rainforests in Nicaragua and Panama, sometimes co-occurring with its closest relative *P. obovoidea.* From this and its widespread distribution across Central and South America *P. tropicalis* is most likely native to this region and has spread with imported tropical crops and ornamentals to other continents. Before being formally described by Aragaki & Uchida (2001) *P. tropicalis* isolates were commonly identified as *P. capsici* and even now many sequences submitted to GenBank as *P. capsici* are of *P. tropicalis* (see appendix S3 in Burgess *et al.* 2021).

In contrast to *P. obovoidea* and *P. tropicalis*, their closest known relative *P. pyriformis* appears to have a limited distribution and has only been recovered, together with *P. obovoidea*, from one lowland rainforest in Panama.

Phytophthora capsici is a harmful pathogen with global distribution in agricultural zones and a wide host range of mainly non-woody host plants (Mchau & Coffey 1995, Erwin & Ribeiro 1996, Drenth & Guest 2004, Roberts *et al.* 2005, Truong *et al.* 2010, Granke *et al.* 2012, Sanogo & Bosland 2013, Enzenbacher *et al.* 2015, Kong *et al.* 2022, Quesada-Ocampo *et al.* 2023, Sanogo *et al.* 2023). A potential origin of *P. capsici* within Central America and the southern USA is indicated by its particularly wide host range among *Fabaceae*, *Cucurbitaceae* and *Solanaceae* species native to Central America; its wide distribution in Central America and the southern USA, where it was first described from *Capsicum annuum* in New Mexico by Leonian in 1922; the fact that it has never been recovered in any of the numerous *Phytophthora* surveys of natural streams and forests across Europe, Asia, Australia and South Africa (Jung *et al.* 1996, 2013a, 2017b, 2019, 2020, Oh *et al.* 2013, Dunstan *et al.* 2016, O'Hanlon *et al.* 2016, Burgess *et al.* 2017, 2021, Corcobado *et al.* 2020, 2023, Seddaiu *et al.* 2020); the frequent occurrence of both mating types in the same horticultural field; and the probable geographic origin of many Clade 2b relatives in Central America.

Phytophthora mexicana, first described in 1923 as a pathogen of tomato (*Solanum lycopersicum*) fruits in Mexico (Erwin & Ribeiro 1996), is a cryptic species with only two known living isolates in culture collections (WOC P646 = CBS 554.88 = ATCC 46731 = IMI 92550 = CPHST BL 24 from Mexico and ex-epitype CBS 149405 = CPHST BL 199 = French Ph213 = S972 from the USA; Abad *et al.* 2023a, Table S1). However, in the multigene phylogenetic analyses of this study, several other isolates previously designated as *P. capsici* (CBS 121656, WPC P1314, CPV302; Table S1) or *P.* aff. *capsici* (ATCC 15427; Yang *et al.* 2017), all originating from Mexico or the USA, grouped with *P. mexicana* (Fig. 3). An origin of *P. mexicana* in Mexico and the southern USA is most likely.

Several isolates obtained in the present study from naturally fallen leaves in three streams running through agricultural areas in Sumatra and isolate CBS 370.72 from New Mexico, previously designated as *P. capsici* (Yang *et al.* 2017), grouped in our multigene phylogeny together separately from *P. capsici* and *P. mexicana* (Fig. 3) and were, hence, designated as *P.* taxon pseudocapsici. Although an origin in Southeast Asia cannot be ruled out, it seems more likely that *P.* taxon pseudocapsici, like its close relatives *P. capsici* and *P. mexicana*, is native to Central America and the southern USA.

Phytophthora multiplex, a new probable hybrid species with *P. theobromicola* as maternal parent, was found widespread in tropical lowland rainforests in Nicaragua and Panama and was also recorded from Costa Rica (isolate WPC P10417; Fig. 3). Along with many other Clade 2b taxa it is probably endemic to Central America.

The recently described *P. theobromicola*, in the past erroneously identified as *P. citrophthora* (Mchau & Coffey 1994), is currently known only for causing black pod disease of cocoa in Brazil (Decloquement *et al.* 2021) and Colombia (Ramírez Martínez *et al.* 2021; Table S1).

The currently undescribed *P.* taxon brasiliensis, previously known as *P. capsici* isozyme group CAP3 and electrophoretic type ET26 (Mchau & Coffey 1995), and sometimes designated as *Phytophthora cf. capsici* FM-2011, is frequently associated with pod rot of cocoa in Brazil (*e.g.* WPC isolates P0622, P0630, P15128 and P15130; isolate LT29; isolate Cp-1 designated as *P. capsici* by Bowers *et al.* 2007; see Table S1) and was also found in the rhizosphere of the native Brazilian tree *Caesalpinia echinata* (isolate WPC P6907). Its phylogenetic position as basal taxon of a cluster comprising *P. frigidophila* from Panama and three Chilean species, *i.e.*, *P. aysenensis*, *P. distorta* and *P. valdiviana* (Fig. 3), supports an origin of *P.* taxon brasiliensis in Brazil.

Phytophthora gloveri, is exclusively known as the causal agent of root rot and stunting of the introduced Virginian tobacco (*Nicotiana tabacum*) in southeastern Brazil (Abad *et al.* 2011) where it is most likely endemic thriving on native South American tobacco species.

Phytophthora taxon subnubulis (isolate L5395) was isolated in 2008 from *Capsicum pubescens* in the montane Oxapampa region of Peru (Hu *et al.* 2020, Winkworth *et al.* 2022) where it is most likely endemic.

Phytophthora aysenensis (Crous *et al.* 2020), *P. distorta* and *P. valdiviana* have all been found exclusively in the cool-temperate

Aysen and Valdivia regions in southern Chile where they are endemic.

Phytophthora amaranthi is the only known Clade 2b species that has not been recorded from the Americas. Appearing suddenly in 2007 in central Taiwan and subsequently spreading rapidly through the entire production area of the native Asian edible amaranth (*Amaranthus tricolor*) resulting in substantial economic losses, *P. amaranthi* appears to be a typical exotic, introduced pathogen (Ann *et al.* 2016). Since many species of the cosmopolitan genus *Amaranthus* are native to North, Central and South America, it seems probable that *P. amaranthi*, like its closest relatives *P. capsici*, *P. gloveri* and *P. mexicana*, originates from the Americas.

Clade 2c taxa

With nine known and 15 new species, Clade 2c is currently the largest of the seven subclades.

Phytophthora multivora is widely distributed in Australia, where it was first described, and in South Africa and Europe. It has also been reported from the Canary Islands, North America and New Zealand, but only once from Asia on nursery stock in Japan (Scott *et al.* 2009, Hansen *et al.* 2012, Hüberli *et al.* 2013, Mrázková *et al.* 2013, Szabó *et al.* 2013, Bienapfl & Balci 2014, Scott & Williams 2014, Puno *et al.* 2015, Rahman *et al.* 2015, Scarlett *et al.* 2015, Jung *et al.* 2016, Burgess *et al.* 2017, 2021, Garbelotto *et al.* 2018, Rodríguez-Padrón *et al.* 2018, Migliorini *et al.* 2019, Rooney-Latham *et al.* 2019, Sims & Garbelotto 2021). Considered to be in equilibrium with the native flora in South Africa (Oh *et al.* 2013, Tsykun *et al.* 2022), *P. multivora* is an emerging aggressive pathogen with a particularly wide host range elsewhere (Scott *et al.* 2009, 2012, Mrázková *et al.* 2013, Szabó *et al.* 2013, Bienapfl & Balci 2014, Migliorini *et al.* 2019, Jung *et al.* 2016, Garbelotto *et al.* 2018, Rodríguez-Padrón *et al.* 2018, Rooney-Latham *et al.* 2019, Sims & Garbelotto 2021). A recent analysis of a global population sample of *P. multivora* confirmed South Africa as its centre of origin (Tsykun *et al.* 2022).

Phytophthora capensis and *P. emzansi* were first described from South Africa (Bezuidenhout *et al.* 2010, Bose *et al.* 2021a). *Phytophthora emzansi* is exclusively known from South Africa where it was isolated independently in the Western Cape Province from plantations of the endemic shrub *Agathosma betulina* (Bezuidenhout *et al.* 2010); from Eerste River and the rhizosphere of the native tree *Afrocarpus falcata* in the afrotemperate Knysna Forest, and *Podocarpus elongata* in Kirstenbosch National Botanical Garden (Bose *et al.* 2021a); and in the province KwaZulu-Natal from soil samples in the Ingeli Forest (Oh *et al.* 2013). Its distinct position in the phylogenetic analyses with *P. capensis* as next - though distant - relative (Fig. 4) and its exclusively amphigynous antheria, unique within Clade 2c, indicate long-term isolated evolution of *P. emzansi*, further supporting an origin in South Africa. *Phytophthora capensis* was isolated from the cultivated endemic shrubs *Olea capensis* and *Curtisia dentate* in the Western Cape Province and was later found in soil samples and streams of two forests and a botanical garden in Eastern Cape Province and KwaZulu-Natal (Bezuidenhout *et al.* 2010, Oh *et al.* 2013). This distribution, long-term isolation indicated by a particularly long branch length in the multigene phylogeny (Fig. 4) and lack of any records from elsewhere suggest that *P. capensis* is native to South Africa.

In contrast, its sister species, *P. pseudocapensis*, has a wide distribution in natural montane forest streams in Java, Sumatra, Sulawesi (this study) and Vietnam (Jung *et al.* 2020, designated as *P. capensis*) and submontane streams in Taiwan (Jung *et al.* 2017c, designated as *P. capensis*) with high genetic variability within and between different populations (Fig. 4) suggesting Southeast Asia as the taxons' centre of origin.

Phytophthora plurivora is almost exclusively known from the Northern Hemisphere where it has the widest distribution of all Clade 2c species commonly occurring in natural ecosystems, nurseries and planting sites across Europe and also reported from many natural ecosystems, nurseries and restoration sites in North America (Jung 2009, Jung & Burgess 2009, Nechwatal *et al.* 2011, Orlikowski *et al.* 2011, Reeser *et al.* 2011, Hansen *et al.* 2012, Milenković *et al.* 2012, Jung *et al.* 2013a, 2016, 2018a, 2019, Mrázková *et al.* 2013, Szabó *et al.* 2013, Bienapfl & Balci 2014, Jankowiak *et al.* 2014, Brazee *et al.* 2016, Parke *et al.* 2014, O'Hanlon *et al.* 2016, Rooney-Latham *et al.* 2019, Corcobado *et al.* 2020, Frankel *et al.* 2020, Matsiakh *et al.* 2020, Seddaiu & Linaldeddu 2020, Seddaiu *et al.* 2020, Rossmann *et al.* 2021, Mora-Sala *et al.* 2022). There are currently only four records from the Southern Hemisphere, from the Valdivia River in Chile (Jung *et al.* 2018b), from soil of an *Austrocedrus chilensis* forest in Patagonia, Argentina (Vélez *et al.* 2020), from *Juglans regia* in New Zealand (isolate WPC P10679 = ICMP 14152 = NZFS 2671; Table S1) and from the rhizosphere of a non-native *Quercus robur* tree in the Blue Mountains Botanic Garden in New South Wales, Australia (Laurence *et al.* 2023). From a microsatellite study of exclusively European and North American isolates, Schöbel *et al.* (2014) suggested a European origin for *P. plurivora*. However, in both Europe and North America *P. plurivora* clearly behaves as an introduced aggressive pathogen, with a particularly wide host range in native plant species causing severe root rot, bark cankers and mortality in nurseries, out-plantings and natural forests and acting as one of the main drivers of current oak and beech declines across Europe (Jung 2009, Jung & Burgess 2009, Nechwatal *et al.* 2011, Orlikowski *et al.* 2011, Milenković *et al.* 2012, Jung *et al.* 2013a, 2016, 2018a, 2019, Mrázková *et al.* 2013, Szabó *et al.* 2013, Bienapfl & Balci 2014, Jankowiak *et al.* 2014, Corcobado *et al.* 2020, Frankel *et al.* 2020, Linaldeddu *et al.* 2020, Seddaiu & Linaldeddu 2020, Seddaiu *et al.* 2020, Mora-Sala *et al.* 2022). Over the past decade *P. plurivora* has been recovered from soil around multiple hardwood tree genera in healthy, natural temperate forests in a remote region of western Nepal (Vettraino *et al.* 2011), and in Yunnan and Taiwan (Huai *et al.* 2013, Jung *et al.* 2017c). It has also been obtained, together with the introduced *P. cactorum* and eight other *Phytophthora* spp., from declining *Malus sieversii* forests in the temperate Tian Shan mountains in Xinjiang, Northwest China (Liu *et al.* 2018, Xu *et al.* 2019). Further, our recent surveys demonstrated an almost ubiquitous distribution of *P. plurivora* in native forests and streams across the Japanese main island of Honshu without any evident association with disease symptoms in the native vegetation. These recent observations form a strong argument for long-term coevolution between *P. plurivora* and the Asian flora, and hence an origin for *P. plurivora* in temperate Asia.

Phytophthora curvata, *P. excentrica*, *P. falcata*, *P. japonensis*, *P. nimia*, *P. oblonga* and *P. vacuola* are seven new endemic Clade 2c species found in the present study in the rhizosphere and streams of native healthy forests across three main islands of Japan, *i.e.*, Honshu, Shikoku and Kyushu. While *P. falcata* occurred on all three islands, other species were found on two (*P. japonensis*, *P. nimia*) or only one island (*P. curvata*, *P. excentrica*, *P. oblonga*, *P. vacuola*). The comparatively small island of Shikoku (*ca*. 18 000 km^2) showed the highest Clade 2c diversity, with six new species detected.

Located in a transitional zone between Southeast Asia and East Asia, Taiwan not only shares the occurrence of *P. citricola* and *P. plurivora* with Japan (Erwin & Ribeiro 1996, Jung & Burgess

2009, Jung *et al.* 2017c) but also the new Clade 2c species *P. pseudocapensis* and *P. catenulata* (previously *P. citricola* VII) with Vietnam (Jung *et al.* 2017c, 2020, this study).

Phytophthora fansipanensis and *P. obturata* are two new endemic Clade 2c species with apparently local vicariant distributions in Vietnam. *Phytophthora fansipanensis* was found in cloud forests on the Fansipan Mountain close to the border with Yunnan, China; *P. obturata* in a subtropical evergreen submontane forest in Ba Vì National Park near Hanoi and a montane *Chamaecyparis* forest on Sau Chua Mountain near Sapa (Jung *et al.* 2020, this study).

Phytophthora macroglobulosa is currently known only from a tropical montane forest on Hainan Island (under its previous designation as *P. citricola*; Zeng *et al.* 2009) which is also located on the Asian continental shelf and, hence, was connected to Vietnam during the Pleistocene where its sister species *P. obturata* thrives in *ca*. 400 km distance in Ba Vì National Park.

Another five Clade 2c species have been recorded in Europe in addition to the introduced *P. multivora* and *P. plurivora*. *Phytophthora acerina* was first described as causing bark cankers, dieback and mortality on native *Acer pseudoplatanus* trees in a managed forest in Northwestern Italy (Ginetti *et al.* 2014). The pathogen has subsequently been found associated with declining riparian *Alnus glutinosa* trees in Sardinia (Seddaiu & Linaldeddu 2020), with root rot and sudden death of olive trees in Northeastern Italy (Linaldeddu *et al.* 2020) and with declining *Quercus suber* trees in a botanical garden in Northern Italy (T. Jung & M. Horta Jung unpubl. results). Due to its high aggressiveness to several major European tree species and its sudden appearance in different regions of Italy *P. acerina* is most likely a recent introduction to Europe. ITS-based records from a stream in Tennessee in 2010 (designated as *P. citricola*; GenBank accession no. MF959536.1) and in 2015 from rhizosphere soil of *Populus fremontii* in California (GenBank accession no. MG707815.1) indicate a scattered distribution in the USA. In New South Wales, Australia, *P. acerina* was isolated in 2017 from a non-native horticultural *Prunus dulcis* tree (isolate VPRI 44117; Burgess *et al.* 2021). The oldest known record of *P. acerina* from 2003 also came from a non-native horticultural *Prunus persica* tree in Taiwan (GenBank ITS accession no. GU111596.1; submitted as *P. citricola*), indicating pathogen spread via the international nursery trade. Since *P. acerina* was recently reported to cause root and collar rot, decline and mortality of native *Metasequoia glyptostroboides* trees in Central China (Liu *et al.* 2022) an origin somewhere in East Asia seems likely.

Phytophthora balkanensis, previously informally designated *P. citricola* E (Jung & Burgess 2009) and as isozyme subgroup and electrophoretic type CIT2-4 (Oudemans *et al.* 1994) was first isolated in 1986 from horticultural *Rubus idaeus* plants in Ireland (Jung & Burgess 2009) and later from nursery stock in Italy (Prigigallo *et al.* 2015) and Croatia (this study). It was also recovered in the present study from soil and streams of beech, oak and alder forests in Bosnia-Herzegovina and Serbia. Outside Europe there are only two known records of *P. balkanensis,* from *R. idaeus* and irrigation water in California (isolates WPC P1321 = ATCC 64809, P1803, P1804) and from *Fragaria* sp. in Taiwan (isolates WPC P6624 = ATCC 66621, P6625, P6627) (Oudemans *et al.* 1994, Bezuidenhout *et al.* 2010, Brazee *et al.* 2017). With a close phylogenetic relationship *P. acerina* and *P. balkanensis* have probably evolved in the same biogeographic region, most likely in East Asia along with their relatives *P. plurivora* and *P. curvata* (Fig. 4).

Phytophthora pachypleura and *P. platani*, are currently known exclusively from Europe. *Phytophthora pachypleura* is plausibly a recently introduced pathogen spreading within the European nursery trade on its only known host *Aucuba japonica* (Henricot *et al.* 2014, Ginetti *et al.* 2015). In our phylogenetic analyses, it formed together with the Japanese *P. falcata* one of three closely related East and Southeast Asian clusters and, hence, is certainly originating in this region.

Phytophthora platani was first isolated in 2013 from the rhizosphere of healthy *Platanus orientalis* trees in two natural riparian forests in Sicily, Italy. More recently it was found causing root rot and aerial bark cankers of a mature *Platanus* × *acerifolia* tree in London, UK, to which it was also pathogenic on inoculation (A. Pérez-Sierra and T. Jung, unpublished results). Whether *P. platani* is specific to *Platanus* trees remains, however, unknown. Its close phylogenetic relationship to a cluster of three species with probable North American origin, *i.e.*, *P. caryae*, *P. limosa* and *P. pini*, indicates that *P. platani* may be also native to North America which, coincidentally, harbours seven endemic *Platanus* species.

Phytophthora pini, first described by Leonian (1925) from roots of *Pinus resinosa* in Minnesota, is widely distributed in nurseries, plantings, streams, forests and agricultural run-off areas across the USA (Ghimire *et al.* 2011, Hong *et al.* 2011, Reeser *et al.* 2011, Bienapfl & Balci 2014, Knaus *et al.* 2015, Sims *et al.* 2015b, Brazee *et al.* 2016, 2017, Yang & Hong 2016, Rooney-Latham *et al.* 2019). It is also being spread widely on ornamental *Rhododendron* and conifer nursery stock in the USA (Hong *et al.* 2011, Knaus *et al.* 2015) and Europe (Lilja *et al.* 2011, Jung *et al.* 2016). Like *P. balkanensis, P. pini* also has a scattered distribution in nursery outplantings in Europe (Lilja *et al.* 2011, Jung *et al.* 2016, this study) and in semi-natural ecosystems in the Balkans where it has been found in forest streams and the rhizosphere of riparian poplar plantations (Milenković *et al.* 2018) and a *Fraxinus angustifolia* tree (this study) in Serbia; and in forest streams and the rhizosphere of riparian *Alnus glutinosa* trees in Bosnia-Herzegovina (this study). Recently it was recorded from *Rhododendron pulchrum* plants in Nanjing, China (Xu *et al.* 2021). Since its sister species *P. limosa* (including the informally designated *P.* taxon *citricola* III and *P. citricola* taxon 22F3; Hong *et al.* 2011, Brazee *et al.* 2017, Yang *et al.* 2017) has so far been found mainly in forests and waterbodies in the USA it seems likely that both species are native to North America. Indeed, the high aggressiveness of *P. pini* and *P. limosa* (as *P. citricola* III) to the common European beech tree, *Fagus sylvatica*, planted as an ornamental in North American parks and in pathogenicity tests (Jung *et al.* 2005, Weiland *et al.* 2010, Kenaley *et al.* 2014), is a strong argument against a European origin of both these pathogens.

Phytophthora caryae was first described from streams in the eastern USA (Brazee *et al.* 2017). Its basal position to *P. limosa* and *P. pini* in the multigene phylogeny of this study (Fig. 4) supports a North American origin of *P. caryae*. The only other reports of *P. caryae* to date are metagenomic records from two forests of *Nothofagus pumilio* and *A. chilensis* in Patagonia (Vélez *et al.* 2020).

Clade 2d

The only known member of this subclade, *P. oleae*, is exclusively known from one olive tree plantation in southern Italy where it appeared suddenly in 2015 causing excessive fruit rot (Ruano-Rosa *et al.* 2018). This strongly suggests a recent introduction. The origin of *P. oleae* and, hence, of Clade 2d remains unknown.

Clade 2e taxa

Clade 2e now comprises the five previously known species *P. acaciae*, *P. acaciivora*, *P. bishii*, *P. elongata* and *P. frigida*, six new

species, *P. amamensis*, *P. borneensis*, *P. celeris*, *P. indonesiensis*, *P. penetrans* and *P. pseudofrigida*, and the informally designated *P.* taxon pseudobisheria, *P.* taxon AUS 2E and *P.* taxon Costa Rica 8.

Phytophthora acaciae, *P. acaciivora* and *P. frigida* were all first described from plantations of exotic *Acacia* and eucalypt species suggesting their spread via the international nursery trade: *P. acaciae* in Brazil recorded from *Acacia mearnsii* native to southeastern Australia (Albuquerque Alves *et al.* 2019); *P. acaciivora* in Vietnam from *A. mangium* native to Maluku, New Guinea and northeastern Queensland (Burgess *et al.* 2020); and *P. frigida* in Brazil from *A. mearnsii* (Albuquerque Alves *et al.* 2016; Dos Santos 2016) and in South Africa both from *A. decurrens*, native to eastern New South Wales and *Eucalyptus smithii* native to southeastern Australia (Maseko *et al.* 2007).

However, while *P. acaciae* may have been introduced to Brazil on *A. mearnsii*, there are currently no records of it from elsewhere, and the co-occurrence of both mating types in Brazil indicates that *P. acaciae* might be indigenous to the area, naturally associated with native neotropical plant species *e.g.*, from the *Acacieae* genera *Acaciella* or *Mariosousa*. The discovery of the new Clade 2e species *P. penetrans* in a healthy tropical lowland rainforest in Panama and the occurrence of its closest relative, the undescribed *P.* taxon Costa Rica 8, in a rainforest in Costa Rica (ITS GenBank accession no. KC479193), increase the possibility of a neotropical origin for *P. acaciae*.

Phytophthora frigida has also been recovered from a stream in Sicily, Italy (Jung *et al.* 2019) where it was certainly introduced. Burgess *et al.* (2017, 2021) considered *P. frigida* native to Australia based on metagenomic records from soil samples in New South Wales and Western Australia (Burgess *et al.* 2017) and on isolations from native forest soils in Queensland and New South Wales (Scarlett *et al.* 2015, Burgess *et al.* 2021). However, isolate W1731 from New South Wales resided in the multigene phylogeny of this study within *P. pseudofrigida* casting doubt on the presence of *P. frigida* in Eastern Australia. Therefore, it seems more likely that *P. frigida* is native to South Africa which is also supported by its wide distribution in both commercial and native forests, the presence of both mating types and the aggressiveness to the non-native trees *A. decurrens* and *E. smithii* (Maseko *et al.* 2007, Bose *et al.* 2018, 2021b).

The recoveries in the present study of *P. pseudofrigida* from four natural streams running through a tropical hill rainforest in Western Sumatra, a montane rainforest in Northern Sumatra and two montane rainforests in Western Java suggest an origin of this new species in Sundaland. This is further supported by the co-occurrence of another new Clade 2e species, *P. indonesiensis*, in the rhizosphere of the same hill rainforest in Western Sumatra where *P. pseudofrigida* was isolated from a forest stream. Also, by our detection of the close relative of *P. pseudofrigida*, *P. acaciivora*, and another new Clade 2e species, *P. celeris*, in the effluents of an *A. crassicarpa* and eucalypt nursery in Central Sumatra established on a site previously inhabited by a natural lowland rainforest. However, the possibility of an Eastern Australian origin of *P. pseudofrigida* cannot be excluded. Since all isolates from Indonesia and the isolate from New South Wales belonged to the A1 mating type further surveys are needed to find the A2 mating type and clarify the centre of origin. *Phytophthora indonesiensis* also occurred in the rhizosphere of a montane tropical rainforest in Sulawesi and a stream running through a lowland rainforest in Northeast Kalimantan. In our multigene phylogeny, the populations from the three Indonesian islands grouped separately with the Kalimantan isolates being basal to the isolates from Sumatra and Sulawesi indicating local evolution and adaptation. This is supported by the considerably lower optimum growth temperature of the montane Sulawesi isolates (Fig. 62). Another new Clade 2e species from Indonesia, *P. borneensis*, was found only in the rhizosphere of a lowland rainforest in East Kalimantan.

Phytophthora bishii thrives on species of *Rosaceae* in the global plant trade: on *Fragaria* × *ananassa* in the USA; *Rosa* sp. in the Netherlands; *Rubus idaeus* in Australia (Abad *et al.* 2008) and Spain (ITS GenBank accession nos. MN134587.1 and MN549026.1). The findings of *P. bishii* on the Southeast Asian *Zingiberaceae* species *Etlingera elatior* planted in Brazil (ITS GenBank accession no. JF917303.1) and in the rhizosphere of a remote, montane natural *Chamaecyparis obtusa* forest in Taiwan (Brasier *et al.* 2010) and its close phylogenetic relationship to *P. borneensis* (Fig. 4) suggest a Southeast or East Asian origin. The informally designated *P.* taxon pseudobisheria is only known from ornamental plants of *Rhododendron* and the North American *Rhus aromatica* in North Carolina and Pennsylvania, respectively (Yang *et al.* 2017; Table S1), and its origin remains unknown although its close relationship to *P. celeris* (Fig. 4) suggests it might be native to Southeast Asia, too.

The new species *P. amamensis*, sister species to *P. indonesiensis* (Fig. 4), has to date been found only in a subtropical monsoon forest on Amami Island in the Ryukyu archipelago, Japan (this study), which suggests that this species may have an East Asian origin.

Phytophthora penetrans is currently only known from a natural, healthy lowland rainforest in Panama suggesting it might be native there and possibly elsewhere in Central America. This is supported by the occurrence of another Clade 2e taxon, the informally designated *P.* taxon Costa Rica 8 (ITS GenBank accession no. KC479193), in a tropical rainforest of the neighboring country Costa Rica.

Phytophthora elongata was first described in Western Australia where it was introduced through mine site rehabilitation plantings. It subsequently spread as an aggressive invasive pathogen on a range of native woody plants and along riparian corridors (Rea *et al.* 2010, Jung *et al.* 2018a). Based on metabarcoding and isolation records from soils of healthy natural ecosystems in New South Wales, Victoria and Tasmania (Dunstan *et al.* 2016, Burgess *et al.* 2017, 2021), an origin of *P. elongata* in Southeastern Australia has been proposed (Burgess *et al.* 2017, 2021). There are only two records of *P. elongata* outside of Australia, as an introduced pathogen on ornamental *Buxus*, *Ilex* and *Rhododendron* in nurseries in Maryland, USA (Bienapfl & Balci 2014) and from natural mangrove leaf litter in a coastal area of the Philippines (Bennett *et al.* 2017). Further surveys of ecosystems across Southeast Asia and Southeastern Australia are needed to clarify its origin. A close relative of *P. elongata*, the undescribed *P.* taxon AUS 2E (previously *P.* taxon elongata-like; Rea *et al.* 2010), has also been found widespread in Western Australia where it might be endemic (Burgess *et al.* 2021).

Clade 2f taxa

Currently, Clade 2f comprises *P. multivesiculata*, the informally designated *P.* taxon aquatilis and *P.* taxon Costa Rica 5, and the three new species *P. angustata*, *P. furcata* and *P. sumatera*.

Phytophthora multivesiculata was first described as causing necroses on stem bases and leaves of *Cymbidium* orchids in the Netherlands (Ilieva *et al.* 1998), and was subsequently isolated from *Cymbidium* plants in New Zealand (Hill 2004), Vietnam (ITS GenBank accession no. DQ835678.1, submitted in 2006; Chern *et al.* 2011), New South Wales (Cunnington *et al.* 2009), Taiwan

(Chern *et al.* 2011) and Hawaii (ITS GenBank accession no. GU258925.1; isolate WPC-P7254), and from *Cymbidium* species and hybrids and the indigenous orchid *Ansellia africana* in South Africa (Bose & Hammerbacher 2023). This is consistent with its being spread very effectively via the international orchid trade. Its hosts and lack of sporangial caducity suggest a co-evolution with the terrestrial (rather than the epiphytic) *Cymbidium* species native to subtropical or tropical montane forests in South and Southeast Asia.

An Asian origin for *P. multivesiculata* is further supported by the natural distributions of its phylogenetic relatives *P. furcata*, exclusively found in a stream and rhizosphere soil of a cloud forest at the Fansipan Mountain in the North of Vietnam; and *P. sumatera* which occurs commonly in streams and rhizosphere soil of montane and lowland rainforests in Northern and Western Sumatra and Java.

Phytophthora angustata was only found in a tropical lower montane rainforest at the Mombacho Volcano in Nicaragua, where it is most probably endemic. Interestingly, the undescribed *P.* taxon Costa Rica 5, for which only an ITS sequence is available (ITS GenBank accession KC479200), was detected in a lowland rainforest of the neighboring country Costa Rica.

Phytophthora taxon aquatilis is currently known only from a single isolate obtained from a stream in Virginia, USA. Its origin remains unknown (Hong *et al.* 2012). However, since the three Clade 2f species with a probable origin in Asia, *P. furcata*, *P. multivesiculata* and *P. sumatera*, produce almost exclusively amphigynous antheridia whereas the antheridia in *P. angustata* and *P.* taxon aquatilis are almost exclusively paragynous (Hong *et al.* 2012), an origin for *P.* taxon aquatilis in Central or North America seems more likely.

Clade 2g taxa

Comprising four new species from Southeast and East Asia the new Clade 2g is currently the second-smallest of the subclades. *Phytophthora proliferata* and *P. inclinata* thrive in the rhizosphere of healthy tropical lowland rainforests in the Vietnamese Cuc Phuong National Park and on Côn Lôn island situated 50 km off the Vietnamese coast on the Asian continental shelf, respectively (Jung *et al.* 2020, this study).

Phytophthora multipapillata has only been recovered from two healthy tropical lowland rainforest sites in East Kalimantan. In the multigene phylogenetic analyses, the two populations grouped separately suggesting potential local evolution and adaptation. Despite extensive surveys, *P. multipapillata* could not be obtained from the adjacent islands of Java, Sumatra and Sulawesi and could, hence, be endemic to the island of Borneo. Noteworthy, its closest relative is *P. inclinata* from Côn Lôn Island which was connected to Borneo via a land bridge during the Pleistocene.

Phytophthora transposita was found in the rhizosphere of healthy *Zanthoxylum ailanthoides* trees in a warm-temperate natural forest on the Japanese Kyushu Island where it is most likely endemic.

Summary: natural biogeography of Clade 2 and its subclades

Based mainly on the indirect evidence of endemism of the taxa presented above the main natural distribution of the subclades is summarized in Fig. 78. Terminology follows the recent update of Wallace' s biogeographic regions by Holt *et al.* (2013).

Clade 2a is native to the Oriental (= Indo-Malayan), Sino-Japanese and Oceanian biogeographic regions ranging from Nepal and India in the West to Japan and Papua New Guinea in the East and Christmas Island in the South. Multiple diversity hotspots occur in the Himalayas, Indochina, Sundaland, Taiwan and Japan (Figs 78, 79). The aerial Clade 2a species *P.* ×*australasiatica* and *P.* ×*vanyenensis* range from Sundaland across the Strait of Makassar to Sulawesi, which is the westernmost island of the transitional biogeographic region of Wallacea (Richardson *et al.* 2012).

Clade 2b is exclusively native to the Americas ranging from boreal Alaska in the North along the temperate and subtropical western regions of the Nearctic via a diversity hotspot of ten species in the transitional tropical Panamanian biogeographic region (= WWF Central America bioregion) and the tropical and temperate regions of eastern South America to the cool-temperate Valdivian and Aysen regions of Chile in the Southwest of the Neotropic realm (Figs 78, 79).

Clade 2c has a disjunct natural distribution in five biogeographic regions. Its main distribution stretches across the Oriental and Sino-Japanese regions from Nepal in the West via Indochina and Sundaland to Taiwan and Japan in the East, with a hotspot of nine species in the Japanese archipelago and another of five species in Southeast Asia and one species, *P. pseudocapensis*, occurring also in Sulawesi. The presence of *P. plurivora* in the Tien Shan mountains of Xinjiang, China is the only known natural distribution of a Clade 2c species in the Palearctic region. An isolated natural Clade 2c centre, comprising *P. capensis*, *P. emzansi* and *P. multivora*, lies in South Africa at the southernmost range of the Afrotropical biogeographic region. Another four Clade 2c species are probably endemic to the Midwest, Atlantic and southern regions of the USA in the eastern part of the Nearctic realm (Figs 78, 79).

The origin of the monospecific Clade 2d is unknown.

The main concentration of Clade 2e, including eight of the 11 known and new species plus *Phytophthora* taxon AUS 2E, stretches along an arc from Tasmania, Victoria, New South Wales and Queensland in the Southeast and East of the Australasian region via Sulawesi in Wallacea, Java, through Sumatra and Kalimantan in the South of the Oriental region to Taiwan and Amami Island in the Southeast of the Sino-Japanese region (Figs 78, 79). A smaller Clade 2e hotspot, currently comprising *P. penetrans* and the undescribed *P.* taxon Costa Rica 8, lies in the Panamanian biogeographic region. *Phytophthora acaciae* appears to be endemic to the southeastern Neotropical region while *P. frigida* most likely originates from South Africa (Figs 78, 79).

With *P. furcata* in Vietnam, *P. sumatera* in Java and Sumatra and a supposed origin of *P. multivesiculata* somewhere in Southeast Asia, Clade 2f has one centre in the Oriental biogeographic region while a second centre, comprising *P. angustata* and the undescribed *P.* taxon Costa Rica 5, lays in the Panamanian region (Figs 78, 79).

Clade 2g has a centre of diversity in the Oriental biogeographic region where three of the four known species occur naturally along a transect from northern Vietnam to Borneo, whereas *P. transposita* is native to Kyushu in the East of the Sino-Japanese region (Figs 78, 79).

Notes on the evolutionary history of Clade 2

Both multigene molecular phylogenetic analyses (Figs 1, S1) indicate an early divergence of Clades 2e and 2f followed by the subsequent divergences of Clades 2d, 2c and 2b, and most recently the splitting of Clades 2a and 2g. However, due to inconsistent results between the BI and ML analyses, it remains unresolved whether Clade 2e or 2f diverged first. The disjunct natural distributions of Clade 2c, Clade 2e and Clade 2f on separate

continents (Figs 78, 79) can only be explained if these subclades evolved before the break-up of the ancient supercontinent Pangea and/or by intercontinental migrations.

In this regard, East Asia and North America were connected via the Beringia land bridges intermittently from the late Cretaceous until the early Pliocene *ca*. 70–5.3 Mya (Gladenkov *et al.* 2002, Brikiatis 2016) and temporarily during the glacial periods of the Pleistocene (Vila *et al.* 2011, Elias & Brigham-Grette 2013). The timing and duration of North Atlantic land bridges is still under debate. While they were long believed to have existed more or less continuously until the early Oligocene *ca*. 30 Mya (McKenna 1983, Tiffney 1985, Davis *et al.* 2002), recent evidence indicates that North America, Greenland and Europe were mainly connected via the De Geer and Thulean routes which existed intermittently between 68 and 56 Mya (Brikiatis 2016). The Isthmus of Panama closed completely at *ca*. 3.5 Mya, fusing the Laurasian North American and the Gondwanan South American Plates, but a volcanic arc in the Panamanian region was already beginning to block the Central American Seaway *ca*. 12–6 Mya (Woodburne 2010, Bacon *et al.* 2015, Bogarín *et al.* 2016). Africa and Asia have been almost continuously connected from 19 Mya via the Gomphotherium landbridge and later the Isthmus of Suez (Harzhauser *et al.* 2007). Intercontinental migrations and interchange account for the relatedness of the East Asian and North American floras (Qian 2002, Lang *et al.* 2007, Baskin & Baskin 2016, Wen 1999, Wen *et al.* 2010, 2016) and for the circum-Pacific or Holarctic distributions of many animal (Morley 2003, Sharma & Giribet 2012, Van Damme & Sinev 2013, Toussaint *et al.* 2017, Kim *et al.* 2018) and plant families and genera, including the Fagaceous genera *Castanea*, *Fagus* and *Quercus* (Denk & Grimm 2009, Hubert *et al.* 2014).

While a potential for intercontinental *Phytophthora* migration is demonstrated by the distribution of *P. uniformis* from the otherwise exclusively Eurasian Clade 7a in Alaska and the Pacific Northwest (Adams *et al.* 2010, Aguayo *et al.* 2013, Jung *et al.* 2017a, b), the fact that there are no intermediate native records for Clades 2e and 2f between their centres in East or Southeast Asia and those in Central America and South Africa (only Clade 2e) argues against their intercontinental migration. In addition, New Guinea, the Moluccas and Sulawesi have never been connected by land bridges, while Western Sulawesi and Sundaland have been separated since *ca*. 45 Mya when rifts opened the Strait of Macassar (MacKinnon *et al.* 1997, Whitten *et al.* 2002, Hall 2017, Michaux 2010, Lohmann *et al.* 2011, Gower *et al.* 2012), thus preventing potential migration between the extant Clade 2e areas in eastern Australia and those in Asia.

Regarding Clade 2c, during the warmer climates of the late Cretaceous and Paleogene (*ca*. 70–23 Mya) the boreotropical vegetation and the Beringia land bridge may have allowed intermittent migration and interchange between the extant native centres in East Asia and North America. However, the Clade 2c subcentre in South Africa is separated from the other Clade 2c areas in Asia and North America by vast distances including semi-arid or arid environments and oceans which would have been major obstacles to migration.

Overall, it seems most likely that Clades 2c, 2e and 2f separated before Pangea split into Gondwana and Laurasia (*ca*. 200 Mya). The disjunct distributions of Clades 2c, 2e and 2f and the often vicariant distributions of species within the subclade centres are most probably a product of fundamentally allopatric, non-adaptive radiation processes due to migration across geographic barriers, the eruption of new geographic barriers (*e.g*. mountain uplift and the separation of islands) and gradual macroclimatic changes, leading to geographic isolation and accumulating genetic drift (Brasier 1986, Kozak *et al.* 2006, Rundell & Price 2009). Suggested examples of fundamentally allopatric speciation are, within Clade 2f, the distributions of *P. angustata* in Nicaragua, *P. furcata* in northern Vietnam and *P. sumatera* in Sundaland; within Clade 2e the distributions of *P. acaciae* in Brazil, *P. penetrans* in Panama, *P. amamensis* on Amami Island, *P. elongata* in southeastern Australia, *P. borneensis* in East Kalimantan and *P. celeris* in Central Sumatra; within Clade 2c the centres in North America, South Africa, Southeast and East Asia, and within Southeast Asia the vicariant distributions of *P. fansipanensis* on the Fansipan Mountain, *P. obturata* in Ba Vì National Park and on Sau Chua Mountain, and *P. macroglobulosa* on Hainan Island; and within Clade 2g, similar to Clade 2c, the centre in Southeast Asia and the occurrence of *P. transposita* in Japan, and within Southeast Asia the vicariant distributions of *P. proliferata* in Cuc Phuong National Park, *P. inclinata* on Côn Lôn Island and *P. multipapillata* in East Kalimantan.

Within the Japanese archipelago, the isolated occurrence of *P. vacuola* in montane *Quercus* and *Alnus* forests in Central Honshu might also reflect allopatric speciation. The co-occurrence of multiple Clade 2c species within other Japanese ecosystems, however, is more likely to result from sympatric events *i.e*., from local adaptive radiation associated with different host plants, microclimates, soil types and microbiomes (Mayr 1942, Brasier 1986, Givnish 1997, 2015, Rundell & Price 2009, Jung *et al.* 2017b). Examples include *P. curvata*, *P. excentrica*, *P. falcata* and *P. japonensis* in a mixed *Quercus-Abies-Torreya-Tsuga* forest in Ichinomata on Shikoku Island; *P. japonensis*, *P. nimia* and *P. oblonga* in a warm-temperate forest in Satayama on Shikoku Island; and *P. falcata*, *P. japonensis* and *P. nimia* in a warm-temperate forest in Takakuma on Kyushu Island.

The more recently diverged Clades 2a, 2b and 2g, in contrast to Clades 2c, 2e and 2f, are exclusively native to Asia (2a, 2g) or the Americas (2b), indicating that Clade 2b and the common ancestor of Clades 2a and 2g most likely diverged after the splitting of Pangea into Gondwana and Laurasia *ca*. 175 Mya. The absence of native Clade 2a and 2g species in the Americas and the fact that all known and new species from these subclades most likely originate in subtropical or tropical regions between India and Japan make a migration from the Americas via Beringia highly unlikely, further supporting the hypothesis that Clades 2a and 2g evolved from their common ancestor in South, Southeast or East Asia.

Clade 2b, on the other hand, most probably evolved in South America since the Valdivian rainforests and *Nothofagus* forests in South Chile, where the *P. aysenensis* - *P. distorta* - *P. valdiviana* complex originates, became isolated by the development of arid and semi-arid environments as a consequence of the Andean uplift between 23 and 12 Mya (Antonelli & Sanmartín 2011, Tecklin *et al.* 2011, Turchetto-Zolet *et al.* 2013), *i.e*., long before the complete closure of the Isthmus of Panama *ca*. 3.5 Mya enabled the migration of soilborne organisms between North and South America. During its subsequent spread to Central and North America as part of the Great American Biotic Interchange (Rull 2011, Bacon *et al.* 2015) Clade 2b probably underwent many allopatric and adaptive radiation events, discussed below. Equally, the possibility of some prior exchange of airborne *Phytophthora* species along the volcanic arc that formed in the Panamanian region *ca*. 12–6 Mya (*cf*. Woodburne 2010, Bacon *et al.* 2015, Bogarin *et al.* 2016) cannot be ruled out.

Since none of the 22 taxa now known from Clade 2b is native to Africa the subclade most probably evolved in South America after its splitting from Africa *ca*. 140 Mya. However, the possibility

that unknown native Clade 2b species exist somewhere in the vast unsurveyed regions between South Africa and the Mediterranean regions of North Africa cannot be ruled out.

Notes on the drivers of radiation, diversity and endemism within Clade 2

In the Pleistocene recurrent lowering of global sea levels during glaciation periods created temporary land bridges connecting the islands of the Sundaland and Con Dao archipelagos in Southeast Asia and the Japanese archipelago in East Asia with each other and, together with other islands on the Asian continental shelf such as Hainan and Taiwan, with the Asian mainland. These periods resulted in gateways for migration and interchange, whereas the intervening warm-humid interglacial periods resulted in isolation and increased hybridisation, speciation and radiation events (Chang-Fu *et al.* 1994, Chung-Fu 1994, Gower *et al.* 2012). Further, on the Asian mainland and adjacent islands, the climate during the glacial periods was cooler and considerably drier than today. This lowered altitudinal zones and forced thermophilic species to retreat into lowland refugia isolated by mountain ranges; and montane and hydrophilic species into "mountain island" refugia surrounded by drier savannahs or grasslands, resulting in disjunct post-Pleistocene populations and radiations (Heaney 1991, Laumonier 1997, MacKinnon *et al.* 1997, Whitten *et al.* 1997, 2002, Hope 2001, Hope *et al.* 2004, Cannon *et al.* 2009, Tian *et al.* 2010, Wurster *et al.* 2010, Ye *et al.* 2016).

These complex processes are considered mainly responsible for the species richness and the high degree of endemism of the flora and fauna of these regions (Chang-Fu *et al.* 1994, Chung-Fu 1994, Laumonier 1997, MacKinnon *et al.* 1997, Whitten *et al.* 1997, 2002, Axelrod *et al.* 1998, Averyanov *et al.* 2003, Roos *et al.* 2004, Van Welzen & Slik 2009, Lohman *et al.* 2011, Van Welzen *et al.* 2011, Richardson *et al.* 2012, Li *et al.* 2013), including the disjunct distribution and high phenotypic diversity of the eight known Asian lineages of *P. ramorum* from Clade 8c (Jung *et al.* 2021). Accordingly, in East and Southeast Asia, the populations of *Phytophthora* in general (Zeng *et al.* 2009, Jung *et al.* 2017a, c, 2020, 2022) and of Clade 2 are very diverse, exhibiting a high degree of endemism. The Japanese archipelago harbours at least 13 native species from Clades 2a, 2c, 2e and 2g of which nine (69.2 %) are most probably endemic (*P. amamensis*, *P. curvata*, *P. excentrica*, *P. falcata*, *P. japonensis*, *P. nimia*, *P. oblonga*, *P. transposita*, *P. vacuola*). In Taiwan two of the eight (25 %) native species from Clades 2a, 2c and 2e are probably endemic (*P. pseudoccultans*, *P.* ×*taiwanensis*). Sundaland is within the origin of 11 species from Clades 2a, 2c, 2e, 2f and 2g of which five (45.5 %) are most likely endemic (*P. borneensis*, *P. celeris*, *P. indonesiensis*, *P. multipapillata*, *P. sumatera*). Currently the second highest recorded degree of probable endemism regarding Clade 2 in Asia is in Vietnam, with eight of the 14 (57.1 %) native species from Clades 2a, 2c, 2e, 2f and 2g (*P. fansipanensis*, *P. furcata*, *P. inclinata*, *P. mekongensis*, *P. multibullata*, *P. obturata*, *P. proliferata*, *P. vietnamensis*).

In Central America 10 of the 14 (71.4 %) native taxa from Clades 2b, 2e and 2f are probable endemics (*P. angustata*, *P. calidophila*, *P. frigidophila*, *P. montana*, *P. multiplex*, *P. penetrans*, *P. pyriformis*, *P. variepedicellata*, *P.* taxon Costa Rica 5 and 8). This is consistent with the role of allopatric speciation and adaptive radiation events during the range expansion of Clade 2b to Central America hypothesised above. Further, as in Southeast and East Asia Central America experienced glacial-interglacial alternation during the Pleistocene with recurrent mean cooling of 5–9 °C and rainfall reductions of 30–50 %, resulting in lowering of altitudinal zones, retraction of rainforest species into isolated refugia surrounded by drier forest and savannah vegetation and, at transitional altitudes, mingling of thermophilic lowland and cooler montane species (Bush & Colinvaux 1990, Piperno 2006, Bush *et al.* 2009, Woodburne 2010).

Today tropical cloud forests form an archipelago of "mountain islands" across Central America with extremely high levels of local endemism (Myers 1969, Luna Vega *et al.* 1999, Rovito *et al.* 2015). Accordingly, five of the ten putatively endemic Clade 2 species in the area are restricted to individual tropical cloud forests (*P. angustata*, *P. calidophila*, *P. frigidophila*, *P. montana*, *P. variepedicellata*). Indeed, the co-occurrence of *P. frigidophila*, *P. montana* and *P. variepedicellata* in the remote cloud forest near the peak of Volcano Baru in Panama may constitute a textbook example of highly localised sympatric radiation driven by adaptation to different host plants or plant tissues. The highest degree of endemism in Clade 2, however, is found in the South of Chile where all three native Clade 2b species recorded, *P. aysenensis*, *P. distorta* and *P. valdiviana*, are probable endemics. This is most likely a consequence of the millions of years of isolation of the perhumid Gondwanan Valdivian rainforests and Southern beech forests by the Pacific Ocean to the west and semi-arid environments to the north and east (Hueck 1966, Armesto *et al.* 1995, Seibert 1996, Hinojosa *et al.* 2006, Antonelli & Sanmartín 2011, Tecklin *et al.* 2011, Turchetto-Zolet *et al.* 2013). It is notable that in Clade 10 the four species from the *P. kernoviae* complex, *P. chilensis*, *P. kernoviae*, *P. pseudochilensis* and *P. pseudokernoviae*, are also considered endemic to the Valdivian rainforests (Jung *et al.* 2022).

Notes on the evolution of lifestyle and adaptive traits within Clade 2

In the early-diverged subclade 2f, all five known taxa are self-fertile ('homothallic'), produce persistent sporangia lacking pedicels (except for *P.* taxon aquatilis) with nonpapillate or less frequently shallow semipapillate apices and internal nested and extended proliferation (except for *P.* taxon aquatilis) (Ilieva *et al.* 1998, Hong *et al.* 2012, this study). These traits probably reflect a more primitive or archaic soil- and waterborne lifestyle focussed on continuous spread and infection with a high dependence on zoospore inoculum and survival in unfavourable environmental conditions via regularly produced oospores; together with potentially constrained genetic variability due to a high frequency of inbreeding, a strategy probably suited to a more uniform environment (*cf.* Brasier 1986, Brasier *et al.* 2003, Jung *et al.* 2011). With optimum growth temperatures of 25 °C and maximum temperatures below 30 °C, *P. angustata*, *P. furcata* and *P. sumatera* are probably adapted to the rhizosphere and streams of montane tropical cloud and rainforests. Having a lower temperature optimum of 20 °C and higher maximum temperatures of 30 and 30–35 °C, *P. multivesiculata* and *P.* taxon aquatilis may be adapted to a temperate or upper montane tropical climate (Ilieva *et al.* 1998, Hong *et al.* 2012).

Since all Clade 2f species and the majority of Clade 2e species share persistent, nonpapillate to shallow semipapillate sporangia, self-fertility and soil- or waterborne lifestyle it can be assumed that they inherited this more primitive evolutionary state from the last common ancestor of all extant Clade 2 species.

In the other early-diverged subclade, 2e, sporangial traits, the breeding system and cardinal temperatures show considerably higher variability than in Clade 2f. A majority of eight Clade 2e

species are intrinsically self-fertile ('homothallic') (Tables S14, S15). However, each species in the cluster of *P. acaciae*, *P. acaciivora*, *P. frigida* and *P. pseudofrigida* has an A1/A2 and therefore possibly more outcrossing-orientated breeding system that may enhance genetic variability and consequently greater potential for adaptation to changing host populations or environmental conditions (*cf*. Brasier 1986). *Phytophthora acaciae*, *P. frigida* and *P. pseudofrigida* also produce asexual chlamydospores, which will further ensure their survival in unfavourable conditions. Chlamydospores are not produced by any of the self-fertile species from Clade 2e, nor any other subclade. Apart from *P. bishii* (Abad *et al.* 2008), ten of the 11 species with available data produce pedicellate sporangia. While eight of the pedicellate species lack sporangial caducity the sporangia of *P. frigida* are reported to be caducous (Maseko *et al.* 2007). *Phytophthora indonesiensis* produces a small proportion (<1 %) of caducous sporangia, potentially enabling, in addition to a predominantly soilborne lifestyle, infection of some aerial plant tissues in its tropical rainforest habitats. Sporangial apices in Clade 2e range from exclusively papillate (*P. acaciae*, *P. acaciivora*, *P. frigida*, *P. pseudofrigida*) and exclusively semipapillate (*P. bishii*, *P. elongata*, *P. penetrans*, *P.* taxon AUS 2E) to predominantly semipapillate (*P. amamensis*, *P. celeris*, *P. indonesiensis*) but with a small proportion of papillate (*P. amamensis*, *P. celeris*, *P. indonesiensis*) and nonpapillate sporangia (*P. amamensis*, *P. celeris*) (Abad *et al.* 2008, Rea *et al.* 2010, Albuquerque Alves *et al.* 2019, Burgess *et al.* 2020, this study). Only *P. borneensis* produces almost equal proportions of nonpapillate and semipapillate sporangia.

With maximum temperatures for growth between 32.5 and 35 °C *P. acaciae*, *P. acaciivora*, *P. borneensis*, *P. celeris* and *P. pseudofrigida* appear adapted to their natural tropical lowland rainforest habitats (Albuquerque Alves *et al.* 2019, Burgess *et al.* 2020, this study). *Phytophthora indonesiensis* isolates from montane rainforests in Sulawesi have significantly lower optimum temperatures than those from lowland rainforests in Borneo and Sumatra (20 *vs*. 25 °C), suggesting local adaptation. With optimum and maximum temperatures of 20 and <30 °C respectively the soilborne *P. elongata* is probably adapted to the temperate climate in southeastern Australia.

The next diverged monospecific lineage of *P. oleae* (Clade 2d) is also characterised by self-fertility and persistent semipapillate sporangia consistent with a soilborne lifestyle in a uniform stable environment.

In the fourth diverged subclade, 2c, sporangial apices are highly variable. Twenty-one of the 24 known and new species have either exclusively semipapillate sporangia or predominantly semipapillate sporangia with a proportion of papillate sporangia (*P. emzansi*, *P. excentrica*, *P. falcata*, *P. limosa*, *P. pini*, *P. platani*) and/or nonpapillate sporangia (*P. balkanensis*, *P. catenulata*, *P. emzansi*, *P. excentrica*, *P. limosa*, *P. oblonga*, *P. pini*) (Bezuidenhout *et al.* 2010, Bose *et al.* 2021a, this study). *Phytophthora capensis* is reported to have exclusively papillate sporangia (Bezuidenhout *et al.* 2010) while *P. vacuola* has predominantly papillate sporangia. *Phytophthora curvata* and *P. pseudocapensis* are unique within Clade 2c showing almost equal proportions of papillate and semipapillate sporangia.

Sixteen of the 17 Clade 2c species examined for pedicels to date have varying proportions of pedicellate sporangia, ranging from 6–11 % in *P. vacuola* and *P. japonensis* to 49–52 % in *P. falcata*, *P. nimia* and *P. obturata*. *Phytophthora curvata* is the only species not producing pedicels. While 18 species are probably exclusively soil- and waterborne, the other six species, *i.e.*, *P. catenulata*, *P. falcata*, *P. nimia*, *P. oblonga*, *P. obturata* and *P. platani*, produce up to 1 % caducous sporangia in water, possibly an adaptation to a partially aerial lifestyle. Indeed *P. platani* has been isolated from cankers of *Platanus* × *acerifolia* 18 m above ground (this study). Further in five of these species (*P. catenulata*, *P. nimia*, *P. oblonga*, *P. obturata*, *P. platani*) the sporangia are commonly formed in large sympodia of up to 8–15 sporangia, also consistent with a partially aerial lifestyle; and (unlike other Clade 2c species) *P. oblonga* commonly produces sporangia on solid agar which are exclusively caducous. It is also notable that, as with all five known species in Clade 2f, internal sporangial proliferation in *P. platani* occurs both in a nested and extended way, whereas in *P. nimia* and *P. oblonga* it is solely extended. Since none of the other 20 Clade 2c species and only two species from Clade 2e (*P. borneensis*, *P. penetrans*) show internal proliferation, the internal proliferation observed in these species has probably evolved both independently and convergently.

As also with Clades 2d, 2f and 2g but in contrast to the other three subclades, all 24 known and new Clade 2c species are intrinsically self-fertile ('homothallic'). The probable natural habitats of 19 taxa are known. Thirteen have maximum temperatures for growth between 27.5 and 30 °C and, hence, are adapted for a soil- or waterborne lifestyle in montane tropical or subtropical forests (*P. catenulata*, *P. fansipanensis*, *P. macroglobulosa*, *P. obturata*, *P. pseudocapensis*) or temperate forests (*P. capensis*, *P. curvata*, *P. emzansi*, *P. falcata*, *P. japonensis*, *P. nimia*, *P. oblonga*, *P. vacuola*) (Bose *et al.* 2021a, this study). The other six species have maximum temperatures between 30 and 32.5 °C consistent with their natural habitats in the soil and streams of subtropical or tropical lowland to lower montane forests (*P. citricola*, *P. limosa*, *P. multivora*, *P. pini*) and/or warm-temperate forests (*P. excentrica*, *P. pini*, *P. plurivora*).

The 19 known and new species with available data in the more recently divergent Clade 2b exhibit a highly variable range of sporangial traits, breeding systems, cardinal temperatures and lifestyles, including the emergence of a more aerial lifestyle. Four species have exclusively semipapillate persistent (*P. gloveri*, *P. mengei*, *P. montana*) or predominantly persistent (*P. siskiyouensis*) sporangia in concordance with a predominantly soilborne lifestyle (Reeser *et al.* 2007, Hong *et al.* 2009, Abad *et al.* 2011, this study). In contrast, nine species produce exclusively papillate (*P. aysenensis*, *P. capsici*, *P. mexicana*) or predominantly papillate (*P. frigidophila*, *P. multiplex*, *P. obovoidea*, *P. pyriformis*, *P. theobromicola*, *P. tropicalis*) sporangia. These are mostly caducous in five species (*P. capsici*, *P. frigidophila*, *P. obovoidea*, *P. pyriformis*, *P. tropicalis*), consistent with an aerial or partially aerial lifestyle (Mchau & Coffey 1995, Erwin & Ribeiro 1996, Aragaki & Uchida 2001, Crous *et al.* 2020, Decloquement *et al.* 2021, this study). High proportions of both papillate and semipapillate sporangia occur in four species. Two of these have persistent or predominantly persistent sporangia consistent with a soil- and waterborne lifestyle (*P. distorta*, *P. valdiviana*) and two partly caducous or mostly caducous sporangia suggesting a partially (*P. amaranthi*; Ann *et al.* 2016) or predominantly aerial (*P. variepedicellata*; this study) lifestyle. *Phytophthora calidophila* and *P.* taxon pseudocapsici are distinct from all other Clade 2b species in producing high proportions of papillate, semipapillate and nonpapillate sporangia which are mostly caducous.

Within Clade 2b, a firm relationship is apparent between lifestyle and breeding system. Among the nine self-fertile and mainly inbreeding species eight have persistent (*P. aysenensis*, *P. glovera*, *P. mengei*, *P. montana*, *P. valdiviana*) or predominantly persistent sporangia (*P. amaranthi*, *P. distorta*, *P. siskiyouensis*) and

a soilborne or predominantly soilborne lifestyle (Reeser *et al.* 2007, Hong *et al.* 2009, Abad *et al.* 2011, Ann *et al.* 2016, Crous *et al.* 2020, this study). Only one self-fertile species, *P. frigidophila*, has an aerial lifestyle. The only known sterile species, *P. theobromicola*, also has persistent sporangia and a soilborne lifestyle (Decloquement *et al.* 2021). In contrast, apart from *P. multiplex*, seven of the nine taxa with an A1/A2 and therefore potentially more outcrossing breeding system (*P. capsici*, *P. calidophila*, *P. obovoidea*, *P. pyriformis*, *P. tropicalis*, *P. variepedicellata*) have caducous sporangia and an aerial or predominantly aerial lifestyle as leaf, fruit and shoot pathogens (Mchau & Coffey 1995, Erwin & Ribeiro 1996, Aragaki & Uchida 2001, this study). This may facilitate their ability to respond to changing host populations and environmental conditions.

In the A1/A2 Clade 2b species, production of chlamydospores is common (*P. multiplex*, *P. obovoidea*, *P. pyriformis*, *P. tropicalis*, *P. variepedicellata*) or infrequent (*P. capsici*, *P. mexicana*) (Mchau & Coffey 1995, Erwin & Ribeiro 1996, Aragaki & Uchida 2001, this study). Together with the formation of dense hyphal aggregations (*P. calidophila*, *P. multiplex*, *P. obovoidea*, *P. pyriformis*, *P. tropicalis*, *P. variepedicellata*, *P.* taxon pseudocapsici), this may further enhance survival during adverse environmental conditions.

Available data on maximum temperatures for growth of 17 Clade 2b taxa are highly variable in range but appear generally consistent with their known natural habitats: 25–27.5 °C in *P. frigidophila* and *P. montana* from the cloud forest at 2 400 m altitude at Volcano Baru in Panama; 27.5–30 °C in *P. variepedicellata* from the same cloud forest at Volcano Baru, *P. distorta* and *P. valdiviana* from the cool-temperate Valdivian rainforests, *P. siskiyouensis* from the cool-temperate Pacific Northwest and subboreal Alaska and *P. mengei* with currently unknown natural habitat; (30–)32–<35 °C in *P. multiplex*, *P. pyriformis*, *P. theobromicola* and *P. tropicalis* from tropical lowland rainforests (Decloquement *et al.* 2021, this study), *P. calidophila* from a tropical lower montane forest, *P. obovoidea* from tropical lowland and montane forests, and *P. amaranthi* and *P. mexicana* with probable but unknown natural subtropical/tropical habitats (Ann *et al.* 2016, this study); and >35 °C in *P. capsici* and *P.* taxon pseudocapsici with unknown natural subtropical/tropical habitats. It is noteworthy that all eight Clade 2b species with aerial or partially aerial lifestyle in tropical lowland and lower montane forests (*P. calidophila*, *P. obovoidea*, *P. pyriformis*, *P. tropicalis*) or unknown natural habitats in tropical or subtropical regions (*P. amaranthi*, *P. capsici*, *P. mexicana*, *P.* taxon pseudocapsici) have maximum growth temperatures above 32 °C; probably an adaptation to hot daytime temperatures in infected aerial plant tissues.

Within Clade 2g, *P. inclinata* and *P. proliferata* have almost equal proportions of papillate and semipapillate sporangia whereas *P. multipapillata* produces predominantly semipapillate sporangia with a smaller proportion of papillate and a few nonpapillate sporangia. *Phytophthora transposita* is both unusual and currently unique in Clade 2g producing a mixture of papillate, semipapillate and nonpapillate sporangia. Proportions of pedicellate sporangia vary from 4 % in *P. proliferata* and *P. transposita* to 46 % in *P. multipapillata*. While *P. inclinata*, *P. multipapillata* and *P. transposita* have exclusively persistent sporangia without internal proliferation *P. proliferata* exhibits rare caducity, possibly enabling a partially aerial lifestyle, and regularly shows internal nested and extended proliferation.

All Clade 2g species share optimum and maximum temperatures of 27.5 and 30–32.5 °C, respectively, consistent with their natural habitats in the rhizosphere of subtropical or tropical lowland to lower montane forests.

The phenotypic and behavioural resemblances between Clade 2g and Clade 2c, *i.e.*, self-fertility ('homothallism') with paragynous antheridia, variable sporangial traits and a soilborne or predominantly soilborne lifestyle are probably best explained by convergent evolution. However, it cannot be ruled out that these traits occurred in the various common ancestors of Clade 2c and the 2b-2g-2a cluster; Clade 2b and the Clade 2g-2a cluster; and Clades 2g and 2a.

In Clade 2a, the evolution towards an aerial lifestyle appears even more advanced than in its sister Clade, 2b. In 11 of the 20 known and newly described taxa with available data the sporangia formed in water are exclusively or predominantly caducous (*P. colocasiae*, *P. insulinativitatica*, *P. mekongensis*, *P. pseudoccultans*, *P. vietnamensis*, *P.* ×*australasiatica*, *P.* ×*taiwanensis*, *P.* ×*vanyenensis*, *P.* taxon awatangi, *P.* taxon germisporangia) while the other nine have partial (*P. botryosa*, *P. himalsilva*, *P. meadii*, *P. occultans*, *P. terminalis*, *P.* taxon himalsilva-like 1) or rare (*P. citrophthora*, *P. multibullata*, *P. pseudocitrophthora*, *P.* ×*lusitanica*) sporangial caducity (Erwin & Ribeiro 1996, Vettraino *et al.* 2011, Man In't Veld *et al.* 2015, Crous *et al.* 2017, Dang *et al.* 2021, this study). The sporangial apices in water are variable ranging from exclusively (*P. himalsilva*, *P. mekongensis*, *P. pseudoccultans*) or predominantly (*P. pseudocitrophthora*, *P. vietnamensis*) papillate and exclusively (*P. colocasiae*) or predominantly (*P. citrophthora*, *P. meadii*) semipapillate to nearly similar proportions of papillate and semipapillate (*P. insulinativitatica*, *P. multibullata*, *P. occultans*, *P. terminalis*, *P.* ×*australasiatica*, *P.* ×*taiwanensis*, *P.* ×*vanyenensis*) or a transition between semipapillate and papillate (*P.* ×*lusitanica*) (Erwin & Ribeiro 1996, Vettraino *et al.* 2011, Man In't Veld *et al.* 2015, Crous *et al.* 2017, Dang *et al.* 2021, this study).

In water, *P. botryosa* produces similar proportions of semipapillate and nonpapillate sporangia and only 12 % papillate sporangia. With *P. meadii*, 23 % of sporangial apices are nonpapillate whereas smaller proportions (up to 10 %) of nonpapillate sporangia are found in *P. citrophthora*, *P. pseudocitrophthora*, *P. vietnamensis*, *P.* ×*australasiatica*, *P.* ×*taiwanensis* and *P.* ×*vanyenensis*.

Eleven of the 20 Clade 2a taxa with available data (*P. botryosa*, *P. colocasiae*, *P. insulinativitatica*, *P. meadii*, *P. mekongensis*, *P. multibullata*, *P.* ×*australasiatica*, *P.* ×*taiwanensis*, *P.* ×*vanyenensis*, *P.* taxon awatangi, *P.* taxon germisporangia) have A1/A2 and therefore potentially more outcrossing orientated breeding system. With the exceptions of *P. mekongensis* and *P.* taxon germisporangia, they also produce chlamydospores as an alternative survival structure (Erwin & Ribeiro 1996, Crous *et al.* 2017, Dang *et al.* 2021, this study). A similar trend occurs in Clade 2b, and appears to be associated with an exclusively or partially aerial lifestyle and adaptation to a more heterogeneous environment. Five taxa are self-fertile and lack chlamydospores (*P. himalsilva*, *P. occultans*, *P. pseudoccultans*, *P. terminalis*, *P.* taxon himalsilva-like 1) (Vettraino *et al.* 2011, Man In't Veld *et al.* 2015, this study). Another four species (*P. citrophthora*, *P. pseudocitrophthora*, *P. vietnamensis*, *P.* ×*lusitanica*; Erwin & Ribeiro 1996, this study) appear to be sterile or have 'silenced' their sexual reproduction systems. In the tropical A1/A2 ('heterothallic') *P. colocasiae*, around one third of isolates examined by Feng *et al.* (2022) in Japan were self-fertile, indicating a high frequency of secondary self-fertility ('secondary homothallism', Brasier 1992), probably giving *P. colocasiae* added genetic and adaptive flexibility. Similarly, self-fertile genotypes have also been reported for *P. colocasiae* isolates from subtropical Taiwan (Ko 1979, Ann *et al.* 1986).

Maximum temperatures for growth in Clade 2a vary between 27.5 and 35 °C, consistent with their natural habitat. *Phytophthora*

colocasiae, *P. insulinativitatica*, *P. meadii*, *P. mekongensis*, *P.* taxon awatangi, *P.* taxon germisporangia and the majority of isolates of the hybrid species *P.* ×*australasiatica*, *P.* ×*taiwanensis* and *P.* ×*vanyenensis* have maximum temperatures for growth above 32.5 °C (Dang *et al.* 2021, this study) consistent with their infecting aerial plant tissues in tropical lowland rainforests or subtropical lowland monsoon forests. Maximum growth temperatures between 30 and 32.5 °C are found in three taxa from upper montane tropical forests (*P. himalsilva*, *P. vietnamensis*, *P.* taxon himalsilva-like 1), two species from subtropical regions (*P. citrophthora*, *P. pseudocitrophthora*), *P. multibullata* from submontane tropical forests and the tropical *P. botryosa* (Vettraino *et al.* 2011, Dang *et al.* 2021, this study), and *P. occultans* and *P.* ×*lusitanica* with unknown natural habitats (Man In't Veld *et al.* 2015, this study). *Phytophthora pseudoccultans* from montane monsoon forests in Taiwan and *P. terminalis* with unknown natural habitat have the lowest maximum temperatures of all known and new Clade 2a taxa, at 27.5–30 and 26–28 °C, respectively (Man In't Veld *et al.* 2015, this study).

In part because of our baiting mainly the forest soil and water environment the natural and potential host ranges of the 43 Clade 2 species described here are mostly unknown. Even for the many previously known Clade 2 species only one or a few host species are known, and these are confined to non-natural or introduced situations. Thus, based on a comprehensive literature review of 34 described Clade 2 species, Brasier *et al.* (2022) demonstrated that in terms of records on crops, ornamentals or forest trees, mainly in the context of the introduction of the host or pathogen, their host ranges varied from very wide (>20 host species, 13.9 %) to medium-wide (6−20 host species, 19.4 %) to narrow (1−5 host species, 66.7 %), most being in the narrow range. Disease types ranged from root rots (72.2 % of 34 species), stem cankers on woody hosts (52.7 %) and leaf/shoot blights, bud rots or fruit rots (38.9 %) to declines and diebacks of forest ecosystems (25 %). Furthermore, 14 of the 34 species (41.8 %) were recorded as thriving as saprotrophs in water bodies (Brasier *et al.* 2022). This compares with 27 of the 43 new Clade 2 species described here (63 %) being recovered from forest streams.

Notes on the relationship between level of heterozygosity, breeding system and interspecific hybridity across the subclades

Heterozygosity data for all taxa examined based on nine nuclear genes and the relationship between mean heterozygosity and breeding system, whether intrinsically self-fertile ('homothallic'), A1/A2 ('heterothallic') or sterile (see Terminology section) are shown in Tables 1–4, S18.

Across all subclades the A1/A2 and sterile taxa showed markedly higher levels of mean nuclear heterozygosity, at 0.4 % and 0.46 % respectively, than the self-fertile taxa at 0.09 % (Table 2). Indeed, across the 56 self-fertile taxa (excluding *P.* taxon aquatilis with 0.42 %) mean heterozygosity ranged from only *ca.* zero to 0.25 (Tables 2–4, S18; see also horizontal bar insert in Fig. 80). Against this benchmark the 25 A1/A2 taxa with suitable data showed a much wider range at zero to 1.27 %, as did the five sterile taxa at 0.09–0.84 % (Tables 2–4, S18; Fig. 80). The A1/A2 and sterile groups therefore included both species with low heterozygosity levels comparable to the self-fertile species, and species with much higher heterozygosity levels (Fig. 80).

Almost all the A1/A2 and sterile taxa occur in Clades 2a and 2b (the exceptions being three A1/A2 taxa in Clade 2e). When the 2a and 2b taxa are ranked for heterozygosity levels (Tables 3–4; Fig. 80), not unexpectedly a relationship is indicated between mean heterozygosity, breeding system and species hybridity. Thus, there appears to be a discontinuity between taxa below and above *ca.* 0.3 % mean heterozygosity. Further, all those >0.3 % are either of A1/A2 type or are sterile.

Previously, isolates representing three of the taxa in the Clade 2a >0.3 % cluster have been designated as some form of species hybrid based on nuclear genotyping by sequencing: isolate BD518, the ex-type of *P.* ×*lusitanica*; isolate VN763 of *P.* ×*australasiatica*; and five isolates of *P.* ×*taiwanensis* (Van Poucke *et al.* 2021). This conclusion of hybridity is further supported here by their respective high mean levels of nuclear heterozygosity at 0.52 %, 0.89 % and 1.09 %. Also, two of them exhibit a high level of mitochondrial

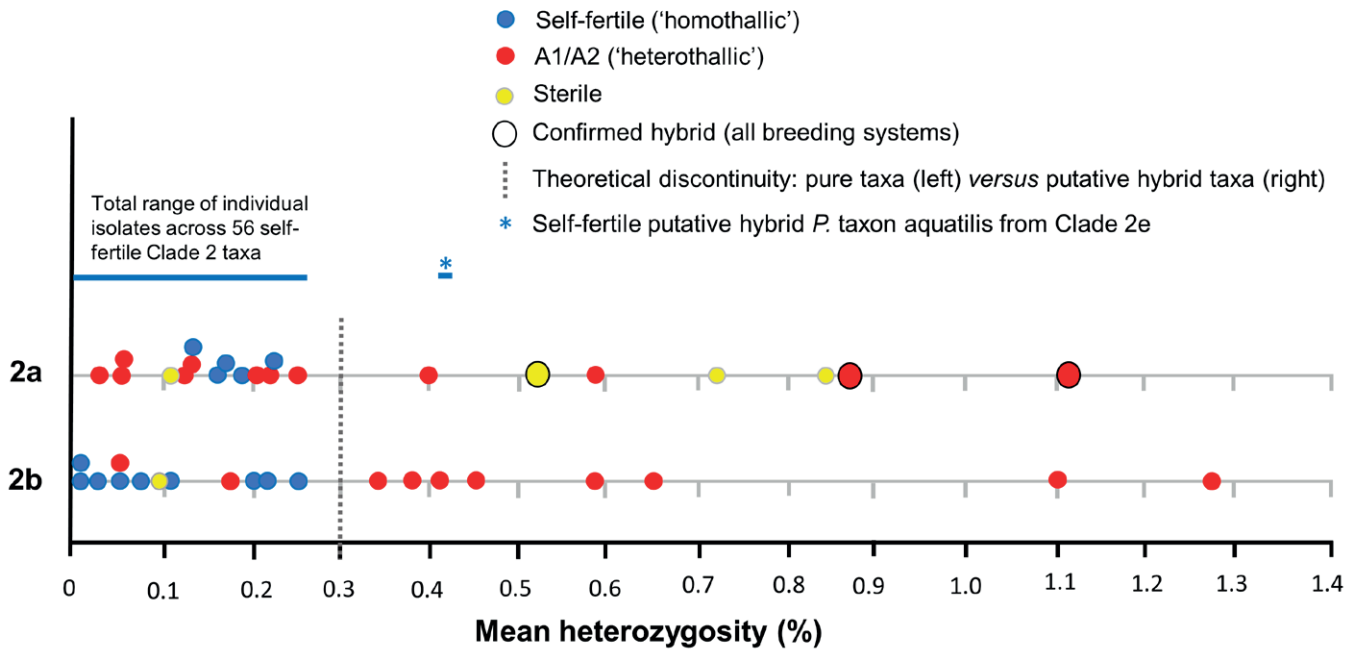

Fig. 80. Distribution of mean nuclear gene heterozygosity *versus* breeding system for the individual taxa in *Phytophthora* Clades 2a and 2b.

Table 3. Relationship between level of heterozygosity across nine nuclear genes (LSU, ITS, *ßtub*, *hsp90*, *tigA*, *rpl10*, *tef-1α*, *enl*, *ras-ypt1*), breeding system and interspecific hybridity in *Phytophthora* subclade 2a.

Taxon	No. of isolates	Mean nuclear heterozygosity (%)	Nuclear heterozygosity range (%)	Breeding system	Hybrid status[1]
P. taxon meadii-like[2]	1	0.03	n/a	A1/A2	Pure
P. taxon awatangi[3]	1	0.05	n/a	A1/A2	Pure
P. insulinativitatica[3]	2	0.06	0.04–0.08	A1/A2	Pure
P. citrophthora	10	0.11	0.01–0.14	Sterile	Pure
P. taxon germisporangia[3]	1	0.12	n/a	A1/A2	Pure
P. botryosa	4	0.13	0.11–0.24	A1/A2	Pure
P. pseudoccultans	3	0.13	n/a	Self-fertile	Pure
P. himalsilva	6	0.16	0.15–0.17	Self-fertile	Pure
P. taxon himalsilva-like 1[4]	1	0.17	n/a	Self-fertile	Pure
P. occultans	3	0.19	0.18–0.22	Self-fertile	Pure
P. meadii	5	0.2	0.14–0.33	A1/A2	Pure
P. colocasiae	3	0.22	0.0–0.29	A1/A2	Pure
P. terminalis	1	0.23	n/a	Self-fertile	Pure
P. multibullata[3]	3	0.25	0.16–0.44	A1/A2	Ambiguous
P. ×*vanyenensis*	12	0.4	0.19–0.78	A1/A2	Ambiguous
P. ×*lusitanica*[5]	3	0.52	0.51–0.53	Sterile	Confirmed
P. mekongensis	5	0.59	0.50–0.71	A1/A2	Probable
P. pseudocitrophthora	7	0.72	0.56–0.79	Sterile	Probable
P. vietnamensis[5]	3	0.84	0.84–0.84	Sterile	Probable
P. ×*australasiatica*	18	0.87	0.65–1.11	A1/A2	Confirmed
P. ×*taiwanensis*	5	1.09	0.89–1.14	A1/A2	Confirmed

[1] 'Pure': isolates assumed to be representative of a near pure species.

Ambiguous: wide range of nuclear heterozygosity levels suggesting that the studied isolates are a mixture of individuals ranging from a near 'pure' non-hybrid status to various hybrid recombinants or introgressants.

Probable: high level of nuclear heterozygosity consistent with all studied isolates being some form of interspecific hybrid; in addition the following can apply: mitochondrial genes show high similarity to one or more other Clade 2a taxa; different mitochondrial genes show high similarity to different other Clade 2a taxa; multiple mitochondrial genotypes.

Confirmed: based on nuclear genotyping by sequencing (Van Poucke *et al.* 2021); in addition high level of nuclear heterozygosity and identity of mitochondrial genes with other (maternal) Clade 2a species.

[2] LSU, *hsp90*, *tigA*, *rpl10* and *tef-1α* not available

[3] LSU, *tigA*, *rpl10*, *tef-1α*, *enl*, *ras-ypt1* not available.

[4] *ras-ypt1* not available.

[5] Isolates studied could be genetically identical or closely related due to local asexual reproduction.

gene identity with another Clade 2a taxon, suggesting possible mitochondrial parentage: *P.* ×*lusitanica* with *P. citrophthora*; and *P.* ×*australasiatica* with *P.* ×*vanyenensis* (Table S19). The taxa *P.* ×*lusitanica*, *P.* ×*australasiatica* and *P.* ×*taiwanensis* have therefore been formally designated in this study as hybrids and are shown in Table 3 and Fig. 80 as confirmed hybrids.

From this it could be conjectured that most if not all of the taxa in the <0.3 % clusters may be 'pure' species, and they are speculatively suggested to be such in Tables 3 and 4; whereas those in the >0.3 % clusters (in addition to *P.* ×*lusitanica*, *P.* ×*australasiatica* and *P.* ×*taiwanensis*) could again be some form of hybrids, whether full allopolyploids, hybrid introgressants or mixed populations of parental species and hybrids. In *P.* ×*vanyenensis*, for example, designated as a hybrid previously (Dang *et al.* 2021), isolates are shown here to have a very wide range in heterozygosity from 0.19−0.78 % (12 isolates, Table 3) and could conceivably be a mixture of a parental species, hybrids and introgressants, as in a hybrid swarm. Indeed, isolate CBS 235.30 of *P.* ×*vanyenensis*, reported by Van Poucke *et al.* (2021) not to be a hybrid, has the second lowest score among the isolates for nuclear heterozygosity (0.26 %). It might therefore be genetically closer to a parent species of a hybrid population. *Phytophthora* ×*vanyenensis* and other taxa in the >0.3 % clusters with a relatively broad spread of heterozygosity values, *i.e.*, *P. obovoidea* and *P. tropicalis*, are therefore speculatively listed as ambiguous in Tables 3 and 4. Taxa above 0.3 % exhibiting more consistent heterozygosity values, such as *P. calidophila*, *P. mekongensis*, *P. multiplex*, *P. pseudocitrophthora*, *P. pyriformis*, *P. vietnamensis* and *P.* taxon pseudocapsici, are listed as probable hybrids (Tables 3, 4).

Table 4. Relationship between level of heterozygosity across nine nuclear genes (LSU, ITS, *ßtub*, *hsp90*, *tigA*, *rpl10*, *tef-1α*, *enl*, *ras-ypt1*), breeding system and interspecific hybridity in *Phytophthora* subclade 2b.

Taxon	No. of isolates	Mean nuclear heterozygosity (%)	Nuclear heterozygosity range (%)	Breeding system	Hybrid status[1]
P. amaranthi[2, 8]	3	0	0.0–0.0	Self-fertile	Pure
P. aysenensis[3, 8]	2	0	0.0–0.0	Self-fertile	Pure
P. gloveri	3	0.01	0.0–0.03	Self-fertile	Pure
P. capsici s. str.[4, 9]	1	0.05	n/a	A1/A2	Pure
P. montana[8]	3	0.05	0.05–0.05	Self-fertile	Pure
P. mengei	3	0.07	0.07–0.07	Self-fertile	Pure
P. theobromicola[5]	4	0.09	0.0–0.27	Sterile	Pure
P. t. mengei-like[6]	1	0.1	n/a	Self-fertile	Pure
P. siskiyouensis	3	0.11	0.0–0.17	Self-fertile	Pure
P. taxon brasiliensis[7]	1	0.17	n/a	A1/A2	Pure
P. distorta[8]	3	0.2	0.2–0.2	Self-fertile	Pure
P. valdiviana	4	0.21	0.21–0.22	Self-fertile	Pure
P. frigidophila[8]	3	0.25	0.25–0.25	Self-fertile	Pure
P. mexicana s. l.	5	0.34	0.22–0.51	A1/A2	Ambiguous
P. tropicalis	15	0.38	0.16–0.61	A1/A2	Ambiguous
P. variepedicellata[8]	5	0.41	0.39–0.42	A1/A2	Probable
P. multiplex	10	0.45	0.31–0.52	A1/A2	Probable
P. obovoidea	21	0.59	0.27–1.12	A1/A2	Ambiguous
P. taxon pseudocapsici	4	0.65	0.46–0.72	A1 /A2	Probable
P. calidophila[8]	3	1.1	1.1–1.1	A1/A2	Probable
P. pyriformis[8]	3	1.27	1.26–1.28	A1/A2	Probable

[1] 'Pure': isolates assumed to be representative of a near pure species.

Ambiguous: wide range of nuclear heterozygosity levels suggesting that the studied isolates are a mixture of individuals ranging from a near 'pure' non-hybrid status to various hybrid recombinants or introgressants.

Probable: high level of nuclear heterozygosity consistent with all studied isolates being some form of interspecific hybrid; in addition the following can apply: mitochondrial genes show high similarity to one or more other Clade 2a taxa; different mitochondrial genes show high similarity to different other Clade 2a taxa; multiple mitochondrial genotypes.

[2] LSU, *enl* and *tef-1α* not available.

[3] *hsp90*, *tigA*, *rpl10*, *tef-1α*, *enl* and *ras-ypt1* not available.

[4] *tigA* and *enl* not available.

[5] LSU, *tigA*, *rpl10*, *enl* and *ras-ypt1* not available.

[6] LSU, *hsp90*, *tigA*, *rpl10*, *enl* and *ras-ypt1* not available.

[7] *ras-ypt1* not available.

[8] Isolates studied could be genetically identical or closely related due to local asexual reproduction.

[9] Low heterozygosity could reflect this being only a single isolate of an otherwise widely distributed, competently A1/A2 outcrossing species.

A further indication of the potential hybridity of the taxa >0.3 % in Clades 2a and 2b comes from close matches in mitochondrial gene profiles (Tables S19, S20). Among the Clade 2a taxa listed as probable hybrids in Table S20, *P. mekongensis* shows high mitochondrial similarity with *P.* ×*vanyenensis*; *P. vietnamensis* with *P.* ×*vanyenensis*; and *P. pseudocitrophthora* with *P. occultans* (Table S19). *Phytophthora pseudocitrophthora* may be identical with the hybrid *P. occultans* × *citrophthora*-related (isolate CBS 111726) informally designated by Van Poucke *et al.* (2021). In Clade 2b, *P. calidophila*, *P. multiplex* and *P. taxon pseudocapsici,* all listed as probable hybrids (Table 4), show high mitochondrial similarity or full identity to *P. variepedicellata, P. theobromicola* and *P. capsici*, respectively (Table S20)*;* and *P obovoidea* and *P. tropicalis,* both listed as ambiguous for hybridity (Table 4), also show high mitochondrial similarity (Table S20).

In Clade 2f, *P.* taxon aquatilis, described as homothallic (self-fertile) by Hong *et al.* (2012), is a unique outlier in the collective heterozygosity profile of all self-fertile Clade 2 taxa (Fig. 80) with a mean nuclear heterozygosity level of 0.42 % (Tables 2, S18). *Phytophthora* taxon aquatilis could therefore also be some form of hybrid. Overall, we consider the higher heterozygosity levels of the taxa listed either as probable hybrids or as ambiguous in Tables 3 and 4 (together with *P.* taxon aquatilis in Clade 2f), plus in some cases mitochondrial co-similarity with other taxa, to be highly indicative of hybridity. However, we consider a higher burden of proof is required.

With the exceptions of *P.* ×*lusitanica*, *P. pseudocitrophthora* and *P. vietnamensis* with sterile or silenced breeding systems, the other confirmed or probable hybrids, *i.e.*, *P. calidophila*, *P. mekongensis*, *P. multiplex*, *P. pyriformis*, *P.* ×*australasiatica* and *P.* ×*taiwanensis*, and the three ambiguous species *P. obovoidea*, *P. tropicalis* and *P.* ×*vanyenensis* exhibit apparently functional A1/A2 breeding systems which, in combination with their novel genomes, may have facilitated their survival and success in competition with their parent species. Whether the confirmed hybrid *P.* ×*lusitanica* and probable hybrids *P. pseudocitrophthora* and *P. vietnamensis* have become sterile as a result of becoming unbalanced allopolyploids needs investigation.

Further, among the putatively 'pure' (*i.e.*, non-hybrid) self-fertile taxa in the Clade 2a and 2b <0.3 % clusters the mean heterozygosity ranges of the self-fertile and A1/A2 taxa are remarkably similar, at *ca*. 0–0.25 % and 0.03–0.22 %, respectively (Fig. 80). This raises the possibility that relative proportions of sexual outbreeding versus inbreeding in each system are also similar. In the self-fertile (and generally assumed more typically inbreeding) species, outbreeding can occur via the fusion of antheridia and oogonia (and subsequently of gametes) between adjacent, genetically dissimilar genotypes, with probably no barrier to this process. In the A1/A2 system, in addition to outcrossing, inbreeding can occur as a result of (i) selfing induced by the interaction of adjacent A1s and A2s and (ii) selfing of individual A1s or A2s in response to other environmental stimuli (Brasier 1971, 1978, 1992, Reeves & Jackson 1974, Zentmyer 1979, Jayasekera *et al.* 2007, Jung *et al*. 2013b). For both breeding systems, frequencies of inbreeding versus outbreeding in native (non-introduced) natural populations also need further investigation.

DISCUSSION

This paper is primarily the product of worldwide surveys searching for endemic species of *Phytophthora* in comparatively underexplored forests and natural ecosystems, and to a lesser extent *Phytophthora* species that were introduced into nurseries and plantations (*cf*. Zeng *et al.* 2009, Brasier *et al.* 2010, Vettraino *et al.* 2011, Jung *et al.* 2016, 2017b, 2018b, 2019, 2020, 2021, 2022, Puglisi *et al.* 2017, Milenković *et al.* 2018). These surveys had three main objectives. Firstly, to identify the geographic origins of *Phytophthoras* which have been highly damaging when introduced into non-native ecosystems, such as *P. cinnamomi, P. lateralis*, *P. ramorum* and *P.* ×*cambivora* (*cf*. Brasier *et al.* 2010, 2012, Jung *et al.* 2021, Shakya *et al.* 2021, Mullet *et al.* 2023) to enhance understanding of their natural breeding systems, host-pathogen relationships and containment by competitors and to potentially obtain new insights for resistance breeding. Secondly, to enhance understanding of the biogeography of the genus, including the origins and spread of its main clades (Jung *et al.* 2017c, 2022). And thirdly, to improve knowledge of *Phytophthora* diversity to better inform and manage international forest biosecurity, including measures aimed at managing pathways of introduction.

In 2009, when only 90 *Phytophthora* species had been formally described, the total number of *Phytophthora* species worldwide was estimated to lie between 200 and 600 (Brasier 2009). Later, Scott *et al.* (2019) estimated between 274 and 378 species. This study, presenting 43 new species and designating three other new taxa, doubles the number of taxa in *Phytophthora* Clade 2 alone from 47 to 93: 79 species and 14 informally designated taxa. It also brings the number of currently known *Phytophthora* species across all twelve clades to around 260 (based on 218 described and accepted species in Brasier *et al.* 2022, Chen *et al.* 2022, Jung *et al.* 2022 and Abad *et al*. 2023a). Moreover, the number of described *Phytophthora* species continues to increase steadily.

The 43 new Clade 2 species are identified based on unique combinations of morphological characters (gametangia, sporangia, chlamydospores, hyphal swellings and aggregations), colony morphology and temperature-growth relations, and a distinct position in the multigene phylogeny. They are distributed across five of the six previously known phylogenetic subclades, 2a–c, e, f, and a new subclade 2g. These now comprise 22 taxa in Clade 2a (6 new and 11 known species plus *P.* taxon awatangi, *P.* taxon germisporangia, *P.* taxon himalsilva-like 1 and 2 and *P.* taxon meadii-like); 22 in Clade 2b (9 new and 9 known species plus *P.* taxon brasiliensis, *P.* taxon mengei-like, *P.* taxon pseudocapsici and *P.* taxon subnulis), 24 in Clade 2c (15 new and 9 known species); 14 in Clade 2e (6 new and 5 known species plus *P.* taxon AUS 2E, *P.* taxon *pseudobisheria* and *P.* taxon Costa Rica 8); six in Clade 2f (3 new and 1 known species plus *P.* taxon aquatilis and *P.* taxon Costa Rica 5); four (all new species) in Clade 2g; and one (*P. oleae*) in Clade 2d. The now substantially revised molecular phylogeny of Clade 2 (Fig. 1) indicates early divergence of subclades 2f and 2e was followed next by a divergence of subclade 2d, then the emergence of subclades 2c and 2b and more recently a separation of subclades 2a and 2g.

We also show here that the six subclades tend to be geographically differentiated (Fig. 78). The three earlier diverged subclades (2e, 2f and 2c) are intercontinental, occurring both in the Americas and in Asia. Clade 2f is present in Southeast Asia and Central America; Clade 2e is circumpacific (Australia, Sundaland, Taiwan, Amami Island, Central America, eastern South America) and most likely also native to South Africa (*P. frigida*); and Clade 2c occurs in eastern North America, Southeast and East Asia and South Africa. This endemism across several continents is probably best explained by the evolution of these subclades on the ancient supercontinent Pangea before it split into Gondwana and Laurasia. Nonetheless, subsequent intercontinental migrations, possibly via ancient land bridges such as Beringia, the Isthmus of Panama and the North Atlantic land bridges, cannot be ruled out (*cf*. Notes on the evolutionary history of Clade 2, above). Emergence before the fragmentation of Pangea would put the age of these three subclades at ~175 Mya or more.

The three most recently diverged subclades, however, appear confined to separate continental regions consistent with their diverging after the splitting of Pangea: 2a and 2g to South and Southeast Asia and 2b to the Americas. Since 13 of the 17 known Clade 2a species and all four known Clade 2g species have been found between India and Japan it is most likely that these subclades evolved within this area, as previously suggested for Clade 2a by Dang *et al.* (2021). The fact that none of the 22 known Clade 2b taxa are native to Africa suggests this subclade probably evolved in South America after its splitting from Africa *ca*. 140 Mya (*cf*. Notes on the evolutionary history of Clade 2, above).

Several hotspots of subclade diversity were highlighted by this study (Fig. 79; and see Notes on the geographical distribution of Clade 2, above). Vietnam together with Indochina as a whole constitutes a hotspot of Clade 2a diversity, with at least seven species. The native forests of Taiwan are another 2a hotspot, with three species including two new probable endemics. Central America is the centre of diversity of Clade 2b, hosting 11 of the 22 known and new taxa. The cool-temperate Aysen and Valdivia regions in southern Chile constitute another 2b hotspot, with three endemic species. Clade 2c has its main centres of diversity in East

and Southeast Asia, with currently 18 confirmed taxa including a plethora of 15 new taxa. Eight 2c taxa including seven new endemics have now been identified in Southeast Asia alone, and the Japanese archipelago hosts at least ten 2c species including eight endemics. The Indonesian archipelago is a hotspot of Clade 2e diversity, with in total five species. Clade 2f has one possible centre in Asia, comprising three species, and a second centre with two species in the Central American Panamanian region. Currently, in the second-least numerous subclade 2g one centre three of the four known species are in a focus between Vietnam and Borneo and the other occurs in Kyushu, Japan.

Some of these diversity hotspots probably reflect allopatric speciation. For example, the different clusters of Clade 2c species in North America, South Africa, Southeast Asia and East Asia seem likely to result from geographic isolation followed by local radiations. The vicariant distributions of the Clade 2c taxa *P. fansipanensis* on the Fansipan Mountain, *P. obturata* in Ba Vì National Park and on Sau Chua Mountain (all in Vietnam); *P. macroglobulosa* on the Chinese Hainan Island; and of the Clade 2g taxa *P. proliferata* in Cuc Phuong National Park in northern Vietnam, *P. inclinata* on Côn Lôn Island and *P. multipapillata* on Borneo, suggest allopatric speciation resulting from local geographic barriers. Other hotspots may reflect local sympatric speciation, for example, the co-occurrence of the Clade 2c species *P. curvata*, *P. excentrica*, *P. falcata* and *P. japonica* in mixed sub-tropical *Quercus-Abies-Torreya-Tsuga*-forests on Shikoku Island, Japan. However, without evidence of the extent of local adaptation of these taxa, in particular their host ranges and their levels of reproductive isolation, it is only possible to speculate.

Interestingly, Clade 2 shows both striking biogeographical similarities and some contrasts to *Phytophthora* Clade 10. Both clades occur naturally, and sometimes co-occur, in northern Indochina, Amami Island, Java, Sulawesi, Eastern Australia, South Africa, the Valdivian region in southern Chile and the Southeast and East of the USA (Hong *et al.* 2011, Oh *et al.* 2013, Yang *et al.* 2016, Brazee *et al.* 2017, Jung *et al.* 2018b, 2020, 2022; Bose *et al.* 2021a; this study). However, none of the known Clade 10 species is native to western North America, Central America or the east and southeast of South America (Jung *et al.* 2022), whereas this vast region is naturally inhabited by at least 19 Clade 2 taxa. Clade 10 is also apparently absent from Taiwan and the main islands of Japan, where at least 18 species from Clade 2 are probably native. Further, whereas Clade 2 species do not appear to be native to Europe, Clade 10 has radiated in Europe, occurring as four extant native species in boreal, subboreal and temperate regions (*P. gallica*, *P. scandinavica*, *P. subarctica* and *P. ukrainensis*; Jung *et al.* 2022). The absence of Clade 2 in Europe could indicate that it never colonised the region. Indeed, none of the 93 known Clade 2 taxa is adapted to particularly low temperatures and only the North American *P. siskiyouensis* is native to subboreal regions. If Clade 2 was originally present in Europe it may have become extinct during the long Pleistocene glaciations (*cf*. Huntley 1993, Latham & Ricklefs 1993, Svenning 2003).

High genomic, phenotypic and behavioural flexibility, in particular an ability to switch between different breeding systems, spore types and lifestyles, is a salient characteristic of the genus *Phytophthora* that is considered to account for its long-term evolutionary success and for its species being highly successful pathogens when introduced into novel ecosystems (Brasier *et al.* 2022). This must also have enabled the Clade 2 subclades to adapt to such a very wide variety of environments and hosts worldwide. Indeed, the current 79 well-characterised species and the five informally designated taxa with suitable data (*P.* taxon aquatilis, *P.* taxon AUS 2E, *P.* taxon awatangi, *P.* taxon germisporangia, *P.* taxon pseudocapsici) display most of the breeding systems, gametangial and sporangial forms, cardinal temperatures, 'lifestyles' and host and substrate characteristics of the genus as a whole (*cf*. Brasier *et al.* 2022; Tables 5–7, S4–S17; and see Notes on adaptive traits of Clade 2, above), although no very low temperature-tolerant species have been identified.

This phenotypic and behavioural breadth can almost be said of the taxa within Clade 2b alone. Breeding systems of the twenty 2b taxa with suitable data range from intrinsically self-sterile ('homothallic') to A1/A2 ('heterothallic') to sexually sterile. Antheridia produced by different taxa are either paragynous, amphigynous or a mixture of both (Tables 5, 6, S7–S9). Sporangiophores formed range from simple to lax or dense sympodia; sporangia range from predominantly papillate and semipapillate to a proportion of nonpapillate, and from caducous to partially caducous to non-caducous (Tables 7, S7–S9). Optimal temperatures for growth in subclade 2b, and indeed in Clade 2 as a whole, range from 20–30 °C and maximum temperatures from 25–35 °C (Tables S7–S9,

Table 5. Breeding system frequency across the subclades of *Phytophthora* Clade 2.

Subclade	No. of taxa	Proportion of taxa (of these % forming chlamydospores)		
		Self-fertile	A1/A2	Sterile
2a	19	21 (0)	58 (83)	21 (0)
2b[1]	18	50 (0)	44 (63)	6 (100)
2c	24	100 (0)	0	0
2d	1	100 (0)	0	0
2e[2]	12	67 (0)	33 (75)	0
2f[3]	5	100 (0)	0	0
2g	4	100 (0)	0	0

[1] No suitable data available for *P.* taxon brasiliensis, *P.* taxon pseudocapsici, *P.* taxon mengei-like and *P.* taxon subnulis.

[2] No data available for *P.* taxon pseudobisheria and *P.* taxon Costa Rica 8.

[3] No data available for *P.* taxon Costa Rica 5.

Table 6. Frequency of paragynous and amphigynous antheridial types among the self-fertile ('homothallic') and the A1/A2 *Phytophthora* taxa in the Clade 2 subclades.

	Self-fertile				A1/A2	
		Proportion of taxa (approx.; %)				
Subclade	No. of taxa	Paragynous	Paragynous and amphigynous	Amphigynous	No. of taxa	Proportion amphigynous (%)
2a[1]	4	0	100	0	11	100
2b[2]	9	11	44.5	44.5	9	100
2c	24	33	63[3]	4	0	n/a
2d	1	100	0	0	0	n/a
2e[4]	8	100	0	0	4	100
2f[5]	5	0	60[6]	40	0	n/a
2g	4	100	0	0	0	n/a

n/a = not applicable.

[1] *P. citrophthora*, *P. pseudocitrophthora*, *P. vietnamensis* and *P.* ×*lusitanica* have sterile breeding systems.

[2] No data available for *P.* taxon brasiliensis, *P.* taxon mengei-like and *P.* taxon subnulis; *P. theobromicola* has a sterile breeding system.

[3] Typically only 0.2–5 % amphigynous types.

[4] No data available for *P.* taxon pseudobisheria and *P.* taxon Costa Rica 8.

[5] No data available for *P.* taxon Costa Rica 5.

[6] Very wide range, from 5–99 % paragynous and from 1–95 % amphigynous types, respectively.

Table 7. Frequency of sporangial types across the subclades of *Phytophthora* Clade 2.

Subclade	No. of taxa	Proportion of taxa (approx.; %)			
		Mainly papillate to semipapillate[1]		Non-papillate to semi- papillate, non-caducous	
		Fully or partly caducous	Non- or rarely caducous	Internal proliferation	No internal proliferation
2a	19	79	21[2]	0	0
2b[3]	19	53[4]	47	0	0
2c	24	0	100[5]	0	0
2d	1	0	100	0	0
2e[6]	11	9[7]	91[8]	0	0
2f[9]	4	0	0	100	0
2g	4	0	100[10]	0	0

[1] Proportion of non-papillate sporangia <20 %.

[2] All four species (*P. citrophthora*, *P. multibullata*, *P. pseudocitrophthora, P.* ×*lusitanica*) show rare caducity.

[3] No data available for *P.* taxon brasiliensis, *P.* taxon mengei-like and *P.* taxon subnulis.

[4] In *P. calidophila* 25 % non-papillate sporangia.

[5] In six species (= 25 %) <1 % of sporangia caducous; in three species (= 12.5 %) internal proliferation occurring.

[6] No data available for *P.* taxon pseudobisheria and *P.* taxon Costa Rica 8.

[7] *P. frigida* is reported to be caducous (Maseko *et al.* 2007).

[8] In *P. indonesiensis* <1 % of sporangia caducous; in two species internal proliferation occurring.

[9] No suitable data available for *P.* taxon aquatilis and *P.* taxon Costa Rica 5.

[10] In *P. multipapillata* (= 25 % of species) <1 % of sporangia caducous; in *P. proliferata* (= 25 % of species) internal proliferation occurring.

Fig. 62), and are generally consistent with the climate a species will experience in its native habitat (*cf.* Notes on the evolution of lifestyle and adaptive traits in Clade 2, above).

Since many of the Clade 2 species examined here were obtained via soil and water baiting in the absence of evident symptoms on local non-woody plants or trees, one can only infer their lifestyles indirectly from their properties *in vitro* and by analogy with similar but behaviourally better-understood taxa in this and other *Phytophthora* clades (*cf.* Brasier *et al.* 2022). On this basis, trends towards 'lifestyle specialisation' within the different subclades can be suggested. In Clade 2a, compared to the other subclades more of the species (~58 %) have an A1/A2 system implying potentially greater outcrossing (Table 5), and 2a also has by far the highest frequency of species with fully or partly caducous sporangia (~79 %; Table 7). This suggests a trend towards being adapted for more heterogeneous environments

and for aerial dispersal and infection. As three species fitting this pattern, *i.e*., *P. botryosa*, *P. colocasiae* and *P. meadii*, are damaging pathogens of tree crops, this combination of characters may also indicate a higher biosecurity risk. Clade 2b is more variable than Clade 2a in many characteristics but also has a relatively high frequency of outcrossing taxa (8 species = 44 %). Within the latter, a degree of specialisation is again indicated, as six of them (75 %) produce caducous sporangia. In contrast, among the ten self-fertile Clade 2b species the majority (70 %) are non-caducous or rarely caducous. Therefore, two somewhat divergent 'lifestyle specialisation' trends may have occurred in Clade 2b. While the more numerically limited Clade 2e also has a mixture of taxa with self-fertile (~67 %) and A1/A2 (~33 %) systems, in this case only one of the known taxa, the A1/A2 *P. frigida*, is caducous (Maseko *et al.* 2007). Clade 2c is particularly distinctive. All 24 species are self-fertile, and all have non-caducous or 'rarely caducous' sporangia. This suggests adaptation for survival in more uniform environments in association with a mainly soil-inhabiting and root-infecting lifestyle. If correct, then this evolutionary 'strategy' may have been so successful that it has been conserved throughout the migration and radiation of Clade 2c into North America, southern Africa and East and Southeast Asia. Its success is also indicated by the later diverged Clade 2g whose known members are in all aspects effectively 'Clade 2c look-alikes'. The five known taxa in Clade 2f are also intrinsically self-fertile, but form sporangia that, while non-caducous, are mostly nonpapillate and internally proliferating. Currently, this is the only Clade 2 subclade in which this type of sporangium, possibly an adaptation for rapid sequential production of sporangia in water, occurs. This subclade could therefore be adapted to relatively environmentally stable riparian conditions. Overall, the above trends are an indication of considerable lifestyle fluidity across Clade 2 as a whole, probably comparable in breadth to that in *Phytophthora* Clade 10 (see Jung *et al.* 2022).

Regarding the species with an A1/A2 breeding system in Clade 2, certain lifestyle features stand out. First, most of these species, together with one sterile species (*P. theobromicola*), were found to produce chlamydospores, but no chlamydospores were formed by any of the self-fertile species (Tables 5, S4–S17). This suggests chlamydospores are an important mode of survival for some outcrossing taxa under adverse environmental conditions or when the other compatibility type is 'absent'. Second, the antheridia formed by the A1/A2 species are consistently amphigynous, whereas those formed by the self-fertile taxa vary (Table 6). This tight association of amphigyny with the A1/A2 breeding system is found across the genus, but the reason has yet to be determined. It could, for example, be associated with delaying or controlling the mixing of cytoplasm between divergent genotypes (*cf*. Brasier 1983). Some of the species in Clade 2 that produce amphigynous antheridia but are self-fertile and potentially more inbreeding (notably subclade 2b, Table 6) may have evolved from outcrossing species, *i.e.* they may be 'secondarily homothallics' (*cf*. Brasier 1992).

Thirdly, it is also notable that Clade 2a has a relatively high frequency of sterile species (4 species, ~21 %). These include the economically important *P. citrophthora* and *P. pseudocitrophthora*, some isolates of which are silent A1s or A2s; *P.* ×*lusitanica* with all known isolates being silent A2s; and *P. vietnamensis* (which was initially recorded here as a silent A1 but later lost the ability to induce gametangial formation in *P. meadii* A2; Table S4, this study). In addition, two informally described outcrossing Clade 2a taxa, *P*. taxon germisporangia and *P*. taxon awatangi, are exclusively of A1 and A2 type, respectively (Dang *et al.* 2021). Collectively, this suggests the sterility of some Clade 2a taxa has resulted from the degeneration or loss of a previously functioning A1/A2 system, perhaps due to changes in environmental conditions favouring clonal or asexual spread, such as colonisation of a novel host or another disturbance event (*cf*. Brasier & Hansen 1992, Brasier 1995). This may also apply to *P. tropicalis* (Clade 2b), in which both outcrossing and sterile isolates occur (Aragaki & Uchida 2001).

Furthermore, within Clade 2a, some single isolates of the Clade 2a taxa *P. colocasiae* and *P. meadii* are not only of A1 or A2 type but are also partially self-fertile (Erwin & Ribeiro 1996, Feng *et al.* 2022). This may occur when an A1 or an A2 isolate carries an extra chromosome of the 'opposite' compatibility type as a result of meiotic non-disjunction (*cf*. Sansome 1980); or, in the case of *P. meadii*, a consequence of 'A1 + A2' polyploidy (Sansome *et al.* 1990). Either way, these features reflect the potentially high inbreeding versus outcrossing flexibility of the A1/A2 compatibility system (Brasier 1992).

Interspecific hybridisation has the potential to generate novel variation and rapid evolution in oomycetes and fungi (Brasier 2000a, 2001, Schardle & Craven 2003, Stuckenbrock 2016) and is being increasingly recognised in both true fungi (Newcombe *et al.* 2000, Gonthier *et al.* 2007, Paoletti *et al.* 2006, Brasier *et al.* 2021) and Phytophthoras (Brasier *et al.* 2004, Man in' t Veld *et al.* 2012, Bertier *et al.* 2013, Nagel *et al.* 2013, Burgess 2015, Jung *et al.* 2017b, c, 2018b, 2020, Van Poucke *et al.* 2021, Mullet *et al.* 2023) including the destructive alder dieback pathogen, *P*. ×*alni* (Brasier *et al.* 1999, Husson *et al.* 2015). Introductions and other anthropogenic disturbance events may create opportunities for hybridisation between previously geographically isolated taxa (Brasier 2001). In this study Clade 2a species *P.* ×*lusitanica*, *P.* ×*australasiatica,* and *P*. ×*taiwanensis* were previously identified as species hybrids based on nuclear genotyping by sequencing (Van Poucke *et al.* 2021). This is further supported here by their high mean nuclear heterozygosity levels (0.52, 0.89 and 1.09 %) and, in the case of *P.* ×*lusitanica* and *P.* ×*australasiatica*, a high level of mitochondrial gene identity with another Clade 2a taxon. They were considered confirmed hybrids in this study and formally designated as such.

Another eight taxa in Clade 2a, five in Clade 2b and one in Clade 2f are also proposed here to be some form of hybrid, based on a nuclear heterozygosity level above 0.3 % and in some cases a high level of mitochondrial gene identity with another Clade 2a taxon. Where their nuclear heterozygosity levels were relatively consistent, they were considered probable hybrids. Where their levels were relatively wide-ranging, they were considered ambiguous hybrids. For example, twelve isolates of *P.* ×*vanyenensis* (identified as a hybrid by Dang *et al.* 2021) exhibited a very wide range in heterozygosity from 0.19–0.78 % and might conceivably represent a hybrid swarm including less heterozygous individuals or introgressants closer to a parent species (*cf.* Brasier *et al.* 2021). The same may apply to *P. tropicalis* and several other taxa. However, because of the often limited sample sizes, lack of evidence of nuclear gene homology with more than one species and uncertainty as to whether only limited introgression, full hybridity or a combination of these could be involved, we consider that with the 'probable' and 'ambiguous' taxa stronger proof of hybridity is required. In particular evidence of comparative genome size and the frequency and distribution of multi-allelic loci (*cf*. Van Poucke *et al.* 2021); and where possible clear evidence of direct association with one or more parent species and some indication of whether hybridity is ancient or ongoing.

The increasing emergence or detection of hybridisation processes including hybrid swarms in Phytophthoras is likely to

challenge the utility of species concepts used in classical taxonomic and biosecurity protocols.

If confirmed, the overall number of hybrid taxa in Clades 2a and 2b could be remarkably high: eight out of 21 taxa (38.1 %) in each subclade. This could conceivably reflect high levels of recent anthropogenic disturbance in the geographic areas they inhabit (*cf*. Brasier 2001). Further, all the putative and confirmed hybrid taxa in Clades 2a and 2b have an A1/A2 compatibility system or are sexually sterile, suggesting the A1/ A2 system favours interspecific hybridisation, and that sterility may be a regular product of it; and all are aerial pathogens, suggesting the 'aerial lifestyle' may also favour hybridisation. No hybrids were detected in Clades 2c, 2d, 2e and 2g. and, apart from *P.* taxon aquatilis from Clade 2f, (suggested here as a possible hybrid) the other 56 self-fertile taxa examined across all seven subclades exhibited a nuclear heterogeneity level <0.3 % and none were suspected to be hybrids.

The many characteristics shared across the eleven major *Phytophthora* clades define them as a strongly biologically cohesive and as a relatively tight evolutionary unit (Brasier *et al.* 2022). Within the *Phytophthora* phylogenetic tree however, the 20 downy mildew (DM) genera form two distinct clades, rendering *Phytophthora* paraphyletic (Cooke *et al.* 2000, Runge *et al.* 2011, Jung *et al.* 2017a, Bourret *et al.* 2018, Scanu *et al.* 2021, Brasier *et al.* 2022, Abad *et al.* 2023a) and the DMs polyphyletic. Although proposals have been made to split *Phytophthora* into multiple genera (Runge *et al.* 2011, Crous *et al.* 2021), the high diversity revealed here within Clade 2 alone adds further support to the conclusion that no major morphological or behavioural synapomorphies exist in the individual clades (or groups of clades) that justify naming them as separate genera (Brasier *et al.* 2022). In much the same vein, a century ago Leonian (1925), when he transferred *P. citrophthora* (Clade 2a) from the genus *Pythiacystis* to *Phytophthora*, stated "This organism is so obviously a *Phytophthora* species that the genus *Pythiacystis* is no longer tenable".

Both accurate taxonomy and a correspondingly accurate understanding of the scale of pathogen diversity are needed to underpin modern plant biosecurity. However, pathogen outbreak data indicate these aspirations currently fall well short of global biosecurity needs. For example, the number of forest epidemics and declines associated with *Phytophthora* species globally has increased rapidly from ca five in the 1960s to 41 in 2022, leading to considerable economic and environmental costs (Brasier *et al.* 2022). It is now widely recognised that such outbreaks are often directly or indirectly attributable to importation of exotic pathogens via the international trade in live plants or parts of plants, in particular rooted plants for planting, with disease often amplified in nurseries and spread by subsequent outplanting of infested stock (Jung & Blaschke 2004, Brasier 2008, Jung 2009, Dehnen-Schmutz *et al.* 2010, Drew *et al.* 2010, Liebhold *et al.* 2012, Santini *et al.* 2013, Jung *et al.* 2016, 2018a, Frankel *et al.* 2020, Riddell *et al.* 2020; Sims & Garbelotto 2021, Rossmann *et al.* 2021). The recent arrival of the NA1 lineage of *P. ramorum* in North America (Mascheretti *et al.* 2009) and of the EU2 in Northern Ireland (Van Poucke *et al.* 2012) are probably linked to specialist trade in Asian plants. Findings that European and North American nurseries are infested with numerous exotic *Phytophthora* species further highlight the risks (*e.g.*, MacDonald *et al.* 1994, Themann *et al.* 2002, Schwingle *et al.* 2007, Moralejo *et al.* 2009, Leonberger *et al.* 2013, Bienapfl & Balci 2014, Parke *et al.* 2014, Jung *et al.* 2016, Rooney-Latham *et al.* 2019, Rossmann *et al.* 2021, Mora-Sala *et al.* 2022).

Of further concern is the fact that under current agreements biosecurity protocols are heavily dependent on lists of specifically named threat organisms. In Europe, for example, extensive lists of organisms of concern are collated from scientific journals, the internet and elsewhere by national and trans-national plant health agencies (*cf*. https://gd.eppo.int/; https://planthealthportal.defra.gov.uk/pests-and-diseases/uk-plant-health-risk-register/). Many, perhaps most of these listed organisms have come to attention because they have already spread beyond their natural range and are causing damage to vulnerable hosts. Unfortunately, numerous highly damaging forest disease outbreaks over the past century have been caused by pathogens virtually unknown to science before their introduction (Brasier 2008, Roy *et al.* 2014, Jung *et al.* 2018a). Prominent examples in the early to mid-20th century were the Dutch elm disease and Chestnut blight pathogens (*e.g.*, Gibbs & Wainhouse 1986, Anagnostakis 1987, Brasier 2000b) and among Phytophthoras, *P. cinnamomi, P.* ×*cambivora* and *P. lateralis* (*e.g.*, Day 1938, Tucker & Milbrath 1942, Crandall & Gravatt 1945, Moreau & Moreau 1952, Hansen *et al.* 2000, Hardham 2005, Jung *et al.* 2018a, Mullet *et al.* 2023). More recently, despite advances in taxonomy and molecular detection, these episodes have continued, including outbreaks caused by the European ash dieback pathogen *Hymenoscyphus pseudoalbidus* and the previously 'unknown' Phytophthoras *P. kernoviae*, *P. multivora*, *P. pinifolia*, *P. plurivora* and *P. ramorum* (*e.g.*, Rizzo *et al.* 2002, Brasier *et al.* 2005, Durán *et al.* 2008, Jung & Burgess 2009, Scott *et al.* 2009, Santini *et al.* 2013, Gross *et al.* 2014, Jung *et al.* 2016, 2018a, b, 2021, Migliorini *et al.* 2019, Corcobado *et al.* 2020, Shakya *et al.* 2021, Brasier *et al.* 2022).

In practice, there is a critical lack of data on the scale of unknown pathogen threats. This amounts to a major forest biosecurity evidence gap. To offset this, forest biosecurity practitioners need to be more involved in active scientific intelligence gathering (Brasier 2005), *i.e.*, in proactively assessing both the scale and the quality of the unknown threats. The 43 previously unknown *Phytophthora* Clade 2 species uncovered by the present surveys indicate the numerical scale of the risks. At least 41 of them (95 %) were found in 'healthy' forests with no noticeable disease symptoms, but owing to the sampling protocols used their native hosts are largely unknown. Any one of them could potentially be a threat to naïve or non-coevolved hosts elsewhere in the world. This applies also to the many previously unknown Phytophthoras being discovered in other clades (*e.g.*, Hong *et al.* 2008, 2010, 2012, Yang & Hong 2013, Scanu *et al.* 2015, 2021, Yang *et al.* 2013, 2014a, b, c, 2016, Jung *et al.* 2017b–d, 2018b, 2020, 2022, Burgess *et al.* 2018, Bose *et al.* 2021a, Chen *et al.* 2022).

To assess the quality of the risks posed by these 'new' Clade 2 Phytophthoras (and those in other clades) we suggest the following. Firstly, their pathogenicity and potential host ranges be tested on a standard range of well-characterised, non-coevolved hosts (*e.g.*, *Rhododendron*, *Eucalyptus*, *Fagus*, *Quercus*, *Castanea* and *Chamaecyparis* spp.), with well characterised *Phytophthora* species as controls. In this regard, in one recent pilot test roots of *Fagus sylvatica* and *Castanea sativa* were highly susceptible to 11 and seven exotic Clade 2 species, respectively (T. Corcobado, T. Majek and T. Jung, unpubl. results). A greater emphasis might be placed on testing A1/A2 species which, theoretically at least, could be more adaptable if introduced together; although even highly specialised self-fertile species can be extremely dangerous when introduced elsewhere (*e.g.*, *P. lateralis* on *Chamaecyparis* spp.; Hansen *et al.* 2000). Secondly, now that the geographic origins of some damaging *Phytophthora* species are beginning to be identified through surveys and subsequent population studies (*e.g.*, *P. cinnamomi* in mixed forests in Taiwan and Vietnam, Shakya *et*

al. 2021; *P. kernoviae* in Valdivian rainforests in Chile, Jung *et al.* 2018b, 2022; *P. lateralis* in Taiwanese cedar forests, Brasier *et al.* 2010, 2012; *P. multivora* in South Africa, Tsykun *et al.* 2022; *P. ramorum* in east Asian laurasilva forests, Jung *et al.* 2021; and *P.* ×*cambivora* in mixed broadleaved forests in Japan, Mullet *et al.* 2023), these developments need to be consolidated by research aimed at understanding their role in the ecosystem including their natural hosts and the mechanisms of host resistance.

The results of this study further emphasise the fact that, for *Phytophthora* at least, the number of scientifically unknown taxa is probably very high, with possibly as many as ~200 to 400 species still to be discovered (Brasier 2009). Therefore, with the continued reliance on lists of named threat organisms, global biosecurity will continue to be on the back foot until measures are more focused on regulating the highest risk pathways of plant movement, such as traded plants, plant collecting and even informal plant-associated tourism (*cf*. Liebhold *et al.* 2012, Brockerhoff *et al.* 2014).

CONCLUSIONS

Comprising 79 described species and 14 informally designated taxa, Clade 2 is currently the largest of the 12 recognised *Phytophthora* clades.

The natural biogeography of Clade 2 includes southeastern and eastern Australia; a large belt stretching from India and Nepal via China and Southeast Asia to Taiwan and the Japanese archipelago; South Africa; the Americas extending from Alaska to the south of Chile, the southeast of Brazil and eastern North America from the Atlantic and the Gulf of Mexico to the US Midwest. Particularly diverse Clade 2 hotspots are found in East and Southeast Asia and Central America.

The evolutionary history of Clade 2 appears to have involved pre-Gondwanan divergence of three of the extant subclades 2c, 2e and 2f, all with disjunct natural distributions on separate continents. They comprise species with a soilborne and aquatic lifestyle and, in Clade 2c, a few partially aerial species. Three other extant subclades, 2a, 2b and 2g, appear to be a result of the post-Gondwanan divergence in Southeast/East Asia and South America respectively. Clade 2g has a soilborne root-infecting lifestyle whereas Clade 2b comprises both soil-inhabiting and aerially disseminated species. Clade 2a has evolved further towards an aerial lifestyle, comprising species which are predominantly or partially airborne. Evidence suggests the currently 93 described and informally designated Clade 2 taxa have resulted from both allopatric non-adaptive and sympatric adaptive radiations. In Clades 2a and 2b over 30 % of the taxa may be hybrids and the hybridity appears to be associated with an A1/A2 breeding system and an aerial lifestyle. Overall, Clade 2 exhibits much of the diversity in breeding systems, morphologies and lifestyles seen across the genus as a whole (*cf*. Brasier *et al.* 2022).

The large number of previously unknown *Phytophthora* species being uncovered in surveys of underexplored ecosystems underlines the risk of relying on lists of known organisms in international biosecurity protocols. Pathogenicity and host range tests of many new taxa are needed to assess the level of risk they pose to global forest biosecurity.

ACKNOWLEDGEMENTS

The authors are grateful to the Project Phytophthora Research Centre Reg. No. CZ.02.1.01/0.0/0.0/15_003/0000453 co-financed by the Czech Ministry for Education, Youth and Sports and the European Regional Development Fund, the Portuguese Science and Technology Foundation (FCT) for co-financing the European BiodivERsA project RESIPATH: Responses of European Forests and Society to Invasive Pathogens (BIODIVERSA/0002/2012) and for financing the Exploratory Project EXPL/AGR-FOR/1304/2012 'Screening of Asian oak species for potential resistance to *Phytophthora* spp.' (QuerResist), the European Union's Horizon 2020 research and innovation programme for financing under grant agreement No. 63564 project POnTE: Pest Organisms Threatening Europe, to the Japanese Society for the promotion of science, KAKEN No. 18H02245, and to Phytophthora Research and Consultancy for co-funding the expeditions to Japan and Taiwan. Travel and subsistence support for C.M.B. was provided by Brasier Consultancy. DNA sequencing of Hungarian, Taiwanese and Chilean isolates was partly supported by the Hungarian Scientific Research Fund (OTKA) grant K101914. This work was in part supported by the U.S. Department of Agriculture, Agricultural Research Service. The authors also thank the administration of the company ARAUCO as the owner of Parque Oncol in Chile, the administration of the company APRIL in Indonesia and the administration of Hoang-Lien National Park in Vietnam for the permission to take samples in their forests. We are grateful to Dr. Atsushi Sakai (FFPRI, Shikoku Research Centre) for his invaluable assistance during the survey in Shikoku, Japan, and to Aneta Bačová, Anna Hýsková, Henrieta Ďatková and Milica Raco (all Mendel University in Brno, Czech Republic), Mariela González and Sebastian Fajardo (both previously Universidad de Concepción), and Diána Seress (HUN-REN CAR, Plant Protection Institute, Hungary) for much appreciated technical support.

DECLARATION ON CONFLICT OF INTEREST

The authors declare that there is no conflict of interest.

REFERENCES

Abad ZG, Abad JA, Coffey MD, *et al.* (2008). *Phytophthora bisheria sp. nov*., a new species identified in isolates from the Rosaceous raspberry, rose and strawberry in three continents. *Mycologia* **100**: 99–110.

Abad ZG, Burgess TI, Bourret T, *et al*. (2023a). *Phytophthora*: taxonomic and phylogenetic revision of the genus. *Studies in Mycology* **106**: 259–348.

Abad ZG, Burgess TI, Redford AJ, *et al.* (2023b). *IDphy*: An international online resource for molecular and morphological identification of *Phytophthora* based on type specimens. *Plant Disease* **107**: 987–998.

Abad ZG, Ivors K, Gallup CA, *et al.* (2011). Morphological and molecular characterization of *Phytophthora glovera sp. nov*. from tobacco in Brazil. *Mycologia* **103**: 341–350.

Adams GC, Catal M, Trummer L (2010). Distribution and severity of alder *Phytophthora* in Alaska. In: *Proceedings of the Sudden Oak Death Fourth Science Symposium* (Frankel SJ, Kliejunas T, Palmieri KM, eds). USDA Forest Service, Albany, California, USA. General Technical Report PSW-GTR-229: 29–49.

Aguayo J, Adams GC, Halkett F, *et al.* (2013). Strong genetic differentiation between North American and European populations of *Phytophthora alni* subsp. *uniformis*. *Phytopathology* **103**: 190–199.

Albuquerque Alves TC, Tessmann DJ, Ivors KL, *et al.* (2016). First report of gummosis caused by *Phytophthora frigida* on Black wattle in Brazil. *Plant Disease* **100**: 2336.

Albuquerque Alves TC, Tessmann DJ, Ivors KL, *et al.* (2019). *Phytophthora acaciae sp. nov*., a new species causing gummosis of Black wattle in Brazil. *Mycologia* **111**: 445–455.

Alvarez LA, Vicent A, De la Roca E, *et al.* (2008). Branch cankers on citrus trees in Spain caused by *Phytophthora citrophthora*. *Plant Pathology* **57**: 84–91.

Anagnostakis SL (1987). Chestnut blight: The classical problem of an introduced pathogen. *Mycologia* **79**: 23–37.

Ann P-J, Huang J-H, Tsai J-N, *et al.* (2016). Morphological, molecular and pathological characterization of *Phytophthora amaranthi sp. nov*. from amaranth in Taiwan. *Journal of Phytopathology* **164**: 94–101.

Ann PJ, Kao CW, Ko WH (1986). Mating-type distribution of *Phytophthora colocasiae* in Taiwan. *Mycopathologica* **93**: 193–194.

Antonelli A, Sanmartín I (2011). Why are there so many plant species in the Neotropics? *Taxon* **60**: 403–414.

Aragaki M, Uchida JY (2001). Morphological distinctions between *Phytophthora capsici* and *P. tropicalis sp. nov*. *Mycologia* **93**: 137–145.

Armesto J, Villagrán C, Arroyo MTK (1995). *Ecología de los bosques nativos de Chile*. Santiago: Editorial Universitaria.

Averyanov LV, Loc PK, Hiep NT, *et al.* (2003). Phytogeographic review of Vietnam and adjacent areas of Eastern Indochina. *Komarovia* **3**: 1–83.

Axelrod DI, Al-Shehbaz I, Raven PH (1998). History of the modern flora of China. In: *Floristic characteristics and diversity of east Asian plants* (Zhang AL, Wu SG, eds). China Higher Education Press/Springer, Beijing: 43–55.

Bacon CD, Silvestro D, Jaramillo C, *et al.* (2015). Biological evidence supports an early and complex emergence of the Isthmus of Panama. *Proceedings of the National Academy of Sciences of the USA* **112**: 6110–6115.

Bai RS, Thomas J (2000). Phytophthora rot - a new disease of vanilla (*Vanilla planifolia* Andrews) in India. *Journal of Spices and Aromatic Crops* **9**: 73–75.

Bandelt H-J, Forster P, Röhl A (1999). Median-joining networks for inferring intraspecies phylogenies. *Molecular Biology and Evolution* **16**: 37–48.

Baskin JM, Baskin CC (2016). Origins and relationships of the mixed mesophytic forest of Oregon-Idaho, China, and Kentucky: Review and synthesis. *Annals of the Missouri Botanical Garden* **101**: 525–552.

Bennett RM, Dedeles GR, Thines M (2017). *Phytophthora elongata* (*Peronosporaceae*) is present as an estuarine species in Philippine mangroves. *Mycosphere* **8**: 959–967.

Bertier L, Leus L, D'hondt L, *et al.* (2013). Host adaptation and speciation through hybridization and polyploidy in *Phytophthora*. *PLoS ONE* **8**: e85385.

Bezuidenhout CM, Denman S, Kirk SA, *et al.* (2010). *Phytophthora* taxa associated with cultivated *Agathosma*, with emphasis on the *P. citricola* complex and *P. capensis sp. nov*. *Persoonia* **25**: 32–49.

Bienapfl JC, Balci Y (2014). Movement of *Phytophthora* spp. in Maryland's nursery trade. *Plant Disease* **98**: 134–144.

Bilodeau GJ, Martin FN, Coffey MD, *et al.* (2014). Development of a multiplex assay for genus- and species-specific detection of *Phytophthora* based on differences in mitochondrial gene order. *Phytopathology* **104**: 733–748.

Blackwell E (1949). Terminology in *Phytophthora*. The Commonwealth Mycological Institute, Kew, Surrey, UK. *Mycological Papers* **30**: 24.

Blair JE, Coffey MD, Park S-Y, *et al.* (2008). A multi-locus phylogeny for *Phytophthora* utilizing markers derived from complete genome sequences. *Fungal Genetics and Biology* **45**: 266–277.

Bogarín D, Pupulin F, Smets E, *et al.* (2016). Evolutionary diversification and historical biogeography of the *Orchidaceae* in Central America with emphasis on Costa Rica and Panama. *Lankesteriana* **16**: 189–200.

Bose T, Hammerbacher A (2023). The first report of *Phytophthora multivesiculata* causing black rot of *Cymbidium* and *Ansellia africana* from South Africa. *Plant Disease* **107**: 588.

Bose T, Hulbert JM, Burgess TI, *et al.* (2021a). Two novel *Phytophthora* species from the southern tip of Africa. *Mycological Progress* **20**: 755–767.

Bose T, Wingfield MJ, Roux J, *et al.* (2018). Community composition and distribution of *Phytophthora* species across adjacent native and non-native forests of South Africa. *Fungal Ecology* **36**: 17–25.

Bose T, Wingfield MJ, Roux J, *et al.* (2021b). *Phytophthora* species associated with roots of native and non-native trees in natural and managed forests. *Microbial Ecology* **81**: 122–133.

Bouckaert R, Drummond A (2017). bModelTest: Bayesian phylogenetic site model averaging and model comparison. *BMC Evolutionary Biology* **17**: 42.

Bouckaert R, Heled J, Kühnert D, *et al.* (2014). BEAST 2: A software platform for bayesian evolutionary analysis. *PLoS Computational Biology* **10**: e1003537.

Bourret TB, Choudhury RA, Mehl HK, *et al.* (2018). Multiple origins of downy mildews and mito-nuclear discordance within the paraphyletic genus *Phytophthora*. *PLoS ONE* **13**: e0192502.

Bowers JH, Martin FN, Tooley PW, *et al.* (2007). Genetic and morphological diversity of temperate and tropical isolates of *Phytophthora capsici*. *Phytopathology* **97**: 492–503.

Brasier CM (1967). *Physiology of reproduction in Phytophthora*. PhD Thesis, University of Hull, UK.

Brasier CM (1971). Induction of sexual reproduction in single A2 isolates of *Phytophthora* species by *Trichoderma viride*. *Nature* **231**: 283.

Brasier CM (1978). Stimulation of oospore formation in *Phytophthora* by antagonistic species of *Trichoderma* and its ecological implications. *Annals of Applied Biology* **89**: 135–139.

Brasier CM (1983). Problems and prospects in *Phytophthora* research. In: *Phytophthora: Its biology, taxonomy, ecology and pathology* (Erwin DC, Bartnicki-Garcia S, Tsao PH, eds). American Phytopathological Society, St. Paul, Minnesota, USA: 353–364.

Brasier CM (1986). The dynamics of fungal speciation. In: *Evolutionary biology of the fungi* (Rayner ADM, Brasier CM, Moore D, eds). Cambridge University Press, Cambridge, UK: 231–260.

Brasier CM (1990). China and the origins of Dutch elm disease: An appraisal. *Plant Pathology* **39**: 5–16.

Brasier CM (1992). Evolutionary biology of *Phytophthora*. Part I: Genetic system, sexuality and the generation of variation. *Annual Review of Phytopathology* **30**: 153–171.

Brasier CM (1995). Episodic selection as a force in fungal microevolution with special reference to clonal speciation and hybrid introgression. *Canadian Journal of Botany* **73**: 1213–1221.

Brasier CM (2000a). Rise of the hybrid fungi. *Nature* **405**: 134–135.

Brasier CM (2000b). Intercontinental spread and continuing evolution of the Dutch elm disease pathogens. In: *The elms: Breeding, conservation and disease management* (Dunne CP, ed.). Kluwer Academic Publishers, Boston, USA: 61–72.

Brasier CM (2001). Rapid evolution of introduced plant pathogens via interspecific hybridization. *Bioscience* **51**: 123–133.

Brasier CM (2005). Preventing invasive pathogens: deficiencies in the system. *The Plantsman (new series)* **4**: 54–57.

Brasier CM (2008). The biosecurity threat to the UK and global environment from international trade in plants. *Plant Pathology* **57**: 792–808.

Brasier CM (2009). *Phytophthora* biodiversity: How many *Phytophthora* species are there? In: *Phytophthoras in Forests and Natural Ecosystems: Fourth Meeting of the International Union of Forest Research Organizations (IUFRO) Working Party S07.02.09* (Goheen EM, Frankel SJ, eds). USDA Forest Service, Pacific Southwest Research Station, Albany, California. General Technical Report PSW-GTR-221: 101–115.

Brasier CM, Griffin MJ (1979). Taxonomy of *Phytophthora palmivora* on cocoa. *Transactions of the British Mycological Society* **72**: 111–143.

Brasier CM, Rayner ADM (1987). Whither terminology below the species level in the fungi? In: *Evolutionary biology of the fungi* (Rayner ADM, Brasier CM, Moore D, eds). Cambridge University Press, Cambridge, UK: 379–388.

Brasier CM, Webber J (2010). Sudden larch death. *Nature* **466**: 824–825.

Brasier CM, Beales PA, Kirk SA, *et al.* (2005). *Phytophthora kernoviae sp. nov*. an invasive pathogen causing bleeding stem lesions on forest trees and foliar necrosis of ornamentals in Britain. *Mycological Research* **109**: 853–859.

Brasier CM, Cooke DEL, Duncan JM (1999). Origins of a new *Phytophthora* pathogen through interspecific hybridisation. *Proceedings of the National Academy of Sciences of the USA* **96**: 5878–5883.

Brasier CM, Cooke DEL, Duncan JM, *et al.* (2003). Multiple new phenotypic taxa from trees and riparian ecosystems in *Phytophthora gonapodyides – P. megasperma* ITS Clade 6, which tend to be high-temperature tolerant and either inbreeding or sterile. *Mycological Research* **107**: 277–290.

Brasier CM, Franceschini S, Forster J, *et al.* (2021). Enhanced outcrossing, directional selection and transgressive segregation drive evolution

of novel phenotypes in hybrid swarms of the Dutch Elm Disease pathogen *Ophiostoma novo-ulmi*. *Journal of Fungi* **7**: 452.

Brasier CM, Franceschini S, Vettraino AM, *et al.* (2012). Four phenotypically and phylogenetically distinct lineages in *Phytophthora lateralis*. *Fungal Biology* **116**: 1232–1249.

Brasier CM, Kirk SA, Delcan J, *et al.* (2004). *Phytophthora alni sp. nov*. and its variants: designation of emerging heteroploid hybrid pathogens spreading on *Alnus* trees. *Mycological Research* **108**: 1172–1184.

Brasier C, Scanu B, Cooke D, *et al.* (2022). *Phytophthora*: an ancient, historic, biologically and structurally cohesive and evolutionarily successful generic concept in need of preservation. *IMA Fungus* **13**: 12.

Brasier CM, Vettraino AM, Chang TT, *et al.* (2010). *Phytophthora lateralis* discovered in an old growth *Chamaecyparis* forest in Taiwan. *Plant Pathology* **59**: 595–603.

Brazee NJ, Wick RL, Hulvey JP (2016). *Phytophthora* species recovered from the Connecticut River Valley in Massachusetts, USA. *Mycologia* **108**: 6–19.

Brazee NJ, Yang X, Hong CX (2017). *Phytophthora caryae sp. nov*., a new species recovered from streams and rivers in the eastern United States. *Plant Pathology* **66**: 805–817.

Brikiatis L (2016). Late Mesozoic North Atlantic land bridges. *Earth-Science Reviews* **159**: 47–57.

Brockerhoff EG, Kimberley M, Liebhold AM, *et al.* (2014). Predicting how altering propagule pressure changes establishment rates of biological invaders across species pools. *Ecology* **95**: 594–601.

Burgess TI (2015). Molecular characterization of natural hybrids formed between five related indigenous Clade 6 *Phytophthora* species. *PLoS ONE* **10**: e0134225.

Burgess TI, Simamora AV, White D, *et al.* (2018). New species from *Phytophthora* Clade 6a: evidence for recent radiation. *Persoonia* **41**: 1–17.

Burgess TI, Dang QN, Le BV, *et al.* (2020). *Phytophthora acaciivora sp. nov*. associated with dying *Acacia mangium* in Vietnam. *Fungal Systematics and Evolution* **6**: 243–252.

Burgess TI, White D, McDougall KM, *et al.* (2017). Distribution and diversity of *Phytophthora* across Australia. *Pacific Conservation Biology* **23**: 1–13.

Burgess TI, Edwards J, Drenth A, *et al.* (2021). Current status of *Phytophthora* in Australia. *Persoonia* **47**: 151–177.

Bush MB, Colinvaux PA (1990). A pollen record of a complete glacial cycle from lowland Panama. *Journal of Vegetation Science* **1**: 105–118.

Bush MB, Correa-metrio AY, Hodell DA, *et al.* (2009). Re-evaluation of climate change in lowland Central America during the Last Glacial Maximum using new sediment cores from Lake Petén Itzá, Guatemala. In: *Past Climate Variability in South America and Surrounding Regions* (Vimeux F, Sylvestre F, Khodri M, eds). *Developments in Paleoenvironmental Research* **14**, Springer, Dordrecht: 113–128.

Cannon CH, Morley RJ, Bush AB (2009). The current refugial rainforests of Sundaland are unrepresentative of their biogeographic past and highly vulnerable to disturbance. *Proceedings of the National Academy of Sciences of the USA* **106**: 11188–11193.

Cassens I, Mardulyn P, Milinkovitch MC (2005). Evaluating intraspecific "network" construction methods using simulated sequence data: Do existing algorithms outperform the Global Maximum Parsimony approach? *Systems Biology* **54**: 363–372.

Cerqueira AO, Luz EDMN, De Souza JT (2006). First record of *Phytophthora tropicalis* causing leaf blight and fruit rot on breadfruit in Brazil. *Plant Pathology* **55**: 296.

Chang-Fu H, Chung-Fu S, Kuoh-Cheng Y (1994). Introduction to the flora of Taiwan, 3: floristics, phytogeography, and vegetation. In: *Flora of Taiwan*. 2nd edition. Editorial Committee of the Flora of Taiwan Second Edition, Taipei, Republic of China: 7–18. https://tai2.ntu.edu.tw/ebooks/FlTaiwan2nd/1.

Chávez-Ramírez B, Rodríguez-Velázquez ND, Chávez-Sánchez ME, *et al.* (2021). Morphological and molecular identification of *Phytophthora tropicalis* causing black pod rot in Mexico. *Canadian Journal of Plant Pathology* **43**: 670–679.

Chee KH (1969). Variability of *Phytophthora* species from *Hevea brasiliensis*. *Transactions of the British Mycological Society* **52**: 425–436.

Chen Q, Bakhshi M, Balci Y, *et al.* (2022). Genera of phytopathogenic fungi: GOPHY 4. *Studies in Mycology* **101**: 417–564.

Chern L-L, Ann P-J, Wang I-T (2011). *Cymbidium* black rot caused by an aberrant strain of *Phytophthora multivesiculata* in Taiwan. *Plant Pathology Bulletin* **20**: 1–10.

Chung-Fu S (1994). Introduction to the flora of Taiwan, 2: geotectonic evolution, paleogeography, and the origin of the flora. In: *Flora of Taiwan*. 2nd edition. Editorial Committee of the Flora of Taiwan Second Edition, Taipei, Republic of China: 3–7. https://tai2.ntu.edu.tw/ebooks/FlTaiwan2nd/1.

Cooke DEL, Drenth A, Duncan JM, *et al.* (2000). A molecular phylogeny of *Phytophthora* and related oomycetes. *Fungal Genetics and Biology* **30**: 17–30.

Corcobado T, Cech TL, Brandstetter M, *et al.* (2020). Decline of European beech in Austria: involvement of *Phytophthora* spp. and contributing biotic and abiotic factors. *Forests* **11**: 895.

Corcobado T, Cech TL, Daxer A, *et al.* (2023). *Phytophthora*, *Nothophytophthora* and *Halophytophthora* diversity in rivers, streams and riparian alder ecosystems of Central Europe. *Mycological Progress* **22**: 50.

Crandall BS, Gravatt GF, Ryan MM (1945). Root disease of *Castanea* species and some coniferous and broadleaf nursery stocks, caused by *Phytophthora cinnamomi*. *Phytopathology* **35**: 162–180.

Crous PW, Wingfield MJ, Burgess TI, *et al.* (2017). Fungal Planet description sheets: 558–624. *Persoonia* **38**: 240–384.

Crous PW, Wingfield MJ, Chooij MJ, *et al.* (2020). Fungal Planet description sheets: 1042–1111. *Persoonia* **44**: 301–459.

Crous PW, Rossman AY, Aime MC, *et al.* (2021). Names of phytopathogenic fungi: A practical guide. *Phytopathology* **111**: 1500–1508.

Cunnington JH, de Alwis SK, Priest M (2009). Some notes on *Phytophthora syringae* and *P. multivesiculata* in Australia. *Australasian Plant Disease Notes* **4**: 42–43.

Dang QN, Pham TQ, Arentz F, *et al.* (2021). New *Phytophthora* species in clade 2a from the Asia-Pacific region including a re-examination of *P. colocasiae* and *P. meadii*. *Mycological Progress* **20**: 111–129.

Das AK, Nerkar S, Kumar A, *et al.* (2016). Detection, identification and characterization of *Phytophthora* spp. infecting *Citrus* in India. *Journal of Plant Pathology* **98**: 55–69.

Davis CC, Bell CD, Mathews S, *et al.* (2002). Laurasian migration explains Gondwanan disjunctions: Evidence from *Malpighiaceae*. *Proceedings of the National Academy of Sciences of the USA* **99**: 6833–6837.

Day WR (1938). Root-rot of sweet chestnut and beech caused by species of *Phytophthora*: 1. Cause and symptoms of disease: its relation to soil conditions. *Forestry* **12**: 101–116.

Dehnen-Schmutz K, Holdenrieder O, Jeger MJ, *et al.* (2010). Structural change in the international horticultural industry: some implications for plant health. *Scientia Horticulturae* **125**: 1–15.

Decloquement J, Ramos-Sobrinho R, Elias SG, *et al.* (2021). *Phytophthora theobromicola sp. nov*.: A new species causing black pod disease on cacao in Brazil. *Frontiers in Microbiology* **12**: 537399.

Denk T, Grimm GW (2009). The biogeographic history of beech trees. *Review of Palaeobotany and Palynology* **158**: 83–100.

Dick MA, Dobbie K, Cooke DEL, *et al.* (2006). *Phytophthora captiosa sp. nov*. and *P. fallax sp. nov.* causing crown dieback of *Eucalyptus* in New Zealand. *Mycological Research* **110**: 393–404.

Dick MW (1990). *Keys to Pythium*. University of Reading Press, Reading, UK.

Donahoo RS, Lamour KH (2008a). Characterization of *Phytophthora* species from leaves of nursery woody ornamentals in Tennessee. *HortScience* **43**: 1833–1837.

Donahoo RS, Lamour KH (2008b). Interspecific hybridization and apomixis between *Phytophthora capsici* and *Phytophthora tropicalis*. *Mycologia* **100**: 911–920.

Dos Santos AF (2016). *Phytophthora frigida*. *Forest Phytophthoras* **6**: 10.5399/osu/fp.6.1.3887. http://journalsoregondigital.org/index.php/ForestPhytophthora/article/view/3887/3710

Dos Santos AF, Tessmann DJ, Alves TCA, *et al.* (2011). Root and crown rot of Brazilian pine (*Araucaria angustifolia*) caused by *Phytophthora cinnamomi*. *Journal of Phytopathology* **159**: 194–196.

Douglas J, Zhang R, Bouckaert R (2021). Adaptive dating and fast proposals: revisiting the phylogenetic relaxed clock model. *PLoS Computational Biology* **17(2)**: e1008322.

Drenth A, Guest DI (eds) (2004). Diversity and management of *Phytophthora* in Southeast Asia. Australian Centre for International Agricultural Research, Canberra, Australia.

Drew J, Anderson N, Andow D (2010). Conundrums of a complex vector for invasive species control: a detailed examination of the horticultural industry. *Biological Invasions* **12**: 2837–2851.

Drummond AJ, Ho SYW, Phillips MJ, *et al.* (2006). Relaxed phylogenetics and dating with confidence. *PLoS Biology* **4**: 699–710.

Dunstan WA, Howard K, Hardy GEStJ, *et al.* (2016). An overview of Australia's *Phytophthora* species assemblage in natural ecosystems recovered from a survey in Victoria. *IMA Fungus* **7**: 47–58.

Durán A, Gryzenhout M, Slippers B, *et al.* (2008). *Phytophthora pinifolia sp. nov*. associated with a serious needle disease of *Pinus radiata* in Chile. *Plant Pathology* **57**: 715–727.

Elias S, Brigham-Grette J (2013). Late Pleistocene glacial events in Beringia. In: *Encyclopedia of Quaternary Science* (Elias S, ed.). 2nd edition. Elsevier, Amsterdam, Netherlands: 191–201.

Enzenbacher TB, Naegele RP, Hausbeck MK (2015). Susceptibility of greenhouse ornamentals to *Phytophthora capsici* and *P. tropicalis*. *Plant Disease* **99**: 1808–1815.

Erwin DC, Ribeiro OK (1996). *Phytophthora diseases worldwide*. APS Press, St. Paul, Minnesota, USA.

Feng W, Hieno A, Otsubo K, *et al.* (2022). Emergence of self-fertile *Phytophthora colocasiae* is a possible reason for the widespread expansion and persistence of taro leaf blight in Japan. *Mycological Progress* **21**: 49–58.

Ferguson AJ, Jeffers SN (1999). Detecting multiple species of *Phytophthora* in container mixes from ornamental crop nurseries. *Plant Disease* **83**: 1129–1136.

Fletcher K, Klosterman SJ, Derevnina L, *et al.* (2018). Comparative genomics of downy mildews reveals potential adaptations to biotrophy. *BMC Genomics* **19**: 8–10.

Fletcher K, Gil J, Bertier LD, *et al.* (2019). Genomic signatures of heterokaryosis in the oomycete pathogen *Bremia lactucae*. *Nature Communications* **10**: 1–13.

Foster ZSL, Albornoz FL, Fieland VJ, *et al.* (2022). A new oomycete metabarcoding method using the *rps10* gene. *Phytobiomes Journal* **6**: 214–226.

Frankel SJ, Conforti C, Hillman J, *et al.* (2020). *Phytophthora* introductions in restoration areas: Responding to protect California native flora from human-assisted pathogen spread. *Forests* **11**: 1291.

Garbelotto MM, Frankel S, Scanu B (2018). Soil- and waterborne *Phytophthora* species linked to recent outbreaks in northern California restoration sites. *California Agriculture* **72**: 208–216.

Garbelotto MM, Lee HK, Slaughter G, *et al.* (1997). Heterokaryosis is not required for virulence of *Heterobasidion annosum*. *Mycologia* **89**: 92–102.

Gerlach WWP, Schubert R (2001). A new wilt of *Cyclamen* caused by *Phytophthora tropicalis* in Germany and the Netherlands. *Plant Disease* **85**: 334.

Ghimire SR, Richardson PA, Kong P, *et al.* (2011). Distribution and diversity of *Phytophthora* species in nursery irrigation reservoir adopting water recycling system during winter months. *Journal of Phytopathology* **159**: 713–719.

Gibbs JN (1978). Intercontinental epidemiology of Dutch elm disease. *Annual Revue of Phytopathology* **16**: 287–307.

Gibbs JN, Wainhouse D (1986). Spread of forest pests and pathogens in the northern hemisphere. *Forestry* **59**: 141–153.

Ginetti B, Moricca S, Squires JN, *et al.* (2014). *Phytophthora acerina sp. nov*., a new species causing bleeding cankers and dieback of *Acer pseudoplatanus* trees in planted forests in Northern Italy. *Plant Pathology* **63**: 858–876.

Ginetti B, Ragazzi A, Carmignani S, *et al.* (2015). Collar rot and crown wilting by *Phytophthora pachypleura* on *Aucuba japonica* in Italian nurseries. *Plant Disease* **99**: 1860.

Givnish TJ (1997). Adaptive radiation and molecular systematics: aims and conceptual issues. In: *Molecular evolution and adaptive radiation* (Givnish TJ, Systma KJ, eds). Cambridge University Press, New York, USA: 1–54.

Givnish TJ (2015). Adaptive radiation versus 'radiation' and 'explosive diversification': why conceptual distinctions are fundamental to understanding evolution. *New Phytologist* **207**: 297–303.

Gladenkov AX, Oleinik AE, Marincovich L, *et al.* (2002). A refined age for the earliest opening of Bering Strait. *Palaeogeography, Palaeoclimatology, Palaeoecology* **183**: 321–328.

Gonthier P, Nicolotti G, Linzer R, *et al.* (eds) (2007). Invasion of European pine stands by a North American forest pathogen and its hybridization with a native interfertile taxon. *Molecular Ecology* **16**: 1389–1400.

Gower DJ, Johnson KG, Richardson JE, *et al.* (eds) (2012). *Biotic evolution and environmental change in Southeast Asia*. The Systematics Association Special Volume Series, Cambridge University Press, New York, USA.

Graham JH, Menge JA (2000). *Phytophthora*-induced diseases. In: *Compendium of Citrus Diseases*. 2nd edition. APS Press, St Paul, MN, USA: 12–15.

Granke L, Quesada-Ocampo L, Hausbeck M (2013). *Phytophthora capsici* in the Eastern USA. In: *Phytophthora a global perspective* (Lamour K, ed.). CABI, Wallingford, UK: 96–103.

Granke LL, Quesada-Ocampo L, Lamour K, *et al.* (2012). Advances in research on *Phytophthora capsici* on vegetable crops in the United States. *Plant Disease* **96**: 1588– 1600.

Gross A, Holdenrieder O, Pautasso M, *et al.* (2014). *Hymenoscyphus pseudoalbidus*, the causal agent of European ash dieback. *Molecular Plant Pathology* **15**: 5–21.

Hall R (2017). Southeast Asia: New views of the geology of the Malay archipelago. *Annual Review of Earth and Planetary Sciences* **45**: 331–358.

Hansen EM, Goheen DJ, Jules ES, *et al.* (2000). Managing Port-Orford-cedar and the introduced pathogen *Phytophthora lateralis*. *Plant Disease* **84**: 4–14.

Hansen EM, Reeser PW, Sutton W (2012). *Phytophthora* beyond agriculture. *Annual Review of Phytopathology* **50**: 359–378.

Hardham AR (2005). *Phytophthora cinnamomi*. *Molecular Plant Pathology* **6**: 589–604.

Harzhauser M, Kroh H, Mandic O, *et al.* (2007). Biogeographic responses to geodynamics: A key study all around the Oligo–Miocene Tethyan Seaway. *Zoologischer Anzeiger* **246**: 241–256.

Heaney LR (1991). A synopsis of climatic and vegetational change in Southeast Asia. *Climatic Change* **19**: 53–61.

Henricot B, Pérez-Sierra A, Jung T (2014). *Phytophthora pachypleura sp. nov*., a new species causing root rot of *Aucuba japonica* and other ornamentals in the United Kingdom. *Plant Pathology* **63**: 1095–1109.

Hill C (2004). First report of *Phytophthora multivesiculata* on *Cymbidium* orchids in New Zealand. *Australasian Plant Pathology* **33**: 603–604.

Hinojosa LF, Armesto JJ, Villagrán C (2006). Are Chilean coastal forests pre-Pleistocene relicts? Evidence from foliar physiognomy, palaeoclimate, and phytogeography. *Journal of Biogeography* **33**: 331–341.

Holt B, Lessard JP, Borregaard MK (2013). An update of Wallace's zoogeographic regions of the world. *Science* **339**: 74–78.

Hong CX, Gallegly ME, Browne GT, *et al.* (2009). The avocado subgroup of *Phytophthora citricola* constitutes a distinct species, *Phytophthora mengei sp. nov*. *Mycologia* **101**: 833–840.

Hong CX, Gallegly ME, Richardson PA, *et al.* (2011). *Phytophthora pini* Leonian resurrected to distinct species status. *Mycologia* **103**: 351–360.

Hong C, Gallegly ME, Richardson PA, *et al.* (2008). *Phytophthora irrigata*, a new species isolated from irrigation reservoirs and rivers in Eastern United States of America. *FEMS Microbiology Letters* **285**: 203–211.

Hong CX, Gallegly ME, Richardson PA, *et al.* (2010). *Phytophthora hydropathica*, a new pathogen identified from irrigation water, *Rhododendron catawbiense* and *Kalmia latifolia*. *Plant Pathology* **59**: 913–921.

Hong CX, Richardson PA, Hao W, *et al.* (2012). *Phytophthora aquimorbida sp. nov*. and *Phytophthora* taxon 'aquatilis' recovered from irrigation reservoirs and a stream in Virginia, USA. *Mycologia* **104**: 1097–1108.

Hope G (2001). Environmental change in the late Pleistocene and later Holocene at Wanda Site, Soroako, South Sulawesi, Indonesia. *Palaeogeography, Palaeoclimatology, Palaeoecology* **171**: 129–145.

Hope G, Kershaw AP, van der Kaars S, *et al.* (2004). History of vegetation and habitat change in the Austral-Asian region. *Quaternary International* **118–119**: 103–126.

Hopple JS, Vilgalys R (1994). Phylogenetic relationships among coprinoid taxa and allies based on data from restriction site mapping of nuclear rDNA. *Mycologia* **86**: 96–107.

Hu J, Shrestha S, Zhou Y, *et al.* (2020). Dynamic extreme aneuploidy (DEA) in the vegetable pathogen *Phytophthora capsici* and the potential for rapid asexual evolution. *PLoS ONE* **15**: e0227250.

Huai WX, Tian G, Hansen EM, *et al.* (2013). Identification of *Phytophthora* species baited and isolated from forest soil and streams in northwestern Yunnan province, China. *Forest Pathology* **43**: 87–103.

Hüberli D (1995). *Analysis of variability among isolates of Phytophthora cinnamomi Rands from Eucalyptus marginata Donn ex Sm. and E. calophylla R. Br. based on cultural characteristics, sporangia and gametangia morphology, and pathogenicity*. Bachelor thesis. Murdoch University, Murdoch, Australia.

Hüberli D, Hardy GEStJ, White D, *et al.* (2013). Fishing for *Phytophthora* from Western Australia's waterways: a distribution and diversity survey. *Australasian Plant Pathology* **42**: 251–260.

Hubert F, Grimm GW, Jousselin E, *et al.* (2014). Multiple nuclear genes stabilize the phylogenetic backbone of the genus *Quercus*. *Systematics and Biodiversity* **12**: 405–423.

Hueck K (1966). *Die Wälder Südamerikas* ('*The forests of South America*'). Gustav Fischer, Stuttgart, Germany.

Huntley B (1993). Species-richness in north-temperate zone forests. *Journal of Biogeography* **20**: 163–180.

Husson C, Aguayo J, Revellin C, *et al.* (2015). Evidence for homoploid speciation in *Phytophthora alni* supports taxonomic reclassification in this species complex. *Fungal Genetics and Biology* **77**: 12–21.

Ilieva E, Man In't Veld WA, Veenbaas-Rijks W, *et al.* (1998). *Phytophthora multivesiculata*, a new species causing rot in *Cymbidium*. *European Journal of Plant Patholo*gy **104**: 677–684.

Jankowiak R, Stępniewska H, Bilański P, *et al.* (2014). Occurrence of *Phytophthora plurivora* and other *Phytophthora* species in oak forests of southern Poland and their association with site conditions and the health status of trees. *Folia Microbiologica* **59**: 531–542.

Jayasekera AU, McComb JA, Shearer BL, *et al.* (2007). *In planta* selfing and oospore production of *Phytophthora cinnamomi* in the presence of *Acacia pulchella*. *Mycological Research* **111**: 355–362.

Jung T (2009). Beech decline in Central Europe driven by the interaction between *Phytophthora* infections and climatic extremes. *Forest Pathology* **39**: 73–94.

Jung T, Burgess TI (2009). Re-evaluation of *Phytophthora citricola* isolates from multiple woody hosts in Europe and North America reveals a new species, *Phytophthora plurivora sp. nov*. *Persoonia* **22**: 95–110.

Jung T, Blaschke M (2004). Phytophthora root and collar rot of alders in Bavaria: distribution, modes of spread and possible management strategies. *Plant Pathology* **53**: 197–208.

Jung T, Nechwatal J (2008). *Phytophthora gallica sp. nov*., a new species from rhizosphere soil of declining oak and reed stands in France and Germany. *Mycological Research* **112**: 1195–1205.

Jung T, Balci Y, Broders KD, *et al.* (2023). *Synchrospora gen. nov*., a new *Peronosporaceae* genus with aerial lifestyle from a natural cloud forest in Panama. *Journal of Fungi* **9**: 517.

Jung T, Blaschke H, Neumann P (1996). Isolation, identification and pathogenicity of *Phytophthora* species from declining oak stands. *European Journal of Forest Pathology* **26**: 253–272.

Jung T, Chang TT, Bakonyi J, *et al.* (2017b). Diversity of *Phytophthora* species in natural ecosystems of Taiwan and association with disease symptoms. *Plant Pathology* **66**: 194–211.

Jung T, Colquhoun IJ, Hardy GEStJ (2013b). New insights into the survival strategy of the invasive soilborne pathogen *Phytophthora cinnamomi* in different natural ecosystems in Western Australia. *Forest Pathology* **43**: 266–288.

Jung T, Durán A, Sanfuentes von Stowasser E, *et al.* (2018b). Diversity of *Phytophthora* species in Valdivian rainforests and association with severe dieback symptoms. *Forest Pathology* **48**: e12443.

Jung T, Hansen EM, Winton L, *et al.* (2002). Three new species of *Phytophthora* from European oak forests. *Mycological Research* **106**: 397–411.

Jung T, Horta Jung M, Cacciola SO, *et al.* (2017d). Multiple new cryptic pathogenic *Phytophthora* species from *Fagaceae* forests in Austria, Italy and Portugal. *IMA Fungus* **8**: 219–244.

Jung T, Horta Jung M, Scanu B, *et al.* (2017c). Six new *Phytophthora* species from ITS Clade 7a including two sexually functional heterothallic hybrid species detected in natural ecosystems in Taiwan. *Persoonia* **38**: 100–135.

Jung T, Horta Jung M, Webber JF, *et al.* (2021). The destructive tree pathogen *Phytophthora ramorum* originates from the Laurosilva forests of East Asia. *Journal of Fungi* **7**: 226.

Jung T, Hudler GW, Jensen-Tracy SL, *et al.* (2005). Involvement of *Phytophthora* spp. in the decline of European beech in Europe and the USA. *Mycologist* **19**: 159–166.

Jung T, La Spada F, Pane A, *et al.* (2019). Diversity and distribution of *Phytophthora* species in protected natural areas in Sicily. *Forests* **10**: 259.

Jung T, Milenković I, Corcobado T, Májek T, *et al.* (2022). Extensive morphological and behavioural diversity among fourteen new and seven described species in *Phytophthora* Clade 10 and its evolutionary implications. *Persoonia* **49**: 1– 57.

Jung T, Nechwatal J, Cooke DEL, *et al.* (2003). *Phytophthora pseudosyringae sp. nov*., a new species causing root and collar rot of deciduous tree species in Europe. *Mycological Research* **107**: 772–789.

Jung T, Orlikowski L, Henricot B, *et al.* (2016). Widespread *Phytophthora* infestations in European nurseries put forest, semi-natural and horticultural ecosystems at high risk of Phytophthora diseases. *Forest Pathology* **46**: 134–163.

Jung T, Pérez–Sierra A, Durán A, *et al.* (2018a). Canker and decline diseases caused by soil- and airborne *Phytophthora* species in forests and woodlands. *Persoonia* **40**: 182–220.

Jung T, Scanu B, Bakonyi, J, *et al.* (2017a). *Nothophytophthora gen. nov*., a new sister genus of *Phytophthora* from natural and semi-natural ecosystems. *Persoonia* **39**: 143–174.

Jung T, Scanu B, Brasier CM, *et al.* (2020). A survey in natural forest ecosystems of Vietnam reveals high diversity of both new and described *Phytophthora* taxa including *P. ramorum*. *Forests* **11**: 93.

Jung T, Stukely MJC, Hardy GEStJ, *et al.* (2011). Multiple new *Phytophthora* species from ITS Clade 6 associated with natural ecosystems in Australia: evolutionary and ecological implications. *Persoonia* **26**: 13–39.

Jung T, Vettraino AM, Cech TL, *et al.* (2013a). The impact of invasive *Phytophthora* species on European forests. In: *Phytophthora a global perspective* (Lamour K, ed.). CABI, Wallingford, UK: 146–158.

Katoh K, Standley DM (2013). MAFFT multiple sequence alignment software version 7: improvements in performance and usability. *Molecular Biology and Evolution* **30**: 772–780.

Kenaley SC, Rose C, Sullivan PJ, *et al.* (2014). Bleeding canker of European beech in southeastern New York State: *Phytophthora* species, spatial analysis of disease, and periodic growth of affected trees. *Journal of Environmental Horticulture* **32**: 113–125.

Kim S, de Medeiros BAS, Byun B-K, *et al.* (2018). West meets East: How do rainforest beetles become circum-Pacific? Evolutionary origin of *Callipogon relictus* and allied species (*Cerambycidae*: *Prioninae*) in the New and Old Worlds. *Molecular Phylogenetics and Evolution* **125**: 163–176.

Knaus B, Fieland V, Graham K, *et al.* (2015). Diversity of foliar *Phytophthora* species on *Rhododendron* in Oregon nurseries. *Plant Disease* **99**: 1326–1332.

Ko WH (1979). Mating-type distribution of *Phytophthora colocasiae* on the island of Hawaii. *Mycologia* **71**: 434–437.

Kone A, Kofke DA (2005). Selection of temperature intervals for parallel-tempering simulations. *Journal of Chemical Physics* **122**: 1–2.

Kong JC, Thanh TAV, Yeo FKS, *et al.* (2022). Characterisation of *Phytophthora capsici* causing foot rot of black pepper (*Piper nigrum* L.) in Julau, Sarawak. *Archives of Phytopathology and Plant Protection* **55**: 1686–1712.

Kozak KH, Weisrock DR, Larson R (2006). Rapid lineage accumulation in a non-adaptive radiation: phylogenetic analysis of diversification rates in eastern North American woodland salamanders (*Plethodontidae*: *Plethodon*). *Proceedings of the Royal Society B* **273**: 539–546.

Kozlov A, Darriba D, Flouri T, *et al.* (2019). RAxML-NG: a fast, scalable and user-friendly tool for maximum likelihood phylogenetic inference. *Bioinformatics* **35**: 4453–4455.

Krishnan A, Joseph L, Roy CB (2019). An insight into *Hevea - Phytophthora* interaction: The story of *Hevea* defense and *Phytophthora* counter defense mediated through molecular signalling. *Current Plant Biology* **17**: 33–41.

Kroon LPNM, Bakker FT, van den Bosch GBM, *et al.* (2004). Phylogenetic analysis of *Phytophthora* species based on mitochondrial and nuclear DNA sequences. *Fungal Genetics and Biology* **41**: 766–782.

Lamour K (ed.) (2013). *Phytophthora a global perspective*. CABI, Wallingford, UK: 96 pp.

Lanfear R, Frandsen P, Wright A, *et al.* (2016). PartitionFinder 2: New methods for selecting partitioned models of evolution for molecular and morphological phylogenetic analyses. *Molecular Biology and Evolution* **34**: 772–773.

Lang P, Dane F, Kubisiak TL, *et al.* (2007). Molecular evidence for an Asian origin and a unique westward migration of species in the genus *Castanea* via Europe to North America. *Molecular Phylogenetics and Evolution* **43**: 49–59.

Latham RE, Ricklefs RE (1993). Continental comparison of temperate-zone tree species richness. In: *Species Diversity in Ecological Communities: Historical and Geographical Perspectives* (Ricklefs RE, Schluter D, eds). The University of Chicago Press, Chicago: 294–314.

Laumonier Y (1997). *The vegetation and physiography of Sumatra*. Geobotany book series vol. 22, Springer Science and Business Media, Dordrecht, Germany: 223 pp.

Leahy RM (2006). *Phytophthora Blight of Pothos*. Plant Pathology Circular No. 401, Florida Department of Agriculture & Conservation Services, Division of Plant Industry: 4 pp.

Legeay J, Husson C, Boudier B, *et al.* (2020). Surprising low diversity of the plant pathogen *Phytophthora* in Amazonian forests. *Environmental Microbiology* **22**: 5019–5032.

Lemoine F, Domelevo Entfellner J, Wilkinson E, *et al.* (2018). Renewing Felsenstein's phylogenetic bootstrap in the era of big data. *Nature* **556**: 452–456.

Leonberger AJ, Speers C, Ruhl G, *et al.* (2013). A survey of *Phytophthora* spp. in Midwest nurseries, greenhouses, and landscapes. *Plant Disease* **97**: 635–640.

Leonian LH (1925). Physiological studies on the genus *Phytophthora*. *American Journal of Botany* **12**: 444–498.

Liebhold AM, Brockerhoff EG, Garrett LJ, *et al.* (2012). Live plant imports: the major pathway for forest insect and pathogen invasions of the US. *Frontiers in Ecology and Environment* **10**: 135–143.

Li C, Hongjin D, Hua P (2013). Diversity and distribution of higher plants in Yunnan, China. *Biodiversity Science* **21**: 359–363.

Lilja A, Rytkönen A, Hantula J (2011). Introduced pathogens found on ornamentals, strawberry and trees in Finland over the past 20 years. *Agricultural and Food Science* **20**: 74–85.

Lin MJ, Ko WH (2008). Occurrence of isolates of *Phytophthora colocasiae* in Taiwan with homothallic behavior and its significance. *Mycologia* **100**: 727–734.

Linaldeddu BT, Bregant C, Montecchio L, *et al.* (2020). First report of *Phytophthora acerina*, *P. pini*, and *P. plurivora* causing root rot and sudden death of olive trees in Italy. *Plant Disease* **103**: 996.

Liu AH, Shang J, Zhang JW, *et al.* (2018). Canker and fine-root loss of *Malus sieversii* (Ldb.) Roem. Caused by *Phytophthora plurivora* in Xinjiang Province in China. *Forest Pathology* **48**: e12462.

Liu D-X, Zhao W-X, Xia J-P, *et al.* (2022). First report of root rot caused by *Phytophthora acerina* on *Metasequoia glyptostroboides* in China. *Plant Disease* **106**: 2270.

Lohman DJ, de Bruyn M, Page T, *et al.* (2011). Biogeography of the Indo-Australian Archipelago. *Annual Review of Ecology, Evolution, and Systematics* **42**: 205–226.

Loyd AL, Benson DM, Ivors KL (2014). *Phytophthora* populations in nursery irrigation water in relationship to pathogenicity and infection frequency of *Rhododendron* and *Pieris*. *Plant Disease* **98**: 1213–1220.

Luna Vega I, Ayala OA, Organista DE, *et al.* (1999). Historical relationships of the Mexican cloud forests: a preliminary vicariance model applying Parsimony Analysis of Endemicity to vascular plant taxa. *Journal of Biogeography* **26**: 1299–1305.

Luongo L, Vitale S, Galli M, *et al.* (2016). Morphological and molecular identification of *Phytophthora tropicalis* as causal agent of crown and root rot on *Albizia julibrissin*. *Journal of Phytopathology* **164**: 959–966.

MacDonald JD, Ali-Shtayeh MS, Kabashima J, *et al.* (1994). Occurrence of *Phytophthora* species in recirculated nursery irrigation effluents. *Plant Disease* **78**: 607–611.

MacKinnon K, Hatta G, Halim H, *et al.* (1997). *The Ecology of Kalimantan*. Ecology of Indonesia Series, vol. III, Oxford University Press, Oxford, UK.

MacMahon PJ, Purwantara A (2004). *Phytophthora* on cocoa. In: *Diversity and Management of Phytophthora in Southeast Asia* (Drenth A, Guest DI, eds). Australian Centre for International Agricultural Research, Canberra, Australia: 104–115.

Man in' t Veld WA, Rosendahl KCHM, Hong C (2012). *Phytophthora* x *serendipita sp. nov*. and *P.* x *pelgrandis*, two destructive pathogens generated by natural hybridization. *Mycologia* **104**: 1390–1396.

Man in' t Veld WA, Rosendahl KCHM, van Rijswick PCJ, *et al.* (2015). *Phytophthora terminalis sp. nov*. and *Phytophthora occultans sp. nov*., two invasive pathogens of ornamental plants in Europe. *Mycologia* **107**: 54–65.

Marks GC, Smith IW (1991). *The cinnamon fungus in Victorian forests. History, distribution, management and control*. Lands and Forests Bulletin No. 31, Department of Conservation and Environment, Melbourne, Australia: 33 pp.

Martin FN, Tooley PW (2003). Phylogenetic relationships among *Phytophthora* species inferred from sequence analysis of mitochondrially encoded cytochrome oxidase I and II genes. *Mycologia* **95**: 269–284.

Mascheretti S, Croucher PJ, Vettraino A, *et al.* (2008). Reconstruction of the sudden oak death epidemic in California through microsatellite analysis of the pathogen *Phytophthora ramorum*. *Molecular Ecology* **11**: 2755–2768.

Maseko B, Burgess TI, Coutinho TA, *et al.* (2007). Two new *Phytophthora* species from South African *Eucalyptus* plantations. *Mycological Research* **111**: 1321–1338.

Matsiakh I, Kramarets V, Cleary M (2020). Occurrence and diversity of *Phytophthora* species in declining broadleaf forests in western Ukraine. *Forest Pathology* **51**: e12662.

Mayr E (1942). *Systematics and the origin of species*. Columbia University Press, New York.

McCarthy CGP, Fitzpatrick DA (2017). Phylogenomic reconstruction of the oomycete phylogeny derived from 37 genomes. *mSphere* **2**: e00095-17.

Mchau GRA, Coffey MD (1994). An integrated study of morphology and isozyme patterns found within a worldwide collection of *Phytophthora citrophthora* and a redescription of the species. *Mycological Research* **98**: 1291–1299.

Mchau GRA, Coffey MD (1995). Evidence for the existence of two subpopulations in *Phytophthora capsici* and a redescription of the species. *Mycological Research* **99**: 89–102.

McKenna MC (1983). Cenozoic paleogeography of North Atlantic land bridges. In: *Structure and development of the Greenland-Scotland Ridge* (Bott MHP, Saxov S, Talwani M, *et al.*, eds). Plenum Press, New York: 351–399.

McRae W (1918). *Phytophthora meadii* n. sp. on *Hevea brasiliensis*. *Memoirs of the Department of Agriculture in India. Botanical Series 9*: 219–273.

Meitz-Hopkins JC, Pretorius MC, Spies CFJ (2014). *Phytophthora* species distribution in South African citrus production regions. *European Journal of Plant Pathology* **138**: 733–749.

Michaux B (2010). Biogeology of Wallacea: geotectonic models, areas of endemism, and natural biogeographical units. *Biological Journal of the Linnean Society* **101**: 193–212.

Migliorini D, Khdiar MY, Rodríguez-Padrón C, *et al.* (2019). Extending the host range of *Phytophthora multivora*, a pathogen of woody plants in horticulture, nurseries, urban environments and natural ecosystems. *Urban Forestry & Urban Greening* **46**: 126460.

Milenković I, Keča N, Karadžić D, *et al.* (2012). Incidence of *Phytophthora* species in beech stands in Serbia. *Folia Forestalia Polonica, series A* **54**: 223–232.

Milenković I, Keča N, Karadžić D, *et al.* (2018). Isolation and pathogenicity of *Phytophthora* species from poplar plantations in Serbia. *Forests* **9**: 330.

Miyasaka SC, Lamour K, Shintaku M, *et al.* (2013). Taro leaf blight caused by *Phytophthora colocasiae*. In: *Phytophthora a global perspective* (Lamour K, ed.). CABI, Wallingford, UK: 104–112.

Moralejo E, Pérez-Sierra A, Alvarez LA, *et al.* (2009). Multiple alien *Phytophthora* taxa discovered on diseased ornamental plants in Spain. *Plant Pathology* **58**: 100–110.

Mora-Sala B, León M, Pérez-Sierra A, *et al.* (2022). New reports of *Phytophthora* species in plant nurseries in Spain. *Pathogens* **11**: 826.

Moreau C, Moreau M (1952). Etude mycologique de la maladie de l'encre du chêne. *Revue de Pathologie Vegetale* **31**: 201–231.

Morley JR (2003). Interplate dispersal paths for megathermal angiosperms. *Perspectives in Plant Ecology, Evolution and Systematics* **6**: 5–20.

Mrázková M, Černý K, Tomšovský M, *et al.* (2013). Occurrence of *Phytophthora multivora* and *Phytophthora plurivora* in the Czech Republic. *Plant Protection Science* **49**: 155–164.

Müller N, Bouckaert R (2020). Adaptive parallel tempering for BEAST 2. *bioRxiv* 10.1101/603514.

Mullet MS, Van Poucke K, Haegemann A, *et al.* (2023). Phylogeography and population structure of the global, wide host-range hybrid pathogen *Phytophthora ×cambivora*. *IMA Fungus* **14**: 4.

Myers CW (1969). The ecological geography of cloud forests in Panama. *American Museum Novitates* **2396**: 1–52.

Nagel JH, Gryzenhout M, Slippers B, *et al.* (2013). Characterization of *Phytophthora* hybrids from ITS clade 6 associated with riparian ecosystems in South Africa and Australia. *Fungal Biology* **117**: 329–347.

Nath VS, Senthil M, Hedge VM, *et al.* (2013). Genetic diversity of *Phytophthora colocasiae* isolates in India based on AFLP analysis. *3 Biotech* **3**: 297–305.

Nechwatal J, Hahn J, Schönborn A, *et al.* (2011). A twig blight of understorey European beech (*Fagus sylvatica*) caused by soilborne *Phytophthora* spp. *Forest Pathology* **41**: 493–500.

Nechwatal J, Schubert R, Gerlach WWP (2014). A presumably exotic *Phytophthora* species causing dieback of *Buxus sempervirens* in Germany and Romania. *Journal of Plant Diseases and Protection* **121**: 193–201.

Newcombe G, Stirling B, McDonald S, *et al.* (2000). *Melampsora* x *columbiana,* a natural hybrid of *M. medusae* and *M. occidentalis*. *Mycological Research* **104**: 261–274.

O'Hanlon R, Choiseul J, Corrigan M, *et al.* (2016). Diversity and detections of *Phytophthora* species from trade and nontrade environments in Ireland. *Bulletin OEPP/EPPO Bulletin* **46**: 594–602.

Oh E, Gryzenhout M, Wingfield BD, *et al.* (2013). Surveys of soil and water reveal a goldmine of *Phytophthora* diversity in South African natural ecosystems. *IMA Fungus* **4**: 123–131.

Orlikowski LB, Ptaszek M, Rodziewicz A, *et al.* (2011). *Phytophthora* root and collar rot of mature *Fraxinus excelsior* in forest stands in Poland and Denmark. *Forest Pathology* **41**: 510–519.

Oudemans P, Coffey MD (1991). A revised systematics of twelve papillate *Phytophthora* species based on isozyme analysis. *Mycological Research* **95**: 1025–1046.

Oudemans P, Förster H, Coffey MD (1994). Evidence for distinct isozyme subgroups within *Phytophthora citricola* and close relationships with *P. capsici* and *P. citrophthora*. *Mycological Research* **98**: 189–199.

Pane A, Cacciola SO, Scibetta S, *et al.* (2009). Four *Phytophthora* species causing foot and root rot of apricot in Italy. *Plant Disease* **93**: 844.

Paoletti M, Buck KW, Brasier CM (2006). Selective acquisition of novel mating type and vegetative incompatibility genes via interspecies gene transfer in the globally invading eukaryote *Ophiostoma novo-ulmi*. *Molecular Ecology* **14**: 249–263.

Parke JL, Knaus BJ, Fieland VJ, *et al.* (2014). *Phytophthora* community structure analyses in Oregon nurseries inform systems approaches to disease management. *Phytopathology* **104**: 1052–1062.

Pattengale ND, Alipour M, Bininda-Emonds ORP, *et al. (*2010). How many bootstrap replicates are necessary? *Journal of Computational Biology* **17**: 337–354.

Patil B, Hedge V, Sridhara S, *et al.* (2022). Multigene phylogeny and haplotype analysis reveals predominance of oomycetous fungus, *Phytophthora meadii* (McRae) associated with fruit rot disease of arecanut in India. *Saudi Journal of Biological Sciences* **29**: 103341.

Pérez-Sierra A, Jung T (2013). *Phytophthora* in woody ornamental nurseries. In: *Phytophthora a global perspective* (Lamour K, ed.). CABI, Wallingford, UK: 166–177.

Pérez-Sierra A, Kalantarzadeh M, Sancisi-Frey S, *et al.* (2015). *Phytophthora siskiyouensis* causing stem lesions and cankers on *Alnus incana*. *New Disease Reports* **31**: 17.

Pérez-Sierra A, Horta Jung M, Jung T (2022). Survey and monitoring of *Phytophthora* species in natural ecosystems: Methods for sampling, isolation, purification, storage, and pathogenicity tests. In: *Plant Pathology. Methods in Molecular Biology, vol. 2536* (Luchi N, ed.). Humana, New York, NY, USA: 23–49.

Peries OS, Dantanarayana DM (1965). Compatibility and variation in *Phytophthora* cultures from *Hevea brasiliensis* in Ceylon. *Transactions of the British Mycological Society* **48**: 631–637.

Peries OS, Fernando TM (1966). Studies on the biology of *Phytophthora meadii*. *Transactions of the British Mycological Society* **49**: 311–325.

Piperno DR (2006). Quaternary environmental history and agricultural impact on vegetation in Central America. *Annals of the Missouri Botanical Garden* **93**: 274–296.

Posada D, Crandall KA (2001). Intraspecific gene genealogies: Trees grafting into networks. *Trends in Ecology and Evolution* **16**: 37–45.

Prigigallo MI, Mosca S, Cacciola SO, *et al.* (2015). Molecular analysis of *Phytophthora* diversity in nursery-grown ornamental and fruit plants. *Plant Pathology* **64**: 1308–1319.

Puglisi I, De Patrizio A, Schena L, *et al.* (2017). Two previously unknown *Phytophthora* species associated with brown rot of Pomelo (*Citrus grandis*) fruits in Vietnam. *PLoS ONE* **12**: e0172085.

Puno VI, Laurence MH, Guest DI, *et al.* (2015). Detection of *Phytophthora multivora* in the Wollemi Pine site and pathogenicity to *Wollemia nobilis*. *Australasian Plant Pathology* **44**: 205–215.

Qian H (2002). Floristic relationships between Eastern Asia and North America: Test of Gray's hypothesis. *The American Naturalist* **160**: 317–332.

Quesada-Ocampo LM, Parada-Rojas CH, Hansen Z, *et al.* (2023). *Phytophthora capsici*: Recent progress on fundamental biology and disease management 100 years after its description. *Annual Review of Phytopathology* **61**: 185–208.

Rahman MZ, Uematsu S, Suga H, *et al.* (2015). Diversity of *Phytophthora* species newly reported from Japanese horticultural production. *Mycoscience* **56**: 443–459.

Rajalakshmy VK, Joseph A, Arthassery S (1985). Occurrence of two mating groups in *Phytophthora meadii* causing abnormal leaf fall disease of rubber in South India. *Transactions of the British Mycological Society* **85**: 723–725.

Rambaut A, Drummond A, Xie D, *et al.* (2018). Posterior summarization in Bayesian phylogenetics using Tracer 1.7. *Systematic Biology* **67**: 901–904.

Ramírez Martínez J, Cárdenas Toquica M, Guevara-Suarez M, *et al.* (2021). Oomycete species associated with *Theobroma cacao* crops in Colombia. *Plant Pathology* **70**: 1695–1707.

Rea AJ, Jung T, Burgess TI, *et al.* (2010). *Phytophthora elongata sp. nov*. a novel pathogen from the *Eucalyptus marginata* forest of Western Australia. *Australasian Plant Pathology* **39**: 477–491.

Reeser PW, Hansen EM, Sutton W (2007). *Phytophthora siskiyouensis*, a new species from soil, water, myrtlewood (*Umbellularia californica*) and tanoak (*Lithocarpus densiflorus*) in southwestern Oregon. *Mycologia* **99**: 639–643.

Reeser PW, Sutton W, Hansen EM, *et al.* (2011). *Phytophthora* species in forest streams in Oregon and Alaska. *Mycologia* **103**: 22–35.

Reeser PW, SuttonW, Hansen EM, *et al.* (2012). A new *Phytophthora* species in ITS Clade 2 killing *Ceanothus* grown for rehabilitation of disturbed forest sites. In: *Phytophthora in Forests and Natural Ecosystems, Proceedings of the 6th Meeting of IUFRO Working Party 7.02.09* (Jung T, Brasier CM, Sánchez ME, *et al.*, eds). University of Córdoba, Spain: 104.

Reeves RJ, Jackson RM (1974). Stimulation of sexual reproduction in *Phytophthora* by damage. *Transactions of the British Mycological Society* **84**: 303–310.

Reyes-Tena A, Huguet-Tapia JC, Lamour KH, *et al.* (2019). Genome sequence data of six isolates of *Phytophthora capsici* from Mexico. *Molecular Plant-Microbe Interactions* **32**: 1267–1269.

Richardson JE, Costion CM, Muellner AN (2012). The Malesian floristic interchange: plant migration patterns across Wallace's Line. In: *Biotic evolution and environmental change in Southeast Asia* (Gower DJ, Johnson KG, Richardson JE, *et al.*, eds). The Systematics Association, Special Volume 82, Cambridge University Press, New York, USA: 138–163.

Riddell CE, Dun HF, Elliot M, *et al.* (2020). Detection and spread of *Phytophthora austrocedri* within infected *Juniperus communis* woodland and diversity of co-associated Phytophthoras as revealed by metabarcoding. *Forest Pathology* **50**: e12602.

Rizzo DM, Garbelotto M, Davidson JM, *et al.* (2002). *Phytophthora ramorum* as the cause of extensive mortality of *Quercus* spp. and *Lithocarpus densiflorus* in California. *Plant Disease* **86**: 205–214.

Roberts PD, Urs RR, French-Monar RD, *et al.* (2005). Survival and recovery of *Phytophthora capsici* and oomycetes in tailwater and soil from vegetable fields in Florida. *Annals of Applied Biology* **146**: 351–359.

Robideau GP, De Cock AW, Coffey MD, *et al.* (2011). DNA barcoding of oomycetes with cytochrome c oxidase subunit I and internal transcribed spacer. *Molecular Ecology Resources* **11**: 1002–1011.

Rodríguez-Padrón C, Siverio F, Pérez-Sierra A, *et al.* (2018). Isolation and pathogenicity of *Phytophthora* species and *Phytopythium vexans* recovered from avocado orchards in the Canary Islands, including *Phytophthora niederhauserii* as a new pathogen of avocado. *Phytopathologia Mediterranea* **57**: 89–106.

Rojic SV, Cancino EL (1975). *Phytophthora cinnamomi* Rands and *Ph. citrophthora* (Smith et Smith) Leonian, causal agents of walnut (*Juglans regia*) collar rot in Chile. *Investigación agrícola* **3**: 201.

Rooney-Latham S, Blomquist CL, Kosta KL, *et al.* (2019). *Phytophthora* species are common on nursery stock grown for restoration and revegetation purposes in California. *Plant Disease* **103**: 448–455.

Roos MC, Keßler PJA, Gradstein SR, *et al.* (2004). Species diversity and endemism of five major Malesian islands: diversity–area relationships. *Journal of Biogeography* **31**: 1893–1908.

Rossmann S, Lysøe E, Skogen M, *et al.* (2021). DNA metabarcoding reveals broad presence of plant pathogenic oomycetes in soil from internationally traded plants. *Frontiers in Microbiology* **12**: 637068.

Rovito SM, Vásquez-Almazán CR, Papenfuss CJ, *et al.* (2015). Biogeography and evolution of Central American cloud forest salamanders (*Caudata*: *Plethodontidae*: *Cryptotriton*), with the description of a new species. *Zoological Journal of the Linnean Society* **175**: 150–166.

Roy BA, Alexander HM, Davidson J, *et al.* (2014). Increasing forest loss worldwide from invasive pests requires new trade regulations. *Frontiers in Ecology and the Environment* **12**: 457–465.

Ruano-Rosa D, Schena L, Agosteo GE, *et al.* (2018). *Phytophthora oleae sp. nov*. causing fruit rot of olive in southern Italy. *Plant Pathology* **67**: 1362–1373.

Rull V (2011). Neotropical biodiversity: timing and potential drivers. *Trends in Ecology and Evolution* **26**: 508–513.

Rundell RJ, Price TD (2009). Adaptive radiation, nonadaptive radiation, ecological speciation and nonecological speciation. *Trends in Ecology and Evolution* **24**: 394–399.

Runge F, Telle S, Ploch S, *et al.* (2011). The inclusion of downy mildews in a multi-locus-dataset and its reanalysis reveals a high degree of paraphyly in *Phytophthora*. *IMA Fungus* **2**: 163–171.

Salamone A, Scarito G, Pane A, *et al.* (2011). Root and basal stem rot of rose caused by *Phytophthora citrophthora* in Italy. *Plant Disease* **95**: 358.

Sanogo S, Bosland PW (2013). Biology and management of *Phytophthora capsici* in the South-western USA. In: *Phytophthora a global perspective* (Lamour K, ed.). CABI, Wallingford, UK: 87–95.

Sanogo S, Lamour K, Kousik S, *et al.* (2023). *Phytophthora capsici*, 100 years later: Research mile markers from 1922 to 2022. *Phytopathology* **113**: 921–930.

Sansome ER (1980). Reciprocal translocation heterozygosity in heterothallic species of *Phytophthora* and its significance. *Transactions of the British Mycological Society* **74**: 175–185.

Sansome ER, Brasier CM, Hamm PB (1990). *Phytophthora meadii* may be a species hybrid. *Mycological Research* **95:** 273–277.

Santini A, Ghelardini L, De Pace C, *et al.* (2013). Biogeographic patterns and determinants of invasion by alien forest pathogens in Europe. *New Phytologist* **197**: 238–250.

Savita GSV, Nagpal A (2012). *Citrus* diseases caused by *Phytophthora* species. *GERF Bulletin of Biosciences* **3**: 18–27.

Scanu B, Hunter GC, Linaldeddu BT, *et al.* (2014). A taxonomic re-evaluation reveals that *Phytophthora cinnamomi* and *P. cinnamomi* var. *parvispora* are separate species. *Forest Pathology* **44**: 1–20.

Scanu B, Jung T, Masigol H, *et al.* (2021). *Phytophthora heterospora sp. nov*., a new pseudoconidia-producing sister species of *P. palmivora*. *Journal of Fungi* **7**: 870.

Scanu B, Linaldeddu BT, Deidda A, *et al.* (2015). Diversity of *Phytophthora* species from declining Mediterranean maquis vegetation, including two new species, *Phytophthora crassamura* and *P. ornamentata sp. nov*. *PLoS ONE* **10**: e0143234.

Scanu B, Webber JF (2016). Dieback and mortality of *Nothofagus* in Britain: ecology, pathogenicity and sporulation potential of the causal agent *Phytophthora pseudosyringae*. *Plant Pathology* **65**: 26–36.

Scarlett K, Daniel R, Shuttleworth LA, *et al.* (2015). *Phytophthora* in the Gondwana Rainforests of Australia World Heritage Area. *Australasian Plant Pathology* **44**: 335–348.

Schardl CL, Craven KD (2003). Interspecific hybridization in plant-associated fungi and oomycetes: a review. *Molecular Ecology* **12**: 2861–2873.

Schoebel CN, Stewart J, Gruenwald NJ, *et al.* (2014). Population history and pathways of spread of the plant pathogen *Phytophthora plurivora*. *PLoS ONE* **9**: e85368.

Schwingle BW, Smith JA, Blanchette RA (2007). *Phytophthora* species associated with diseased woody ornamentals in Minnesota nurseries. *Plant Disease* **91**: 97–102.

Scott P, Williams N (2014). Phytophthora diseases in New Zealand forests. *New Zealand Journal of Forestry* **59**: 14–21.

Scott P, Bader MK-F, Burgess T, *et al.* (2019). Global biogeography and invasion risk of the plant pathogen genus *Phytophthora*. *Environmental Science & Policy* **101**: 175–182.

Scott PM, Burgess TI, Barber PA, *et al.* (2009). *Phytophthora multivora sp. nov*., a new species recovered from declining *Eucalyptus*, *Banksia*, *Agonis* and other plant species in Western Australia. *Persoonia* **22**: 1–13.

Scott PM, Jung T, Shearer BL, *et al.* (2012). Pathogenicity of *Phytophthora multivora* to *Eucalyptus gomphocephala* and *Eucalyptus marginata*. *Forest Pathology* **42**: 289–298.

Seddaiu S, Brandano A, Ruiu PA, *et al.* (2020). An overview of *Phytophthora* species inhabiting declining *Quercus suber* stands in Sardinia (Italy). *Forests* **11**: 971.

Seddaiu S, Linaldeddu BT (2020). First report of *Phytophthora acerina*, *P. plurivora*, and *P. pseudocryptogea* associated with declining common alder trees in Italy. *Plant Disease* **104**: 1874.

Seibert P (1996). *Farbatlas Südamerika - Landschaften und Vegetation* (*'Colour atlas South America - landscapes and vegetation*'). Eugen Ulmer, Stuttgart, Germany: 288 pp.

Shakya SK, Grünwald NJ, Fieland VJ, *et al.* (2021). Phylogeography of the wide-host range panglobal plant pathogen *Phytophthora cinnamomi*. *Molecular Ecology* **30**: 5164–5178.

Sharma PP, Giribet G (2012). Out of the Neotropics: Late Cretaceous colonization of Australasia by American arthropods. *Proceedings of the Royal Society B* **279**: 3501–3509.

Shrestha S, Hu J, Fryxell RT, *et al.* (2014). SNP markers identify widely distributed clonal lineages of *Phytophthora colocasiae* in Vietnam, Hawaii and Hainan Island, China. *Mycologia* **106**: 676–685.

Shrestha SK, Zhou Y, Lamour K (2013). Oomycetes baited from streams in Tennessee 2010–2012. *Mycologia* **105**: 1516–1523.

Sims LL, Goheen E, Kanaskie A, *et al.* (2015a). Alder canopy dieback and damage in Western Oregon riparian ecosystems. *Northwest Science* **89**: 34–46.

Sims LL, Garbelotto M (2021). *Phytophthora* species repeatedly introduced in Northern California through restoration projects can spread into adjacent sites. *Biological Invasions* **23**: 2173–2190.

Sims LL, Sutton W, Reeser P, *et al.* (2015b). The *Phytophthora* species assemblage and diversity in riparian alder ecosystems of western Oregon, USA. *Mycologia* **107**: 889–902.

Smith IW, Cunnington J, Pascoe I (2006). Another new? species of *Phytophthora* on alder 'down under' (Australia). In: *Progress in research on Phytophthora siseases of forest yrees* (Brasier CM, Jung T, Osswald W, eds), Forest Research, Farnham, Hampshire, UK: Poster 30.

Spies CFJ, Meitz-Hopkins JC, Langenhoven SD, *et al.* (2014). Two clonal lineages of *Phytophthora citrophthora* from citrus in South Africa represent a single phylogenetic species. *Mycologia* **106**: 1106–1118.

Stöver BC, Müller KF (2010). TreeGraph 2: Combining and visualizing evidence from different phylogenetic analyses. *BMC Bioinformatics* **11**: 7.

Stukenbrock EH (2016). The role of hybridization in the evolution and emergence of new fungal plant pathogens. *Phytopathology* **106**: 104–112.

Studholme DJ, Panda P, Sanfuentes von Stowasser E, *et al.* (2019). Genome sequencing of oomycete isolates from Chile supports the New Zealand origin of *Phytophthora kernoviae* and makes available the first *Nothophytophthora* sp. genome. *Molecular Plant Pathology* **20**: 423–431.

Sukumaran J, Holder MT (2010). DendroPy: A Python library for phylogenetic computing. *Bioinformatics* **26**: 1569–1571.

Sukumaran J, Holder MT (2015). SumTrees: Phylogenetic tree summarization. https://github.com/jeetsukumaran/DendroPy [accessed 18 Oct 2023].

Svenning J-C (2003). Deterministic Plio-Pleistocene extinctions in the European cool-temperate tree flora. *Ecology Letters* **6**: 646–653.

Szabó I, Lakatos F, Sipos G (2013). Occurrence of soilborne *Phytophthora* species in declining broadleaf forests in Hungary. *European Journal of Plant Pathology* **137**: 159–168.

Tamura K, Stecher G, Kumar S (2021). MEGA11: Molecular Evolutionary Genetics Analysis version 11. *Molecular Biology and Evolution* **38**: 3022–3027.

Tecklin D, DellaSala DA, Luebert F, *et al.* (2011). Valdivian temperate rainforests of Chile and Argentina. In: *Temperate and boreal rainforests of the world* (DellaSala DA, ed.). Island Press, Washington, Covelo, London: 132–153.

Tian S, López-Pujol J, Wang H-W, *et al.* (2010). Molecular evidence for glacial expansion and interglacial retreat during Quaternary climatic changes in a montane temperate pine (*Pinus kwangtungensis* Chun ex Tsiang) in southern China. *Plant Systematics and Evolution* **284**: 219–229.

Themann K, Werres S, Lüttmann R, *et al.* (2002). Observations of *Phytophthora* spp. in water recirculation systems in commercial hardy ornamental nursery stock. *European Journal of Plant Pathology* **108**: 337–343.

Thines M, Choi Y–J (2016). Evolution, diversity and taxonomy of the *Peronosporaceae*, with focus on the genus *Peronospora*. *Phytopathology* **106**: 6–18.

Tiffney BH (1985). The Eocene North Atlantic land bridge: Its importance in tertiary and modern phytogeography of the northern hemisphere. *Journal of the Arnold Arboretum* **66**: 243–273.

Toussaint EFA, Hendrich L, Hájek J, *et al.* (2017). Evolution of Pacific Rim diving beetles sheds light on Amphi-Pacific biogeography. *Ecography* **40**: 500–510.

Truong NV, Liew ECY, Burgess LW (2010). Characterisation of *Phytophthora capsici* isolates from black pepper in Vietnam. *Fungal Biology* **114**: 160–170.

Tsykun T, Prospero S, Schoebel CN, *et al.* (2022). Global invasion history of the emerging plant pathogen *Phytophthora multivora*. *BMC Genomics* **23**: 153.

Turchetto-Zolet AC, Pinheiro F, Salgueiro F, *et al.* (2013). Phylogeographical patterns shed light on evolutionary process in South America. *Molecular Ecology* **22**: 1193–1213.

Tucker CM, Milbrath JA (1942). Root rot of *Chamaecyparis* caused by a species of *Phytophthora*. *Mycologia* **34**: 94–103.

Tyson JL, Fullerton RA (2007). Mating types of *Phytophthora colocasiae* from the Pacific region, India and South-east Asia. *Australasian Plant Disease Notes* **2**: 111–112.

Uchida J, Kadooka CY (2013). Distribution and biology of *Phytophthora tropicalis*. In: *Phytophthora a global perspective* (Lamour K, ed.). CABI, Wallingford, UK: 178–186.

Van Damme K, Sinev AY (2013). Tropical Amphi-Pacific disjunctions in the *Cladocera* (*Crustacea*: *Branchiopoda*). *Journal of Limnology* **72(s2)**: 209–244.

Van Poucke K, Franceschini S, Webber JF, *et al.* (2012). Discovery of a fourth evolutionary lineage of *Phytophthora ramorum*: EU2. *Fungal Biology* **116**: 1178–1191.

Van Poucke K, Haegeman A, Goedefroit T, *et al.* (2021). Unravelling hybridization in *Phytophthora* using phylogenomics and genome size estimation. *IMA Fungus* **12**: 16.

Van Welzen PC, Parnell JAN, Slik JWF (2011). Wallace's Line and plant distributions: two or three phytogeographical areas and where to group Java? *Biological Journal of the Linnean Society* **103**: 531–545.

Van Welzen PC, Slik JWF (2009). Patterns in species richness and composition of plant families in the Malay Archipelago. *Blumea* **54**: 166–171.

Vélez ML, La Manna L, Tarabini N, *et al.* (2020). *Phytophthora austrocedri* in Argentina and co-inhabiting Phytophthoras: Roles of anthropogenic and abiotic factors in species distribution and diversity. *Forests* **11**: 1223.

Vettraino AM, Brasier CM, Brown AV, *et al.* (2011). *Phytophthora himalsilva sp. nov*. an unusually phenotypically variable species from a remote forest in Nepal. *Fungal Biology* **115**: 275–287.

Vettraino AM, Franceschini S, Vannini A (2010). First report of *Buxus rotundifolia* decline caused by *Phytophthora citrophthora* (R. & E. Sm.) Leonian in Italy. *Plant Disease* **94**: 272.

Vila R, Bell CD, Macniven R, *et al.* (2011). Phylogeny and palaeoecology of *Polyommatus* blue butterflies show Beringia was a climate-regulated gateway to the New World. *Proceedings of the Royal Society B* **278**: 2737–2744.

Wang J, Presser JW, Goss EM (2016). Nuclear DNA content of the hybrid plant pathogen *Phytophthora andina* determined by flow cytometry. *Mycologia* **108**: 899–904.

Waterhouse GM (1963). Key to the species of *Phytophthora* de Bary. *Mycological Papers* **92**: 1–22.

Weiland JE, Nelson AH, Hudler GW (2010). Aggressiveness of *Phytophthora cactorum*, *P. citricola* I, and *P. plurivora* from European beech. *Plant Disease* **94**: 1009–1014.

Wen J (1999). Evolution of Eastern Asian and Eastern North American disjunct distributions in flowering plants. *Annual Review of Ecology and Systematics* **30**: 421–455.

Wen J, Ickert-Bond S, Nie Z-L, *et al.* (2010). Timing and modes of evolution of eastern Asian-North American biogeographic disjunctions in seed plants. In: *Darwin's Heritage Today: Proceedings of the Darwin 2010 Beijing International Conference* (Long M, Gu H, Zhou Z, eds). Higher Education Press, Bejing, China: 252–269.

Wen J, Nie Z-L, Ickert-Bond SM (2016). Intercontinental disjunctions between eastern Asia and western North America in vascular plants highlight the biogeographic importance of the Bering land bridge from late Cretaceous to Neogene. *Journal of Systematics and Evolution* **54**: 469–490.

White TJ, Bruns T, Lee S, *et al.* (1990). Amplification and direct sequencing of fungal ribosomal RNA genes for phylogenetics. In: *PCR Protocols: A Guide to Methods and Applications* (Innes MA, Gelfand DH, Sninsky JJ, *et al.*, eds). Academic Press, San Diego, California, USA: 315–322.
Whitten T, Damanik SJ, Anwar J, *et al.* (1997). *The Ecology of Sumatra*. Ecology of Indonesia Series, Vol. I, Oxford University Press, Oxford, UK.
Whitten T, Mustafa M, Henderson GS (2002). *The Ecology of Sulawesi*. Ecology of Indonesia Series, Vol. IV, Oxford University Press, Oxford, UK.
Winkworth RC, Neal G, Ogas RA, *et al.* (2022). Comparative analyses of complete *Peronosporaceae* (*Oomycota*) mitogenome sequences – insights into structural evolution and phylogeny. *Genome Biology and Evolution* **14**: evac049.
Woodburne MO (2010). The Great American Biotic Interchange: Dispersals, tectonics, climate, sea level and holding pens. *Journal of Mammalian Evolution* **17**: 245–264.
Wurster CM, Bird MI, Bull ID, *et al.* (2010). Forest contraction in north equatorial Southeast Asia during the last glacial maximum. *Proceedings of the National Academy of Sciences of the USA* **107**: 15508–15511.
Xu J, Yang X, Li Y, *et al.* (2019). *Phytophthora* species from Xinjiang Wild apple forests in China. *Forests* **10**: 927.
Xu J, Yang X, Li Y, *et al.* (2021). First report of *Phytophthora pini* causing foliage blight and shoot dieback of *Rhododendron pulchrum* in China. *Plant Disease* **105**: 1229.
Yang X, Hong C (2016). Diversity and populations of *Phytophthora*, *Phytopythium* and *Pythium* species recovered from sediments in an agricultural run-off sedimentation reservoir. *Plant Pathology* **65**: 1118–1125.
Yang X, Hong C (2013). *Phytophthora virginiana sp. nov*., a high-temperature tolerant species from irrigation water in Virginia. *Mycotaxon* **126**: 167–176.
Yang X, Hong C (2018). Differential usefulness of nine commonly used genetic markers for identifying *Phytophthora* species. *Frontiers in Microbiology* **9**: 2334.
Yang X, Balci Y, Brazee NJ, *et al.* (2016). A unique species in *Phytophthora* clade 10, *Phytophthora intercalaris sp. nov*., recovered from stream and irrigation water in the eastern USA. *International Journal of Systematic and Evolutionary Microbiology* **66**: 845–855.
Yang X, Copes WE, Hong CX (2013). *Phytophthora mississippiae sp. nov*., a new species recovered from irrigation reservoirs at a plant nursery in Mississippi. *Journal of Plant Pathology and Microbiology* **4**: 180.
Yang X, Copes WE, Hong CX (2014a). Two novel species representing a new clade and cluster of *Phytophthora*. *Fungal Biology* **118**: 72–82.
Yang X, Gallegly ME, Hong CX (2014b). A high-temperature tolerant species in clade 9 of the genus *Phytophthora*: *P. hydrogena sp. nov*. *Mycologia* **106**: 57–65.
Yang X, Richardson PA, Hong C (2014c). *Phytophthora* ×*stagnum nothosp. nov*., a new hybrid from irrigation reservoirs at ornamental plant nurseries in Virginia. *PLoS ONE* **9**: e103450.
Yang X, Tyler BM, Hong C (2017). An expanded phylogeny for the genus *Phytophthora*. *IMA Fungus* **8**: 355–384.
Ye Z, Chen P, Bu W (2016). Terrestrial mountain islands and Pleistocene climate fluctuations as motors for speciation: A case study on the genus *Pseudovelia* (*Hemiptera*: *Veliidae*). *Scientific Reports* **6**: 33625.
Zeng H-C, Ho H-H, Zheng F-C (2009). A survey of *Phytophthora* species on Hainan Island of South China. *Journal of Phytopathology* **157**: 33–39.
Zentmyer GA (1979). Stimulation of sexual reproduction in the A2 mating type of *Phytophthora cinnamomi* by a substance in avocado roots. *Phytopathology* **69**: 1129–1131.
Zentmyer GA (1988). Origin and distribution of four species of *Phytophthora*. *Transactions of the British Mycological Society* **91**: 367–378.
Zhang KM, Zheng FC, Li YD, *et al.* (1994). Isolates of *Phytophthora colocasiae* from Hainan Island in China: evidence suggesting an Asian origin of this species. *Mycologia* **86**: 108–112.

Supplementary Material: https://studiesinmycology.org/

Fig. S1. Fifty percent majority rule consensus phylogram derived from maximum likelihood analysis of a concatenated thirteen-locus (LSU, ITS, *βtub*, *hsp90*, *tigA*, *rpl10*, *tef-1α*, *enl*, *ras-ypt1*, *cox1*, *cox2*, *nadh1*, *rps10*) dataset of *Phytophthora* major Clade 2. Maximum Likelihood bootstrap values (in %) are indicated but not shown below 60 %. *Phytophthora infestans* and *P. pseudosyringae* from Clades 1c and 3, respectively, were used as outgroup taxa (not shown). (EpT), (NT) and (T) denote ex-epitype, ex-neotype and ex-type isolates. Scale bar indicates 0.02 expected changes per site per branch.
Fig. S2. Fifty percent majority rule consensus phylogram derived from maximum likelihood analysis of a concatenated thirteen-locus (LSU, ITS, *βtub*, *hsp90*, *tigA*, *rpl10*, *tef-1α*, *enl*, *ras-ypt1*, *cox1*, *cox2*, *nadh1*, *rps10*) dataset of *Phytophthora* Clade 2a. Bootstrap values (in %) are indicated but not shown below 60 %. *Phytophthora infestans* and *P. pseudosyringae* from Clades 1c and 3, respectively, were used as outgroup taxa (not shown). (EpT), (NT) and (T) denote ex-epitype, ex-neotype and ex-type isolates. Scale bar indicates 0.01 expected changes per site per branch.
Fig. S3. Fifty percent majority rule consensus phylogram derived from maximum likelihood analysis of a concatenated thirteen-locus (LSU, ITS, *βtub*, *hsp90*, *tigA*, *rpl10*, *tef-1α*, *enl*, *ras-ypt1*, *cox1*, *cox2*, *nadh1*, *rps10*) dataset of *Phytophthora* Clade 2b. Bootstrap values (in %) are indicated but not shown below 60 %. *Phytophthora infestans* and *P. pseudosyringae* from Clades 1c and 3, respectively, were used as outgroup taxa (not shown). (EpT) and (T) denote ex-epitype and ex-type isolates, respectively isolates. Scale bar indicates 0.01 expected changes per site per branch.
Table S1. Details of isolates from *Phytophthora* major Clades 2, 3 and 7 included in the phylogenetic, morphological, growth-temperature and biogeography studies.
Table S2. Overview of PCR conditions and details of primers used for amplification and sequencing of *Phytophthora* isolates.
Table S3. GenBank accession numbers of *Phytophthora* isolates included in the phylogenetic, morphological and growth-temperature studies.
Table S4. Morphological characters and dimensions (mean ± SD; µm), cardinal temperatures (°C) and temperature-growth relations (mm/d) on V8-juice agar of *Phytophthora* species from subclade 2a (1st set).
Table S5. Morphological characters and dimensions (mean ± SD; µm), cardinal temperatures (°C) and temperature-growth relations (mm/d) on V8-juice agar of *Phytophthora* species from subclade 2a (2nd set).
Table S6. Morphological characters and dimensions (mean ± SD; µm), cardinal temperatures (°C) and temperature-growth relations (mm/d) on V8-juice agar of *Phytophthora* species from subclade 2a (3rd set).
Table S7. Morphological characters and dimensions (mean ± SD; µm), cardinal temperatures (°C) and temperature-growth relations (mm/d) on V8-juice agar of *Phytophthora* species from subclade 2b (1st set).
Table S8. Morphological characters and dimensions (mean ± SD; µm), cardinal temperatures (°C) and temperature-growth relations (mm/d) on V8-juice agar of *Phytophthora* species from subclade 2b (2nd set).
Table S9. Morphological characters and dimensions (mean ± SD; µm), cardinal temperatures (°C) and temperature-growth relations (mm/d) on V8-juice agar of *Phytophthora* species from subclade 2b (3rd set).
Table S10. Morphological characters and dimensions (mean ± SD; µm), cardinal temperatures (°C) and temperature-growth relations (mm/d) on V8-juice agar of *Phytophthora* species from subclade 2c (1st set).
Table S11. Morphological characters and dimensions (mean ± SD; µm), cardinal temperatures (°C) and temperature-growth relations (mm/d) on V8-juice agar of *Phytophthora* species from subclade 2c (2nd set).
Table S12. Morphological characters and dimensions (mean ± SD; µm), cardinal temperatures (°C) and temperature-growth relations (mm/d) on V8-juice agar of *Phytophthora* species from subclade 2c (3rd set).
Table S13. Morphological characters and dimensions (mean ± SD; µm), cardinal temperatures (°C) and temperature-growth relations (mm/d) on V8-juice agar of *Phytophthora* species from subclade 2c (4th set).
Table S14. Morphological characters and dimensions (mean ± SD; µm), cardinal temperatures (°C) and temperature-growth relations (mm/d) on V8-juice agar of *Phytophthora* species from subclades 2d (only *P. oleae*) and 2e (1st set).

Table S15. Morphological characters and dimensions (mean ± SD; µm), cardinal temperatures (°C) and temperature-growth relations (mm/d) on V8-juice agar of *Phytophthora* taxa from subclade 2e (2nd set).
Table S16. Morphological characters and dimensions (mean ± SD; µm), cardinal temperatures (°C) and temperature-growth relations (mm/d) on V8-juice agar of *Phytophthora* taxa from subclade 2f.
Table S17. Morphological characters and dimensions (mean ± SD; µm), cardinal temperatures (°C) and temperature-growth relations (mm/d) on V8-juice agar of *Phytophthora* species from subclade 2g.
Table S18. Heterozygosity across nine nuclear gene regions (LSU, ITS, *ßtub*, *hsp90*, *tigA*, *rpl10*, *tef-1α*, *enl*, *ras-ypt1*), breeding systems and hybrid status of 46 *Phytophthora* taxa in subclades 2c, 2d, 2e, 2f and 2g.
Table S19. Pairwise sequence identities (%) for the mitochondrial *cox1*, *cox2*, *nadh1* and *rsp10* genes between eight *Phytophthora* Clade 2a species with ambiguous, probable or confirmed hybrid status and their closest matches.
Table S20. Pairwise sequence similarities (%) for the mitochondrial *cox1*, *cox2*, *nadh1* and *rsp10* genes between six *Phytophthora* Clade 2b taxa with ambiguous or probable hybrid status and their closest matches.